H. Sawada • M. Araki • N.A. Chappell
J.V. LaFrankie • A. Shimizu (Eds.)

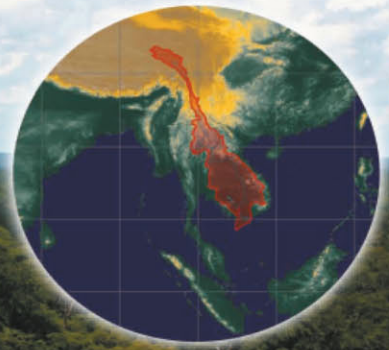

Forest Environments in the Mekong River Basin

Springer

H. Sawada, M. Araki, N.A. Chappell, J.V. LaFrankie, A. Shimizu (Eds.)
Forest Environments in the Mekong River Basin

H. Sawada, M. Araki, N.A. Chappell,
J.V. LaFrankie, A. Shimizu (Eds.)

Forest Environments in the Mekong River Basin

With 145 Figures, Including 37 in Color

Springer

Haruo Sawada, Ph. D.
Forestry and Forest Products Research Institute
1 Matsunosato, Tsukuba, Ibaraki 305–8687, Japan

Makoto Araki
Forestry and Forest Products Research Institute
1 Matsunosato, Tsukuba, Ibaraki 305–8687, Japan

Nick A. Chappell, Ph. D.
Lancaster Environment Centre, Lancaster University
Lancaster LA1 4YQ, UK

James V. LaFrankie, Ph. D.
Center for Tropical Forest Science, Smithsonian Tropical Research Institute
National Institute of Education
1 Nanyang Walk, Jurong, Singapore

Akira Shimizu, Ph. D.
Forestry and Forest Products Research Institute
1 Matsunosato, Tsukuba, Ibaraki 305–8687, Japan

ISBN 978-4-431-46500-3 Springer Tokyo Berlin Heidelberg New York

Library of Congress Control Number: 2007921191

This work is subject to copyright. All rights are reserved, whether the whole or part of the material is concerned, specifically the rights of translation, reprinting, reuse of illustrations, recitation, broadcasting, reproduction on microfilms or in other ways, and storage in data banks. The use of registered names, trademarks, etc. in this publication does not imply, even in the absence of a specific statement, that such names are exempt from the relevant protective laws and regulations and therefore free for general use.

Springer is a part of Springer Science+Business Media
springer.com

© Springer 2007
Printed in Japan

Typesetting: SNP Best-set Typesetter Ltd., Hong Kong
Printing and binding: Shinano Inc., Japan

Printed on acid-free paper

Foreword

Deforestation and forest degradation have continued over a long period of time, and the deterioration of forest environment management services is becoming one of the biggest concerns in the world. Especially in large continental river basins, selfish political attitudes and individual interests in some regions predispose other regions to problems downstream and bring about international issues. The Mekong is just such a river basin and its water is the most important resource, interdependent with the forest conditions in the region. The lives of millions of people are sustained by the water of the Mekong River, and mutual understanding on water resource management is essential in this region. Consequently, appropriate environment management to control water resources is required of each country along with scientific knowledge of forest management, including forest hydrology.

The Mekong River Commission (MRC) was established in 1995 to jointly manage shared water resources and develop the economic potential of the river by the governments of Cambodia, Laos, Thailand, and Vietnam. However, very limited operational forest management for water resources is being conducted based on reliable sources of information.

International cooperation in science and technology has progressed in Southeast Asia. One such activity, the research project "Changes of Water Cycle in the Mekong River Basin" (CWCM), has been conducted by the Forestry Administration (FA) of Cambodia, the Forestry and Forest Products Research Institute (FFPRI) of Japan, and several universities, since 2002.

Advanced observation systems of atmospheric flux, ground water levels, soil water movement, and stable isotope variation as well as satellite remote sensing technologies were introduced for the continuous monitoring of the forest environment. The project has produced much new information about the forest environment of Cambodia. To honor their efforts, the Cambodian government awarded the Japanese researchers the medal of the Chevalier of the Order of Sahametrei in June 2005 as a tribute to their ongoing activities. In December 2005, the members of the project organized the international conference titled "Forest Environment in Continental River Basins; with a focus on the Mekong River" as an International Union of Forest Research Orgnizations (IUFRO) meeting with the support of the FFPRI.

Participants from more than 10 countries attended, most of whom live in the Mekong River basin. Mr. Ty Sokhun, Head of FA, introduced the meeting as the first

international conference in the field of forest research in Cambodia. Because very little knowledge of this region had been available to the public, interest was raised among many international researchers, and much new information was exchanged during the meeting of 160 participants, including Cambodian university students.

I find the chapters of this book, comprising the papers presented and collected at the conference, most exciting. Even as recently as 10 years ago, who would have guessed that this kind of scientific data could be obtained from the Mekong River basin? One of the most pleasing features of this book is the original data and views presented by the authors, which fill in the gaps in the forest data of the world.

Motoaki Okuma
President
FFPRI

Preface

The Mekong River runs through six countries, from China to Vietnam, and the usage and management of water resources are different in each country. The Mekong River Commission (MRC) plays an important role in collecting various kinds of information about the lower Mekong and in strengthening the integrated water resources management capacity. However, the history of each country in the region is quite complex, and the scientific knowledge of water resources is still very limited in some areas.

Although adequate information on forest hydrology is lacking in some countries, the practical knowledge of others is quite useful in this region because of the many similarities in their natural environments. As a result, we organized an international International Union of Forest Research Orgnizations (IUFRO) conference, "The Forest Environment in Continental River Basins; with a focus on the Mekong River," so that scientists in related fields could meet and share their knowledge of the region for the purpose of good forest management with a focus on water resources.

We were greatly pleased that the meeting provided a good opportunity not only for researchers but also for many university students to learn of the research activities on forest ecosystems, hydrology, and forest management. It was the first such conference on forest research in Cambodia, and there were several difficulties that had to be overcome. However, it proved enjoyable for everyone to work together to make the conference a success.

We believe the conference was productive and has resulted in this volume, among other things, which we are proud to present to our colleagues around the world. The book consists of three parts, each contributing to a better understanding of the Mekong River basin: forest hydrology, forest management, and forest ecology. The chapters of the book are based on full papers that were collected after the conference, with each paper being sent to two peer reviewers. The papers were designated as either research papers or technical papers, according to the evaluations of the reviewers.

We would like to acknowledge IUFRO and IUFRO-J for their understanding and support of the conference. We are grateful to the Forestry Administration (FA) of Cambodia and to the Japan International Cooperation Agency in Cambodia for their valuable contributions to the conference. The FA opened a secretariat's office and assigned full-time assistants to the conference. We express our thanks to the Forestry

and Forest Products Research Institute (FFPRI) and staff members who helped the editors to accomplish their goal. We also thank staffs of Springer Japan for keeping in close contact with us and making possible the publication of this book.

Haruo Sawada
Makoto Araki
Nick Chappell
James LaFrankie
Akira Shimizu
Editors

Editorial Board

Editors:
Sawada, Haruo
Araki, Makoto
Chappell, Nick A.
LaFrankie, James V.
Shimizu, Akira

Assistant Editors:
Furuya, Naoyuki
Ito, Eriko
Kabeya, Naoki

Reviewers:
Araki, Makoto
Awaya, Yoshio
Chappell, Nick A.
Furuya, Naoyuki
Hattori, Sigeaki
Hirabuki, Yoshihiko
Ito, Eriko
Kanzaki, Mamoru
LaFrankie, James V.
Mochida, Haruyuki
Ohnuki, Yasuhiro
Ohta, Seiichi
Sawada, Haruo
Seino, Tatsuyuki
Shimizu, Akira
Shimizu, Takanori
Shinomiya, Yoshiki
Suzuki, Masakazu
Tamai, Koji
Tsuboyama, Yoshio
Tsuchiya, Toshiyuki
Tsuyuki, Satoshi

Contents

Foreword V

Preface VII

Editorial Board IX

Contributors XV

Color Plates XXI

Part I Forest Hydrology

Runoff Processes in Southeast Asia: Role of Soil, Regolith, and Rock Type 3
N.A. Chappell, M. Sherlock, K. Bidin, R. Macdonald, Y. Najman, and G. Davies

Impact of Land-Use Development on the Water Balance and Flow Regime of the Chi River Basin, Thailand 24
K. Boochabun, S. Vongtanaboon, A. Sukrarasmi, and N. Tangtham

Evaluation of Evapotranspiration in Forested Areas in the Mekong Basin Using GIS Data Analysis 36
S. Sawano, N. Hotta, H. Komatsu, M. Suzuki, and T. Yayama

Severe Drought Resulting from Seasonal and Interannual Variability in Rainfall and Its Impact on Transpiration in a Hill Evergreen Forest in Northern Thailand 45
T. Kume, H. Takizawa, N. Yoshifuji, N. Tanaka, K. Tanaka, C. Tantasirin, and M. Suzuki

Factors Affecting Interannual Variability in Transpiration in a Tropical Seasonal Forest in Northern Thailand: Growing Season Length and Soil Drought 56
N. Yoshifuji, N. Tanaka, C. Tantasirin, and M. Suzuki

Scale Dependency of Hydrological Characteristics in the Upper Ping River Basin, Northern Thailand 67
K. Kuraji, K. Punyatrong, I. Sirisaiyard, C. Tantasirin, and N. Tanaka

Year-Round Observation of Evapotranspiration in an Evergreen Broadleaf Forest in Cambodia 75
T. Nobuhiro, A. Shimizu, N. Kabeya, Y. Tsuboyama, T. Kubota, T. Abe, M. Araki, K. Tamai, S. Chann, and N. Keth

Measurements of Wind Speed, Direction, and Vertical Profiles in an Evergreen Forest in Central Cambodia 87
K. Tamai, A. Shimizu, T. Nobuhiro, N. Kabeya, S. Chann, and N. Keth

Stomatal Response Characteristics of Dry Evergreen and Dry Deciduous Forests in Kampong Thom, Cambodia 97
K. Daikoku, S. Hattori, A. Deguchi, Y. Fujita, M. Araki, and T. Nobuhiro

Changes of Vertical Soil Moisture Conditions of a Dry Evergreen Forest in Kampong Thom, Cambodia 112
M. Araki, A. Shimizu, J. Toriyama, E. Ito, N. Kabeya, T. Nobuhiro, B. Tith, S. Pol, S. Lim, S. Khorn, P. Pith, S. Det, S. Ohta, and M. Kanzaki

Stable Isotope Studies of Rainfall and Stream Water in Forest Watersheds in Kampong Thom, Cambodia 125
N. Kabeya, A. Shimizu, S. Chann, Y. Tsuboyama, T. Nobuhiro, N. Keth, and K. Tamai

Runoff Characteristics and Observations on Evapotranspiration in Forest Watersheds, Central Cambodia 135
A. Shimizu, N. Kabeya, T. Nobuhiro, T. Kubota, Y. Tsuboyama, E. Ito, M. Sano, S. Chann, and N. Keth

Part II Forest Management

Object-Oriented Land Cover Classification Based on Two Satellite Images Obtained in One Dry Season in Cambodia 149
N. Furuya, H. Saito, S. Preap, B. Tith, and M. Meas

Land Cover Change Mapping of the Mekong River Basin Using NOAA Pathfinder AVHRR 8-km Land Dataset 159
H. Saito, Y. Sawada, N. Furuya, and S. Preap

Effect of Forest Cover Change on Sedimentation in Lam Phra Phloeng Reservoir, Northeastern Thailand 168
K. Lorsirirat

Seasonally Flooded Community Forest on the Banks of the Songkhram River: A Research Framework 179
T. Sasaki, S. Worrapornpan, and S. Seesang

Part III Forest Ecology

Forest Environment of Vietnam: Features of Forest Vegetation and Soils ... 189
V.T. Phuong

Principal Forest Types of Three Regions of Cambodia: Kampong Thom, Kratie, and Mondolkiri 201
A. Tani, E. Ito, M. Kanzaki, S. Ohta, S. Khorn, P. Pith, B. Tith, S. Pol, and S. Lim

Comparison of the Leaf Area Index (LAI) of Two Types of Dipterocarp Forest on the West Bank of the Mekong River, Cambodia 214
E. Ito, S. Khorn, S. Lim, S. Pol, B. Tith, P. Pith, A. Tani, M. Kanzaki, T. Kaneko, Y. Okuda, N. Kabeya, T. Nobuhiro, and M. Araki

Open Woodland Patches in an Evergreen Forest of Kampong Thom, Cambodia: Correlation of Structure and Composition with Microtopography 222
R. Hiramatsu, M. Kanzaki, J. Toriyama, T. Kaneko, Y. Okuda, S. Ohta, S. Khorn, P. Pith, S. Lim, S. Pol, E. Ito, and M. Araki

Use of ASTER Optical Indices to Estimate Spatial Variation in Tropical Seasonal Forests on the West Bank of the Mekong River, Cambodia..... 232
E. Ito, S. Lim, S. Pol, B. Tith, P. Pith, S. Khorn, A. Tani, M. Kanzaki, T. Kaneko, Y. Okuda, and M. Araki

Soils Under Different Forest Types in the Dry Evergreen Forest Zone of Cambodia: Morphology, Physicochemical Properties, and Classification 241
J. Toriyama, S. Ohta, M. Araki, M. Kanzaki, S. Khorn, P. Pith, S. Lim, and S. Pol

Soil Moisture Conditions in Four Types of Forests in Kampong Thom, Cambodia 254
M. Araki, J. Toriyama, S. Ohta, M. Kanzaki, E. Ito, B. Tith, S. Pol, S. Lim, S. Khorn, P. Pith, and S. Det

Apparent Change in Soil Depth and Soil Hardness in Forest Areas in Kampong Thom Province, Cambodia 263
Y. Ohnuki, C. Kimhean, Y. Shinomiya, S. Sor, J. Toriyama, and S. Ohta

Effect of Soil Water Content on Water Storage Capacity: Comparison Between the Forested Areas in Cambodia and Japan..... 273
Y. Shinomiya, M. Araki, J. Toriyama, Y. Ohnuki, A. Shimizu, N. Kabeya, T. Nobuhiro, C. Kimhean, and S. Sor

Influence of Large Seasonal Water Level Fluctuations and Human Impact on the Vegetation of Lake Tonle Sap, Cambodia 281
Y. Araki, Y. Hirabuki, D. Powkhy, S. Tsukawaki, C. Rachna, M. Tomita, and K. Suzuki

Subject Index 295

Contributors

Abe, Toshio
Forestry and Forest Products Research Institute (FFPRI), Tsukuba, Japan

Araki, Makoto
Forestry and Forest Products Research Institute (FFPRI), Tsukuba, Japan

Araki, Yuji
Graduate School of Environment and Information Sciences, Yokohama National University, Yokohama, Japan

Bidin, Kawi
School of Science and Technology, University Malaysia Sabah, Kota Kinabalu, Malaysia

Boochabun, Kanokporn
Research and Applied Hydrology Group, Hydrology Division, Office of Hydrology and Water Management, Royal Irrigation Department, Bangkok, Thailand

Chann, Sophal
Forest and Wildlife Science Research Institute (FWSRI), Forestry Administration, Phnom Penh, Cambodia

Chappell, Nick A
Lancaster Environment Centre, Lancaster University, Lancaster, United Kingdom

Daikoku, Kenichi
Graduate School of Bioagricultural Sciences, Nagoya University, Nagoya, Japan

Davies, Gemma
Lancaster Environment Centre, Lancaster University, Lancaster, United Kingdom

Deguchi, Aiko
Graduate School of Bioagricultural Sciences, Nagoya University, Nagoya, Japan

Det, Seila
Forest and Wildlife Science Research Institute (FWSRI), Forestry Administration, Phnom Penh, Cambodia

Fujita, Yuji
Graduate School of Bioagricultural Sciences, Nagoya University, Nagoya, Japan

Furuya, Naoyuki
Forestry and Forest Products Research Institute (FFPRI), Tsukuba, Japan

Hattori, Shigeaki
Graduate School of Bioagricultural Sciences, Nagoya University, Nagoya, Japan

Hirabuki, Yoshihiko
Faculty of Liberal Arts, Tohoku Gakuin University, Sendai, Japan

Hiramatsu, Reiko
Faculty of Agriculture, Kyoto University, Kyoto, Japan

Hotta, Norifumi
Graduate School of Agricultural and Life Sciences, The University of Tokyo, Tokyo, Japan

Ito, Eriko
Forestry and Forest Products Research Institute (FFPRI), Tsukuba, Japan

Kabeya, Naoki
Forestry and Forest Products Research Institute (FFPRI), Tsukuba, Japan

Kaneko, Takayuki
Graduate School of Agriculture, Kyoto University, Kyoto, Japan

Kanzaki, Mamoru
Graduate School of Agriculture, Kyoto University, Kyoto, Japan

Keth, Nang
Forest and Wildlife Science Research Institute (FWSRI), Forestry Administration, Phnom Penh, Cambodia

Khorn, Saret
Forest and Wildlife Science Research Institute (FWSRI), Forestry Administration, Phnom Penh, Cambodia

Kimhean, Chansopheaktra
Forest and Wildlife Science Research Institute (FWSRI), Forestry Administration, Phnom Penh, Cambodia

Komatsu, Hikaru
Institute of Industrial Sciences, The University of Tokyo, Tokyo, Japan

Kubota, Tayoko
Forestry and Forest Products Research Institute (FFPRI), Tsukuba, Japan

Kume, Tomonori
Kasuya Research Forest, Kyushu University, Fukuoka, Japan

Kuraji, Koichiro
University Forest in Aichi, The University of Tokyo, Aichi, Japan

Lim, Sopheap
Forest and Wildlife Science Research Institute (FWSRI), Forestry Administration, Phnom Penh, Cambodia

Lorsirirat, Kosit
Office of Hydrology and Water Management, Royal Irrigation Department, Bangkok, Thailand

Macdonald, Ray
Lancaster Environment Centre, Lancaster University, Lancaster, United Kingdom

Meas, Makara
Forest and Wildlife Science Research Institute (FWSRI), Forestry Administration, Phnom Penh, Cambodia

Najman, Yani
Lancaster Environment Centre, Lancaster University, Lancaster, United Kingdom

Nobuhiro, Tatsuhiko
Forestry and Forest Products Research Institute (FFPRI), Tsukuba, Japan

Ohnuki, Yasuhiro
Kyushu Research Center, Forestry and Forest Products Research Institute (FFPRI), Kumamoto, Japan

Ohta, Seiichi
Graduate School of Agriculture, Kyoto University, Kyoto, Japan

Okuda, Youichirou
Graduate School of Agriculture, Kyoto University, Kyoto, Japan

Pith, Phearak
Forest and Wildlife Science Research Institute (FWSRI), Forestry Administration, Phnom Penh, Cambodia

Pol, Sopheavuth
Forest and Wildlife Science Research Institute (FWSRI), Forestry Administration, Phnom Penh, Cambodia

Powkhy, Dourng
Peace In Tour Angkor, Siem Reap, Cambodia

Preap, Sam
Forest and Wildlife Science Research Institute (FWSRI), Forestry Administration, Phnom Penh, Cambodia

Punyatrong, Kowit
Department of National Park Wildlife and Plant Conservation, Bangkok, Thailand

Rachna, Chay
Authority for the Protection of the Site and Management of Angkor and Region of Siem Reap, Angkor Conservation Compound, Siem Reap, Cambodia

Saito, Hideki
Kyushu Research Center, Forestry and Forest Products Research Institute (FFPRI), Kumamoto, Japan

Sano, Makoto
Forestry and Forest Products Research Institute (FFPRI), Tsukuba, Japan

Sasaki, Taro
International Cooperation Center for Agricultural Education (ICCAE), Nagoya University, Nagoya, Japan

Sawada, Yoshito
Forestry and Forest Products Research Institute (FFPRI), Tsukuba, Japan

Sawano, Shinji
Graduate School of Agricultural and Life Sciences, The University of Tokyo, Tokyo, Japan

Seesang, Sunan
Sukhothai Thammathirat Open University, Nonthaburi, Thailand

Sherlock, Mark
Lancaster Environment Centre, Lancaster University, Lancaster, United Kingdom

Shimizu, Akira
Forestry and Forest Products Research Institute (FFPRI), Tsukuba, Japan

Shinomiya, Yoshiki
Shikoku Research Center, Forestry and Forest Products Research Institute (FFPRI), Kochi, Japan

Sirisaiyard, Issara
The 7th Watershed Development Office, Department of National Park Wildlife and Plant Conservation, Chiang Mai, Thailand

Sor, Sethik
Forest and Wildlife Science Research Institute (FWSRI), Forestry Administration, Phnom Penh, Cambodia

Sukrarasmi, Apichat
PAL Consultants Company Limited, Bangkok, Thailand

Suzuki, Kunio
Graduate School of Environment and Information Sciences, Yokohama National University, Yokohama, Japan

Suzuki, Masakazu
Graduate School of Agricultural and Life Sciences, The University of Tokyo, Tokyo, Japan

Takizawa, Hideki
College of Bioresource Sciences, Nihon University, Fujisawa, Japan

Tamai, Koji
Kyushu Research Center, Forestry and Forest Products Research Institute (FFPRI), Kumamoto, Japan

Tanaka, Katsunori
Frontier Research Center for Global Change, Yokohama, Japan

Tanaka, Nobuaki
Japan Science and Technology Agency/CREST, Kawaguchi, Saitama, Japan
Graduate School of Agricultural and Life Sciences, The University of Tokyo, Tokyo, Japan

Tangtham, Nipon
Faculty of Forestry, Kasetsart University, Bangkok, Thailand

Tani, Akihiro
Graduate School of Agriculture, Kyoto University, Kyoto, Japan

Tantasirin, Chatchai
Department of Conservation, Aculty of Forestry Kasetsart University, Bangkok, Thailand

Tith, Bora
Forest and Wildlife Science Research Institute (FWSRI), Forestry Administration, Phnom Penh, Cambodia

Tomita, Mizuki
Department of Environmental Information, Tokyo University of Information Sciences, Chiba, Japan

Toriyama, Jumpei
Graduate School of Agriculture, Kyoto University, Kyoto, Japan

Tsuboyama, Yoshio
Forestry and Forest Products Research Institute (FFPRI), Tsukuba, Japan

Tsukawaki, Shinji
Institute of Nature and Environmental Technology, Kanazawa University, Kanazawa, Japan

Vongtanaboon, Sukanya
Faculty of Science and Technology, Rajabhat Phuket University, Phuket, Thailand

Vu Tan, Phuong
Research Centre for Forest Ecology and Environment (RCFEE) of Forest Science Institute of Vietnam, Hanoi, Vietnam

Worrapornpan, Supaporn
Healthy Public Policy Foundation, Bangkok, Thailand

Yayama, Tomoko
Graduate School of Agricultural and Life Sciences, The University of Tokyo, Tokyo, Japan

Yoshifuji, Natsuko
Japan Science and Technology Agency/CREST, Kawaguchi, Saitama, Japan
Graduate School of Agricultural and Life Sciences, The University of Tokyo, Tokyo, Japan

Color Plates

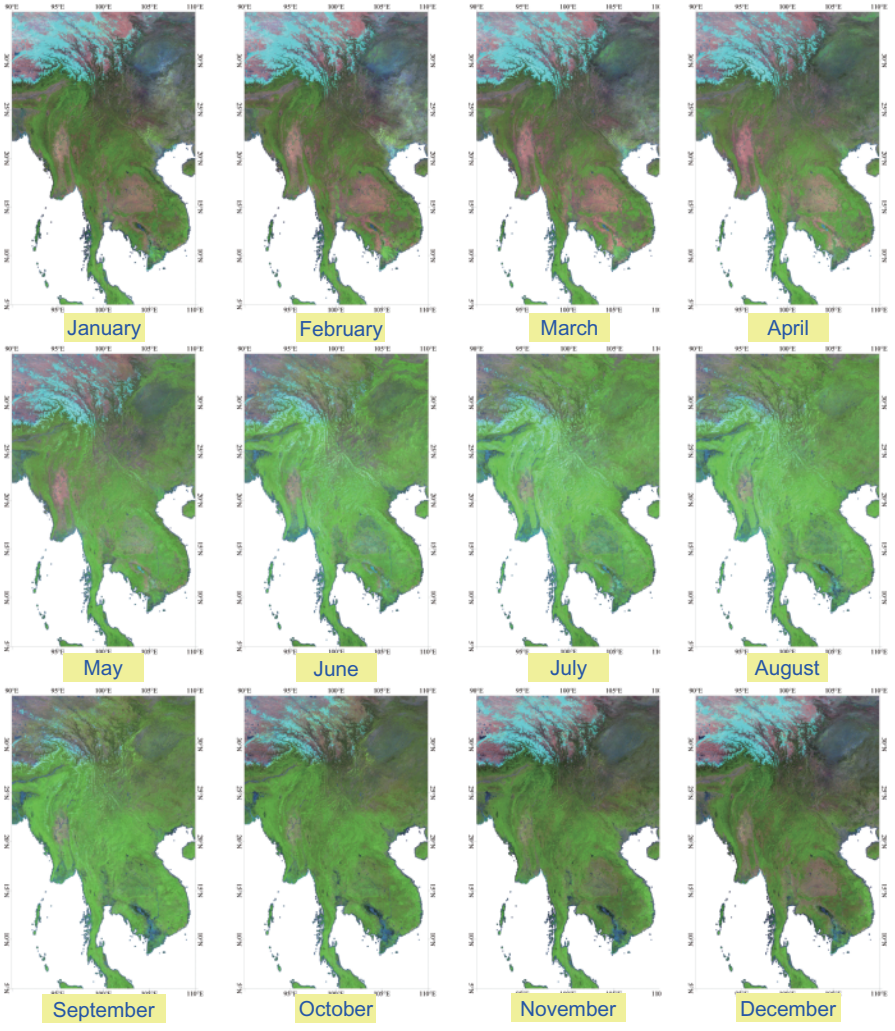

1. Cloud-free images of the Mekong River Basin processed by the Forestry and Forest Products Research Institute (FFPRI) of Japan (middle of each month)

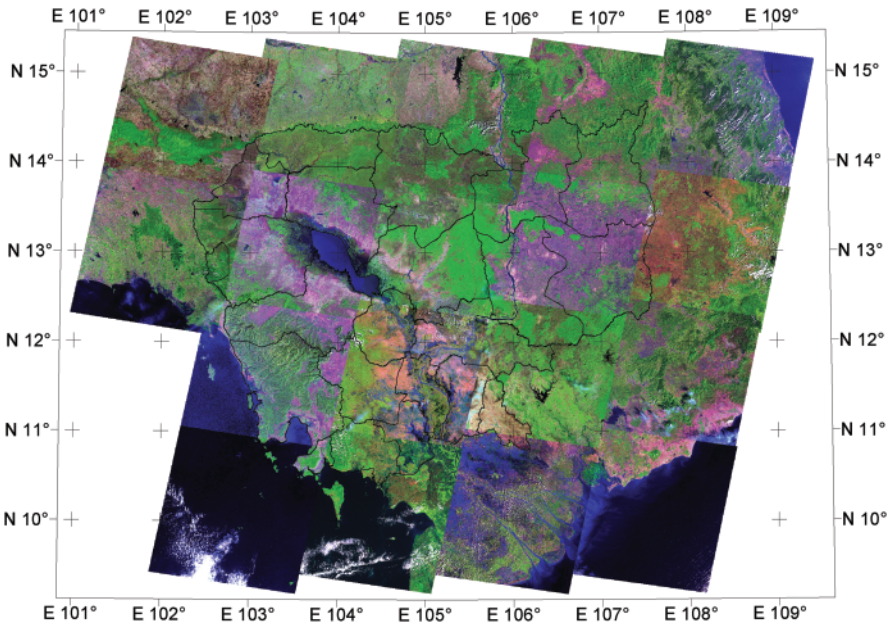

2. Landsat ETM+ mosaic image of Cambodia (Black lines show the boundaries of province of Cambodia)

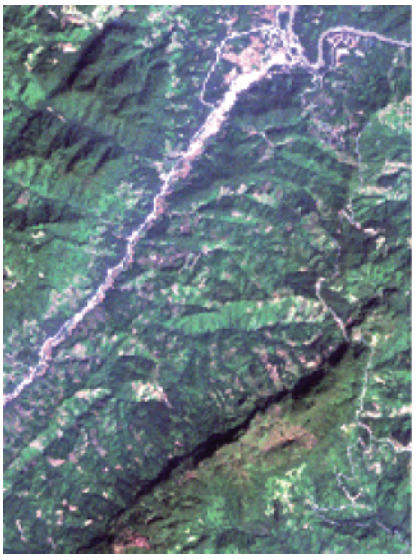

3. Satellite image of shifting cultivation

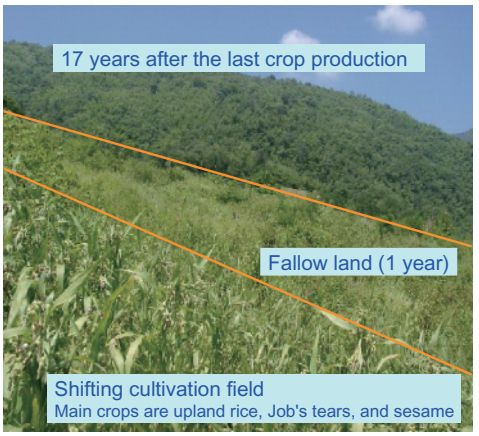

4. Field site of shifting cultivation

Experimental watershed in Cambodia (1)

5. Fetch and pyrgeometer (longwave radiometer)

6. Tower area including observation shed from a 40-m height

7. Gate to the tower site

8. Meteorological observation tower (see chapters 7, 8, 12)

Experimental watershed in Cambodia (2)

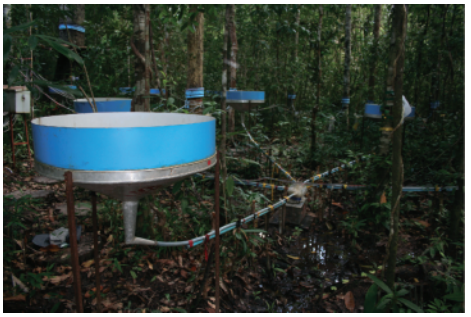

9. Interception plot

10. Measuring velocity of stream flow

11. Measuring velocity of stream flow

12. Measuring cross section of a stream

Forests and soils in Kampong Thom, Cambodia

13. Dry evergreen forest

14. Acrisols

15. Mixed forest

16. Podzols

17. Dry deciduous forest

18. Arenosols

19. Swamp forest

20. Histosols

Forests and soils in Mondulkiri and Kratie, Cambodia

21. A hill evergreen forest and its soil in Mondulkiri

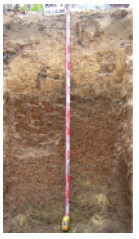

22. A deciduous forest and its soil in Kratie

Dry evergreen forest in Kampong Thom, Cambodia

23. Deep soil profile

24. Forest in observation area

International Conference on Forest Environment in Continental River Basins with a Focus on the Mekong River, Phnom Penh, Cambodia 2005

25. Opening ceremony

26. Presentation and discussion

27. Participants

Excursion tour after the conference

28. Flooded forest in Tonle Sap Lake (1)

29. Flooded forest in Tonle Sap Lake (2)

30. Observation plot

31. Angkor Wat, a World Heritage Site

Part I
Forest Hydrology

Runoff Processes in Southeast Asia: Role of Soil, Regolith, and Rock Type

Nick A. Chappell*, Mark Sherlock, Kawi Bidin, Ray Macdonald, Yani Najman, and Gemma Davies

Abstract. Runoff processes govern the river hydrograph form, location of return-flow and biogeochemical water quality of tropical forest watersheds. This study reviews the literature on runoff processes from tropical rainforests and applies it to the situation in tropical Southeast Asia. The impact of clay mineralogy on permeability and thence water pathways within the soil, and the role of deep pathways with unconsolidated geological materials (regolith) or permeable rock (solid geology) are emphasised, and a new perceptual model, DELTAmodel, presented. Lastly, the implications of these findings for runoff processes within the Mekong Basin are discussed.

1. Introduction

Runoff processes determine the pathways that rainfall takes en route to a river. Within tropical regions, such as Southeast Asia (Fig. 1a), our knowledge of these water pathways is mostly derived from experiments conducted on individual hillslopes perhaps 10 to 300 m in length (Bonell 2004). This approach forms the discipline of hillslope hydrology (Kirkby 1978; Anderson and Burt 1990). Most of this research has been conducted within temperate environments, but some studies have been undertaken within the equatorial, seasonal, and dry tropics. This work has shown the presence of several types of runoff process within these globally important hydroclimatic regions. Some of the key phenomena and pathways identified are (i) a dominance of infiltration-cum-subsurface flow over overland flow in the generation of channel flow (Dubreuil 1985**;** Chappell et al. 1999a,b, 2004b; Bonell 2004; Chappell 2005a); (ii) the importance of lateral flow in organic near-surface layers (Bonell and Gilmour 1978; Bonell et al. 1981); (iii) the presence of "natural soil pipes" which route a proportion of water rapidly through hillslope soils (Baillie 1975; Jones 1990; Chappell et al. 1998; Chappell and Sherlock 2005); and (iv) the effects of soil compaction by vehicles or construction activities on the proportion of overland flow at local scales (Malmer and Grip 1990; Van der Plas and Bruijnzeel 1993; Ziegler et al. 2004).

Whilst it has been relatively easy to show that these pathways exist, it remains difficult to quantify the role of each pathway in the generation of riverflow within a specific headwater basin, let alone in areas where there are no experimental hillslope results nearby (Sherlock et al. 1995; McDonnell 2003; Chappell and Sherlock 2005). Indeed, the issue of how to generalise hillslope-scale observations to areas without

* Lancaster Environment Centre, Lancaster University, Lancaster, United Kingdom
E-mail: n.chappell@lancaster.ac.uk

direct observations of each runoff pathway is now at the forefront of scientific hydrology. Some scientists attempt to undertake this generalisation using maps of analogue information such as soil type (Nyabeze 2005), while others seek to abstract the resultant effects of different water pathways from hydrograph form (Kokkonen et al. 2003). As yet, neither method provides a perfect solution. Maps of soil type, for example, are classified primarily by a range of edaphic and pedological factors, not just factors controlling runoff processes (FAO-UNESCO 1990; Chappell and Ternan 1992; Soil Survey Staff 1999). Equally, different runoff pathways can give similar hydrograph forms, so that is not easy to identify which are the dominant runoff pathways purely from hydrograph analysis (Chappell 2005b). Despite these limitations, we believe that some information about runoff pathways is contained within maps of terrain characteristics, such as soil type or geology.

Even if our knowledge of runoff processes in tropical regions such as Southeast Asia is incomplete, we have still a duty to disseminate the existing data and theory, as it is these pathways that underpin many environmental processes. Clearly, runoff pathways control the time that water takes to reach rivers (Chappell et al. 2004b) and, thereby, whether the channel capacity is exceeded and flooding produced. They also affect the moisture status of soils in time and space and, thereby, the natural distribution of plants (Gibbons and Newbery 2003) and the agricultural productivity of soils (Baron et al. 1998). Further, they affect the migration of nutrients which affect soil edaphic status, plant distribution, and river water quality; this is particularly important where land-use change accelerates the loss of nutrients from soils to rivers (Chappell et al. 2004c). The movement of other solutes, such as agricultural pesticides and leaking industrial wastes, through soils and rocks towards rivers is similarly regulated by water pathways (Racke et al. 1997). Runoff pathways on the land surface, namely overland flow and channel flow, also regulate the amount of sediment mobilised and transported. Changes to these surface runoff pathways, therefore, affect the sediment load of tropical streams and rivers (Chappell et al. 2004b,c).

These environmental responses to spatial variations in runoff pathways have been shown to have major impacts in Southeast Asia (Bruijnzeel 1990; Chappell et al. 2004b,c). This region is particularly important for environmental research because of the rate of loss of the natural forest vegetation (Drigo 2004), the rapid industrial and urban development in the region, the rapid population growth, and the impact of this region on global climate (Chen and Houze 1997; Schneider 1998; Neale and Slingo 2003).

Given the overriding importance of runoff pathways and the Southeast Asia region, this study seeks to add to our knowledge of the controls on the spatial distribution of runoff pathways in this region of the equatorial and seasonal tropics. There are several key controls affecting the relative significance of each runoff pathway (Dunne et al. 1975). The controls include (i) rainfall characteristics (Smith 2004; Bidin and Chappell 2006), (ii) the magnitude of evapotranspiration relative to precipitation, (iii) surface and outcrop/rockhead topography (Kirkby 1975; O'Loughlin 1981; Zaslavski and Sinai 1981; Burt and Butcher 1985; Freer et al. 2002), (iv) the nature of the local soil and regolith and rock types, (v) the catchment depth/area relation (Blösch and Sivapalan 1997), (vi) the form and density of the channel network (Gregory 1976; Walsh 1996), and sometimes (vii) vegetation (Ziegler and Giambelluca 1998; Roberts

2000). Within this study, we focus on observations of the role of soil type, regolith type, and rock type on likely runoff pathways within Southeast Asia.

Ideally, we would restrict our observations on runoff pathways to tropical Southeast Asia. As there have been so few hillslope hydrology studies (i.e., studies with at least permeability and soil-water measurements) in Southeast Asia (Fig. 1a), we need to extend our analyses to include hillslope hydrology findings to the whole of the wet and seasonally wet tropics (Fig. 1b); although this still only gives a modest dataset of

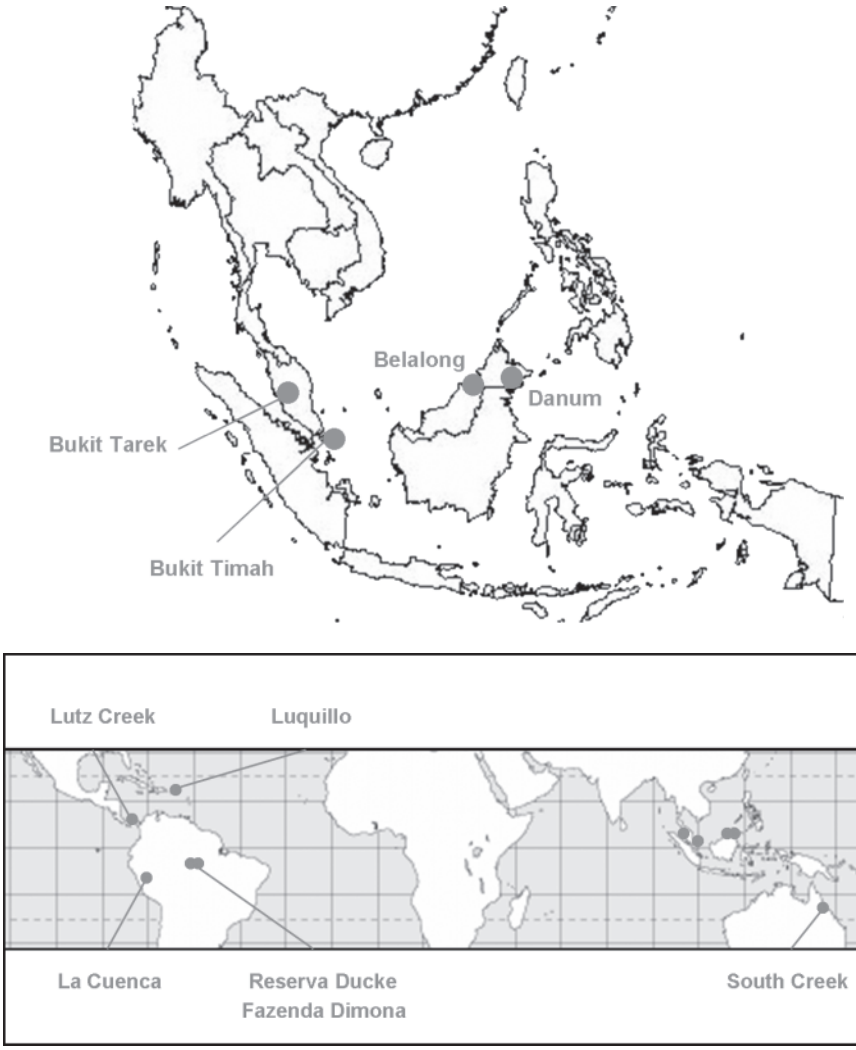

FIG. 1. Approximate location and distribution of published hillslope hydrology studies in Southeast Asia (**a**) and the whole of the humid tropics (**b**)

ten sites. These hillslope experiments have been conducted at South Creek, Australia (Bonell and Gilmour 1978; Bonell et al. 1981, 1983), Reserva Ducke, Brazil (Nortcliff and Thornes 1981), Fazenda Dimona, Brazil (Hodnett et al. 1997), Ulu Belalong, Brunei (Dykes and Thornes 2000), Bukit Tarek, Peninsular Malaysia (Noguchi et al. 1997), Danum, East Malaysia (Sinun et al.1992; Chappell et al. 1998, 1999a,b, 2004a; Chappell and Sherlock 2005), Luquillo, Puerto Rico (Schellekens 2000), Lutz Creek, Panama (Godsey et al. 2004; Kinner and Stallard 2004), La Cuenca, Peru (Elsenbeer and Lack 1996), and Bukit Timah, Singapore (Sherlock et al. 1995, 2000; Chappell and Sherlock 2005). Others have attempted to generalise the runoff pathways illustrated in these studies (Chappell and Ternan 1992; Elsenbeer 2001; Bonell 2004), particularly in the upper layers of the ground; we attempt to add to this work.

2. Effect of Soil Type

The strict definition of a soil as comprising only a topsoil (A horizon) and a subsoil (B horizon) is used here, where the underlying strata are defined as the parent material. Sometimes the parent material is rock, in other places it is a layer of unconsolidated geological materials or "regolith" overlying the rock. The regolith layer can be up to 50 m in depth in granitic terrains of Southeast Asia (Twidale 2005). In tropical regions, the unconsolidated material that forms the regolith can be in situ weathered rock or fluvial, alluvial, or colluvial sediments. Beneath the regolith (or directly beneath the soil) is the rock, which should be defined as it is not only a parent material for the soil, but is sometimes an important route for water—an issue which is often overlooked in tropical hillslope hydrology (Bonell 2004).

Soil type is classified using a range of edaphic and pedological characteristics (FAO-UNESCO 1990; Soil Survey Staff 1999). Hydrological characteristics affecting runoff pathways, notably permeability, porosity, and soil moisture status, are only one set of the many factors. Thus, a perfect correlation between hydrological characteristics and soil type should not be expected (Chappell and Ternan 1992). Note also that the classification of soil type is often incorrectly confused with the soil textural class, which is simply the mix of different particle sizes that make up each soil horizon.

2.1. Dominant Soil Type in Southeast Asia

Within the tropics, the dominant soil type is the Ferralsol group (USDA equivalent: Oxisol), and it covers 20% of the tropics, covering most of Amazon and Congo basins (Driessen and Dudal 2001). Ferralsol is, however, not very extensive in Southeast Asia or humid West Africa, where the dominant soil type is the "Acrisol-Alisol group" (USDA equivalent: Ultisol) (FAO-UNESCO 1976, 1990, 2004; Driessen and Deckers 2001; Fig. 2). In 1990, the Alisol group was newly defined and some Acrisol group soils, namely the more-unstable, base-poor soils, were reclassified as Alisol soils (FAO-UNESCO 1990). Strictly, Alisol soils can be distinguished from post-1990 Acrisol soils by the cation-exchange capacity being less than 24 $cmol^{+}kg^{-1}$ clay, as a result of the presence of unstable 2:1 clays (e.g., smectite). As a consequence, these soils have a poor soil structure in comparison to post-1990 Acrisol soils. The pre-1990

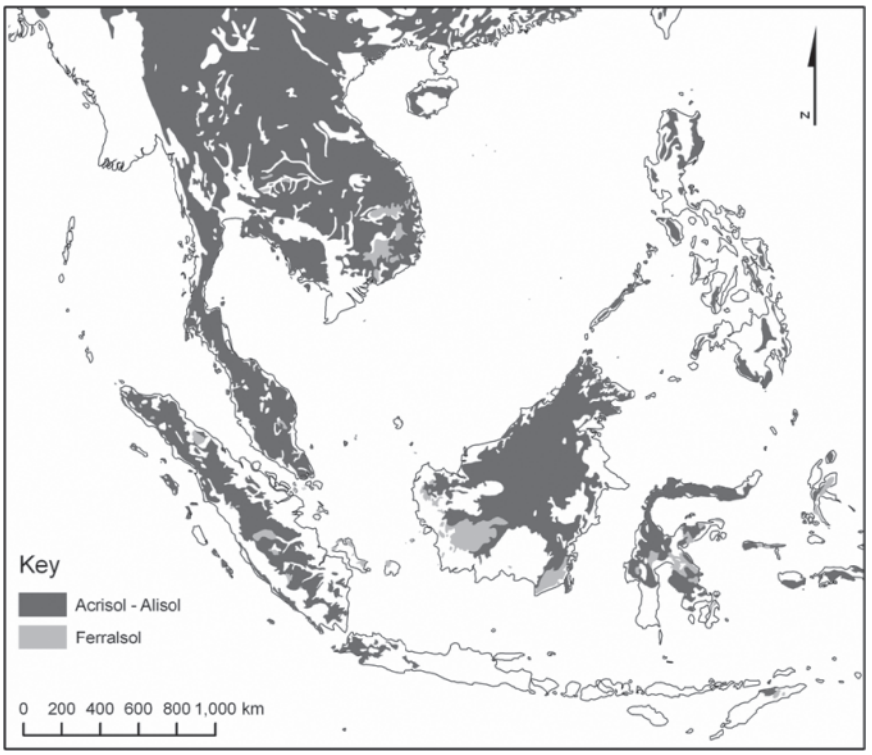

FIG. 2. Spatial extent of the Acrisol-Alisol (*dark grey*) and Ferralsol (*light grey*) soil groups in Southeast Asia (90°–130° E and 23.4° N to 12° S). [Adapted from FAO-UNESCO (2004) using ArcGIS version 9.1 (ESRI, Redlands, CA, USA)]

Acrisol soil group (Fig. 2) has, however, not yet been remapped into Alisol soils and post-1990 Acrisol soil. We, therefore, refer to the pre-1990 Acrisol soils mapped in Fig. 2 as the Acrisol-Alisol group.

2.2. Tropical Hillslope Hydrology Studies and Soil Type

Figure 1a,b shows the locations of the key hillslope hydrology studies (i.e., studies with at least permeability and soil-water measurements) published in the international literature. Six out of ten are on Acrisol-Alisol soils, the dominant soil of Southeast Asia (Sherlock et al. 1995; Noguchi et al. 1997; Chappell et al. 1998; Dykes and Thornes 2000; Schellekens 2000; Kinner and Stallard 2004). A further two studies (Bonell and Gilmour 1978; Elsenbeer and Lack 1996) have results from a mix of Acrisol-Alisol and other soils. There are only two studies on the dominant Ferralsol soil of the tropics, namely Nortcliff and Thornes (1981) and Hodnett

et al. (1997), and only one that includes this soil with others (Bonell and Gilmour 1978).

Elsenbeer (2001) suggested that water pathways within tropical soils form a continuum from a Ferralsol end-member with predominantly vertical flow in the soil to an Acrisol end-member with predominantly lateral flow in the soil. This excellent start to a generalisation of water pathways using soil type does, however, have some significant inconsistencies. First, the water pathways for Danum (see Fig. 4 in Elsenbeer 2001) are placed by Elsenbeer (2001) in the intermediate category between the Acrisol and Ferralsol end-members. As the Danum experiments were conducted on Alisol soils (Chappell et al. 1999b), the less well drained soils of the pre-1990 Acrisol class (Driessen and Decker 2001; Driessen and Dudal 2001), they should have a greater, not smaller, proportion of lateral flow than the post-1990 Acrisols. The observations of Chappell and Sherlock (2005) confirm this. Second, Elsenbeer (2001) classifies the Bukit Tarek soils as being part of the Ferralsol end-member, whereas they are Acrisol soils (Yusop 1996; Noguchi et al. 1997). Third, the soil at Bukit Timah is derived from a granite regolith very similar to that of Bukit Tarek. As the Acrisol soil at Bukit Timah has a significant proportion of vertical flow, although not total domination (Chappell and Sherlock 2005), we are more likely to expect a similar situation for Bukit Tarek. Last, the South Creek hillslope experiments were conducted on a range of soils including Ferralsols (Bonell et al. 1981, 1983) and, therefore, should not be all classified as in the Acrisol end-member class. We suggest that there may be a new model/generalisation that does not produce these major inconsistencies.

2.3. New Generalisation of Water Pathways in Tropical Acrisol-Alisol and Ferralsol Soils

We know that Alisol soils are distinguished from Acrisol soils on the basis of their clay mineralogy. Driessen and Deckers (2001) and Driessen and Dudal (1991) clearly showed that the internal drainage characteristics (notably permeability) of Ferralsol soils vary from very good to poor depending on clay mineralogy. Driessen and Dudal (1991, p. 161) state that Ferralsols with a clay mineralogy dominated by gibbsite are well drained, those dominated by 2:1 clays (e.g., smectite) have poor drainage, and kaolinite gives an intermediate state. Clay mineralogy affects soil permeability via its effects on the aggregate stability and structure of the soils (Driessen and Dudal 1991).

If we now consider the flow pathways at the sites that gave inconsistencies in the Elsenbeer (2001) model of soil type–flow pathways, we can see that the same soil type can have a wide range of proportions of vertical to lateral flow (Chappell and Sherlock 2005), and clay mineralogy may be the cause. The Alisol soil at Danum, with its high proportion of 2:1 clays (Chappell et al. 1999b), gives a high proportion of lateral flow of approximately 60% of total percolation (Chappell and Sherlock 2005). In contrast, the Acrisol of Bukit Timah, with a dominance of kaolinite (Rahman 1992), has less than 10% lateral flow (Chappell and Sherlock 2005). Some of the highest rates of soil permeability published are for the Amazonian site of Nortcliff and Thornes (1981). Even given the uncertainties associated with permeability data (Chappell and Ternan 1997; Sherlock et al. 2000), such high permeabilities strongly

suggest no impediment to vertical drainage in the soil. A clay mineralogy dominated by gibbsite is indeed expected at this locality (Norcliff, personal communication). This observation contrasts with the Ferralsols associated with Acrisols in the South Creek catchment in tropical northeast Australia, where marked discontinuities in the soil permeability profile and significant volumes of lateral flow in the soil have been monitored (Bonell and Gilmour 1978; Bonell et al. 1981, 1983). Thus, at this site, the Ferralsols are expected to be dominated by kaolinitic or even 2:1 clays. By examining these key case studies, we would tentatively suggest a new model of the interactions between soil type, clay mineralogy, permeability, and flow direction (Fig. 3). Because of our suggested interaction between clay mineralogy and permeability, we call this model the ^{clay}K model (Fig. 3). Given the observations of flow direction at a range of sites, we can now tentatively add these locations to our perceptual model (Fig. 3). These placements are, however, preliminary and require further testing.

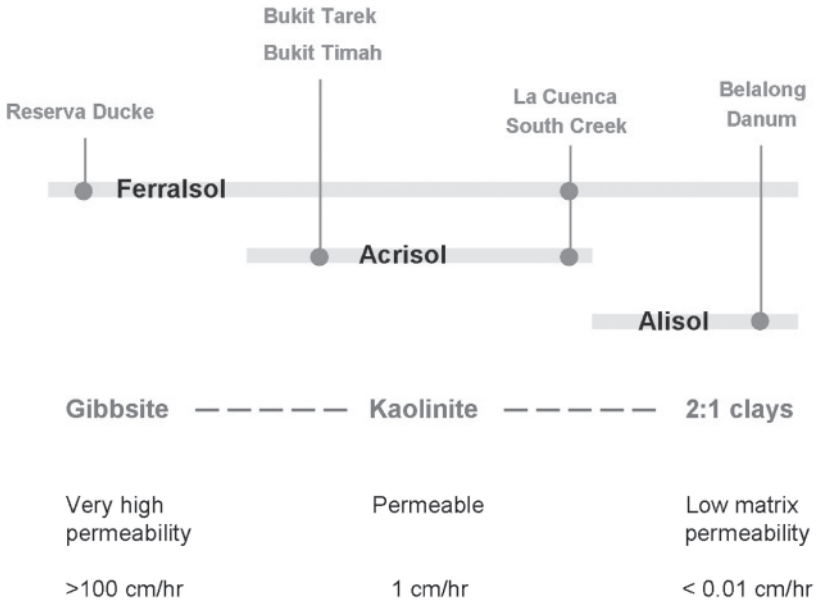

FIG. 3. The ^{clay}K model showing the range and end-members of subsoil permeability expected from the clay mineralogy of the three key soils of the humid tropics: Ferralsol, Acrisol, and Alisol soils. Locations with Ferralsol soils dominated by gibbsite have very high subsoil permeabilities, well in excess of 100 cm h^{-1} (e.g., Reserva Ducka, Brazil). Sites with Acrisol soils dominated by kaolinite clays have permeable subsoils (approximately 1 cm h^{-1}), e.g., Bukit Timah, Singapore, and Bukit Tarek, Peninsular Malaysia. Alisol soils are dominated by 2:1 clays (e.g., smectite) and have low matrix permeabilities (<0.01 cm h^{-1}) in their subsoil strata, as observed at Kuala Belalong, Brunei, and Danum, East Malaysia. The Ferralsol and Acrisol soils of La Cuenca, Peru, and South Creek, Australia, have subsoil permeabilities intermediate between the Bukit Timah and Danum sites, so are expected to have a clay mineralogy intermediate between kaolinite dominated and 2:1 clay dominated

Arguably, this model is slightly more robust than it needs to be, given that by far the most dominant soil present in Southeast Asia, as opposed to the whole of the tropics, is the Acrisol-Alisol group. Thus, it is the hydrological differences between these Acrisol and Alisol soils that are the most important. The inclusion of this other important soil does, however, allow wider comparisons with other flow pathway behaviour (e.g., Nortcliff and Thornes 1981). Given that the current map of Southeast Asian soils (FAO-UNESCO 1976, 2004) does not distinguish between Acrisol soils and Alisol soils, the observed hydrological differences between these two soils suggest that such a map is needed.

Most hillslope hydrological studies end the analysis of runoff pathways at this point, in that they only consider waterpath direction and magnitude within the soil (i.e., A and B horizons). At many locations, rainfall percolates much deeper than the soil before returning to form streamflow. Thus the analysis of runoff pathways at any location should consider whether a significant proportion of the rainfall is able to percolate into a deeper regolith or rock.

3. Effect of Regolith Type

In some landscapes, lithomorphic soils dominate, where only a topsoil (A horizon) directly overlying an impermeable rock is present, i.e., there are no subsoil or regolith layers. The steep mountain slopes of the Himalayas are a good example. Within Southeast Asia, lithomorphic soils such as Leptosols are rare (FAO-UNESCO 1976), with soils having a permeable subsoil and permeable deeper strata being common. Unfortunately, comprehensive maps of the extent, depth, and hydrological properties of regolith for the whole of Southeast Asia have not been produced. We do, however, know that weathering and mass movement of some rock types leads to a regolith that may be both deep and permeable. Tropical weathering of granitic rock in Southeast Asia and Australasia certainly leads to the development of a permeable regolith that can be 10–60 m in depth (Twidale 2005; Campbell 1997; Melinda et al. 2004). This regolith is normally described as saprolite. The granitic rock from which this saprolite is developed is shown in Fig. 4, for which we have abstracted the felsic and intermediate plutonic rocks from the Wakita et al. (2004) digital map of East and Southeast Asia. Granitic rocks with their deep permeable regoliths occur at many locations in Southeast Asia, and in some areas, notably Malay Peninsula (West Malaysia and Singapore), they are very extensive (Fig. 4). Furthermore, new hydrological analysis of watersheds on the Malay Peninsula would indicate that the presence of this regolith has a large impact on river hydrograph form (Chappell et al. 2004c; Chappell et al., in preparation) as a result of the deeper pathways within the regolith.

Quaternary materials are often unconsolidated. They have a very wide range of hydrological properties given that they can be produced by a wide range of geomorphological processes, including fluvial deposition, slope wash, mass movement, marine inundation, and glacial deposition. Where sediments are coarse (i.e., sands, gravels, and larger materials) and are not capped by impermeable soils (e.g., Gleysols), then percolation will move to depth within these regolith materials, before returning to generate riverflow. The impact on the hydrograph could be similar to that of the granite saprolite. Within Southeast Asia, Quaternary sediments are quite

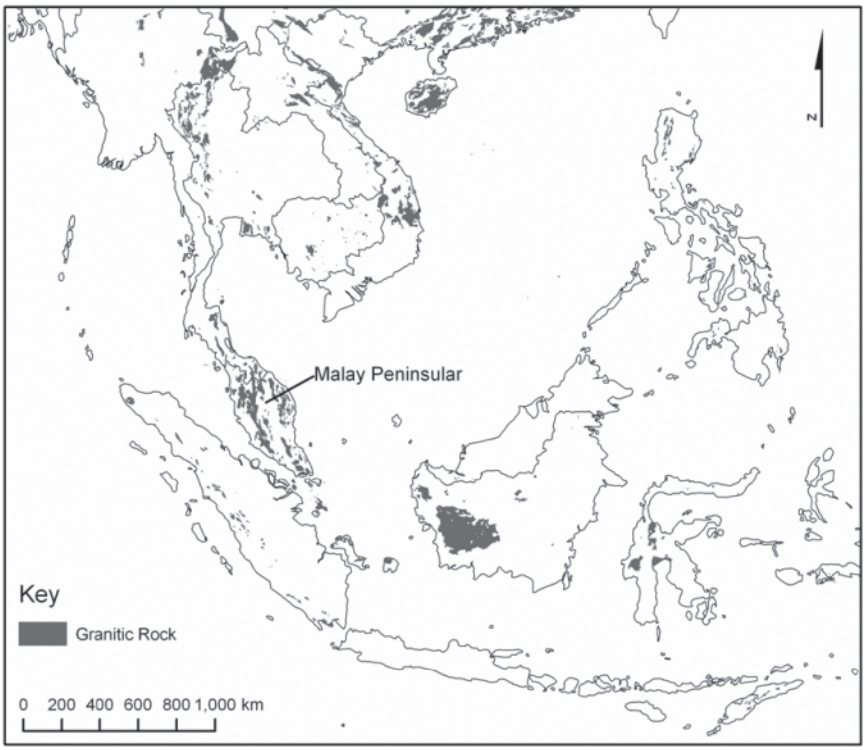

FIG. 4. Spatial extent across Southeast Asia (90°–130° E and 23.4° N to 12° S) of the acid/intermediate plutonic rocks (notably granite) shown in *dark grey*. [Adapted from the digital data of Wakita et al. (2004) using ArcGIS version 9.1 (ESRI, Redlands, CA, USA)]

extensive (Fig. 5). Within the "Mekong Lowland" (Gupta 2005), which comprises much of Cambodia, and also in the Central Plain of Thailand extensive areas of sandy sediments have developed as a result of inundation by the Mekong and Chao Phraya rivers, respectively (Tien et al. 1988; Chiem 1993). In locations where these sediments are not capped by Gleysols (see FAO-UNESCO 1976, 2004) or marine muds (see Phienwej and Nutalaya 2005), and some relief is present to allow drainage, rainfall can percolate to depth within the sediments. There may be indications of this deeper flow within the damped hydrographs of the Stung Chinit experimental basin in Cambodia (see the hydrograph in Shimizu et al. 2005). Indeed, the sandy layers of the Quaternary sediments in Mekong Lowland, the Central Plain of Thailand, and other areas of Southeast Asia (see Fig. 5) are classified as an "aquifer" by Struckmeier and Richts (2004) and Phienwej and Nutalaya (2005), i.e., a substantial groundwater body having both a high permeability and porosity.

Where the depth of Quaternary sediments becomes substantial, perhaps several hundreds of metres (Shroder 1993; Najman 2006), the sediments become more consolidated and, with age, lithified to what might be described as rock, rather than regolith. The boundary between the regolith (or drift geology) and rock is often very indistinct in Quaternary materials.

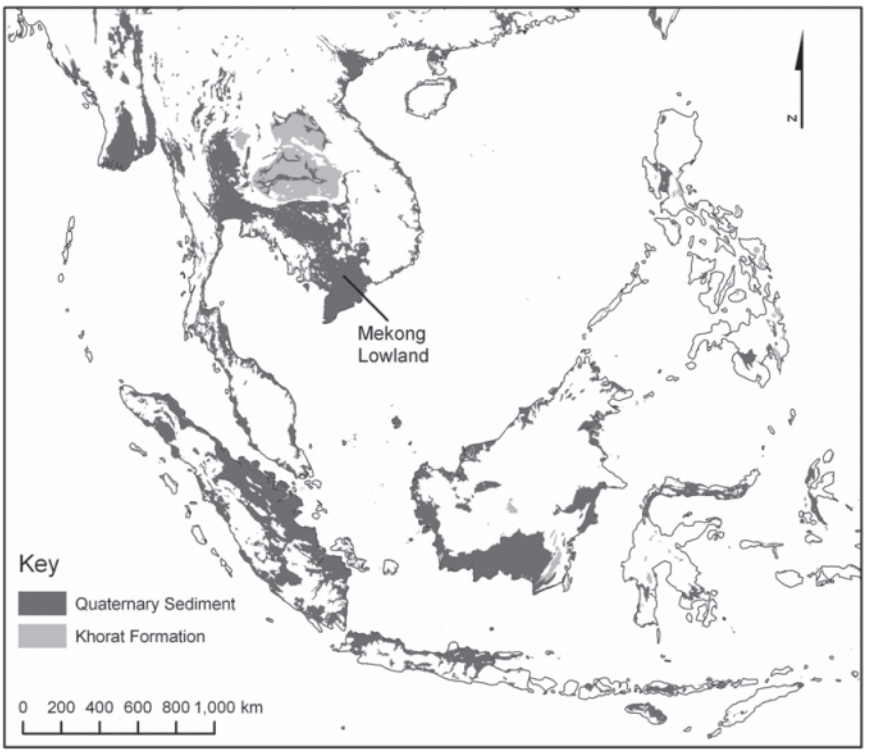

Fig. 5. Spatial extent across Southeast Asia (90°–130° E and 23.4° N to 12° S) of the Quaternary sediments (*dark grey*) and the Khorat Formation (*light grey*) of Northeast Thailand. [Adapted from the digital data of Wakita et al. (2004) using ArcGIS version 9.1 (ESRI, Redlands, CA, USA)]

If a significant proportion of the areas mapped as granitic rock (see Fig. 4) and Quaternary sediment (see Fig. 5) do indeed have deep permeable regoliths, then rainfall will percolate to depth (i.e., 2–10 m or even 2–50 m) in many areas of Southeast Asia. Other geological formations found in Southeast Asia may also have permeable regoliths (Struckmeier and Richts 2004). The possibility of the presence of a deeper water pathway, therefore, needs to be considered at any study locality. Furthermore, there is a need to develop a map of the extent of deep permeable regoliths across the whole of Southeast Asia.

4. Effect of Rock Type

Whilst deep permeable regoliths seem to play an important role in the rainfall-runoff behaviour of some key areas in Southeast Asia, the extent of permeable rock seems to be much more limited. On a global basis, sandstone formations and carbonate rocks are the most extensive rocks with significant permeability and hence potential for deep-water pathways (Zektser and Everett 2004). The spatial extent of carbonate rocks in Southeast Asia is relatively limited (Gillieson 2005), as is the extent of

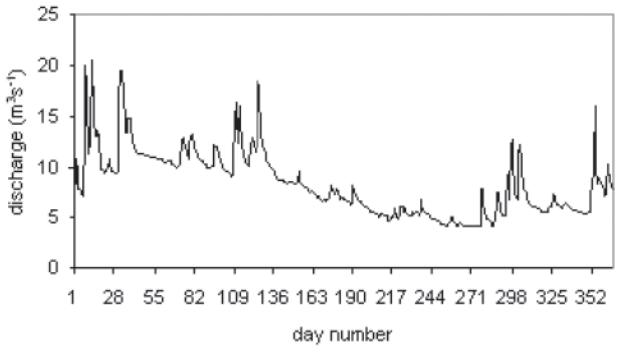

FIG. 6. Hydrograph of the 1033 km^2 watershed of River Kennet (United Kingdom) gauged at Theale during 2004. (Data supplied by the National River Flow Archive, UK)

onshore sedimentary basins dominated by sandstone. One locally important sandstone basin forms the Khorat Plateau of Northeastern Thailand (Heggemann et al. 1994; Racey et al. 1996). The geology is shown in Fig. 5. Although the solid geology may be an important deep groundwater resource (Struckmeier and Richts 2004; Zektser and Everett 2004), its rivers, part of the Mekong system, do not appear to be significantly damped (Douglas 2005; Mekong River Commission 2005), which would have indicated a deep pathway through the rock; this may be because relatively impermeable evaporite deposits cap the upper strata of the Khorat Formation (Carter and Bristow 2003). In other regions of the world, the movement of rainfall deep into permeable rock significantly damps the river hydrograph; see, for example, the long tails on the river hydrograph of the River Kennet in the United Kingdom, which is affected by the underlying Cretaceous chalk aquifer (Fig. 6).

For much of Southeast Asia, the solid geology is important not for the internal water pathways but as the parent material for the overlying regoliths and soils.

5. Generalisation, Limits, and Research Needs

We are acutely aware that the analysis we have presented so far is limited by the lack of availability of (i) hillslope hydrological studies available for particular combinations of soil, regolith, and rock and (ii) a map of the spatial extent of deep permeable regoliths (and their hydrological properties). Attempts at a generalisation of the relationship between water pathways and soil, regolith, and rock type within the humid tropics (Chappell and Ternan 1992; Elsenbeer 2001; Bonell 2004; Chappell and Sherlock 2005) are, however, valuable if only to highlight existing deficiencies and the need for ongoing and future research.

As a way of highlighting the possibility that deeper pathways exist within any tropical catchment under investigation, we propose that water pathway systems fall into four categories. The first, a "type I system," has a lithomorphic soil (A horizon) directly overlying an impermeable rock (an "aquifuge": Todd and Mays 2005). This situation is typical of the steep slopes of the Himalayas but also occurs over smaller areas of East Asia, e.g., in the Chinese headwaters of the Mekong River (FAO-UNESCO 1977).

The runoff system that is likely to be much more extensive in Southeast Asia is the type II system. This situation is the same as a type I system, except that the soils are fully developed (e.g., Acrisol-Alisol, Ferralsol soils). Thus, water movement is expected in the subsoil as well as the topsoil, with percolation reaching a few metres into the ground. The flow pathways within the Baru and W8S5 catchments at Danum, Malaysian Borneo (Chappell et al. 1998; Chappell and Sherlock 2005) extend into subsoil horizons but cannot reach further, given that the solid geology is relatively impermeable and a regolith layer is lacking.

Of equal importance in Southeast Asia, given the extent of the mapped geology associated with regolith (see Figs. 4, 5), are type III systems. These systems have fully developed soils formed from deep permeable (or partially permeable) regolith overlying an impermeable solid geology. Good examples of type III hillslope hydrological study sites are Bukit Tarek (Noguchi et al. 1997) and Bukit Timah (Chappell and Sherlock 2005), which have Acrisol soils and a deep permeable granite saprolite.

The type IV water pathway system has fully developed soils and the presence of a regolith, but it also has permeable rock. Because of a lack of hillslope hydrological studies on rock aquifers in Southeast Asia, we are unable to cite a good example, but expect that such systems do exist at some localities (see Fig. 6). As this conceptualisation of the role of different strata to runoff pathways considers the presence/absence of four strata (i.e., topsoil, subsoil, regolith, and permeable rock) and results in four system types, we describe it as the Delta model, where delta is the fourth letter of the Greek alphabet. This conceptualisation or perceptual model (see Beven 2001 for the definition) is shown in Fig. 7.

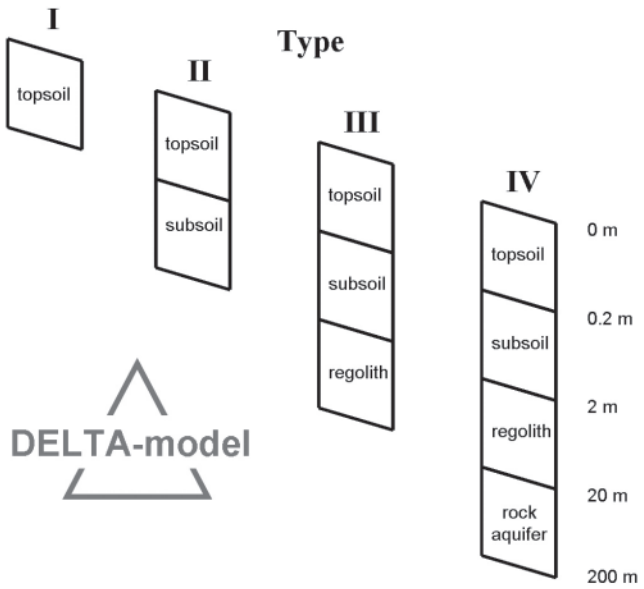

Fig. 7. Schematic representation of the Delta model, where water pathway systems are classified according to the presence of as many as four strata (topsoil, subsoil, regolith, and solid rock) with the names *type I* to *IV*. Example depths and the logarithmic depth scale are given

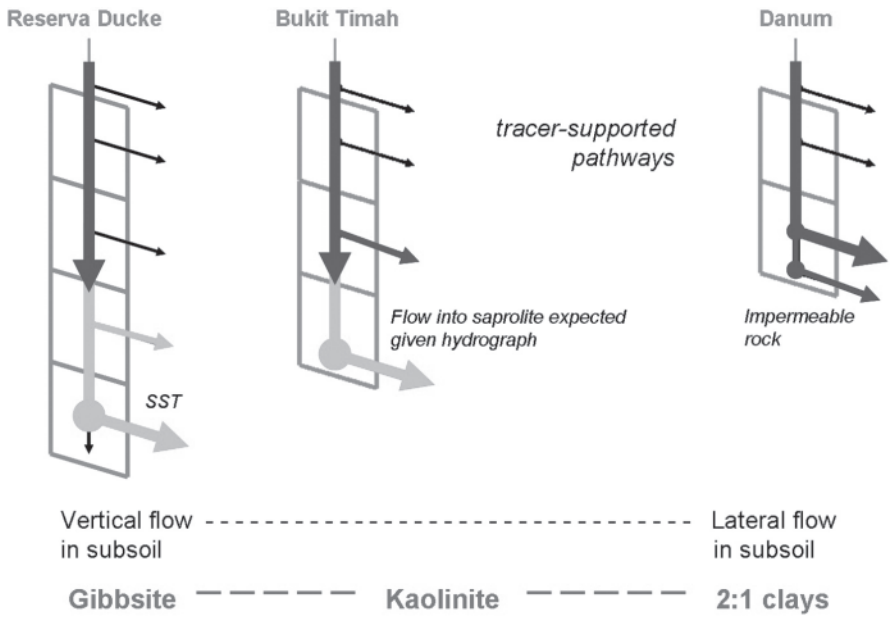

FIG. 8. The combined ^{clay}K model and Delta model showing the flow pathways for three key experimental sites across the humid tropics: Reserva Ducka (Nortcliff and Thornes 1981), Bukit Timah, and Danum (Chappell and Sherlock 2005). The *uppermost box* always represents the topsoil (see Fig. 7). The effect on the flow direction in the subsoil (i.e., vertical or lateral flow-dominated systems) together with the gradation from gibbsite to kaolinite to 2:1 clays is shown on the *x*-axis. The *dark grey arrows* show more certain flow pathways than the *light grey arrows*, and *arrow width* gives an estimate of the magnitude of the flow. Most certain pathways are derived from observations of tracer migration (Chappell and Sherlock 2005). There are no quantitative observations of the vertical flow into the underlying sandstone (SST) at Reserva Ducke or underlying granite saprolite at Bukit Timah, although significant qualitative evidence supports this hypothesis

To illustrate the utility of both the ^{clay}K and Delta model for comparing and generalising the results of runoff pathway studies, Fig. 8 shows the observed flow pathways within three experimental studies covering a range of situations found in the humid tropics.

We are presenting what we believe is a new perceptual model, which by definition is a simplification of reality (Beven 2001); this means that there will be omissions, uncertainties, and possibly errors with this approach. First, even if the ^{clay}K concept were to hold, soil permeability varies considerably within the same soil horizon of the same soil type at any one locality (Nielsen et al. 1973; Bonell et al. 1983; Chappell and Ternan 1992; Chappell and Sherlock 2005). Any one hillslope may exhibit a very different local permeability pattern and, thereby, flow pattern from a "typical" or representative site.

Second, soils are classified according to a range of physicochemical characteristics, not just hydrological characteristics. As a consequence, we should not expect there to be a perfect correlation between soil type and permeability or pathway direction (Chappell and Ternan 1992).

Third, small-scale soil maps such as the FAO-UNESCO (2004) digital map are gross simplifications of the way in which soil types change over several kilometres, let alone over a few hundred metres. Key changes in soil types along a soil catena, the sequence of associated soils found along hillslope transects (Milne 1935), impact on the resultant behaviour of the whole hillslope but are not shown on small-scale maps (Chappell and Ternan 1992).

Fourth, tropical hillslope studies have shown the importance of phenomena such as percolines and natural soil pipes to runoff behaviour at hillslope scale (Bunting 1961; Baillie 1975; Jones 1990; Chappell et al. 1998, 2001). We know that such features are present within many tropical soils and certainly within the Acrisol-Alisol soils that dominate in Southeast Asia (Chappell and Sherlock 2005; Chappell et al. 2006). There is, however, insufficient research to be able to predict the hydrological impact of these phenomena for a particular soil type or locality.

Fifth, even where maps of regolith can be derived, considerable spatial variability in the depth and hydrological properties of the materials is expected, given their diverse formation processes.

Sixth, factors other than soil, regolith, and rock types affect runoff pathways but are not explicitly considered, e.g., the degree and dynamics of saturation within the subsurface. For example, where an extensive regolith is permanently saturated in an area of very low relief, as may be the case in parts of the lower Mekong, such strata may not play a part in the rainfall-runoff pathways. Other factors that would be expected to impact on runoff pathways in Southeast Asia include the rainfall characteristics (Robinson and Sivapalan 1997), surface topography, outcrop/rockhead topography (i.e., shape of the upper surface of the impermeable rock), and vegetation.

Seventh, the vertical to lateral flow ratio and the residence time of the water within a catchment system changes with scale. For example, as catchment scale increases from a few hectares to thousands of kilometres square, then there is a tendency for residence time to increase as the depth:area relationship reduces.

Last, the different techniques used to estimate the direction and magnitude of water pathways within individual experimental hillslopes can give very different results (Sherlock et al. 2000; McDonnell 2003; Chappell and Sherlock 2005). So, the findings that we are trying to correlate with soil, regolith, or rock type may themselves not be an accurate representation of the flow pathways.

All these issues need to be considered in improving our conceptualisation of runoff processes within Southeast Asia, which explains why we have yet to release our preliminary version of a conceptual model (i.e., a numerical version of a perceptual model: Beven 2001) for testing by others. Following further development, including comparisons with physics-based model simulations at the hillslope-scale (cf. Chappell and Binley, 1992), we will make the conceptual model available for testing with the tropical hillslope data of other investigators.

6. Implications for Runoff Processes in the Mekong Basin

The Mekong drainage basin is the largest in Southeast Asia at 795 000 km^2. It is also strategically important given that its riverflow is sourced from six nations (Cambodia, China, Lao PDR, Myanmar, Thailand, and Vietnam). There are, however, very few

studies detailing the runoff processes within this basin. We are able to make some comments on the likely runoff processes within the Mekong Basin, given (i) the proceeding analysis of hillslope studies from around the humid tropics, (ii) the interpretation of available Geographic Information System (GIS) data for soils and rocks (see Figs. 2, 4, 5), and (iii) the tentative perceptual models of the relationship between flow pathways and the soil, regolith, and rock type (see Figs. 3, 7, 8). Such comments are certainly no replacement for the field experimental studies that are needed within the basin.

The dominant soil type in the Mekong basin, as in Southeast Asia as a whole, is the Acrisol-Alisol group (FAO-UNESCO 1976, 1977, 2004). If the proceeding analysis of Alisols being dominated by lateral flow and Acrisols having mostly vertical flow is accurate, this will have an impact in the Mekong. Existing soil data, notably cation-exchange capacity (CEC) and clay content, should be reexamined or new data collected that allow (i) specific research hillslopes or watersheds to be classified as either Alisol or (post-1990) Acrisol, and (ii) the derivation of a Mekong soil map that distinguishes these two soil groups.

Cambodia and hence to the lower reaches of the Mekong basin are largely underlain by Quaternary sediments, some of which are coarse fluviatile deposits (Tien et al. 1988; Chiem 1993). In these areas, a dominance of Acrisol over Alisol soils would mean that rainfall would be expected to percolate through soils into and through these sediments before reaching rivers. If this is the case, the study of the hydrological characteristics and response of regolith at a depth of several metres is important to any catchment hydrological research in this region.

Within this same downstream sector of the Mekong basin, the presence of Gleysol (USDA Aquic suborders) and Fluvisol (USDA Fluvent) over the Mekong delta and along most of the Cambodian sections of the main channel of the River Mekong and Tonle Sap tributary (FAO-UNESCO 1976, 2004) is equally significant for hydrological study and interpretation. Gleysols and most Fluvisols are slowly permeable (Driessen and Deckers 2001; Driessen and Dudal 1991); this means that within the Mekong floodplain areas (approximately 10 km on either side of the main channels) either (i) the underlying regolith parent material is also locally slowly permeable or (ii) the soil would restrict vertical percolation to the regolith strata. Either situation would mean that rapid routing of rainfall to the main river via the topsoil (or even surface) pathways would be expected within these floodplain areas. These areas would effectively behave like a type I flow pathway regimen. Direct field monitoring is required to confirm the role of this pathway along the lower Mekong floodplain.

The other region of the Mekong basin containing Gleysols along main channels, and indeed Gleyic Acrisols/Gleyic Alisols across most of the area, is the Khorat Plateau (FAO-UNESCO 1976; see Fig. 6). The presence of these less-permeable soils may be the result of the less-permeable evaporite upper strata of underlying rock that form the parent material (Carter and Bristow 2003). This observation would also support the idea that the Mae Nam Mun River system is hydrologically isolated from the deep aquifer beneath the Khorat Plateau. Further study is needed to identify the possibility of connections of this deep aquifer with the surface drainage.

In the northern headwater of the Mekong, north of the Tropic of Capricorn, the downstream reaches have Fluvisol soils, while the extreme headwaters and steep valley slopes have poorly developed, lithomorphic soils in complexes of Lithosols,

Xerosols, Kastanozems, and Rankers (FAO-UNESCO 1997, 2004). A very shallow or type I flow pathway system would be expected in these lithomorphic soils.

Given that the Ferralsol is the dominant soil of the tropics, it is worth noting the extent of this soil in the Mekong basin. Very few areas of the Mekong are mapped as being dominated by Ferralsol soils. The only areas are in the extreme southeast of the basin where parts of the Tonle Srepok and Dak Dear basins (Vietnam) have Ferralsol soils (FAO-UNESCO 1976, 2004; see Fig. 2) developed on basaltic rocks (Wakita et al. 2004).

In summary, understanding the spatial patterns of runoff processes within the Mekong requires further work to isolate the regions of Alisol soil from Acrisol soil, particularly where the presence of Acrisol soil would allow much percolation of rainfall to depth within the extensive regoliths of the Mekong lowlands. Further study of the effect of Gleysols and Fluvisols, particularly in the same Mekong lowlands, is similarly important, in this case to identify the presence and role of near-surface and hence rapid rainfall-runoff pathways.

7. Conclusions

This analysis has examined the role of soil, regolith, and rock type on runoff pathways within tropical Southeast Asia. Direct observations of runoff pathways should always be a key element of such analyses, but there are insufficient published hillslope hydrology studies for the Southeast Asian region to make robust generalisations. As a result, we have attempted generalisations of water pathway to soil–regolith–rock linkages for studies undertaken throughout the whole humid tropics (i.e., wet tropics and seasonally wet tropics). We then examined the spatial patterns of soil–regolith–rock information for the whole Southeast Asia region available from the latest sources (FAO-UNESCO 2004; Wakita et al. 2004) to assess the importance of each stratum and the potential interactions between the strata. Throughout, we have acknowledged the considerable uncertainties within (i) the data sources (GIS data and experimental results) and (ii) our generalisations. Implicit within this is also our focus on only one factor affecting runoff pathways, namely the soil–regolith–rock system; we acknowledge the additional role of factors such as the rainfall regimen, topography, and channel network. It is, however, our view that generalisations from a wider range of observations and conditions from the whole humid tropics might give insight into phenomena within Southeast Asia or indeed its largest watershed, the Mekong, where sufficient local observations are absent.

It is hoped that we have demonstrated that previous generalisations (or perceptual models) of flow pathways in the humid tropics have significant inconsistencies. A new model (^{clay}K) is proposed which addresses the inconsistencies in the soil component by utilising clay mineralogy. Where permeable regoliths or rocks are present, and we show where these may be present, rainfall may percolate to a considerable depth before returning to form riverflow. Very often hillslope hydrological studies and larger-scale hydrological modelling exercises have ignored these deeper pathways (Bonell 2004; Chappell et al. 2005). Thus, there is a second reason for understanding the role of surficial geology (i.e., regolith) and solid geology in rainfall-runoff research. To highlight the role of these deeper strata, we propose a new model called the Delta

model. For the moment, this remains a perceptual model (i.e., a qualitative description of ideas: Beven 2004). With more data and analysis, we hope that this could become a conceptual model (i.e., a quantitative description of key ideas: Beven 2004). Our aim is to encourage new quantitative field research into the role and interaction of soil, regolith, and rock strata on runoff pathways.

The analysis of the data sources (GIS data and experimental results) has highlighted the potential importance of Acrisol-Alisol soil groups and regolith associated with granitic rock and Quaternary sediments within Southeast Asia. These are important considerations for hydrological research within the Mekong basin, but this subregion also has relatively extensive regions of slowly permeable soils overlying the Quaternary sediments (i.e., the regolith underlying Cambodia) and a deep aquifer system within the solid geology of the Khorat Plateau. The nature of the interaction between deeper hydrological systems and the surface hydrology where there are impeding layers (perhaps considered as "aquitards": Todd and Mays 2005) must be clarified.

Our main point is that field observations are needed to support the ideas forwarded and that this research needs to take a holistic approach to the hydrology of soils, regoliths, and rock.

References

Anderson MG, Burt TP (1990) Process studies in hillslope hydrology. Wiley, Chichester

Baillie IC (1975) Piping as an erosion process in the uplands of Sarawak. J Trop Geogr 41:9–15

Baron JS, Hartman MD, Kittel TGF, Band LE, Ojima DS, Lammers RB (1998) Effects of land cover, water redistribution, and temperature on ecosystem processes in the South Platte Basin. Ecol Appl 8:1037–1051

Beven KJ (2001) Rainfall-runoff modelling: a primer. Wiley, Chichester

Bidin K, Chappell NA (2006) Characteristics of rain-events at an inland locality in Northeastern Borneo. Hydrol Process 20:3835–3850

Blöschl G, Sivapalan M (1997) Process controls on regional flood frequency: Coefficient of variation and basin scale. Water Resour Res 33:2967–2980

Bonell M (2004) Runoff generation in tropical forests. In: Bonell M, Bruijnzeel LA (eds) Forests, water and people in the humid tropics. Cambridge University Press, Cambridge, pp 314–406

Bonell M, Gilmour DA (1978) The development of overland flow in a tropical rainforest catchment. J Hydrol 39:365–382

Bonell M, Gilmour DA, Sinclair DF (1981) Soil hydraulic properties and their effect on surface and subsurface water transfer in a tropical rainforest catchment. Hydrol Sci Bull 26:1–18

Bonell M, Gilmour DA, Cassells DS (1983) A preliminary survey of the hydraulic properties of rainforest soils in tropical north-east Queensland and their implications for the runoff process. In: De Ploey J (ed) Rainfall, simulation, runoff and soil erosion. Catena Suppl 4:57–78

Bruijnzeel LA (1990) Hydrology of moist tropical forest and effects of conversion: a state of the art review. UNESCO, Paris

Bunting BT (1961) The role of seepage moisture in soil formation, slope development, and stream initiation. Am J Sci 259:503–518

Burt TP, Butcher DP (1985) Topographic controls of soil moisture distributions. J Soil Sci 36:469–486

Campbell EM (1997) Granite landforms. J R Soc W Aust 80:101–112

Carter A, Bristow C (2003) Linking hinterland evolution and continental basin sedimentation using detrital zircon thermochronology: a study of the Khorat Plateau Basin, Eastern Thailand. Basin Res 15:271–285
Chappell NA (2005a) Water pathways in humid forests: myths vs. observations. Suiri Kagaku 48:32–46
Chappell NA (2005b) Modelling tropical forest watersheds: setting realistic goals. ETFRN News 45:25–28
Chappell NA, Binley AM (1992) The impact of rain forest disturbance upon near-surface groundwater flow: modelling of hillslope flow experiments. Ann Geophys 10(II):c330
Chappell NA, Ternan JL (1992) Flow-path dimensionality and hydrological modelling. Hydrol Process 6:327–345
Chappell N, Ternan L (1997) Ring permeametry: design, operation and error analysis. Earth Surf Process Landf 22:1197–1205
Chappell NA, Sherlock MD (2005) Contrasting flow pathways within tropical forest slopes of Ultisol soil. Earth Surf Process Landf 30:735–753
Chappell NA, Franks SW, Larenus J (1998) Multi-scale permeability estimation in a tropical catchment. Hydrol Process 12:1507–1523
Chappell NA, McKenna P, Bidin K, Douglas I, Walsh RPD (1999a) Parsimonious modelling of water and suspended-sediment flux from nested-catchments affected by selective tropical forestry. Philos Trans R Soc Lond B 354:1831–1846
Chappell NA, Ternan JL, Bidin K (1999b) Correlation of physicochemical properties and sub-erosional landforms with aggregate stability variations in a tropical Ultisol disturbed by forestry operations. Soil Tillage Res 50:55–71
Chappell NA, Bidin K, Sherlock MD, Lancaster JW (2004a) Parsimonious spatial representation of tropical soils within dynamic, rainfall-runoff models. In: Bonell M, Bruijnzeel LA (eds) Forests, water and people in the humid tropics. Cambridge University Press, Cambridge, pp 756–769
Chappell NA, Douglas I, Hanapi JM, Tych W (2004b) Source of suspended-sediment within a tropical catchment recovering from selective logging. Hydrol Process 18:685–701
Chappell NA, Nik AR, Yusop Z, Tych W, Kasran B (2004c) Spatially-significant effects of selective tropical forestry on water, nutrient and sediment flows: a modelling-supported review. In: Bonell M, Bruijnzeel LA (eds) Forests, water and people in the humid tropics. Cambridge University Press, Cambridge, pp 513–532
Chappell NA, Bidin K, Fowell M, Solera M, Tych W, Vongtanaboon S (2005) Towards a macro-hydrology of the humid tropics: implications for GCM simulations. In: Abstracts of the Royal Meteorological Society conference 2005, Exeter University, 12–16 September 2005, p 10
Chappell NA, Vongtanaboon S, Jiang Y, Tangtham N (2006) Return-flow prediction and buffer designation in two rainforest headwaters. For Ecol Manag 224:131–146
Chiem NH (1993) Geo-pedological study of the Mekong Delta. Southeast Asian Stud 31:158–186
Chen SS, Houze RA (1997) Interannual variability of deep convection over the tropical warm pool. J Geophys Res 102(D22):25783–25795
Douglas I (2005) The Mekong river basin. In: Gupta A (ed) The physical geography of Southeast Asia. Oxford University Press, Oxford, pp 193–218
Driessen PM, Deckers J (2001) Lecture notes on the major soils of the World. World soil resources report 94. FAO, Rome
Driessen PM, Dudal R (1991) The major soils of the world: lecture notes on their geography, formation properties and use. Agricultural University Wageningen and Katholieke Universiteit Leuven, The Netherlands
Drigo R (2004) Trends and patterns of tropical land use change. In: Bonell M, Bruijnzeel LA (eds) Forests, water and people in the humid tropics. Cambridge University Press, Cambridge, pp 9–39

Dubreuil PL (1985) Review of field observations of runoff generation in the tropics. J Hydrol 80:237–264
Dunne T, Moore TR, Taylor CH (1975) Recognition and prediction of runoff-producing zones in humid regions. Hydrol Sci Bull 3:305–327
Dykes AP, Thornes JB (2000) Hillslope hydrology in tropical rainforest steeplands in Brunei. Hydrol Process 14:215–235
Elsenbeer H (2001) Hydrologic flowpaths in tropical soilscapes–a review. Hydrol Process 15:1751–1759
Elsenbeer H, Lack A (1996) Hydrometric and hydrochemical evidence for fast flowpaths at La Cuenca, Western Amazonia. J Hydrol 180:237–250
FAO-UNESCO (1976) Soil map of the world, sheet IX. FAO, Rome
FAO-UNESCO (1977) Soil map of the world, sheet VIII-3. FAO, Rome
FAO-UNESCO (1990) Soil map of the world. Revised legend. Soils Bulletin 66. FAO, Rome
FAO-UNESCO (2004) Digital soil map of the world and derived soil properties. FAO, Rome
Freer J, McDonnell JJ, Beven KJ, Peters NE, Burns DA, Hooper RP, Aulenbach B, Kendall C (2002) The role of bedrock topography on subsurface storm flow. Water Resour Res 38:1269
Gibbons JM, Newbery DM (2003) Drought avoidance and the effect of local topography on trees in the understorey of Bornean lowland rain forest. Plant Ecol 164:1–18
Gillieson D (2005) Karst in Southeast Asia. In: Gupta A (ed) The physical geography of Southeast Asia. Oxford University Press, Oxford, pp 157–176
Godsey S, Elsenbeer H, Stallard R (2004) Overland flow generation in two lithologically distinct rainforest catchments. J Hydrol 295:276–290
Gregory KJ (1976) Drainage networks and climate. In: Derbyshire E (ed) Geomorphology and climate. Wiley, London, pp 289–315
Gupta A (2005) Landforms of Southeast Asia. In: Gupta A (ed) The physical geography of Southeast Asia. Oxford University Press, Oxford, pp 38–64
Heggemann H, Helmcke D, Gottingen, Tietze KW (1994) Sedimentary evolution of the Mesozoic Khorat Basin in Thailand. Zentbl Geol Palaont Teil 1 (Stuttgart 1992) 11/12:1267–1285
Hodnett MG, Vendrame I, Marques Filho A De O, Oyama MD, Tomasella J (1997) Soil water storage and groundwater behaviour in a catenary sequence beneath forest in central Amazonia: I. Comparisons between plateau, slope and valley floor. Hydrol Earth Syst Sci 1:265–278
Jones JAA (1990) Piping effects in humid lands In: Higgins CG, Coates DR (eds) Groundwater geomorphology. Special paper 252. Geological Society of America, Boulder, CO, pp 111–138
Kinner DA, Stallard RF (2004) Identifying storm flow pathways in a rainforest catchment using hydrological and geochemical modelling. Hydrol Process 18:2851–2875
Kirkby MJ (1975) Hydrograph modelling strategies. In: Peel R, Chisholm M, Haggett P (eds) Processes in physical and human geography. Heinemann, Boston, pp 69–90
Kirkby MJ (1978) Hillslope hydrology. Wiley, Chichester
Kokkonen TS, Jakeman AJ, Young PC, Koivusalo HJ (2003) Predicting daily flows in ungauged catchments: model regionalization from catchment descriptors at the Coweeta Hydrologic Lab. Hydrol Process 17:2219–2238
Malmer A Grip H (1990) Soil disturbance and loss of infiltrability caused by mechanised and manual extraction of tropical rainforest in Sabah, Malaysia, For Ecol Manag 38:1–12
McDonnell JJ (2003) Where does water go when it rains? Moving beyond the variable source area concept of rainfall-runoff response. Hydrol Process 17:1869–1875
Mekong River Commission (2005) Overview of the hydrology of the Mekong Basin. Mekong River Commission, Vientiane

Melinda F, Rahardjo H, Han KK, Leong EC (2004) Shear strength of compacted soil under infiltration condition. J Geotech Geoenviron Eng 130:807–817
Milne G (1935) Some suggested units of classification and mapping, particularly for East African soils. Soil Res 4:183–198
Najman Y (2006) The detrital record of orogenesis: a review of approaches and techniques used in the Himalayan sedimentary basins. Earth-Sci Rev 74:1–72
Neale R, Slingo J (2003) The maritime continent and its role in the global climate: a GCM study. J Climate 16:834–848
Nielsen DR, Biggar JW, Ehr KT (1973) Spatial variability of field-measured soil-water properties. Hilgardia 42:215–259
Noguchi S, Abdul Rahim N, Baharuddin K, Tani M, Sammori T, Morisada K (1997) Soil physical properties and preferential flow pathways in a tropical rain forest, Bukit Tarek, Peninsular Malaysia. J For Res 2:115–120
Nortcliff S, Thornes JB (1981) Seasonal variations in the hydrology of a small forested catchment near Manaus, Amazonas, and the implications for its management. In: Lal R, Russell EW (eds) Tropical agricultural hydrology. Chichester, Wiley
Nyabeze WR (2005) Calibrating a distributed model to estimate runoff for ungauged catchments in Zimbabwe. Phys Chem Earth 30:625–633
O'Loughlin EM (1981) Saturation regions in catchments and their relation to soil and topographic properties. J Hydrol 53:229–246
Phienwej N, Nutalaya, P (2005) Subsidence and flooding in Bangkok. In: Gupta A (ed) The physical geography of Southeast Asia. Oxford University Press, Oxford, pp 358–378
Racke KD, Skidmore MW, Hamilton DJ, Unsworth JB, Miyamoto J, Cohen SZ (1997) Pesticide fate in tropical soils. Pure Appl Chem 69:1349–1371
Racey A, Love MA, Canham A, Goodall JGS, Polachan S, Jones PD (1996) Stratigraphy and reservoir potential of the Mesozoic Khorat Group, NE Thailand. Part 1: Stratigraphy and sedimentary evolution. J Petrol Geol 19:5–40
Rahman A (1992) Soils of Singapore. In: Gupta A, Pitts J (eds) Physical adjustments in a changing landscape: the Singapore story. Singapore University Press, Singapore, pp 144–189
Roberts J (2000) The influence of physical and physiological characteristics of vegetation on their hydrological response. Hydrol Process 14:2885–2901
Robinson JS, Sivapalan M (1997) Temporal scales and hydrological regimes: implications for flood frequency scaling. Water Resour Res 33:2981–2999
Schellekens J (2000) Hydrological processes in a humid rain forest: a combined experimental and modelling approach. PhD thesis. Vrije Universiteit, Amsterdam
Schneider N (1998) The Indonesian throughflow and the global climate system. J Climate 11:676–689
Sherlock MD, Chappell NA, Greer T (1995) Tracer and Darcy-based identification of subsurface flow, Bukit Timah forest, Singapore. Singapore J Trop Geol 16:197–215
Sherlock MD, Chappell NA, McDonnell JJ (2000) Effects of experimental uncertainty on the calculation of hillslope flow paths. Hydrol Process 14:2457–2471
Shimizu A, Kabeya N, Nobuhiro T, Kubota T, Tsuboyama Y, Ito E, Sano M, Chann S, Keth N (2005) Study on runoff characteristics in forest watersheds, Central Cambodia. In: Proceedings of the international conference on forest environment in continental river basins; with a focus on the Mekong River, Phnom Penh, Cambodia, 5–7 December 2005, pp 33–34
Shroder JF (1993) Himalaya to the sea: geology, geomorphology and the Quaternary. Routledge, London.
Sinun W, Meng WW, Douglas I, Spencer T (1992) Throughfall, stemflow, overland flow and throughflow in the Ulu Segama rain forest, Sabah, Malaysia. Philos Trans R Soc Lond Ser B 335:389–395

Smith MB, Koren VI, Zhang Z, Reed SM, Pan JJ, Moreda F (2004) Runoff response to spatial variability in precipitation: an analysis of observed data. J Hydrol 298:267–286

Soil Survey Staff (1999) Soil taxonomy: a basic system of soil classification for making and interpreting soil surveys, 2nd edn. United States Department of Agriculture, Washington, DC

Struckmeier W, Richts A (2004) Groundwater resources of the world. Special edition. BGR, Hannover and UNESCO, Paris

Todd DK, Mays LW (2005) Groundwater hydrology, 3rd edn. Wiley, Hoboken

Tien PC, An LD, Bach LD (1988) Geology of Cambodia, Laos and Vietnam: explanatory note. Geological Survey of Vietnam, Hanoi

Twidale CR (2005) Granitic Terrains. In: Gupta A (ed) The Physical Geography of Southeast Asia. Oxford University Press, Oxford, pp123–141

Van der Plas MC, Bruijnzeel LA (1993) The impact of mechanized selective logging of lowland rain forest on topsoil infiltrability in the upper Segama area, Sabah, Malaysia. IAHS Publ 216:203–211

Wakita K, Okubo Y, Bandibas JC, Lei X, Schulte MJD (2004) Digital geologic map of East and Southeast Asia, 1:2,000,000, 2nd edn. Geological Survey of Japan, Tsukaba

Walsh RPD (1996) Drainage density and network evolution in the humid tropics: evidence from the Seychelles and the Windward Islands. Z Geomorphol 103:1–23

Yusop Z (1996) Nutrient cycling in secondary rainforest catchments of Peninsular Malaysia. PhD thesis. University of Manchester, Manchester

Zaslavski D, Sinai G (1981) Surface hydrology: IV. Flow in sloping, layered soil. J Hydrol Div (HYI):53–64

Zektser IS, Everett LG (2004) Groundwater resources of the world and their use. IHP-VI. Series on groundwater no. 6. UNESCO, Paris

Ziegler AD, Giambelluca TW (1998) The influence of revegetation efforts on hydrologic response and erosion, Kahoolawe Island, Hawaii. Land Degrad Dev 9:189–206

Ziegler AD, Giambelluca TW, Tran LT, Vana TT, Nullet MA, Fox J, Tran Duc Vien, Pinthong J, Maxwell JF, Evett S (2004) Hydrological consequences of landscape fragmentation in mountainous Northern Vietnam: evidence of accelerated overland flow generation. J Hydrol 287:124–146

Technical Report

Impact of Land-Use Development on the Water Balance and Flow Regime of the Chi River Basin, Thailand

Kanokporn Boochabun*, Sukanya Vongtanaboon, Apichat Sukrarasmi, and Nipon Tangtham

To analyze the relationships between land-use changes and water balance and flow regimes in the Chi River basin, Thailand, we used historical data of annual rainfall and seasonal and annual flow from 1951 to 2003, which corresponded to land-use changes derived from Landsat imagery acquired between 1973 and 2003. We found that during the past 52 years the forested area in the Chi River basin has declined by 20%, whereas agricultural areas, paddy fields, and urban areas have expanded rapidly. Upland agriculture (maize, cassava) fluctuated from more than 36% in 1973 to less than 20% in 2000, with a notable drop in cassava cultivation. In contrast, sugarcane cultivation increased during the past 5 years because of increased market demands, and rice fields were expanded from 20% to 42% in 2000. Although annual rainfall in the Chi River basin has tended to decrease, we found an insignificant relationship between land-use changes, in particular, the depletion of forested areas, and annual rainfall. We also found an insignificant relationship between the water budget component and land-use changes, with a rather small effect on seasonal and annual flows of the basin.

1. Introduction

Land-use changes have the potential to greatly affect the hydrology of an area. The hydrological roles of forests have been studied extensively in western and some Asian countries. Although some studies have been conducted in Thailand (Tangtham 1994), in-depth investigations with empirical predictions are still lacking. In fact, there has been a good deal of controversy in scientific circles over the past several decades on the relationship between forests and rainfall, between forests and water yields, and between soil erosion and sedimentation control in Thailand (Ruangpanit 1971; Niyom 1980; Janmahasatien 1986; Euvananon 1994). Empirical findings on these topics have mainly been reported by university researchers. Unfortunately, however, long-term records of changes in water yields corresponding to land-use changes are rare. It is

* Research and Applied Hydrology Group, Hydrology Division, Office of Hydrology and Water Management, Royal Irrigation Department, Bangkok, Thailand
E-mail: b_kanokporn@yahoo.com

thus rather difficult to derive valid conclusions, and in many cases more-reliable data are required to gain more conclusive findings (Tangtham 1994).

Rainfall is generally thought to be generated by monsoonal effects (Technical Data and Information Committee 1986). International evidence and simulation models suggest two conditions under which forests generate rainfall. First, montane forests at very high altitudes (≥2000 m) can harvest clouds. In Thailand, this has been confirmed at Doi Pui. Lekavijit (1982) investigated the effects of high-altitude evergreen forests on rainfall in Chiang Mai Province, northern Thailand. He recorded about 50 mm/year of additional annual rainfall in forested areas compared to cleared areas at the same altitude. Second, the deforestation of vast tracts of land, i.e., >250 000 km^2, could reduce the probability of rainfall from water cycling (Lekavijit 1982).

Changes and variation in annual rainfall patterns in different regions of Thailand were also studied by Wongvitavas (1989), although he did not investigate the relationship between rainfall and forest depletion. Wongvitavas (1989) recorded sharp decreases in annual rainfall in the central, northern, and southwestern regions of the country. The same was true in the east, whereas the northeastern and southeastern regions showed a slight downward trend in rainfall.

Kanae et al. (2001) investigated the variation in rainfall and the land-use changes in northeastern Thailand in 2000 using a time-series analysis and hydrological modeling. They detected significant decreases in precipitation over Thailand only in the time series of monthly precipitation in September. The amounts of precipitation recorded at many meteorological stations in September have decreased by approximately 100 mm/month (an approximately 30% relative change) over the past three or four decades. Meteorological modeling of rainfall during August–September and land cover in 1992–1994 showed that September rainfall in the northeast decreased by approximately 26 mm/month (7%), whereas in some other parts of this region rainfall decreased by as much as 88 mm/month (29%). However, rainfall in August was unchanged. Kanae et al. (2001) explained that light southwest monsoons in September were the cause of lower September rainfall in the northeast. The model also indicated that deforestation caused reduced surface roughness, and the changes in surface albedo affected the weakening of southwest monsoons in this area.

It is thought that forests may add water vapor to the air via evapotranspiration and may increase rainfall in arid zones (Chunkao 1979). High-altitude forests can increase the likelihood of cold and warm air masses mixing and consequently may contribute to condensation; this is especially true for mountainous forest areas where air temperature is usually low. Chunkao (1979) concluded that forests may have some effect on rainfall in addition to affecting topographic conditions and monsoon air circulation.

When large areas of forest are encroached, their natural functions can be altered, often resulting in the natural phenomena of floods and drought (Bunkert 1983). Similarly, Tangkitjavisuth (1979) found that forest encroachment in northeastern Thailand can result in drought and flood, as was recently evidenced by severe temperature fluctuations in this region. Prachaiyo (1983) also supported the idea that large deforested areas inhibit the creation of water vapor or atmospheric moisture, resulting in arid weather, because forests may add water vapor to the air by evapotranspiration and may increase rainfall in arid zones. Flow records for the Chi River

indicate periods of severe flooding during the rainy season and drought during the dry period, which may have been the result of forest encroachment, as suggested by Tangkitjavisuth (1979).

Small-scale experiments have demonstrated that forest clearance leads to an increase in water yield, but it is unclear if this result holds for larger river basins (>1000 km^2). No widespread changes in rainfall totals or patterns were found in the 12 100 km^2 Nam Pong catchment in northeast Thailand between 1957 and 1995, despite a reduction in the area classified as forest from 80% to 27% during the past three decades (Wilk et al. 2000). No detectable changes were found in any other water balance terms or in the dynamics of the recession of flow at the end of the rainy season. When a hydrological model calibrated using data from the period before deforestation was applied for the last years of the study period (1987–1995), the runoff generation was underestimated by approximately 15%, indicating increased runoff generation after deforestation. However, this was mainly the result of the hydrological response during one single year in the first period, when the flow/rainfall (*Q/P)* ratio was very low. When this year was excluded, neither analysis based on the hydrological model revealed any significant change in the water balance as a result of deforestation. More detailed land-use analyses revealed that shade trees were left on agricultural plots, and there were several abandoned areas in which secondary growth could be expected; this may have accounted for the results (Wilk et al. 2000).

The conversion of natural forest and agricultural areas to urbanized areas in the Chi River basin has resulted in a significant increase in impervious surfaces in the landscape. In developed areas, surface runoff is not able to infiltrate into the soil because of the prevalence of impermeable surfaces, which results in a high peak volume of water reaching the channel system within a relatively short period of time. Thus, land-use information can be used to estimate the effect of forest conversion on water balance and flow regimes in the Chi River basin. Our goal was threefold: to explore the land-use changes in the Chi River basin, to investigate the relationship between land-use changes and rainfall flow, and to evaluate the effect of land-use development on the water balance. Here, we attempt to summarize our empirical findings in the Chi River basin related to these three topics. We hope that the information compiled here will contribute to the formulation of national and regional policy on forest and land resource management.

2. Site and Data

The Chi River basin, which is located in northeast Thailand, drains into the Mun River and Mekong River. The altitude of this 47 818 km^2 basin is 200 m, and most topographic features are of the Korat Plateau. Deciduous and evergreen forests are the main forest types, covering 20% of the area. Seventy-five rain-gauge stations are distributed throughout the basin, and one streamflow station is located at outlet E.20A in Maha Chana Chai, Yasothon Province.

Percentage forest cover data for the Chi River basin were derived from Landsat images acquired in 1974, 1978, 1979, 1989, 1991, and 1993, which were interpreted by the Royal Forestry Department. Land-use data for the Chi River basin were gathered from land-use maps created in 1973, 1978, and 1982, which were provided by the

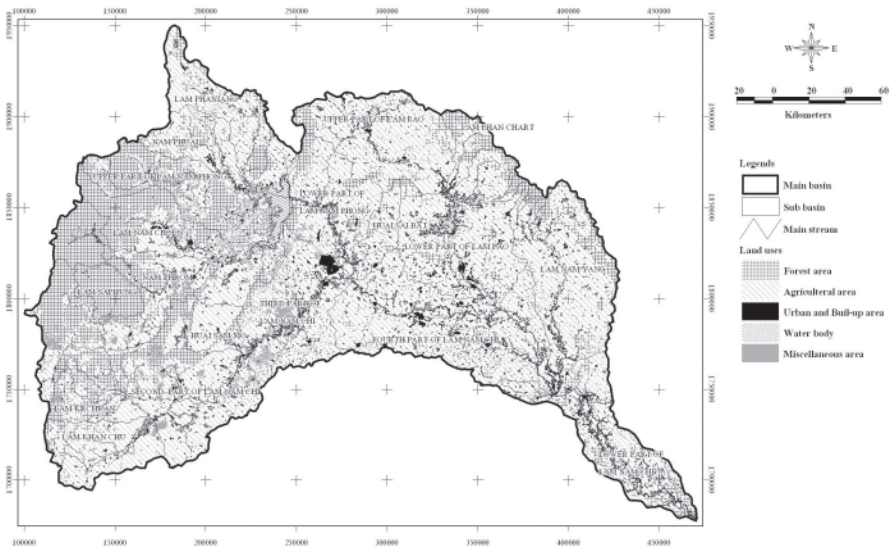

Fig. 1. Land use of Chi River basin in 2000

Faculty of Forestry, Kasetsart University, and in 1990, 1994, and 2000, provided by the Land Development Department and the Office of Agricultural Statistics. Land-use data from 2000 are shown in Fig. 1.

Historical data of the annual rainfall and seasonal and annual flow between 1951 and 2003, which were compiled by the Royal Irrigation Department (2003) and correspond to land-use changes from 1973 to 2003, were used to analyze the relationships between land-use changes and the water balance and flow regime of the Chi River basin. We analyzed the effect of land-use development on rainfall distribution, rainfall flow variation, water balance, and flow regime.

3. Research Methods

Our strategy for investigating the effect of land-use development on the water balance and flow regime of the Chi River basin involved a series of experiments. The first step was to evaluate the historical rainfall amount and distribution in the Chi River basin up to the present and analyze the effect of land-use development on the amount of rainfall. The catchment flow variation was then analyzed to determine the effect of land-use changes and variation in rainfall on discharge and water loss in terms of water balance. Finally, we examined the effect of land-use development on streamflow timing.

3.1. Analysis of Land-Use Changes

The rate of land-use change in years for which it was not recorded can be evaluated using the equation of Wacharakitti (1975):

$$A = P(1 + r)^n$$

where A is the area of land use in a given year, P is the area of land use in the first year, r is the increasing or decreasing proportion of land-use area per year; and n is the time difference between the 2 years.

3.2. Rainfall Flow Analysis

The amount and distribution of rainfall in the Chi River basin were explored to assess the spatial and temporal rainfall patterns in the catchment. To decrease the effect of rainfall on flow and to show the effect of land-use changes on flow, we applied a moving average for the time-series data to analyze the rainfall and flow variation in the catchment.

3.3. Relationship Between Land-Use Changes and Water Balance

We used regression analysis to determine the relationship between land-use changes and rainfall flow.

Water balance was evaluated as follows:

$$Et = R - Q \pm \Delta S$$

where Et is evapotranspiration (mm/year), R is rainfall (mm/year), Q is discharge (mm/year), and ΔS is the soil moisture gradient. The relationship between land-use changes and water balance was also analyzed using regression.

4. Results and Discussion

4.1. Land-Use Changes in the Chi River Basin

During the past 52 years, the forested area in the Chi River basin has declined by 20% while the agricultural areas, paddy fields, and urban areas have expanded rapidly. Upland agriculture (maize, cassava) fluctuated from >36% in 1973 to <20% in 2000, with a notable drop in cassava cultivation. In contrast, the area of sugarcane cultivation increased during the last 5 years because of increased market demand, and rice fields expanded from 20% to 42% by 2000. Disturbed forestland in the basin has been converted into agricultural use. Reservoir construction also facilitated an increase in agriculture. Land-use changes during 1973–2000 in the Chi River basin are shown in Fig. 2 and Table 1.

4.2. Relationship Between Land-Use Changes and Variation in Rainfall

The range of annual rainfall in the Chi River basin from 1952 to 2003 was 932–1647 mm, with an average rainfall of 1324 mm/year. The amount of rainfall was less

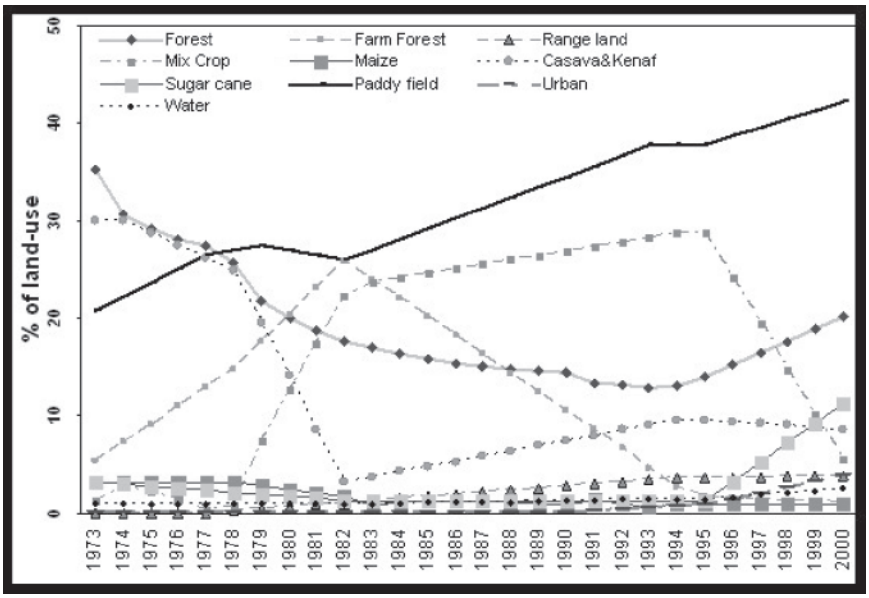

Fig. 2. Changes of various land use in the Chi River basin during 1973–2000

in the western area of the basin and gradually increased in the east as a result of monsoons and tropical typhoons (Fig. 3).

During the past 52 years, with the 20% decline in the forested area of the Chi River basin and rapid expansion of agricultural, paddy, and urban areas, the average annual rainfall has also decreased by 2 mm/year. During the rainy season, rainfall decreased by 3 mm, especially in July–September, the wettest months in this area. The time-series analysis revealed a declining trend in annual rainfall (Fig. 4).

Although the annual rainfall in the Chi River basin tended to decrease, we found an insignificant relationship between land-use changes, in particular, the depletion of forested areas, and annual rainfall. This finding corresponds to the results of Wilk et al. (2000), who reported no widespread changes in rainfall totals and patterns in the 12 100 km^2 Nam Pong catchment in northeast Thailand between 1957 and 1995, despite a reduction in the area classified as forest from 80% to 27% during the past three decades.

4.3. Relationship Between Land-Use Changes and Flow Variation

From the streamflow data for 1974–2003 at station E.20A (47 818 km^2 basin area) in Maha Chana Chai, Yasothon Province, the average streamflow was 8979 million m^3/year. The amount of discharge in the basin was 14% of the rainfall. The high flow was 7045 million m^3, or 79% of the total flow, and the low flow was 1933 million m^3, or 21% of the total flow. Thus, the variation in flow was quite high.

TABLE 1. Land-use change during 1973–2000 in the Chi River basin (drainage area, 49 477 km^2)

Year	Forest		Mixed crop land		Agriculture				Urban	Water
	Forest	Farm forest	Range land	mixed Crop	Maize	Cassava & kenaf	Sugar cane	Paddy field		
1973	35.20	5.35	0.00	1.22	3.17	30.00	3.19	20.78	0.12	0.97
1974	30.56	7.23	0.00	2.69	3.17	29.97	2.98	22.30	0.12	0.97
1975	29.13	9.12	0.00	2.30	3.17	28.71	2.77	23.70	0.12	0.97
1976	28.16	11.01	0.00	1.44	3.16	27.45	2.56	25.11	0.12	0.98
1977	27.49	12.90	0.00	0.28	3.16	26.20	2.35	26.51	0.13	0.98
1978	25.79	14.79	0.29	0.78	3.16	24.94	2.14	27.00	0.13	0.98
1979	21.73	17.58	0.50	7.44	2.81	19.50	1.93	27.43	0.13	0.97
1980	19.96	20.36	0.71	12.71	2.45	14.05	1.73	26.95	0.13	0.96
1981	18.66	23.15	0.92	17.51	2.09	8.60	1.53	26.47	0.13	0.95
1982	17.68	25.93	0.95	22.17	1.74	3.16	1.32	25.98	0.13	0.94
1983	16.91	24.00	1.34	23.71	0.87	3.69	1.32	27.05	0.13	0.98
1984	16.30	22.07	1.57	24.16	1.09	4.23	1.31	28.12	0.13	1.02
1985	15.81	20.14	1.76	24.61	1.23	4.77	1.31	29.19	0.13	1.06
1986	15.42	18.20	1.97	25.07	1.26	5.30	1.30	30.25	0.13	1.10
1987	15.09	16.27	2.17	25.52	1.22	5.84	1.30	31.32	0.13	1.14
1988	14.81	14.34	2.39	25.97	1.12	6.38	1.29	32.39	0.13	1.19
1989	14.58	12.41	2.59	26.42	0.98	6.91	1.28	33.45	0.13	1.23
1990	14.39	10.48	2.80	26.88	0.80	7.45	1.28	34.52	0.13	1.27
1991	13.26	8.55	3.01	27.33	1.38	7.98	1.27	35.59	0.31	1.31
1992	13.21	6.61	3.23	27.78	0.88	8.52	1.27	36.66	0.49	1.35
1993	12.86	4.68	3.44	28.24	0.68	9.06	1.26	37.72	0.67	1.39
1994	12.99	2.75	3.65	28.69	1.00	9.59	1.26	37.79	0.85	1.44
1995	13.93	1.71	3.68	28.70	1.00	9.60	1.26	37.80	0.88	1.44
1996	15.18	1.59	3.70	24.08	0.98	9.40	3.25	38.68	1.48	1.65
1997	16.44	1.47	3.73	19.46	0.96	9.20	5.24	39.56	2.09	1.86
1998	17.69	1.34	3.75	14.84	0.94	9.00	7.22	40.44	2.69	2.08
1999	18.95	1.22	3.78	10.22	0.92	8.80	9.21	41.32	3.30	2.29
2000	20.2	1.1	3.8	5.6	0.9	8.6	11.2	42.2	3.9	2.5

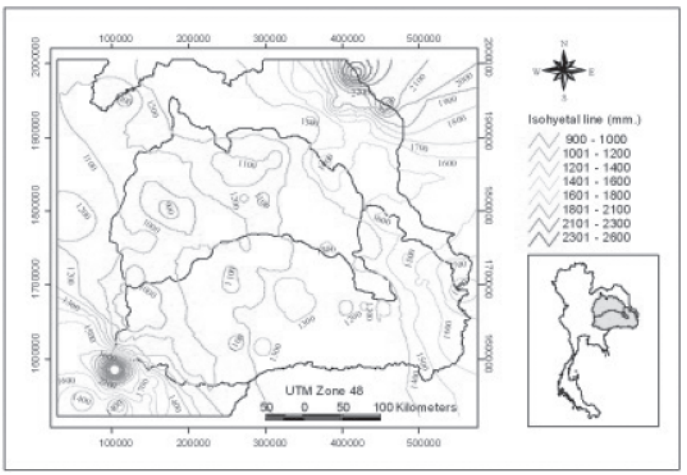

FIG. 3. Isohyetal map in eastern part of Thailand

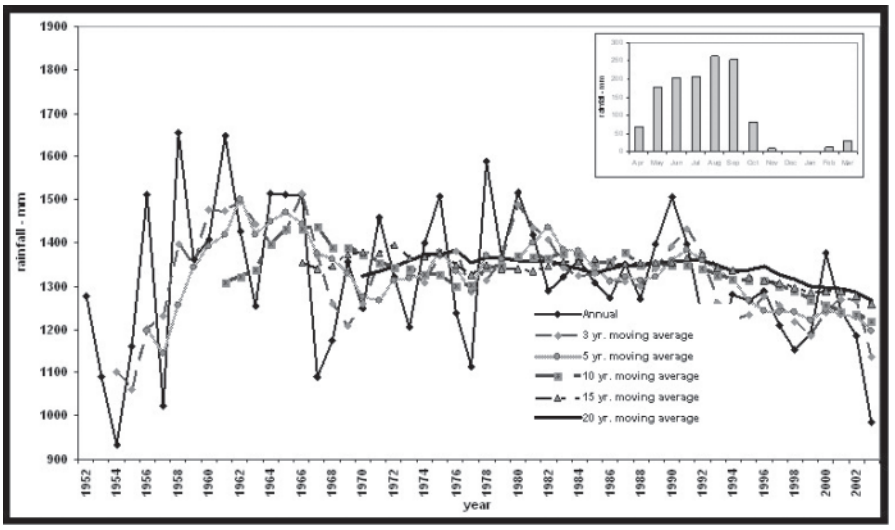

FIG. 4. Variation of annual rainfall and moving average with difference time series

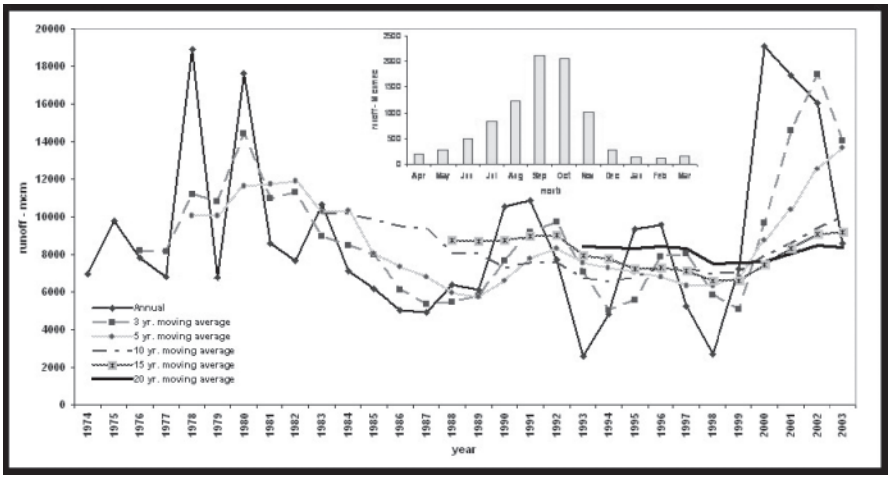

FIG. 5. Variation of annual runoff and moving average with difference time series

Over the past 52 years, the annual streamflow has increased by 1 million m^3/year, indicating a small increase in river discharge, whereas the high flow tended to increase by 47 million m^3/year. This finding corresponds with the data of Wilk et al. (2000), who found increased runoff generation following deforestation.

Monthly flow during the rainy season in the Chi River basin was relatively high, whereas flow tended to decrease during the dry season, which is characterized by extremely low rainfall. Thus, the flow analysis of the Chi River showed frequent flooding during the rainy season and drought during the dry period.

The time-series analysis indicated that the annual flow in the Chi River tended to decrease during the first 25 years and then increased for the last 5 years (Fig. 5).

Although the annual flow in the basin tended to rise during these last years, an insignificant relationship between land-use changes was found, with little effect on seasonal and annual flows.

4.4. Effect of Land-Use Changes on the Water Balance of the Chi River Basin

Land-use changes are related to hydrological processes. Yearly flow patterns depend on both precipitation and evapotranspiration, as well as on the soil characteristics of the catchment. As a result of the land-use changes in the Chi River basin, the parameters of the water balance equation have changed slightly (Table 2).

Time-series variations in rainfall, runoff, and evapotranspiration with changes in the percent forested area are shown in Fig. 6. As the forested area decreased from 31% in 1974 to 13% in 1995, all water balance components also tended to decrease. The average annual rainfall was 1306 mm, providing 14% discharge and 86% evapotranspiration or 1118 mm/year, which was quite high compared to the amount of rainfall. Annual evapotranspiration varied between 71% and 95%.

Because we investigated evapotranspiration simply by using water balance equations and measuring transpiration rates, and deep seepage was not taken into con-

Table 2. Percentage of land-use area and parameters of water balance equation during 1974–2000 in the Chi River basin

Year	Forest (%)	Rainfall (mm)	Flow (mm)	Et (mm)
1974	31	1400	145.34	1254
1975	29	1508	204.90	1303
1976	28	1237	164.31	1072
1977	27	1114	142.70	971
1978	26	1588	395.65	1192
1979	22	1367	141.56	1226
1980	20	1517	368.84	1148
1981	19	1420	179.62	1241
1982	18	1289	160.56	1128
1983	17	1320	222.83	1098
1984	16	1361	149.50	1212
1985	16	1307	128.52	1178
1986	15	1272	105.37	1167
1987	15	1352	103.18	1248
1988	15	1271	133.23	1138
1989	15	1398	127.91	1271
1990	14	1505	220.88	1284
1991	13	1398	226.85	1171
1992	13	1227	161.93	1065
1993	13	1156	53.99	1102
1994	13	1281	100.95	1180
1995	14	1266	195.17	1071
1996	15	1288	200.55	1088
1997	16	1210	109.39	1101
1998	18	1154	56.92	1097
1999	19	1191	151.83	1039
2000	20	1376	399.39	977

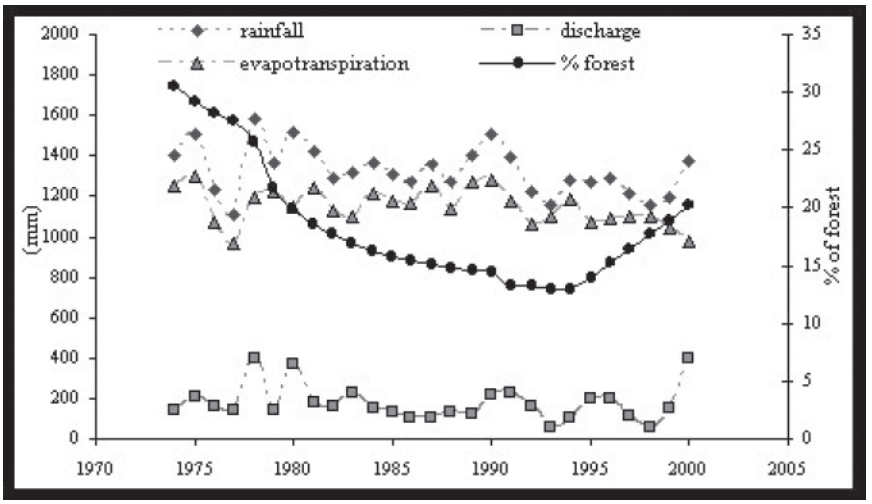

FIG. 6. Time-series variation of water balance components and percentage of forest area in the Chi River basin

sideration, the estimated amount of water loss (1118 mm/year) may be excessive. Thus, future work should consider deep seepage in calculating evapotranspiration using the water balance method because deforestation opens the ground to receive more rainfall and decreases evapotranspiration loss, which in turn may increase the amount of groundwater recharge. However, the evapotranspiration estimated here can be used as a relative value because all evapotranspiration values using the water balance method have the same deep seepage rate. The evapotranspiration loss estimated by the water balance indicated that almost all types of forests in Thailand consume >1000 mm/year of water if annual rainfall is not inhibited by drought (Suwanarat 1981; Chotibal 1982; Tangtham 1991). A comparison of all evapotranspiration values is possible to analyze the variation in losses according to land-use changes, forest area effects, and other factors.

In the Chi River basin, significant changes in land use have occurred over very long time periods. We discovered that land-use changes in the Chi River basin had an effect on decreasing the annual discharge and low flow. The area of bare land, mixed cropland, paddy fields, urban areas, and reservoirs were related to lower discharge and higher evapotranspiration. In contrast, the conversion of forestland into maize, cassava, and sugarcane showed a positive nonsignificant relationship with discharge, leading to a reduction in evapotranspiration.

The correlation coefficient of the relationship between evapotranspiration and decreased forest area was very low and nonsignificant. Rainfall, annual discharge, high flow, and low flow were not significantly related to the decreased forested area. Annual discharge and seasonal flow depended on the amount of rainfall, especially in the rainy season. Thus, neither analysis based on the hydrological model could reveal any significant change in the water balance terms resulting from deforestation, which corresponds with the results of Wilk et al. (2000).

These results of insignificant effects of land-use change on water balance in the basin were comparable to those reported by Sutthipibul (1987) and Tangtham and Sutthipibul (1988). These authors compared the changes in average regional rainfall to changes in forest cover in northeastern Thailand between 1951 and 1984. Yearly statistical analyses showed an insignificant relationship between monthly, seasonal, and annual rainfall patterns and the remaining forested areas. Thus, the authors found no correlation between rainfall parameters and the percentage of remaining forested area, although annual rainfall generally exhibited a weak negative trend during the period under consideration. When considering time trends, statistical parameters obtained using moving averages for 10-, 15-, 20-, 25-, and 30-year periods indicate that rainfall has decreased significantly as the forested area has decreased, whereas the number of rainy days has increased significantly (see Fig. 4).

5. Conclusion

During the past 52 years, the forested area in the Chi River basin has declined by 20%, whereas agricultural, paddy, and urban areas have expanded rapidly. Upland agriculture (maize, cassava) fluctuated from >36% in 1973 to <20% in 2000, with a notable drop in cassava cultivation. In contrast, the area of sugarcane production increased during the past 5 years because of the increased market demand, and rice fields expanded from 20% to 42% by 2000.

Although the annual rainfall in the Chi River basin tended to decrease, we found an insignificant relationship between land-use changes, in particular the depletion of forested area, and annual rainfall. Moreover, an insignificant relationship between the water budget component and land-use changes was found, with a minimal effect on seasonal and annual flows. Annual streamflow tended to increase, indicating increased runoff generation following deforestation.

The relationship between evapotranspiration and decreased forested area was not significant. Rainfall, annual discharge, high flow, and low flow were not related to decreased forested area. Annual discharge and seasonal flow depended on the amount of rainfall, especially during the rainy season. Thus, neither analysis based on the hydrological model could reveal any significant change in the water balance terms as a result of deforestation.

However, land-use development over the past 52 years has altered the flow regime by shifting the quartile and half flows to earlier dates and shortening the flow interval by 5%, although there was an insignificant effect on high flow interval parameters. Deforestation in the Chi River basin could thus shorten both the amount and timing of water flow in the summer.

References

Bunkert S (1983) Drought-insect outbreak. Vanasarn 41:263–278

Chotibal N (1982) The influence of the physical characteristics of watersheds and deforestation on streamflow in eastern Thailand. MS thesis. Kasetsart University, Bangkok

Chunkao K (1979) Micrometeorology. Department of Conservation, Faculty of Forestry, Kasetsart University, Bangkok

Euvananon S (1994) Impact of land-use changes on streamflow and suspended sediment of Pasak Basin. MS thesis. Kasetsart University, Bangkok
Janmahasatien R (1986) Soil and water losses from the terraced reforestation at Angkhang Highland, Chiang Mai. MS thesis. Kasetsart University, Bangkok
Kanae S, Oki T, Musiake K (2001) Impact of deforestation on regional precipitation over the Indochina Peninsula. J Hydrometeorol 2:51–70
Lekavijit Y (1982) The role of hill-evergreen forests on hydrological processes at Doi Pui in Chiang Mai. MS thesis. Kasetsart University, Bangkok
Niyom W (1980) Streamflow characteristics from forests and shifting cultivation areas at Sakaerat Environment Experiment Station. MS thesis. Kasetsart University, Bangkok
Prachaiyo B (1983) The losses after the destruction of forests. Paper presented at the 1983 National Forestry Conference, Royal Forestry Department, Bangkok
Royal Irrigation Department (2003) Hydrological data. Hydrological Division, Office of Hydrology and Water Management, Royal Irrigation Department, Bangkok
Ruangpanit N (1971) The effect of crown cover on surface runoff and soil erosion in hill evergreen forest. MS thesis. Kasetsart University, Bangkok
Sutthipibul V (1987) Effects of diminishing forest areas on rainfall amount and distribution in northeastern Thailand. MS thesis. Kasetsart University, Bangkok
Suwanarat R (1981) Water balance in hill-evergreen forest, Doi Pui, Chiang Mai. MS thesis. Kasetsart University, Bangkok
Tangkitjavisuth V (1979) The relationship between economic factors and rates of deforestation in Sakearat Environmental Research Station Area. MS thesis. Kasetsart University, Bangkok
Tangtham N (1991) Khao Yai Ecosystems: the hydrological role of Khao Yai National Park. Thail J For 9:172–195
Tangtham N (1994) The hydrological roles of forests in Thailand. TDRI Q Rev 9(3): 27–32
Tangtham N, Sutthipibul V (1988) Effects of diminishing forest areas on rainfall amount and distribution in northeastern Thailand. FRIM-IHP-UNESCO regional seminar on tropical forest hydrology, vol 4. UNESCO, Kuala Lumpur, Malaysia, pp 421–430
Technical Data and Information Committee (1986) Data and information for weather modification in Thailand. Ministry of Agriculture and Cooperatives, Bangkok, Thailand
Wacharakitti S (1975) Tropical forest land-use evolution/Northern Thailand. PhD dissertation. Colorado State University, Fort Collins, CO
Wilk J, Andersson L, Plermkamon V (2000) Hydrological impacts of forest conversion to agriculture in a large river basin in northeast Thailand. Hydrol Process 15(14): 2729–2748
Wongvitavas P (1989) Rainfall in Thailand. Technical document 551.582-04-1989. Meteorological Department, Bangkok

Evaluation of Evapotranspiration in Forested Areas in the Mekong Basin Using GIS Data Analysis

Shinji Sawano*, Norifumi Hotta, Hikaru Komatsu, Masakazu Suzuki, and Tomoko Yayama

We assessed evapotranspiration in the Mekong River basin with a focus on the distribution of forested areas using geographic information system (GIS) datasets. We developed a new model to estimate evapotranspiration, a major component of the forest water budget. The model calculates transpiration (including forest floor evaporation) and interception loss separately. Transpiration was calculated based on the Priestley–Taylor equation. Interception loss assumed a constant interception ratio. After clarifying distributions of climatic conditions and forested area in the basin, we calculated the evapotranspiration rate distribution. We then identified significant factors to consider in accurate estimation of evapotranspiration by comparing evapotranspiration rates based on the model and those based on the original form of the Priestley–Taylor equation. Consequently, we concluded that the contribution of evergreen and deciduous broadleaf forests in the southern part of the basin is one of the dominant components of evapotranspiration from the whole basin, because those forests are distributed in an area with high evaporative potential and the forests cover a large area. Furthermore, it is essential to evaluate the transpiration control of evergreen broadleaf forests in the lower part of the basin because of decreases in soil moisture during the dry season.

1. Introduction

The Mekong River, with a basin of about 800 000 km^2 and a length of 4500 km, flows through six countries. Proper water resource management in the Mekong River basin is essential given the increased demand for irrigation water in recent years (Kamoto 2004). Water resource distributions need to be evaluated in the context of topographic, climatic, and vegetation conditions, which vary widely in the Mekong River basin (Kazama et al. 2001; Kite 2001). The evaluation of water resources in forested areas is particularly essential because such areas are being altered at a rapid pace by various land-use practices (Mekong River Commission 2003), and numerous forest types exist in the Mekong River basin. In this study, we used geographic information

* Graduate School of Agricultural and Life Sciences, The University of Tokyo, Tokyo, Japan
E-mail: ssawano@fr.a.u-tokyo.ac.jp

system (GIS) datasets to evaluate evapotranspiration in the Mekong River basin, a major component of the water budget, focusing on the distribution of forested areas.

2. Materials and Methods

2.1. Dataset

Elevation and gradient data were used to clarify the topographic characteristics of the basin. The 30-arcsec digital elevation dataset GTOPO30 provided by the US Geological Survey (USGS) was processed to yield gradient data. The MOD12Q1 dataset classified from the MODIS data using the University of Maryland method (Hansen et al. 2000) provided land cover data, including forest-type distributions. A model was developed that required monthly meteorological data to estimate evapotranspiration. Therefore, we processed International Satellite Land Surface Climatology Project (ISLSCP) Initiative 1 data (Meeson et al. 1995), which contained 6-hourly data with a spatial resolution of 1.0° × 1.0° for 1987 and 1988, to obtain monthly meteorological data. We subsequently interpolated the temperature data to 30-arcsec data using the temperature lapse rate (0.6°C 100 m^{-1}) and the difference in elevation between 1.0° ×1.0° and 30 arcsec. Latent heat flux data from ISLSCP and GEWEX Asian Monsoon Experiment (GAME) reanalysis data (Yatagai et al. 2000) with a spatial resolution of 2.5° × 2.5° from April to October 1998 were used for model comparison.

2.2. The Model

A model was developed to estimate evapotranspiration in forested areas, which is a major component of the forest water budget. The model calculated transpiration (including forest floor evaporation) and interception evaporation separately. Transpiration was calculated based on the Priestley–Taylor (PT) equation (Priestley and Taylor 1972), and interception loss was assumed to be a fixed proportion of the rainfall. Evapotranspiration from forested areas was estimated using the following equation:

$$\begin{aligned} E &= E_t + E_i \\ &= \alpha \frac{\Delta}{\Delta + \gamma} R_n + \beta P \end{aligned} \tag{1}$$

where α is the Priestley–Taylor constant, R_n is net radiation (MJ m^{-2}), Δ is the gradient of saturated vapor pressure with temperature, γ is the psychrometric constant, β is the interception ratio, and P is monthly precipitation. The PT equation required net radiation as input data; as only solar radiation data were available, we converted it to net radiation data. In forested areas, net radiation was set at 0.8 times the solar radiation (Komatsu et al. 2007).

Evapotranspiration from other vegetation types and water surfaces was estimated using the original form of the PT equation with $\alpha = 1.26$. The net radiation levels were set at 0.65 and 0.6 times the solar radiation levels for other vegetation types and water surfaces, respectively (Otsuki et al. 1989; Takase and Sato 1989).

2.3. Estimating Evapotranspiration

Water availability and plant phenology in the Mekong basin vary seasonally. We evaluated the effects of seasonal changes in the forested areas of the basin by considering three experimental conditions: no seasonal change (case 1), water availability changed seasonally (case 2), and water availability and plant phenology varied seasonally (case 3). In case 1, we gave α and β constant values of 0.8 and 0.15, respectively, based on previous studies (Kuraji and Tanaka 2002; Komatsu 2005).

In case 2, we evaluated the effect of a reduction in soil water on evapotranspiration by using a bucket model, which is usually used in a General Circulation Model (Manabe 1969). Precipitation in the Mekong basin is regulated by southwest and northeast monsoons (Matsumoto 1997). A marked dry season is caused by northeast monsoons; we classified it to be from November to April. The rainy season, dominated by southeast monsoons, occurs between middle May and early October. Most of the precipitation in the Mekong basin is observed in this period. A reduction in soil water during the dry season would affect evapotranspiration. The effect on transpiration of a reduction in soil water can be expressed as follows:

$$\alpha' = \alpha\left(\frac{W}{W_{\mathrm{MAX}}}\right) \tag{2}$$

where W is the current water content in a tank and W_{MAX} is the maximum water content of the tank. The W_{MAX} of forested areas was set at 150 mm, the original value used in the Bucket Model (Manabe 1969). The W_{MAX} of the surface soil layer ($\leqq$0.25 m) was investigated by Kondo (1993): that of clay was estimated as 89.7 mm and that of loam was estimated as 107.0 mm. We set the W_{MAX} of other areas at 100 mm, the average of the W_{MAX} for clay and loam estimated by Kondo (1993).

Plant phenology is affected by thermal conditions and water availability. In case 3, we express the effect of thermal conditions on plant phenology using α, which is parameterized in Japan (Sawano 2003) as follows:

$$\alpha = 0.0129 \times T + 0.296 \tag{3}$$

where T is monthly temperature. Deciduous forests in the Mekong usually defoliate in the dry season. We set β at 0.15 during periods of canopy cover (May–October) and at 0 for periods of defoliation (November–April).

3. Results and Discussion

3.1. The Basin Characteristics Expressed by the Dataset

The upper Mekong basin is located on the Tibetan Plateau and is 6000 m or more above sea level (asl). The elevation of the basin decreases with distance downstream. The Mekong delta, i.e., the mouth of the Mekong River, lies at 0 m asl (Fig. 1a). Figure 1b shows the distribution of annual mean temperatures based on ISLSCP temperature data. Annual mean temperature in the Mekong River basin increases with distance

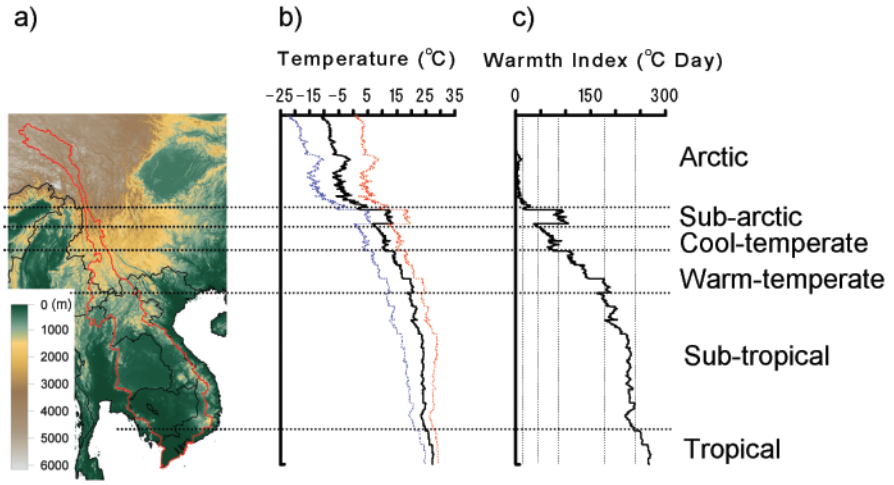

FIG. 1a–c. Characteristics of the Mekong River basin. **a** Elevation map; **b** annual mean temperature, maximum monthly temperature, and minimum monthly temperature calculated for each latitude; **c** warmth index calculated for each latitude

downstream and ranges from −15°C on the Tibetan Plateau to 25°C at the mouth. The difference between the maximum and minimum monthly temperatures, i.e., the index of the degree of change in temperature, is about 20°C in the upper part of the basin and decreases with proximity to the river mouth, where the difference is about 5°C. Figure 1c shows the climatic division in the Mekong basin using the Warmth Index (Kira 1971); according to this division, the Mekong basin encompasses a wide range of climatic zones, from subarctic to tropical.

3.2. *Forest-Type Distributions*

Figure 2 shows the land-use distribution in the Mekong basin, as obtained from the MOD12Q1 data. We investigated the characteristics of forested area distribution, categorized into five types: evergreen or deciduous broadleaf, evergreen or deciduous needle leaf, and mixed forest. The evergreen and deciduous broadleaf forest types were dominant in the basin. Broadleaf and mixed forests were mainly distributed in the lower part of the basin, although both were present in all parts of the basin. In contrast, needle leaf forests were mainly distributed in the upper part of the basin. Figure 3 shows the distribution of evergreen broadleaf forests, classified by gradient and elevation. Evergreen broadleaf forests were widely distributed from 0 to 4600 m in elevation and from 0° to 32° in gradient. The climatic zone in the Mekong changed with elevation. Evergreen broadleaf forests categorized by MOD12Q1 may contain some forest types with different evapotranspiration characteristics because evapotranspiration characteristics are strongly affected by climatic and topographic conditions.

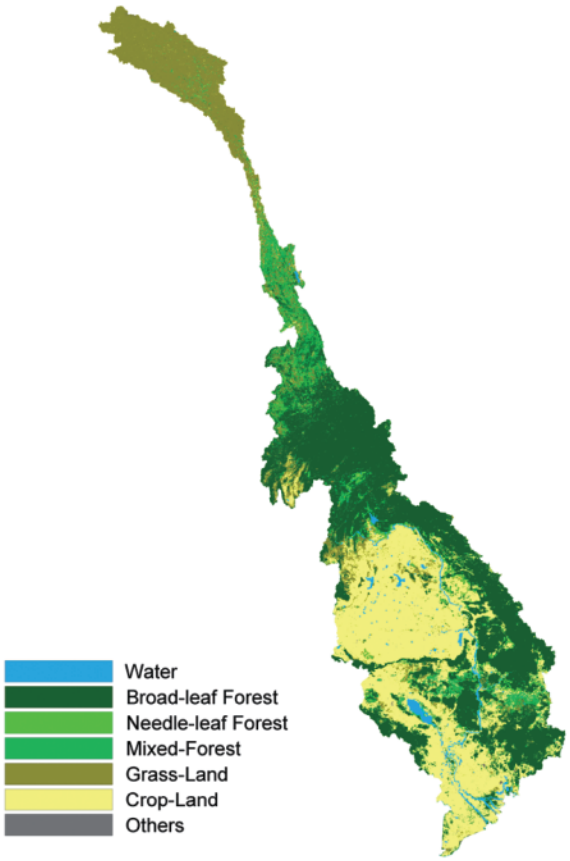

FIG. 2. Land-use distribution map of the Mekong River basin, categorized for seven land-use types

3.3. Distribution of Evapotranspiration

The distribution of the estimated evapotranspiration in cases 1, 2, and 3 can be seen in Fig. 4a, b, and c, respectively. In case 1, evapotranspiration was overestimated, with distributions ranging from 400 mm year^{-1} in the upper basin to 1800 mm year^{-1} in the lower basin. The high evapotranspiration rates of around 1800 mm year^{-1} were distributed in northeast Thailand, Cambodia, and in the Mekong delta, which is located in Vietnam. The evapotranspiration estimated in case 1 was nearly equal to the potential evapotranspiration predicted using the Budyko method (Kondo 1994).

In cases 2 and 3, the estimated evapotranspiration ranged from 180 mm year^{-1} in the upper basin to 1400 mm year^{-1} in the lower basin, except at the water surface. Evapotranspiration rates ranging from 700 to 1000 mm year^{-1} were widely distributed, and rates over 1000 mm year^{-1} were distributed in the southern part of the basin. The higher rates of evapotranspiration, excluding the water surfaces, were distributed in the western part of Cambodia. These estimates for cases 2 and 3 were about 400–

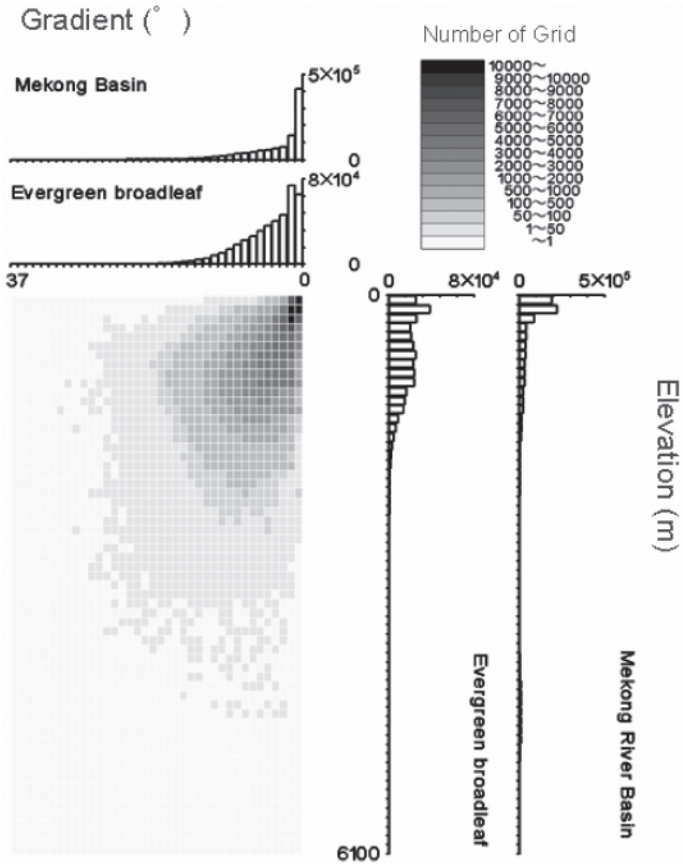

FIG. 3. Distribution of number of grids in evergreen broadleaf forest counted for every gradient and elevation

500 mm year^{-1} lower than those for case 1. The effect of reduced soil water content on evapotranspiration was particularly apparent in the lower parts of the basin, an area of high evaporative potential. Differences in the estimates for cases 2 and 3 appeared north of the subtropical zone, where the differences between minimum and maximum monthly temperature increased. The differences ranged from 70 mm year^{-1} in the lower basin to 200 mm year^{-1} north on the national border between Laos and China. The effect of decreases in temperature on transpiration activity in the dry season appeared stronger than that of decreases of soil water content.

3.4. Model Comparison

Figure 5 shows a comparison between the estimated evapotranspiration in case 3 and the latent heat flux in ISLSCP and GAME reanalysis data to compare model performance. We compared the values at middle and lower parts of the basin, where climatic zones and water availability differed significantly. In the middle of the basin, the

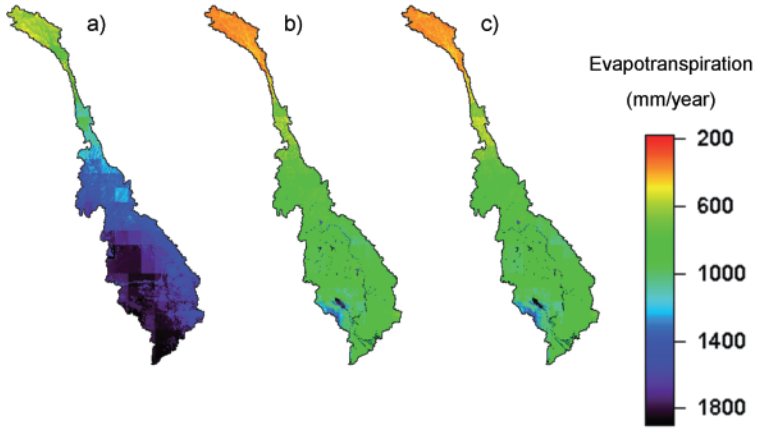

FIG. 4. Distributions of estimated evapotranspiration in the Mekong River basin: **a** case 1; **b** case 2; **c** case 3

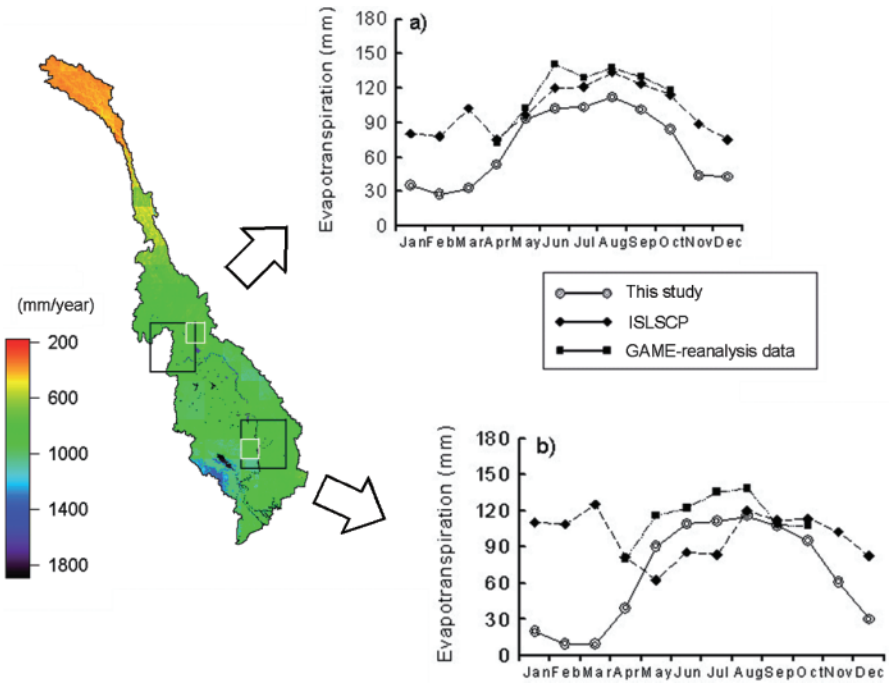

FIG. 5. Comparison of evapotranspiration from this study, International Satellite Land Surface Climatology Project (ISLSCP), and GEWEX Asian Monsoon Experiment (GAME) reanalysis data: midbasin (**a**) and lower basin (**b**). The *white and black boxes* indicate the spatial resolution of ISLSCP and GAME reanalysis data, respectively. We extracted an evergreen forest pixel (30-arcsec) from the same area as both the ISLSCP and GAME reanalysis data for comparison in the case 3 simulation

values estimated by our model, as with the ISLSCP and GAME reanalysis data, had a summer season peak. On the whole, our model estimates were lower than the ISLSCP and GAME reanalysis data, and the difference was remarkable in the dry season. In the lower part of the basin, both our model estimates and the GAME reanalysis data showed a summer season peak, but the ISLSCP data differed from our model in seasonal trend. In the rainy season, our model estimates plotted between the ISLSCP and GAME reanalysis data. In the dry season, the relationship between our model and the ISLSCP data was the same as in the middle part of the basin. Evapotranspiration in forested areas in northern Thailand, out of the Mekong River basin, peaked in the late dry season (Tanaka et al. 2003). Our model requires further development to better understand the effect of water availability on evapotranspiration in evergreen forest types in the dry season. Previous studies (Nemani et al. 1993; Nishida et al. 2003) have indicated that remote sensing methods are effective in quantifying seasonal change in evergreen forest evaporation resistance on a large scale.

4. Conclusions

We evaluated evapotranspiration in the Mekong River basin, focusing on forested areas using GIS datasets. After clarifying distributions of climatic conditions and forested areas in the basin, we calculated the distributions of evapotranspiration rates in the basin using a new model based on the Priestley–Taylor equation. We identified the dominant factors to be considered for the accurate estimation of evapotranspiration by comparing evapotranspiration rates estimated by the model with variations in calculation conditions. Consequently, we came to the following conclusions. The contribution of evergreen and deciduous broadleaf forests in the southern part of the basin is a dominant component of evapotranspiration from the whole basin, because those forests are distributed in the area with the highest evaporative potential and they cover a large area. Furthermore, it is essential to evaluate the effect of soil moisture reduction on transpiration in evergreen broadleaf forests in the dry season.

Acknowledgments. This study was supported by "Assessment of the Impact of Global-Scale Change in Water Cycles on Food Production and Alternative Policy Scenario" of the AFFRCS (Agriculture, Forestry and Fisheries Research Council Secretariat). We thank Dr. Akira Shimizu of the FFPRI (Forestry and Forest Products Research Institute) for providing the opportunity to conduct this study and Dr. Tomonori Kume and Ms. Natsuko Yoshifuji, both of the University of Tokyo, for valuable discussions.

References

Hansen MC, Defries RS, Townsend JRG, Sohlberg R (2000) Global land cover classification at 1 km spatial resolution using a classification tree approach. Int J Remote Sens 21: 1331–1364

Kamoto M (2004) Challenges of the Mekong River Commission (in Japanese with English abstract). J Jpn Soc Hydrol Water Resour 17:181–199

Kazama S, Sawamoto M, Nawarathana NB (2001) Basic study on the evaluation of water resources in the Mekong River Basin (in Japanese with English abstract). Ann J Hydraulic Eng JSCE 45:19–24
Kira T (1971) Seitaigaku kara mita shizen (in Japanese). Kawadeshobo, Tokyo
Kite G (2001) Modeling the Mekong: hydrological simulation for environmental impact studies. J Hydrol 253:1–13
Komatsu H (2005) Forest categorization according to dry-canopy evaporation rates in the growing season: comparison of the Priestley–Taylor coefficient values from various observation sites. Hydrol Process 19:3873–3896
Komatsu H, Hashimoto S, Kume T, Yoshifuji N, Hotta N, Suzuki M (2007) Seasonal trends in the solar radiation/net radiation ratio above a *Cryptomeria japonica* plantation forest. Bulletin of Tokyo University forest, accepted
Kondo J (1993) A new bucket model for predicting water content in the surface soil layer (in Japanese with English abstract). J Jpn Soc Hydrol Water Resour 6:344–349
Kondo J (1994) Sekai no suimonkikou. In: Kondo J (ed) Mizukankyo no kishogaku. Asakurashoten, Tokyo, pp 308–322
Kuraji K, Tanaka N (2003) Rainfall interception studies in the tropical rainforest J Jpn For Soc 185:18–28 (in Japanese with English abstract)
Manabe S (1969) Climate and the ocean. 1: The atmospheric circulation and the hydrology of the Earth's surface. Mon Weather Rev 97:739–774
Matsumoto J (1997) Seasonal transition of summer rainy season over Indochina and adjacent monsoon region. Adv Atmos Sci 14:231–245
Meeson BW, Corprew FE, McManus JMP, Myers DM, Closs JW, Sun KJ, Sunday DJ, Sellers PJ (1995) ISLSCP Initiative 1.Global data sets for land-atmosphere models, 1987–1988. Published on CD-ROM by NASA (USA_NASA_GDAAAC_ISLSCP_001.-USA_NASA_GDAAC_ISLSCP_005
Mekong River Commission (2003) State of the basin report. Mekong River Commission, Phnom Penh. pp 185–204
Nemani RR, Pierce L, Running SW, Goeard S (1993) Developing satellite-derived estimates of surface moisture status. J Appl Meteorol 32:548–557
Nishida K, Nemani RR, Glassy JM, Running SW (2003) Development of an evapotranspiration index from Aqua/MODIS for monitoring surface moisture status. IEEE Trans Geosci Remote Sensing 41:493–501
Otsuki K, Miura T, Takase K (1989) Evapotranspiration, vol 7. Evapotranspiration in large-scale area (in Japanese). J JSIDRE 57:133–139
Priestley CHB, Taylor RJ (1972) On the assessment of surface heat flux and evaporation using large-scale parameters. Mon Weather Rev 100:81–92
Sawano S (2003) Simple model for evaluating the evapotranspiration of a forested area in Japan (in Japanese). MS thesis. University of Tokyo, Tokyo, Japan
Takase K, Sato K (1989) Evapotranspiration, vol 6. Evapotranspiration in crop land (in Japanese). J JSIDRE 57:75–80
Tanaka K, Takizawa H, Tanaka N, Kosaka I, Yoshifuji N, Tantasirin C, Piman S, Suzuki M, Tangtham N (2003) Transpiration peak over a hill evergreen forest in northern Thailand in the late dry season: assessing the seasonal changes in evapotranspiration using a multilayer model. J Geophys Res 108:4533
Yatagai A, Yamazaki N, Horikama H, Takahashi K, Ueda H, Aonashi K, Sumi K, Takeuchi Y, Tada H (2000) About GAME reanalysis data (in Japanese). J Jpn Soc Hydrol Water Resour 13:486–495

Severe Drought Resulting from Seasonal and Interannual Variability in Rainfall and Its Impact on Transpiration in a Hill Evergreen Forest in Northern Thailand

Tomonori Kume*, Hideki Takizawa, Natsuko Yoshifuji, Nobuaki Tanaka, Katsunori Tanaka, Chatchai Tantasirin, and Masakazu Suzuki

Our previous study revealed that a hill evergreen forest in the Kog-Ma experimental watershed in northern Thailand, which is influenced by Asian monsoon cycles, transpired actively even in the late dry season. In this study, the impact of severe drought on the transpiration of this forest was investigated using data measured at the site over 8 years that showed seasonal and interannual variation in rainfall. To this aim, the impacts of soil drought on sap flow and water potential were examined during severe drought conditions. This site showed large interannual variation in the total amount of annual rainfall and in the length of the dry period. An unusually severe drought occurred in the late dry seasons of 1998 and 2004 as a result of the small amount of annual rainfall and a prolonged dry period coinciding with El Niño. Under the detected severe drought conditions in the late dry season of 2004, noticeable symptoms of water stress were apparent only in the smallest study tree. Decreases in sap flow velocity and water potential caused by soil drought were not apparent in larger trees. Deeper root systems of larger trees may explain the lower impact of severe drought on transpiration in larger trees. Transpiration in this forest could be maintained actively even under unusually severe drought conditions.

1. Introduction

Deforestation in peninsular Indochina influences the regional water balance through changes in evapotranspiration (Kanae et al. 2001). Thus, to assess the effects of deforestation on the regional environment, it is first necessary to understand the processes of evapotranspiration from forests in the region. However, few studies have reported the seasonal and interannual variation in evapotranspiration and the determining factors of evapotranspiration in the Indochina region (e.g., Pinker et al. 1980; Giambelluca et al. 1996; Tanaka et al. 2003).

* Kasuya Research Forest, Kyushu University, Fukuoka, Japan
E-mail: kumett@forest.kyushu-u.ac.jp

Hill evergreen forest is the dominant vegetation type in northern Thailand and is influenced by the Asian monsoon (Sri-Ngernyuang et al. 2003). Our previous study revealed that the hill evergreen forest in the Kog-Ma experimental watershed in northern Thailand transpired actively even in the late dry season based on a numerical model; the model was validated with latent heat fluxes measured by the eddy covariance method (Tanaka et al. 2003). This finding implies that the seasonal trend in evapotranspiration in the hill evergreen forest type is mainly controlled by the atmospheric evaporative demand and that soil drought in the late dry season has little influence on seasonal trends in evapotranspiration. However, the impact of severe drought resulting from interannual rainfall variability on transpiration has not been investigated.

This study was undertaken to examine the impact of severe drought on transpiration in a hill evergreen forest in northern Thailand. Interannual variation in rainfall at the Kog-Ma experimental watershed was determined using continuous micrometeorological measurements, which commenced in 1997. Under the detected severe drought conditions, we assessed the impact of soil drought on sap flow and water potential in two large trees and two smaller trees. We confirmed the impact of soil drought on sap flow and water potential using a water supply treatment on an individual tree in which symptoms of water stress were apparent.

2. Site and Measurements

2.1. Site

This study was conducted in a subwatershed of the Kog-Ma experimental watershed, situated 1265–1420 m above mean sea level on Mount Pui (18°48′ N, 98°54′ E) near Chiang Mai, northern Thailand. The seasonal changes in both air temperature and rainfall show that this area has three seasons: a rainy season, an early (cool) dry season, and a late (hot) dry season. The study watershed is covered with hill evergreen forest at a continuous canopy height of approximately 25–40 m. The dominant plant family is the Fagaceae, including *Lithocarpus*, *Quercus*, and *Castanopsis*. The leaf area index is approximately 4.5 $m^2 m^{-2}$ with small seasonal fluctuations.

2.2. Micrometeorological Measurements

A 50-m-tall meteorological tower and instruments for measuring meteorological factors over the canopy have been in place at the study area since February 1997. Air temperature and relative humidity were measured at 43.4 m using a thermohygrograph (HMP45A; Vaisala, Helsinki, Finland). Downward and upward shortwave radiation (MS402; Eko Instruments, Tokyo, Japan) and downward and upward longwave radiation (MS201F; Eko Instruments) were measured at 50.5 m. Volumetric soil water content (θ) was measured at depths of 0.1–0.5 m below the forest floor near the tower using a time domain reflectometry sensor (CS-615; Campbell Scientific, Logan, UT, USA). Data were collected every 5 s, with 10-min means recorded in a data logger (CR23X; Campbell Scientific). Rainfall was measured using a tipping-bucket rain gauge (20-cm diameter and 0.5-mm tip resolution; Ohta Keiki, Tokyo, Japan) in an open space.

Table 1. Characteristics of sample trees selected for measurement of water potentials and sap flows in September 2003

	Family	Species	Height (m)	Stem diameter at breast height (cm)	Crown projected area (m^2)
CL	Lauraceae	*Cinnamomum porrectum* (large)	29.8	51.9	78.1
LL	Fagaceae	*Lithocarpus elegans*	25.4	28.5	95.9
LS	Fagaceae	*Lithocarpus elegans*	4.8	4.0	6.7
CS	Lauraceae	*Cinnamomum porrectum* (small)	1.4	1.3[a]	0.4

[a] Stem diameter at base

2.3. Water Potential and Sap Flow Measurements

To investigate the impact of severe drought on tree transpiration, we selected two large and two small evergreen trees that were adjacent to the tower and represented the two dominant species at this site (Table 1). Diurnal variation in the leaf water potential (Ψ_{leaf}) was measured with a pressure chamber (PMS Instruments, Corvallis, OR, USA). One to three sun-exposed leaves in the upper crown of each tree were sampled every 3 h in the period from predawn to sunset. The measurements of stem water potential (Ψ_{stem}) were substituted with the measurements of Ψ_{leaf} on the branches from the lowest crown of each tree, which were artificially prevented from transpiring by covering the branches under aluminum foil and plastic bags, according to the methods of Landsberg et al. (1976). Measurements were conducted on 4–5 November 2002 (early dry season), 2–3 March 2003 (late dry season), 2–3 September 2003 (rainy season), 16–17 November 2003 (early dry season), and 7–8 March 2004 (late dry season).

At the same time, sap flow velocity was measured using a thermal heat pulse method or a stem heat balance method, depending on the stem diameter. A thermal heat pulse sensor (HP-1; Hayashi Denko, Tokyo, Japan) was inserted into the large *Cinnamomum porrectum* (CL), the large *Lithocarpus elegans* (LL), and the smaller *L. elegans* (LS), which had thick stems. Measurements were conducted continuously with a data logger (CR10X; Campbell Scientific). A gauge for the stem heat balance method (SGA 10; Dynamax, Houston, TX, USA) was attached to the smaller *C. porrectum* (CS), which had the thinnest stem, and the measurements were recorded with a data logger (CR10X) for several days before and after the water potential measurements in September 2003, November 2003, and March 2004.

3. Results

3.1. Seasonal and Interannual Variability in Micrometeorological Elements

3.1.1. Total Amount of Annual Rainfall

Figure 1 shows the interannual variation in rainfall at the Kog-Ma experimental watershed and rainfall records monitored by the Thai Meteorological Department

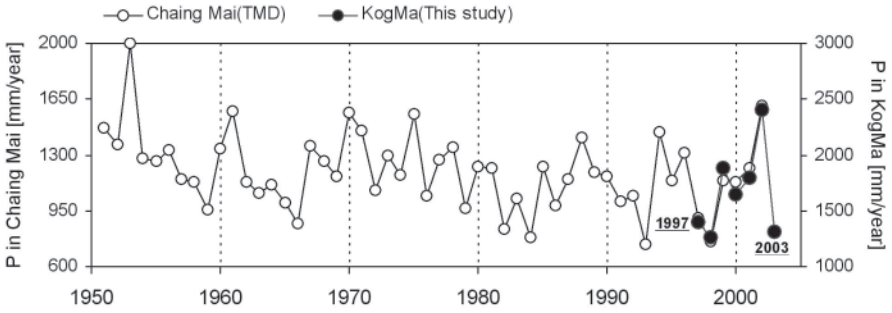

FIG. 1. Interannual variations in rainfall (*P*) at the Kog-Ma watershed and long-term rainfall records in Chaing Mai city. *Black circles* represent annual rainfall measured at Kog-Ma watershed in this study; *open circles* represent rainfall records monitored at the nearest meteorological observatory, Thailand Meteorological Department (TMD) in Chaing Mai. Note: Rainfall in Kog-Ma is represented using the *right vertical axis*

(TMD) at the nearest meteorological observatory situated 312 m above mean sea level in Chiang Mai (18°47′ N, 98°59′ E). The patterns of interannual variation in rainfall at the study site corresponded to the rainfall pattern recorded by the TMD, although the amount of annual rainfall recorded at the observatory was lower than at Kog-Ma, because rainfall is dependent on altitude. These data suggest that the annual rainfall at the site in 2002 was greater than in the previous 20 years and that the annual rainfall at the site in 2003 was as low as that measured in 1997 and 1998, when an unusually severe drought occurred in Southeast Asia coinciding with the El Niño event of 1997–1998 (Walsh and Newbery 1999; Wang and Weisberg 2000).

3.1.2. General Micrometeorological Elements

Rainfall and soil water content were generally higher from May to October (the rainy season) and lower from November to April (the dry season). Correspondingly, solar radiation and the vapor pressure deficit (VPD) were generally less from May to October (rainy season) and greater from November to April (dry season). The dry periods, defined according to Whitmore (1994) as periods with a sliding 30-day total rainfall of less than 100 mm, appeared consistently in each year, and the dry periods never extended more than 1 month in the period from June to September (see Fig. 3a). Moreover, Fig. 3a shows large year-to-year differences in the length of the dry period, which spanned approximately 3–7 months each year. The amounts of preceding rainfall for 90 days in the late dry seasons of 1998 and 2004 were significantly lower than those in the other years because of the small annual rainfall amount and the prolonged dry period in 1997–1998 and 2003–2004. These results suggest that an unusually severe drought occurred in the late dry season of 1998 and 2004 at this site, although soil water measurements at depths of 0.1–0.5 m were not distinctively different in the late dry seasons of 1998, 2004, and other years (Fig. 2). A physical

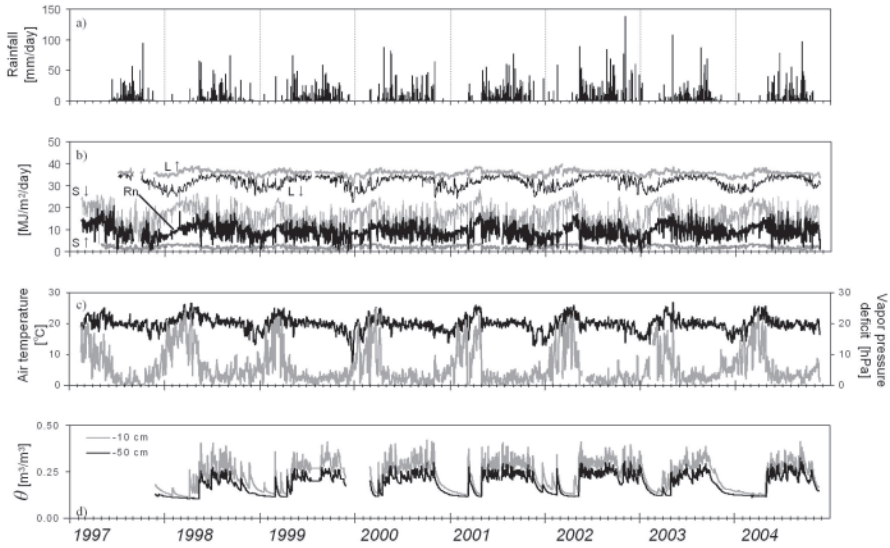

FIG. 2. Time-series daily micrometeorological elements of daily rainfall (**a**), downward and upward short-wave radiation ($S\swarrow$, $S\nearrow$, respectively), downward and upward long-wave radiation ($L\swarrow$, $L\nearrow$, respectively), and net radiation (Rn) (**b**), air temperature (*black line*) and vapor pressure deficit (*gray line*) (**c**), and volumetric soil water content (θ) in Kog-Ma experimental watershed, northern Thailand (**d**)

interpretation of the rainfall during the preceding 90 days is discussed in a later section.

3.2. Impacts of Severe Drought on Sap Flow Velocity and Water Potential

In this study, changes in sap flow velocity and water potential following seasonal transitions were examined in two periods: November 2002 to March 2003 (wet year) and September 2003 to March 2004 (drought year; see Fig. 3b). In both periods, diurnal peaks of the sap flow velocities in CL, LL, and LS during the late dry season were larger or very similar to the peaks from the rainy and early dry seasons (Fig. 4b,c). The sap flow velocity peaks in CS during the late dry season were very similar to those from the early dry season, whereas the leaf fall in CS occurred in the early dry season in 2003, and the difference in these peaks in CS between rainy and early dry seasons was probably caused by leaf fall (Fig. 4c). Thus, it was difficult to detect an apparent decrease in sap flow velocities caused by severe drought even in the drought year. Further, symptoms of water stress were not apparent in the minimum Ψ_{leaf} at midday in the four trees in the late dry season for both the wet and drought years, although the minimum Ψ_{leaf} at midday in the four trees decreased following the seasonal transition from the rainy and early dry season to the late dry season. On the other hand, predawn Ψ_{stem} in CS significantly decreased to −1.1 MPa in the late

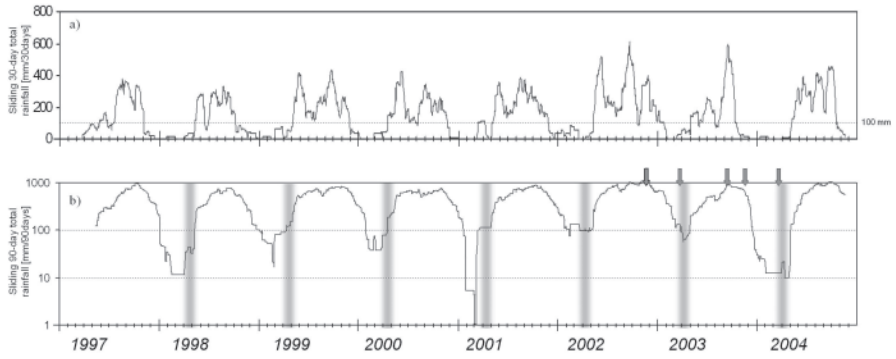

FIG. 3. Rainfall during the preceding 30 and 90 days: (**a**) sliding 30-day total rainfall and (**b**) sliding 90-day total rainfall in the period from 1997 to 2004. A period from March to April (the late dry season) is screened by a *gray belt*. *Vertical arrows* represent the timing of the water potential measurement

dry season of the drought year (Fig. 4e); this value was the lowest of any of the study specimens during the two measurement years. The predawn Ψ_{stem} corresponds to the soil water potential in contact with the roots (e.g., Bucci et al. 2004). These results suggest that soil drought was more severe in the late dry season of 2004 and that CS may have suffered from soil drought.

To confirm whether CS suffered from water stress as a result of soil drought, we began supplying water to CS on 9 March 2004 (Fig. 5). After seven water supply treatments, the predawn Ψ_{stem} increased from −1.1 MPa on 8 March to −0.14 MPa on 13 March, and the minimum Ψ_{stem} at midday increased from −1.3 MPa on 8 March to −0.4 MPa on 13 March (Fig. 5c). The diurnal peaks in sap flow velocity also increased gradually from 9 to 13 March (Fig. 5b). The recovery of sap flow velocity and water potential in CS after water supplementation confirmed that the reductions in sap flow velocity and predawn Ψ_{stem} were caused by stomatal closure due to soil drought (e.g., Davies and Zhang 1991; Meinzer et al. 1995).

Furthermore, the reduction in sap flow velocity in CS caused by soil drought ranged from 30% to 40% at a given atmospheric evaporative demand, when the reduction in sap flow velocity was defined according to Pataki et al. (2000) as follows:

$$\text{Reduction} = 1 - \frac{f_{\text{late}}(\text{VPD})}{f_{\text{early}}(\text{VPD})}$$

where $f_{\text{late}}(\text{VPD})$ is the predicted sap flow velocity at a given VPD using the relationship between sap flow velocity and VPD in the late dry season, and $f_{\text{early}}(\text{VPD})$ is the predicted sap flow velocity at a given VPD using the relationship between sap flow velocity and VPD in the early dry season. Soil drought caused reductions in sap flow velocity in CL and LL of approximately 10% and a reduction in LS of approximately 30%. Thus, the degree of reduction in sap flow velocity caused by soil drought differed by tree size. However, significant reductions in sap flow velocity were not observed in the trees in the late dry season of the wet year.

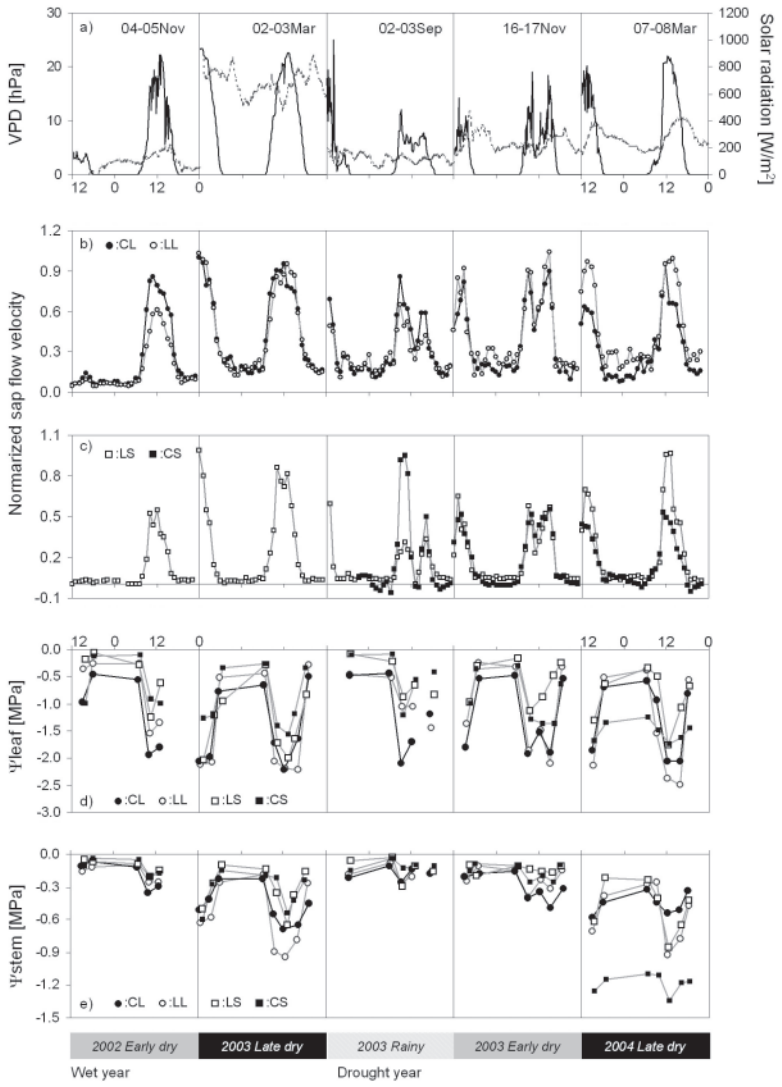

FIG. 4. Diurnal and seasonal variations in (**a**) solar radiation (*black line*) and vapor pressure deficit (*dotted lines*), (**b**) normalized sap flow velocity in large *Cinnamomum porrectum* (*CL*) (*black circles*) and *Lithocarpus elegans* (*LL*) (*open circles*), (**c**) normalized sap flow velocity in *Lithocarpus elegans* (*LS*) (*open squares*) and small *Cinnamomum porrectum* (*CS*) (*black squares*), (**d**) leaf water potentials (ψ_{leaf}), and (**e**) stem water potentials (ψ_{stem}) in four individuals. Sap flow velocities in the wet year were normalized by the maximum value in the period from November 2002 to March 2003 in each tree. Sap flow velocities in the drought year were normalized by the maximum values in the period from September 2003 to March 2004 in each tree

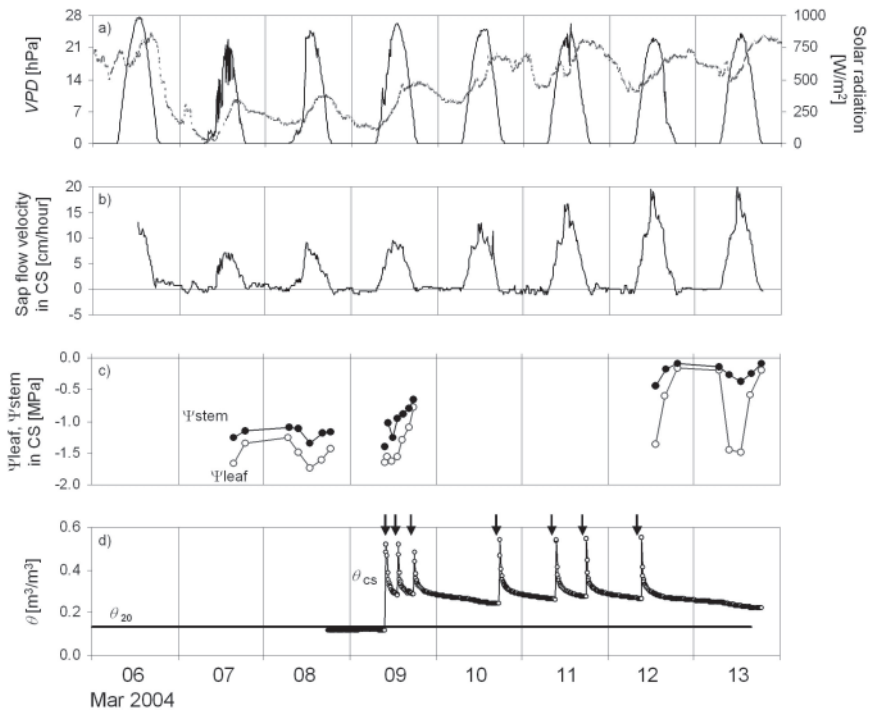

Fig. 5a–d. Recovery of sap flow and water potential in CS after water supply treatment. Diurnal variations in (**a**) solar radiation (*black line*) and vapor pressure deficit (*VPD*) (*dotted line*), (**b**) sap flow velocities in CS, (**c**) yleaf (*open circles*) and ystem (*black circles*) in CS, and (**d**) soil water contents measured at 20 cm below the ground near the tower (θ_{20}) and around CS at the depth of 20 cm (θ_{cs}), located about 20 m north of the tower. *Vertical arrows* represent the times at which water supply treatments were conducted

4. Discussion

The amount of rainfall preceding the late dry seasons of 1997 and 2004 was significantly smaller than the rainfall preceding the late dry season in the other year because of the low annual rainfall and the prolonged dry period (see Fig. 3). Under the drought conditions in the late dry season of 2004, the reductions in sap flow velocity and predawn Ψ_{stem} were only significant in CS among the trees in our study (see Figs. 4, 5). The recovery of sap flow velocity and water potential in CS after water supply treatments showed that the reductions in the late dry season in the drought year were caused by stomatal closure due to soil drought. On the other hand, larger trees continued to transpire even in the late dry season of the drought year (see Fig. 4).

In this study, the sliding 90-day rainfall total was used as the index representing the degree of soil drought (see Fig. 3). For a physical interpretation of the sliding total rainfall, Fig. 6 shows the sliding total rainfall with the number of days sliding from 30 to 120 in 30-day steps and predawn Ψ_{stem} (i.e., soil water potential) for each water

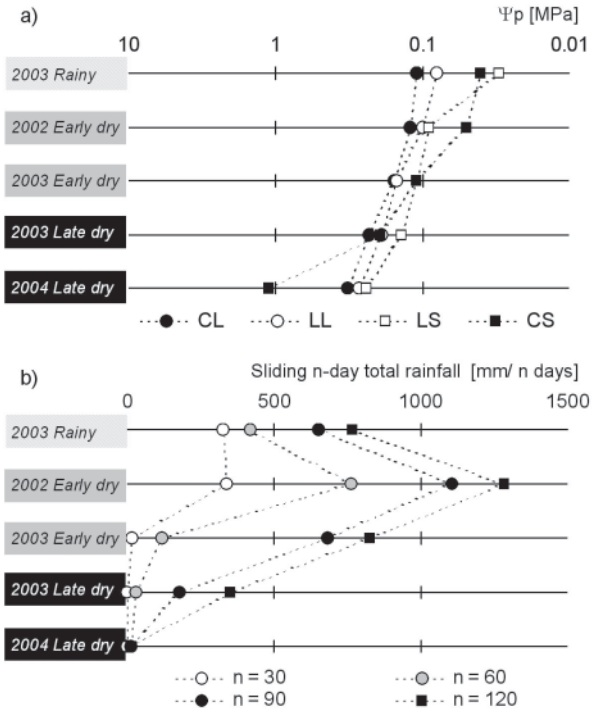

FIG. 6. Predawn ψ stem (ψp) (**a**) and sliding n-day total rainfall (**b**) at each water potential measurement term. The n-day moved from 30 to 120 days in 30-day steps. Values are shown in ascending order of the average ψ p in four individual trees at each measurement term

potential measurement term. When the sliding total rainfall encompassed only 30 or 60 days, the tendency for soil in the late dry season to be drier in 2003 than 2004 was not evident. However, this tendency was apparent when the sliding total rainfall encompassed more than 90 days. This finding suggests that the soil condition during the late dry season is related to the amount of rainfall during the preceding 90 or more days and that the soil layer at this site has a capacity to hold rainfall from the preceding 90 or more days.

Stream flow at this site has never been interrupted, even in the late dry season (Tanaka et al. 2003), suggesting that there may be moisture deeper within the subsurface (i.e. regolith) to maintain transpiration over the late dry season. A numerical analysis using a soil–plant–atmosphere–continuum model shows that a rooting depth of more than 4–5 m is needed to maintain transpiration in the late dry season under unsaturated soil conditions (Tanaka et al. 2004). The possibility of trees establishing such a deep root system at this site was supported by a penetration test, which showed that the soil became harder at a depth of 4–5 m (Tanaka et al. 2004). The sap flow observed at the top of the watershed ridge, where the groundwater table (i.e., saturated soil water) may rarely appear, also showed active transpiration in the late dry season (N. Yoshifuji, personal communication). These results suggest that there is an

unsaturated water reserve in the deep soil layer and that the roots in larger trees in this evergreen forest can reach this depth to maintain transpiration even in the late dry season of drought years.

A high demand for water by trees can in some cases lead to the development of a deep and extensive root system (Cermák et al. 1993). Canadell et al. (1996) showed that a tropical evergreen tree is likely to have a deep rooting depth, with the maximum ranging from 2.0 to 18.0 m (average, 7.3 ± 2.8 m). Such a deep root system seems to develop over decades or centuries. The roots of a small tree such as CS would likely not reach such depths. Usually, the shallower portions of soil are drier than the deeper portions during no-rain periods (e.g., Hodnett et al. 1995). The dry soil in the shallower soil layer could lead to more significant decreases in transpiration in smaller trees than in larger trees during the late dry season, particularly during unusually severe drought conditions such as those recorded at this site. The lowest predawn Ψ_{stem} in CS in the late dry season of the drought year (−1.1 MPa) supports evidence that severe dry soil appeared in the shallower soil layer (see Fig. 4). On the other hand, the developed deep root system in larger trees could explain the lower impact of severe drought on transpiration in larger trees, allowing canopy-scale transpiration at this site to be maintained actively even in the late dry season of an unusually severe drought. Transpiration from larger trees is thought to contribute most to the total transpiration because of the high leaf area index of the upper canopy and the intense solar radiation and VPD to which the upper canopy is exposed.

Acknowledgments. This study was supported by CREST (Core Research for Evolution Science and Technology) of JST (Japan Science and Technology Agency). We are grateful to Professor Taikan Oki of the University of Tokyo, and to Professor Nipon Tangtham of Kasetsart University, for providing the opportunity to conduct this study. Some measurements were supported by Dr. Izumi Kosaka of Japan conservation engineers and Dr. Shoji Hashimoto of the Forestry and Forest Products Research Institute. Fruitful discussions with Mr. Norifumi Hotta and Dr. Shinji Sawano, both from the University of Tokyo, and Dr. Hikaru Komatsu of Kyushu University, are also greatly appreciated.

References

Bucci SJ, Scholz F, Goldstein G, Meinzer FC, Hinojosa JA, Hoffmann WA, Franco AC (2004) Processes preventing nocturnal equilibration between leaf and soil water potential in tropical savanna woody species. Tree Physiol 24:1119–1127

Canadell J, Jackson RB, Ehleringer JR, Mooney HA, Sala OE, Schulze E-D (1996) Maximum rooting depth for vegetation types at the global scale. Oecologia (Berl) 108:583–595

Cermák J, Matyssek R, Kucera J (1993) Rapid response of large, drought-stressed beech trees to irrigation. Tree Physiol 12:281–290

Davies WJ, Zhang J (1991) Root signals and the regulation of growth and development of plants in drying soil. Annu Rev Physiol Plant Mol Biol 42:55–76

Giambelluca TW, Tran LT, Ziegler AD, Menard TP, Nullet MA (1996) Soil-vegetation-atmosphere processes: simulation and field measurement for deforested sites in northern Thailand. J Geophys Res 101:25867–25885

Hodnett MG, Pimentel da Silva L, da Rocha HR, Cruz Senna R (1995) Seasonal soil water storage changes beneath central Amazonian rainforest and pasture. J Hydrol 170: 233–254

Kanae S, Oki T, Mushiake K (2001) Impact of deforestation on regional precipitation over the Indochina Peninsula. J Hydrometeorol 2:51–70

Landsberg JJ, Blanchard TW, Warrit B (1976) Studies on the movement of water through Apple Trees. J Exp Bot 27:79–596

Meinzer FC, Goldstein G, Jackson P, Holbrook NM, Gutierrez MV, Cavelier J (1995) Environmental and physiological regulation of transpiration in tropical forest gap species: the influence of boundary layer and hydraulic properties. Oecologia (Berl) 101:514–522

Pataki DE, Oren R, Smith WK (2000) Sap flux of co-occurring species in a western subalpine forest during seasonal soil drought. Ecology 81:2557–2566

Pinker RT, Thompson OE, Eck TF (1980) The energy balance of a tropical evergreen forest. J Appl Meteorol 19:1341–1350

Sri-Ngernyuang K, Kanzaki M, Mizuno T, Noguchi H, Teejuntuk S, Sungpalee C, Hara M, Yamakura T, Sahunalu P, Dhanmanonda P, Bunyavejchewin S (2003) Habitat differentiation of Lauraceae species in a tropical lower montane forest in northern Thailand. Ecol Res 18:1–14

Tanaka K, Takizawa H, Tanaka N, Kosaka I, Yoshifuji N, Tantasirin C, Piman S, Suzuki M, Tangtham N (2003) Transpiration peak over a hill evergreen forest in northern Thailand in the late dry season: assessing the seasonal changes on evapotranspiration using a multilayer model. J Geophys Res 108:4533

Tanaka K, Takizawa H, Kume T, Xu J, Tantasirin C, Suzuki M (2004) Impact of rooting depth and soil hydraulic properties on the transpiration peak of an evergreen forest in northern Thailand in the late dry season. J Geophys Res 109:D23107

Walsh RPD, Newbery DM (1999) The ecoclimatology of Danum, Sabah, in the context of the world's rainforest regions, with particular reference to dry periods and their impact. Philos Trans R Soc Lond B 354:1869–1883

Wang C, Weisberg RH (2000) The 1997–98 El Niño evolution relative to previous El Niño events. J Climate 13:488–501

Whitmore TC (1994) An introduction to tropical rain forests. Oxford University Press, Oxford

Factors Affecting Interannual Variability in Transpiration in a Tropical Seasonal Forest in Northern Thailand: Growing Season Length and Soil Drought

Natsuko Yoshifuji*, Nobuaki Tanaka, Chatchai Tantasirin, and Masakazu Suzuki

Tropical seasonal forests play an important role in global and regional carbon cycling and climates. Annual transpiration and primary productivity in tropical seasonal forests should be affected by the growing season length and physiological controls during the growing season. We investigated the year-to-year variations in the transpiration period as a measure of the growing season length in a teak (*Tectona grandis* Linn. f.) plantation in northern Thailand using sap flux measurements obtained over a 4-year period and examined the effect of soil drought on transpiration during the mid-growing season. The beginning and end of the transpiration period differed appreciably between years, corresponding to differences in the timing of soil moisture changes. These differences resulted in approximately 60 days interannual variation in the length of the transpiration period during the observation period, indicating that soil moisture changes are a major cause of large interannual variation in the transpiration period. Transpiration control caused by soil drought was sometimes observed during the transpiration period. The results suggest that soil moisture has two potential impacts on annual transpiration at this site; through modification of the length of the transpiration period, and through physiological control during the transpiration period. This regime contrasts with temperate deciduous forests and hill evergreen forests, another typical forest type in Thailand.

1. Introduction

Tropical forests are an important latent energy source, having a strong influence on both global and regional climates (Lean and Warrilow 1989; Kanae et al. 2001). They also play a significant role in the global carbon budget (Melillo et al. 1993; Malhi and Grace 2000). In tropical regions in Southeast Asia, large areas are characterized by seasonal rainfall under the influence of the Asian monsoon (Matsumoto 1997) and their exposure to seasonal drought. There are several types

* Japan Science and Technology Agency/CREST, Kawaguchi, Saitama, Japan, Graduate School of Agricultural and Life Sciences, The University of Tokyo, Tokyo, Japan
E-mail: natsuko@fr.a.u-tokyo.ac.jp

of forests in this region (Rundel and Boonpragob 1995) including evergreen and drought deciduous, which drop their leaves in the dry season. In deciduous forests, transpiration and primary productivity are affected by the transition between growing and dormant seasons, as well as physiological controls and meteorological conditions during the growing season (e.g., Schmid et al. 2000; Wilson and Baldocchi 2000). The impact of changes in the growing season length on annual transpiration and primary productivity are likely to be critical, especially in tropical forests, because of their large energy fluxes throughout the years. However, assessment of this impact along with that of physiological controls and atmospheric conditions on the annual energy and carbon budget in tropical deciduous forests has received less attention than that in temperate and boreal deciduous forests (Black et al. 2000; Wilson and Baldocchi 2000; White and Nemani 2003; Barr et al. 2004).

This study examines the possible effect of changes in soil moisture on transpiration through modification of the transpiration period and physiological control during the growing season in a tropical seasonal forest in northern Thailand. This is a preliminary study aimed at quantifying the impact of inter-annual variations in growing season length and physiological control on annual transpiration. We determine the length of the transpiration period in a teak (*Tectona grandis* Linn. f.) plantation in northern Thailand by sap flux measurements obtained over a 4-year period and examine the response of the beginning and end of transpiration to soil moisture changes. We also investigate transpiration control resulting from soil drought during the growing season. The outcomes show two potential effects of soil moisture changes on interannual variation in the transpiration of tropical seasonal forests.

2. Site and Methods

2.1. Site Description

The study was conducted in an even-aged teak (*T. grandis*) stand planted in 1968 in the Mae Moh plantation, Lampang province, northern Thailand (18°25′ N, 99°43′ E, 380 m above sea level). The teak trees were planted on an almost flat area, and tree density around the study site was about 360 trees ha^{-1}. Mean annual temperature and precipitation at the study site for the period 2000–2004 were 25.8°C and 1284 mm, respectively. The climate in this area is influenced by Asian monsoons, which produce highly seasonal variations in precipitation. There is a clear dry season from November to April, which between 2000 and 2004 had a mean monthly rainfall less than 100 mm. The soil in the Mae Moh plantation is classified as Loamy Paleustults (Thai classification).

2.2. Meteorological and Soil Moisture Measurements

Incident solar radiation above the canopy (S_0) was measured with a silicon pyranometer (LI200X; Li-Cor, Lincoln, NE, USA) at a height of 22 m using a research tower situated in the study site. Incident solar radiation below the canopy (S_b) was likewise

measured with a pyranometer (MS401; EKO, Tokyo, Japan) situated on the forest floor at a height of about 0.5 m, approximately 30 m away from the tower. Both radiation data were measured every 5 s, and their 10-min averages were recorded with a data logger (CR10X; Campbell Scientific, Logan, UT, USA).

Air temperature and relative humidity above the canopy were measured at a height of 26 m with an aspirated psychrometer (HMP45D; Vaisala, Helsinki, Finland) installed on the tower and recorded every 10 min with a data logger (SQ1250; Grant Instruments, Cambridge, UK). The vapor pressure deficit (VPD) was calculated from the air temperature and relative humidity. Rainfall was measured with a self-made storage-type rain gauge in an open site about 500 m away from the tower. A tipping bucket (no. 34T; Ohta Keiki, Tokyo, Japan) with a data logger (Hobo Event; Onset Computer, Bourne, MA, USA) was also installed beside the rain gauge, and the time of tip was recorded to give the time distribution of rainfall.

Volumetric soil water content (θ; $m^3 m^{-3}$) at depths of 0.1, 0.2, 0.4, and 0.6 m near the tower was measured with a time domain reflectometer (TDR; CS-615, Campbell Scientific) and a data logger (CR10X; Campbell Scientific) at 60-min intervals. The relative extractable water in a 0–0.6 m soil layer (Θ) was computed as described in Kumagai et al. (2004); Θ ranges from 0 to 1, corresponding to the driest and wettest conditions of the soil during the observation period, respectively.

2.3. Transpiration Measurement Using the Heat Pulse Method

Heat pulse velocity (HPV; cm h^{-1}) was measured as an index of tree transpiration using heat pulse sensors (HP-1; Hayashi Denko, Tokyo, Japan) consisting of three vertically aligned probes: a heater probe and upstream and downstream thermistor probes. Heat pulse sensors were inserted into the outer xylem of tree stems at a height of about 1.5 m. A heat pulse tracer was released every 20 min. The time at which the temperature difference between the two thermistor probes returned to 0 following the heat pulse was recorded on a data logger (CR10X; Campbell Scientific). HPV was calculated as described in Closs (1958).

Five *T. grandis* trees near the tower were selected for the HPV measurements. The mean height and diameter at breast height of the sample trees were 18 m and 20 cm, respectively, belonging to the dominant classes around the study site. Three sensors were installed in two trees in May 2000 then reinstalled in different positions once or twice until February 2004. Sensors were installed in the remaining three trees in November 2001. HPV data from February 2001 to February 2005 were used in this study.

2.4. Determination of the Transpiration Period

For each day, the mean daytime HPV(V_d) was computed by averaging the measurements obtained between 0600 and 1800, while the maximum nighttime HPV(V_{n_max}) was defined as the maximum value obtained between 0000–0400 and 2000–2400 on the same day. The dates of commencement and dormancy of tree transpiration were determined for each sample tree as the dates when the V_d became higher and lower than the V_{n_max}, respectively. Thus, the transpiration period of

each observation year was defined as the period from the onset to end of tree transpiration, which was obtained by averaging the dates of both events for all sample trees.

In the long-term continuous measurements, HPV values tended to decrease gradually because of a decline in water transport ability around the implanted sensors, which might have been caused by deposition of resin in the xylem vessels around the sensors or by cavitation (Smith and Allen 1996). To remove the influence of this phenomenon in the present study, we calculated the relative V_d (V) of each sample tree as follows:

$$V = \frac{V_d - V_{d_\min}}{V_{d_\max} - V_{d_\min}} \tag{1}$$

where $V_{d_\min}$ is the minimum value of V_d throughout the entire observation period, and $V_{d_\max}$ is the maximum value of V_d in each observation period, i.e., periods I, II, III, and IV (described later).

2.5. Determination of Changes in Leaf Area Index (LAI)

According to Beer's law (Holst et al. 2004), transmittance of incident radiation through a canopy exponentially decreases with increasing LAI, indicating that radiative transmittance ($R_t = S_b/S_0$) can be a signal of temporal change in LAI. We calculated the daily R_t (R_{td}) by averaging the R_t when the zenith angle was more than 75°, so as to reduce the impacts of the zenith angle and direct radiation on R_t (Yoshifuji et al. 2006). The relative daily radiative transmittance (ϕ) was then calculated using R_{td} as follows:

$$\phi = \frac{R_{td_\mathrm{avg}} - R_{td_\min}}{R_{td_\max} - R_{td_\min}} \tag{2}$$

where R_{td_avg}, $R_{td_\min}$, and $R_{td_\max}$ are the 15-day-moving average of R_{td} and minimum and maximum values during the observation period, respectively. Because ϕ ranges from 0 to 1 and is inversely correlated with changes in LAI, we used $1 - \phi$ as an index of the changes in LAI.

3. Results and Discussion

3.1. Rainfall Patterns and Soil Moisture Variations

Daily rainfall, daily mean air temperature, daily mean VPD, and Θ for 4 years from February 2001 to February 2005 are shown in Fig. 1. Rainfall has clear seasonality, showing rainy and dry seasons. VPD and Θ also show clear seasonal variations, corresponding to the rainfall seasonality, in contrast with the relatively small seasonal variation in incident solar radiation and air temperature.

The rainy season commenced from the end of April and continued through to the beginning of May every year, and was accompanied by a decline in VPD and an increase in Θ, which was generally high during the rainy season but sometimes

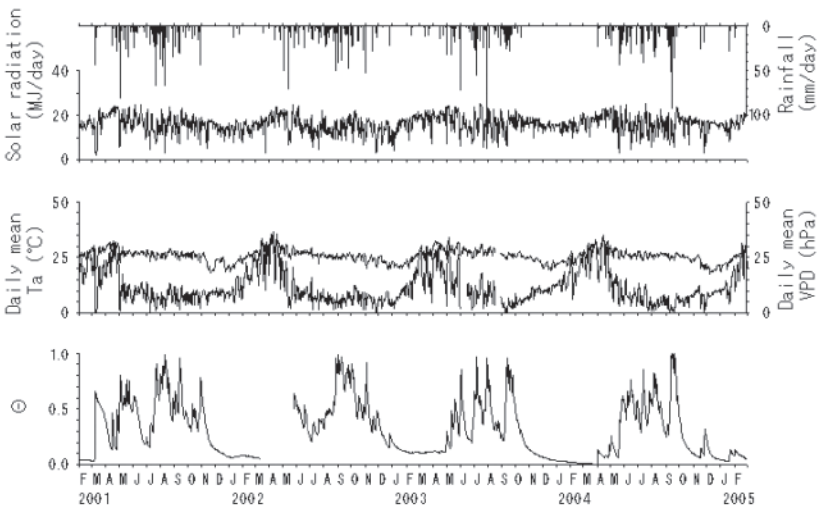

FIG. 1. Yearlong climate data for the Mae Moh teak plantation between February 2001 and February 2005. From the *top*, this figure shows the daily rainfall, the daily total solar radiation, daily mean air temperature (Ta, *thin line*) with daily mean vapor pressure deficit (VPD, *bold line*), and daily mean relative extractable water (Θ)

showed a significant decline. After the end of the rainy season, Θ declined to its minimum value in the late dry season. Despite the similar timing of commencement, the end of the rainy season differed appreciably from year to year. In 2001, rainfall events had ended by the end of October; however, in 2002, rainfall was noted even in November and December, and the decline in Θ was relatively slow. In 2003 and 2004, the finish of rainfall events occurred earlier than in 2001 and 2002, around the middle of October in 2003 and at the end of September in 2004, and the decline in Θ was also earlier than in 2001 and 2002. It is notable that heavy rainfall events with 117 mm rain in 6 days were observed in March 2001 before commencement of the rainy season, causing a marked increase in Θ; however, no such heavy rainfall events, with an accompanying large increase in Θ, were observed during the dry season in the other 3 years.

According to the commencement and end of the rainy seasons, four specific periods were defined: I, II, III, and IV (March 2001 to February 2002, March 2002 to February 2003, March 2003 to February 2004 and March 2004 to February 2005, respectively), for use in the following analysis.

3.2. Seasonal and Interannual Variations in Transpiration in Relation to Soil Moisture Changes

Figure 2 shows seasonal changes in tree transpiration described by V against the changes in $1 - \phi$, the index of changes in LAI, and Θ from March 2001 to February 2005. Increases in V and $1 - \phi$ showed that an increase in transpiration accompanied

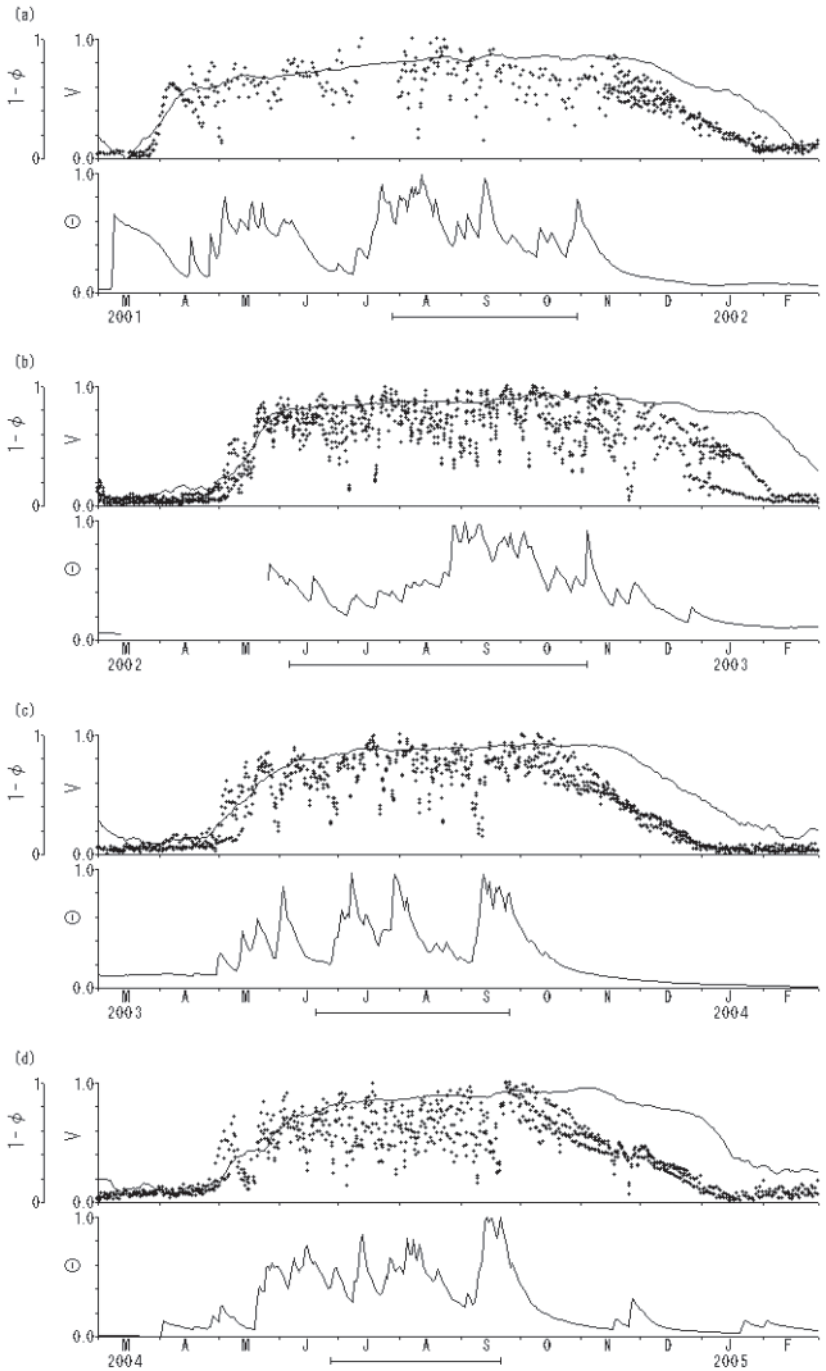

FIG. 2. Seasonal variations in the relative mean daytime heat pulse velocities (V) of each of the sample trees (*dot plot*) with $1 - \phi$ (line, ϕ: relative daily radiative transmittance) and daily mean relative extractable water (Θ) for (**a**) period I (March 2001 to February 2002), (**b**) period II (March 2002 to February 2003), (**c**) period III (March 2003 to February 2004), and (**d**) period IV (March 2004 to February 2005). Mid-growing seasons (*horizontal bars*) are also indicated

leaf unfolding every year; however, the timing was different between years. In periods II, III, and IV, transpiration increased with leaf unfolding in May (Fig. 2b–d), corresponding to the increase in Θ at the beginning of the rainy season (Fig. 2c,d). On the other hand, in period I, an increase in transpiration and leaf unfolding was observed in March, before commencement of the rainy season, following the large increase in Θ (Fig. 2a) caused by the exceptionally heavy rainfall events at the beginning of the month (see Fig. 1). This observation indicates that enhanced soil moisture advanced leaf unfolding, causing earlier commencement of transpiration. Induction of leaf flushing as a result of irrigation and an exceptional rainfall event during the dry season have also been reported for all leafless trees, except dormant stem succulents, in a tropical semideciduous forest in Costa Rica (Borchert and Rivera 2002), suggesting that increases in soil moisture can be a key factor in leaf flushing of tropical trees.

V declined earlier than $1 - \phi$ in line with the decrease in Θ in the dry season every year, revealing that transpiration started to decline early in the dry season in response to the soil moisture reduction, even though LAI remained high, and stopped in the dry season before the completion of leaf fall (Fig. 2). The timing of the decline and end of transpiration also differed appreciably between years, declining and ending earlier in periods III and IV than periods I and II in line with the earlier decline in Θ (Fig. 2). The decline in transpiration in advance of leaf fall implies that transpiration declined primarily as a result of a decline in stomatal conductance, which depends on meteorological factors such as soil moisture and photosynthetic capacity (Matsumoto et al. 2005). Yoshifuji et al. (2006) investigated the effects of meteorological factors on the decline in tree transpiration early in the dry season before the commencement of leaf fall in this site and found an effect of reductions in Θ. It is likely that soil moisture reductions reduce stomatal conductance, resulting in a decline in transpiration, which, after a time lag, is followed by the fall of senescent leaves. These findings indicate that the timing of the decline and end of transpiration are affected by differences in the timing of soil moisture reduction. Thus, differences in soil moisture changes are a major cause of the year-to-year variations in the beginning and end of transpiration in this site, though further inspection using much more long-term data or an experiment controlling soil moisture, for example, by irrigation, is required.

As a result of modification of the beginning and end of transpiration, year-to-year variations in the length of the transpiration period spanned about 60 days during the 4-year observation period (Fig. 3). The transpiration period was the longest in period I because of the advanced commencement of transpiration and was shorter in periods III and IV than periods I and II due to the earlier end of transpiration. This variation in the length of the transpiration period was much larger than the variation in growing season length previously reported in temperate deciduous forests, though the method employed was different from in this study: 3- and 5-day variations in the carbon uptake period were observed from 1997 to 1999 in beech stands in France and Denmark, respectively (Granier et al. 2002), and 6- to 10-day and 5- to 10-day differences in leaf emergence with carbon uptake and offset of photosynthesis were reported from 1991 to 1995 in the Harvard Forest in Massachusetts (Goulden et al. 1996). The large variation in the length of the transpiration period at this site implies

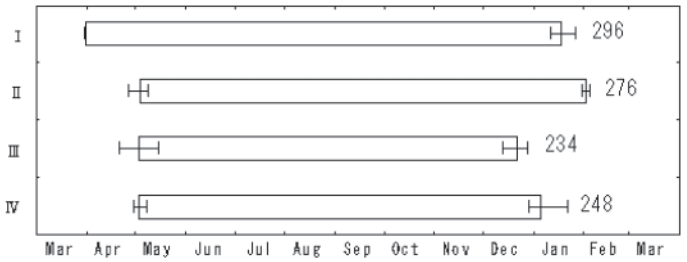

FIG. 3. Transpiration period (*thick open bar*) with individual differences over sample trees (*thin bars*) for period I (March 2001 to February 2002), period II (March 2002 to February 2003), period III (March 2003 to February 2004), and period IV (March 2004 to February 2005). *Numbers* represent the lengths of each transpiration period in days

a profound potential impact on energy and carbon exchange on an annual time scale (Yoshifuji et al. 2006).

3.3. The Effect of Soil Drought on Transpiration in the Rainy Season

The transpiration rate was the highest with significant variation after reaching the fully leafed canopy until Θ started to decline at the end of the rainy season, during which time Θ sometimes fell to around 0.2 (see Fig. 2). We determined the mid-growing season to be from the day when $1 - \phi$ reached 0.8, which was assumed as the commencement of the fully leafed canopy, to the initial day of the decline in Θ at the end of the rainy season, as shown in Fig. 2. Transpiration during the mid-growing season is likely to account for the largest portion of the annual transpiration. To examine the effect of soil drought on transpiration during the mid-growing season, we selected two continuous months including the day with the minimum Θ from the mid-growing season of each observation year, and determined the relationship between the V averaged over the sample trees and mean daytime (0600–1800) VPD over the range of Θ (Fig. 4). Here, V values measured when the daily mean S_0 was below $200\,\mathrm{Wm^{-2}}$ were discriminated because low incident radiation reduces the tree transpiration rate regardless of Θ and VPD. The mean V showed a similar positive correlation with VPD when $\Theta > 0.24$ (Fig. 4); however, it declined when $\Theta \leq 0.24$ at the same VPD value compared to when $\Theta > 0.24$, as observed in periods II and III (Fig. 4b,c). This indicates that transpiration was suppressed because of soil moisture reduction, probably through stomatal control. In the mid-growing season in periods I and IV, Θ did not fall to 0.24, and transpiration control from soil drought was not observed (Fig. 4a,d). It was also elucidated that a soil drought strong enough to cause transpiration suppression sometimes occurred during the transpiration period. This observation suggests that the extent of soil drought during the transpiration period has a potential impact on annual transpiration.

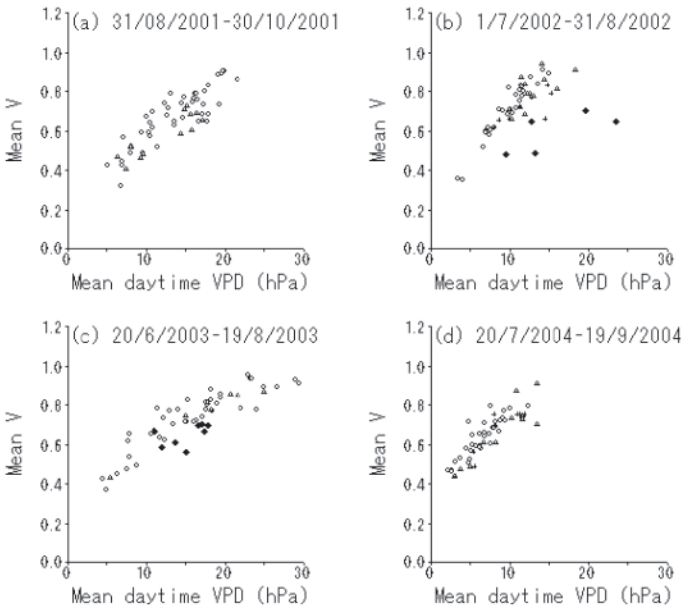

FIG. 4. The relative mean daytime heat pulse velocities averaged over sample trees (mean V) over the range of the mean daytime vapor pressure deficit (VPD) in two continuous months including the day with the minimum Θ selected from each mid-growing season: (**a**) from 31 August to 30 October 2001, (**b**) from 1 July to 31 August 2002, (**c**) from 20 June to 19 August 2003, and (**d**) from 20 July to 19 September 2004. Symbols represent the range of daily mean relative extractable water (Θ): *closed diamonds* for $\Theta \leq 0.24$, *crosses* for $0.24 < \Theta \leq 0.3$, *open triangles* for $0.3 < \Theta \leq 0.4$, and *open circles* for $0.4 < \Theta$. Data when daily mean solar radiation was below 200 Wm^{-2} were discriminated

4. Conclusion

Based on 4 years of monitoring data, we examined seasonal and interannual variations in transpiration of a teak (*T. grandis*) plantation in northern Thailand in relation to soil moisture changes. The correlation between the beginning and end of transpiration and soil moisture change indicates that large interannual differences in transpiration period were induced by modification in soil moisture change. As a result, year-to-year variations in the length of transpiration period spanned about 60 days, implying a profound potential impact on annual transpiration. The occurrence of transpiration control due to soil drought during the transpiration period revealed that the extent of soil drought during the transpiration period also has a potential impact on annual transpiration.

This research suggests that soil moisture change has two potential impacts on annual transpiration at this site: through modification of the length of the transpiration period, and through physiological control during the transpiration period. This result contrasts with temperate deciduous forests where onset and offset of carbon uptake correlates with soil and air temperature (Baldocchi et al. 2005). These findings

also contrast with hill evergreen forests, another typical forest type in Thailand influenced by the monsoon (Rundel and Boonpragob 1995), where transpiration peaks in the late dry season because of little water stress and increased evaporative demand (Tanaka et al. 2003; Kume et al. 2006). Further clarification is necessary to quantify the extent to which the interannual variation in energy, water, and carbon budget is caused by the potential impacts of soil moisture change through large variations in the length of the transpiration period and through stomatal control during the transpiration period.

Acknowledgments. This work was supported by CREST (Core Research for Evolutional Science and Technology) of JST (Japan Science and Technology Agency) and GEWEX (Global Energy and Water Cycle Experiment) Asian Monsoon Experiment-Tropics (GAME-T). We thank Hikaru Komatsu (Kyushu University) and Tomonori Kume (The University of Tokyo) for their useful critiques. We are also grateful to Jakkit Chaiyanet (Kasetsart University, Thailand), Masatoshi Aoki (Tokyo University of Agriculture and Technology) and Samakkee Boonyawat (Kasetsart University, Thailand) for their support during this project and to the Thai Forest Industry Organization for providing us with the opportunity to conduct this study.

References

Baldocchi DD, Black TA, Curtis PS, Falge E, Fuentes JD, Granier A, Gu L, Knohl A, Pilegaard K, Schmid HP, Valentini R, Wilson K, Wofsy S, Xu L, Yamamoto S (2005) Predicting the onset of net carbon uptake by deciduous forests with soil temperature and climate data: a synthesis of FLUXNET data. Int J Biometeorol 49: 377–387

Barr AG, Black TA, Hogg EH, Kljun N, Morgenstern K, Nesic Z (2004) Inter-annual variability in the leaf area index of boreal aspen-hazelnut forest in relation to net ecosystem production. Agric For Meteorol 126:237–255

Black TA, Chen WJ, Barr AG, Arain MA, Chen Z, Nesic Z, Hogg EH, Neumann HH, Yang PC (2000) Increased carbon sequestration by a boreal deciduous forest in years with a warm spring. Geophys Res Lett 27:1271–1274

Borchert R, Rivera G (2002) Modification of vegetative phenology in a tropical semideciduous forest by abnormal drought and rain. Biotropica 34:27–39

Closs RH (1958) The heat pulse method for measuring rate of sap flow in a plant stem. N Z J Sci 1:281–288

Goulden ML, Munger JW, Fan SM, Daube BC, Wofsy SC (1996) Exchange of carbon dioxide by a deciduous forest: response to interannual climate variability. Science 271:1576–1578

Granier A, Pilegaard K, Jensen NO (2002) Similar net ecosystem exchange of beech stands located in France and Denmark. Agric For Meteorol 114:75–82

Holst T, Hauser S, Kirchgäßner A, Matzarakis A, Mayer H, Schindler D (2004) Measuring and modeling plant area index in beech stands. Int J Biometeorol 48:192–201

Kanae S, Oki T, Musiake K (2001) Impact of deforestation on regional precipitation over the Indochina Peninsula. J Hydrometeorol 2:51–70

Kumagai T, Katul GG, Saitoh TM, Sato Y, Manfroi OJ, Morooka T, Ichie T, Kuraji K, Suzuki M, Porporato A (2004) Water cycling in a Bornean tropical rainforest under current and projected precipitation scenarios. Water Resour Res 40(1):W01104

Kume T, Takizawa H, Yoshifuji N, Tanaka K, Tantasirin C, Tanaka N, Suzuki M (2006) Impact of soil drought due to seasonal and inter-annual variability of rainfall on sap flow and water status of evergreen trees in a tropical monsoon forest in northern Thailand. For Ecol Manag (in press)
Lean J, Warrilow DA (1989) Simulation of the regional climate impact of Amazon deforestation. Nature (Lond) 342:411–413
Malhi Y, Grace J (2000) Tropical forests and atmospheric carbon dioxide. Trends Ecol Evol 15:332–337
Matsumoto J (1997) Seasonal transition of summer rainy season over Indochina and adjacent monsoon region. Adv Atmos Sci 14:231–245
Matsumoto K, Ohta T, Tanaka T (2005) Dependence of stomatal conductance on leaf chlorophyll concentration and meteorological variables. Agric For Meteorol 132:44–57
Melillo JM, McGuire AD, Kicklighter DW, Moore B III, Vorosmarty CJ, Schloss AL (1993) Global climate change and terrestrial net primary production. Nature (Lond) 363: 234–240
Rundel PW, Boonpragob K (1995) Dry forest ecosystem of Thailand. In: Bullock SH, Mooney HA, Medina E (eds) Seasonally dry tropical forests. Cambridge University Press, Cambridge, pp 93–123
Schmid HP, Grimmond CSB, Cropley F, Offerle B, Su H (2000) Measurements of CO_2 and energy fluxes over a mixed hardwood forest in the mid-western United States. Agric For Meteorol 103:357–374
Smith DM, Allen SJ (1996) Measurement of sap flow in plant stems. J Exp Bot 47: 1845–1852
Tanaka K, Takizawa H, Tanaka N, Kosaka I, Yoshifuji N, Tantasirin C, Piman S, Suzuki M, Tangtham N (2003) Transpiration peak over a hill evergreen forest in northern Thailand in the late dry season: Assessing the seasonal changes in evapotranspiration using a multiplayer model. J Geophys Res 108:4533
White MA, Nemani RR (2003) Canopy duration has little influence on annual carbon storage in the deciduous broad leaf forest. Global Change Biol 9:967–972
Wilson KB, Baldocchi DD (2000) Seasonal and interannual variability of energy fluxes over a broadleaved temperate deciduous forest in North America. Agric For Meteorol 100:1–18
Yoshifuji N, Kumagai T, Tanaka K, Tanaka N, Komatsu H, Suzuki M, Tantasirin C (2006) Inter-annual variation in growing season length of a tropical seasonal forest in northern Thailand. For Ecol Manag 229:333–359

Scale Dependency of Hydrological Characteristics in the Upper Ping River Basin, Northern Thailand

Koichiro Kuraji*, Kowit Punyatrong, Issara Sirisaiyard, Chatchai Tantasirin, and Nobuaki Tanaka

The scale dependence of the hydrological characteristics of a river basin was studied using three watersheds with different scales in northern Thailand. The discharge per unit area in the medium-scale watershed (Mae Chaem) had only small interannual changes even though large interannual changes occurred in the rainfall. The discharge per unit area in the small-scale watershed (Mae Tia) was about twice as large as in the medium-scale watershed and had larger interannual changes that were correlated with the interannual changes in rainfall. The long-term trend of discharge per unit area showed no distinct trend in either medium- or small-scale watersheds, whereas there was a distinct decreasing trend of low flow in the small-scale watershed. In the medium-scale watershed, however, this decreasing trend did not appear, suggesting that the land cover change in the uplands may have an influence on the discharge per unit area in the small-scale watershed, but only a minor influence on the discharge per unit area in the medium-scale watershed. The discharge per unit area in the microscale watershed (Huay Kog-Ma) was the largest and had the smallest seasonal change among the three watersheds. Even in the dry season, there was significant water flow in the microscale watershed.

1. Introduction

In high-elevation areas of the Upper Ping river basin, northern Thailand, shifting cultivation and dry season irrigation for cabbage and garlic farming are widespread among the hill tribes. Because of the increasing water demand for irrigation of the paddy fields and fruit farms in the dry season, and the large interannual variation of rainfall, as well as the duration of the dry period, downstream regions frequently suffer water shortages (Kuraji and Kowit 2000). People in the downstream areas perceive the upstream farmers as water consumers, but the relationship between upstream land cover change and downstream dry season flow volume has not been fully studied in this region.

* University Forest in Aichi, The University of Tokyo, Aichi Japan
E-mail: kuraji@uf.a.u-tokyo.ac.jp

One of the issues is the scale dependence of the hydrological characteristics of the river basin. It is well known that, in microscale (0.01–1 km^2), there will be distinct changes in hydrology if one changes the land cover in the catchments, but at present it is not known if this theory is applicable to small- (1–100 km^2) and medium-scale (100–10 000 km^2) catchments. It is important to understand the scale dependence of the hydrological characteristics of the river basin in this region.

The objective of this study was to compare the hydrological characteristics of three different scale catchments to understand the scale dependence of hydrology in the Upper Ping River basin. The scale dependence of the impact of land cover change on river discharge was also examined.

2. Study Sites and Methods

Three watersheds of different scales [Mae Chaem (medium scale, 3853 km^2), Mae Tia (small scale, 65 km^2), and Huay Kog-Ma (microscale, 0.0879 km^2) were selected as the study sites (Fig. 1, Table 1). We examined the long-term rainfall and runoff data obtained in these watersheds.

Rainfall in Mae Chaem watershed has been observed manually at several points by the Thai Meteorological Department (TMD), Royal Forestry Department (RFD), and Air Force over a long period. Long-term rainfall data observed in Doi Inthanon [2565 meters above sea level (m.a.s.l.)], the highest point in Thailand), and Huay Bong (810 m.a.s.l.) were used in this study. In 1997, the Global Energy and Water Experiment

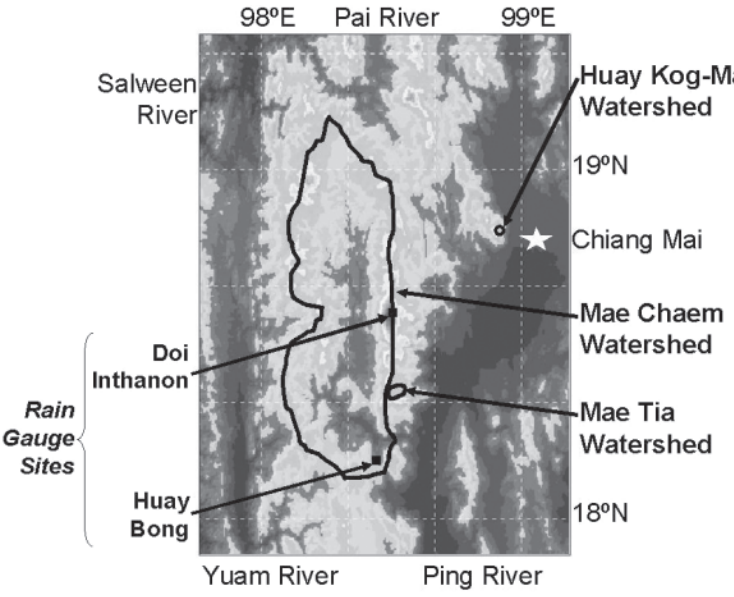

FIG. 1. Location of the three watersheds and rain gauges. *Light grey*, high elevation; *dark grey and black*, low-elevation areas. In the Thai language, *doi* means mountain, *mae* means "river," and *huay* means "stream." The two rain gauge locations used in this study are also shown

TABLE 1. Three different scale watersheds (top) and two rain gauge stations (bottom) used in this study

Scale	Name	Area (km^2)	Natural vegetation	Human impact
Medium	Mae Chaem	3853	HEF, MDF, DDF, pine	Yes
Small	Mae Tia	65	HEF, MDF, DDF, pine	Yes
Micro	Huay Kog-Ma	0.0879	HEF	No

HEF, hill evergreen forest; MDF, mixed deciduous forest; DDF, dry dipterocarp forest

Elevation	Name	m.a.s.l.	Mean annual rainfall	Operation organization
High	Doi Inthanon	2565	2540 mm	Air Force, GAME (Nov. 1997)
Low	Huay Bong	810	1038 mm	RFD, GAME (Nov. 1999)

m.a.s.l., Meters above sea level; GAME, Global Energy and Water Experiment (GEWEX) Asian Monsoon Experiment; RFD, Royal Forestry Department

(GEWEX) Asian Monsoon Experiment (GAME) project selected Mae Chaem watershed as one of the intensive observation river basins, and 15 automatic recording rain gauges were installed in 1997, which have been operating up to the present. To analyse the long-term trend in rainfall, we checked the relationship between manual observation data and automatically recorded GAME rain gauge data. The data shown in the following section are the combined data from both the manual and automatic recording rain gauges.

The river discharge in Mae Chaem and Mae Tia was measured by the Royal Irrigation Department (RID) and the Department of Energy Development and Promotion (DEDP), while the river discharge in Huay Kog-Ma was measured by the study group.

3. Results and Discussion

3.1. Scale Dependence of Hydrological Characteristics

Figure 2 shows the long-term annual rainfall and discharge per unit area in these watersheds. Rainfall in Mae Chaem watershed is characterized by the evident increase in altitude during the rainfall (Kuraji et al. 2001, 2004). Rainfall in Doi Inthanon is the highest in Mae Chaem watershed, whereas the rainfall in Huay Bong is about one-half or one-third of the rainfall in Doi Inthanon. Rainfall anywhere in Mae Chaem watershed and the surrounding area may be intermediate between the two rain gauge stations. Figure 2 shows a large interannual fluctuation in rainfall in both higher and lower areas. The differences between the maximum and minimum annual rainfall in Doi Inthanon and Huay Bong are 1731.5 mm (71% of annual mean) and 735.8 mm (68% of annual mean), respectively. The coefficients of variation in annual rainfall from 1980 to 1992 in Doi Inthanon and Huay Bong are 11.2% and 15.6%, respectively, showing that the relative amplitude of the interannual variation in Huay Bong rainfall was larger than that in Doi Inthanon.

The annual discharge per unit area in Mae Chaem, Mae Tia, and Huay Kog-Ma watersheds is strongly dependent on the size of the watershed. The largest annual discharge per unit area was observed in the smallest watershed (Huay Kog-Ma), because the mean elevation of the smaller watershed is higher than that of the larger

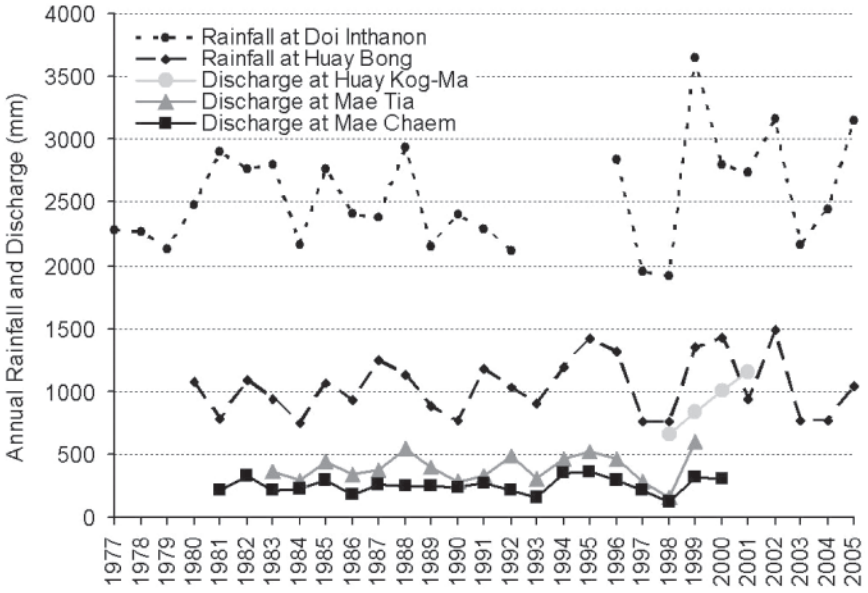

Fig. 2. Annual rainfall and discharge per unit area in Mae Chaem, Mae Tia, and Huay Kog-Ma watersheds. Rainfall data were a combination of observations by manual and automatic recording rain gauges at Huay Bong (810 m) and Doi Inthanon (2565 m) in Mae Chaem watershed

watersheds and the mean rainfall in the smaller watershed is larger than that in the larger watershed. The interannual fluctuations of the annual discharge per unit area in Mae Chaem watershed are relatively small compared to the rainfall fluctuation, whereas the fluctuations of discharge per unit area in Mae Tia and Huay Kog-Ma watersheds are larger than that in Mae Chaem watershed. The differences between the maximum and minimum annual discharge per unit area in Mae Chaem, Mae Tia, and Huay Kog-Ma are 243.9, 443.1, and 501.9 mm, respectively, smaller than the amplitude of fluctuation in the annual rainfall. The smaller fluctuation of the discharge per unit area than the fluctuation of rainfall can be explained by the large water storage capacity of the watersheds occurred because of the relatively small interannual change in evapotranspiration (Tanaka et al. 2004). The coefficients of variation in annual discharge per unit area from 1983 to 1999 in Mae Chaem and Mae Tia are 25.0% and 28.4%, respectively, showing that the relative amplitude of the interannual variation in Mae Chaem discharge per unit area was smaller than that in Mae Tia. Data for only 4 years are available for the annual discharge in Huay Kog-Ma, but the amplitude of the interannual fluctuation is the largest.

In 1998, minimum annual discharge per unit area was observed in both Mae Chaem and Mae Tia watersheds owing to less rainfall in 1997 and 1998. In this region, low minimum flow will occur because of the combination of two factors: less rainfall during the previous rainy season, and delay in the onset of the rainy season in the current year.

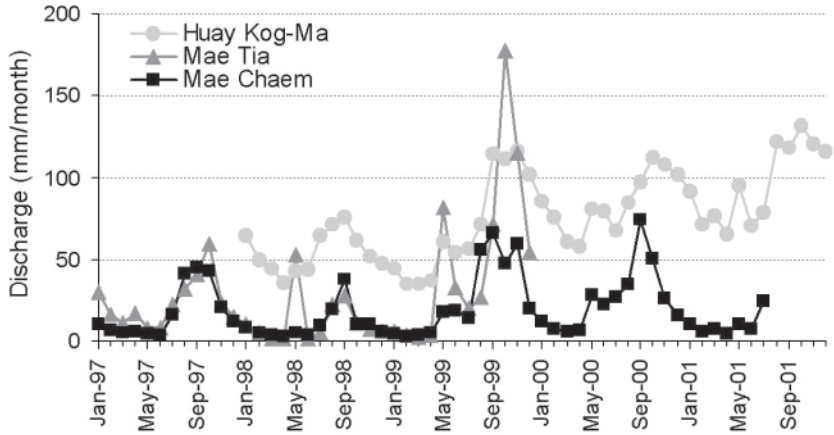

FIG. 3. Monthly discharge per unit area in the three watersheds from 1997 to 2001

Figure 3 shows the monthly discharge per unit area observed in the three watersheds. In the dry season (from November to April), the discharge per unit area tends to decrease in the three watersheds, and the discharge per unit area in Mae Tia and Mae Chaem was nearly zero at the end of each dry season. In Huay Kog-Ma, however, 40 mm/month or more of the discharge per unit area was in streams even at the end of the dry season in 1998 and 1999 (1997 and 1998 are extraordinarily dry years). The existence of the large amount of discharge per unit area in the very dry period in Huay Kog-Ma is explained not by the scaling effect but by the hydrogeological effect. The role of deep-water pathways within permeable unconsolidated materials in damping the river hydrography would be critical in Huay Kog-Ma. The water demand for transpiration of the Hill Evergreen Forest in Huay Kog-Ma during the dry season is also supplied by the water storage in the watershed (Tanaka et al. 2004).

Figure 4 shows the daily hydrograph recordings observed in the three watersheds during 1998 and 1999. In 1998, the initial condition of the watershed was dry owing to the lower rainfall in the 1997 rainy season. The rainfall in the 1998 rainy season was also less than normal, and the initial condition in 1999 was also dry. The rainy season in 1999 started earlier than usual and there was more rainfall in the rainy season.

From Fig. 4, it is found that the amplitude of the seasonal change in daily discharge per unit area is less than one order in Huay Kog-Ma, about two orders in Mae Chaem, and about three orders in Mae Tia. The small amplitude of the microscale Huay Kog-Ma may be explained by its geological conditions. The amplitude of the medium-scale Mae Chaem is smaller than that of the small-scale Mae Tia as a result of the averaging effects of basin heterogeneity. In 1998, the discharge per unit area in the three watersheds was similar in value only during September because of the difference in initial conditions (very dry) and lower rainfall during the rainy season. In 1999, however, the discharge per unit area was similar from mid-May to October despite the similar initial difference in conditions compared with 1998; this may have occurred because

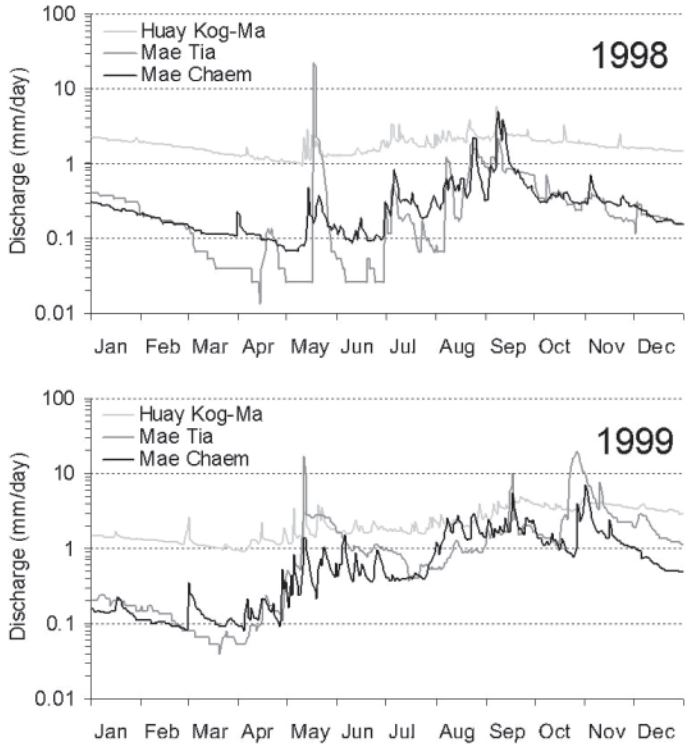

Fig. 4. Daily discharge per unit area in 1998 and 1999 in the three watersheds

of the abundance of rain in the early rainy season, which can dissipate the effect of the initial difference in conditions.

3.2. Scale Dependence of the Impact of Land Cover Change on River Discharge

Figure 5 shows the long-term trends in annual discharge per unit area and annual minimum flow in Mae Chaem and Mae Tia watersheds. The trends in annual discharge per unit area in both the rivers show no distinct increase or decrease. The trend in annual minimum flow in Mae Chaem also shows no distinct change, whereas the trend in Mae Tia shows a distinct decrease. From 1983 to 1988, the minimum flow in Mae Tia was about two times higher than that in Mae Chaem, which corresponds with the ratio of the annual discharge per unit area between Mae Chaem and Mae Tia. After 1989, however, the minimum flow in Mae Tia is almost the same or lower than that in the Mae Chaem for some years. This timing in the change of minimum flow in Mae Tia corresponds with the agricultural transformation in the high-elevation area in this region. From the mid-1990s, the introduction of the hill irrigation system increasingly enabled the farmers to undertake dry season cultivation. Irrigational water use in the dry season is one of the reasons for the decrease in the minimum

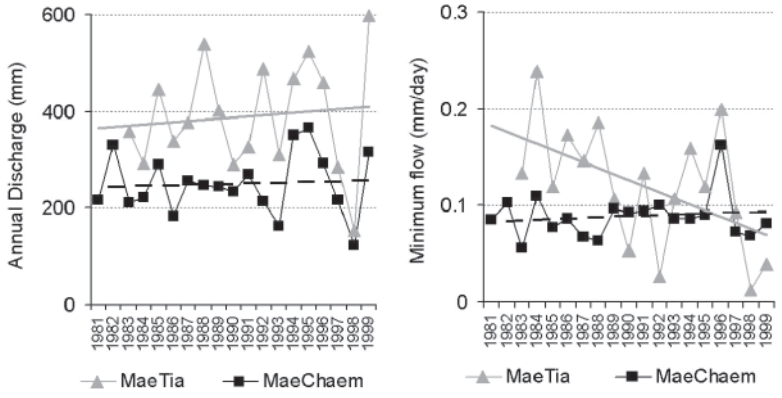

FIG. 5. Long-term series of annual discharge per unit area (*left*) and minimum flow (*right*) in Mae Chaem and Mae Tia watersheds

flow of Mae Tia. In Mae Chaem, however, the minimum flow shows no change because the agricultural transformation in Mae Chaem occurred on a relatively small scale with respect to the 3853 km^2 watershed.

4. Conclusion

The scale dependence of the hydrological characteristics of the river basin was studied in three watersheds with different scales in northern Thailand. The discharge per unit area in the medium-scale watershed had only small interannual changes corresponding to a large interannual change in rainfall. The discharge per unit area in the small-scale watershed was about twice that of the medium-scale watershed and had larger interannual changes, corresponding to changes in interannual rainfall. The long-term trend of discharge per unit area showed no distinct trend in both medium- and small-scale watersheds, while there was a distinct decreasing trend of low flow in the small-scale watershed. In the medium watershed, however, this decreasing trend did not appear, suggesting that the land cover change in the uplands may have an influence on the discharge per unit area in the small-scale watershed. There was only a minor influence on the discharge per unit area in the medium-scale watershed. The discharge per unit area in the microscale watershed (Huay Kog-Ma) was the largest and had the smallest seasonal change among the three watersheds. There was significant water flow in the microscale watershed, even in the dry season.

It was concluded that the rainfall–runoff response and long-term trend of discharge per unit area and low flow in the medium-, small-, and microscale catchments are very different from each other. It was difficult to apply any conclusion obtained in one scale to the other scale catchments. It may be doubtful if one can apply the "land cover change influences on discharge per unit area" hypothesis to medium- or large-scale catchments.

Acknowledgment. This work has been supported by a CREST project (Effects of rainfall variability on water cycle and ecosystem in tropical forest under Asian monsoon climate).

References

Kuraji K, Kowit P (2000) Hydro-meteorological research and its application to watershed management for solving local conflict over water in Mae Tia watershed, Northern Thailand. In: Proceedings of the fresh perspectives on hydrology and water resources in Southeast Asia and the Pacific, Christchurch, New Zealand, pp 189–196

Kuraji K, Kowit P, Suzuki M (2001) Altitudinal increase in rainfall in Mae Chaem watershed, Thailand. J Meteorol Soc Jpn 79:353–363

Kuraji K, Kowit P, Issara S (2004) Six years intensive rainfall observation in Mae Chaem Watershed, Northern Thailand. The 6th international study conference on GEWEX in Asia and GAME, Kyoto, Japan. GAME CD-ROM publication no. 11, T3KK09 Aug 04 160237

Tanaka K, Takizawa H, Kume T, Xu J, Chatchai T, Suzuki M (2004) The impact of rooting depth and soil hydraulic properties on the transpiration peak of an evergreen forest in northern Thailand in the late dry season. J Geophys Res 109:D23107

Year-Round Observation of Evapotranspiration in an Evergreen Broadleaf Forest in Cambodia

Tatsuhiko Nobuhiro*, Akira Shimizu, Naoki Kabeya, Yoshio Tsuboyama, Tayoko Kubota, Toshio Abe, Makoto Araki, Koji Tamai, Sophal Chann, and Nang Keth

We conducted a year-round observation of meteorological elements using a meteorological observation tower 60 m in height to evaluate evapotranspiration in an evergreen broadleaf forest watershed in central Cambodia. The period of observation was from November 2003 to October 2004. Solar radiation was consistent throughout the year. The integrated values of net radiation and downward and upward shortwave radiation were 5.09, 6.79, and 0.76 GJ m^{-2} $year^{-1}$, respectively. The temperature observed above the forest canopy was lowest and highest in the first and latter half of the dry season, respectively. The mean air temperature was 26.4°C. The saturation deficit was high in the late dry season (>30 hPa) and low during the rainy season (<25 hPa). The evapotranspiration rate was estimated from these observed meteorological parameters using the heat-balance method incorporating the Bowen ratio. The evapotranspiration rate was higher in the dry season than in the rainy season. Seasonal variation in evapotranspiration corresponded to the variation in the saturation deficit above the forest canopy. The amount of year-round evapotranspiration was 1139.7 mm. The water budget calculations from observation data suggested a water loss of 1202.8 mm for the experimental watershed. Thus, the observed evapotranspiration and water loss amounts were similar.

1. Introduction

The forested area of the Indochina Peninsula is declining because of deforestation, development for farmland, and other land use changes. Downstream on the Mekong River, which flows through the peninsula, the ratio of forested area in Cambodia is comparatively higher than that in neighboring countries (Narith 1997). The forest is widely distributed in the southwest and northeast mountainous areas of the country

* Forestry and Forest Products Research Institute (FFPRI), Tsukuba, Japan
E-mail: tatuhiko@ffpri.affrc.go.jp

and is also distributed in the north to central flatlands. Therefore, evaluating the river water derived from the forested areas is important for water supplies in Cambodia and the Mekong downstream area.

Some studies have been conducted on hydrological processes and water resources on the Indochina Peninsula. For example, evaporation in agricultural fields was observed in Thailand (Shah et al. 1986; Hayashi and Vorasoot 1989; Watanabe et al. 2004). Pinker et al. (1980b) performed measurements of energy and water balance in an evergreen forest in Thailand. Kabeya et al. (2004) analyzed the water confluence of the Tonle Sap and Mekong using a stable oxygen isotopic ratio. However, little research concerning the water resources of forested areas in Cambodia has been undertaken.

For this reason, we designated experimental watersheds in evergreen-forested areas to evaluate water resources in Cambodia. To understand water use in downstream regions, it is important to know the amount of water loss from forested watersheds. Using the water balance concept at the watershed level, the amount of water loss is estimated by subtracting the amount of runoff from precipitation in the watershed. However, the water loss obtained from water budget observations is not adequate in terms of daily variation analysis, because the low temporal resolution does not provide sufficiently detailed information. As most water loss from a watershed occurs via the process of evapotranspiration, we constructed a 60-m-high meteorological observation tower in an evergreen forested watershed in Cambodia to estimate the evapotranspiration rate as representative data for this region. Seasonal variations in meteorological components were also investigated. We then analyzed the relationship between the evapotranspiration rate and each meteorological element.

2. Site Description

The experimental watershed O Thom I is located in the Kampong Thom Province of central Cambodia (Fig. 1). The O Thom I River is a branch of the Stung Chinit River, which drains into Tonle Sap Lake. The area of the O Thom I watershed is 137 km^2, with an altitude between 46 and 273 m. The vegetation of the experimental watershed consisted of evergreen broadleaf trees, such as dipterocarps. Dominant species near the observation tower were *Myristica iners*, *Anisoptera costata*, *Dipterocarpus costatus*, and *Vatica odorata*. The forest surrounding the observation tower consisted of three canopy stories: overstory, secondary story, and lower story. The mean diameter at breast height and mean tree height of overstory trees were 39.6 cm and 27.2 m, respectively.

A 60-m-high meteorological observation tower was set up in the northeast part of the O Thom I watershed (12°44′ N, 105°28′ E). The topography near the tower was very flat. The leaf area index (LAI) varied within a range of 4 to 5, peaking in June and then gradually decreasing. Even in the dry season, the LAI maintained 80% of its peak value (Ito et al. 2004). Investigation of the forest soil layer suggested that the forest soil type was Acrisol (Ohta et al. 2004) and that its depth was 4–9 m (Ohnuki et al. 2004) in the O Thom I watershed.

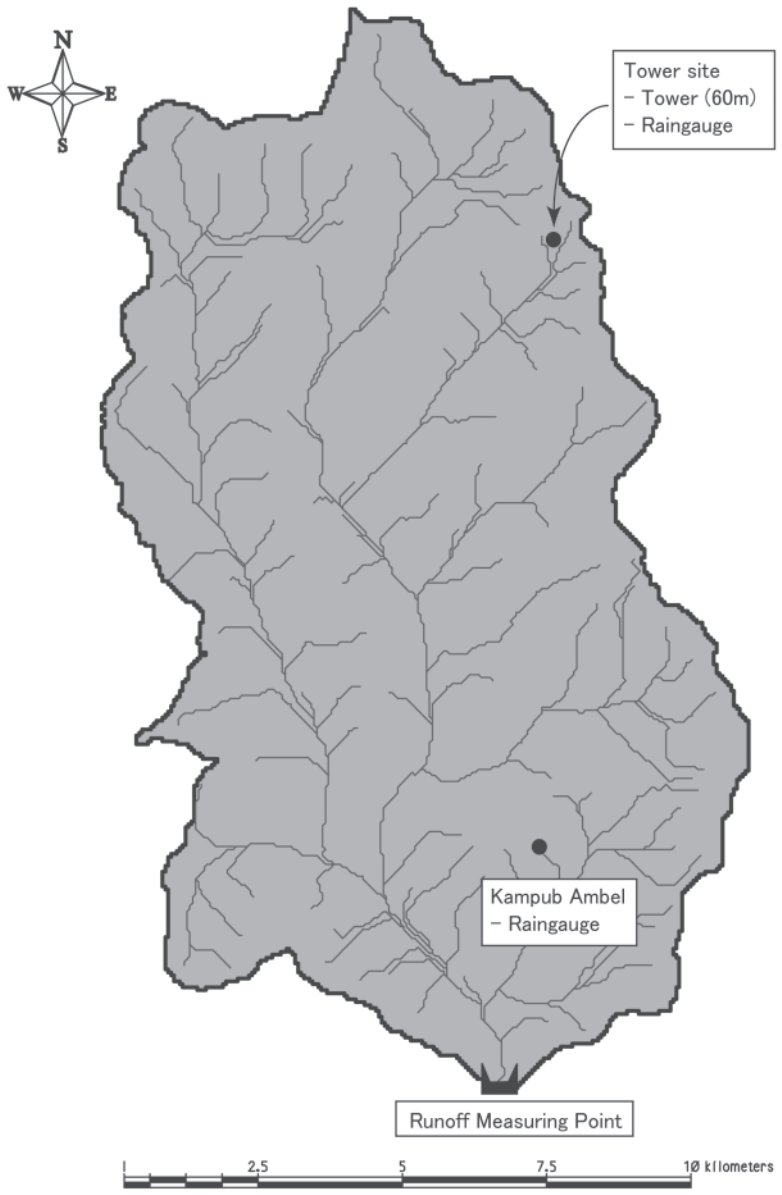

Fig. 1. Location of observation points in the O Thom I watershed

3. Methods

To determine the latent heat flux from the forested area, various observations were performed in a tropical monsoon region. In the Kog-Ma watershed located in northern Thailand, evapotranspiration-related measurements have been made in a hill evergreen forest using the eddy correlation technique (Tanaka et al. 2004). In the Chao Phraya River basin in the north part of this country, the eddy correlation method was also applied to estimate surface fluxes with several land covers (Toda et al. 2002). This method is widely used to estimate evapotranspiration with equipment such as a supersonic anemometer–thermometer (SAT) and digital temperature and humidity sensors with quick responses. However, in using this method for long-term observations, problems such as maintaining a supply of electricity to power the equipment, verifying the acquired data, and generally maintaining the system can occur. It was therefore difficult to perform measurements continuously at the outset of our observations in the experimental watershed in Cambodia.

We used the temperature and water vapor pressure profiles to estimate evapotranspiration. We employed the heat-balance method incorporating the Bowen ratio, which measures the energy budget above the forest canopy from the profiles of potential temperature and water vapor pressure. The data required to perform the analyses were collected using equipment installed on a 60-m-high meteorological observation tower (Fig. 2). A rain gauge (RG-2M; Onset, Bourne, USA) and pyranometers (CM3;

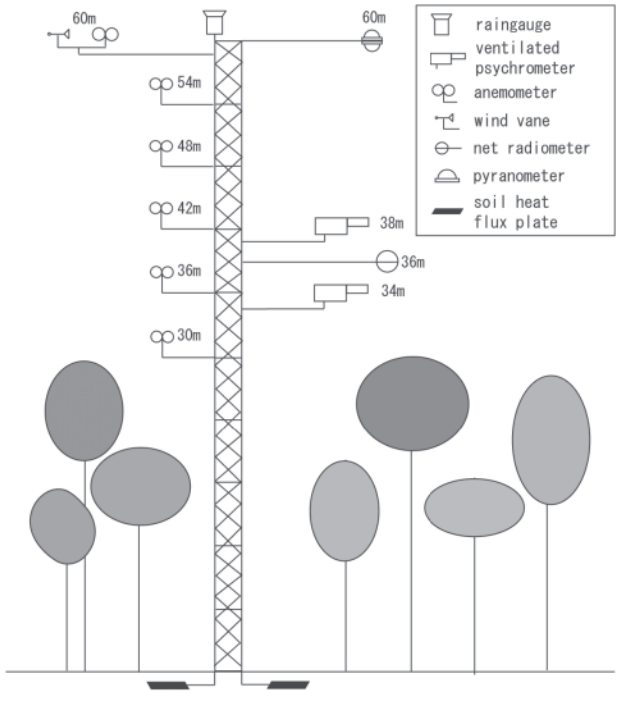

Fig. 2. Schematic diagram of the 60-m-high meteorological observation tower

Kipp & Zonen, Delft, Netherlands) were installed 60 m above the ground, at the top of the tower. Two ventilated psychrometers (MH-020T; Eko, Tokyo, Japan) were installed above the forest canopy at 34 and 38 m. A net radiometer (Q7.1; REBS, Seatle, USA) was placed at a height of 36 m. Two heat flux plates (MF-180M; Eko, Tokyo, Japan) were installed under the forest soil at a depth of 2 cm near the tower. A wind vane (03301-5; Young, Traverce, USA) and an anemometer (03101-5; Young, Traverce, USA) were placed at a height of 38 m from October 2003 to September 2004, after which they were moved to a height of 60 m. Anemometers were also installed at 30, 36, 42, 48, and 54 m. Atmospheric pressure was observed at Kbal Domrey, 20 km away from the tower site. Another rain gauge was installed at Kampub Ambel village (12°39′ N, 105°28′ E), in the southern part of the watershed, and at Bak Snar (12°32′ N, 105°17′ E), located 30 km southwest, close to the point where runoff measurements were made in the Stung Chinit River. Details of the runoff observations are described by Kabeya et al. (2007). Shallow wells were made near the tower, and the groundwater level was measured each day.

The period of observation was from November 2003 to October 2004. Before this time, a preliminary investigation was made in October 2003. All measurements were taken at 10-s intervals and recorded as 10-min averages (or cumulative values) using a data logger (CR10X; Campbell, North Logan, USA). A combination of interchangeable batteries and solar cell panels was used to supply electricity. The wet bulbs of the ventilated psychrometers were checked weekly and refilled with water as required. Verification of the ventilated psychrometers was performed once every 3 months. The ventilated psychrometers were set at the same altitude and calibrated using an Assmann psychrometer. Missing values of net radiation were estimated from shortwave radiation. On occasions when temperature elements were lacking, evapotranspiration was estimated using multiple regression containing variables such as net radiation, saturation deficit, and wind speed in the dry and rainy season.

The heat-balance method incorporating the Bowen ratio was used to estimate evapotranspiration (Hattori 1985). This method relies on the following relationship:

$$Rn = H + \lambda E + G + J + B + A \tag{1}$$

where Rn is the net radiation, H is the sensible heat flux, λE is the latent heat flux, λ is the heat of water vaporization, G is the ground heat flux, J is the change in heat storage, B is the quantity of heat required for CO_2 fixation, and A is advection. In this study, J, B, and A were negligible. We measured H, λE, and G, which are the main elements of the heat-balance component. The diffusion coefficients of the latent and sensible heat fluxes can be considered equal at the boundary layer; thus, using the Bowen ratio (β), the latent heat flux can be estimated from Eq. 1 as follows:

$$\lambda E = \frac{Rn - G}{1 + \beta} \tag{2}$$

where

$$\beta = \frac{H}{\lambda E} \tag{3}$$

The Bowen ratio can then be calculated by measuring the wet- and dry-bulb temperatures at two heights (34 and 38 m):

$$\beta = \frac{\gamma(TD_1 - TD_2)}{(\delta + \gamma)(TW_1 - TW_2) - \gamma(TD_1 - TD_2)} \tag{4}$$

where γ is the psychrometric constant, $(TD_1 - TD_2)$ is the difference in temperature between the dry bulbs at the two heights, δ is the gradient of the saturated vapor pressure curve, and $(TW_1 - TW_2)$ is the temperature difference between the wet bulbs at the two heights.

4. Results and Discussion

The evapotranspiration processes of forested areas (e.g., transpiration, evaporation of intercepted water, etc.) may be dependent on many meteorological factors, such as radiation energy, air temperature, saturation deficit, and soil moisture (Green 1993; Hattori et al. 1993; Granier et al. 1996; Cienciala et al. 2000). Therefore, it is important to obtain basic information on those components in Cambodian forested areas.

Figure 3 shows the seasonal variation of precipitation at Bak Snar, near the gauging point at Stung Chinit. The rainy season in this region ran from May to October, with the remaining period representing the dry season. Approximately 94% of the precipitation occurred during the rainy season (May to October 2004).

The daytime net radiation (*Rn*), downward shortwave radiation (*Sd*), and upward shortwave radiation (*Su*) averaged every 10 days are shown in Fig. 4. Although these radiation energy components were affected by precipitation or cloud cover, the amount of net radiation in the rainy season was similar to that in the dry season; thus, consistent radiation energy was supplied to the forest crown surface throughout the year. The integrated values of net radiation and downward and upward shortwave radiation for a 1-year period were 5.09, 6.79, and 0.76 GJ m^{-2} $year^{-1}$, respectively.

Albedo is influenced by the leaf water content, LAI, solar elevation angle, and other factors. Seasonal variation in albedo was estimated from the integrated shortwave radiation balance during the daytime (Fig. 5). Albedo was higher in the dry season than in the rainy season. The variation in albedo ranged from 0.093 to 0.127. This result corresponded to the range of 0.098–0.183 in a dry evergreen forest in Thailand

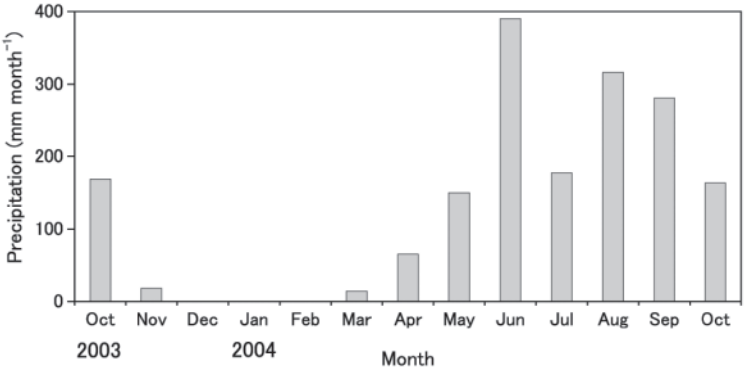

Fig. 3. Seasonal variation in precipitation at Bak Snar

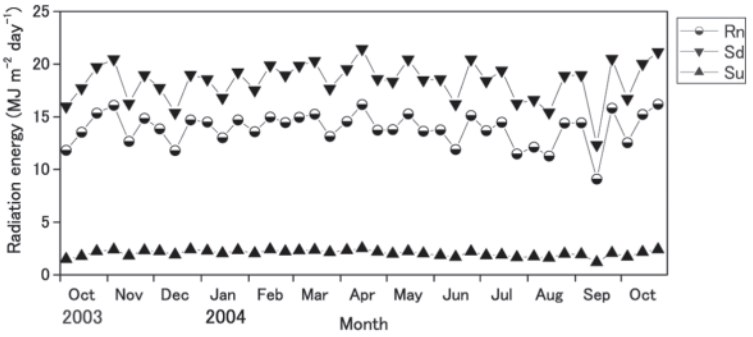

Fig. 4. Seasonal variation in radiation energy components

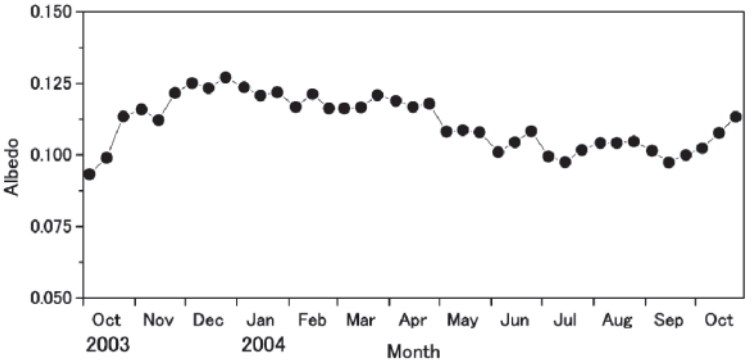

Fig. 5. Seasonal variation in albedo observed at 60 m above the ground

(Pinker et al. 1980a) and 0.098–0.136 in an Amazonian tropical rainforest (Culf et al. 1995). Culf et al. (1995) also indicated that the seasonal variation in albedo at low latitudes was not affected by the solar elevation angle. Given that the LAI retained 80% of its peak value even in the dry season, it has been considered that albedo is mainly affected by the seasonal variation in leaf water conditions (Mooney et al. 1977; Hunt et al. 1987).

The daily maximum and mean air temperatures observed at 34 m in height during the observation period are shown in Fig. 6. Maximum air temperature was highest at the end of the dry season (>35°C); in the rainy season, it was <35°C. However, the lowest temperature was observed during the first half of the dry season. The mean air temperature during the observation period was 26.4°C.

The daily maximum and mean saturation deficit were calculated from dry- and wet-bulb temperatures observed at 34 m in height (Fig. 7). The saturation deficit near the canopy layer was highest (>30 hPa) under fine weather conditions in the late dry season and was relatively low (<25 hPa) throughout the rainy season. The daily maximum saturation deficit corresponded mostly with the daily maximum temperature.

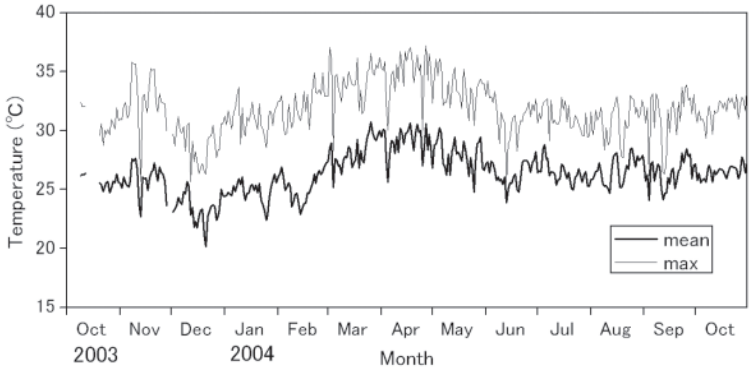

Fig. 6. Seasonal variation in temperature observed at 34 m above the ground

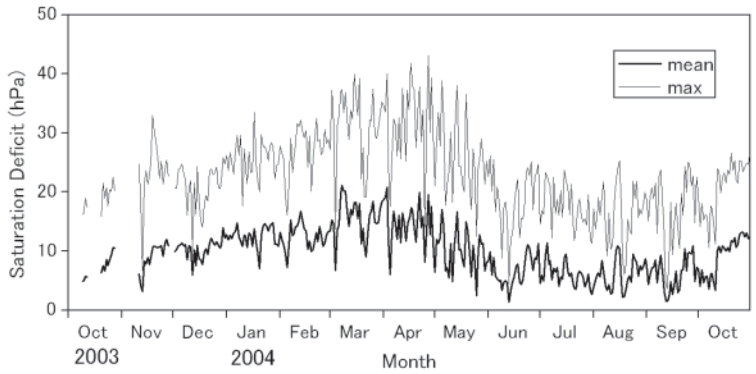

Fig. 7. Seasonal variation in the saturation deficit (hPa) observed at 34 m above the ground

Figure 8 shows the seasonal variation in the groundwater level measured in shallow wells near the observation tower (January–October 2004). The groundwater level close to the stream channel (no. 6) was highest; groundwater levels decreased with distance from the stream. At site no. 9, which was at the highest altitude and furthest from the stream, the groundwater level was about 3 m below the surface (Araki et al. 2007). The groundwater level in all wells was lowest at the end of the dry season and increased following rainfall events. Therefore, it is thought that the soil water content remained at a high level throughout the rainy season and decreased gradually during the dry season.

The seasonal variation in evapotranspiration is shown in Fig. 9. The amount of year-round evapotranspiration during the observation period (November 2003–October 2004) was estimated to be 1139.7 mm. The daily evapotranspiration rate was higher in the dry season than in the rainy season. Although the soil water content declined during the dry season, the maximum evapotranspiration rate appeared in

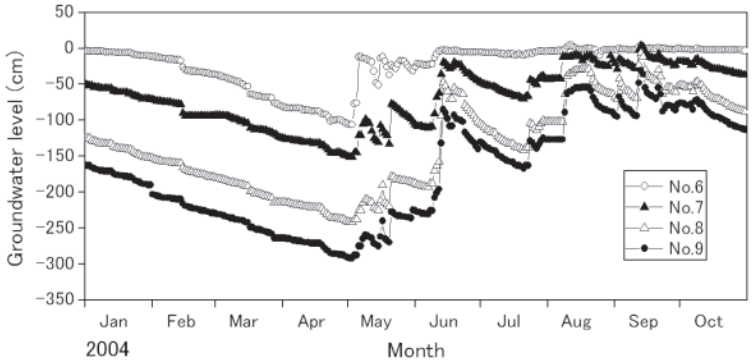

FIG. 8. Seasonal variation in groundwater level at sites near the observation tower

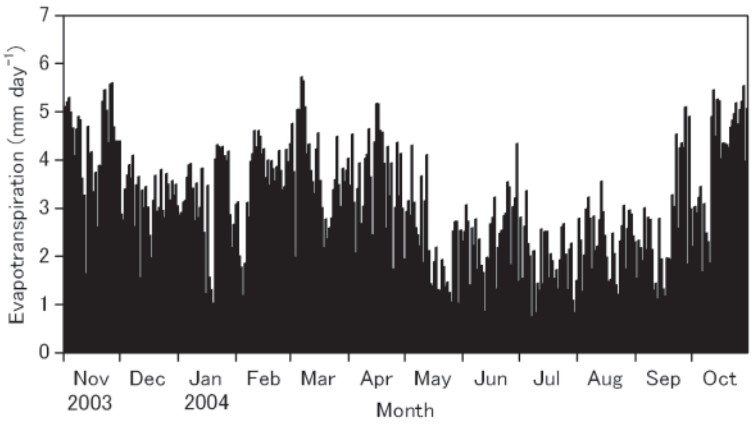

FIG. 9. Seasonal variation in daily evapotranspiration rate

the dry season during the year. This result was similar to the tendency of latent heat flux obtained in a hilly evergreen forest of northern Thailand (Tanaka et al. 2003). Furthermore, the occurrence of a high transpiration rate in the dry season was in agreement with the result obtained in northern Australia (O'Grady et al. 1999). As a result of comparing seasonal variation in evapotranspiration with meteorological elements, the fluctuation pattern of peak values in evapotranspiration corresponded with the variation in the peak of the maximum saturation deficit.

The observed evapotranspiration was compared with the water budget obtained from the runoff measurements. Studies investigating water budgets in forest stands are generally conducted on a much larger scale, encompassing entire catchment areas (Doley 1981; Oyebande 1988; Kuraji 1996). As deep seepage exists and a part of the discharge cannot be accurately described by observation of the rivers in this area, the watershed with the deepest channel position was selected. Consequently, the chosen Stung Chinit watershed, containing the tower site, produced the maximum amount

of runoff among all experimental watersheds. Runoff from Stung Chinit watershed was 362.6 mm in 2004 (Kabeya et al. 2005); precipitation at Bak Snar, the precipitation observation point near the stream flow measurement point of Stung Chinit, was 1565.4 mm. Based on these observations, the amount of water loss was considered to be 1202.8 mm. The evapotranspiration observed at the tower site, 1139.7 mm, was similar to the water loss, considering the existence of deep seepage.

5. Summary

We observed the seasonal variation in evapotranspiration and various meteorological parameters in an evergreen broadleaf forest watershed in Cambodia. There was very little precipitation during the dry season. Solar radiation was consistent throughout the year. The integrated values of net radiation and downward and upward shortwave radiation were 5.09, 6.79, and 0.76 GJ m^{-2} $year^{-1}$, respectively. Albedo ranged from 0.093 to 0.127 and was higher in the dry season than in the rainy season. The temperature observed above the forest canopy was lowest and highest in the first and latter half of the dry season, respectively. The mean air temperature was 26.4°C. The saturation deficit was high in the late dry season (>30 hPa) and low during the rainy season (<25 hPa). The groundwater level was lowest at the end of the dry season, and it increased to be near the soil surface, corresponding to precipitation events. The evapotranspiration rate was estimated from these observed meteorological parameters using the heat-balance method incorporating the Bowen ratio. Although the soil water content declined gradually during the dry season, the evapotranspiration rate was higher in the dry season than in the rainy season. The fluctuation pattern of peak values in evapotranspiration corresponded with the variation in the peak of the maximum saturation deficit. The amount of year-round evapotranspiration was 1139.7 mm. The water budget calculations from observation data suggested a water loss of 1202.8 mm for the experimental watershed. Thus, the observed evapotranspiration and water loss amounts were similar.

Acknowledgments. This study was funded by the Research Revolution 2002 Project of MEXT (Ministry of Education, Culture, Sports, Science and Technology) and the Assessment of the Impact of Global-Scale Change in Water Cycles on Food Production and Alternative Policy Scenario of AFFRCS (Agriculture, Forestry and Fisheries Research Council Secretariat), Japan.

References

Araki M, Shimizu A, Toriyama J, Ito E, Kabeya N, Nobuhiro T, Bora T, Sopheavuth P, Sopheap L, Saret K, Phearak P, Saila D, Ohta S, Kanzaki M (2007) Changes of vertical soil moisture conditions of a dry evergreen forest in Kampong Thom, Cambodia. In: Sawada H, Araki M, Chappell NA, La Frankie JV, Shimizu A (eds) Forest Environments in the Mekong River Basin. Springer, Tokyo, pp 112–124

Cienciala E, Kučera J, Malmer A (2000) Tree sap flow and stand transpiration of two *Acacia mangium* plantations in Sabah, Borneo. J Hydrol 236:109–120

Culf AD, Fisch G, Hodnett MG (1995) The albedo of Amazonian forest and ranch land. J Climate 8:1544–1554

Doley D (1981) Tropical and subtropical forests and woodlands. In: Kozlowski TT (ed) Water deficits and plant growth, vol VI. Academic Press, New York, pp 209–323
Granier A, Huc R, Barigah ST (1996) Transpiration of natural rain forest and its dependence on climatic factors. Agric For Meteorol 78:19–29
Green SR (1993) Radiation balance, transpiration and photosynthesis of an isolated tree. Agric For Meteorol 64:201–221
Hattori S (1985) Explanation on derivation process of the equations to estimate evapotranspiration and problems on the application to forest stand (in Japanese). Bull For For Prod Res Inst 332:139–165
Hattori S, Tamai K, Abe T (1993) Effects of soil moisture and vapor pressure deficit on evapotranspiration in a hinoki plantation (in Japanese). J Jpn For Soc 75:216–224
Hayashi Y, Vorasoot N (1989) Spatial distribution of actual evapotranspiration rate in northeast Thailand during the dry season. Jpn Agric Res Q 22:260–267
Hunt ER, Rock BN, Nobel PS (1987) Measurement of leaf relative water content by infrared reflectance. Remote Sens Environ 22:429–435
Ito E, Araki M, Kanzaki M, Ohta S, Kaneko T, Tani A, Hiramatsu R, Toriyama J, Okuda Y (2004) Leaf area index in tropical seasonal forests in Kompong Thom, Cambodia. In: Sawada H, Chann S, Shimizu A, Araki M (eds) Proceedings of the international workshop on forest watersheds 2004, Phnom Penh, Cambodia, 29 October 2004, pp 28–32
Kabeya N, Kubota T, Shimizu A, Nobuhiro T, Tsuboyama Y, Chann S, Tith N (2004) Research on stable oxygen isotopic ratios of river water around the confluence of the Tonle Sap and the Mekong. In: Proceedings of the international conference on advances in integrated Mekong River management, Lao PDR, Vientiane, 25–27 October 2004, pp 143–149
Kabeya N, Shimizu A, Nobuhiro T, Chann S, Keth N, Abe T, Kubota T, Tsuboyama Y (2005) Observation of precipitation and discharge amounts in Cambodian forested catchments (in Japanese). Trans Jpn For Soc 116:437
Kabeya N, Shimizu A, Chann S, Tsuboyama Y, Nobuhiro T, Keth N, Tamai K (2007) Stable isotope studies of rainfall and stream water in forest watersheds in Kampong Thom, Cambodia. In: Sawada H, Araki M, Chappell NA, LaFrankie JV, Shimizu A (eds) Forest Environments in the Mekong River Basin. Springer, Tokyo, pp 125–134
Kuraji K (1996) Water balance studies on moist tropical forested catchments (in Japanese). J Jpn For Soc 78:89–99
Mooney HA, Ehleringer J, Björkman O (1977) The energy balance of leaves of the evergreen desert shrub *Atriplex hymenelytra*. Oecologia (Berl) 29:301–310
Narith H (1997) Asia–Pacific forestry sector outlook study: country paper on some aspects of forestry in Cambodia. APFSOS/WP/18. Food and Agriculture Organization of the United Nations, Rome, Italy
O'Grady AP, Eamus D, Hutley LB (1999) Transpiration increases during the dry season: patterns of tree water use in eucalypt open-forest of northern Australia. Tree Physiol 19:591–597
Ohnuki Y, Shinomiya Y, Kimhern C, Sor S (2004) Distribution of soil depth at forested areas in three provinces in Cambodia. In: Sawada H, Chann S, Shimizu A, Araki M (eds) Proceedings of the international workshop on forest watersheds 2004, Phnom Penh, Cambodia, 29 October 2004, pp 37–42
Ohta S, Toriyama J, Kanzaki M (2004) Forest soil and its properties in Kompong Thom, Cambodia. In: Sawada H, Chann S, Shimizu A, Araki M (eds) Proceedings of the international workshop on forest watersheds 2004, Phnom Penh, Cambodia, 29 October 2004, pp 20–23
Oyebande L (1988) Effects of tropical forest on water yield. In: Reynolds ERC, Thompson FB (eds) Forests, climate, and hydrology: regional impacts. UNESCO, Paris, France, pp 16–50
Pinker RT, Thompson OE, Eck TF (1980a). The albedo of tropical evergreen forest. Q J R Meteorol Soc 106:551–558

Pinker RT, Thompson OE, Eck TF (1980b) The energy balance of a tropical evergreen forest. J Appl Meteorol 19:1341–1350
Shah M, Bhatti MA, Jensen JR (1986) Crop coefficient over a rice field in the central plain of Thailand. Field Crop Res 13:251–266
Tanaka K, Takizawa H, Tanaka N, Kosaka I, Yoshifuji N, Tantasirin C, Piman S, Suzuki M, Tangtham N (2003) Transpiration peak over a hill evergreen forest in northern Thailand in the late dry season: assessing the seasonal changes in evapotranspiration using a multilayer model. J Geophys Res 108:4533
Tanaka K, Takizawa H, Kume T, Xu J, Tantasirin C, Suzuki M (2004) Impact of rooting and soil hydraulic properties on the transpiration peak of an evergreen forest in northern Thailand in the late rainy season. J Geophys Res 69:D23107
Toda M, Nishida K, Ohte N, Tani M, Musiake K (2002) Observations of energy fluxes and evapotranspiration over terrestrial complex land covers in the tropical monsoon environment. J Meteorol Soc Jpn 80:465–484
Watanabe K, Yamamoto T, Yamada T, Sakuratani T, Nawata E, Noichana C, Sributta A, Higuchi H (2004) Changes in seasonal evapotranspiration, soil water content, and crop coefficients in sugarcane, cassava, and maize fields in Northeast Thailand. Agric Water Manag 67:133–143

Measurements of Wind Speed, Direction, and Vertical Profiles in an Evergreen Forest in Central Cambodia

Koji Tamai*, Akira Shimizu, Tatsuhiko Nobuhiro, Naoki Kabeya, Sophal Chann, and Nang Keth

The wind characteristics of speed, direction, and vertical profile were studied to determine the effects of undulations in the local topography and canopy surface on flux observations made from a tower in an evergreen forest in Kompong Thom Province, Cambodia. Three seasonal patterns of wind speeds and directions were identified. The first occurred in December and January and was characterized by northerly monsoons that persisted all day, as well as a diurnal variation in wind speed, with a maximum and minimum around noon and near sunset, respectively. A second pattern, in February, was characterized by southerly to westerly prevailing monsoon winds, along with an easterly mountain wind observed in the early morning. Wind speed was low throughout the day. The third pattern was similar to the second but included brief, strong winds associated with squalls. Thus, regional effects on circulation were limited, and monsoon winds were found to dominate the meteorological system above the evergreen forest of central Cambodia. In the forest, the estimated roughness length and zero plane displacement height averaged 18.3 m and 7.5 m, respectively, and the average canopy height was 27.2 m. The dependence of roughness length and zero plane displacement height on the wind direction was within the standard deviation. Thus, the undulating canopy surface had little effect on the tower flux observations.

1. Introduction

The Mekong River flows from the Tibetan plateau, through Laos, Myanmar, Cambodia, and Vietnam, and into the South China Sea. A large proportion of the Mekong basin is forested, and this is believed to have a marked effect on the water cycle. Therefore, we studied latent heat flux in central Cambodia using an observation tower to estimate forest water yields. Tower fluxes have generally been found to be influenced at several scales by undulating canopy and land surfaces. Accordingly, observations of representative sensible heat flux from evergreen forests should ideally exclude the

* Kyushu Research Center, Forestry and Forest Products Research Institute (FFPRI), Kumamoto, Japan
E-mail: a123@ffpri.affrc.go.jp

influence of local topography and canopy surface undulations around observation towers. In the present study, wind speed and direction were monitored to estimate local topographic influences on the meteorological system around an observation tower. The dependence of the roughness length and zero plane displacement height on wind direction was also investigated to assess the effects of canopy surface undulations around the tower on the flux observations.

2. Site Description and Observation Methods

Observations were made in a forest located in the O Thom I basin (12°44′ N, 105°28′ E; 88 m above sea level), in Kompong Thom Province, Cambodia. The elevation of the basin ranges from 46 to 273 m, and the basin covers approximately 137 km^2. The basin topography is very flat. A 60-m-high tower was built in the middle of a flat plain surrounded for many kilometers in all directions by similar forest. Evergreen trees, such as *Vatica odorata*, *Calophyllum inophyllum*, and species of Myristicaceae, dominate the surrounding forest. The maximum tree height is about 45 m, and the average height of the upper canopy trees is 27.2 m.

The equipment on the tower included a wind vane and an anemometer (03101 LRM Young Wind Sentry; Campbell Scientific, Logan, U.S.A.) at 38 m for the analysis of wind speed and direction characteristics. Anemometers (03001 LRM Young Wind Sentry; Campbell Scientific) were located at 54, 48, 42, 36, and 30 m for analysis of the wind profile to estimate the zero plane displacement height and roughness length. The average wind speed and direction were recorded in a data logger (CR10X; Campbell Scientific) at 10-min intervals. Wind speed and direction data were collected from 7 December 2003 until 23 July 2004, and wind profile analysis data were collected from 1 to 10 August 2004 (rainy season) and 11 to 20 March 2005 (dry season).

3. Seasonal Variation in Wind Speed and Direction

The wind speeds and directions observed at a height of 38 m were used in the analysis. Figure 1 shows the seasonal variation in the daily average and maximum wind speed (U_{avg} and U_{max}, respectively) and the most frequent wind direction each day (θ_{fre}). The following three patterns appeared frequently:

(A) $U_{avg} > 2\,m\,s^{-1}$, $U_{max} = 4–6\,m\,s^{-1}$, and θ_{fre} = northeast or north
(B) $U_{avg} \approx 1\,m\,s^{-1}$, $U_{max} = 2–4\,m\,s^{-1}$, and θ_{fre} = south
(C) $U_{avg} = 1–2\,m\,s^{-1}$, $U_{max} = 4–8\,m\,s^{-1}$, and θ_{fre} = southwest

Pattern A appeared on most days between 7 December 2003 and 16 January 2004. Pattern B was seen on many days between 17 January and 2 April 2004, except for three periods when pattern A recurred: 22–25 January, 10–14 February, and 7–9 March. Subsequently, pattern C occurred frequently. However, the border between the periods dominated by patterns B and C was not as clear as that between patterns A and B.

Chang (1984) examined the monsoon circulation in Southeast Asia and found that the northeast monsoon is established in late November and weakens in spring. In summer, the southwest monsoon extends from the Indian Ocean to east of the

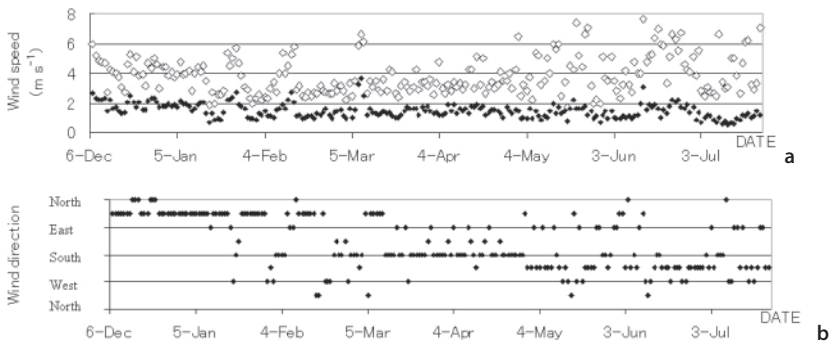

FIG. 1a,b. Seasonal variation in wind speed and direction. **a** Daily averaged and maximum wind speed: ◇, maximum wind speed; ◆, averaged wind speed. **b** Daily most frequent wind direction

Philippines. The average onset date of the summer monsoon in Cambodia is before 20 May. The westerlies are deepest in southern Thailand, Cambodia, and southern Vietnam. Our observations agreed well with those of Chang (1984).

4. Diurnal Variation in Wind Speed and Direction

The data for 10 consecutive days were examined in detail for each pattern. The days examined for patterns A to C were 31 December–9 January, 17–26 February, and 10–19 June (periods A to C, respectively). Wind speed and direction for each hour are shown in Tables 1 and 2, respectively. There are 60 values for each hour because each period consisted of 10 days and readings were taken every 10 min.

4.1. Diurnal Variation in Wind Speed

Figure 2 shows the diurnal variations in wind speed in periods A to C. In period A, wind speeds (U) were maximal from 1000 to 1200 and minimal from 1800 to 2000, whereas in period B, $U < 2\,m\,s^{-1}$ for 92% of the recorded data. Wind speeds $>3\,m\,s^{-1}$ were observed only once in period B. Period C was distinguished by low wind speeds, with rare gusts exceeding $5\,m\,s^{-1}$; wind speeds in the ranges of $0–1\,m\,s^{-1}$ and $>4\,m\,s^{-1}$ were more frequent than in period A. Wind speeds $>5\,m\,s^{-1}$ were observed ten times in period C, at various times between 1400 and 2400. The wind directions on each occasion had a westerly component, i.e., southwest (seven times), west (twice), and northwest (once), and southwesterly winds generally prevailed throughout period C [Table 2(c)].

4.2. Diurnal Variation in Wind Direction

The wind direction (θ) in period A was almost constantly from the north or northeast [Table 2(a)], whereas diurnal variation was clearly evident in periods B and C. In period B, θ was from the east at 0700 to 0800 and moved clockwise to the west by

Table 1. Diurnal patterns of wind speed

(a) December 31–January 9																									
5– m/s																									0
4–5 m/s										6	3	4	1												14
3–4 m/s								1	25	39	37	23	11	5	1										142
2–3 m/s	10	18	21	33	42	38	36	49	35	15	20	33	37	26	13	5	3					2	9	6	451
1–2 m/s	50	42	39	27	18	22	24	10					11	24	37	41	40	9	2	21	36	46	46	54	599
0–1 m/s														5	9	14	17	51	58	39	24	12	5		234
Hour	0				4				8				12				16				20				Sum
(b) February 17–26																									
5– m/s																									0
4–5 m/s																									0
3–4 m/s	1																								1
2–3 m/s	16	19	9	8	4	1		2	12	16	15	6	1	2	1	3	2				1	2	1	2	123
1–2 m/s	40	37	38	35	35	44	43	35	33	40	36	34	37	34	27	33	29	20	10	18	16	23	31	48	776
0–1 m/s	3	4	13	17	21	15	17	23	15	4	9	20	22	24	32	24	29	40	50	42	43	35	28	10	540
Hour	0				4				8				12				16				20				Sum
(c) June 10–19																									
5– m/s														1			1		5				1	2	10
4–5 m/s	1	4		1	1			1			2	2	2	9	3	3		2		3	2		5	1	42
3–4 m/s	5	2	4	2	3	6	3	1	2	3	11	18	11	14	18	14	7	5	5	3	5	3	10	10	165
2–3 m/s	2		6	7	8	1	2	5	14	18	13	19	32	16	20	20	20	9	8	11	11	12	7	10	271
1–2 m/s	28	30	23	21	15	30	28	31	22	26	19	11	10	18	16	15	16	34	22	18	16	18	12	20	499
0–1 m/s	24	24	27	29	33	23	27	22	22	13	15	10	5	2	3	8	16	10	20	25	26	27	25	17	453
Hour	0				4				8				12				16				20				Sum

Data are wind speed in each range and each hour

Table 2. Diurnal patterns of wind speed

(a) January 9–December 31																									
North	1											1	4	23	27	29	47	53	56	56	55	37	15	7	411
Northeast	49	54	56	59	57	59	58	55	52	48	47	49	49	26	25	23	13	3		2	5	23	44	51	907
East	10	6	4	1	3	1	2	5	8	12	13	10	7	9	4	1							1	2	99
Southeast														2											2
South																									0
Southwest																									0
West																									0
Northwest															4	4		4	4	2					18
Hour	0				4				8				12				16				20				Sum
(b) 17–26 February																									
North				1	1						2	2	4	3	4	2				1	2	2			24
Northeast	3	3		7	11	15	12	8	4	8	5	1	3	1	4	1	1		4	5		3	4	5	108
East	3	5	9	3	4	19	25	34	19	7	11	4	2	3	6	6	3	5	2	1	4		1	1	177
Southeast	8	9	15	24	28	14	15	9	24	19	12	12	6	5	11	3	5	4	6	8	4		1		242
South	34	39	30	22	16	12	8	9	12	22	20	9	8	5	5	5	4	5	3	4	8	11	13	19	323
Southwest	12	4	6	3					1	4	9	14	14	18	9	8	11	6	6	12	16	25	35	23	236
West											1	10	15	17	15	19	28	34	32	15	19	15	5	12	237
Northwest												8	8	8	6	16	8	6	7	14	7	4	1		93
Hour	0				4				8				12				16				20				Sum
(c) June 10–19																									
North	1	1	2	2	1					1	1	1		1			3		1		2		1		18
Northeast	4		6	10	4	3	8	3	6	4	1			1			6	4	5	1	5	1	3	1	76
East	1	3	7	11	15	22	15	9	10	1							1	7	10	10	3	6	1	2	134
Southeast	9	9	9	11	16	15	14	9	6	4	1	1	1					1	3	3	5	2	4	5	128
South	7	14	15	12	7	7	10	16	18	20	15	11	10	14	14	16	12	16	14	16	16	7	15	17	319
Southwest	18	12	10	4	2	5	7	13	14	14	17	27	30	25	30	27	29	28	24	19	23	30	22	10	440
West	16	11	5	5	11	7	5	9	6	9	21	16	15	16	10	11	6	3	3	7	6	12	13	20	243
Northwest	4	10	6	5	4	1	1	1		7	4	4	4	3	6	6	3	1		4		2	1	5	82
Hour	0				4				8				12				16				20				Sum

Data are wind direction at each direction and hour

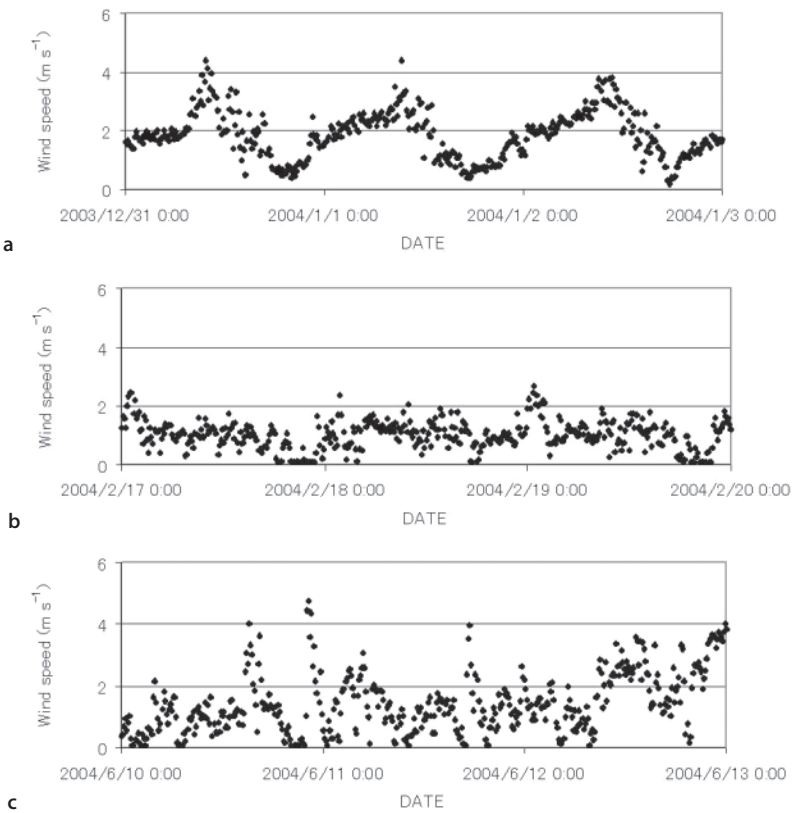

Fig. 2. Diurnal fluctuation of wind speed: **a** pattern A; **b** pattern B; **c** pattern C

1700 to 1900. Subsequently, θ shifted counterclockwise to the east by the next morning. Throughout period B, the winds were most frequently from the southeast, southwest, west, or south. In period C, θ was from the south or southwest at all times, except at 0600, when θ was from the east; the most frequent θ was from the southwest, but south and west were almost as frequent. Thus, the prevailing winds were from the south and west throughout periods B and C.

A 658-m peak is located 28 km northeast of the observation site. The east wind that prevailed in the early morning in periods B and C is thought to have been a mountain wind from this peak. These mountain winds were not observed in period A because they were overpowered by strong monsoon winds of about 2 m s^{-1}. Two processes may have contributed to the prevailing southerly and westerly winds in periods B and C. These winds may correspond to the monsoon winds from the north in period A, or they may form as valley winds that correspond to the early morning mountain wind. Although Lake Tonle Sap and the Gulf of Siam are located to the south and west of the study site, there is no valley near the tower. Therefore, the first process more likely describes the manner in which the prevailing winds formed.

5. Summary of Wind Speed and Direction Characteristics

The wind speed and direction phenomena observed from December 2003 to July 2004 can be summarized as follows. December was the dry season and a north wind blew from inland throughout the day, caused by the monsoon. Wind speeds fluctuated, and were maximal around 1000 to 1200 and minimal from 1800 to 2000. Beginning in late January, the direction of the monsoon gradually changed from north to between south and west; the last monsoon wind from the north was on March 10. The monsoon winds from the west to the south were not as strong as those from the north, and thus the local topography resulted in weak east winds in the early morning during these periods. At the start of the rainy season in May, brief strong winds caused by squalls were observed on some afternoons.

Morooka et al. (2002) and Saitoh et al. (2005) observed the diurnal and seasonal variation in wind directions and wind speed on Borneo. They reported that the wind speed fluctuated between a minimum at sunrise and a maximum at 1500 to 1600. There was a sea wind in the morning and a mountain wind in the afternoon, and the wind speeds were high from December through February as a result of the northeast monsoon.

By comparison, in the O Thom I basin, diurnal variation in wind speed was evident only during the northerly monsoon, and the influence of the local topography was apparent only in the early morning, when the monsoon winds were weak. Consequently, the seasonal variation in the monsoon exceeded the diurnal variation that resulted from the local topography. Our results may reflect the fact that the local topography was more homogeneous and farther from the ocean than that in Borneo.

6. Characteristics of the Roughness Length and Zero Plane Displacement Height Wind Profiles

In general, when atmospheric stability is neutral, the vertical wind profile over a forest canopy can be expressed as follows:

$$U(z) = \frac{U*}{\kappa} \ln\left(\frac{z-d}{z_0}\right) \quad (1)$$

where z is the observation height (m), U(z) is the wind speed ($m\,s^{-1}$) at height z, U_* is the friction velocity ($m\,s^{-1}$), d is the zero plane displacement height (m), z_0 is the roughness length (m), and κ is the von Karman constant. The parameters d and z_0 can be estimated as follows. First, d is determined to maximize the correlation coefficient between U(z) as the dependent variable and ln(z–d) as the independent variable. The slope and intercept of the resulting linear function are calculated to give $\frac{U*}{\kappa}$ and $\frac{U*}{\kappa}\ln(z_0)$, respectively. Then, z_0 is calculated from these values.

The stability length $\left(\frac{z-d}{L}\right)$ used to judge atmospheric stability is defined as follows:

$$\frac{z-d}{L}=\frac{\kappa g H(z-d)}{c_p \rho U_*{}^3 T} \tag{2}$$

where H is the sensible heat flux ($w\,m^{-1}$) reported by Shimizu et al. (2004), ρ is the air density ($kg\,m^{-3}$), and C_p is the specific heat of air at constant pressure ($J\,kg^{-1}\,m^{-3}$).

The averages and standard deviations of the roughness length (z_0) and zero plane displacement height (d) were calculated as 7.5 ± 6.6 m and 18.3 ± 6.9 m, respectively, when neutral stability was applied; atmospheric stability is judged to be neutral when the stability length is between –0.1 and 0.1 (Nakamura and Mahrt 2001) The numbers used to estimate the z_0 and d were 289 and 317 in the rainy and dry season, respectively. The average heights are 28% and 67%, respectively, of the average overstory height (h) of 27.2 m. Hattori (1985) reported values of $z_0\,h^{-1} = 0.02–0.14$ and $d\,h^{-1} = 0.61–0.92$ for coniferous forests. Arya (1988) noted that z_0 for forests is "several meters" and d is 70%–80% of the average canopy height. The ratios of $d\,h^{-1}$ (0.55) in this study are almost within the ranges noted by Hattori (1985) and Arya (1988). Malhi et al. (1998) determined the ratio of dh^{-1} as 0.67 in Central Amazonian rainforest, which is similar to this study. However, $z_0\,h^{-1}$ is greater than the maximum of the range reported by Hattori (1985); z_0 is in agreement with Arya (1988).

Figure 3 shows the dependence of z_0 and d on wind direction. Although the average z_0 and d in each direction vary, the standard deviations of z_0 and d are so great that the variations in z_0 and d in each direction are within the range of the standard deviations. Therefore, the dependence of z_0 and d on wind direction was not clearly established. No effects of canopy topography and land cover on tower observations were identified in this study. The short observation period in this study and the monsoon system cause the frequent wind directions to be only north-northeast and west-southwest. Moreover, the variation of d and z_0 in each wind direction is supposed to include the effect by wind speed dependency.

More detailed analysis will be performed in further studies.

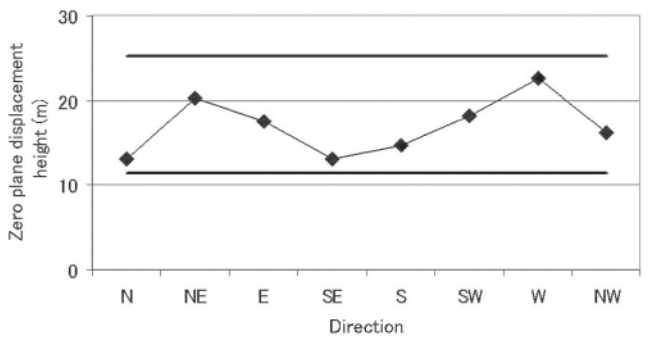

Fig. 3a,b. Dependency of zero plane displacement height and roughness length on wind direction. **a** Zero plane displacement height. *Upper and lower horizontal lines* show the range of total averaged height and standard deviation (18.3 ± 6.9 m). The variation of averaged height in each wind direction is within the range of standard deviation. **b** Roughness length. *Upper and lower horizontal lines* show the range of total averaged length and standard deviation (7.5 ± 6.6 m). The variation of averaged length in each wind direction is almost within the range of standard deviation

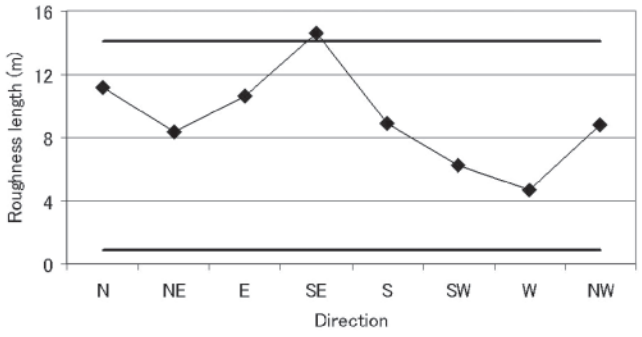

FIG. 3a,b. *Continued*

7. Conclusion

Regional patterns of circulation appear to be rarely caused by local topography, and the monsoons apparently dominate the meteorological system in the evergreen forest region of central Cambodia. Roughness length and zeroplane displacement height appeared to be independent of wind direction in this study. Thus, local topography and the undulating canopy surface around the tower had little effect on the tower flux observations. This observation indicates that flux has little spatial variation caused by local topography and the undulating canopy surface. Thus, the tower established in the evergreen forest is very suitable for observations of representative sensible heat fluxes from the evergreen forest of central Cambodia.

Acknowledgments. This study was funded by the Research Revolution 2002 Project of MEXT (Ministry of Education, Culture, Sports, Science and Technology), Japan.

References

Arya SP (1988) Introduction to micrometeorology. Academic Press, London

Chang J (1984) The monsoon circulation of Asia. In: Yoshino M (ed) Climate and agricultural land use in monsoon Asia. University of Tokyo Press, Tokyo, Japan, pp 3–34

Hattori S (1985) Explanation on the derivation process for equations to estimate evapotranspiration and problems with their application to forest stands (in Japanese). Bull For For Prod Res Inst 332:139–165

Malhi Y, Nobre AD, Grace J, Kruijt B, Pereira MG, Culf A, Scott S (1998) Carbon dioxide transfer over a Central Amazonian rain forest. J Geophys Res 103D:31593–31612

Morooka T, Kuraji K, Kumagai T, Suzuki M (2002) Characteristics of wind profile and turbulent flow above the tropical rain forest in Lambir National Forest, Sarawak* (in Japanese). Trans Jpn For Soc 113:151

* Title translated by the author

Nakamura R, Mahrt L (2001) Similarity theory for local and spatially averaged momentum fluxes. Agric For Meteorol 108:265–279
Saitoh TM, Kumagai T, Ohashi M, Morooka T, Suzuki M (2005) Nighttime CO_2 flux over a Bornean tropical rainforest (in Japanese). J Jpn Soc Hydrol Water Resour 18:64–72
Shimizu A, Nobuhiro T, Kabeya N, Tamai K, Kubota T, Tsuboyama Y (2004) Some observations on evapotranspiration in an evergreen broad-leaf forest watershed, Cambodia. In: Proceedings of the international conference on advances in integrated Mekong River management, Lao PDR, Vientiane 25–27 October 2004, pp 130–136

Stomatal Response Characteristics of Dry Evergreen and Dry Deciduous Forests in Kampong Thom, Cambodia

Kenichi Daikoku*, Shigeaki Hattori, Aiko Deguchi, Yuji Fujita, Makoto Araki, and Tatsuhiko Nobuhiro

We explored diurnal and seasonal variations in stomatal conductance in dry evergreen and dry deciduous forests in Cambodia and examined the stomatal response characteristics at two sites using a Jarvis-type model. Although stomatal conductance had maximum values at 9:00 (0900) or 10:00 (1000) in the morning and decreased continuously during the evening, transpiration showed peak values in the daytime and minimum values in the morning or evening at both sites in correspondence with the vapor pressure deficit. Stomatal conductance decreased in the rainy season to the late dry season; the pattern was clearer in the dry evergreen forest than in the dry deciduous forest. Stomatal conductance and volumetric soil water content had similar seasonal patterns, although these patterns differed between the dry evergreen and dry deciduous forests. The seasonal patterns of stomatal conductance and transpiration were different in the dry evergreen forest in the rainy season as a result of the moist air conditions. Clear differences were observed in maximum stomatal conductance and the function of the vapor pressure deficit between the two sites. In particular, compared to the results of other studies, the two sites showed large differences in their responses to the vapor pressure deficit. The functions of photosynthetically active radiation and the vapor pressure deficit showed wide daily change, suggesting that these factors may greatly impact the diurnal change of stomatal conductance. The vapor pressure deficit and volumetric soil water content also showed large seasonal variations and remarkable differences in function. The vapor pressure deficit had a large influence on stomatal conductance in the early dry season, whereas volumetric soil water content had a large effect in the late dry season.

1. Introduction

In the Mekong River basin, population increases and rapid economic development have led to deforestation that may threaten water resources and alter runoff characteristics. To forecast changes in water resources, the actual situation of the water cycle

* Graduate School of Bioagricultural Sciences, Nagoya University, Nagoya, Japan
E-mail: i051003d@mbox.nagoya-u.ac.jp

must be clarified. As forests cover an extensive area of the basin, forest transpiration plays a major role in the water cycle.

Stomata regulate the interaction of evaporative water exchange between plants and the atmosphere and may respond to several environmental variables. Therefore, stomatal conductance (g_s) is an important element in quantitative evaluations of transpiration from a forest to the air. A number of studies have examined stomatal conductance and associated variables. Observational studies have highlighted the interactions between the leaf surface and environmental factors, such as solar radiation, air temperature, and humidity (Roberts et al. 1990), and have provided large data sets benefiting model-based studies.

Jarvis-type (Jarvis 1976) and Ball-type (Ball et al. 1987) models have been used to model g_s and to examine the influence of environmental factors and functional modifications (Avissar et al. 1985; Massman and Kaufmann 1991). However, most studies have focused on spatial and vertical distributions of g_s based on parameters of land surface models or multilayer vegetation–air exchange models (Dolman et al. 1991). In contrast, few studies have highlighted the interaction between seasonal stomatal behavior and seasonal changes in environmental variables. Kosugi et al. (1995) minimized the overestimation of modeled g_s in spring and winter by using fitted model parameters for each season, but they did not detail why the parameters changed seasonally. Matsumoto et al. (2005) introduced a function representing the leaf chlorophyll concentration in a Jarvis-type model. The model was more accurate in autumn but still produced overestimates in spring. Moreover, studies that have focused on seasonal changes of g_s have mainly concentrated on temperate forests, and thus the seasonal behavior of stomata in tropical forests remains unclear.

Studies of various regions have indicated that light, soil and atmospheric moisture, and temperature conditions are the primary environmental variables affecting g_s (Kosugi 1995; Sirisampan et al. 2003). Several studies have compared maximum g_s (g_{smax}) and stomata response characteristics to changes in each of these environmental variables in diverse regions, seasons, and species. Kelliher et al. (1995) compared g_{smax} and maximum canopy conductance in various districts, and Körner (1994) reviewed g_{smax} in vegetation zones worldwide. However, few observational studies have collected data on g_s and local microclimates in seasonal tropical forests. Furthermore, comprehensive studies on leaf physiological traits of tropical trees do not exist for the Southeast Asian realms (Junrbandt et al. 2004). Fanjul and Barradas (1985) observed a pronounced midday closure of stomata in April caused by increased vapor pressure deficit (*VPD*) and low leaf water potential in tropical deciduous forests. However, their observations were only conducted in the dry season, and few studies have measured g_s year-round. Therefore, g_{smax} patterns and the influences of environmental variables such as light, soil and atmospheric moisture, and temperature on the seasonal behavior of stomata in seasonal tropical forests are largely unknown.

In this study, we examined g_s in dry evergreen (E_f) and dry deciduous (D_f) tropical seasonal forests, which are typical forest types in Cambodia. No previous studies have detailed the g_s characteristics of Cambodian tree species. Thus, we sought to assess the status of diurnal and seasonal changes in g_s of tree species in Cambodia and to clarify the characteristics of stomatal response to environmental factors in dry evergreen and dry deciduous forests.

2. Materials and Methods

2.1. Research Site

The study was conducted in Kampong Thom Province, central Cambodia (12°07′ N, 105°04′ E), in two plots approximately 5 km apart and having almost the same climatic conditions. The study sites were at altitudes less than 200 m above sea level. One plot was named E_f and the other was D_f. The E_f and D_f plots had mean tree heights of approximately 35.9 and 19.4 m and stem densities of 617 and 240 trees ha^{-1}, respectively. The leaf area indices (*LAI*, single-sided) ranged from 2.84 and 0.52 $m^2 m^{-2}$ in the dry season to 4.31 and 0.95 $m^2 m^{-2}$ in the rainy season at E_f and D_f, respectively. The D_f plot is a very sparse forest in comparison to deciduous forests in Cambodia. The D_f forest type consists of deciduous species but is not completely defoliated in the dry season. Annual rainfall measured at a height of 60 m on an observation tower was 1663.2 mm from May 2004 to April 2005, with the rainy season extending from May to November. The main soil type at both sites was an Acrisol.

2.2. Plant Material

Measurements of transpiration and g_s were conducted at six trees of five species at E_f and five trees of five species at D_f. At E_f, we examined *Mangifera dupperreana*, *Syzygium* spp., *Drypetes* sp., Myrsinaceae, and *Elaeocarpus*; at D_f, we examined *Dipterocarpus obtusifolius*, *Gluta laccifera*, *Parinari annamensis*, *Syzygium* spp., and *Calophyllum* sp.

2.3. Measurements of Stomatal Conductance, Transpiration, and Microclimates

Transpiration (T_r) and g_s were measured with a steady-state diffusion porometer (LI-1600; Li-Cor, Lincoln, NE, USA), which also measured photosynthetically active radiation (*PAR*), air temperature (T_a), and relative humidity. The vapor pressure deficit (*VPD*) was calculated from T_a and relative humidity by the following equation:

$$VPD = e_s(T_a)\left(1 - \frac{R_h}{100}\right) \quad (1)$$

where R_h is the relative humidity and $e_s(T_a)$ is the saturated vapor pressure at T_a.

Measurements were carried out on the same leaves every hour during three experimental periods: 29 November–1 December 2003 in the early dry season, 6–9 September 2004 in the rainy season, and 5–6 March 2005 in the late dry season. Hourly volumetric soil water content (*WC*) was measured with a soil moisture gauge (UIZ-ECH; Uizin, Tokyo, Japan) and a Decagon ECHO probe (Decagon, Pullman, WA, USA) at depths of 20, 50, 100, 150, 200, and 250 cm at E_f from December 2003 and also at 30 and 100 cm from May 2003 at D_f. We used data for the 150-cm depth at E_f and the 100-cm depth at D_f because these data sets had fewer missing observations during the steady-state diffusion porometer observations. We measured 2- to 3-m heights of

relatively light-exposed leaves. Thus, the measured leaves were beneath the upper canopy at E_f and at the surface of the canopy at D_f.

2.4. Modeling Procedure

A Jarvis-type model, which predicts the g_s proposed by Jarvis (1976), was applied for this analysis. Jarvis described the relationship between g_s and local climate in this model, where g_{smax} is reduced by functions associated with environmental variables. Previous studies have proposed numerous variables, including solar radiation, photon flux density, T_a, *VPD*, leaf water potential, *WC*, and atmospheric CO_2 concentration (Jarvis 1976; Stewart 1988; Sirisampan et al. 2003), and equations for each function (Avissar et al. 1985; Dolman and Van Den Burg 1988; Winkel and Rambal 1990). We used the variables *PAR*, *VPD*, T_a, and *WC* to estimate g_s and each functional form, expressed as follows:

$$g_s = g_{smax} \cdot f(PAR) \cdot f(T_a) \cdot f(VPD) \cdot f(WC) \tag{2}$$

$$f(PAR) = \frac{PAR}{PAR + \frac{g_{smax}}{k1}} \tag{3}$$

$$f(T_a) = \left(\frac{T_a - T_{min}}{T_{opt} - T_{min}} \right) \left(\frac{T_{max} - T_a}{T_{max} - T_{opt}} \right)^{\left(\frac{T_{max} - T_{opt}}{T_{opt} - T_{min}} \right)} \tag{4}$$

$$f(VPD) = \frac{1}{1 + \left(\frac{VPD}{VPD_{0.5}} \right)^{k2}} \tag{5}$$

$$f(WC) = 1 - \exp(WC_{min} - WC)^{k3} \tag{6}$$

where g_{smax} is the maximum stomatal conductance; T_{min}, T_{opt}, and T_{max} represent the minimum, optimum, and maximum T_a, respectively; $VPD_{0.5}$ is the *VPD* value when the function of *VPD* is equal to 0.5; WC_{min} is the minimum *WC*; and $k1$, $k2$, and $k3$ are coefficients showing the curvature of the response curve. The functions for *PAR*, T_a, and *VPD* have been referred to by Jarvis (1976) and Kosugi et al. (1995). A logarithmic function was fitted to *WC*. To determine parameter values, we used a nonlinear least squares technique in Microsoft Excel solver, which minimizes the root mean square errors (*RMSE*) between measured and predicted g_s. Table 2 shows nomenclatures in this study.

3. Results and Discussion

3.1. Diurnal and Seasonal Variations in Stomatal Conductance, Transpiration, and Environmental Factors

Diurnal and seasonal changes in mean g_s, T_r, *PAR*, *VPD*, T_a, and *WC* for two forests are shown in Fig. 1. Stomatal conductance followed a typical daily pattern (variation in each cell); peak values of g_s were recorded at approximately 1000 at E_f and 0900 at

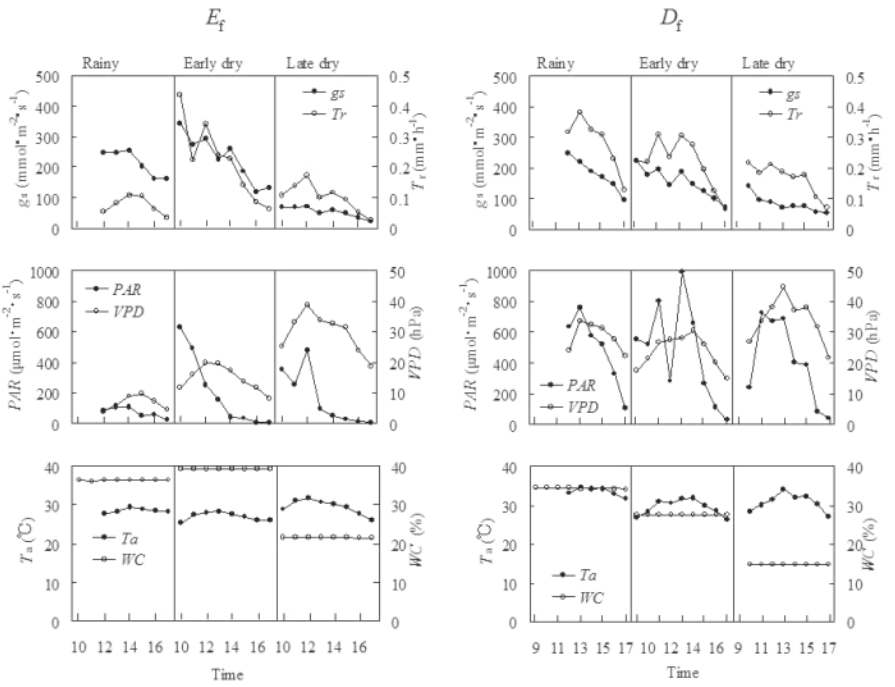

FIG. 1. Diurnal and seasonal changes in stomatal conductance (g_s) and micrometeorology at E_f (*dry evergreen forest, left*) and D_f (*dry deciduous forest, right*)

D_f, which marked the beginning of measurement and start of continuous decrease, respectively. The same diurnal pattern has been commonly reported from intraday measurements of g_s using porometers (Dolman and Van Den Burg 1988; Roberts et al. 1990; Juhrbandt et al. 2004). Körner (1994) noted that the most frequent diurnal change approximates a triangular shape, whereby *PAR* largely controls stomatal opening in early morning, followed by the reduction of g_s by the *VPD*, and later "time-dependent reduction" in the late afternoon. Transpiration showed maximum values in the daytime (1200–1400) and minimum values in the morning or evening at both sites; this pattern was almost identical to that of *VPD*. The transpiration peak appeared later than the peak of g_s because transpiration is influenced by not only g_s but also by *VPD*. The value of *PAR* at E_f was very weak compared to that at D_f, and more than 80% of the observation data was less than 200 $\mu mol\, m^{-2}\, s^{-1}$. This observation indicates that low-intensity light arrived at the lower layer of E_f, which had a denser canopy and much higher *LAI* than D_f. The *VPD* increased until 1200 and stayed within a narrow range from 1200 to 1400 before decreasing in the evening. *WC* was approximately constant all day and thus did not affect the diurnal variation in g_s. The diurnal T_a ranged from 31.8° to 25.5°C at E_f and from 36.4° to 26.4°C at D_f. Diurnal patterns of g_s, T_r, *VPD*, T_a, and *WC* were generally similar at the two forests, with the exception of the *PAR* pattern.

Stomatal conductance was high in the rainy season and low in the dry season (see Fig. 1; comparison between cells in horizontal row). The average g_s values in the rainy, early dry, and late dry seasons were 214, 230, and 54 mmol m^{-2} s^{-1} at E_f and 178, 152, and 82 mmol m^{-2} s^{-1} at D_f, respectively. The limitation of g_s was confirmed in the late dry season and was clearer at E_f than at D_f. Roberts et al. (1990) reported that g_s was lowest when the soil water potential reached its annual low; therefore, seasonal change in g_s at the sites may have been mostly influenced by *WC*. Both g_s and *WC* at our sites had minimum values in the late dry season. Moreover, *WC* at our sites showed similar seasonal patterns to g_s: 39.3% in the early dry season, >36.4% in the rainy season, and >21.6% in the late dry season at E_f.; 34.4% in the rainy season, >27.4% in early dry season, and >14.7% in the late dry season at D_f. The seasonal pattern of T_r was similar to that of g_s at D_f, although the patterns of g_s and T_r at E_f showed significant differences in the rainy season. Because the *VPD* at E_f was less than 10 hPa even at midday in the rainy season, transpiration would be limited by the moist air condition. The seasonal change in *PAR* was different at the two sites, with relatively high *PAR* in the dry season at E_f and lesser seasonal variation at D_f. The different seasonal change of *PAR* was explained by the greater *LAI* change, 2.84 to 4.31 at E_f and 0.52 to 0.95 at D_f, and the different measurement position beneath the upper canopy at E_f and at the surface of the canopy at D_f. The *VPD* indicated drastic seasonal change at E_f of 6.6, 14.6, and 29.6 hPa on average in the rainy, early dry, and late dry seasons, respectively. At D_f, *VPD* was consistently higher than at E_f, with values of 28.4, 23.5, and 33.9 hPa on average in the rainy, early dry, and late dry seasons, respectively. The value of *VPD* did not fall below 10 hPa at D_f even in the rainy season because of the high temperature and radiation reflecting the forest's sparse canopy. Little seasonal change occurred in T_a, which constantly stayed above 25°C. Differences in forest structure and measurement position between the two forests largely explained the differences in *PAR* and *VPD*.

3.2. Stomatal Responses to Environmental Factors and Determination of Model Parameters

To clarify stomatal behavior in response to environmental factors at each site, we investigated response characteristics found in our study and in previous studies using the Jarvis-type model. Figure 2 shows the relationships between the environmental variables and g_s observed at the sites (dots) and the fitting lines estimated by the model (lines). The E_f and D_f sites had g_{smax} values of 884 and 557 mmol m^{-2} s^{-1}, respectively. Stomata tended to close as *VPD* exceeded about 10 hPa at E_f and 30 hPa at D_f. Stomatal conductance showed light saturation and a hyperbolic response to *PAR*. The *PAR* value of light saturation was approximately 800 µmol m^{-2} s^{-1} at both E_f and D_f. Very narrow ranges of T_a were obtained; T_a values were higher at D_f than at E_f, with mean values of 31.0°C and 28.5°C, respectively. Hence, changes in T_{min} and T_{max} appear to have minimal impact on changes in g_s. Values of T_{opt} were slightly higher at D_f than at E_f. Stomatal conductance decreased logarithmically as *WC* declined. The g_s values at E_f showed a marked decline at *WC* less than 30%. The g_s values at D_f tended to gradually decrease if *WC* was less than 20%, but no drastic limitation of g_s was evident for the range of observation at D_f.

The model parameters fitted to the observation results are shown in Table 1. The *RMSE* values were 110.0 and 115.9 mmol m^{-2} s^{-1} at E_f and D_f, respectively. Matsumoto

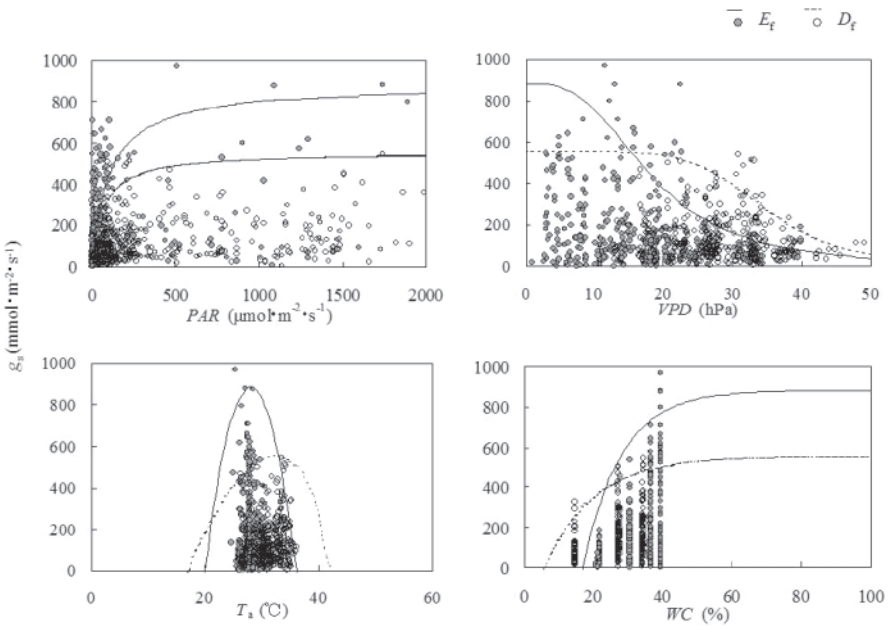

FIG. 2. Relationships between stomatal conductance (g_s) and the observed variables (*dots*) and fitted model equations (*lines*). *PAR*, photosynthetically active radiation; *VPD*, vapor pressure deficit; T_a, air temperature; *WC*, volumetric soil water content

TABLE 1. Fitted parameter values of the model

Parameter	E_f	D_f	Unit
g_{smax}	884	557	mmol m^{-2} s^{-1}
T_{min}	20.0	16.9	°C
T_{opt}	28.0	32.3	°C
T_{max}	36.0	41.2	°C
$k1$	8.3	8.0	
$VPD_{0.5}$	18.1	35.0	hPa
$k2$	3	6	
WC_{min}	17	6	%
$k3$	0.09	0.07	
RMSE	110.0	115.9	mmol m^{-2} s^{-1}

et al. (2005) calculated *RMSE* between predicted and measured g_s for 10 *Quercus serrata* trees and obtained a range from 36 to 87 mmol m^{-2} s^{-1}. Although our calculations included five or six species in each forest and did not consider physiological factors such as leaf nitrogen, leaf age, and chlorophyll concentration, the model predicted diurnal and seasonal trends of g_s, which suggests that the functional form in the model was appropriate.

To clarify the stomatal response characteristics at our sites, we compared the parameters in the model with those of other studies in various regions (Figs. 3–6) using error bars to evaluate the individual differences. Several data were read from figures in the paper. The g_{smax} values of our sites were relatively large compared to the average g_{smax} for various vegetation types and twice as large as those found for other tropical deciduous or tropical seasonal forests (Fig. 3). The $VPD_{0.5}$ and VPD values of the declining points at E_f were as low as those of temperate secondary forest, and the values at D_f were as high as those at similar types of tropical deciduous forest (Fig. 4). Oren et al. (1999) compared the sensitivity of the parameters of VPD, which was defined as the gradient ratio of the function, and

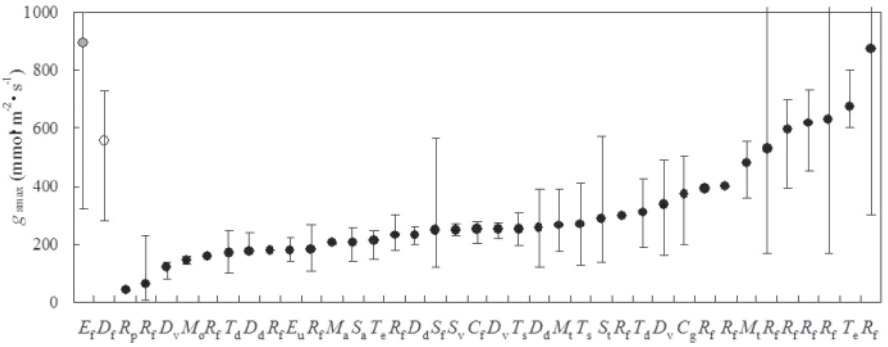

FIG. 3. Values of maximum stomatal conductance (g_{smax}) for various forest types. E_f, dry evergreen forest site; D_f, dry deciduous forest site; R_p, red pine trees; R_f, tropical rainforest; D_v, desert vegetation; M_o, monsoonal forest; T_d, temperate deciduous forest; D_d, tropical dry deciduous forest; E_u, *Eucalyptus* forest; M_a, mangrove forest; S_a, semiarid vegetation; T_e, temperate evergreen forest; S_f, temperate secondary forest; S_v, swamp vegetation; C_f, coniferous forest; T_s, tundra shrubs; M_t, Mediterranean trees; S_t, subalpine trees; C_g, temperate dry continental grassland (Fetcher 1979; Fanjul and Barrades 1985; Roberts et al. 1990; Winkel and Rambal 1990; Dolman et al. 1991; Massman and Kanfumann 1991; Körner 1994; Kosugi 1995; Reich et al. 1999; Kuno and Arai 2002; Matsuo and Kosugi 2002; Miki et al. 2002; Sirisampan et al. 2003; Juhrbandt et al. 2004; Iwata 2005)

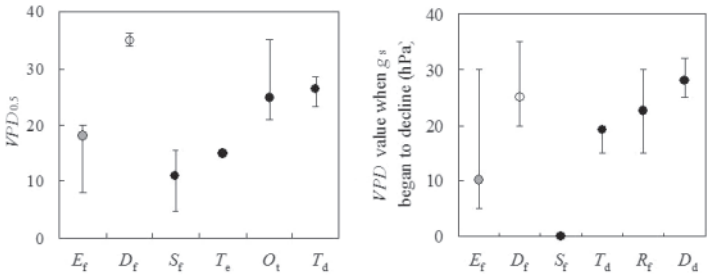

FIG. 4. Comparison of vapor pressure deficit (VPD) for various forest types. E_f, dry evergreen forest site; D_f, dry deciduous forest site; S_f, temperate secondary forest; T_e, temperate evergreen forest; O_t, oak trees; T_d, temperate deciduous forest; R_f, tropical rainforest; D_d, tropical dry deciduous forest (Fanjul and Barrades 1985; Dolman and Van Den Burg 1988; Furukawa 1995; Sirisampan et al. 2003; Hiyama et al. 2005; Iwata 2005)

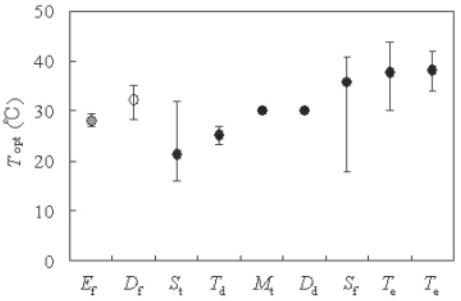

FIG. 5. The parameter T_{opt} (optimal air temperature) for various forest types. E_f, dry evergreen forest site; D_f, dry deciduous forest site; S_t, is subalpine trees; T_d, temperate deciduous forest; M_t, Mediterranean trees; D_d, tropical dry deciduous forest; S_f, temperate secondary forest; T_e, temperate evergreen forest (Fanjul and Barrades 1985; Winkel and Rambal 1990; Massman and Kanfumann 1991; Kosugi 1995; Sirisampan et al. 2003; Hiyama et al. 2005; Iwata 2005)

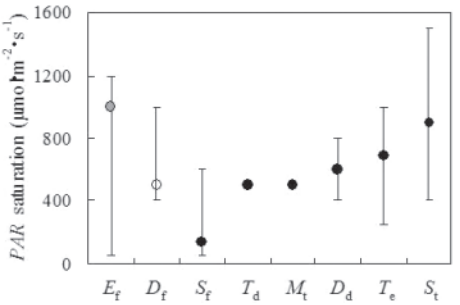

FIG. 6. The value of photosynthetically active radiation (*PAR*) saturation for various forest types. E_f, dry evergreen forest site; D_f, dry deciduous forest site; S_f, temperate secondary forest; T_d, temperate deciduous forest; M_t, Mediterranean trees; D_d, tropical dry deciduous forest; T_e, temperate evergreen forest; S_t, subalpine trees (Fanjul and Barrades 1985; Winkel and Rambal 1990; Massman and Kanfumann 1991; Kosugi 1995; Sirisampan et al. 2003; Iwata 2005)

reported that sensitivity would be higher in species with larger g_s. At our sites, g_{smax} was larger and g_s had a higher gradient ratio to *VPD* at E_f than at D_f. Hamada (2002) compared various regions from the tropics to the subarctic with regard to parameters that indicated sensitivity to *VPD*; the study showed that g_s tended to respond more sensitively in humid regions. Because the value of *VPD* at D_f was constantly more than 10 hPa, the continual dryness of the air could have caused g_s insensitivity to *VPD* at D_f. Hamada also indicated that warmer regions tend to have higher T_{opt}, which agrees with the higher T_{opt} and mean T_a at D_f (Fig. 5). The *PAR* value of light saturation at both sites was as high as that at other sites (Fig. 6).

The g_s responses at E_f and D_f were significantly different, despite being from contiguous sites. Clear differences were evident in g_{smax} and $VPD_{0.5}$ at the two sites. Responses to *VPD* particularly differed between the two sites, compared to findings of previous studies. Fanjul and Barradas (1985) suggested that sensitivity to *VPD* may be a useful adaptation to lower ambient humidity, also noting that active leaves with

Table 2. Nomenclature

D_f	Dry deciduous forest
E_f	Dry evergreen forest
g_s	Stomatal conductance (mmol m^{-2} s^{-1})
g_{smax}	Maximum stomatal conductance (mmol m^{-2} s^{-1})
LAI	Leaf area index (m^2 m^{-2})
PAR	Photosynthetically active radiation (μmol m^{-2} s^{-1})
T_a	Air temperature (°C)
T_{max}	Maximum air temperature for stomata opening (°C)
T_{min}	Minimum air temperature for stomata opening (°C)
T_{opt}	Optimum air temperature for stomata opening (°C)
T_r	Transpiration (mm h^{-1})
VPD	Vapor pressure deficit (hPa)
$VPD_{0.5}$	VPD value when g_s becomes 50% of g_{smax} (hPa)
WC	Volumetric soil water content at a depth of 150 cm at E_f and 100 cm at D_f (%)
WC_{min}	Minimum WC for stomata opening (%)

high radiation requirements in an arid environment indicate the presence of physiological adaptations to tolerate water stress. However, although stomatal closure may improve the water status of trees, a reduction in photosynthesis is also likely to occur (Jarvis and Morison 1981). These results indicate that the response of g_s to VPD may be the main cause of contrasting g_s responses to the environment at E_f and D_f, but the relationships among g_s, transpiration, and photosynthesis require further clarification.

3.3. Comparison Among Environmental Factors

We quantified the effect of each meteorological factor and compared the factors in relation to diurnal and seasonal changes in g_s by applying the Jarvis-type model. When a factor has a strong influence on stomata, the function of the factor in the Jarvis-type model has a large variation. Therefore, we evaluated the range of the function value as the influence of the meteorological factor. Figure 7 shows diurnal variation of the function of PAR, VPD, T_a, and WC in two forests. The functions of PAR and VPD changed substantially during the day. The daily range of the function of PAR was 0.85–0.04 at E_f and 0.94–0.30 at D_f. The influence of radiation was high at E_f compared to D_f because measurements at E_f were taken at a lower layer of canopy and PAR was limited. In contrast, the function of VPD had a daily range of 0.92–0.44 at E_f and 0.95–0.19 at D_f; the influence of VPD was higher at D_f than at E_f. However, little daily variation occurred in the function of T_a, and no daily variation was observed in the function of WC at either forest. Because each variable affecting stomatal behavior in the model was independent, the variance of each function was expressed dependently with g_s. Therefore, variabilities in the functions of PAR and VPD indicated that they have a major impact on the diurnal change in g_s; furthermore, the stability of the function of T_a indicated that T_a is always close to the optimum condition.

The seasonal mean values of each function are shown in Fig. 8. Remarkable seasonal changes were observed in VPD and WC functions, and the seasonal pattern of

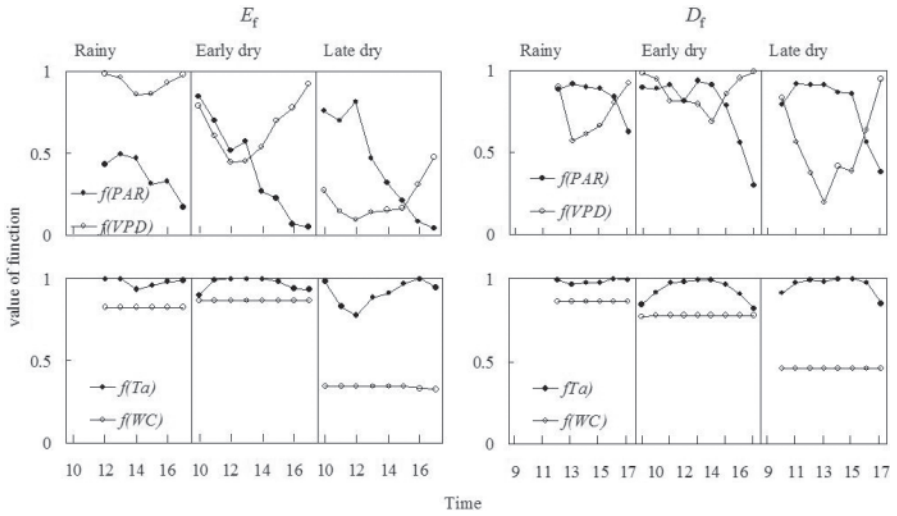

FIG. 7. Diurnal change in model functions at E_f (*left*) and at D_f (*right*)

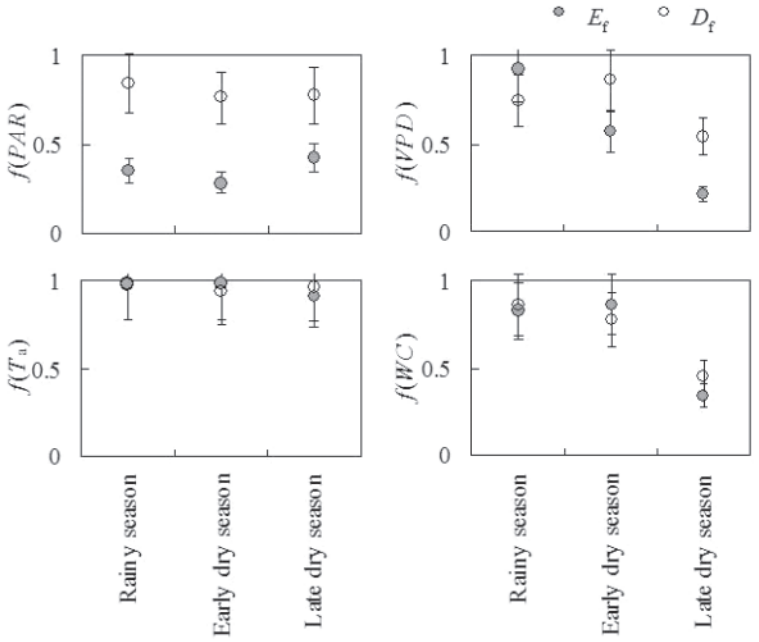

FIG. 8. Seasonal change in model functions

VPD differed between the two sites. At E_f the function of *VPD* decreased as drying proceeded from 0.92, 0.57, and 0.22 in the rainy, early dry, and late dry seasons, respectively; in contrast, the function of *VPD* was 0.75 and 0.86 in the rainy and early dry seasons and 0.54 in the late dry season at D_f. Because *VPD* values differed between E_f and D_f when g_s began to decline, the function of *VPD* at E_f decreased in the early dry season, while that at D_f did not vary until the late dry season. The function of *WC* was 0.82 at E_f and 0.86 at D_f in the rainy season and declined in the early and late dry seasons from 0.87 to 0.34 and from 0.78 to 0.46 at E_f and D_f, respectively. Because the function of *WC* showed a logarithmic decrease, the limitation effect became strong only in the late dry season when dryness became severe. Variation in the function of *PAR* was 0.35, 0.28, and 0.42 at E_f and 0.98, 0.94, and 0.96 at D_f in the rainy, early dry, and late dry seasons, respectively. Stomata tended to open in correspondence with increments of *PAR* by defoliation in the late dry season at E_f. The function of T_a was almost constant, ranging from 0.9 to 1.0 in both forests during the three seasons.

The magnitude of influence for each environmental function on seasonal change of g_s was $VPD > WC > PAR > T_a$. The influence of *VPD* and *WC* on seasonal change of g_s was about four and eight times greater than that of *PAR* and T_a, respectively. Matsumoto et al. (2005) compared the variability of each function and reported that the functions of *VPD* and T_a ranged from approximately 0.6 to 1.0 and 0.5 to 1.0, respectively. They also indicated that the variability in g_s depended on meteorological variables in the order of photon flux density > *VPD* > leaf temperature > soil matrix suction in a warm-temperate area and that the order did not change seasonally. Contrasting ranges were evident at our sites; *VPD* had a wider range and T_a had a narrower range. At our sites, the conditions of the rainy and dry seasons clearly appeared, and soil and air water conditions strongly influenced the seasonal variation of g_s. Our results showed that air and soil water drought have a great impact on g_s in different seasons, with *VPD* important in the early dry season and *WC* important in the late dry season. Moreover, the different seasonal changes in g_s between E_f and D_f were mainly caused by variation in the function of *VPD*, because *VPD* values differed between E_f and D_f when g_s began to decline.

4. Conclusions

We examined diurnal and seasonal changes in g_s for tree species in Cambodia and clarified the stomatal response characteristics to environmental factors in both dry evergreen and dry deciduous forests using a Jarvis-type model. Peak values of g_s were recorded at 0900 or 1000 and decreased continuously in the evening. Transpiration showed maximum values in the daytime and minimum values in the morning or evening at both sites, and the pattern was almost identical to that of *VPD*. Because the measured leaves were beneath the upper canopy of E_f, more than 80% of the observation data of *PAR* at E_f was less than $200\,\mu mol\,m^{-2}\,s^{-1}$. The seasonal change in g_s was high in the rainy season and limited in the late dry season; this feature was clearer at E_f than at D_f. The volumetric soil water content at our sites showed similar seasonal patterns as g_s and reflected the different seasonal patterns in g_s between E_f and D_f. The seasonal pattern of T_r was similar to that of g_s at D_f, although the patterns of g_s and T_r at E_f indicated a significant difference in the rainy season as a result of

the moist air conditions. *VPD* drastically increased from the rainy to late dry seasons at E_f, while that at D_f did not fall below 10 hPa even in the rainy season. Microclimate variables, particularly *PAR* and *VPD*, clearly differed between the two forests because of differences in forest structure; the dense canopy at E_f contrasted with the sparse canopy at D_f.

The g_s responses at E_f and D_f had significant differences despite the contiguous locations of the sites. Clear differences were evident in g_{smax} and $VPD_{0.5}$ at the two sites. The different responses to *VPD* between the two sites were particularly large compared to those at sites of other studies. This finding suggests that the differing g_s responses to environment conditions at E_f and D_f were mainly caused by the g_s response to *VPD*. Because the value of *VPD* at D_f was constantly more than 10 hPa, the continual dryness of the air could have caused insensitivity of g_s to *VPD* at D_f.

The functions of *PAR* and *VPD* changed greatly on a diurnal basis, indicating their major impact on the diurnal change in g_s. Remarkable seasonal changes were observed in the functions of *VPD* and *WC*. The function of *VPD* changed from 0.92 to 0.57 between the rainy and early dry seasons at E_f and from 0.86 to 0.54 between the early and late dry seasons at D_f, respectively. The function of *WC* declined between the early and late dry seasons from 0.87 to 0.34 and 0.78 to 0.46 at E_f and D_f, respectively.

The results also indicated that air and soil water drought have great impact on g_s in different seasons, with *VPD* having a greater influence in the early dry season and *WC* being influential in the late dry season. Furthermore, differing seasonal changes in g_s between E_f and D_f were likely caused by variation in the function of *VPD*, because stomatal response to *VPD* differed between E_f and D_f. High *VPD* even in the rainy season at D_f suggests that stomata can be open even under high *VPD* conditions to perform photosynthesis. As stomatal closure may ameliorate the water status of trees but also reduce photosynthesis, the relationships among g_s, transpiration, and photosynthesis require further clarification.

Acknowledgments. We thank Eriko Ito of the Forestry and Forest Products Research Institute and Mamoru Kanzaki of Kyoto University for their help in collecting *LAI* data and identifying tree species. We are also grateful to Drs. Akira Shimizu, Naoki Kabeya, and Koji Tamai for assisting with the observations. This study was funded by the Research Revolution 2002 Project of MEXT (Ministry of Education, Culture, Sports, Science and Technology), Japan.

References

Avissar R, Avissar P, Hahrer Y, Bravdo BA (1985) A model to simulate response of plant stomata to environmental conditions. Agric For Meteorol 34:21–29

Ball JT, Woodrow IE, Berry JA (1987) A model predicting stomatal conductance and its contribution to the control of photosynthesis under different environmental conditions. In: Biggens I (ed) Progress in photosynthesis research, vol IV. Proceedings of the VII international congress on photosynthesis. Martinus-Nijhoff, Dordrecht, Netherlands, pp 221–224

Dolman AJ, Van Den Burg GJ (1988) Stomatal behavior in an oak canopy. Agric For Meteorol 43:99–108

Dolman AJ, Gash JHC, Roberts J, Shuttleworth WJ (1991) Stomatal and surface conductance of tropical rainforest. Agric For Meteorol 54:303–318
Fanjul L, Barrades VL (1985) Stomatal behavior of two heliophile understorey species of a tropical deciduous forest in Mexico. J Appl Ecol 22:943–954
Fetcher N (1979) Water relations of five tropical tree species on Barro Colorado Island. Panama. Oecologia (Berl) 40:229–233
Furukawa A (1995) Final reports of research projects by The Global Environment Research Fund, E-2. Diversity of wildlife in tropical forest ecosystems: (1) Ecophysiological diversity in the formation of a crown (in Japanese). Global Environment Department, Tokyo, pp 70–87.
Hamada S (2002) An evapotranspiration characteristic of a Japanese red pine forest in Siberia and regionality of canopy conductance model parameters (in Japanese). Masters thesis. Iwate University, Morioka, Japan
Hiyama T, Kochi K, Kobayashi N, Sirisampan S (2005) Seasonal variation in stomatal conductance and physiological factors observed in a secondary warm-temperature forest. Ecol Res 20:333–346
Iwata N (2005) Scale-up procedure for transpiration in a secondary broad-leaved forest (in Japanese). Masters thesis, Nagoya University, Nagoya, Japan
Jarvis PG (1976) The interpretation of the variations in leaf water potential and stomatal conductance found in canopies in the field. Philos Trans R Soc Lond B 273:593–610
Jarvis PG, Morison JIL (1981) The control of transpiration and photosynthesis by stomata. In: Jarvis PG, Mansfield TA (ed) Stomatal physiology. Cambridge University Press, London, pp 247–279
Juhrbandt J, Leuschner C, Holscher D (2004) The relationship between maximal stomatal conductance and leaf traits in eight Southeast Asian early successional tree species. For Ecol Manag 202:245–256
Kelliher FM, Leuning R, Raupach MR, Shulze E-D (1995) Maximum conductances for evaporation from global vegetation types. Agric For Meteorol 73:1–16
Körner C (1994) Leaf diffusive conductances in the major vegetation types of the globe. In: Schulze E-D, Caldwell MM (eds) Ecophysiology of photosynthesis. Ecological studies, vol 100. Springer, Berlin, pp 463–490
Kosugi Y (1995) Measurement and modeling of stomatal conductance (in Japanese). J Jpn Soc Hydrol Water Resour 8:221–230
Kosugi Y, Kobashi S, Shibata S (1995) Modeling stomatal conductance in leaves of several temperate evergreen broadleaf trees. J Jpn Soc Reveget Tech 19:245–255
Kuno H, Arai K (2002) Effects of temperature and relative humidity on gas exchange rates of five species of broad-leaved trees (in Japanese with English summary). J Jpn Soc Reveget Tech 28:20–25
Massman WJ, Kanfumann MR (1991) Stomatal response to certain environmental factors: a comparison of models for subalpine trees in the Rocky Mountains. Agric For Meteorol 54:155–167
Matsumoto K, Ohta T, Tanaka T (2005) Dependence of stomatal conductance on leaf chlorophyll concentration and meteorological variables. Agric For Meteorol 132:44–57
Matsuo N, Kosugi Y (2002) Seasonal variation of the leaf-scale control of gas exchange in a temperate broad-leaved forest (in Japanese with English summary). J Jpn Soc Reveget Tech 28:14–19
Miki N, Hirai A, Sakamoto K, Nishimoto T, Yoshikawa K (2002) Diurnal change of stomatal conductance, transpiration rate, and photosynthetic rate in *Pinus densiflora* Sieb. et Zucc. saplings on different soil water conditions (in Japanese with English summary). J Jpn Soc Reveget Tech 28:103–108
Oren R, Sperry JS, Katul GG, Pataki DE, Ewers BE, Phillips N, Schäfer KVR (1999) Survey and synthesis of intra- and interspecific variation in stomatal sensitivity to vapour pressure deficit. Plant Cell Environ 22:1515–1526

Reich PB, Ellsworth DS, Walters MB, Vose JM, Gresham C, Volin JC, Bowman D (1999) Generality of leaf trait relationships: a test across six biomes. Ecology 80:1955–1969
Roberts J, Cabral OMR, De Aguiar LF (1990) Stomatal and boundary-layer conductances in an Amazonian terra firme rain forest. J Appl Ecol 27:336–353
Sirisampan S, Hiyama T, Hashimoto T, Fukushima Y (2003) Diurnal and seasonal variations in stomatal conductance in a secondary temperate forest (in Japanese with English summary). J Jpn Soc Hydrol Water Resour 16:113–130
Stewart JB (1988) Modeling surface conductance of pine forest. Agric For Meteorol 43:19–35
Winkel T, Rambal S (1990) Stomatal conductance of some grapevines growing in the field under a Mediterranean environment. Agric For Meteorol 51:107–121

Changes of Vertical Soil Moisture Conditions of a Dry Evergreen Forest in Kampong Thom, Cambodia

Makoto Araki*, Akira Shimizu, Jumpei Toriyama, Eriko Ito, Naoki Kabeya, Tatsuhiko Nobuhiro, Bora Tith, Sopheavuth Pol, Sopheap Lim, Saret Khorn, Phearak Pith, Seila Det, Seiichi Ohta, and Mamoru Kanzaki

Changes of soil water conditions in a soil profile were observed and estimated using a one-dimensional vertical soil water movement model for a dry evergreen forest area of Kampong Thom Province, Cambodia. The research site was in a dry evergreen forest where a meteorological observation tower had been established. Soil water matric potentials were measured at 20-, 50-, 100-, 150-, 200-, and 250-cm depths in an observation plot. Groundwater levels were observed at the site. Soil water matric potentials at each observation depth in a soil profile were simulated using a one-dimensional water movement model that was based on Richards' equation. Results of observations and simulation revealed the following. (1) The site's water-saturated zone was close to the ground surface during the rainy season. Water conditions in the unsaturated zone, which was above the groundwater level, were influenced strongly by groundwater. The groundwater level was 400 cm deep even in the dry season. The entire soil profile, from the surface to the bottom, never dried completely. (2) At the beginning of the rainy season, at the surface and subsurface depths of 20 cm and 50 cm, respectively, soil matric potentials were increased by rainfall events, which often supply water to the ground surface. Meanwhile, matric potentials at 200 and 250 cm depths were influenced directly by groundwater; they retained high potential values even during the dry season. In the middle zone, at depths of 100 and 150 cm, the soil was quite dried; the minimum matric potentials in the rainy season resembled those of the surface zone. (3) At the beginning of the dry season, matric potentials at 20- and 50-cm depths decreased because of soil water loss by transpiration of trees and evaporation from the ground surface. Matric potentials at 100- 150-, 200-, and 250-cm depths were positive because the groundwater level, which was raised to 50 cm deep during the rainy season, remained 100 cm deep during that period. (4) Soil water movement along the soil profile at the observation site was simulated using a one-dimensional vertical soil water movement model. Results of the simulation accorded well with observations of soil water conditions in both rainy and dry seasons. The model based on Richards' equation was applicable to this research area, a dry evergreen forest area.

* Forestry and Forest Products Research Institute (FFPRI), Tsukuba, Japan
E-mail: makot@ffpri.affrc.go.jp

1. Introduction

Water resources from the Mekong River are necessary to support the 56 million residents of the Mekong River basin. For that reason, elucidation of the water cycle of the forest area in the Mekong River basin is an important issue for effective utilization of water resources. Soil water conditions serve an important role in water conservation functions of forests, just as groundwater does. Fundamental forest soil water information must be accumulated with the intention of estimating the role of forests in the water cycle. As one component of that information, changes of vertical soil moisture conditions were observed and estimated for a dry evergreen forest area of Kampong Thom Province, Cambodia.

In this study, groundwater levels that indicated changes of the water-saturated zone and vertical soil water conditions as a main factor of soil water movements were observed through the seasons. Characteristics of soil water conditions were clarified using observation data; typical vertical soil water movement patterns were simulated using a one-dimensional soil water movement model based on Richards' equation for saturated and unsaturated soils (Richards 1931). Shimizu et al. (1995) studied unsaturated flow at different vegetation sites in Japan.

Those studies contribute basic data to hydrological research on forests in the Mekong River basin and contribute to estimative methods of soil water conditions over wide areas. Those results contribute to remote sensing hydrology through provision of soil water characteristic parameters that were applied to satellite data.

2. Site and Methods

2.1. Observation Site and Measuring Methods

Observation sites were located in dry evergreen forest areas of a flat landscape in Kampong Thom province in central Cambodia (Fig. 1). Dipterocarp trees were dominant in the site area. Major species at the site were *Vatica odorata, Myristica* species, *Anisoptera costata*, and *Dipterocarpus costatus* (Tani et al. 2007). The mean diameter at breast height and mean tree height of overstory trees were, respectively, 39.6 cm and 27.2 m (Nobuhiro et al. 2007). The mean annual temperature at the study area is 27°C. Annual rainfall is 1300–1900 mm with a pronounced dry season from November through February. The ground elevation was 90 m above sea level, geological conditions were quaternary sandy sediments, and geomorphological features were almost flat or slightly undulating. At this research site, a dry evergreen forest area, the soil profile consisted of a thin organic litter layer, with underlying A, B, and C horizons. The respective soil colors of the A and B horizons were dull orange or brown and light brownish-gray. The soil texture of the surface horizon was loamy sand; the subsurface horizon had a sandy loam texture. Deeper horizons had a sandy clay loam texture. The soil type was determined as Haplic Acrisols through observation of soil profile morphology and analyses of soil samples (Toriyama et al. 2007).

Groundwater levels were measured every morning with alarm measuring-tape observation wells from January 2004. In this report, groundwater levels at the soil water matric potential measuring point were estimated from the groundwater level

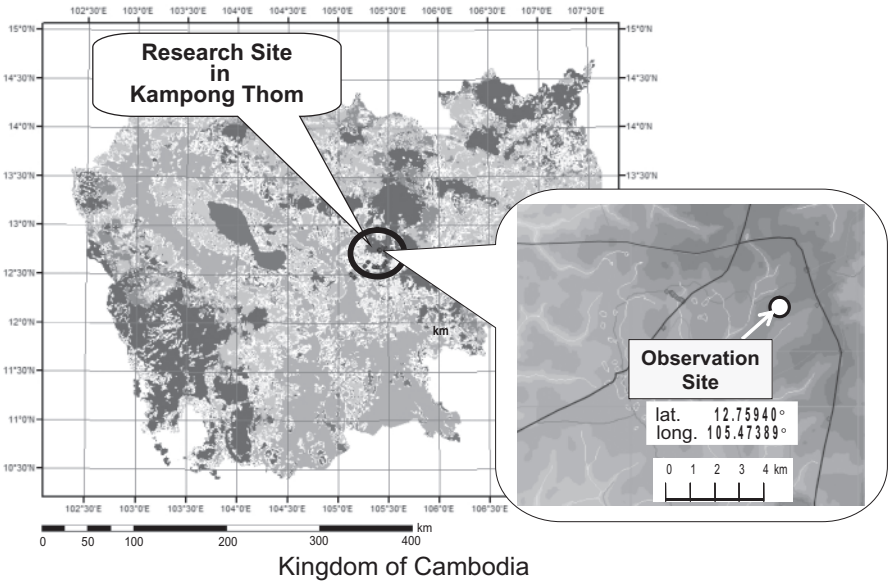

Fig. 1. Location of the observation site

of a nearest well and two other wells. Those three wells and soil observation points were serial along a very low gradient slope.

The soil water suction was measured automatically every hour at points of 20-, 50-, 100-, 150-, 200-, and 250-cm depths along a soil profile using an automatic tensiometer (UIZ-SMT; Uizin, Co., Ltd., Tokyo, Japan). In this chapter, soil water suction is called the matric potential. Although observations were begun in December 2003, data in 2004 were used for this analysis because data were approximately sufficient for it. Soil core samples were collected from the soil profile and measured using a constant head permeameter method to determine saturated hydraulic conductivity. In addition, the pressure-chamber method was used to measure soil water characteristics and other soil physical properties.

A meteorological observation tower and interception measuring plot were also located at the observation site. Groundwater observation wells and soil water measuring gauges were set in that observation site (Nobuhiro et al. 2007).

2.2. One-Dimensional Vertical Soil Water Movement Model

Soil water matric potentials at each observation depth in a soil profile were simulated using a one-dimensional water movement model that was based on Richards' equation. For this simulation, the following data were used: observed soil profile morphology, measured soil physical properties from soil sample analyses, onsite observed precipitation data, and groundwater levels at observation wells. Simulation periods were the beginning of the rainy season, May 2004, when several rainfall events were

recorded, and the beginning of the dry season, October–December 2004, when the rainless period started.

Initially, simulation of the rainy season specifically emphasized modeling the infiltration process and wetting of each soil horizon. At the beginning of the dry season, the simulation specifically addressed prediction of the reduced water matric potential at each soil horizon. After those simulations, comparisons between simulations and observation data represented relationships between measured parameters of soil physical properties as internal factors and environmental conditions as external factors: precipitation, groundwater level, etc.

3. Results and Discussion

3.1. Seasonal Change of Groundwater Level

Measured values of the groundwater level in saturated zones are presented in Fig. 2. Generally, the rainy season occurs during May–October; the dry season is from November to April (Top et al. 2004). The groundwater level increased day by day after the start of the rainy season and was recorded as 50 cm deep, the maximum, in August and September in both 2004 and 2005. After the start of the dry season, the groundwater level decreased each day; finally, it recorded a minimum in late April to early May.

During the rainy season in May it rained several times, but the groundwater level was recorded as minimum. A delayed response pertains between rainfall and the groundwater rise; for that reason, groundwater levels were lowest in May. Groundwater levels in May were 230–300 cm deep in both 2004 and 2005. In April–May the groundwater level was 240–280 cm deep; it was steady around 250 cm deep. The number of rainfall events and amount of precipitation were not steady in the early rainy season of June–July. Groundwater levels did not rise steadily; instead, they

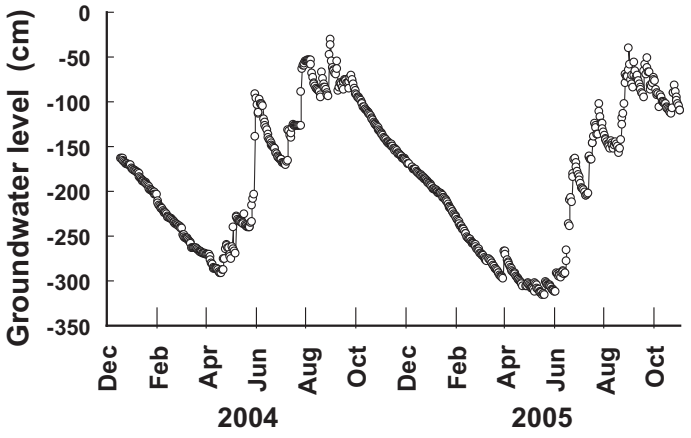

Fig. 2. Change of groundwater level at observation point

exhibited rapid fluctuations. In the middle of the rainy season, during August–September, groundwater levels were 50 cm deep, which is very close to the ground surface. After the dry season started, in mid-October to December, the groundwater level dropped from 100 cm to 150 cm deep. It had been decreasing slowly each day during 2 months; rapid fluctuation was not apparent. Those results can be summarized as follows.

The water-saturated zone was close to the ground surface during the rainy season at this site. Therefore, the water condition in the unsaturated zone was influenced by groundwater, although it was above the groundwater level. The groundwater level remained at 300 cm deep, even in the dry season. The total soil profile, from the surface to the bottom, did not dry completely.

3.2. Soil Water Matric Potentials at the Beginning of the Rainy Season and Dry Season

Changes of soil water conditions along a soil profile that were derived from vertical soil water movement are presented in Fig. 3. Immediately before the rainy season, on 1 May 2004, when the groundwater level was minimal, soil matric potentials were—650, −600, −720, −670, −130, and −50 cmH_2O, respectively, at 20-, 50-, 100-, 150-, 200-, and 250-cm depths. Matric potentials at the 200- and 250-cm depth indicated values that were derived from capillary rise of groundwater, which was 300 cm deep. The matric potentials reflected the water capillary rise from the groundwater surface in the soil profile zone, which is deeper than 200 cm. In the zone of the soil profile shallower than 50 cm deep, where groundwater was not supplied sufficiently by capillary rise, the matric potentials were decreased by drying. At 100- and 150-cm

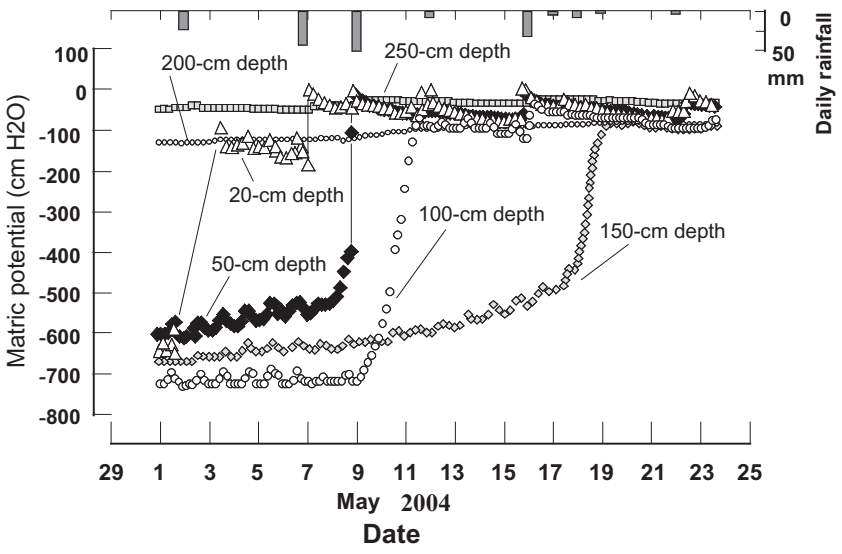

Fig. 3. Observed soil water matric potentials at a soil profile: start of the rainy season

depths, the matric potentials were too low to be estimated from capillary rise from groundwater. Those values were nearly equal to those at the 20-cm and 50-cm depths. Capillary rise was incapable of reaching zones that were less than 150 cm deep because the soil texture was sandy; it had insufficient clay and silt contents to retain fine pores, which facilitate the capillary rise of groundwater.

In the afternoon of 1 May 2004, 23 mm precipitation was recorded. Its supplied water raised the soil matric potential at the 20-cm depth from −650 cmH_2O to −140 cmH_2O. On 7 May, about 40 mm precipitation raised the matric potential at the 20-cm depth to −30 cmH_2O. The 50-mm precipitation recorded on 8 May raised the matric potential at 50-cm depth to −30 cmH_2O as well. In the deep profile zone, the 250-cm depth, the matric potential rose according to the rising groundwater level by daily precipitation; it reached −27 cmH_2O. In the middle profile zone, 100–150 cm in depth, the soil was dried: matric potentials at 100-cm and 150-cm depths were steady at −600 to −700 cmH_2O during the same periods. Those steady values resulted from the constant demand for soil water for transpiration through the root systems of trees. The water supply from groundwater through the capillary rise was limited to depths that were close to the groundwater level. It was unable to reach the middle zone above 150 cm deep. The groundwater level was regulated not only by water that infiltrated from the upper soil horizons but was also influenced over a wide area as a watershed. In other words, changes of groundwater levels were influenced spatially by precipitation in the watershed. Water infiltration rates of surface soil were lower than for other forests in this area (Ohnuki et al. 2007). Therefore, it took a long time to redistribute rainfall to soil water in deeper zones. During the dry season, the actual water storage capacity (WSC) had been increased (Shinomiya et al. 2007), and soil had held much WSC at the beginning of the rainy season. Also for those reasons, the potential levels at 100 cm and 150 cm deep were steadily low. Therefore, rising matric potentials require sufficient cumulative precipitation after the start of the rainy season. The matric potential at the 100-cm depth had become −90 cmH_2O on 11 May, when 8-mm precipitation was recorded. Cumulative precipitation reached 60 mm by 19 May, and the matric potential at the 150-cm depth rose to −80 cmH_2O. Finally, when the cumulative precipitation had become 100 mm on 31 May, matric potentials were greater than −100 cmH_2O throughout the soil profile. By the end of May, the early rainy season, the entire soil profile showed a wet condition by rainfall events. However, the groundwater level was stable at the 250-cm depth during this period. Then, soil water infiltrated vertically according to a hydraulic gradient that was affected mainly by gravitational potential. Regarding soil water matric potentials during October–December 2004, the early dry season is represented in Fig. 4. After only 3-mm precipitation was recorded on 10 October, no precipitation occurred until 24 November 2004. On 25 November, it rained 5 mm. There was less than 1-mm of rainfall on each day of 26 November and 2 December 2004. After those rainfall events, no rainfall events occurred through March 2005.

The matric potential at 20-cm depth was −30 cmH_2O on 10 October. By 15 December, it had decreased to −750 cmH_2O. During that period, the matric potential at the 50-cm depth was −50 cmH_2O. It decreased to −790 cmH_2O, during which time the groundwater level decreased from 80 to 170 cm deep. Then, matric potentials at 100-, 150-, 200-, and 250-cm depths were from 20 to −60 cmH_2O, from 70 to −6 cmH_2O, 110 to 25 cmH_2O, and 160 to 70 cmH_2O, respectively, during 10 October–15 December. Soil matric

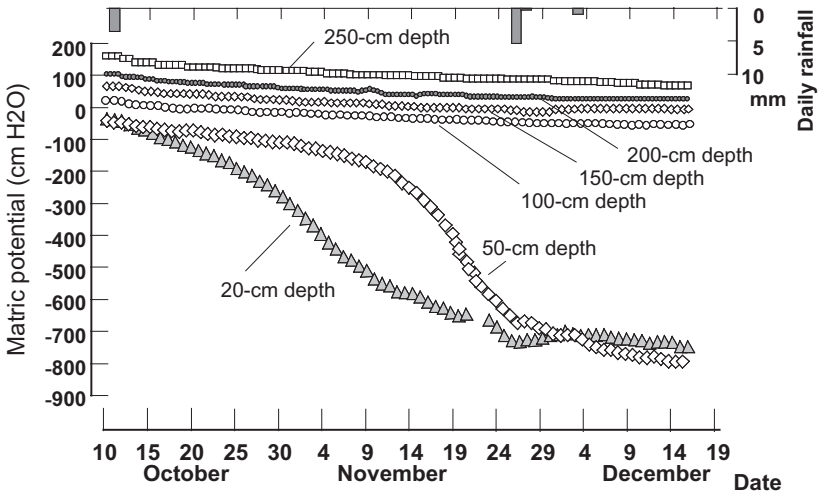

FIG. 4. Observed soil water matric potentials at a soil profile: start of the dry season

potentials recorded positive pressure conditions in soil profile zones deeper than 100 cm. Each matric potential reflected differences of the groundwater level. Soil was moist or wet in the soil profile during the dry season. Therefore, transpiration had not decreased extremely and continued at a high rate (Nobuhiro et al. 2007).

3.3. Saturated-Unsaturated Flow Model Application

At the beginning of the rainy season, in May 2004, when it began to rain and rainfall events occurred several times, soil matric potentials were estimated using the simulation model. In addition, at the beginning of the dry season, during October to December 2004 when rainfall stopped, soil matric potentials were estimated. The periods of simulation were identical to those of the observations already described. The simulation model that was applied to estimation of soil water matric potentials is represented in the following subsection.

3.3.1. Model Equations

One-dimensional water movement in saturated-unsaturated porous medium is generally described using a modified form of Richards' equation (Richards 1931) using Darcy's law (Eq. 2) and the equation of continuity for water (Eq. 3) as follows.

$$\frac{\partial \theta}{\partial t} = \frac{\partial}{\partial x}\left[K\left(\frac{\partial h}{\partial t} + \cos\beta \right) \right] - Sink \tag{1}$$

In that equation, h is the water pressure head, θ is the volumetric water content, t is time, x is the spatial coordinate (positive upward), $Sink$ is the sink term and root water uptake, β is the angle between the flow direction and the vertical axis (for example, $\beta = 0°$ for vertical flow, 90° for horizontal flow, and $0° < \beta < 90°$ for inclined flow), and K is the unsaturated hydraulic conductivity function (Eq. 4).

Darcy's law is expressed as the following:

$$q = K\, grad H \tag{2}$$

Therein, H is the hydraulic head ($H = h + x$); q is the soil water flux.

The equation of continuity for water is the following:

$$\frac{\partial \theta}{\partial t} = \frac{\partial q}{\partial x} - Sink \tag{3}$$

The equation of van Genuchten (1980) was used as a soil moisture characteristic curve.

$$\theta(h) = \begin{cases} \theta_r + \dfrac{\theta_s - \theta_r}{\left[1 + |\alpha h|^n\right]^m} & h < -2\,\text{cm} \\ \theta_s & h \geq -2\,\text{cm} \end{cases} \tag{4}$$

The unsaturated hydraulic conductivity function is the following

$$K = K_s \times S^l [1 - (1 - S^{1/m})^m]^2 \tag{5}$$

Therein, $m = 1 - 1/n$, $n > 1$, and K_s is the saturated hydraulic conductivity. Parameter l associated with pore connectivity was estimated as about 0.5 as an average for many soils (Mualem 1976). Furthermore, α and n are fitting parameters.

As defined below, S is the effective water content or degree of saturation.

$$S = \frac{\theta - \theta_r}{\theta_s - \theta_r} \tag{6}$$

In that equation, θ_r and θ_s, respectively, denote the residual and saturated water contents.

3.3.2. Space and Time Discretization

Actual calculations were performed using HYDRUS-1D (Simunek et al. 1998). The basic method of discretization was explained generally.

The soil profile is first discretized into 13 adjoining elements. A mass-lumped linear finite-element scheme was used for discretization of the mixed form of the Richards' equation (Eq. 1) as follows:

$$\frac{\theta_i^{j+1,k+1} + \theta_i^j}{\Delta t} = \frac{1}{\Delta x}\left(K_{i+\frac{1}{2}}^{j+1,k} \frac{h_{i+1}^{j+1,k+1} - h_i^{j+1,k+1}}{\Delta x_i} - K_{i-\frac{1}{2}}^{j+1,k} \frac{h_i^{j+1,k+1} - h_{i-1}^{j+1,k+1}}{\Delta x_{i-1}} \right) + \frac{K_{i+\frac{1}{2}}^{j+1,k} - K_{i-\frac{1}{2}}^{j+1,k}}{\Delta x} - Sink_i^j \tag{7}$$

In the equation above, the following pertain.

$$\Delta t = t^{j+1} + t^j,\ \Delta x = \frac{x_{i+1} + x_{i-1}}{2},\ \Delta x_i = x_{i+1} - x_i,\ \Delta x_{i-1} = x_i - x_{i-1},$$

$$K_{i+\frac{1}{2}}^{j+1,k} = \frac{K_{i+1}^{j+1,k} + K_i^{j+1,k}}{2},\ K_{i-\frac{1}{2}}^{j+1,k} = \frac{K_i^{j+1,k} + K_{i-1}^{j+1,k}}{2}$$

Table 1. Parameters of soil physical properties

Depth (cm)	Ks ($cm\,s^{-1}$)	θs ($m \cdot m^{-3}$)	Θr ($m \cdot m^{-3}$)	Δx (cm)
0–20	1.472×10^{-3}	0.444	0.001	20
20–40	7.551×10^{-4}	0.362	0.001	20
40–60	1.020×10^{-3}	0.396	0.001	20
60–80	7.300×10^{-4}	0.401	0.001	20
80–100	1.608×10^{-3}	0.374	0.067	20
100–120	9.371×10^{-4}	0.381	0.01	20
120–140	1.164×10^{-3}	0.409	0.01	20
140–180	4.643×10^{-4}	0.376	0.01	20
180–200	1.086×10^{-3}	0.401	0.01	20
200–260	3.639×10^{-4}	0.394	0.01	20

Ks, saturated hydraulic conductivity; θs, saturated volumetric water content; Θr, residual soil water content; Δx, vertical increment of mesh

Therein, subscripts $i - 1$, i, and $i + 1$ indicate positions in the finite difference mesh, and superscripts k and $k + 1$, respectively, denote the previous and current iteration levels. Superscripts j and $j + 1$, respectively, represent the previous and current time levels. Equation 6 is based on a fully implicit discretization of the time derivative. It is solved using a Picard iterative solution scheme. The output time step time for calculation is 60 min and mesh size is 20 cm. Boundary conditions were determined using the observed values: evaporation from the forest floor (Hattori et al. 2004), the evapotranspiration rate and rainfall (Nobuhiro et al. 2007), and the groundwater level (see Fig. 2). In addition, the root distribution was determined through soil profile surveys to 260-cm depth and used as the root parameter. The evaporation rate was $0.5\,mm \cdot day^{-1}$, transpiration was $4.5\,mm \cdot day^{-1}$ during the beginning of the rainy season, and $0.1\,mm \cdot day^{-1}$ and $5.2\,mm \cdot day^{-1}$, respectively, during the beginning of each dry season. It was assumed that evaporation occurred on the surface of the forest floor. It was further assumed that transpiration occurred along the soil profile to 260-cm depth during the daytime (0600–1800) but ceased during rainfall events. Parameters are shown in Table 1 for this simulation.

3.3.3. Simulation Results

Soil water matric potentials at 20-, 60-, 100- 160-, 200-, and 260-cm depths, which correspond approximately to observation points, were estimated using the simulation model.

Actual observation results of the beginning of the rainy season were well reproduced by estimation results (Fig. 5). Data for the matric potential at surface soil profiles indicate that the 20-cm depth was increased rapidly from the initial dried condition ($-600\,cmH_2O$) after the rainfall event on the afternoon of 1 May. This estimation was too rapid a response compared with actual observation results. However, after early steps, the increasing matric potential of estimation agreed well with the observation results in terms of the response time and amount. In addition, at 60-cm depth, the matric potential was raised rapidly from the initial dried condition after a

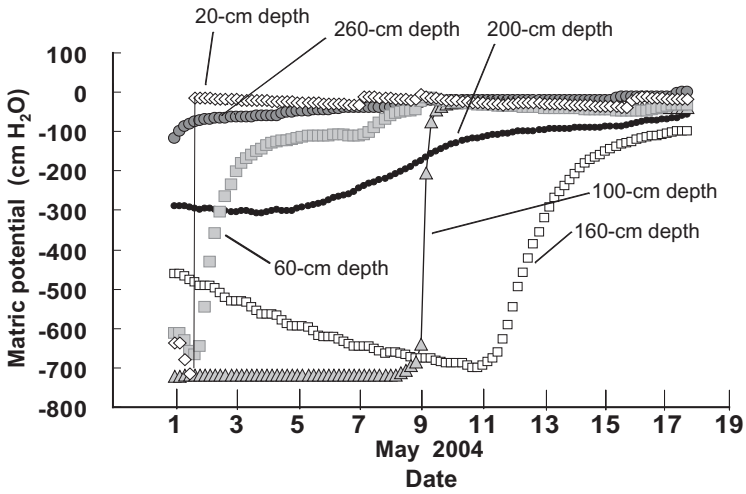

FIG. 5. Simulated soil water matric potentials at a soil profile: start of the rainy season

rainfall event in early May. After those steps, the matric potential of estimation agreed well with observed results. Matric potential at 100-cm depth indicated an overly dried condition: $-700\,cmH_2O$. However, it rose gradually, just as with actual observations, by infiltration of rainfall water. The matric potential at the 160-cm depth, where groundwater exerted no influence, rose through infiltration of rainfall and agreed well with actual observations. In a deeper zone, with 200- and 260-cm depths, the soil profile was wet and matric potentials were high because of the water supply from groundwater. Those estimation results also agreed well with actual observations. Estimations showed a gentle increase of the matric potential curve.

Estimation results for the beginning of the dry season, 10 October to 15 December 2004, are presented in Fig. 6. Actual observed results in that period for soil moisture conditions decreased steadily because of the lack of precipitation. Matric potentials at 20- and 60-cm depths were about $-30\,cmH_2O$ on 10 October; profiles showed wet conditions then. At the end of the estimation period on 15 December, those matric potentials were, respectively, $-820\,cmH_2O$ and $-750\,cmH_2O$. Those results accorded well with actual observations. Estimated curves of the 20-cm depth represented a decreasing trend from the time it started. The curve ceased declining and became steady when matric potentials reached $-800\,cmH_2O$. Simultaneously, the estimation curve of 60-cm depth showed a gradually declining trend from the start point; it subsequently began a rapid decline. Finally, it became steady. Those estimations accorded well with actual observations. Then, estimation of the model was confirmed also for the dry season. Meanwhile, estimation results of 100-cm depth started at $-20\,cmH_2O$, which was an almost saturated condition, similarly to those of the upper two horizons. It decreased gradually, i.e., it dried slowly. Observed drying curves were more gently sloping than the estimated ones. Actual observation data at points deeper than 150-cm depth, i.e., 150-, 200-, and 250-cm depths, represented positive pressures at the start time because the groundwater level was 80 cm deep. Groundwater levels

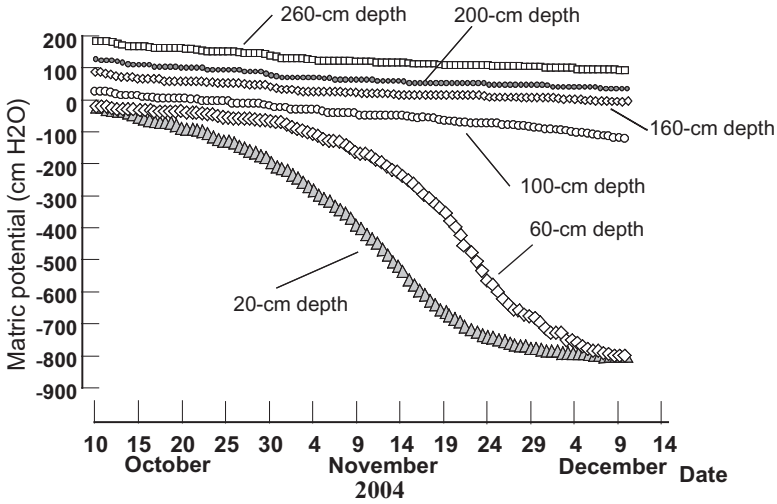

Fig. 6. Simulated soil water matric potentials at a soil profile: start of the dry season

decreased gradually; finally reaching 160-cm depth. States of soil water matric potentials at points deeper than 160-cm depth were mostly reproduced using the estimation model. Estimation of soil moisture conditions in the fluctuation zone of groundwater level requires exact groundwater level data.

Thus, results obtained using a one-dimensional vertical soil water movement model accorded well with actual observation data in an alluvial plain area central Cambodia during both rainy and dry seasons. Those results showed that the estimation model reproduced water movements exactly with observed precipitation, soil properties, and boundary conditions derived from soil profile investigations and analyses of soil samples. Predicted data from estimation models are fundamental information to evaluate wide-area soil water conditions and corroborate satellite data. It will produce important validation data for remote sensing. In the next step, when two-dimensional or three-dimensional behavior of groundwater is analyzed, these results are expected to improve prediction accuracy.

4. Summary

Changes of the soil water matric potential at each soil horizon in a profile had different patterns. At the surface and subsurface, at 20- and 50-cm depths, soil matric potentials increased because of rainfall events that often supplied water to the ground surface at the beginning of the rainy season. Matric potentials at 200-cm and 250-cm depths were influenced directly by groundwater, which maintained high potential values even in the dry season. The potentials did not rise rapidly, even in the rainy season, because groundwater levels did not rise soon after the start of the rainy season. In the middle depth zone, at 100-cm and 150-cm depths, soil was thoroughly dried and matric potentials were minimal in the dry season, just as they were at the

surface zone; these were derived mainly from evapotranspiration of trees. Furthermore, because the capillary rise of groundwater was limited by distance from the groundwater level, the water supply from groundwater was insufficient in that zone. In addition, in that zone, matric potentials did not increase soon after the start of the rainy season. The minimum infiltration rate prevented a smooth water supply to deeper zones. Consequently, the actual water storage capacity increased during the dry season. For that reason, matric potentials must increase when the accumulated precipitation reaches some amount. Matric potentials at 20-cm and 50-cm depths decreased gently but steadily at the beginning of the dry season, as derived through soil water loss by transpiration of trees and evaporation from the ground surface. Matric potentials at 100-, 150-, 200-, and 250-cm depths were positively affected by groundwater because groundwater levels that were raised to 50 cm deep during the rainy season remained at 100 cm deep until the beginning of the dry season. Groundwater levels were recorded as deeper than 200 cm in January–February, and minimum levels were recorded in May. Therefore, even in the dry season, matric potentials at the 200-cm and 250-cm depths were not too low for tree growth.

According to predicted results of soil water movement along a soil profile in the observation site, results obtained using a one-dimensional vertical soil water movement model accorded well with observed soil water conditions of the soil profile in both rainy and dry seasons. This model, based on Richards' equation, has applicability to this research area: a dry evergreen forest area of Cambodia. In this report, observed morphological features of the soil profile, analyzed soil physical properties, observed precipitation, and groundwater level were used for parameters and boundary conditions. Agreement of the results of simulation estimations and actual observations was found. Therefore, the estimation model is inferred to be useful for application to Cambodian forests.

Acknowledgments. We thank Mr. Chann Sophal and the staff of Forestry Administration for their arrangement and assistance in field surveys in the Cambodian forests. This research was carried out as a part of a research project Model Development for the Prediction of Water Resources Changes due to Natural Variation and Human Modification in the Asia Monsoon Region, funded by the Ministry of Education, Culture, Sports, Science, and Technology, Japan.

References

Hattori S, Deguchi A, Daikoku K (2004) Characteristics of transpiration in leaf-scale and forest floor evaporation in dry evergreen and dry deciduous forests in O Thom I watershed. In: Sawada H, Chann S, Shimizu A, Araki M (eds) Proceedings of the international workshop on forest watersheds 2004, Phnom Penh, Cambodia, 29 October 2004, pp 67–72

Mualem Y (1976) A new model for predicting the hydraulic conductivity of unsaturated porous media. Water Resour Res 12(3):513–522

Nobuhiro T, Shimizu A, Kabeya N, Tsuboyama Y, Kubota T, Abe T, Araki M, Tamai K, Chann S, Keth N (2007) Year-round observation of evapotranspiration in an evergreen broadleaf forest in Cambodia. In: Sawada H, Araki M, Chappell NA, LaFrankie JV, Shimizu A (eds) Forest Environments in the Mekong River Basin. Springer, Tokyo, pp 75–86

Ohnuki Y, Kimhean C, Shinomiya Y, Sor S, Toriyama J, Ohta S (2007) Seasonal change of soil depth and soil hardness at forested areas in Kampong Thom Province, Cambodia. In: Sawada H, Araki M, Chappell NA, LaFrankie JV, Shimizu A (eds) Forest Environments in the Mekong River Basin. Springer, Tokyo, pp 263–272

Richards LA (1931) Capillary conduction of liquids through porous mediums. Physics 1:318–333

Shimizu A, Kitahara H, Mashima Y (1995) Change of soil moisture in areas with different vegetation and result of artificial precipitation experiment. IUFRO World Congress XX:24

Shinomiya Y, Araki M, Toriyama J, Ohnuki Y, Shimizu A, Kabeya N, Nobuhiro T, Kimhean C, Sor S (2007) Effect of soil water content on water storage capacity: comparison between the forested areas in Cambodia and Japan. In: Sawada H, Araki M, Chappell NA, LaFrankie JV, Shimizu A (eds) Forest Environments in the Mekong River Basin. Springer, Tokyo, pp 273–280

Simunek J, Sejna M, van Genuchten MT (1998) Simulating water flow, heat, and solute transport in one-dimensional variably saturated media. U.S. Salinity Laboratory, USDA, ARS, Riverside, CA

Tani A, Ito E, Kanzaki M, Ohta S, Khorn S, Pith P, Tith B, Pol S, Lim S (2007) Principal forest types of three regions of Cambodia: Kampong Thom, Kratie, and Mondolkiri. In: Sawada H, Araki M, Chappell NA, LaFrankie JV, Shimizu A (eds) Forest Environments in the Mekong River Basin. Springer, Tokyo, pp 201–213

Top N, Mizoue N, Kai S (2004) Estimating forest biomass increment based on permanent sample plots in relation to woodfuel consumption. J For Res 9:117–123

Toriyama J, Ohta S, Araki M, Kanzaki M, Khorn S, Pith P, Lim S, Pol S (2007) Soils under different forest types in the dry evergreen forest zone in Cambodia: morphology, physicochemical properties, and classification. In: Sawada H, Araki M, Chappell NA, LaFrankie JV, Shimizu A (eds) Forest Environments in the Mekong River Basin. Springer, Tokyo, pp 241–253

van Genuchten MT (1980) A closed-form equation for predicting the hydraulic conductivity of unsaturated soils. Soil Sci Soc Am J 44:892–898

Stable Isotope Studies of Rainfall and Stream Water in Forest Watersheds in Kampong Thom, Cambodia

Naoki Kabeya*, Akira Shimizu, Sophal Chann, Yoshio Tsuboyama, Tatsuhiko Nobuhiro, Nang Keth, and Koji Tamai

Stable isotopes, such as deuterium (D) and oxygen-18 (^{18}O), are widely used in hydrology as environmental tracers because they move with the water itself. Information obtained from stable isotope data can improve our understanding of the processes associated with the source of water and system dynamics and also provide quantitative estimates related to flow dynamics and transport parameters. In this chapter, stable isotope ratios (δD, $\delta^{18}O$) of rainfall and stream water were studied from 2003 in four forest watersheds in the Kampong Thom Province of Cambodia. The stable isotope ratios of rainfall during the dry season from November to April lined up below the local meteoric water line (LMWL), implying that rainfall during the dry season may be affected by secondary evaporation during its descent. When these data were discarded, the slope and the intercept of the LMWL were 7.95 and 9.11, respectively, and close to those of the global meteoric water line (GMWL). The volumetric weighted means of δD and $\delta^{18}O$ values in rainfall were –6.7‰ and –43.9‰, respectively. During the period from January to March, when little rainfall occurred, the δD values of stream water were near the volumetric weighted mean of δD in the rainfall. During the period from April to December, when a considerable amount of rain fell, the temporal variation in δD in rainfall was less evident in stream water. The range of variation in the δD value of stream water differed among the watersheds, which may indicate that the residence time of stream water differs from watershed to watershed.

1. Introduction

Stable isotopes, such as deuterium (D) and oxygen-18 (^{18}O), are widely used in hydrology as environmental tracers because they move with the water itself. Information obtained from stable isotope data can improve our understanding of the processes associated with the source of water and system dynamics, and provide quantitative estimates related to flow dynamics and transport parameters (Yurtsever and Araguás-Araguás 1993).

* Forestry and Forest Products Research Institute (FFPRI), Tsukuba, Japan
E-mail: kabeya@ffpri.affrc.go.jp

The Global Network of Isotopes in Precipitation (GNIP) database compiled by the International Atomic Energy Agency and World Meteorological Organization (IAEA/WMO) has provided data on monthly isotope precipitation variability at more than 100 stations worldwide during the past 40 years (Rozanski et al. 1993). Araguás-Araguás et al. (1998) described the spatial and temporal variability of stable isotope composition in precipitation over the Southeast Asian region using the GNIP dataset. In the Indochina Peninsula, observation data from GNIP have been recorded in Bangkok, Ko Sichang, and Ko Samui, Thailand; Luang-Prabang, Laos; and Yangoon, Myanmar. Yoshimura et al. (2003) reported short-term (1–10 days) variability in precipitation isotope content in Bangkok, Sukhothai, and Chiangmai, Thailand. However, stable water isotope data from Cambodia, which is in the central part of the Indochina Peninsula, have not previously been reported.

In the research described here, stable isotope ratios from rainfall and stream water were investigated from 2003 in four forest watersheds in the Kampong Thom Province of Cambodia. The aims were to establish the elementary relationship between D and ^{18}O values in rainfall called the local meteoric water line (LMWL) and to characterise the temporal variations in D and ^{18}O isotopes in rainfall and stream water.

2. Site and Methods

2.1. Study Area

This research was conducted in four forest watersheds in the Kampong Thom Province in central Cambodia. The locations of these four watersheds are shown in Fig. 1. The drainage areas of the O Toek Loork, O Thom I, O Thom II, and Stung Chinit watersheds are 4 km^2, 137 km^2, 126 km^2, and 3659 km^2, respectively; their altitude ranges are 89–142 m, 46–273 m, 19–74 m, and 19–653 m, respectively. The geology of the O Toek Loork, O Thom I, and O Thom II watersheds is characterised as sandy alluvium. In the Stung Chinit watershed, sandy alluvium is also dominant, but basalt occurs in the northern part and shale is present in the southern part of the watershed. The climate is governed by two monsoons, the cool, dry northeastern monsoon from November to March and the humid southwestern monsoon from May to October. The streams at the water level observation points of the four watersheds flow perennially, even though there is little rain from December to February. The elevations and drainage areas of these watersheds, and the locations of recording instruments, are shown in Table 1. Flow velocity measurements were carried out under various water level conditions at each stream water level observation site. Rating curves were then constructed from the velocity observations. Rainfall was recorded by tipping bucket rain gauges (RG2-M; Onset, Bourne, USA). In addition, air temperature and relative humidity were observed by a thermo-hygrometer (Datamini 3631; Hioki, Ueda, Japan) at the Kbal Domrey Forest Office (about 110 m above sea level), located near the centre of the Stung Chinit watershed.

2.2. Water Sampling

Rainfall was collected at Kbal Domrey Forest Office and sampled in a 30-l plastic bottle through a 21-cm-diameter funnel. To prevent isotopic fractionation due to

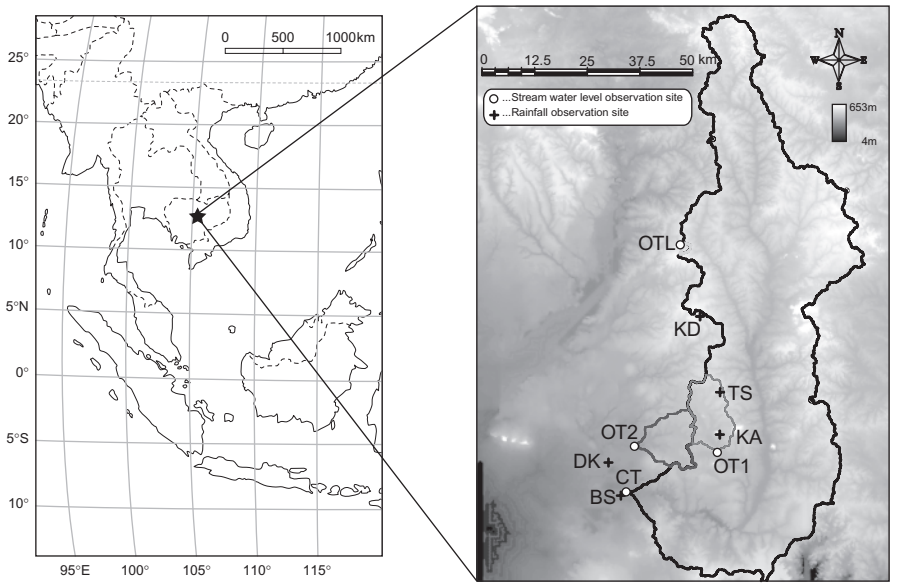

FIG. 1. Location of four experimental forest watersheds in Kampong Thom, Cambodia. Abbreviations for the observation site names in this figure are given in Table 1

TABLE 1. The elevations and drainage areas of the four study watersheds and the allocation of instruments

Site name	Instruments	Altitude (m)	Drainage area (km^2)
Stream water level observation sites			
O Toek Loork (OTL)	S, P_1	89–142	4
O Thom I (OT1)	S, P_1	46–273	137
O Thom II (OT2)	S, P_1	19–74	126
Stung Chinit (CT)	B, P_2	19–653	3659
Rainfall observation sites			
Tower site (TS)	R		
Bak Snar Nursery Forest (BS)	R		
Dorng Kda (DK)	R		
Kampub Ambel (KA)	R		
Kbal Domrey Forest Office (KD)	R, P_1, P_2, Th		

S, staff gauge; B, buzzer-type water level gauge (million water level, Yamayo, Tokyo, Japan); P_1, pressure gauge (MC 1100 WA, STS Sirnach, Switzerland), 0–5 m range, ±0.1% FS; P_2, pressure gauge (mini-TROLL, Air brown Fort Collins, USA), 0–20 m range, ±0.1% "Full scale"; R, tipping bucket rain gauge (RG2-M, On-set), 1 fall equals 0.2 mm; Th, Thermo-hygrometer (Datamini 3631, Hioki)

evaporation, an oil film was poured into the rainfall collector. The sample was protected by the oil film as soon as it entered the collector. Stream water was sampled at each of the four watershed water level sites. The sampling interval for rainfall and stream water was once every 2 or 3 months.

2.3. Stable Isotope Analysis

A mass spectrometer (MAT252; Thermo Scientific, Waltham, USA) was used for hydrogen and oxygen isotope analysis of the water samples. The H_2–H_2O equilibrium method with a Pt catalyst and the CO_2–H_2O equilibrium method in water were used to measure the hydrogen and oxygen isotopic ratios, respectively. The hydrogen and oxygen isotopic ratios were generally expressed in delta units, δD and $\delta^{18}O$, and defined in relation to Vienna standard mean ocean water (V-SMOW), as given by the following equation:

$$\delta D_{sa} = \left(\frac{(D/H)_{sa}}{(D/H)_{re}} - 1 \right) * 1000‰ \mathrm{V-SMOW}$$
$$\text{and} \quad \delta^{18}O_{sa} = \left(\frac{\left(^{18}O/^{16}O\right)_{sa}}{\left(^{18}O/^{16}O\right)_{re}} \right) * 1000‰ \mathrm{V-SMOW} \tag{1}$$

where the subscripts *sa* and *re* refer to the sample and standard values, respectively. The analytical precision of the δD and $\delta^{18}O$ measurements was ±0.4‰ and ±0.02‰, respectively.

2.4. Global and Local Meteoric Water Lines

The isotopic compositions of water can be compared to a well-known relationship, the meteoric water line (MWL), which defines the worldwide relationship between average oxygen and hydrogen isotopic ratios in natural waters (Craig 1961):

$$\delta D = 8\delta^{18}O + 10 \tag{2}$$

The relationship between the oxygen and hydrogen isotopic ratios of the natural water in any particular area is defined as the local meteoric water line (LMWL), and the generalised MWL is then often described as the global meteoric water line (GMWL). The GMWL is essentially a global average of many local meteoric water lines, each controlled by local climatic factors, including the origin of the vapour mass, secondary evaporation during rainfall, and the seasonality of precipitation. These local factors affect both the intercept value, called the deuterium excess, and the slope of the relationship. The LMWL is used as basic information when discussing water cycle processes in a particular area, and for regional or local investigations, it is important to compare surface water and groundwater data with a LMWL (Clark and Fritz 1997).

Dansgaard (1964) first proposed the use of the *d* value to characterise the intercept, called deuterium excess, in global precipitation. The *d* value is defined for a slope of 8 and is calculated for any precipitation sample as follows:

$$d = \delta D - 8\delta^{18}O \tag{3}$$

On a global basis, *d* averages to about 10‰ V-SMOW, but varies regionally as a result of variations in humidity, wind speed, and sea surface temperature (SST) during primary evaporation (Clark and Fritz 1997). Thus, the *d* value mainly

represents a kinetic effect produced by "primary evaporation" when the water evaporates from the sea surface (Dansgaard 1964), although it is altered by "secondary evaporation" from rain as it descends, in some arid regions (Clark and Fritz 1997). In the Asian monsoon region, where the origin of precipitation water vapour changes seasonally, the fluctuation in *d* values of precipitation is large (Kondoh and Shimada 1997), and this fluctuation has the potential to be an effective tracer for estimating the residence time of stream water, spring water, and subsurface water (Kabeya et al., 2007).

2.5. Secondary Evaporation During Rainfall

As already noted, the slope of the MWL for global precipitation is very close to 8. This slope can be affected by evaporation that occurs after condensation. If rain is falling through a dry air column above the ground, some of this rain will evaporate, imparting kinetic fractionation on the drop (Ehhalt et al. 1963). Ehhalt et al. (1963) showed that evaporation during rainfall would shift water away from the MWL along an evaporation slope of less than 8. Thus, rainfall affected by secondary evaporation is aligned below the MWL. Rainfall amount and relative humidity have been examined as atmospheric factors that produce secondary evaporation (Dansgaard 1964; Yurtsever and Gat 1981; Rozanski et al. 1993; Clark and Fritz 1997). In this study, the saturation deficit, which is a more primary atmospheric factor of evaporation, was calculated from the observed temperature and humidity in the field. The relationship between the saturation water vapour pressure and temperature was examined using the following equation by Murray (1967), which is accurate in the range of normal temperature:

$$e_s(T) = 6.1078 \exp\left(\frac{aT}{T+b}\right) \tag{4}$$

where T is temperature (°C), e_s (T) is saturation water vapour pressure (hPa) at T (°C), and the two parameters are a = 17.2693882 and b = 237.3, respectively. The saturation deficit was calculated by the saturation water vapour pressure and relative humidity as follows:

$$SD = e_s\left(1 - \frac{RH}{100}\right) \tag{5}$$

where SD is the saturation deficit (hPa) and RH is relative humidity (%). The observed values at the Kbal Domrey Forest Office were used for T and RH. These values are recorded at 1-h intervals; monthly mean values were used to calculate the monthly mean saturation deficit.

3. Results and Discussion

3.1. Stable Isotopic Composition and Seasonal Variations of Rainfall

A linear relationship between δD and $\delta^{18}O$ values was found for rainfall (Fig. 2):

$$\delta D = 6.82\ \delta^{18}O + 1.24 \quad R^2 = 0.98 \text{ (LMWL using all data)} \tag{6}$$

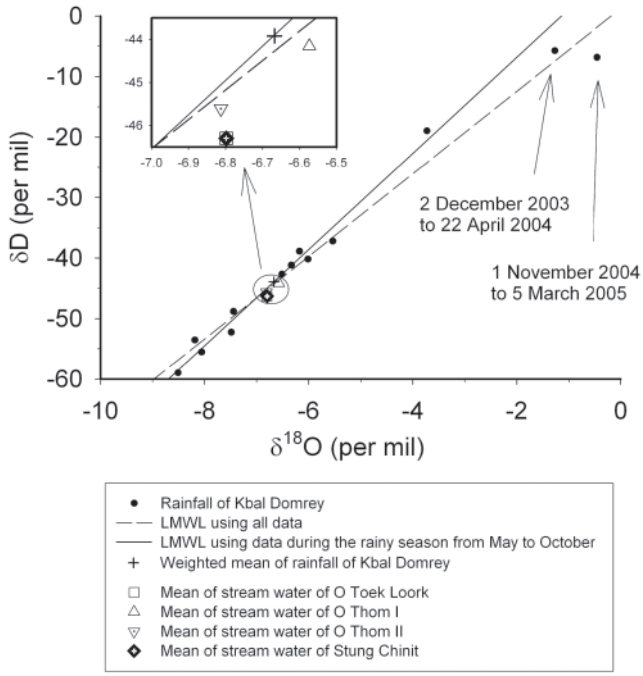

FIG. 2. The isotopic composition of rainfall and stream waters in the experimental forest watersheds, Kampong Thom, Cambodia

$$\delta D = 7.95\ \delta^{18}O + 9.11 \quad R^2 = 0.98 \text{ (LMWL using data collected during the rainy season from May to October)} \tag{7}$$

The slope of the LMWL using all data was 6.82, which was less than that of the MWL (with an assumed slope equal to 8). The δD and $\delta^{18}O$ values of the following two periods were higher than for other data, namely 2 December 2003 to 22 April 2004, and 1 November 2004 to 5 March 2005 (see Fig. 2). These rainfall samples might have been affected by secondary evaporation during their descent because these data were aligned below the LMWL. When they were discarded from the analysis, the slope and the intercept of LMWL became 7.95 and 9.11, respectively, which were closer to those of the GMWL.

The effect of secondary evaporation on δD and $\delta^{18}O$ values of rainfall has been observed in arid regions such as Bahrain (Dansgaard 1964; Yurtsever and Gat 1981) and northern Oman (Clark and Fritz 1997) and in semiarid regions such as Pretoria, South Africa (Ehhalt et al. 1963) and Calgary, Canada (Peng et al. 2004). These studies have indicated the effects of secondary evaporation on rain in rainfall events of less than 5 mm (Peng et al. 2004), 10 mm (Yurtsever and Gat 1981), and 20 mm (Clark and Fritz 1997). At the Kbal Domrey Forest Office in the dry season, from November to April, the monthly rainfall amount was 10 mm or less from November to February, but was approximately 20–100 mm in March and April (Fig. 3). On the other hand, peak values of the monthly mean saturation deficit showed seasonal variation of

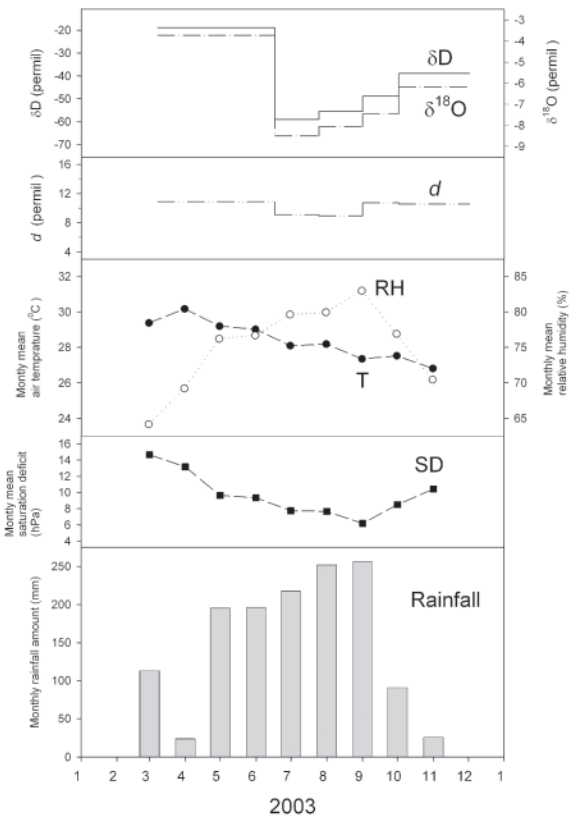

FIG. 3. Seasonal variations of deuterium (δD), oxygen-18 ($\delta^{18}O$), *d* value, air temperature, relative humidity, saturation deficit, and the amount of rainfall at the Kbal Domrey Forest Office in 2003

14–15 hPa in March and April. Similar seasonal variation of the saturation deficit was observed at the tower site, and the daily mean and maximum saturation deficits during March and April were about 10–20 hPa and 30–40 hPa, respectively (Nobuhiro et al., 2007). These results suggest that rainfall in the late dry season (March to April) is strongly influenced by secondary evaporation.

Seasonal variations in δD, $\delta^{18}O$, and *d* values in rainfall at the Kbal Domrey Forest Office in 2003 are shown in Fig. 3; seasonal variations in monthly mean air temperature, monthly mean relative humidity, monthly mean saturation deficit, and monthly rainfall amount are also shown. The highest monthly mean air temperature was 30°C in April; it then decreased and was 27°C in November. The lowest monthly mean relative humidity was 64% in March, and the highest was 83% in September. The annual rainfall for 2003 was 1370.2 mm; there was no rain in January, February, or December. The monthly rainfall exceeded 190 mm for the 5 months from May to September, with the highest value (256 mm) in September; this was also the month with the highest monthly mean relative humidity. Similar increasing and decreasing tendencies were seen in the variations of monthly rainfall and monthly mean relative humidity.

The δD and $\delta^{18}O$ values of rainfall indicated low values ranging from −55.5‰ to −60.0‰ for δD and −8.0‰ to −8.5‰ for $\delta^{18}O$ during the period from July to

September, when the amounts of rainfall were relatively large (see Fig. 3). However, no clear relationship was apparent between the seasonal variations in air temperature and the δD or $\delta^{18}O$ value of rainwater. Dansgaard (1964) reported the global distribution of stable isotopes in precipitation and discussed the two effects that influence the isotopic composition of precipitation, namely, temperature and precipitation amount. At low latitudes, the precipitation amount effect accounts for the variations, whereas seasonal variation at high latitudes is ascribed to the temperature effect (Dansgaard 1964). The precipitation amount effect shows a linear relationship between the amount of precipitation and the isotopic composition of precipitation observed from the tropical to midlatitude regions. Because the study site is located at low latitude, the precipitation amount effect would be expected to be dominant, which was found to be the case.

The *d* value variation in rainfall was very small, ranging from 8.9 to 10.9 (see Fig. 3). In the Asian monsoon region, where the origin of precipitation water vapour changes seasonally, the fluctuation in *d* values of precipitation is large (Kondoh and Shimada 1997). However, in our study area, there was only a very small amount of rainfall in the winter monsoon season from November to March. Thus, the variation in *d* values of the rainfall was very small because rainfall came from water vapour affected only by the summer monsoon.

3.2. Stable Isotopic Composition and Seasonal Variation of Stream Water

Mean δD and $\delta^{18}O$ values of rainfall and stream water from 29 January 2003 to 24 July 2005 are shown in Table 2. The volumetric weighted means of δD and $\delta^{18}O$ values in rainfall were −43.9‰ and −6.7‰, respectively. Mean δD and $\delta^{18}O$ values of stream water in each watershed were close to this value (see Fig. 2).

Seasonal variations in δD values in rainfall and stream water during 2003 are shown in Fig. 4. Seasonal variation in $\delta^{18}O$ is omitted because a linear relationship was demonstrated between δD and $\delta^{18}O$ values. The stable isotope ratio of the rainfall in 2003 was highest at −20‰ during the period from March to mid-June. The value from the middle of June to the end of July was as low as −60‰. Then, the value rose gradually and the value from October to the end of November was −40‰. During the period from December to February when little rain fell, δD values of stream water were near

Table 2. Mean isotopic ratios of rainfall and stream waters from January 29, 2003 to July 24, 2005

	n	$\delta^{18}O$ (‰)		δD (‰)	
		Mean	SD	Mean	SD
Rainfall at Kbal Domrey	13	−6.7[a]	2.6	−43.9[a]	17.6
Stream water of O Toek Loork	15	−6.8	0.2	−46.3	1.4
Stream water of O Thom I	14	−6.6	1.6	−44.2	12.1
Stream water of O Thom II	16	−6.8	1.6	−45.6	12.6
Stream water of Stung Chinit	15	−6.3	0.7	−43.7	5.0

n, sampling time

[a] Volumetric weighted mean

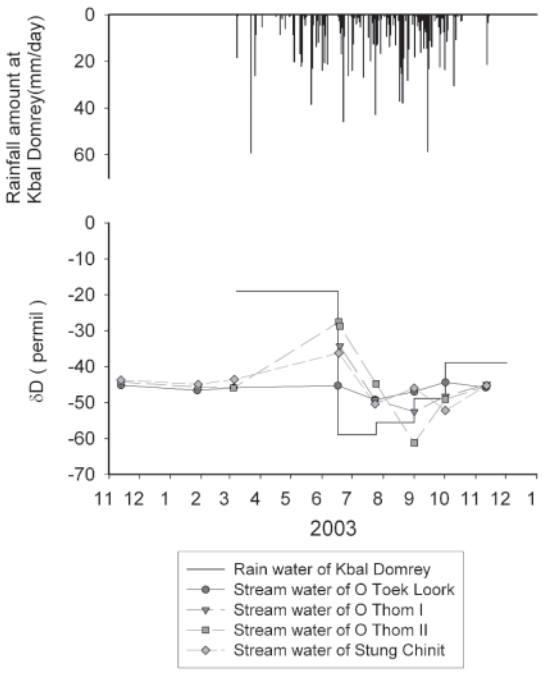

FIG. 4. Seasonal variations in the δD value for rainfall and stream waters and daily rainfall amount in 2003

the volumetric weighted mean of δD in rainfall. During the period from March to November when there was a considerable amount of rainfall, temporal variation in δD values in rainfall were less evident in stream water. Moreover, the range of δD variation in stream water differed between watersheds, implying that the residence time of stream water may differ from watershed to watershed.

4. Conclusions

Stable isotope ratios of rainfall and stream water were examined to characterise the stable isotope compositions and seasonal variations of rainfall and stream water in Cambodia.

Rainfall during the dry season from November to April was aligned below the LMWL, implying that rainfall during the dry season might have been affected by secondary evaporation during its descent. When these data were discarded, the slope and the intercept of LMWL were found to be 7.95, and 9.11, respectively, close to those of the GMWL. This relationship provides fundamental information on stable isotope tracers in Cambodia.

Seasonal variations in δD and $\delta^{18}O$ values in rainfall were large and were mainly controlled by the precipitation amount effect. However, seasonal variation of the *d* value of rainfall was relatively small because rainfall in this area came only from water vapour affected by the summer monsoon. Seasonal variation in δD in rainfall was less evident in stream water from forest watersheds with various drainage areas

(4–3659 km^2). This result shows that seasonal variations in δD and $\delta^{18}O$ values have the potential to provide an effective tracer to better understand the hydrological processes in Cambodian forest watersheds.

Acknowledgments. We thank Mr. Ty Sokun, General Director, Forest Administration of Cambodia, and Mr. Tith Nara, Forest and Wildlife Science Institute, Forest Administration of Cambodia. We also thank Drs. Toshio Abe and Tayoko Kubota, Forest Hydrology Laboratory, Forestry and Forest Product Research Institute of Japan, for their support in the field. This study was funded by the "Research Revolution 2002 Project" of MEXT (Ministry of Education, Culture, Sports, Science and Technology) and the "Assessment of the Impact of Global-Scale Change in Water Cycles on Food Production and Alternative Policy Scenario" of AFFRCS (Agriculture, Forestry and Fisheries Research Council Secretariat), Japan.

References

Araguás-Araguás L, Froehlich K, Rozanski K (1998) Stable isotope composition of precipitation over Southeast Asia. J Geophys Res 103:28721–28742

Clark I, Fritz P (1997) Tracing the hydrological cycle. In: Clark I, Fritz P (eds) Environmental isotopes in hydrogeology. CRC Press, Boca Raton, FL, pp 35–61

Craig H (1961) Isotopic variations in meteoric waters. Science 133:1702–1703

Dansgaard W (1964) Stable isotopes in precipitation. Tellus 16:436–468

Ehhalt D, Knot K, Nagel JF, Vogel JC (1963) Deuterium and oxygen 18 in rain water. J Geophys Res 68:3775–3780

Kabeya N, Katsuyama M, Kawasaki M, Ohte N, Sugimoto A (2007) Estimation of mean residence times of subsurface waters using seasonal variation in deuterium excess in a small headwater catchment in Japan. Hydrol Process (in press) [doi:10.1002/hyp.6231]

Kondoh A, Shimada J (1997) The origin of precipitation in eastern Asia by deuterium excess. J Jpn Soc Hydrol Water Resour 10:627–629

Murray FW (1967) On the computation of saturation vapour pressure. J Appl Meteorol 6:203–204

Nobuhiro T, Shimizu A, Kabeya N, Tsuboyama Y, Kubota Y, Abe T, Araki M, Tamai K, Chann S, Keth N (2007) Year-round observation of evapotranspiration in an evergreen broadleaf forest in Cambodia. In: Sawada H, Araki M, Chappell NA, LaFrankie JV, Shimizu A (eds) Forest Environments in the Mekong River Basin, Springer, Tokyo, pp 75–86

Peng H, Mayer B, Harris S, Krouse HR (2004) A 10-yr record of stable isotope ratios of hydrogen and oxygen in precipitation at Calgary, Alberta, Canada. Tellus 56B:147–159

Rozanski K, Araguás-Araguás L, Gonfiantini R (1993) Isotopic patterns in modern global precipitation. In: Swart PK, Lohmann KC, McKenzie J, Savin S (eds) Climate change in continental isotopic records. Geophysical monograph series, vol 78. American Geophysical Union, Washington, DC, pp 1–36

Yoshimura K, Oki T, Ohte N, Kanae S (2003) A quantitative analysis of short-term ^{18}O variability with a Rayleigh-type isotope circulation model. J Geophys Res 108:4647

Yurtsever Y, Araguás-Araguás L (1993) Environmental isotope applications in hydrology: an overview of the IAEA's activities, experiences, and prospects. In: Peters NE, Hoehn E, Leibundgut C, Tase N, Walling DE (eds) Tracers in hydrology. International Association of Hydrological Sciences (IAHS) publication 215. IAHS Press, Wallingford, pp 3–20

Yurtsever Y, Gat JR (1981) Atmospheric waters. In: Gat JR, Gonfiantini R (eds) Stable isotope hydrology: deuterium and oxygen-18 in the water cycle. Technical report series 210. IAEA, Vienna, pp 103–142

Runoff Characteristics and Observations on Evapotranspiration in Forest Watersheds, Central Cambodia

Akira Shimizu*, Naoki Kabeya, Tatsuhiko Nobuhiro, Tayoko Kubota, Yoshio Tsuboyama, Eriko Ito, Makoto Sano, Sophal Chann, and Nang Keth

We measured precipitation, runoff, and several meteorological factors associated with evapotranspiration in evergreen broadleaf forest watersheds in Kampong Thom Province, central Cambodia. All the studied watersheds have flat topography, with *Vatica odorata* and *Mynistica iners* as the primary plant species. The mean tree height in the upper crown layer was 27 m and the maximum tree height was 45 m. Meteorological factors were observed from a 60-m-high meteorological observation tower. The heat budget method, which incorporates the Bowen ratio, was used to calculate the energy balance above the forest canopy. To estimate evapotranspiration, meteorological data were collected during two sampling periods: October 2003, near the end of the rainy season, and March 2004, in the middle of the dry season. Average daily evapotranspiration levels calculated for the late rainy season and middle of the dry season were 4.4 mm/day and 4.9 mm/day, respectively. A continuous simulation model (modified HYCY model) was then applied with the obtained streamflow data for the watersheds. Evapotranspiration calculated using the tower observations was included as a model parameter. The estimated runoff matched observed runoff comparatively well for small watersheds. The model parameters varied in correspondence with the watershed size.

1. Introduction

The Mekong River is an international waterway that passes through a range of climatic zones. This river originates on the Tibetan Plateau and flows into the South China Sea after passing through several countries including Myanmar, Laos, Thailand, Cambodia, and Vietnam. In the Mekong River basin, increased farming to support a rapidly growing population has led to a dramatic reduction in forest area. Illegal logging and wood collection are also increasing throughout the entire Asian monsoon area, including Cambodia, and the destruction and degradation of forests may alter the water cycle of the whole river basin. According to Cambodian government statistics (Narith 1997), the forested area in Cambodia declined from 74% in

* Forestry and Forest Products Research Institute (FFPRI), Tsukuba, Japan
E-mail: akiraxx@ffpri.affrc.go.jp

the 1970s to 58% in 1993. Despite this reduction, Cambodia still has a high percentage of forested land compared to adjacent countries. Because the forests of Cambodia are representative of the vegetation types that occur throughout the entire Indochina Peninsula, research results from Cambodia will reflect water cycle characteristics of tropical monsoon forest areas in the Mekong River basin. The relatively well-preserved state of Cambodian forests indicates the pivotal role these forests play in the water cycle in Cambodia and in surrounding regions. Moreover, relatively little research has documented forests in Cambodia as compared with forests in neighbouring countries such as Thailand (Yoshifuji et al. 2006). Further detailed study of the water environment of forests in Cambodia's Mekong basin is clearly needed, especially considering the regional influence of this river system. In this study, we investigated the runoff characteristics of forest watersheds in Cambodia using observational data and model applications.

2. Site Description

2.1. Location and Topography

Compared with many other Southeast Asian countries, Cambodia has a relatively large area of lowland forests. However, even in these forest stands, disturbances such as selective cutting and illegal felling are increasing, and secondary forests have developed in many areas.

We chose the Stung Chinit River watershed (12°32′ N, 105°17′ E) and surrounding areas in Kampong Thom Province in central Cambodia as the study area (Fig. 1). The Stung Chinit River is a branch of the Sap River, which connects the Mekong River to Lake Tonle Sap, Cambodia's largest lake (Asian Development Bank 2004). Figure 2 presents the topography and boundaries of the study watersheds based on Geographic Information System (GIS) data and field surveys. Our study area included the O Thom I (12°36′ N, 105°28′ E), O Thom II (12°37′ N, 105°17′ E), O Toek Loork

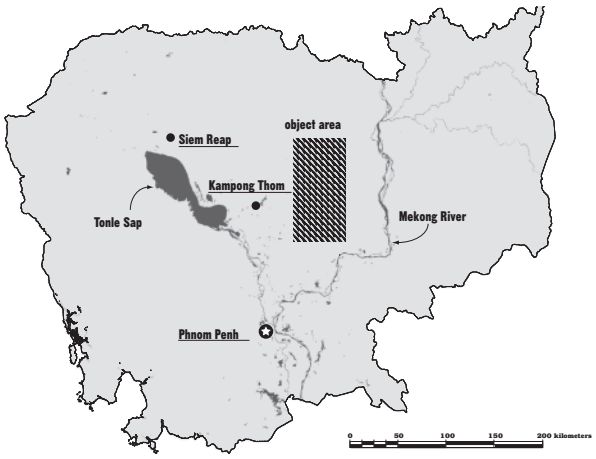

Fig. 1. Objective area in Cambodia

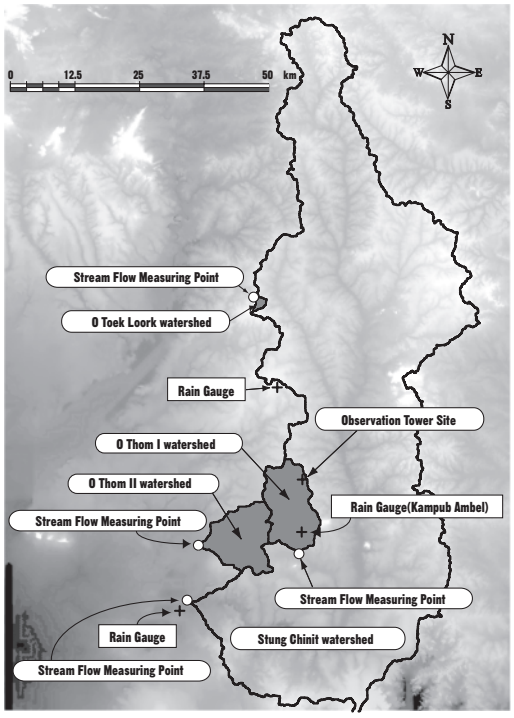

FIG. 2. Objective watersheds and the observation points

(13°03′ N, 105°23′ E), and Chinit watersheds. Table 1 lists the geographic features of each watershed.

The O Thom I and O Thom II rivers are tributaries of the Stung Chinit River. The O Thom I watershed, which is relatively undisturbed by logging (maximum tree height, 45.1 m), was selected as an appropriate site for the study of evapotranspiration. A 60-m-high observation tower with equipment for measuring various meteorological characteristics was erected in the northeast section of the O Thom I watershed. A rain interception measurement plot (25×25 m) was constructed close to the observation tower.

2.2. Vegetation

The vegetation at the experimental watershed consisted of an evergreen broadleaf forest dominated by species of Myristicaceae, *Vatica odorata*, and *Calophyllum inophyllum*. We analyzed the vegetation structure in the rain interception plot located close to the meteorological observation tower in greater detail. Table 2 shows the results of this analysis. The forest surrounding the observation tower consisted of overstory trees, secondary story trees, and lower story trees. The stem density at the site was 1600/ha; however, pole timbers in the lower story were not present at a very high density. The forest canopy was composed of overstory and secondary story timber. The lower story had an average regeneration condition. The frequency distributions of the diameter at breast height and tree height showed clear distinctions among the overstory, secondary story, and lower story (Fig. 3). Although the

Table 1. Geographic features of each watershed

Name	Elevation (m)	Watershed area (km^2)
O Toek Loork	89–142	4
O Thom I	46–273	137
O Thom II	19–74	126
Stung Chinit	19–653	3659

Table 2. Forest composition

	DBH (cm)	H (m)	Number of sterns (N/fm)	C_L (m)	C_D (m)
Piot	12.32	11.28	1600	—	—
Maximum tree[a]	119.40	45.10	(16)	28.60	19.11
Overstory (H > 20 m)	39.60	27.20	96	12.52	7.61
Secondary story (H > 10 m)	12.42	14.05	416	7.43	3.78
Lower story (H < 10 m)	6.67	7.26	1088	—	—

DBH, diameter at breast height; H, mean tree height; C_L, mean crown length; C_D, mean crown diameter

[a] Maximum tree included in overstory

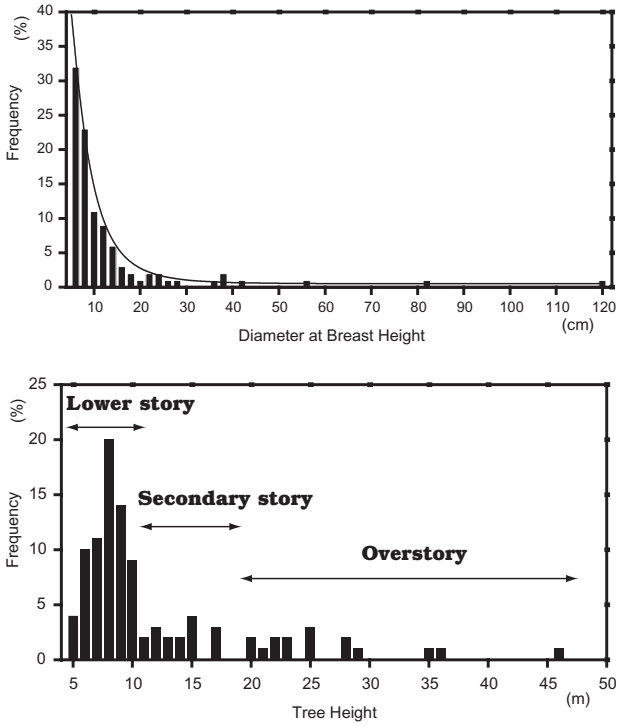

Fig. 3. Distribution of tree diameter and height

upper-canopy trees were relatively low in density, they covered a large area of the canopy, with some secondary layer trees filling crown space gaps between trees in the upper canopy. Lower layer trees had high density but contributed relatively little to the crown area. The dominant species in the overstory were *Myristicaceae* sp., *V. odorata*, and *C. inophyllum*; less-common species included *Maesa* sp. and *Syzigium* sp. In the secondary layer, the main species were *Tarenna* sp. and *Diospyros bejaudi*. The lower layer additionally contained a *Gardenia* species. Because the species of *Myristicaceae* was present in all three vegetation layers, it was considered to be the dominant species at the study site.

3. Methods

In this study, we combined separately observed evapotranspiration and runoff data as in the study by Shimizu et al. (2003). First, we measured several meteorological factors associated with evapotranspiration as well as precipitation and runoff. Second, watershed characteristics concerned with the rainfall–runoff process were analyzed by inputting the obtained evapotranspiration into a model. Below, we describe the methods in order of the meteorological observations, water measurement observations, and model outline including Geographic Information System (GIS) data.

3.1. Meteorological Observations and Evapotranspiration

The Bowen ratio energy balance method (BREB), which measures the energy budget above the canopy, was used to estimate evapotranspiration (Hattori 1985). The data required to perform the analyses were collected using equipment installed on the 60-m-high meteorological observation tower. As a preliminary observation, wind velocity, temperature, and humidity were measured over the forest canopy layer at the study site to determine the height at which the heat budget observation instruments should be installed. Based on these measurements, the height of the lowest observation instrument was >34 m, which corresponded with the height of the forest crown. The rain gauge and pyranometer (upward and downward) were installed 60 m above the ground, at the top of the tower. Anemometers were placed at four different levels (42, 38, 36, and 30 m), and a wind vane was placed at a height of 38 m. Rainfall was also measured at Kampub Ambel Village, located 10 km south of the observation tower. Ventilated psychrometers were installed at two different heights (38 and 34 m). A net-radiometer was placed at 36 m. Two heat flux plates were laid under the soil at a depth of 2 cm. All the variables just described were measured at 10-s intervals, and the average value (or cumulative value recorded over a 10-min period) was recorded using a data logger. Because an AC power supply was not available at the study site, a combination of interchangeable batteries and solar cell panels was used to supply power. The wet-bulb of the ventilated psychrometer was checked weekly and refilled with water as required.

3.2. Rainfall–Runoff Observations

Precipitation and runoff were observed to analyze the rainfall–runoff process at several experimental watersheds (arranged as shown in Fig. 2). Precipitation was

observed using a tipping-bucket-type rain gauge; 10-min interval data were accumulated in the data logger and retrieved periodically. To examine runoff, the water level of stream flow was recorded twice daily using a staff gauge. An automatic water level gauge fixed to the river channel bottom continuously measured water level variation. The amount of runoff was obtained from water level fluctuation based on the discharge rating curve. Discharge rating curves were created using stream cross-section survey data and flow velocity measured at numerous times from low water to flood levels.

3.3. Runoff Model

Runoff analysis was conducted using a modified HYCY model capable of considering thick soil and deep unconsolidated geology. The HYCY model is a conceptual model that can describe river channel runoff, evapotranspiration, subsurface runoff (including deep pathways), and rainfall interception (Fukushima 1988). Observed evapotranspiration was used as a model parameter, and runoff fluctuation was calculated for two watersheds (O Thom II and Chinit) in which streamflow had been observed year-round. In addition, large-area GIS information such as the vegetation coverage ratio in the object watersheds was also collected, and characteristics of each experimental watershed were analyzed using these GIS data.

4. Results and Discussion

4.1. Evapotranspiration Characteristics

Diurnal and seasonal changes in evapotranspiration were calculated by applying the heat budget method in combination with the Bowen ratio, using data collected from the forest meteorological tower. The data required for the calculation of evapotranspiration were collected during both rainy and dry seasons. Variations in meteorological conditions during two periods, October 2003, which was representative of the late rainy season, and March 2004, which was representative of the middle dry season, are summarized as follows.

1. The daily mean atmospheric temperature, measured at a height of 38 m on the observation tower, ranged from 25.2°C during the latter half of the rainy season to 27.1°C in the middle of the dry season. No differences in the minimum air temperatures were recorded during the two observation periods. In contrast, the maximum air temperature was much higher during the dry season. The dry season was also characterized by much greater diurnal temperature variation.
2. Comparing peak values obtained for downward shortwave radiation under fine weather conditions revealed similar and consistent radiation levels of 800–1000 kW/m^2 for the two sampling periods. This result indicates that almost the same amount of daily shortwave energy occurs during the rainy season as during the dry season.
3. The albedo during the rainy and dry seasons ranged from 0.1 to 0.12. These values agree well with the results reported for other tropical forests (Giambelluca et al. 1999).

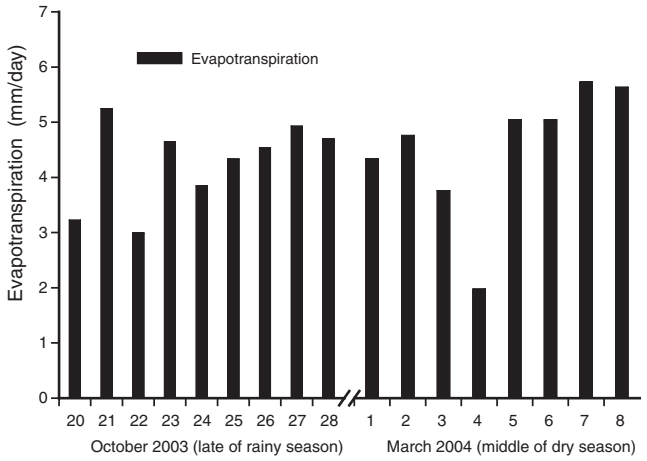

Fig. 4. Evapotranspiration of dry season and rainy season

4. The mean wind speed did not differ significantly between the two observation periods. Maximum daily wind speeds occurred mainly in the daytime during both the rainy and dry seasons. During the rainy season, the diurnal variation pattern of wind speed was almost the same every day, and the wind direction was mostly toward the north/northeast. During the dry season, the wind speed pattern differed almost every day, and the wind direction was highly variable.

5. Diurnal and seasonal changes in evapotranspiration were calculated by applying the heat budget method in combination with the Bowen ratio, using data collected from the forest meteorological tower. The average daily evapotranspiration values calculated for the late rainy season and the middle of the dry season were 4.4 and 4.9 mm/day, respectively (Fig. 4).

4.2. Land-Use Characteristics

Although the measured results from the afore-mentioned experimental plot are considered typical of the forest stand composition in the object watersheds, the land-use and vegetation coverage situations in the experimental watersheds are fundamental information necessary for the analyses. Therefore, we calculated land-use rates for the object watersheds using existing GIS data. The GIS data were linked with a topographic map having 50-m digital elevation model (DEM) data and including information on soil type and geology as well as vegetation (Araki et al. 2004). The watershed geology is dominated by alluvium and basalt, and there is some crystalline schist and other constituents. There are four main soil types distributed in the watersheds.

Figure 5 illustrates the results of the GIS analyses. At the Chinit watershed, which has a large basin area, about 85% of the whole area is woodland, 60% is evergreen forest in wilderness areas, and 10% is deciduous forest. At the O Thom II watershed, woodland occupies 50% or more of the area, but many grassland and shrub areas are

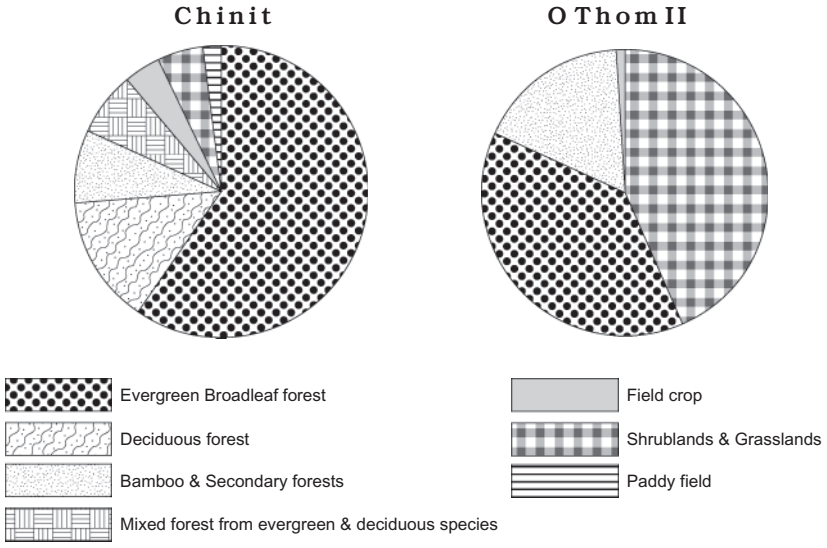

Fig. 5. Coverage ratio in Chinit and O Thom II

present and the vegetation rates differ slightly from those in other watersheds. These differences likely reflect the relative flatness of the O Thom II watershed compared to other watersheds and the proximity of a village.

4.3. Modified HYCY Model

The evapotranspiration data obtained by tower observations (Nobuhiro et al., 2007) were used as a parameter in HYCY model calculations of watershed runoff for comparison with observational data. This model is a type of conceptual model that was originally developed for temperate-zone forests in Japan, and necessary parameters are determined using the storage function model ($S = KQ^P$, where S is storage depth, Q is runoff, and K and P are parameters), channel system model, effective rainfall model, and rainfall interception model (11 parameters in all). Because there is a deep permeable regolith in central Cambodia, we modified the original model by adding an interflow tank to separate interflow and deep subsurface pathways(Fig. 6). Several parameters were determined theoretically, whereas others such as transpiration, evaporation from interception stores, and some runoff factors were determined by observation results.

The recently developed SVAT-HYCY model (Ma and Fukushima 2002) calculates runoff in a large basin by linking an individual HYCY model in unit grids and can be used for analyses of broad areas. However, in this study, we used the concentrated-type model to analyze the fitness of this type of model and compare with watershed characteristics. Moreover, the study watersheds were of suitable size for the HYCY model, ranging from 100 to 4000 km^2.

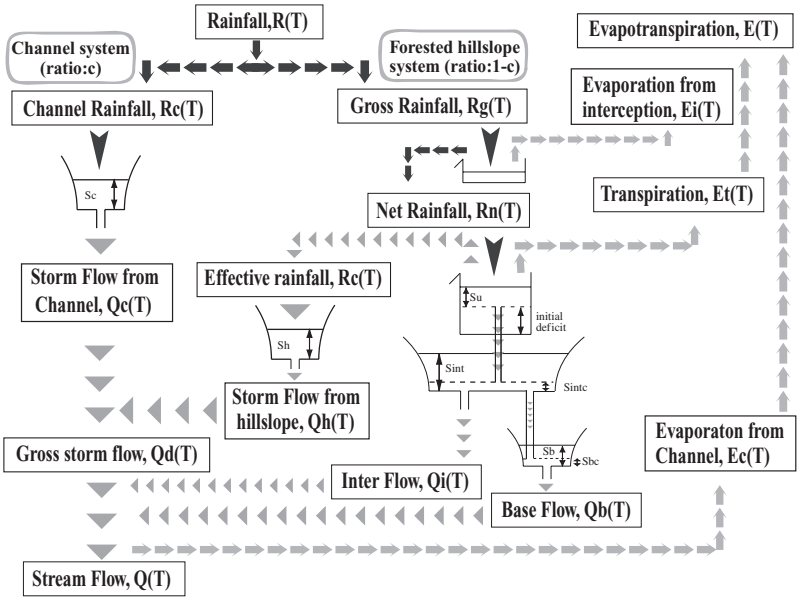

Fig. 6. Modified HYCY model

4.4. Simulation Results

The evapotranspiration computed from the afore-mentioned weather data was used in the HYCY model calculation of watershed runoff, and the results were compared with observation data for the experimental watersheds. The model was also calculated with rainfall observations for 2004. Figure 7 shows the calculation results for Chinit and O Thom II. The estimated runoff matched observed runoff comparatively well in both watersheds, reproducing the fundamental change in runoff in response to rainfall. These results suggest that this modified HYCY model, which describes deep subsurface pathways and shallow subsurface flow using divided compartments, has sufficient parameterization for forest watersheds of this size. Therefore, the representation of evapotranspiration obtained by micrometeorological observations (dry and rainy seasons) was assumed to be appropriate.

However, for the Chinit watershed, which was the largest experimental watershed, some differences in the lag of peak flow and runoff shape were observed, such as over-estimates at the start of the dry season. This finding contrasts with the good reproduction of runoff behavior in the O Thom II watershed. The calculating system of the model may not adequately compute time delays in river channels. Consequently, direct application of this model is considered appropriate for watersheds of approximately 100 km^2. However, as the basin area becomes large, and the storage, channel flow velocity, and mixture of numerous branches gradually start to influence the amount of runoff, some limitations may arise for simple applications of concentrated systems in a large river basin. Thus, if the research purpose is only to improve the runoff reproducibility for a large watershed, a distributed model constructed of

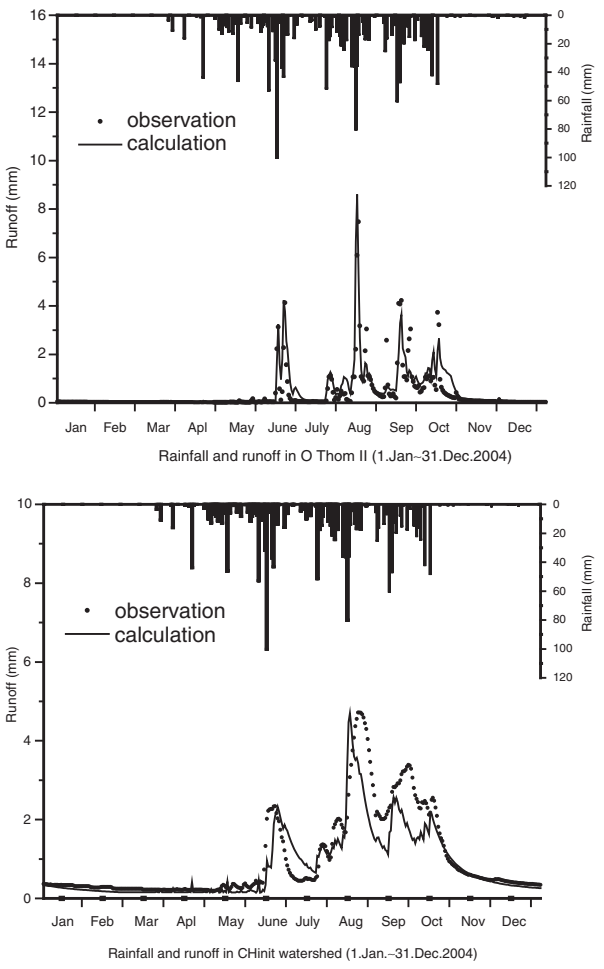

FIG. 7. Results of model application in Chinit and O Thom II River (2004)

linkages of individual HYCY model runoff in unit grids, such as the SVAT-HYCY, should also be considered. The representativeness of precipitation data and the effects of object watershed sizes must also be considered.

Although the calculation accuracy deteriorates as the size of the watershed increases, a single concentrated-type model can be used to examine differences in model parameters and compare watersheds. In this analysis, the behavior of the runoff parameter of the base tank appeared to reflect an increasing trend in base runoff in a larger basin area. That is, because the vertical location of a river channel becomes deeper relative to the ground surface as the object watershed increases in size, a larger watershed can take up the amount of runoff from deeper parts of the groundwater as river flow in the flat alluvial zone of Cambodia. This result is clear from the annual water balance

results for the four experimental watersheds; the smallest experimental watershed had the smallest amount of runoff. In the largest watershed, the river channel was 8 m deep or more from the ground surface, while the river channel was only about 2 m deep in the smallest watershed. The difference in model parameters could reflect such subsurface characteristics in these watersheds, although the effect of vegetation was not clearly confirmed, as it was expressed only by the evapotranspiration term containing the amount of rainfall interception. Evapotranspiration was expressed as an average value of watershed vegetation. Distribution-type models such as TOPMODEL (Beven 1997; Tsuboyama 1997) or the SVAT-HYCY model should be used for more detailed analyses of vegetation effects. Because a concentrated-type model such as the HYCY can more correctly reproduce the amount and tendency of runoff with relatively little information, this type of model is effective for predicting runoff or analyzing river basins in areas such as Cambodia where data records are sparse. Thus, concentrated- or distribution-type models must be chosen appropriately in correspondence with the research purpose (Ao et al. 2000).

Acknowledgments. This study was funded by the "Research Revolution 2002 Project" of MEXT (Ministry of Education, Culture, Sports, Science and Technology) and the "Assessment of the Impact of Global-Scale Change in Water Cycles on Food Production and Alternative Policy Scenario" of AFFRCS (Agriculture, Forestry and Fisheries Research Council Secretariat), Japan.

References

Ao T, Takeuchi K, Ishidaira H (2000) On problems and solutions of the Muskingham–Cunge method applied to a rainfall runoff model. Annu J Hydraulic Eng JSCE 44:139–144

Araki M, Ito E, Ohta S, Kanzaki M, Toriyama J, Kaneko T, Hiramatsu R, Okuda Y, Saret K, Phearak I, Sopheap L, Sopheavuth P, Saila D, Bora T (2004) Forest vegetation and soil conditions in Kampong Thom, Cambodia. In: Proceedings of the international conference on advances in integrated Mekong River management, Lao PDR, Vientiane 25–27 October 2004, pp 182–188

Asian Development Bank (ADB) (2004) Greater Mekong subregion atlas of the environment. Asian Development Bank and United Nations Environment Program, Manila

Beven KJ (1997) TOPMODEL: a critique. Hydrol Process 11:1069–1085

Fukushima, Y. (1988) A model of river flow forecasting for a small forested mountain catchment. Hydrol Process 2:167–185

Giambelluca TW, Fox J, Yarnasarn S, Onibutr P, Nullet MA (1999) Dry-season radiation balance of land covers replacing forest in Thailand. Agric For Meteorol 95:53–65

Hattori S (1985) Explanation on derivation process of equations to estimate evapotranspiration problems on the application to forest stand. Bull For For Prod Res Inst 332:139–165

Ma X, Fukushima Y (2002) Numerical model of river flow formation from small to large scale river basins. In: Singh VP, Frevert DK (eds) Mathematical model of large watershed hydrology. Water resources publications 891. LLC, Englewood, Colorado pp 433–470

Narith H (1997) Asia–Pacific Forestry Sector outlook study: country paper on some aspects of forestry in Cambodia. APFSOS/WP/18. Food and Agriculture Organization of the United Nations, Rome

Nobuhiro T, Shimizu A, Kabeya N, Tsuboyama Y, Kubota T, Abe T, Araki M, Tamai K, Chann S, Keth N (2007) Year-round observation of evapotranspiration in an evergreen broadleaf forest in Cambodia. In: Sawada H, Araki M, Chappell NA, LaFrankie JV, Shimizu A (eds) Forest Environments in the Mekong River Basin, Springer, Tokyo, pp 75–86

Shimizu A, Shimizu T, Miyabuhi Y, Ogawa Y (2003) Evapotranspiration and runoff in a forest watershed, western Japan. Hydrol Process 17:3125–3139

Tsuboyama Y (1997) Topographic controls on stormflow generation in a small forested catchment. In: Abstracts, American Geophysical Union (AGU) fall meeting, San Francisco, California, H22B-05, December

Yoshifuji N, Kumagai T, Tanaka K, Tanaka N, Komatsu H, Suzuki M, Tantasirin C (2006) Inter-annual variation in growing season length of a tropical seasonal forest in Thailand. For Ecol Manag 229:333–339

Part II
Forest Management

Object-Oriented Land Cover Classification Based on Two Satellite Images Obtained in One Dry Season in Cambodia

Naoyuki Furuya*, Hideki Saito, Sam Preap, Bora Tith, and Makara Meas

Some regions of the Mekong River basin still have considerable forest resources, but the pressure for exploiting these resources is very high. Changes of forest cover may strongly affect the water circulation of this region. Therefore, it is important to monitor changes of land cover of this region. In this study, we tested an object-oriented classification method to create a land cover classification map in Cambodia. A commercial object-oriented image analysis software package (eCognition) was used in this analysis. In an object-oriented classification method, the success of classification depends largely on the result of image segmentation. In this study, we overcame the difficulty in image segmentation by combining temporal images acquired in the early and late dry season. The overall accuracy was 0.70, and the Khat statistics value was 0.60. Although the accuracy was moderate, the discrimination between evergreen and deciduous forest types was good. However the mixed or the degraded land cover types were still hard to distinguish from each other. Using images taken in different phenological stages made it possible to both segment the images accurately and classify objects appropriately in an object-oriented classification process.

1. Introduction

Forest resources in the Mekong River basin are still undergoing a remarkable decline and degradation. The changes being made in the forest cover of this region may have a large impact on water circulation and the ecosystem. Cambodia and Laos, which occupy large parts of the middle and lower Mekong River basin, are still covered with rich forest resources (FAO 2005). Therefore, monitoring of these forests and land cover change is one of the urgent tasks for this region.

* Forestry and Forest Products Research Institute (FFPRI), Tsukuba, Japan
E-mail: nfuruya@ffpri.affrc.go.jp

Utilization of satellite images is thought to be a unique and efficient tool to monitor the changes of forest cover over time at regional and landscape scales. In Cambodia, the monsoon season brings long and clear rainy and dry seasons. In the rainy season, it is hard to get clear images because of the clouds, but in the dry season there is a greater possibility to obtain clear images. Broad-leaved evergreen and deciduous tree species are widely distributed in this region. These vegetation types also show unique seasonal change patterns, especially in the dry season. Therefore, temporal images acquired in the dry season make it possible to discriminate these forest cover types.

In some countries, forest and land cover maps have been created at a national level by human interpretation using medium spatial resolution satellite images such as Landsat and SPOT [e.g., National Office of Forest Inventory and Planning (NOFIP) 1992; Ministry of Public Works and Transportation, Kingdom of Cambodia and Japan International Cooperation Agency, Japan (MPWT & JICA) 2003]. However, the quality of such maps depends on the knowledge, techniques, and experiences of the technicians who made them. It is efficient to utilize the seasonal pattern of spectra in multitemporal satellite images, but it is difficult to use multitemporal images simultaneously in practical human interpretation task.

Automatic or semiautomatic methods for creating forest and land cover classification maps have also been tried (Foody and Hill 1996). Land cover maps have been created by adapting a pixel-based classification method to single or multiple images in time series (Oetter et al. 2001; Schriever and Congalton 1995; Wolter et al. 1995), and adapting an object-oriented classification method to middle spatial satellite images was also tested (Yijun and Hussin 2003). However this object-oriented classification method has not yet been tested for discriminating evergreen and deciduous forest types using multitemporal satellite images. This object-oriented classification method has some advantages; for example, texture information extracted from objects becomes available for classification. Moreover, inevitable errors in handling the multitemporal images can be reduced.

Therefore, in this study an object-oriented classification method was tested for creating a land cover map in Cambodia using temporal satellite images acquired in the early and late dry seasons.

2. Study Site

The study site (100 km × 100 km) is located in the central part of Cambodia in the Mekong River basin [approximately 13°02′ N, 105°09′ E (scene center, Fig. 1)]. The area is inside a single Landsat satellite scene with Path : Row = 126 : 51 and is suitable for this study because it contains typical land cover types. Evergreen and deciduous forests are distributed widely in this area. Some disturbances, such as logging, construction of operation roads, and clearing lands for agriculture, are visible in the forest area. Paddy fields are also distributed near villages and along the main roads. The topography is rather flat, and the altitude of the highest point within the study

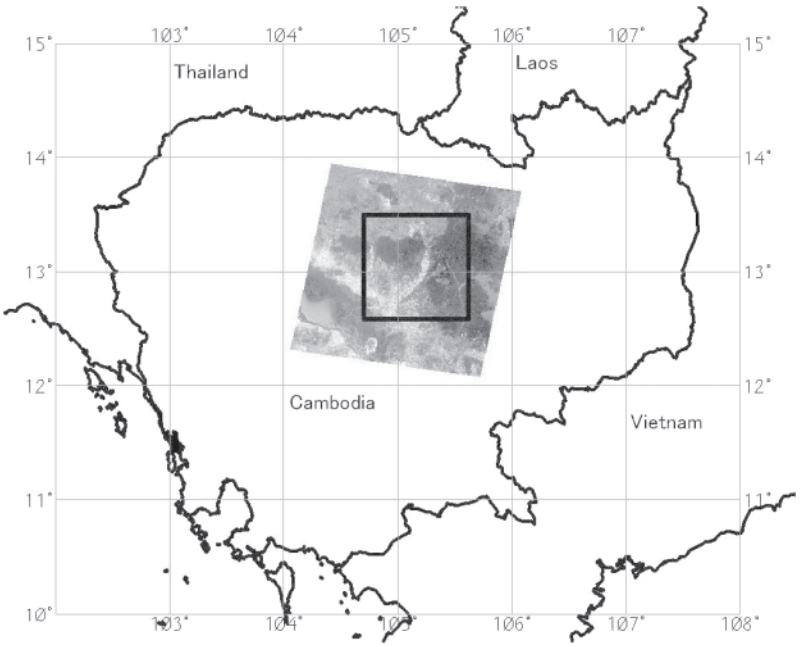

Fig. 1. Location of the study area

area is around 300 m a.s.l. Therefore, topographic effects were not considered in this study.

3. Materials

To minimize the effects of temporal change in this region and utilize seasonal spectral change, two satellite images captured in the same dry season were used for the study (Fig. 2). Two satellite images that were captured by an optical sensor, the Enhanced Thematic Mapper plus (ETM+) onboard Landsat 7 satellite, were used in this study. One was taken in the early dry season (2 December 2001) and the other was taken in the late dry season (20 February 2002).

To evaluate the results of our classification scheme, we used an existing map in digital form prepared by the Ministry of Public Works and Transportation, Kingdom of Cambodia and Japan International Cooperation Agency (2003). The 2003 map was created by human interpretation of satellite images obtained around the year 2000.

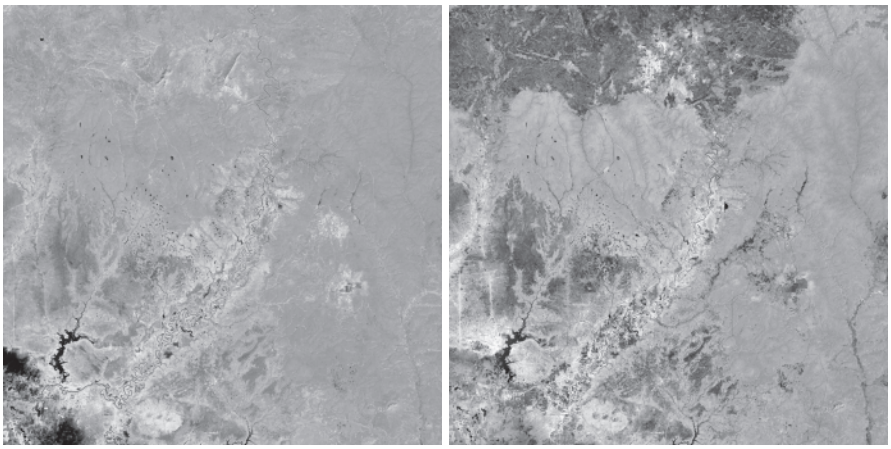

Fig. 2. Landsat 7 ETM+ satellite images (100 km × 100 km): *left*, Dec. 2, 2001; *right*, Feb. 20, 2002

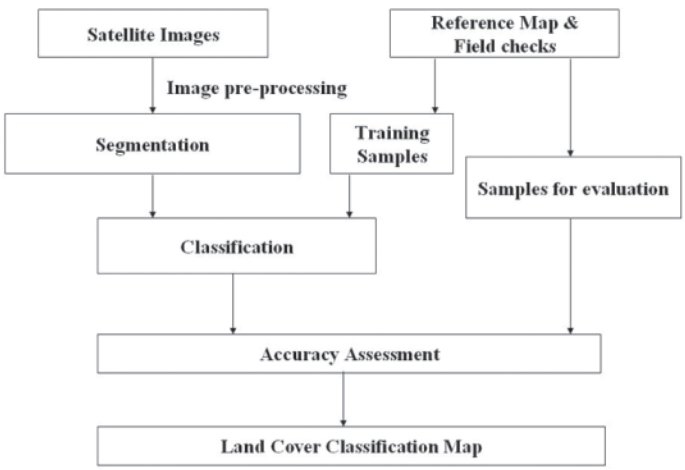

Fig. 3. Flowchart of image processing for land cover classification

4. Methodology

Figure 3 shows a flowchart of our study. In the first step, to analyze the two images at once, the images were geometrically registered and radiometrically normalized with each other. In the second step, land cover objects were produced using an image segmentation algorithm. In the third step, created objects were classified through a nearest neighbor classification method using the training samples carefully chosen from a field check and the 2003 map. Lastly, the classification results were compared with the land cover in the 2003 map.

4.1. Image Preprocessing

First, two satellite images were geometrically registered to the 2003 map using ground control points (GCPs). The root mean square error (RMSE) was within 1 pixel. Then, the satellite image was resampled to 25×25 m pixel size using the nearest neighbor interpolation method. Second, pseudo-invariant features were collected from the evergreen forests, artificial objects, and water bodies in both images. Regression lines were calculated for all bands. The 2002 image was then radiometrically adjusted to the 2001 image using the regression lines (Chavez 1988; Hall et al. 1991; Schott et al. 1988).

4.2. Object-Oriented Classification Method

Object-oriented classification was done with a commercial image analysis software package (eCognition version 4.0; Definiens Imaging 2004). In this process, the image is first divided (segmented) into small objects, i.e., small pieces of land cover, and then the objects are classified into land cover classes using information of selected features extracted from training samples. Therefore, the accuracy of the classification depends on the accuracy of the image segmentation (Definiens Imaging 2004).

The image segmentation algorithm used by eCognition is a region-growing method that starts with one pixel and gradually expands the region by combining with neighboring objects with high homogeneous features (Benz et al. 2004; Definiens Imaging 2004). The algorithm calculates and compares the heterogeneity between two neighboring objects and post-combined new objects. If the difference of heterogeneity (based on both color and shape) is below a certain threshold, the objects are merged. In this algorithm, the user selects several parameters, such as the bands to be used and their weights, the heterogeneity threshold [called the scale parameter (SP)], weights for the color and shape heterogeneity balance (color + shape = 1.0), and weights for the compactness and smoothness balance for shape heterogeneity (compactness + smoothness = 1.0).

4.2.1. Image Segmentation

To minimize the atmospheric effects at short wavelengths, only the red band (TM band 3) was selected in the visible wavelength for the analysis. As a result, a total of eight bands (bands 3, 4, 5, and 7 = 4 bands $\times$ 2 images) were used for image segmentation. The same weight was given to each band for segmentation. By trial and error, we selected the parameters for image segmentation so that the minimum size of land cover objects was maintained. The selected values were SP = 10, color = 0.9, shape = 0.1, and compactness and smoothness = 0.5. The result of image segmentation is shown in Fig. 4. Populated areas were heterogeneous, which probably resulted in the creation of small objects. On the other hand, in the evergreen forest areas, objects were likely to be integrated into large objects.

4.2.2. Classification Method

Objects were classified by a simple nearest neighbor classification method, which uses representative features of land cover categories (Definiens Imaging 2004). Objects are

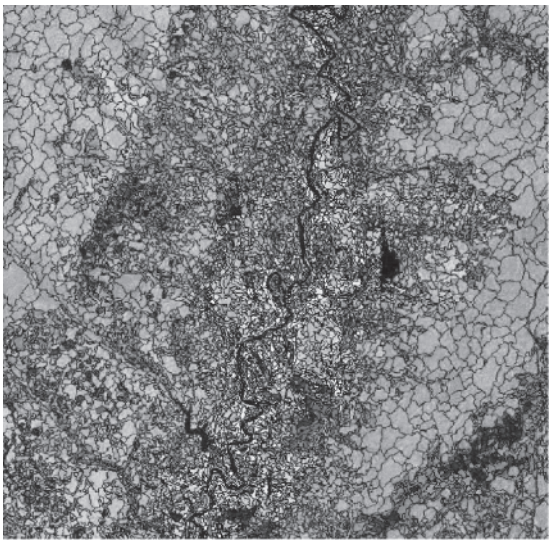

FIG. 4. Result of image segmentation (1 km × 1 km). *Lines* show the boundaries of created objects

TABLE 1. Land cover categories

Land cover category	Varieties included
Evergreen forests	
Deciduous forests	With burnt and unburnt above-ground biomass (in the late dry season)
Mixed forests	Mixed with broadleaved evergreen and deciduous forest types
Shrub lands	Inundated and not inundated (in the early dry season)
Grasslands	Inundated (in the early dry season), burnt and unburnt (in the late dry season)
Agricultural lands	Paddy fields, crop fields
Barren lands	Barren land, sand bank, rock outcrop
Water bodies	Ponds and rivers

automatically categorized to land cover categories with the nearest feature in the feature space. Land cover categories were defined according to the varieties of local land cover in this region (Table 1). Categories such as grasslands and sparse dry deciduous forests, in which grasses grow, are likely to suffer from wildfires in the late dry season. Similarly, some categories, such as grasslands and shrubs, suffer from inundation in the early dry season but not in the late dry season. Therefore, some categories need to be subdivided by occurrence of wildfire and inundation events. Training samples also need to be separately collected from the different land varieties according to the local conditions (Table 1). Selected features for classification were simple mean values of objects from bands 3 to 5 and 7 of both images. The means of the original bands were thought to be adequate because in this study detailed categories were defined according mainly to the differences of seasonal spectral pattern. Figure 5 shows such seasonal variations of spectra for some typical forest cover categories.

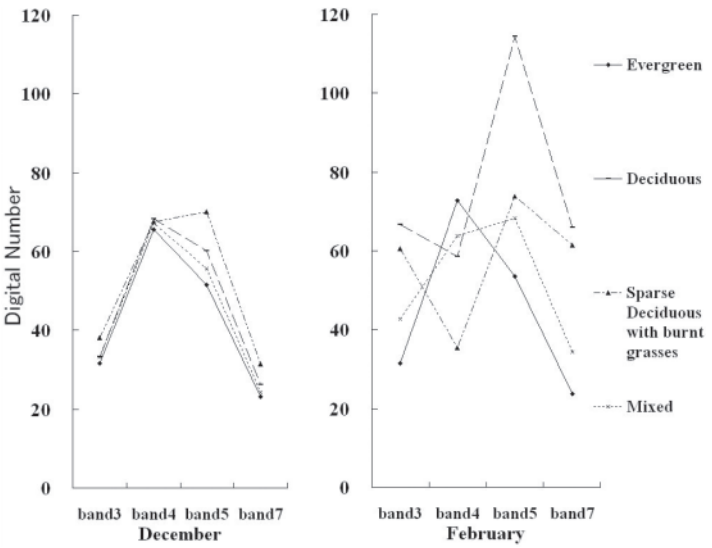

Fig. 5. Spectral patterns of typical forest cover types

4.3. Evaluation Method

The 2003 map was used to evaluate the classification result. The land cover category types from both the created map and the 2003 map were compared at random sampling points. The accuracy of the produced land cover map was assessed quantitatively using samples at random seed points and by visual inspection. A confusion matrix was created, and the overall accuracy and a Khat statistics value were calculated (Congalton 1991).

5. Results

5.1. Results of Classification

A land cover classification map of the study area (Fig. 6) shows a large evergreen forest patch in the eastern part, deciduous forests in the northern part, and mixed forests of evergreen and deciduous forest types in the transition area between evergreen and deciduous forest types. Paddy fields are distributed along the main roads in the west, and shrub lands are distributed between the paddy fields and forest areas. Shrub lands and grasslands seem to be expressed well in the inundation areas in the southwest.

5.2. Accuracy Assessment

Table 2 shows the confusion matrix produced by comparing the classification result with the 2003 map. The overall accuracy was 0.70 and the Khat statistics value was 0.60. This classification result was moderately accurate. The accuracy of the evergreen

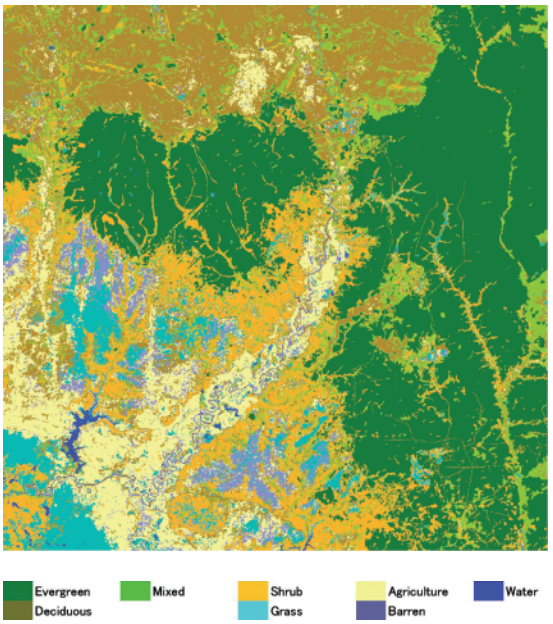

Fig. 6. Land cover classification map

Table 2. A confusion matrix

Classification	Reference									Accuracy
	EF	DF	MF	S	G	AG	B	W	Total	(%)
Evergreen forests (EF)	3230	5	67	85	0	0	0	0	3387	95.36
Deciduous forests (DF)	44	881	119	230	35	248	23	7	1587	55.51
Mixed (MF)	237	101	117	161	17	26	8	10	677	17.28
Shrub (S)	173	9	29	425	33	75	44	2	790	53.80
Grasslands (G)	3	18	1	118	190	166	26	11	533	35.65
Agricultural lands (AG)	6	48	3	85	33	1014	31	8	1228	82.57
Barren lands (B)	2	57	0	37	18	96	78	6	294	26.53
Water bodies (W)	1	0	0	4	7	9	0	31	52	59.62
Total	3696	1119	336	1145	333	1634	210	75	8548	
Accuracy (%)	87.4	78.7	34.8	37.1	57.1	62.1	37.1	41.3		

forest type, which was spread over a large area, was high. The accuracy of deciduous forests was also good. Therefore, this classification method is sufficiently efficient for dividing evergreen and deciduous forest types. On the other hand, the mixed forests were confused with evergreen and deciduous forest types and also with shrub lands. Shrub lands, grasslands, and agricultural lands were also likely to be confused, apparently because these land cover types easily become dry and show similar spectral and seasonal change patterns in the dry season, and because they are likely to appear at similar places in complex mixture forms. The 2003 map also seemed to be more simplified in the process of human visual interpretation than the created land classification map. Therefore, the vegetation patches that remained in the agricultural lands and the degraded land cover patches in the evergreen and deciduous forests are likely to be neglected in the 2003 map. This consideration may also worsen the accuracy of our classification result.

6. Discussion

As mentioned earlier, the accuracy of object-oriented classification depends largely on the success of image segmentation. However, varieties of land cover coexist in the actual world in complex spatial combinations. In particular, it is hard to uniformly divide those land covers with slight differences using satellite images acquired in the growing season. However, in the late dry season, degraded forests or deciduous forests show dry features and the spectral differences become large. Therefore, those land covers seem to be more easily discriminated in the late dry season than in the growing season. On the other hand, the differences among poor vegetation types are hard to identify in the late dry season because they are not sufficiently great in the image, and in some cases the vegetation is likely to have suffered from wildfires. Therefore, although it is difficult to segment an image accurately using only the late dry season image, using two images acquired in the early and the late dry season makes it possible to segment the entire image into meaningful land cover objects. Utilization of temporal images is efficient not only in the image segmentation process but also in the classification process. Utilization of temporal images makes it possible to use seasonal spectral change patterns in the classification process. Also, in the case of land cover information for land cover in one image, for example, in the case of fire and in the case of inundation, those land covers become able to be classified using information from the other scene. Object-oriented classification is also expected to be more robust to noise caused by multitemporal image analysis.

7. Conclusions

In this study we tested an object-oriented classification method to create a land cover classification map in Cambodia. The discrimination between evergreen and deciduous forest types was adequately good. However, the mixed or degraded land cover types were still hard to discriminate from each other. There is still some room for discussion of the validity of image segmentation and the features selected for classification. However, our results show that the object-oriented classification method has at least some ability for large-scale mapping. In object-oriented

classification, the first segmentation process is the key for successful classification. Therefore, we need to pay more attention to creating adequate objects from images. One method for accurately segmenting an image is to use multitemporal images that show different phenological stages.

Acknowledgments. This study was funded by the "Research Revolution 2002 Project" of MEXT (Ministry of Education, Culture, Sports, Science and Technology) and the "Assessment of the Impact of Global-Scale Change in Water Cycles on Food Production and Alternative Policy Scenario" of AFFRCS (Agriculture, Forestry and Fisheries Research Council Secretariat), Japan. We are grateful to the Japan International Cooperation Agency (JICA). The digital map was provided by JICA for study purpose.

References

Benz UC, Hofman P, Willhauck G, Lingenfelder I, Heynen M (2004) Multi-resolution, object-oriented fuzzy analysis of remote sensing data for GIS-ready information. ISPRS J Photogramm Remote Sens 58:239–258

Chavez PS (1988) An improved dark-object subtraction technique for atmospheric scattering correction of multispectral data. Remote Sens Environ 24:459–479

Congalton RG (1991) A review of assessing the accuracy of classifications of remotely sensed data. Remote Sens Environ 37(1):35–46. Definens Imaging GmbH, Munich, Germany

Definiens Imaging (2004) eCognition version 4 object oriented image analysis user guide.

FAO (2005) Global forest resources assessment 2005. FAO Forestry Paper 147. FAO, Rome

Foody GM, Hill RA (1996) Classification of tropical forest classes from Landsat TM data. Int J Remote Sens 17(12):2353–2367

Hall FG, Strebel DE, Nickeson JE, Goez SJ (1991) Radiometric rectification: toward a common radiometric response among multidate, multisensor images. Remote Sens Environ 35:11–27

Ministry of Public Works and Transportation, Kingdom of Cambodia and Japan International Cooperation Agency, Japan (2003) Meta-database-Cambodia Reconnaissance Survey Digital Data JICA, Tokyo, Japan

National Office of Forest Inventory and Planning (NOFIP) (1992) Forest cover and land use in Lao PDR. Final report on the nationwide reconnaissance survey. Report no. 5. NOFIP, Vientiane, Laos

Oetter DR, Cohen WB, Berterretche M, Maiersperger TK, Kennedy RE (2001) Land cover mapping in an agricultural setting using multiseasonal Thematic Mapper data. Remote Sens Environ 76:139–155

Schott JR, Salvaggio C, Volchok WJ (1988) Radiometric scene normalization using pseudoinvariant features. Remote Sens Environ 26:1–16

Schriever JR, Congalton RG (1995) Evaluating seasonal variability as an aid to cover-type mapping from Landsat Thematic Mapper data in the Northeast. Photogramm Eng Remote Sens 61:321–327

Wolter PT, Mlandenoff DJ, Host GE, Crow TR (1995) Improved forest classification in the Northern Lake States using multi-temporal Landsat imagery. Photogramm Eng Remote Sens 61:1129–1143

Yijun C, Hussin YA (2003) Object-oriented classifier for detection tropical deforestation using LANDSAT ETM+ in Berau, East Kalimant, Indonesia. Map Asia Conference 2003 Kuala Lumpur, Malaysia

Land Cover Change Mapping of the Mekong River Basin Using NOAA Pathfinder AVHRR 8-km Land Dataset

Hideki Saito*, Yoshito Sawada, Naoyuki Furuya, and Sam Preap

The objective of this study was to produce land cover maps for the period between 1982 and 2000 using the Normalized Differential Vegetation Index (NDVI) data from the National Oceanic and Atmospheric Administration (NOAA) Pathfinder Advanced Very High Resolution Radiometer (AVHRR) 8-km land dataset for monitoring forest cover changes in the Mekong River basin. Time-series analysis, named Local Maximum Fitting with Kalman Filter (LMF-KF), was applied to the NDVI data to remove noise such as clouds and produce cloudfree images at 10-day intervals. Multitemporal metrics such as annual mean, maximum, minimum, standard deviation, and range were calculated using LMF-KF-processed NDVI data. Classification was performed to produce land cover maps based on signatures from the multitemporal metrics of the NDVI time-series data. The GLC2000 land cover database produced by the Joint Research Center of the European Commission was used as training data for the first classification, which is for the year 2000. Then, the results of the first classification were used as training data for the next classification, which is the previous year. Consequently, classification results for the period between 1982 and 2000 were obtained. It was found that the total forested area was stable in the classification images, whereas the proportion of deciduous forest area had increased.

1. Introduction

A land cover map has an important role in environmental studies as a base map for forest management, wildlife conservation, and water cycle modeling. The study area is located in the Mekong River basin, where forests have been destroyed and degraded by human impact such as commercial logging, shifting cultivation, and expansion of agricultural fields and urban areas, even though biodiversity-rich forests support the life of local residents and wildlife. This area has also been affected by flooding and severe water shortage. Therefore, sustainable forest management is important not only for forest resources but also for water resources.

* Kyusyu Research Center, Forestry and Forest Products Research Institute (FFPRI), Kumamoto, Japan
E-mail: rslsaito@ffpri.affrc.go.jp

There are several advantages to using satellite remote sensing to create forest cover maps on a broad and continuous scale. Especially, it is an efficient method for producing regional- or global-scale maps such as for the Mekong River basin. The Advanced Very High Resolution Radiometer (AVHRR) data of the National Oceanic & Atmospheric Administration (NOAA) have been used for land cover mapping (Defries and Hansen 1994; DeFries et al. 1998; Loveland et al. 2000; Hansen et al. 2000). In many cases, AVHRR 1-km data are used for regional or local land cover mapping, whereas the NOAA Pathfinder AVHRR 8-km land (PAL) dataset is used for global land cover classification (DeFries et al. 1995, 1998; DeFries and Chan 2000). In the present study, the PAL 8-km dataset was used for local-scale mapping because it is the only one from which 20-year land cover data can be extracted.

However, Awaya et al. (2004) described some remaining effects such as sensor degradation and atmospheric distortion in the normalized differential vegetation index (NDVI) images of the PAL dataset and suggested a correction algorithm for NPP estimation. In the present study, to overcome these problems, local maximum fitting with Kalman filter (LMF-KF) modeling and filtering was used (Sawada et al. 2005). It was useful for NOAA Pathfinder data to correct the differences in sensitivity of the AVHRR sensors as well as to remove the effect of clouds and other noise (Sawada et al. 2004). To apply LMF-KF to NOAA Pathfinder data is an effective approach for long-term land cover monitoring.

This chapter describes a methodology for creating a regional land cover map of the for the period between 1982 and 2000 using the PAL 8-km dataset.

2. Study Area

The test area selected is on the Indochina Peninsula and covers Myanmar, Thailand, Laos, Cambodia, and Vietnam (latitude 4°–30°N, longitude 90°–110°E). China was excluded from the test area because the vegetation in southern China differs from that in Southeast Asia. Evergreen forest, deciduous forest, shrub land, and grassland are found in the study area. Mangrove and swamp forests are found around estuaries and large lakes, and along the coast. Shifting cultivation activities and degraded forests are found in mountainous regions such as the northern part of Thailand and Laos. The climate is tropical monsoon ("Am" in the Köppen system).

3. Materials

NDVI data from the PAL 8-km land dataset used in the present study were downloaded from NASA's ftp site (ftp://disc1.gsfc.nasa.gov/data/avhrr/). This dataset, produced as part of the NOAA/NASA Pathfinder AVHRR Land (PAL) program, contains global and continental monthly and 10-day composites of channels 1, 2, 4, and 5 and the normalized difference vegetation index (NDVI) at 8 km and 1° resolution. The data, derived from the Advanced Very High Resolution Radiometers (AVHRR) on the "afternoon" NOAA operational meteorological satellites (NOAA-7, -9, -11), cover the period from 1981 to 1994 (covered period was extended to 2001). The Pathfinder Program produces long-term datasets processed in a consistent manner for global change research, as described in the dataset file Readme.pal.

The NDVI, which is related to the proportion of absorbed photosynthetically active radiation, is calculated from atmospherically corrected reflectance from visible and near-infrared AVHRR channels as follows:

$$\text{NDVI} = (\text{CH2} - \text{CH1}) / (\text{CH2} + \text{CH1}) \quad (1)$$

where CH1 is the reflectance in the visible wavelengths (channel 1, 0.58–0.68 μm) and CH2 is the reflectance in the reflective infrared wavelengths (channel 2, 0.725–1.1 μm). The principle behind this is that channel 1 is in a part of the spectrum where chlorophyll causes substantial absorption of incoming radiation, and channel 2 is in a spectral region where spongy mesophyll leaf structure leads to considerable reflectance (Tucker 1979; Jackson et al. 1983; Tucker et al. 1991).

The compositing process is applied to the dataset to remove much of the cloud cover present in the daily dataset. The composite is generated by comparing the NDVI values for each 8-km bin from 10 consecutive daily datasets. Because the original data at the edge of a scan may contain distortion and bidirectional effect biases, only the data within 42° of the nadir are used in the composite. The pixel with the highest NDVI for the 10 days is chosen as the date for inclusion in the composite (Agbu and James 1994). This compositing process is effective for removing most of the clouds and atmospheric contaminants, thus providing as close to a cloudfree field in each of the data layers as is possible. However, in areas of persistent cloudiness such as tropical regions, cloudy pixels will remain.

The GLC2000 land cover database (http://www-gvm.jrc.it/glc2000/defaultGLC2000.htm), produced by JRC (Joint Research Centre of the European Commission) based on SPOT VEGETATION data, was used as training data. Terrain information is important for large-scale land cover mapping. In this study, GTOPO30 (http://edc.usgs.gov/products/elevation/gtopo30/gtopo30.html), which was developed through a collaborative effort led by staff at the U.S. Geological Survey's EROS Data Center, was used with NOAA data for land cover classification.

4. Methods

4.1. Noise Reduction of NOAA NDVI Data

The LMF-KF time-series analysis was applied to the NDVI data to remove noise such as haze and clouds and produce noisefree images at 10-day intervals. LMF-KF is a modified methodology of the LMF (local maximum filtering) model processing, which assumes that the seasonal change for each pixel is modeled by the sum of cyclic functions. Parameters for LMF-KF are estimated using the Kalman filter algorithm (Sawada et al. 2005). The LMF-KF model processing can produce cloudfree data, which makes it possible to extract the features of seasonal changes for each year.

4.2. Multitemporal Metrics

Multitemporal metrics shown in Table 1 were calculated from LMF-KF-processed NDVI data. These metrics have a relationship with the vegetation phenology.

Table 1. Multitemporal metrics

Annual mean NDVI image	One-channel image with the mean of pixel values through 1 year
Annual maximum NDVI image	One-channel image with the largest pixel value through 1 year
Annual minimum NDVI image	One-channel image with the smallest pixel value through 1 year
Annual standard deviation NDVI image	One-channel image with the standard deviation of pixel value through 1 year
Annual range of NDVI image	One-channel image with the range of pixel value through 1 year

NDVI, normalized differential vegetation index

Table 2. Cover type integration table for GLC2000

Cover types in this analysis	Original cover types of GLC2000
Evergreen forest	Evergreen forest, degraded forest, mangrove, swamp, shrub (mainly evergreen)
Deciduous forest	Deciduous forest, shrub (mainly deciduous), shrub (dry or burnt)
Grassland and crop field	Grassland, cropland, cultivated (nonirrigated), cultivated (irrigated), bare areas, artificial surfaces
Snow and ice	Snow and ice
Water bodies	Water bodies
N.A.	No data/ocean area

4.3. Tree Model Classification

Classification was performed to create land cover maps based on signatures derived from the multitemporal metrics of NDVI time-series data and DEM (Digital Elevation Model) data from GTOPO30. A tree model algorithm included in the statistics and data mining software S-PLUS (Insightful Corp., Seattle, WA USA) was used for classification. The cover types of the land cover map were as follows: evergreen forest, deciduous forest, grassland, and crop field. Cover types of the GLC2000 were integrated as shown in Table 2. In this study, procedures were repeated to retrieve past land cover maps, as shown in Fig. 1.

The tree model of a land cover classification was produced. For the initial tree model, the reclassified GLC2000 map was used for a dependent variable (as training data), and multitemporal metrics of NDVI for the year 2000 and DEM data were used for independent variables to make the tree model for the 2000 land cover map, which is shown as Model2000 in Fig. 1. In this process, all the pixels in the test area excluding the ocean were used. Then, classification for the 2000 land cover map (LC2000 in Fig. 1) was performed using Model2000 and the multitemporal metrics for the year 2000 and DEM. For the year 1999, the resultant land cover map (LC2000) was used for a dependent variable, and multitemporal metrics of NDVI for the year 1999 and DEM were used for the independent variables to make the tree model for the 1999

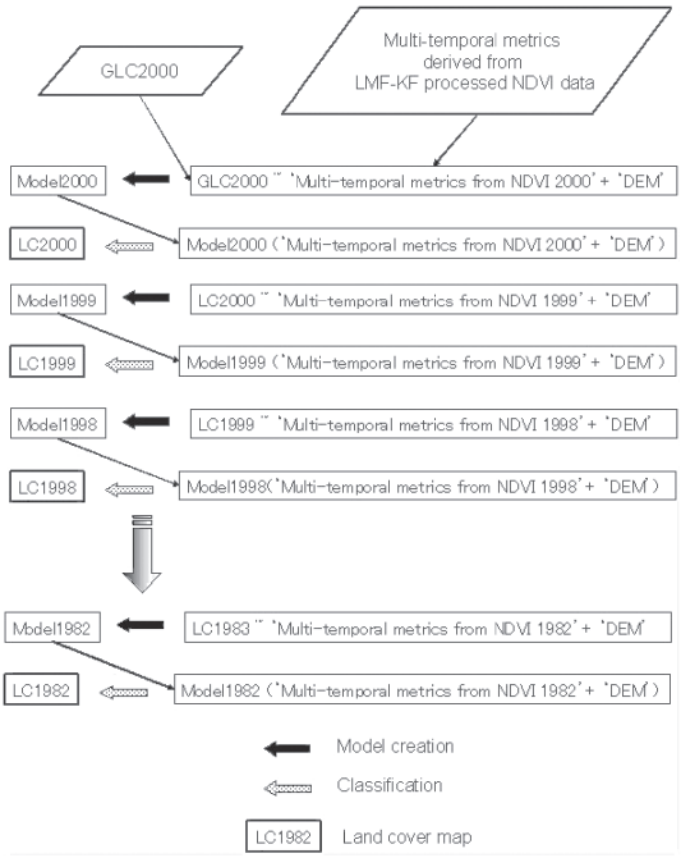

Fig. 1. Flowchart of tree model classification to retrieve past land cover maps

land cover map, which is shown as Model1999 in Fig. 1. These procedures were repeated until the 1982 land cover map was created, which is shown as LC1982 in Fig. 1.

5. Results

Chronological profiles of processed NDVI data were successfully retrieved by LMF-KF model processing (Fig. 2). The LMF-KF-processed NDVI data in this study would successfully retrieve the seasonal changes of each vegetation type. Therefore, the annual minimum value of NDVI could be used as multitemporal metrics, whereas it is difficult to calculate the annual minimum value from a monthly maximum composite image. These results support an earlier proposal, which pointed out the capability of the LMF-KF to remove noises from time-series NDVI data (Sawada et al. 2005). However, Fig. 2 also shows that NDVI data between 1991 and 1994 seemed to

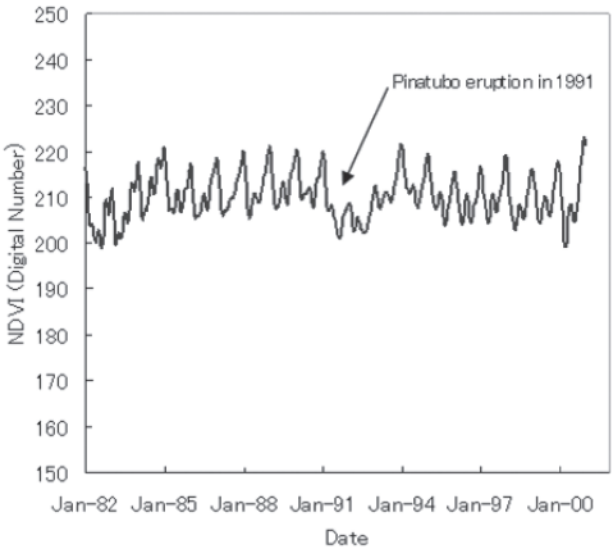

FIG. 2. Interannual and seasonal change profile of local maximum fitting with Kalman filter (LMF-KF)-processed normalized differential vegetation index (*NDVI*)

be affected by a huge eruption of Mt. Pinatubo in the Philippines in 1991. It was confirmed that the performance capability of LMF-KF is not sufficiently high to remove a strong effect on NDVI data such as a large-scale eruption.

Figure 3 shows land cover maps for the period between 1982 and 2000. Classification results between 1995 and 2000 were similar to GLC2000; however, deciduous forest area in the results between 1991 and 1994 was slightly smaller. On the other hand, Fig. 4 shows that the total forested area was stable, while the proportion of deciduous forest area had increased. It was found that the results of the recursive tree model classification using multitemporal metrics were relatively robust. However, validation of the classification results has not yet been carried out.

Even without systematic validation, the absence of deciduous forest in the northern part of Lao PDR was considered to be an unreasonable result. The result is presumably because degraded forests were reclassified as evergreen forest during the integration of land cover types and many degraded forests comprised deciduous forests. To avoid this problem, it is necessary to develop a classification scheme adapted to the PAL 8-km dataset. Satellite remote sensing has some limitations: (a) difference in spectral signature among land cover (or forest) types caused by the signature itself and sensor performance, and (b) mixture rate of land cover types within pixels, which is caused by spatial resolution (map scale) and extent of homogeneous area of land cover patches. Coarse spatial resolution data would be strongly affected by these limitations. On the other hand, it is generally accepted that the boundaries of most vegetation communities are zones of gradual transition, or ecotones, which can be termed as soft or fuzzy (Millington and Alexander 2000). Therefore, boundaries

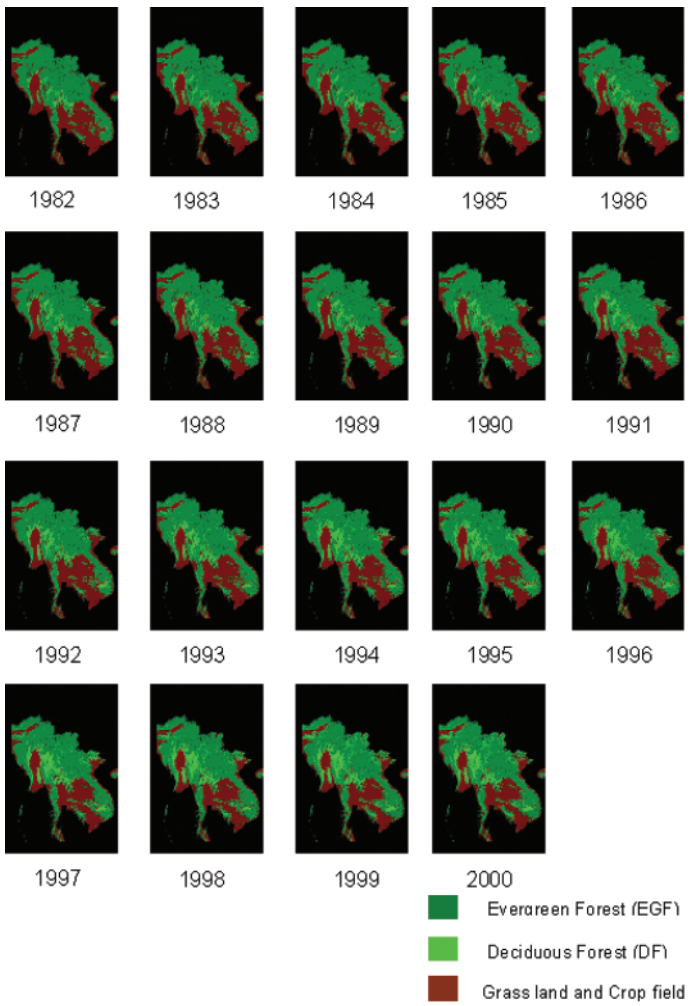

FIG. 3. Land cover maps classified using NOAA Pathfinder AVHRR 8-km land (PAL) images

between evergreen forests, mixed deciduous forests, and deciduous forests would be soft or fuzzy lines. It is important to decide on the classification scheme, especially the number of classification types to be defined.

Even with these limitations, the feasibility of retrieving land cover maps of the Mekong basin for a 20-year period was confirmed in this study. This finding is useful for retrieving land cover for a long period, and the maps could be used for regional-scale modeling. However, validation has not been conducted, and misclassification seems to accumulate process by process. For more accurate land cover maps, it would be necessary to insert a validation and feedback algorithm into the repeated procedure represented in this study and construct a validation dataset for the test area.

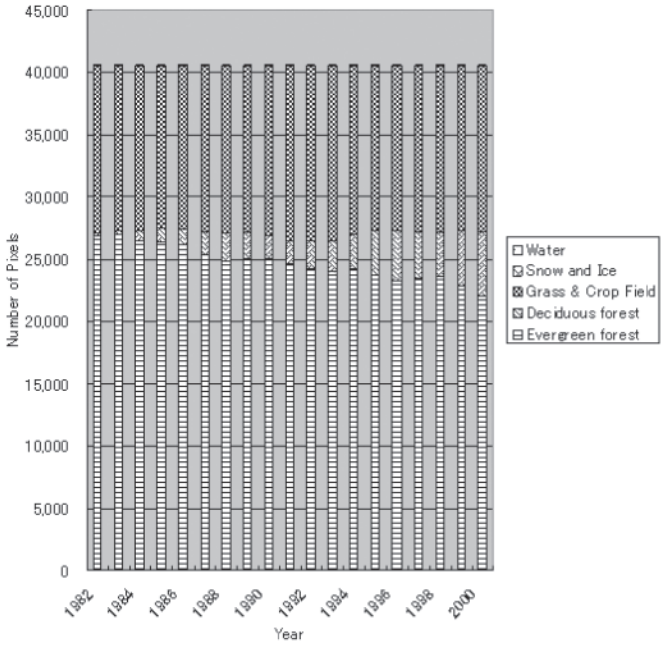

FIG. 4. Interannual changes in number of pixels for each class

Acknowledgments. This study was funded by the "Research Revolution 2002 Project" of MEXT (Ministry of Education, Culture, Sports, Science and Technology) and the "Assessment of the Impact of Global-Scale Change in Water Cycles on Food Production and Alternative Policy Scenario" of AFFRCS (Agriculture, Forestry and Fisheries Research Council Secretariat), Japan.

References

Agbu PA, James ME (1994) The NOAA/NASA Pathfinder AVHRR land data set user's manual. Goddard Distributed Active Archive Center, NASA, Goddard Space Flight Center, Greenbelt, MD

Awaya Y, Kodani E, Tanaka K, Liu J. Zhuang D, Meng Y (2004) Estimation of the global net primary productivities using NOAA image and meteorological data: changes between 1988 and 1993. Int J Remote Sens 25:1597–1613

DeFries R, Chan JC (2000) Multiple criteria for evaluating machine learning algorithms for land cover classification from satellite data. Remote Sens Environ 74:503–515

DeFries R, Hansen M (1994) NDVI derived land cover classification at a global scale. Int J Remote Sens 4:3567–3586

DeFries R, Hansen M, Townshend J (1995) Global discrimination of land cover types from metrics derived from AVHRR Pathfinder data. Remote Sens Environ 54:209–222

DeFries R, Hansen M, Townshend J, Sohlberg R (1998) Global land cover classification at 8 km spatial resolution: the use of training data derived from Landsat imagery in decision tree classifiers. Int J Remote Sens 19:3141–3168

Hansen MC, DeFries R, Townshend JRG, Sohlberg GR (2000) Global land cover classification at 1 km spatial resolution using a classification tree approach. Int J Remote Sens 21:1331–1364

Jackson RD, Slater PN, Pinter PJ (1983) Discrimination of growth and water stress in wheat by various vegetation indices through clear and turbid atmospheres. Remote Sens Environ 15:187–208

Loveland TR, Reed BC, Brown JF, Ohlen DO, Zhu Z, Yang L, Merchant JW (2000) Development of a global land cover characteristics database and INBG DISCover from 1 km AVHRR data. Int J Remote Sens 21:1303–1330

Millington AC, Alexander RW (2000) Vegetation mapping in the last three decades of the twentieth century. In: Alexander R, Millington AC (eds) Vegetation mapping. Wiley, Chichester

Sawada H, Sawada Y, Makara M (2004) NDVI and thermal data to reveal environmental changes in forest area for twenty years in the Mekong river basin. In: Proceedings of international conference on advances in integrated Mekong River management, 25–27 Oct. 2004, Vientiane, the Lao PDR, pp 59–65

Sawada Y, Mitsuzuka N, Sawada H (2005) Development of a time-series model filter for high revisit satellite data. In: Veroustraete F, Bartholome' E, Verstraeten WW (eds) Proceedings of the 2nd international VEGETATION users conference, Antwerp, Belgium 24–26 March 2004. Office for Official Publication of the European Communities, pp 83–89

Tucker CJ (1979) Red and photographic infrared linear combinations for monitoring vegetation. Remote Sens Environ 8:127–150

Tucker CJ, Newcomb WW, Los SO, Prince SD (1991) Mean and inter-year variation of growing-season normalized difference vegetation index for the Sahel 1981–1989. Int J Remote Sens 12:1113–1115

Technical Report

Effect of Forest Cover Change on Sedimentation in Lam Phra Phloeng Reservoir, Northeastern Thailand

Kosit Lorsirirat

To predict the lifespan of Lam Phra Phloeng Reservoir, in which the capacity has been reduced by sedimentation, both sediment inflow volumes generated from upstream areas of the catchment and deposition in the reservoir were calculated. The rating curve of the relationship between discharge and sediment at station M.145 from 1996 to 2000 obtained using water level discharge and a sediment estimation (LQS) showed that the annual sediment volume resulting from inflow to the Lam Phra Phloeng catchment (820 km^2) was 0.36553 Mm^3 (million cubic meters). The siltation rate and annual sediment volume in the reservoir were obtained for a series of periods. During the first period, from 1970 to 1983, the annual sediment volume was 2.23 Mm^3 and the erosion rate was 2.72 mm/year/km^2. This period coincided with a 73.57% decrease in forest area. The second period, from 1983 to 1991, had a lower annual sediment volume of 1.625 Mm^3 and a lower erosion rate of 1.98 mm/year/km^2. The forest area increased 1.05% during this period. In the recent period, from 1991 to 2000, the annual sediment volume was 0.36553 Mm^3 and the erosion rate was 0.445 mm/year/km^2. These low rates were associated with a 4.95% increase in forest area. Since the 1960s, the agriculture of Thailand has shifted from subsistence farming to a cash crop culture to develop the social economy. This shift has resulted in the conversion of forests to cultivated lands. As a result, rapid deforestation has occurred, and soil erosion in crop fields has become a serious problem with regard to resource degradation. Soil erosion from crop fields has generally been recognized since the old days. According to statistics, the area of forest in Thailand decreased from 29.1 million hectares (ha) (56.7% of the total land) in 1961 to 13 million hectares (25%) in 1998. Relative to the FAO statistical database for 2005, the area of crop fields increased from 1 million hectares (2% of the total land) in 1962 to 4.6 million hectares (9%) in 1999, and the area of paddy fields also increased from 6.7 million hectares (13%) to 10.5 million hectares (21%). The most deforested region is northeast Thailand.

Office of Hydrology and Water Management, Royal Irrigation Department, Bangkok Thailand
E-mail: kositl@mail.rid.go.th

1. Introduction

Siltation and sedimentation are widespread problems affecting the viability of water supply systems in Thailand and most other countries of the region. Siltation of catchment reservoirs is a significant problem because of rapid economic and population growth. Water supply is and will increasingly be a critical issue (Kosit 1992). Sediment accumulation in reservoirs of the northeastern regions of Thailand has intensified. Decreases in the storage capacity of reservoirs because of sediment accumulation hinder water operations in irrigated areas. Thus, plans for water resource management are developed successfully by considering sedimentation and erosion. This study of the Lam Phra Phloeng Catchment conducted by the Royal Irrigation Department (RID) focuses on one of the most serious sedimentation problems in Thailand. The goal of this research was to understand how hydrological data can be used in the calculation of the volume of sediment generated by sources over the entire catchment and deposited in the reservoir as a sink, to obtain values comparable to observed data from reservoir surveys. The parameters for water level discharge and the sediment estimation (LQS), such as sediment volume yielded from bank erosion and channel incision, were calculated for use by the RID, and the lifespan of the reservoir was calculated following United States Bureau of Reclamation (USBR) methods (USBR 1974).

Concerns about water resource management, specifically catchment-scale decision making, can be addressed with information on the hydrological processes of sediment generation and storage of individual catchments. Such a case study of sedimentation, represented by observed data, can be applied to the planning and development of water resources. The objectives of this study were to estimate siltation and sedimentation rates and predict the lifespan of the Lam Phra Phloeng Reservoir.

2. Study Site and Methods

This study was conducted as part of the Lam Phra Phloeng dam project, which was located in the Lam Phra Phloeng Catchment at 14°30'34" N and 101°50'28" E in Nakhon Ratchasima province, in the northeastern region of Thailand (Fig. 1). The catchment area is approximately 820 km^2, and the annual inflow averages 241.93 Mm^3 (million cubic meters). The average at station M.145 was 99.55 Mm^3. The climate of the study area is typically tropical savannah affected by monsoon; the annual rainfall is about 1140 mm/year and ranged from 925 to 1491 mm/year over the period from 1990 to 2000. Most of the rainfall (80%) occurs from May to September. The soil texture is predominantly silty loam with gently undulating loam soil. Some of the forested areas are protected, but gradual encroachment of upland agriculture into the forested area is evident. Most of the water supplied from upland catchment areas in Wang Nam Kaew District is taken into the paddy field systems, which results in increased evaporation and infiltration of water at the beginning of the wet season. The field intake causes a reduction in the flow velocity of river water and increases sediment deposition in the riverbed. Finally, the district serves as an effective sink zone for eroded material generated from the entire catchment.

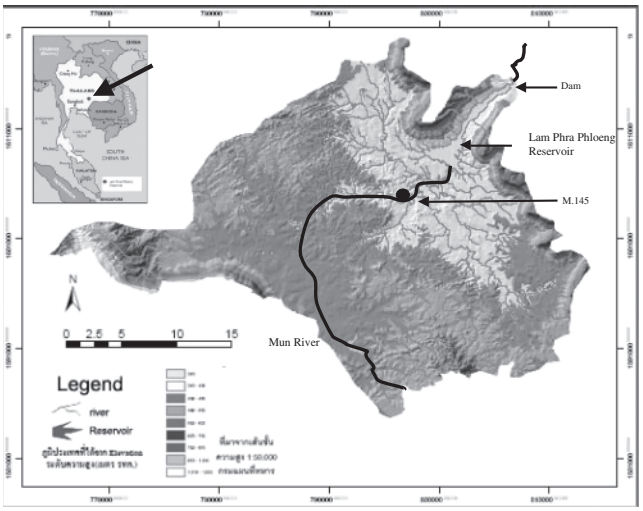

Fig. 1. Study area in Lam Phra Phloeng Catchment located in P. Nakhon Ratchasima, Thailand

The data required for this study can be derived from topographic, soil, and land-use cover classification maps managed by the Land Development Department (LDD) and forest maps managed by the Royal Forestry Department (RFD). The hydrological data set, including rainfall, runoff, sediment, and contour maps of the reservoir, was provided by the RID.

2.1. Methods

We considered sediment sources associated with the changing forest area within the catchment in four different years: 1974, 1979, 1985, and 1991 (Fig. 2). The sediment sink was assessed from hydrological measurements and surveys of reservoir sedimentation in 1983, 1991, and 1998 (Table 1). Thus, hydrological measurements have been carried out to determine the relationship between discharge and sediment yield from the Lam Phra Phloeng Catchment area. Monthly runoff data at station M.145, located upstream of the catchment, were used for sediment inflow data from 1996 to 2000 and to estimate the sediment discharge from the entire catchment area from 1990 to 2000.

2.2. Determination of Reservoir Lifespan

We used the empirical area-reduction method of the USBR (USBR 1974) to determine the distribution of sediment deposition in the reservoir. The trap efficiency of the reservoir sediment deposition rate was calculated from the relationship between the capacity inflow and the trapped sediment value. The trap efficiency was calculated as 0.4445 by comparing the capacity inflow with the trapped sediment value from the Brunes curve. Approximately 96% of the sediment inflow was predicted to be deposited and stored in the reservoir. The annual sediment volume accumulated in the

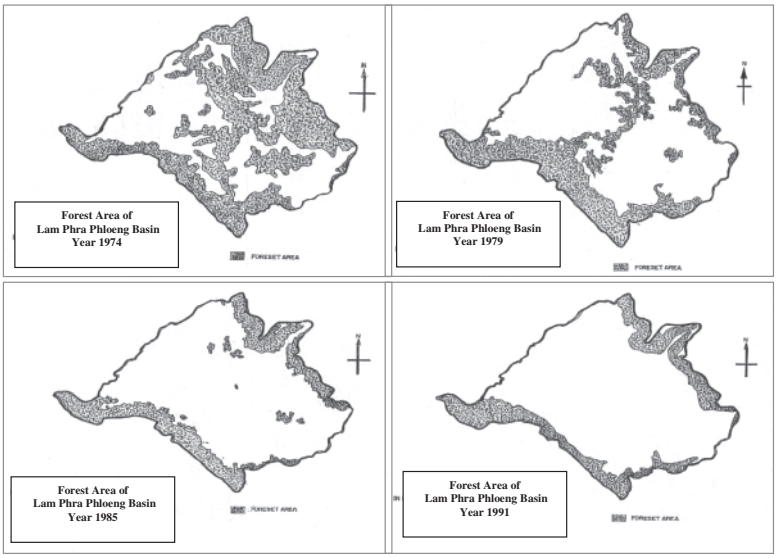

FIG. 2. Change of forest area in Lam Phra Phloeng Catchment years 1974, 1979, 1985, and 1991

TABLE 1. Forest cover and reservoir sedimentation

Year	Forest area (%)	Capacity (Mm^3)	Annual sediment yield (Mm^3/km^2/year)
1970	95.41	150.00	—
1974	72.77	—	
1979	50.94	—	
1983	21.84	121.00	2.23
1985	21.52	—	
1991	20.54	108.00	1.63
1998	25.59	105.45	0.37

reservoir was calculated as 1.94 mm/km^2/year, which reduced the water storage capacity of the reservoir. The distribution of sediment deposition in the reservoir was estimated using the empirical area-reduction method. The resulting total annual sediment inflow was 1.6250 Mm^3/year. From these estimates, the reservoir's lifespan was predicted as 32 years after its completion in 1970.

3. Results and Discussion

3.1. Sediment Inflow to the Reservoir

Deforestation reduced the forested area by about 51.25% from 1974 to 1985. The forested area declined from 531 km^2 to only 160.25 km^2 (Kosit 1992). We explored the calculation of sediment volume for any specified period using a number of methods, including continuous integration. As a result, the 820 km^2 of the entire catchment area

TABLE 2. Mean annual runoff at station M.145 (Mm^3)

Year	April	May	June	July	August	September
1990	—	—	—	—	—	8.63
1991	0.35	10.03	10.84	5.15	11.60	31.52
1992	0.29	5.08	2.84	7.67	13.28	5.43
1993	3.79	2.74	4.06	1.08	2.31	27.16
1994	2.58	10.82	8.70	12.54	7.54	5.80
1995	2.20	5.10	2.70	6.70	15.90	55.20
1996	3.67	10.57	8.39	7.00	9.90	52.96
1997	1.98	2.70	1.41	1.57	3.27	14.0
1998	0.56	5.36	1.31	1.09	6.50	7.54
1999	4.33	29.86	6.23	4.53	6.60	24.05
2000	11.11	16.23	9.82	9.24	14.20	24.20
Mean	3.08	9.85	5.63	5.65	9.11	23.32

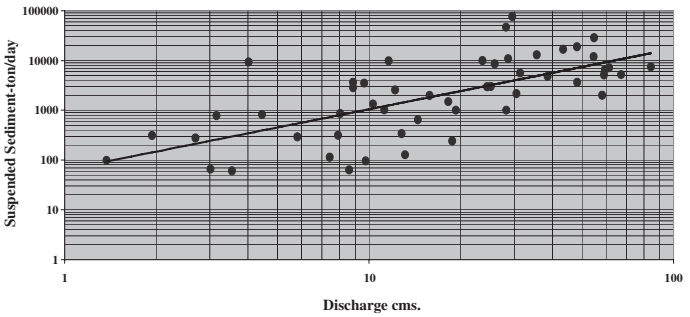

FIG. 3. Sediment volume plotted against discharge in 1996–2000 at station M.145

included 10.78 km^2 as reservoir water surface and 809.3 km^2 as reservoir catchment area of Lam Phra Phloeng, which produced a total of 241.93 Mm^3 in discharge. Given that the unit weight is 1.2685 tons/m^3, sediment inflow to the reservoir was estimated at 0.36553 Mm^3. The runoff yield in the Lam Phra Phloeng River basin was estimated from runoff records from gauging stations. The results show that the runoff yield at the hydrological stations averaged 9.48 l/s/km^2, and annual discharge at station M.145 averaged 99.55 Mm^3 or 3.15 cm over a period of 10 years. These measures can be formulated as a ratio representing the annual discharge in the study area (Table 2). The discharge data from station M.145 were from 1991 to 2000, and the sediment data were from 1996 to 2000. The water level and sediment yield results were plotted against discharge in Fig. 3.

A rating curve was used to determine sediment inflow to the reservoir. We analyzed the relationship between sediment and discharge using the LQS program. This calculation provided a rating curve of relationships between discharge (Q_w) and sediment concentration (Q_{sed}), which was obtained from the observed hydrological data. We used the curve to integrate the total sediment weight over a period of 5 years. All coefficients were determined using nonlinear regression and were substituted into the following equation:

Table 2. *Continued*

October	November	December	January	February	March	Annual
72.67	5.14	1.59	1.63	0.68	0.83	—
20.86	1.73	0.51	0.48	0.20	0.72	93.97
24.11	4.62	1.15	0.67	0.39	0.70	66.20
19.57	2.22	1.03	0.58	0.43	0.77	65.72
4.03	0.94	0.55	0.39	0.25	0.05	54.19
28.60	4.70	2.60	1.50	1.70	1.10	128.00
50.67	13.88	4.88	3.70	2.76	2.69	171.06
7.63	1.12	0.54	0.43	0.06	0.00	34.72
9.28	1.47	1.31	0.90	0.67	—	—
55.20	15.34	4.03	2.72	3.09	2.21	158.19
24.94	5.09	2.84	2.24	1.71	2.35	123.96
28.87	5.11	1.91	1.38	1.08	1.14	**99.55**

$$Q_{sed} = 70.018(Q_w)^{1.5094} \ (r^2 = 0.6461) \quad (1)$$

where Q_w = cubic meters per second (cms) and Q_{sed} = tons per day.

The results from station M.145 indicated that the average annual sediment was 144 843.8 tons/year. The sediment yield varied from 34.33 to 1047.36 tons/year/km^2 over the period from 1996 to 2000, and the average sediment yield was about 434.964 tons/year/km^2. The volume of sediment yielded from the effective catchment area of 820 km^2 was represented as the sediment volume deposited in the reservoir. The effective catchment area was calculated by subtracting the reservoir area, 10.78 km^2, from the entire catchment area. The gross sediment volume calculated from sediment concentration, 356 670 tons/year, plus an additional 30% of bedload (sediment transported continuously along the riverbed, carried forward by rolling, sliding, or hopping on the floor), yielded 463 671 tons/year. This volume estimate was not obtained by direct measurements, but rather by the estimation of the total sediment inflow minus the suspended sediment in the reservoir. In Thailand, using the unit weight of sediment as 1.2685 tons/m^3, the gross annual sediment can be converted to 0.36553 Mm^3.

Reservoir sedimentation can be derived from previous reservoir surveys by contour mapping (see Table 1). In 1970, 1970 to 1983, 1983 to 1991, and 1991 to 1998, the reservoir capacities were 150.00 Mm^3, 121 Mm^3, 108 Mm^3, and 105.45 Mm^3, respectively. The sediment yield varied inversely with forest cover area. Thus, although the forest cover from 1970 to 1983 and from 1983 to 1991 decreased to 73.75% and 1.30%, respectively, the sediment yield increased to 2.23 Mm^3 and 1.63 Mm^3, respectively. In contrast, during the period from 1991 to 1998, forest cover increased by 4.95% and the sediment yield decreased to a level of 0.37 Mm^3. This phenomenon coincided with previous studies of soil and water losses from various land uses in different regions of Thailand. For instance, soil loss from forest land, agriculture land, agroforestry, forest plantations, and para rubber varied from 0.1 to 4.5, 0.8 to 123.4, 0.1 to 13.0, 3 to 5, and 5 to 7 ton/hectare (t/ha)/year, respectively, as shown in Table 3.

This rate of sediment delivery is broadly comparable with the rates of sediment yield produced by selective felling of the Batangsi watershed in Peninsular Malaysia, where disturbance of the steep granitic slopes produced 2826 t/km^2/year during the

Table 3. Soil and water losses from various land uses in different regions

Land use	Location	Rainfall (mm)	Slope (%)	Soil characteristics	Soil loss (t/ha/year)	Runoff (mm)
Northern region						
Forest land						
-Hill evergreen	Chiangmai	2100	20–30	SC, SCL: granite	0.0	
-Mixed deciduous	Lampang	1400		SC, SC: limestone	1.0	
-Mixed deciduous With teak	Lampang	1400		SC, SC: shale, Sandstone	0.9	
-Dry dipterocarp	Lampang	1400		SC: shale, slate	0.5	
-Dry hill evergreen	Lampang	1400		SCL: shale, slate	3.1	
-Teak plantation	Chiangmai	36			3.6	
-Terraced forest Plantation	Chiangmai	1200	40–60	Limestone	0.9	14
-Forest plantation	Chiangmai	1200	40–60	Limestone	3.6	42
Shifting cultivation	Chiangmai	2100	20–25	SL, SCL: granite	0.8	
Agroforestry						
-Forest, coffee	Chiangmai	2100	20–25	SL, SCL: granite	0.1	
-Fruit tree, coffee	Chiangmai	2000	54	SL, SCL: granite	13.0	170
Upland agriculture						
-Maize	Chiangmai		36		52.0	
-Rice	Chiangmai		36		99.0	
-Beans	Chiangmai		36		31.0	
-Sesame	Chiangmai		36		91.0	
Conservation farming						
On slopes						
-Traditional	Mae Hongson	1351	30–40		32.3	135
-Hedgerow	Mae Hongson	1351	30–40		8.2	113
-Grass strip	Mae Hongson	1351	30–40		6.3	106
-Hillside ditch	Chaiang Rai	1650	20–50	C: granite	62.0	60
-Natural forest	Chaiang Rai	1650	20–50	C: granite	18.0	38
-Bench terrace	Chiangmai	1200	25	SL: granite	6.0	25
-Hillside ditches	Chiangmai	1200	35	SL: granite	13.0	22
-Contour bund	Chiangmai	1200	35	SL: granite	8.8	20
Northeastern region						
Agricultural land						
-Maize (no till)	Sakon Nakon	940	9	L: sdeletal	15.5	320
-Maize (cultivated)	Sakon Nakon	940	9	Silicious	23.6	282
-Bare soil	Sakon Nakon	940	9		24.8	357
-Maize (no till)	Kalasin	1199	6	Pairintra	16.4	221
-Maize (cultivated)	Kalasin	1199	6	L: silicious	17.9	224
-Bare soil	Kalasin	1199	6		20.9	282
-Maize (conventional)	Chaiyaphum	1542	27	Sandstone + shale	70.1	240
-Maize (cultivated)	Chaiyaphum	1542	27	Lignt C	85.6	253
-Bare soil	Chaiyaphum	1542	27		123.4	427
-Kenaf	Khon Kaen	1200	5	Yasothon series	5.0	308
-Bare soil	Khon Kaen	1200	5	Yasothon series	11.7	467

Table 3. *Continued*

Land use	Location	Rainfall (mm)	Slope (%)	Soil characteristics	Soil loss (t/ha/year)	Runoff (mm)
Forest land						
-Dry mixed deciduous	Sakon Nakon	940	9	L: skeletal	2.4	85
-Dry evergreen	Chaiyaphum	1542	27	Sandstone + shale	3.8	38
-Dry evergreen	Chaiyaphum	1009	27	Loght C	2.3	
-Mixed deciduous	Kalasin	1199	6	L: silicious	4.5	38
-Dry evergreen	Pak Chong		56		0.2	
Vegetative erosion control						
-Bare soil	Pak Chong	902	9	Pak Chong series	57.0	456
-Contour planting	Pak Chong	901	9	Pak Chong series	0.4	18
-Maize + cover crop	Pak Chong	902	9	Pak Chong series	0.2	11
-Maize + grass strip	Pak Chong	902	9	Pak Chong series	0.0	3
Eastern region						
Cassava with vegetation control						
-Bare	Sri Racha	1031	9	SL	64.0	367
-Crop rotation	Sri Racha	1031	9	SL	1.4	57
-Grass strip	Sri Racha	1031	9	SL	9.0	46
-Bare	Rayong	720	9	Fine L	96.3	661
-Ploughed up, down	Rayong	720	9	Fine L	75.3	637
-Residue of last crop	Rayong	720	9	Fine L	39.5	456
Intercropping and mechanical control						
-Bare	Rayong	1140	8	SL	33.4	524
-Sorghum + groundnut	Rayong	1140	8	SL	6.8	121
-Cassava + black bean	Royong	1140	8	SL	13.5	172
-Cassava + furrowing Cross-slope	Royong	1140	5	SL	4.6	142
Southern region						
Natural forest						
-Moist evergreen	Krabi	1200	30–35		1.0	
Forest plantation						
-Terraced *Parkia* sp.	Krabi	1200	30–35	Sandstone	4.0	
-Unterraced *Parkia* sp.	Krabi	1200	30–35	Sandstone	5.0	
-Unterraced *Litsia* sp.	Krabi	1200	30–35	Sandstone	3.0	
Para rubber Plantation						
-Terraced	Krabi	1200	30–35		5.0	
-Unterraced	Krabi	1200	30–35		7.0	
Western region						
Natural forest						
-Dry dipterocarp	Kanchanaburi	1644	30	SCL	0.1	9.6
-Bamboo	Kanchanaburi	1644	30	SCL	0.1	8.1

Table 3. *Continued*

Land use	Location	Rainfall (mm)	Slope (%)	Soil characteristics	Soil loss (t/ha/year)	Runoff (mm)
Agroforestry						
-Rice in D. *alatus*	Kanchanaburi	1644	30	SCL	0.0	9.4
-Maize in D. *alatus*	Kanchanaburi	1644	30	SCL	0.3	8.6
-Cotton in A. *indica*	Kanchanaburi	1355	20	SCL	3.9	89.4
-Maize in P. *javanica*	Kanchanaburi	1355	20	SCL	3.9	86.5
-Maize in E. *camal-dulensis*	Kanchanaburi	1355	20	SCL	3.2	124.4
-Maize in *L. leuco-cephala*	Kanchanaburi	1355	20	SCL	2.6	86.0
Vegetative control						
-Maize + grass strip	Kanchanaburi	1355	20	SCL	0.3	26.0
-Maize + grass + terrace	Kanchanaburi	1355	20	SCL	0.2	23.0
-Conventional	Kanchanaburi	1355	20	SCL	0.4	33.0

SL, sandy loam; SCL, sandy clay loam; SC, sandy clay; CL, clay loam; C, clay; L, loamy
Source: Thai Forest Sector Master Plan

immediate post-felling period (Lai 1992). The rates are, however, much larger than the 1600 t/km^2/year observed when lowland forest in Borneo was selectively logged (Douglas et al. 1999). The decline in sediment delivery as the landscape and forest recovered, increasing from 21% to 26% forest cover between 1983 and 1998, is to be expected with reforestation by natural regeneration (Douglas et al. 1995; Evans and Turnbull 2004), but the sediment yield of about 500 t/km^2/year remains high in comparison to other partially forested watersheds in Southeast Asia (Sidle et al. 2006).

Hydrographic surveys are the most commonly used method for surveying reservoirs, and they are based on range lines. A rangeline survey requires that beacons be established along each bank to mark the ends of the range lines. The positions of the beacons are established by triangulation, which can be relatively expensive and time consuming. However, range-line surveys do not require particularly sophisticated equipment and are best suited to the resources and skills in this study. The depth of water along a range line is normally measured using an echo sounder with continuous chart readout mounted on a boat or using a measuring rod in shallow water. The measured depths are related to an average water surface elevation. Position-fixing equipment is required to guide the survey vessel along the range line and locate its position when each depth measurement is taken.

By comparing the 1970 contour map (reservoir capacity = 150.00 Mm^3) with reservoir surveys from 1970 to 1983 (reservoir capacity = 121 Mm^3), 1983 to 1991 (reservoir capacity = 108 Mm^3), and 1991 to 1998 (reservoir capacity = 105.45 Mm^3), sediment volume in the reservoir was 29 Mm^3 with an annual sediment input of 2.23 Mm^3 and a depth of erosion rate of 2.72 mm/year/km^2 in the first 13 years. During the second period, the input was 13 Mm^3 in 8 years, or 1.625 Mm^3 annually; the calculated depth of the erosion rate was 1.63 mm/km^2/year. These data represent maximal rates of

sedimentation when 73.57% of the forested area was reduced from 1970 to 1983. Over the period from 1983 to 1991, the forested area decreased only slightly (1.30%), and from 1991 to 1998, the forested area increased by about 4.95% (Arthorn and Somchai 1999); as expected, the sedimentation rate was lower (see Table 1). The total annual sediment was estimated as 0.365553 Mm^3 from the data at station M.145. Over the period from 1970 to 1983, the sediment yield was 2.23 Mm^3/km^2/year; from 1983 to 1991 the sediment yield was 1.63 Mm^3/km^2/year; and from 1991 to 1998, the sediment yield was 0.37 Mm^3/ km^2/year.

3.2. Reservoir Lifespan Prediction

Using the empirical area-reduction method, reservoir sedimentation patterns can yield a relationship between reservoir depth and capacity. The total capacity of the Lam Phra Phloeng Reservoir was 108 Mm^3, with the dead storage at least 240.00 m (a.s.l.). The total annual sediment inflow was measured in reservoir surveys in 1983 and 1991 at 1.6250 Mm^3. Given the sediment accumulation in the Lam Phra Phloeng Reservoir, a lifespan can be computed using the foregoing equation. The result suggests that the lifespan of the reservoir will be 11 years after the second survey in 1991. For further study, to consider the linkages among soil erosion, sources of sediment in upstream areas, and downstream sedimentation sinks in the reservoir, Geographic Information System (GIS) and soil erosion control techniques should be established to develop an integrated plan for catchment management.

4. Conclusion

The volume of sediment yielded from the Lam Phra Phloeng Catchment and the decreasing reservoir capacity caused by sedimentation were measured. Our main findings were the following:

1. The siltation rate and annual sediment volume in the reservoir changed through time. In the first period, from 1970 to 1983, annual sediment volume was 2.23 Mm^3 and the erosion rate was 2.72 mm/year/km^2 because 73.57% of the forested land area had been altered. In the second period, from 1983 to 1991, the forested area increased by 1.05% and sediment inputs declined; the annual sediment volume was 1.625 Mm^3 and the erosion rate was 1.98 mm/year/km^2. In the most recent period, from 1991 to 2000, the forested area increased by 4.95%, the annual sediment volume further declined to 0.36553 Mm^3, and the erosion rate was only 0.445 mm/year/km^2.
2. The total annual sediment inflow was 1.6250 Mm^3/year, so the reservoir lifespan was predicted to come to an end in 2002, 11 years after the second survey in 1991.

One of the major problems in water resource management is sedimentation in reservoirs, which affects reservoir lifespan, flooding, drought, and all sectors of water consumption in the downstream land areas. Our research in Thailand indicates the role of forested lands as an efficient alternative to other land uses. To improve water yields, it is essential not to focus only on the water body. Water resource planning and related concerns require a holistic approach to watershed management to control reservoir sedimentation.

References

Arthorn C, Somchai N (1999) Environmental study of Lam Phra Phloeng Reservoir Sedimentation. Hydrology Division, Royal Irrigation Department, Thailand

Douglas I, Greer T, Sinun W, Anderton S, Bidin K, Spilsbury M, Suhaimi J, Sulaiman A (1995) Geomorphology and rain forest logging. In: McGregor DFM, Thompson DA (eds) Geomorphology and land management in a changing environment. Wiley, Chichester, pp 309–320

Douglas I, Bidin K, Balamurugan G, Chappell NA, Walsh RPD, Greer T, Sinun W (1999) The role of extreme events in the impacts of selective tropical forestry on erosion during harvesting and recovery phases at Danum Valley, Sabah. Philos Trans R Soc Lond Sers B Biol Sci 354:1749–1761

Evans J, Turnbull J (2004) Plantation forestry in the tropics, 2nd edn. Oxford University Press, Oxford

FAO Statistical Database (2005) FAOSTAT-Agriculture. [online] http://faostat.fao.org/faostat/

Kosit L (1992) Effect of basin characteristics and forest cover on reservoir sedimentation in northeastern Thailand. Kaseatsat University, Thailand

Lai FS (1992) Sediment and solute yields from logged, steep upland catchments in Peninsular Malaysia. PhD thesis. University of Manchester, Manchester

Sidle RC, Ziegler AD, Negishi JN, Nik AR, Siew R, Turkelboom F (2006) Erosion processes in steep terrain: truths, myths, and uncertainties related to forest management in Southeast Asia. For Ecol Manag 224(1-2):199–225

USBR (1974) Design of small dams. United States Department of the Interior, United States Bureau of Reclamation, Washington, DC (revised reprint 1974)

Seasonally Flooded Community Forest on the Banks of the Songkhram River: A Research Framework

Taro Sasaki*, Supaporn Worrapornpan, and Sunan Seesang

The Songkhram River is a 420-km-long tributary of the Mekong River and is the last remaining, free-flowing, undammed Mekong tributary in northeast Thailand. This chapter seeks to clarify the framework of competition and harmony in land use of the seasonally flooded community forest on the banks of the Songkhram River. In a study of Thai forest policy, we identified two kinds of policy: a strong policy for excluding illegal farmers from the national forest, and a realistic response to the farmers involving a partial release of national forestland and community forestry. The participation of local people in forest management should be a key factor for solving the land problem in the national forest. The seasonally flooded forest in the Songkhram River Basin grows at the periphery of agricultural land and lies between water resources and agricultural land geographically. While flooded, the land is unsuitable for agriculture, but this prevents deforestation and provides rich natural resources for the local inhabitants.

1. Introduction

Any discussion of the management of natural resources tends to be in the context of the antagonism between the central government and local communities. The nationalization of forest by the central government has faced policy implementers with land tenure issues that reflect the conflict between traditional land use and nationalization. The policy makers tacitly agreed that local people should be settled in fixed villages or moved out of the national forests. These political conditions cannot be treated in the same way, and we must consider the condition of natural resources and geographic land types.

This chapter considers the forest on the banks of the Songkhram River. The Songkhram River flows through Udon Thani, Sakon Nakhon, and Nongkhai provinces of northeastern Thailand to join the Mekong River in Nakhon Phanom Province. This 420-km-long tributary of the Mekong River has a catchment area of 12 367 km^2. It is

* International Cooperation Center for Agricultural Education (ICCAE), Nagoya University, Nagoya, Japan
E-mail: tsasaki@agr.nagoya-u.ac.jp

the last remaining, free-flowing, un-dammed Mekong tributary in northeast Thailand and is important as a store of aquatic biodiversity.

The Department of the Promotion and Development of Energy of the Ministry of Science, Technology, and the Environment proposed constructing a dam on the Songkhram River to prevent flooding and provide water for irrigation. The project was rejected by the National Environment Board (NEB) in 1994. In reaching this decision, local communities had strongly protested against this project, especially on learning of the impact of the Pak Mun Dam on the livelihoods of local people. This protest movement was supported by nongovernmental organizations (NGOs), as well as by people from various sectors in Udon Thani, Sakon Nakhon, and Nakhon Phanom, and academics from Bangkok (Pinkaew 2002).

The debate led to field studies of the Songkhram River. Using 1 : 50 000 aerial photographs, Supranee (2000) revealed that the riparian forest areas were limited to the floodplain and that major changes from riparian forest to agricultural lands had occurred. Suthep and Bunrak (2001) identified land-use changes by comparing Landsat TM images obtained in March 1989 and 1998; they reported that water resources had increased 110%, 35% of the forest area and 47% of the bamboo forest had changed to agricultural land, and the human communities had expanded by 57.3%. Suwit et al. (1987) described the economic changes for communities in the Songkhram River Basin from 1932 to 1987. They conducted field studies in three provinces, Sakon Nakhon, Nakhon Phanom, and Nong Khai, and identified three important factors that contributed to the change in the village economy: rapid population growth as a result of the improved government public health service, the construction of roads to connect the villages with other towns, and the introduction of cash crops, such as kenaf and cassava, in the villages.

These studies revealed the land-use change within the framework of competition between agricultural land use and forest conservation. However, the people's relationship with forests and forest products is still not clear, so those frameworks have treated only a very narrow view of the situation. The main objective of this chapter was to determine the characteristics of forestland use on the banks of the Songkhram River and provide the basic framework needed for conducting field research in this area. To achieve this, we examined the history of the Thai forest policy sector to explain the general pressure on forestland in Thailand and studied community forestry on the banks of the Songkhram River using secondary data and field interviews, focusing on the characteristics of seasonally flooded forest. For secondary data, the booklet "Tambon Agricultural Development Plan" was obtained from the Tambon Administrative Organization and the Provincial Agriculture Office, Department of Agricultural Extension. Fieldwork was conducted in community forests sampled from "the complete list of community forests" (Provincial Forest Office).

2. History of Forest Resource Policies

2.1. Custom of Chap chon and National Forests

The forest resource policy in Thailand can be classified into three areas: forest conservation, immigration, and reforestation. Forest conservation policy is based on legislation concerning forest management and conservation, which has been accom-

panied by the establishment of target areas. The policy objective is based mainly on forest conservation through the expulsion of people from the national forest. Although these policies have stopped deforestation, they have not facilitated conservation and reforestation. Reforestation was begun through government and immigration policies to break the stagnation in forest conservation, which was unsuccessful in gaining the cooperation of local villagers.

Special feature articles have been published, such as "Land issues: the past, the present and the future" in *Economics and Society*, the Bulletin of the National Economic Social Development Board (NESDB). These articles classify land issues in Thailand into three types: those concerning the landless, the peasants, and land tenure. The issue of land tenure does not mean that people do not have enough land to cultivate, but that farmland exists inside national forests where land acquisition is prohibited by the land law. The World Bank estimates that 1 million households are living inside the national forests (NESDB 1980).

The government formed the National Committee on Land Classification in 1960 and classified land into National Conservation Forests (*pa thawon*) comprising 25.9 million ha and farmland and other types comprising 25.3 million ha. National Conservation Forests were converted into National Reserved Forests (*pa saguan*) on enacting the National Reserved Forest Act in 1964. National Conservation Forests were designated on a register of title deeds and require a land survey for ratification. Article 14 of the Reserved Forest Act states, "Within the National Reserved Forests, no person shall occupy, possess, exploit or inhabit the land, develop, clear, burn the forest, collect the forest products or cause by any other means whatsoever any damage to the nature of the National Reserved Forests"; consequently, the acquisition of forestland is prohibited. However, the designation of National Reserved Forests is nationalization by declaration, so the government cannot gain the understanding of local people regarding the status of national forests. In fact, people enter national forests to cultivate land and cause deforestation.

The scope of this issue can be deduced from statistical data. In 1998, the total area of National Reserved Forests was 23.0 million ha (1221 sites), and that of national parks was 4.4 million ha (87 sites), but the actual forested area was less that half the area of national forests, only 12.9 million ha. Parts of the national forests are used as project areas for agrarian reform. Excluding this use, the statistics are enough to grasp the influence of people inside national forests.

The acquisition of land inside a national forest was promoted by the custom of *Chap chon*. *Chap chon* are possession rights, which are approved by investing capital (funds or labor) in land that is not owned and by utilizing the land for a certain length of time. Suehiro (1981) points out that "This resulted in the establishment of a dual system of rights to state land, with the government continuing to retain legal rights of ownership, while the squatters possessed practical rights with respect to occupancy and cultivation." This dual system spread from the central delta to the periphery, and the property system under modern law has been promoted by legal ratification after the fact.

As the aforementioned policies illustrate, two main kinds of policies exist: a strong policy for excluding illegal farmers from national forest, and a realistic response to the farmers involving the partial release of national forestland.

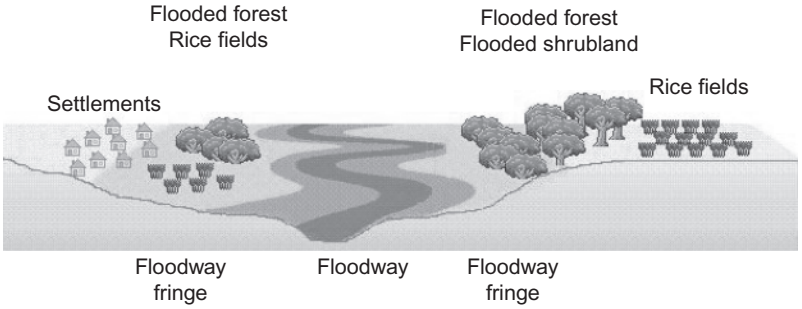

Fig. 1. Land use in the floodplain of the Songkhram River

2.2. Decentralization and Forestry Management

A centralized local administration system aims at domestic control and maintenance of order in Thailand. Therefore, even if a system of "local administration" in which a central power controls one end of the administrative organ were to exist, no form of "local autonomy" as decentralization has developed. However, the rapid development of the Thai economy during the second half of the 1980s brought about the request that concrete administration measures be implemented at the district level, and this impetus has caused a mismatch with measures promoted by the central government.

In cooperation with the United States Agency for International Development (USAID) and the National Energy Committee, the Royal Forest Department carried out the Village Woodlot Project for three years beginning in 1981. This was a pilot project that addressed the shortage of firewood and charcoal wood, with the ultimate aim of investigating the possibility of systematic firewood and charcoal wood production. The project also had social benefits. However, the project was intended to reclaim firewood and charcoal wood, and it did not answer the request of local residents for use of the forest. For example, the forest is also a place that has religious value for local residents, and nonwood forest products are also extracted. Therefore, the collection of firewood and charcoal wood led to land reclamation by exotic species such as eucalyptus, and it became clear that a fundamental part of the life of local residents could not be maintained. Subsequently, forest management by local residents who oppose centralized management was demanded. After conducting village surveys, society recognized the need for forestry management by local residents, especially in the northern region, and a measure to allow forestry management by local residents was confirmed in the forestry policy of the second half of the 1980s.

The *tambon* administrative unit was recognized as an autonomous organization that reflects local residents' intentions. In the local administrative organization, in a typical rural area, the administrative unit positioned at the bottom end of the top-down administration system is a "village" (*mu ban*), and the higher-ranking administrative unit is the *tambon*. Approximately 6400 *tambon* administrative units cover about 97% of the country and encompass about 70% of the population. The "*tambon*

council" (*sapha tambon*) was responsible for executing the policy of the centralized administration in the *tambon* administrative unit. By 1994, *tambon* councils and *tambon* local government law were enforced as part of an administrative reform, and in March 1995, the "*tambon* local government" (*ongkan borihan suan tambon*) was established to set up local autonomy with juridical responsibility. By acquiring the status of a "juridical person" in Article 6 of the law, under the law, the *tambon* local government owns and manages real estate like an individual, which allows more flexible land management. In Article 67, the "protection of natural resources and environment, management, and preservation" is mentioned explicitly. The seventh clause states, "A *tambon* self-governing body has a duty to perform the following matters in the area administered by the *tambon*, based on legal regulations." Concerning the rights and duties in connection with managing natural resources, which make local people the main stakeholders, legal maintenance has advanced in recent years.

The participation of local people in forest management has the potential to solve the land problem in national forests. It has developed into a civil movement, which also involves NGOs, without remaining in a narrow frame, defined as government and local residents. The framework for citizens' participation in municipal affairs has also increased, as seen by the debate over ratification of an article in the community forest bill.

3. Seasonally Flooded Forest in the Songkhram River Basin

3.1. Community Forestry in the Songkhram River Basin

Based on a study of Thai forest policy, we identified a conflict between traditional land use and the nationalization of forestland. This situation can differ at specific sites, so we chose to overview the situation concerning community forestry in the Songkhram River Basin.

The water level of the Mekong River and its tributaries rises quickly during the rainy season from May to October. As shown in Fig. 1, the forest and settlements are flooded, and villagers are limited by the water for 2 to 3 months from July to September. This flooding has the benefit of enriching the area with nutrients and aquatic species. In the dry season, villages use the floodplain as a resource for collecting non-timber forest products, such as vegetables, mushrooms, and bamboo shoots.

According to the provincial forestry office in Nakhon Phanom, deforestation in Nakhon Phanom Province is not as serious as it is in other provinces of northeast Thailand. One of the reasons is that the remaining land is not suitable for agriculture. Referring to the discussion over the struggle between the custom of *Chap chon* and national forests, it should be noted that the seasonally flooded forest in the Songkhram River Basin is located on the periphery of agricultural land. These forests are situated between the water resources of the Songkhram River and agricultural land; this was the result of the pressure the local people placed on land resources suitable for agriculture.

Another reason is the participation of local people in forest management. The interests of the government have shifted from "how to control the people in the

national forest" to "how to empower the local people for managing the forest." Based on data from the provincial office of the Royal Forest Department in Nakhon Phanom, in 1999, 705 community forestry sites existed in Nakhon Phanom, with an area of 77 478 *rai* (12 396 ha) managed by 409 villages. Similar data for Sakon Nakhon in 2003 indicated 86 722 *rai* (13 875 ha) of community forest managed by 883 villages in 126 *tambon*, and 239 of the 889 villages have already received government assistance. It also revealed that 404 villages did not have community forestry. Therefore, 68% of the villages had an opportunity to manage or use forest resources in Sakon Nakhon. These data show the deep link between the people and natural resources, especially community forestry. Now, the actual situation of local people in the Songkhram River Basin is discussed.

3.2. Overview of the Field Survey

A recent study of the Songkhram River was conducted by the Thai Baan Research Team with the support of the World Conservation Union (IUCN) Water and Nature Initiative (WANI). The study involved 240 villagers from four villages in the Sri Songkhram district of Nakhon Phanom Province. The study utilized the local knowledge of ecology, the management of natural resources, local history, the social economy, and livelihoods. They adopted a methodology called Participatory Learning and Action (PLA). This approach gave villagers the opportunity to conduct research on natural resources, which helped them to discover how rich their resources were, and provided them with the opportunity to hold village workshops, empowering them to become active. In all, they identified 124 fish species, 79 types of fishing gear, and 208 botanical species (plants and trees), and analyzed the utility of each species.

To conduct our field survey, we had a discussion with Mr. Rattapol Pituckthepsombat, who is part of the Conservation and Use of Natural Resources for Sustainable Biodiversity in the Klong Watershed Project of the IUCN. He explained the geographic situation, told us that he worked with communities near the Songkhram River, and introduced us in some villages so that we could interview villagers. The following is an overview of our trans-site survey.

The state of community forestry was classified into three types based on the nature of villager participation: the village conducts traditional forest management with government support (e.g., Tha Koon village), the village has just started forest management with government support (e.g., Yang Ngoy village), and the village conducts traditional, spontaneous forest management (e.g., Tha Bo village).

Tha Koon village is in Argadamnoy district, Sakon Nakhon Province. This village gave the school the right to manage 69 *rai* (11.0 ha) of forest. In their original agreement, the school served to protect the forest around the school. The agreement holds that cutting wood and burning forest are prohibited, the school will teach the villagers how to conserve forest, the villagers can use nontimber forest products (NTFPs), and that if the villagers need to use timber in the forest, they must get permission from the school. The school uses the forest for science class activities and community development. The main occupation in the village is fisheries. Some of the villagers work at contract farming, growing watermelons. The community has a forest area of 15 *rai* (2.4 ha), which is cared for by the school. Cultural forest covers 35 *rai* (5.6 ha). The land right is *Nor Sor* 3 *Kor* and *Sor Po Kor 4-01*. Local problems have included

flooding, and the sale of water rights by the village headman, which prevented the villagers from fishing.

Yang Ngoy village is in Sri Songkhram district, Nakhon Phanom Province. In this village, the village headman is interested in fresh swamp forest with an area of 280 *rai* (44.8 ha). They used the forest for fishing and had started to conserve the forest in 1991. In the past, this area was paddy fields and outsiders came to clear trees in the area. Consequently, in 1992, they held a village meeting, and asked the governor to register the area to protect the natural forest. The agreement between villagers holds that burning and destroying forest are prohibited, using the forest for NTFPs is allowed, dead trees can be used, and that the villagers are responsible for taking care of the forest, which is managed by a village committee.

Tha Bo village is in Sri Songkhram district, Nakhon Phanom Province. Tha Bo is home to six ethnic groups: Thai, Lao, Nyaw, Soe, Chinese, and Vietnamese. They started forest conservation in 2002, which resulted from a meeting after a small dam caused damage to paddy fields. They have agreed that fishing in the canal is prohibited, burning forest is prohibited, and that they can use NTFPs. The forest area is about 1000 *rai* (160 ha) and the cultural forest is 2 *rai* (0.32 ha). When the IUCN came to the village, they established a savings group and used the interest from the savings fund for conservation activities by the Fresh Swamp Forest Conservation group. They expanded their activities to a nearby village. This village action started as the idea of a 54-year-old villager, Mrs. Boonterm Narongsilp. She learned to value the rich resources in the area's inundated forest. The biodiversity provided her with bamboo, mushrooms, and a wide range of vegetables and herbs that have fed villagers for decades. Mrs. Narongsilp has been a keen researcher in her own right. She explored the forest to collect herbal plants, tested their medicinal value, and made notes on what she found to consult with experts later. She also studied the local fish and fish-catching tools used by the villagers. She makes her house available as a study center in the village. She put the knowledge she gained on display as an exhibition so that interested people and villagers could learn more about their livelihoods.

As a result of surveying these three villages, we found that people collect firewood and NTFPs regularly and that clear collection rules exist; the floodplain and flooded forest become fishing grounds in the rainy season, and are thus unsuitable for rice farming, so no anthropogenic deforestation occurs; small check dams prevent flooding inside the village, but also lead to the exhaustion of fishery resources; the government sector has only recently become aware of the traditional community forestry, so the land is still being measured; and in some villages, the villagers plant trees in the dry season to help manage the community forest.

4. Results and Discussion

This chapter sought to clarify the framework related to land use in the seasonally flooded community forest on the banks of the Songkhram River in terms of competition and harmony. In our study of Thai forest policy, we identified two kinds of policy: a strong policy for excluding illegal farmers from national forest, and a realistic response to the farmers involving the partial release of national forestland and supporting community forestry. The participation of the local people in forest

management will be the key to resolving the land problem in national forests. The seasonally flooded forest in the Songkhram River Basin is adjacent to the agricultural land. Geographically, it is located between the water resources and the agricultural land. The flooding makes this land unsuitable for agriculture, while preventing deforestation and providing rich natural resources for the local people.

Discussion of the management of natural resources tends to be held in the context of antagonism between the central government and local communities. Nevertheless, in the case of the Songkhram River Basin, the seasonal flooding provides a buffer zone along the riverbank and eases that antagonism. This is part of the reason the local people participate in forest management. Further detailed field research is needed based on this basic framework.

Acknowledgments. This study was funded by the "Assessment of the Impact of Global-Scale Change in Water Cycles on Food Production and Alternative Policy Scenario" of AFFRCS (Agriculture, Forestry and Fisheries Research Council Secretariat), Japan.

References

NESDB (1980) Panaha Thidin Thamkin: Adit, Pajuban, Anakhot. Sedthakit lae Sangkhom 17(4):413–426

Pinkaew L (2002) Competing discourses and practices of "Civil Society": a reflection on the environmental movement in Thailand and some implications for the Mekong Region. Paper presented at the Mekong dialogue workshop: international transfer of river basin development experience, Brisbane, 2 September 2002

Suehiro A (1981) Land reform in Thailand: the concept and background of the Agricultural Land Reform Act of 1975. Institute of Developing Economies. Developing Economies 19(4):314–347

Supranee S (2000) Studies on changes and distribution of riparian forest areas in the flood plain of the Songkhram River using aerial photographs and geographic information systems. Master's thesis. Khon Kaen University, Khon Kaen

Suthep C, Bunrak P (2001) Land use monitoring in Sri Songkhram wetland area. Paper presented at the 22nd Asian conference on remote sensing, Singapore, 5–9 November 2001

Suwit T, Chob D, Surat W (1987) Economic change in Songkhram River Basin communities from A.D.1932 to the present. Faculty of Humanities and Social Science, Khon Kaen University, Khon Kaen

Part III
Forest Ecology

Technical Report

Forest Environment of Vietnam: Features of Forest Vegetation and Soils

Vu Tan Phuong

Accounting for 57% of its entire national area, the forests and forestland of Vietnam cover about 19 million hectares (ha), of which 12.6 million ha is covered by forests (MARD 2005). Because of its diverse climate conditions and complicated topography, Vietnam has a wide range of vegetation and soil types. The forest vegetation includes six major types: (i) evergreen and semideciduous broad-leaved forests, (ii) deciduous forests, (iii) bamboo and palms, (iv) coniferous forests, (v) open broad-leaved forests, and (vi) scrub. Forest soils comprise 14 major soil groups and 31 soil units. The major soil groups include Arenosols, Salic Fluvisols, Thionic Greysols, Acrisols, Ferralsols, and Leptosols. Of those soil groups, Acrisols cover the largest area, followed by Ferralsols and Thionic Fluvisols.

1. Introduction

Because of its favourable location and conditions, Vietnam has a wide variety of vegetation and soils. A study of forest vegetation classification in Vietnam was first carried out and published by Rollet in 1953, followed by Tran Ngu Phuong in 1970 and Thai Van Trung in 1978. The most comprehensive description of Vietnamese forest vegetation was made by Thai Van Trung. Since then, no detailed and systematic studies on forest vegetation classification have been done for the entire country.

Although forest and forestlands occupy a large fraction of the country's land area, the forest areas in Vietnam have decreased dramatically during the last 60 years, particularly during 1943–1990. The main reason for that decrease was the exploitation of timber and conversion of forestland into agricultural land. Since 1990, forest cover has greatly improved because of efforts exerted by the government and international support for reforestation and forest protection for natural regeneration.

This chapter is intended to provide general information about forest resources and forestry in Vietnam, with an emphasis on forest vegetation and soils. Its data are

Research Centre for Forest Ecology and Environment (RCFEE) of Forest Science Institute of Vietnam, Hanoi, Vietnam
E-mail: fuongvt@hn.vnn.vn

derived mainly from available documents on forest vegetation and soils classification in Vietnam.

2. Land and Environment

2.1. Geographic Location

The Socialist Republic of Vietnam is located in the centre of Southeast Asia, with an area of 329 241 km^2, a coastline 3260 km long, and a land border of 4510 km. It is 1650 km long on its north–south axis; from east to west, it is widest at 600 km and narrowest at 50 km.

Vietnam shares borders with China in the north, with Laos and Cambodia in the west, and with the South China Sea and Gulf of Thailand in the east and south. About three-fourths of Vietnam's area is classified as mountainous and hilly areas.

2.2. Climate and Ecological Zones

Vietnam is wholly located in the tropical belt of the Northern Hemisphere, perhaps somewhat more tropical than equatorial. This location imparts high temperatures to Vietnam. The annual average temperature is 22°–27°C. Every year has about 100 rainy days, with average rainfall of 1500–2000 mm. The relative humidity is about 80%.

Vietnam is strongly influenced by northeasterly monsoons; therefore, the average temperature is lower than that of other countries of the same latitudes in Asia. The monsoon system also changes the tropical and humid characteristics of Vietnamese nature. In general, Vietnam has a hot season with many rains and a cool, dry season. Accordingly, the climate in the northern provinces (from Hai Van Pass to the northern areas) changes markedly during the four seasons. In the southern provinces, the temperature is higher and the climate is more stable than in the northern provinces.

Figure 1 shows that Vietnam is divisible into eight ecological zones: these are (i) Northeastern, (ii) Northwestern, (iii) Red River Delta, (iv) North Central Coast, (v) South Central coast, (vi) Central highlands, (vii) Southeastern, and (viii) Mekong Delta.

2.3. Population and Religion

The Vietnamese population as of 2004 was about 80 million people of 54 different ethnic groups, in which the Kinh ethnic group is the majority, occupying nearly 90% of the whole population. The remainder, more than 10%, is the population of 53 groups.

Vietnam is a multiethnic country. Throughout its history, Vietnamese culture has been influenced by different cultures of many countries. Buddhism comes from India, Confucianism and Taoism come from China, Catholicism and Protestantism come from the West, etc. Despite the number of religions, no religious conflicts occur in Vietnam. The religions in Vietnam are in harmony with each other for the general development.

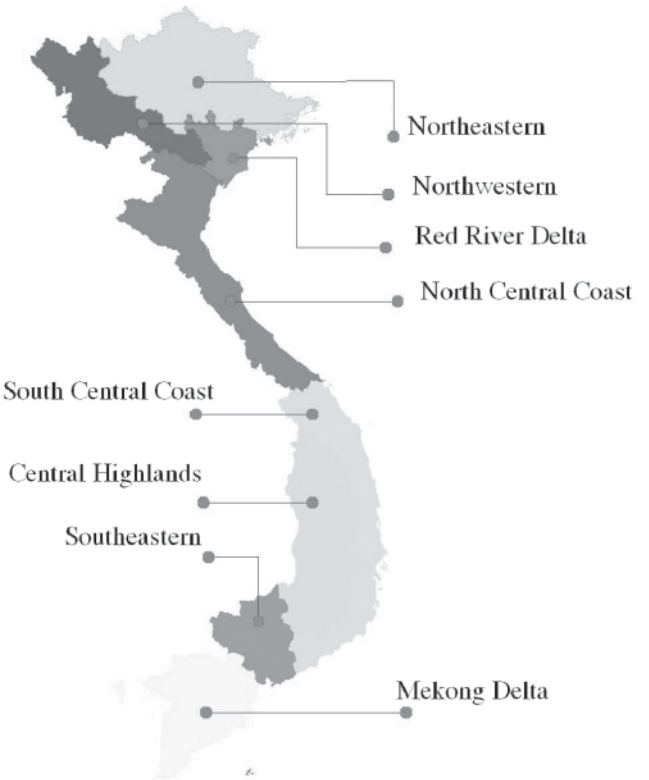

FIG. 1. Ecological zones of Vietnam

3. Forest Area and Function

The total forest and forestland area of Vietnam is about 19 million ha, accounting for 57% of total country area, of which 12.6 million ha is covered by forests. The remainder, 6.4 million ha, includes nonforested areas in forest regions.

Forested areas of Vietnam decreased dramatically during 1943–1990, from 14 million ha, accounting for 43% of national territory in 1943, to 9.2 million ha, estimated as 28% in 1990 (Fig. 2). Since 1990, forest cover in Vietnam has increased. The forest cover as of 2005 is about 38% (about 12.6 million ha; MARD 2005), but Vietnam has a national policy to increase forest coverage to 43% by 2010 through reforestation. Of these existing forest areas, about 10.1 million ha are natural forests and 2 million ha are planted forests.

Presently, forests in Vietnam are classified into three types according to their function: production, protection, and special-use forests. According to statistical data issued by the Ministry of Agriculture and Rural Development (MARD) in 2005, the respective areas of the three kinds of forests can be described as follows:

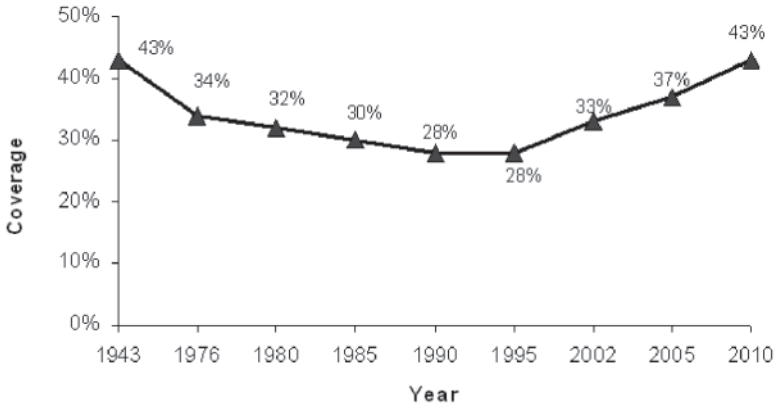

Fig. 2. Forest area (coverage) change, 1943–2010

- Production forests occupy about 4.5 million ha, in which 3.1 million ha are natural forests and about 1.4 million ha are plantations. Production forests include different functions, such as supplying timber, pulp, chipping, and mining poles.
- Protected forest areas are about 6.2 million ha, of which 5.3 million ha are natural forests and 0.9 million ha are planted forest. The protection forests consist of four types: (i) headwater protection forests, (ii) wind- and sand-shielding protection forests, (iii) tide-shielding and sea encroachment prevention forests, and (iv) environmental protection forests (Law on Forest Protection and Development 2004).
- Special-use forests occupy roughly 1.9 million ha, of which about 1.8 million ha is natural forest and the remaining is planted forest. Such forests are intended mainly for protecting and conserving biodiversity. This forest type includes national parks, protected areas, and natural reserves. About 108 national parks and nature reserves have been established throughout the country.

However, regarding the areas of three kinds of forests, MARD is reconsidering the area allocations of each forest type. There is a growing tendency to shrink protection forests while increasing the production forest areas.

4. Forest Vegetation

Because of its diverse climatic and soil conditions, Vietnam has a wide range of vegetation types, with about 2084 native species. Forest vegetation classification was researched and published by Rollet (1953); subsequently, Tran Ngu Phuong (1970) and Thai Van Trung (1978) classified the forest vegetation of Vietnam into groups, types, and subtypes. The following sections describe the main forests and vegetation types.

4.1. Evergreen and Semideciduous Broad-Leaved Forests

1. Closed evergreen lowland forests are found in southern Vietnam, where high rainfall compensates for effects of the short dry season, encouraging the growth of a

closed moist forest. Three storeys are distinguishable, as well as an undergrowth of bushes and regeneration. Dipterocarpaceae often predominate in the upper storey, sometimes attaining a height of more than 50 m. The most common species are *Hopea* spp., *Dipterocarpus costatus, D. alatus, D. dyeri, D. turbinatus, Anisoptera cochinchinensis,* and *Shorea vulgaris*. Other families are also represented in the upper storey, particularly Ebenaceae and Leguminosae such as *Sindora cochinchinensis* and *Dalbergia cochinchinensis*, Guttiferae, and Meliaceae.

Further north, deciduous trees become more frequent, some losing their leaves for a few days in the dry season (e.g., *Dipterocarpus dyeri* and *D. turbinatus*), some for slightly longer (e.g., *Shorea talura, Sterculia* spp. and *Sindora cochinchinensis*), and some for several months (e.g., *Tetrameles nudiflora* and *Bombax* spp.). Other species or genera common in northern Vietnam are *Cinnamomum, Litsea, Lindera, Phoebe, Endospermum chinense, Pometia tomentosa*, and *Dipterocarpus tonkinensis*.

After forest clearance, young closed secondary forests develop, which consist of species such as *Lagerstroemia* spp., *Peltophorum dasyrachis, Cratoxylon* spp., *Canarium* spp., *Dillenia* spp., *Aporosa* spp., *Dipterocarpus intricatus, Xylia xylocarpa, Sindora cochinchinensis, Careya sphaerica, Mallotus* spp., and *Trema* spp. On red soils, bamboos quickly cover disturbed ground again; on sandy soils, recolonisation is very slow.

2. Closed mountain forests. Mountain forests, marked by the absence of dominating trees and an abundance of epiphytes, gradually replace lowland forests. Dipterocarpaceae gradually disappear, with *Hopea odorata* up to 800 m, *Shorea obtusa* up to 900 m, and *Dipterocarpus obtusifolius* up to 1200 or 1300 m in degraded forests. Lauraceae (*Phoebe cuneata, Lindera* spp., *Litsea* spp., *Cinnamomum* spp.), Fagaceae (*Castanopsis* spp., *Lithocarpus* spp., *Quercus* spp.), Magnoliaceae, Juglandaceae, and conifers have become major components of this type of vegetation. Although some conifers are found in unmixed stands, others, such as *Taxus baccata*, *Podocarpus* spp., *Pinus dalatensis*, *Libocedrus* spp., and *Glyptostrobus* spp., tend to be scattered among other species. Above 1700 m in the northern part of the country, mountain forests dominate, with Fagaceae, Ericaceae, and conifers (*Pinus krempfii, P. armandii, Fokienia hodginsii*, and *Keteleeria davidiana*). After clearance, this type of forest is replaced by stands of *Macaranga denticulata, Mallotus cochinchinensis, Trema velutina, Rhus semialata, Styrax* spp., or bamboo.

3. Swamp forests have developed in areas that are more or less permanently covered by freshwater. Vast areas of this type of forest are found in the Mekong floodplains, although large areas of such forests have been drained and cleared for rice culture. Species and genera such as *Eugenia, Elaeocarpus, Sterculia, Adina cordifolia, Calophyllum inophyllum*, and *Sandoricum indicum* are found in these forests along with many palm species. Pure stands of the *Livistona cochinchinensis* palm are sometimes found. Unmixed forests of *Melaleuca leucadendron* are found behind the mangrove swamps in areas not reached by the brackish waters. *Melaleuca cajuputi* are found in overexploited valley bottoms or on humus-rich soils, forming open stands with *Stenochlaena palustris*, *Polybotrya appendiculata*, and *Alstonia spathulata* bushes. On sandy soils, *Ilex godajam* and a number of other species are found in combination with *Melaleuca*.

4. Mangrove swamps cover large areas in the southeastern extremity of Vietnamese lands. To date, 36 “true mangrove” and 73 “associate” species have been

identified. Species of the *Rhizophora* and *Bruguiera* genera make up three-quarters of the thriving forests. In the southeastern area, mangrove species are dominated by Rhizophoracea (*R. apiculata, Bruguiera parviflora*, etc.), Sonneratiaceae (*S. caseolaris, S. alba*, etc.), and Arecacea/Palmeae (*Nypa fruticans, Phoenix paludosa*). In contrast, in northern areas, the dominant mangrove species belong to Avicenniaceae (*Avicennia marina*) and *Myrsinaceae (Aegiceras corniculatum, Lumnitzera racemosa, Kandelia obovata*) (Do Dinh Sam et al. 2005a).

Two less widespread types of evergreen forest are noteworthy:

5. Riparian forests are common on narrow slopes along rivers, with *Cynometra* spp., *Crudia* spp., *Crataeva nurvula, Dipterocarpus alatus, Hopea odorata, Hydnocarpus* spp., *Nauclea* spp., *Eugenia fluviatilis*, and *Telectadium* spp.

6. Coastal forests are commonly found in sandy areas near the ocean, with *Calophyllum inophyllum, Terminalia catappa, Canavalia* spp., *Guettarda speciosa, Cycas rumphii, Hibiscus tiliaceus, Cerbera* spp., *Morinda* spp., *Scaevola* spp., and *Heritiera littoralis*.

4.2. Deciduous Forests

1. "Semiclosed" forests are dominated by various species of the *Lagerstroemia* genus. They represent a transition between closed evergreen forests and open forests. *Lagerstroemia angustifolia*, but also *L. macrocarpa, L. floribunda, L. duperreana*, and *L. thorelii* predominate, along with *Xylia xylocarpa, Sindora cochinchinensis*, and *Vitex pubescens*. Bamboos, particularly *Oxytenanthera* spp., often dominate the undergrowth. This type of forest is very sensitive to clearing, as suggested by the open-forest species. A pure combination of *Terminalia tomentosa* and *Xylia xylocarpa* is often encountered in valley bottoms.

2. Moist deciduous forests and semideciduous lowland forests are found in combination in northern Vietnam. Dipterocarpaceae, Leguminosae, Meliaceae, and Sapindaceae predominate in the tree layer of semideciduous forests. Two types of moist deciduous forest are distinguishable in higher areas, in which bamboos predominate, the other in lower areas. The families best represented are Leguminosae, Verbenaceae, and Combretaceae. After clearing, shrub vegetation develops, with either *Eupatorium* spp. or *Saccharum arundinaceum*. Repeated fires engender the development of open forests.

4.3. Bamboo and Palms

Bamboos are natural undergrowth species in deciduous forests. They invade abandoned cropland on rich basaltic soils and schistose slopes. In closed forest areas, the most common species are *Bambusa arundinacea* and *Oxytenanthera* spp., whereas only the latter is found in "semiclosed" forests. In mixed dry open forests, *Arundinaria falcata* is found in 1- to 2-m-tall pure stands, which are burnt off during the dry season. Other bamboo species of Vietnam are *Sinocalamus latiflorus, Dendrocalamus hamiltonii, Phyllostachys* spp., *Schizostachyum funghomii*, and *Arundinaria amabilis*.

4.4. Coniferous

Conifers are a major component of mountain forests. Various species are found in many forests but do not make up pure stands, apart from *Dacrydium pierrei* and *Fokienia hodginsii*. Two species of conifer, *Pinus krempfii* and *Glyptostrobus* spp., are endemic to Vietnam, the latter being a small tree found in marshy areas. To date, about 50 conifers have been found, of which 33 species are native (Nguyen Hoang Nghia 2004).

The most widespread species of pine are *Pinus merkusii* and *P. khasya*, which make up large stands in the north near the frontier with Laos and in the southern provinces. Another stand is reported in the northern part of Kontum Province. A single block of about 100 000 ha, mostly dominated by *Pinus khasya*, covers the Langbian Mountains between 1100 and 1700 m. In addition, *P. griffithii* is reported in the mountains of the Hue region. In open forests, *P. merkusii* is often mixed with *Dipterocarpus obtusifolius*.

4.5. Open Broad-Leaved Forests

Typical open dipterocarp forests are confined to submoist warm climates with a dry season of 5–6 months and annual rainfall of 1000–1500 mm. These climatic conditions are particularly favourable to the outbreak of fires and rapid soil degradation. Certain forests of this type seem to have become stabilised on skeletal soils of schistose origin (with *Shorea siamensis* and *Terminalia tomentosa*). In Vietnam, open forests are generally found above 500 m, although they exist also in the southeastern lowlands. Rollet (1953) distinguishes the following types:

1. Pure or almost pure stands of *Shorea siamensis* on rocky or skeletal soils are very open and wholly deciduous, with thorny ground vegetation.
2. Pure or almost pure open stands of *Dipterocarpus obtusifolius* are probably the remains of old closed forests on sandy soils. *Irvingia* and *Parinari* are sometimes present. The shrub layer is sparse, but the grass cover is unbroken. *Shorea obtusa, S. talura*, and *S. siamensis* gradually appear.
3. The most degraded type of open forest, on white sandy soils, is made up of stands of *Dipterocarpus intricatus* accompanied by shrubs such as *Randia tomentosa* and *Buchanania reticulate*, which dominate a herbaceous layer. These combinations develop into richer stands if no fires affect them. *Acacia intsii, Memecylon edule, Ochrocarpus* spp., *Eugenia brachiata, Capparis beneolens, Melanorrhea laccifera*, and *Irvingia oliveri* are also found in this type of vegetation. Open stands of *Dipterocarpus intricatus* or *D. obtusifolius* are also sometimes found.
4. Dry mixed formations are the most common type, and are generally found on slightly loamy soils with a thick laterite layer, so that it is hard for water to penetrate in the rainy season. The species in the dominant storey are *Dipterocarpus tuberculatus, Shorea obtusa*, and *Terminalia tomentosa*, as well as *Cratoxylon formosum, Terminalia mucronata, T. chebula, Careya sphaerica, Adina sessilifolia, Vitex pubescens, Shorea talura, Diospyros* spp., *Canarium subulatum*, and *Phyllanthus emblica*. Barring the occurrence of fires, a dry closed forest develops, particularly in inhabited regions, with *Shorea obtusa, S. talura, Dipterocarpus intricatus*, and *Cratoxylon* spp.

as frequent species. In overlogged forests or drier areas, many thorny shrubs such as *Ziziphus cambodianus, Gardenia* spp., *Randia tomentosa, Acacia intsii, Combretum quadrangulare, Feroniella* spp., and *Terminalia moluccana* appear.

4.6. Scrub

After the clearance of forests growing on red basaltic soils, an open scrub vegetation develops, composed mainly of *Careya sphaerica* accompanied by *Phyllanthus emblica, Albizia procera, Grewia elatostemoides, Bauhinia* spp., *Pinus* spp., *Canarium* spp., *Dillenia* spp., *Wrightia annamensis, Symplocos racemosa*, and *Hymenodictyon excelsum*. On very degraded soils, the predominant species are *Rhus* spp., *Careya sphaerica*, *Aporosa* spp., and *Wendlandia glabrata*. On sandy and shallow soils, particularly sandstone hilltops, secondary vegetation is scrub, with such species as *Rhodamnia trinerva, Vaccinium, Cinnamomum, Eugenia* spp., and *Melastoma* spp. On dry and sandy degraded soils, scrub vegetation becomes thorny, with such species as *Acacia intsii, Gardenia* spp., *Capparis beneolens*, and *Ziziphus cambodianus*. It often takes many years for forests to recolonise abandoned cropland.

In some places in southern Vietnam, particularly in the Pleiku and Dalat regions, shrubs can grow to heights of 4–5 m, and are mainly *Grewia paniculata, Aporosa* spp., *Eugenia* spp., *Careya sphaerica, Phyllanthus emblica, Engelhardtia* spp., *Wendlandia* spp., and *Melastoma* spp. In northern areas, scrub plants are smaller, normally between 1–2 m high, and formed by overexploitation of forests. The dominant species are *Rhodomyrtus tomentosa*, *Melastoma* spp., *Aporosa sphaerasperma, Cratoxylum maingayi, Eupatorium odoratum, Wendlandia paniculata, Randia spinosa*, etc.

The Forest Inventory and Planning Institute (FIPI) uses a different classification system. The system classifies Vietnamese vegetation into ten types: evergreen forests, coniferous forests, deciduous forests, semideciduous forests, limestone forests, bamboo, plantation, mangroves, melaleuca, and bush/grass. This system is being applied in the country for forest inventory and forest area data.

5. Forest Soils

According to soil classification data, the soils of Vietnam include 14 major soil groups and 31 soil units. The major soil groups that cover considerable areas and closely relate to the forestry sector are Acrisols, estimated as about 60% of total land area, followed by Ferralsols with about 10%, Thionic Fluvisols[1], about 6%, and Salic Fluvisols, roughly 3%. Two other soils that are also found in forestland area are Arenosols and Leptosols, but these soils are less common compared to others, less than 1.7% each (Vietnam Soil Association 1996; Nguyen Ngoc Binh 1996). The detailed areal quantities of major soil groups and their distribution are shown in Table 1. The following list provides general information about these major soil groups:

[1] According to FAO/UNESCO, these soil groups are put into soil unit but the Vietnamese classification considers it as a major soil group

Table 1. Major soil group areas in Vietnam

Major soil group name	Code	Area (ha)	Percent of land area
Arenosols	AR	533 434	1.70
Salic Fluvisols	Fls	971 356	3.10
Thionic Fluvisols	FLt	1 863 128	5.95
Fluvisols	FL	3 400 059	10.85
Gleysols	GL	452 418	1.44
Histosols	HS	24 941	0.08
Andosols	AN	171 402	0.55
Luvisols	LV	112 939	0.36
Lixisols	LX	42 330	0.14
Calcisols	CL	5 527	0.02
Acrisols	AC	19 970 642	63.72
Ferralsols	FR	3 014 594	9.62
Alisols	AL	280 714	0.90
Leptosols	LP	495 727	1.58

1. **Acrisols (AC).** This largest soil group area is about 19.9 million ha, accounting for 63% of the total national land area. It is widely distributed in hilly, mountainous, and plain areas. Forest types on these soils are evergreen broadleaved forests (Nguyen Ngoc Binh 1996).

Five soil units are identified for this group: Haplic Acrisols, Plinthic Acrisols, Gleyic Acrisols, Ferralic Acrisols, and Humic Acrisols.

Haplic Acrisols develop mainly on acidic magma and sandstone and concentrated mostly in the southeastern, central highlands, and midlands of the northern area. This soil is acidic, poor in nutrients, dry, and is used commonly for agriculture because it is distributed in flat areas and has good drainage.

Plinthic Acrisols are found mainly in midlands of the northern area. The soil is rather compact, with bulk density of 1.3–1.6 g/cm^3. It is also acidic and poor in humus and other nutrients.

Gleyic Acrisols are found in the midlands of the northern, central highland, and southeastern areas. The soil properties vary greatly by region but are normally found in hollow and low topography areas. These soils are mainly used for rice cultivation.

Ferralic Acrisols are distributed throughout the country and occupy the largest area, about 6.8 million ha. The soil fertility is distinct depending on parent materials. However, this soil is acidic, with low base saturation and poor to medium nutrient content. This soil is used commonly for forestry.

Humic Acrisols are found at altitudes of 400 m or more in northeast, northwest, and central highlands. The special feature of this soil is that its 4%–10% humus content is quite rich.

2. **Ferralsols (FR).** This soil covers an area of about 3.1 million ha, accounting for 10% of the national area. It is distributed commonly in hilly and mountainous areas, from altitudes of 50 m up to 1000 m above sea level. The main forest types found on

these soils are evergreen broad-leaved forests dominated by leguminous and dipterocarp species (Nguyen Ngoc Binh 1996).

Three soil units found for this group are Rhodic Ferralsols, Xanthic Ferralsols, and Humic Ferralsols.

Rhodic Ferralsols occupy about 8% of the total land area and are distributed mainly in the central highland, southeastern, north central and northeastern areas. The main features of the soil are that it is brownish red, with pH values or 4.5–5.2, high density of 2.5–2.9, low bulk density of 0.7–1 g/cm^3, low base saturation of less than 50%; and high humus content in the surface layer, with little phosphate and potassium.

Xanthic Ferralsols are commonly found in northeastern, northwestern, north central, southeastern, and central highland areas. The soil is brownish yellow and forms in moist tropical and high rainfall condition. It is moderately deep, with good water drainage and medium soil nutrients.

Humic Ferralsols are distributed at altitudes of 700–900 m or even 2000 m. This soil is developed on base and neutral magma rock and limestone. The soil is acidic and very low in base saturation. Potassium and phosphate in the soils are very poor, but total N and humus contents are rich.

3. **Thionic Fluvisols (FLt).** Covering an area of about 1.9 million ha, accounting for 5.7%, this soil is found commonly in the Mekong delta. The notable feature of this soil is that it contains a sunfidic and sunfuric horizon. It is subdivided into two soil units: Proto Thionic Gleysols and Orthi Thionic Fluvisols. Typical vegetation on this soil is *Melaleuca* spp. and grasses (*Eleocharis ochorostachyo, E. dulis, Lepironia bancana*, etc.).

The main characteristics of the soils are that the soils have high contents of organic matter and a low decomposition rate. Total N is rather high, total phosphate is medium to poor, but available phosphate is extremely poor, and total potassium is normally rich. The soil is very acidic and mainly contains clay particles.

The soils are used for both agriculture and forestry, but mostly for agriculture, which is estimated at about 80% of its area. In forestry, the most suitable species for plantation establishment are *Melaleuca* spp. and *Eucalyptus* spp.

4. **Salic Fluvisols (SFl).** This soil is affected by seawater; the area of this soil distribution is estimated at 0.97 million ha, occupying about 3% of the total country area. It is distributed in coastal areas throughout the country, but concentrates mostly on the coast of southeastern areas. The typical forests appearing on this area are mangrove forests.

Three soil units are Gleyic Salic Fluvisols, Haplic Salic Fluvisols, and Molli Salic Fluvisols.

The first type occupies about 11% of this soil group and is not mature. The soil is neutral or slightly alkaline. The organic content is rather high. Its texture is from medium in the north to heavy in the south.

The second is about 15% of this group and is found in low areas along the coast and river estuaries. The content of Cl^- in the soil is greater than 25% and EC (Electric Conductivity) normally higher than 4 ms/cm. Soil nutrients are in medium to rich grade, particularly in the southeastern area. In addition, the soil is heavy texture and deeper in southeastern areas. However, in the north, the soil is medium texture and sand can be found at the depths of less than 100 cm from the surface.

The last one, Molli Salic Fluvisols, has the greatest area of distribution, about 75% of the group, and is distributed mainly in the Mekong delta. Content of Cl^- is less than 25% and EC smaller than 4 ms/cm. The soil is neutral, but its pH value increases in deeper layers. Humus and N content are moderate.

Land uses in this area are a combination of agriculture, forestry, and fishery. The mangrove forests in this area play an important role in protecting the coast and dams. However, high benefits accruing to shrimp farming have encouraged the conversion of mangrove forests for shrimp farming. The destructive effects of that conversion pose a pending challenge.

5. **Arenosols (AR):** This soil group covers roughly 0.5 million ha, accounting for about 1.6% of land area. It is distributed mainly in coastal areas, particularly in central Vietnam. Natural vegetation cover on these soils are grasses (*Funbystylis sphathaceae*, *F. sericeae*, *Scirpus junciformis*) and shrubs (*Eugenia* spp., *Desmodium ovalium, Nepenthes annamensis)*.

The group is further divided into five soil units: Luvic Arenosols, Rhodic Arenosols, Haplic Arenosols, Cambic Arenosols, and Gleyic Arenosols. However, the first three types are commonly found in forestry.

Generally, the soil is known as poor soil in terms of fertility. It is commonly used for forestry as protection forest (sand shielding protection forests). The main tree species suitable to this soil are *Casuarina equisetifolia* and *Acacia* spp. (Do Dinh Sam et al. 2005b).

6. **Leptosols (LP).** The area of this group is about 0.5 million ha. This soil is distributed mainly in the central highland, north central, and south central areas. It is formed by erosion after the clearance of vegetation cover. Most areas with this soil are not in use and are covered by scattered shrubs and grasses. This group contains only one soil unit, Lithic Leptosols. For forestry, some *Acacia* species are planted on this soil, but they show low productivity.

References

Nguyen Ngoc Binh (1996) Forest soils of Vietnam (in Vietnamese). Agriculture Publishing House, Hanoi

Nguyen Hoang Nghia (2004) Some coniferous tree species in Vietnam (in Vietnamese). Agriculture Publishing House, Hanoi

Ministry of Agriculture and Rural Development (MARD) (2005) Decision no. 1970/QD/BNN-KL on promulgation of the state of national forest for the year of 2005, MARD, Hanoi

Tran Ngu Phuong (1970) Initial research results of northern forests (in Vietnamese). Science and Technology Publishing House, Hanoi

Rollet B (1953) Note sur les forêts claires du sud de l'Indochine. Boise et Forêts des Tropiques no. 31. Nogent-sur-Marne, France

Do Dinh Sam, Nguyen Ngoc Binh, Ngo Dinh Que, Vu Tan Phuong (2005a) Overview of mangrove forests in Vietnam (in Vietnamese). Agriculture Publishing House, Hanoi

Do Dinh Sam, Ngo Dinh Que, Vu Tan Phuong (2005b) Forestland evaluation systems in Vietnam (in Vietnamese). Science and Technology Publishing House, Hanoi

The Socialist Republic of Vietnam (2004) Law on forest protection and development. Article 4: forest classification (in English)
Thai Van Trung (1978) Vegetation cover of Vietnam (in Vietnamese). Science and Technology Publishing House, Hanoi
Vietnam Soil Association (1996) Vietnam soils (in Vietnamese). Agriculture Publishing House, Hanoi

Principal Forest Types of Three Regions of Cambodia: Kampong Thom, Kratie, and Mondolkiri

Akihiro Tani*, Eriko Ito, Mamoru Kanzaki, Seiichi Ohta, Saret Khorn, Phearak Pith, Bora Tith, Sopheavuth Pol, and Sopheap Lim

We enumerated all trees 10 cm or more in DBH with respect to DBH, height, and species identity in 29 circular plots of 20-m radius from Kampong Thom, Kratie, and Mondolkiri Provinces, Cambodia. The composition data were analyzed using cluster analysis with group-averaging protocol, and Sorensen's similarity index based on basal area data and the resulting clusters were also described with respect to height structure and indicator species. We found four main clusters corresponding to traditional qualitative forest types known as evergreen forest, deciduous forest, hill evergreen forest, and swamp forest. The evergreen cluster was further divided into two stand types of dry evergreen forest and two stand types of secondary evergreen forest. The deciduous forest cluster was divided into three stand types of deciduous dipterocarp forest and a mixed deciduous forest. We describe the correspondence between the forest stand types of our study and the many regional names previously used for the different forest types in varying classification systems. Some of the stand types, for example, an evergreen forest overtopped by deciduous dipterocarp (*Dipterocarpus intricatus*) or by a pine (*Pinus merksii*), and a *D. obtusifolius* stand on seasonally waterlogged habitat, seemed to be unique in Cambodia. The application of this method and the needs of regional forest mapping are discussed.

1. Introduction

Cambodia is part of the Indochina bioregion as defined by MacKinnon and MacKinnon (1986) together with Vietnam, Laos, Thailand, and Myanmar. The southern border of this region was described by Whitmore (1984) as falling at the Kangar-Pattani Line, south of which the climate is wetter and less seasonal. Ashton (1991) suggested that the western boundary of the bioregion lies west of the India-Burma border where the climate is drier. The Indochina bioregion corresponds to the area east and north of these two lines and south of the tropical boundary. Forest coverage in Cambodia is at 52.9%, and Cambodia remains one of the more forested countries of the Indochina bioregion (Food and Agriculture Organization 2001). It is

* Graduate School of Agriculture, Kyoto University, Kyoto, Japan
E-mail: tanimark@kais.kyoto-u.ac.jp

particularly worth noting that Cambodia still has forest in the lowland plains, as opposed to Thailand and Vietnam, where the remaining forests are mostly in mountainous areas.

Civil war halted the modern geographic study of Cambodian forests that had been successfully begun with the work of Rollet (1972) and Legris and Blasco (1972). In the 1990s, after the termination of civil war, forest studies were focused on the legal systems and forest management and utilization (The World Bank 1996; Hong-Narith 1997; KimPhat 2000; KimPhat et al. 1999). In the same decade, progress in remote sensing technology allowed a new detailed approach to forest phenology and physiognomy (Forest Cover Monitoring Project 1998). However, ground-based studies of forest composition are still few.

Comparative studies of adjacent forests in Vietnam, Laos, Myanmar, Thailand, and India have been carried out on a national basis, but as in Cambodia, these have been often descriptive and not always specifically applicable to Cambodia because of differences in climate and biogeography [Stamp 1925; Champion 1936; Rollet 1953; Vidal 1960; Ogawa et al. 1961; Royal Forest Department (RFD) 1962; Smitinand 1966, 1977; Schmid 1974; Kutintara 1975; Trung 1978; Bunyavejchewin 1983, 1985; Santisuk 1988]. These differences have led to each country having different terminology for forest types even when the forests are evidently very similar. Common terminology used in India, Myanmar, and Thailand, such as "dry evergreen forest," "mixed deciduous forest," and "dry dipterocarp forest," is not used in Cambodia, Laos, and Vietnam. Added to this, the ecoregion approach of Wikramanayake et al. (2002) recognized six ecoregions in Cambodia: "Southeastern Indochina Dry Evergreen Forest," "Central Indochina Dry Forest," "Cardamom Mountains Rain Forest," "Southern Annamites Montane Rain Forest," "Tonle Sap Freshwater Swamp Forest," and "Tonle Sap-Mekong Peat Swamp Forest." This kind of inconsistency has led to confusion and inconvenience in efforts at forest mapping.

To overcome this situation, a reconsideration of forests in the Indochina bioregion based on numerical vegetation data is required. Fortunately, forests in Cambodia still cover more than 50% of her land and remain in relatively good condition, and thus vegetation study in this country can also contribute to the revision of forest vegetation in this bioregion.

The first objective of this study is to extract principal forest types through numerical analysis of species composition data. The second is to precisely identify the extracted forest types in classification systems proposed by Rollet (1972) for Cambodia, RFD (1962) and Santisuk (1988) for Thailand, Stamp (1925) for Myanmar, Vidal (1960) for Laos, and/or Ashton (1991), and Vidal 1997 for the continental Southeast Asia Indochina bioregion.

2. Study Areas and Methods

The Mekong Secretariat (1994) reported that the total forest area of 11.3 million hectares (ha) was divided into 10.6 million ha dry land forest and 0.7 million ha wet edaphic forest. Dry land forest includes 4.8 million ha evergreen forest, 4.3 million ha deciduous forest, and small areas of coniferous forest, mixed forest, and secondary forest. In this study, we mainly focus on these dry land forests.

In 1997, the Department of Forestry and Wildlife made a vegetation map from satellite images, and the map shows that the evergreen forest is dominant in western side of Me-Kong River and the deciduous forest is dominant in eastern side (Fig. 1). The former forest composes a part of the Southeastern Indochina Dry Evergreen Forest and the latter composes a part of the Central Indochina Dry Forest. The map shows that evergreen forest also exists along the northeastern border with Laos and the eastern border with Vietnam; these forests are a part of the Southern Annamites Montane Rain Forest.

We selected three study areas in contrasting situations. The first is the Kampong Thom study area (KPT), which is in an evergreen forest zone, the second is the Kratie study area (KTE), in a deciduous forest zone, and the last, the Mondolkiri study area (MDK), is in a mountainous zone. Annual rainfall ranges from about 1600 mm to more than 2200 mm, and the climate becomes more humid in the eastern area. The altitude of MDK is higher than that of the other study area, so the annual mean temperature there is lower than that in KPT and KTE (Table 1).

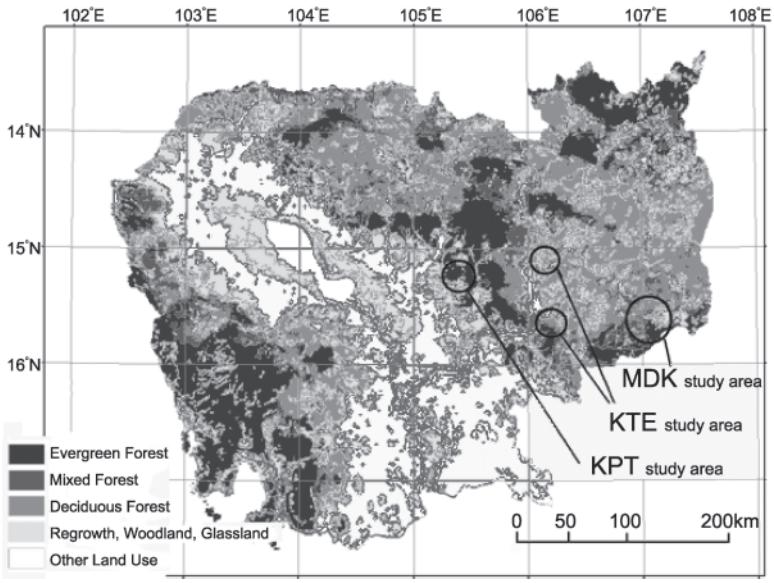

Fig. 1. Vegetation map of Cambodia and the location of the study areas: Kampong Thom (*KPT*), Kratie (*KTE*), and Mondolkiri (*MDK*). (Source: Forest Cover Monitoring Project 1998)

Table 1. Physical settings of three study areas

Study area	Annual rainfall (mm)	Annual mean temperature (°C)	Elevation range of plots (m)	Main soil type
Kampong Thom	1570	27	70–140	Acrisols
Kratie	1800	27	40–120	Plinthosols
Mondolkiri	2250	20	200–900	Ferralsols

We set 12 circular plots of 20-m radius each in KPT (designated KPT1 to –8, –11 to –14), 8 plots in KTE (KTE1 to –8), and 9 plots in MDK (MDK1 to –9). Within each plot, all trees ≥10 cm in diameter at breast height (DBH) were measured and identified to species level. Voucher specimens of all trees were collected and deposited in the Laboratory of Tropical Forest Resources and Environment, Kyoto University. Information was also taken for bamboo, for which we recorded the number of culms and the maximum and minimum DBH. The basal area of the clump is the product of the number of culms and the mean culm basal area. Bamboos were not identified to the species level and were pooled as a single class. Enumerations were conducted from February 2003 to March 2005.

The plots were clustered by the group averaging method using Sorensen distance measurement. Indicator species were extracted by the indicator species analysis (Dufrene and Legendre 1997). These analyses were conducted by PC-ORD Version 4 for Windows (MjM Software Design, Gleneden Beach, OR, USA; McCune and Mefford 1999) based on species total basal area data.

3. Results

Twenty-nine plots were divided into four main clusters that correspond to conventional forest types (Fig. 2): evergreen forest (12 plots), montane forest (2 plots), deciduous forest (14 plots), and swamp forest clusters (1 plot).

3.1. Evergreen Clusters

The principal indicator species for evergreen forest were *Diospyros bejaudii* (Ebenaceae), *Sindora siamensis* (Fabaceae), *Syzygium grande* (Myrtaceae), and five other species (Table 2). The indicators for the deciduous cluster were *Xylia xylocarpa* (Fabaceae) and other two species (Table 2). The evergreen and deciduous clusters could be more finely divided, and we recognized ten stand types (see Fig. 2), each with indicator species (Table 3). The preliminary names of the stand types follow the forest classification system of Thailand (RFD 1962).

3.1.1. Dry Evergreen Forest (DEF1, DEF2)

DEF1 was tall forest, and its canopy height reached to 40 m. The forest was structurally complex and with more than three vertical layers: emergent, canopy, and lower canopy. Indicator species of the evergreen cluster, *Dipterocarpus costatus* and *Anisoptera costata*, dominated the upper canopy layer. Another indicator species of DEF1, *Vatica odorata*, was a dominant species of the lower canopy layer.

DEF2 differed in that the continuous canopy layer of evergreen species such as *Vatica odorata* and *Syzygium* spp. was overtopped by a deciduous species, *Dipterocarpus intricatus*, or a conifer, *Pinus merksii* (Table 4). The canopy height of DEF2 was 20–25 m, shorter than DEF1, and the basal area density was also smaller than that of DEF1 (Fig. 3).

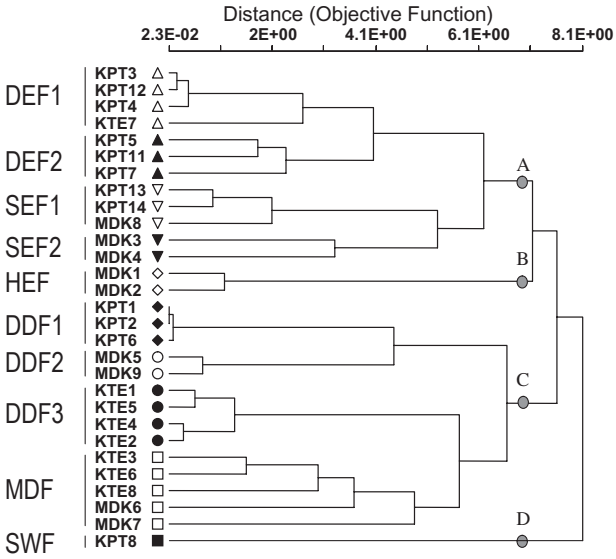

FIG. 2. Dendrogram obtained by the cluster analysis for 29 stands of Cambodia. *KPT*, *KTE*, and *MDK* in plot names indicate the three research areas: Kampong Thom, Kratie, and Mondolkiri, respectively. Four main clusters, evergreen, montane, deciduous, and swamp, are defined by *A*, *B*, *C*, and *D* points, respectively, in the dendrogram. *SWF*, swamp forest; *DEF1*, dry evergreen forest type 1; *DEF2*, dry evergreen forest type 2; *SEF1*, secondary evergreen forest type 1; *SEF2*, secondary evergreen forest type 2; *HEF*, hill evergreen forest; *DDF1–DDF3*, deciduous dipterocarp forest types 1–3; *MDF*, mixed deciduous forest

TABLE 2. List of indicator species of evergreen forest cluster and deciduous forest cluster

Cluster	Family	Species	Life form[a]		P[b]
Evergreen forest	Ebenaceae	*Diospyros bejaudii*	E	M	0.001
	Myrtaceae	*Syzygium* sp. 14	E	M	0.002
	Leguminosae	*Sindora siamensis*	E	M	0.003
	Myrtaceae	*Syzygium grande*	E	M	0.003
	Dipterocarpaceae	*Vatica odorata* subsp. *Brevipetiolata*	E	M	0.007
	Dipterocarpaceae	*Dipterocarpus costatus*	E	T	0.022
	Annonaceae	*Mitrella mesnyi*	E	S	0.042
	Rhizophoraceae	*Carallia brachiata*	E	M	0.043
	Dipterocarpaceae	*Anisoptera costata*	E	T	0.047
Deciduous forest	Leguminosae	*Xylia xylocarpa*	D	T	0.003
	Combretaceae	*Terminalia mucronata*	D	T	0.004
	Rubiaceae	*Mitragyna rotundifolia*	D	T	0.034

[a] Abbreviations of life form: E, evergreen species including briefly deciduous; D, deciduous; S, small tree (<20 m maximum height); M, middle tree (20–30 m); T, large tree (>30 m)

[b] Proportion of randomized trials with indicator value equal to or exceeding the observed indicator value: P = (1 + number of runs >= observed) / (1 + number of randomized runs)

Table 3. List of indicator species of each stand type

Stand type	Family	Species	Life form		*P*
Dry evergreen forest (type 1), DEF1	Dipterocarpaceae	*Vatica odorata* subsp. *brevipetiolata*	E	M	0.001
	Myrtaceae	*Syzygium oblatum*	E	M	0.004
	Capparidaceae	*Capparis sepiara*	E	S	0.019
	Dipterocarpaceae	*Anisoptera costata*	E	T	0.029
	Ebenaceae	*Diospyros* sp. 01			0.039
Dry evergreen forest (type2), DEF2	Verbenaceae	*Vitex* sp. 2			0.001
	Guttiferae	*Calophyllum calaba* var. *bracteatum*	E	M	0.003
	Myrtaceae	*Syzygium grande*	E	M	0.006
	Dipterocarpaceae	*Dipterocarpus intricatus*	D	M	0.023
	Pinaceae	*Pinus merksii*	E	M	0.033
	Dipterocarpaceae	*Shorea roxburgii*	E	T	0.033
	Myrtaceae	*Tristaniopsis burmanica* var. *rufescens*	E	S	0.033
		Unidentified sp. 42			0.033
	Annonaceae	*Polyalthia* sp. 1			0.034
		Unidentified sp. 75			0.034
	Euphorbiaceae	*Aporosa filicifolia*		S	0.041
Secondary evergreen forest (type 1), SEF1	Irvingiaceae	*Irvingia malayana*	E	T	0.003
	Elaeocarpaceae	*Elaeocarpus poilanei*	E		0.032
	Meliaceae	*Sandoricum koetjape*	E	M	0.032
Secondary evergreen forest (type 2), SEF2	Lauraceae	*Phoebe* sp. 01			0.012
	Moraceae	*Ficus* sp. 3			0.012
	Ulmaceae	*Gironniera subaequalis*		M	0.012
	Rubiaceae	*Mentadina trichotoma*	E	M	0.012
	Myrtaceae	*Syzygium* sp. 14	E	M	0.014
	Moraceae	*Artocarpus lakoocha*	D	M	0.032
Hill evergreen forest, HEF	Lauraceae	*Cinnamomum litseafolium*		S	0.010
	Theaceae	*Eurya nitida* var. *nitida*	E	S	0.010
	Proteaceae	*Helicia formosana* var. *formosana*	E	S	0.010
	Fagaceae	*Lithocarpus aggregatus pseudo-magneinii*	E	M	0.010
	Fagaceae	*Lithocarpus vestitus*	E	M	0.010
	Theaceae	*Schima wallichii*	E	M	0.010
	Hypericaceae	*Cratoxylum cochinchinense*	D	M	0.025
Deciduous dipterocarp forest (type 1), DDF1	Anacardiaceae	*Gluta laccifolia*	E	M	0.001
	Dipterocarpaceae	*Dipterocarpus obtusifolius*	D	M	0.013
	Theaceae	*Anneslea fragrans*	E	M	0.046
Deciduous dipterocarp forest (type 2), DDF2	Dipterocarpaceae	*Shorea siamensis*	D	M	0.004
	Fagaceae	*Quercus kerii*	D	S	0.011
	Loganiaceae	*Strychnos nux-vomica*	E	M	0.011
Deciduous dipterocarp forest (type 3), DDF3	Dipterocarpaceae	*Shorea obtusa*	D	M	0.001
	Dipterocarpaceae	*Dipterocarpus tuberculatus*	D	M	0.024
	Rubiaceae	*Mitragyna rotundifolia*	D	M	0.049
Mixed deciduous forest, MDF	Leguminosae	*Xylia xylocarpa*	D	T	0.016
	Flacourtiaceae	*Homalium tomentosum*	D	M	0.020
	Bambusoides	Bamboo species	E		0.023

TABLE 4. Structural properties and dominant species of each stand type D max and H max, maximum stem diameter and maximum tree height in each stand type, respectively

Stand type	Number of plots	Fisher's α	Basal area (m^2/ha)	D max (cm)	H max (m)	Dominant species in basal area (m^2/ha)	
DEF1	4	15.4	32.0	128.0	41.4	*Dipterocarpus costatus*	7.17
		9.4–27.1	27.8–37.4	91.7–128.0	30.9–41.4	*Vatica odorata brevipetiolata*	5.25
						Anisoptera costata	5.13
DEF2	3	14.4	23.0	87.2	26.2	*Dipterocarpus intricatus*	2.54
		12.5–16.7	18.0–31.1	48.1–87.2	25.5–26.2	*Pinus merksii*	2.20
						Syzygium grande	1.90
SF1	3	14.3	38.9	157.2	42.8	*Irvingia malayana*	9.19
		9.8–17.5	30.1–46.3	111.1–157.2	26.5–42.8	*Goniothalamus multiovulatus*	5.35
						Sandoricum koetjape	2.61
SF2	2	14.3	33.0	77.3	31.6	*Gironniera subaequalis*	4.30
		12.6–16.0	28.2–37.8	76.6–77.3	30.4–31.6	*Ficus altissima*	3.48
						Elaeocarpus chinensis	2.76
HEF	2	9.5	29.3	67.5	27.1	*Lithocarpus aggregatus pseudo-magneinii*	8.31
		5.9–13.1	29.1–29.4	44.4–67.5	22.4–27.1	*Schima wallichii*	7.77
						Lithocarpus vestitus	1.81
DDF1	3	2.9	9.7	64.7	19.6	*Dipterocarpus obtusifolius*	4.63
		1.6–5.1	7.9–12.5	49.6–64.7		*Gluta laccifolia*	3.35
						Parinari annamensis	0.61
DDF2	2	6.8	20.4	50.6	26.9	*Shorea siamensis*	10.65
		3.9–9.6	19.4–21.5	42.8–50.6	24.4–26.9	*Dipterocarpus obtusifolius*	1.95
						Terminalia mucronata	1.23
DDF3	4	4.5	12.2	60.4	25.0	*Shorea obtusa*	3.46
		2.1–6.4	6.5–20.8	32.4–60.4	15.0–25.0	*Dipterocarpus tuberculatus*	2.95
						Terminalia tomentosa	1.39
MDF	4	5.2	20.9	78.2	32.1	*Terminalia mucronata*	2.42
		3.0–8.9	11.0–32.0	60.9–78.1	23.5–32.1	*Bamboo* spp.	2.17
						Lagerstroemia ovalifolia	1.63
SWF	1	1.2	15.4	30.0	17.2	*Melaleuca cajuputi*	15.02
						Parinari annamensis	0.15
						Vitex sp. 02	0.12

The range of values in each stand type is shown in the second line

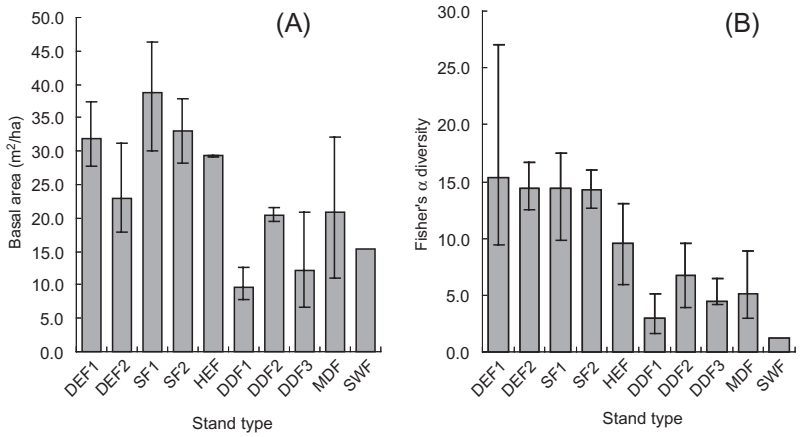

FIG. 3. Averaged basal area density (**A**) and Fisher's α index of species richness (**B**) of each stand type. Evergreen forest cluster showed higher values than deciduous forest cluster in both basal area density and species richness

3.1.2. Secondary Evergreen Forest (SEF1 and SEF2)

Five plots set in secondary forests formed one cluster within the evergreen forest cluster and were further divided into two stand types. Basal area density and species diversity of these two stand types were as high as in dry evergreen forest (see Fig. 3). *Irvingia malayana* (Irvingiaceae) was the dominant species in SEF1. There was no obvious dominant species in SEF2. Most trees were evergreen, and *Pelthophorum dasyrrhachis* (Fabaceae), a known pioneer after shifting cultivation, was frequently recorded in these SEFs. The altitude of the SEF2 plots ranged from 450 to 700 m a.s.l. while that of SEF1 was 80–220 m a.s.l..

3.2. Montane Forest Cluster

This cluster consisted of only two plots, and both plots were defined as hill evergreen forest (HEF) based on the RFD (1962) definition. The plots from the mountainous area in Mondolkiri (>800 m a.s.l.) were all clustered as HEF and formed a consistent forest type. Most species were evergreen with little overlap with the DEF. In general, these hill forests were thought not to be pf primary nature, but rather were likely fallow stands after shifting cultivation. *Schima wallichii* (Theaceae) and *Lithcarpus* spp. (Fagaceae) were dominant (see Table 4).

3.3. Deciduous Cluster

The deciduous forest cluster was indicated by *Xylia xylocarpa* and other two species (see Table 2). The cluster was further divided into four stand types, three deciduous dipterocarp forests and a mixed deciduous forest.

3.3.1. Deciduous Dipterocarp Forest (DDF1, DDF2, DDF3)

Deciduous forests were divided into four stand types, and three of them were named deciduous dipterocarp forests because of the dominance of Dipterocarpaceae.

DDF1 was an almost pure forest of *Dipterocarpus obtusifolius*. This forest was further distinguished by the lowest basal area and poorest species richness among all stand types (see Fig. 3).

DDF2 was located in a mountainous area in the north of the Mondolkiri study area (500–750 m a.s.l.). The dominant species was the deciduous species *Shorea siamensis* (Dipterocarpaceae).

DDF3 consisted of the plots of the Kratie study area (similar stand types were also observed around the KPT study area). The dominant species were all deciduous dipterocarps: *Dipterocarpus tuberculatus*, *Shorea obtusa*, and *Shorea siamensis* (see Table 4).

3.3.2. Mixed Deciduous Forest (MDF)

Five plots were clustered as MDF. In general, they were distinguished principally by the presence of deciduous species, the absence of dipterocarps, and the conspicuous presence of bamboo (RFD 1962). The main species are *Lagerstroemia* spp. (Lythraceae), *Xylia xylocarpa*, and *Dalbergia* spp. (Fabaceae) (see Table 4). Plot MDK7 had a low similarity with the other MDF plots, owing chiefly to the dominance by *Lagerstroemia calyculata*.

3.4. Swamp Forest Cluster

Only one plot was classified into this cluster and it was named swamp forest (SWF). SWF was an almost pure forest of *Melaleuca cajuputi* (Myrtaceae) (Table 4). The species is distributed in swamps and on compact sandy soils in the KPT study area. The indicator species could not be defined for the stand type because only one plot was included in the stand type, but *M. cajuputi* was exclusively dominant in this forest.

4. Discussion

As shown here, 29 plots were divided into four main clusters. These four clusters, evergreen forest, deciduous forest, montane forest, and swamp forest, seemed to correspond to the ecoregions named by Wikramanayake et al. (2002) as “Southeastern Indochina Dry Evergreen Forest”, “Central Indochina Dry Forest”, “Southern Annamites Montane Rain Forest”, and “Tonle Sap-Mekong Peat Swamp Forest”, respectively. We, therefore, discuss by these clusters focusing on the comparison of classification systems in the Indochina bioregion.

4.1. Evergreen Forest Cluster

Most of the plots of the evergreen forest cluster fell geographically within the Southeastern Indochina Dry Evergreen Forest Ecoregion. This ecoregion occurs in a broad band across northern and central Thailand into Laos, Cambodia, and Vietnam. The

term "dry evergreen forest" has usually been applied to forests in this region (RFD 1962; Smitinand 1966; Ashton 1991). However, the forest type was also called by different names such as "les forêts denses humides sempervirentes de plaine" in Cambodia (Rollet 1972), "evergreen dipterocarp forest" in Myanmar (Stamp 1925), "dense humid semi-décidue" in Laos (Vidal 1960), and "semi-evergreen forest" in whole Indochina bioregion (Vidal 1997). DEF1 and DEF2 correspond to these types in their structural complexity with more than three vertical layers and in their evergreen dominant dipterocarp species, at least in the lower canopy layer.

One difference between the composition of DEF1 and DEF2 and the conventional description of dry evergreen forest is the variable composition of the upper canopy. Following Vidal (1997), we would anticipate some main deciduous species comprising 30%–40% of the upper canopy, including species with a determinate leafless period such as *Lagerstroemia* spp. However, in DEF1 we found few leafless trees even at the end of the dry season, whereas the upper canopy of DEF2 was characterized by the deciduous canopy species *Dipterocarpus intricatus*, which is normally recognized as a main species of deciduous dipterocarp forest. Furthermore, *Pinus merksii* also occurred frequently in DEF2, often in mixed association with *D. intricatus* (see Table 4).

The plots classified as SEF were closely clustered with the DEF, and the two stand types shared some evergreen species, such as *Diospyros bejaudii* (Ebenaceae), although the SEF had few evergreen dipterocarps. *Irvingia malayana* (Irvingiaceae) was the dominant tree of SEF1 (see Table 4), and it is one of the characteristic species of DEF (Vidal 1997). Even though these SEFs probably developed after shifting cultivation, the basal area and species diversity were as high as in dry evergreen forest.

4.2. Hill Evergreen Forest Cluster

The composition of the montane plots, with its domination by Theaceae and Fagaceae, easily corresponds to the "hill evergreen forest" of RFD (1962), but other names include "lower montane oak forest" (Santisuk 1988), "les forêts dense a fagacees et lauracees" (Vidal 1960), "oak forest" (Stamp 1925), and "les forêts dense d'altitude" (Rollet 1972). These forests are certainly more variable and complex in composition than the relatively uniform nomenclature would suggest, but little has yet been done to disentangle the variation.

4.3. Deciduous Forest Cluster

In Cambodia, most deciduous forests were dry dipterocarp forest, which is the main forest formation of the central Indochina dry forest ecoregion. According to Wikramanayake et al. (2002), this ecoregion covers more area in mainland Southeast Asia than any other ecoregion. This type of forest has been called "indaing" in Myanmar (Stamp 1925) and "forêt claire" in Laos (Vidal 1960), with other names including "dry dipterocarp forest" (Kutintara 1975), "dry deciduous dipterocarp forest" (Smitinand 1977), as well as "deciduous dipterocarp forest" (RFD 1962).

DDF1 seems to correspond to "claires, peuplement a *Dipterocarpus obtusifolius*" as named by Rollet (1972). In addition to three plots sampled in KPT, there were large patches of the same forest stand in the northern part of KPT Province (around 104°52′ E,

13°00′ N). In other countries, however, few cases were reported, except in Vietnam (Ministry of Forestry 1995; Chinh et al. 1996). Although *Dipterocarpus obtusifolius* is classified as a deciduous tree, the trees in DDF1 have never been leafless in the past three years. Actually, the forests were waterlogged in the rainy season and dry up in the dry season. Such harsh conditions are likely related to the formation of these species-poor open woodlands (Hiramatsu et al., 2007).

The indicator species of DDF2, *Shorea siamensis*, *Quercus kerii*, and *Strychnos nux-vomica*, are common in DDF, especially in drier habitat conditions (Bunyavejchewin 1983). DDF3 is a typical deciduous dipterocarp forest, and this stand type could be seen in Thailand, Myanmar, Vietnam, and all over the Indochina region.

MDF is another stand type of deciduous forest in Indochina bioregion. The main species are *Xylia xylocarpa*, *Lagerstroemia* spp., and *Pterocarpus macrocarpus*, and bamboos tend to join them. Although *Tectona grandis* (teak) also tend to be dominant in MDF of Myanmar, north Thailand, and Laos, there was no natural *Tectona grandis* (teak) distribution in Cambodia (Wikramanayake et al. 2002). The species composition of the MDF stand type consists of *Xylia xylocarpa*, *Terminalia tomentosa*, and *Homalium tomentosum* (see Table 4) and showed high affinity with MDF in Myanmar and Thailand.

4.4. Swamp Forest Cluster

Melaleuca cajuputi is mostly located in swamps and also on the deposits of sand near the coast (Suzuki and Niyomdham 1992). The stand sampled by this study was located far from the coastline and might be one of the most inland populations in Southeast Asia (Hiramatsu et al., 2007).

5. Conclusion

Our numerical classification of sample plots taken from three study areas clearly showed the existence of four main forest clusters: evergreen, deciduous, montane, and swamp forests. Further subdivision of the evergreen and deciduous forests yielded ten stand types. Some of these stand types, for example, DEF1, DDF2, DDF3, and SWF, were easily identified to one of the categories of past forest classification done in Cambodia and surrounding countries. On the other hand, it was difficult to find forest categories corresponding to DEF2 and DDF1 in surrounding countries. These stand types may be unique to Cambodia. Two secondary forests, SEF1 and SEF2, also need to be examined more because the variation of dominant species in these secondary forests could not be fully covered by the present study. The evergreen forests of Cardamom Mountains and mixed forests of Preah Vihear Province might be quite different from the forests treated in this study (Rollet 1972; Forest Cover Monitoring Project 1998). Further sampling is necessary for the comprehensive understanding and precise classification of Cambodian forests.

In summary, this initial attempt at numerical classification, although limited in scale, nonetheless clearly demonstrates the ability of small plots to distinguish forest types that correspond to the traditional qualitative typologies in Southeast Asia. Future avenues to pursue include efforts to expand the scale of these enumerations

so that a greater part of Cambodian forests can be represented, to further analyze the distinctions and variation among basic forest types, and to improve the correspondence between this ground-based quantitative enumeration and the rapidly improving approaches based on remote sensing.

Acknowledgments. We sincerely thank Mr. Chan Sophal and the staff of the Forestry Administration for their kind support during our survey in the Cambodian forests. Thanks are also due to Mr. Makoto Araki, Forestry and Forest Products Research Institute, for his support for our research work. This research was carried out as a part of "Model Development for the Prediction of Water Resources Changes due to Natural Variation and Human Modification in the Asia Monsoon Region (Research Revolution 2002)," funded by the Japanese Ministry of Education, Culture, Sports, Science, and Technology.

References

Ashton PS (1991) Towards a regional classification of the humid tropics of Asia. Tropics 1:1–12

Bunyavejchewin S (1983) Analysis of the tropical dry deciduous forest of Thailand: I. Characteristics of the dominance-types. Nat Hist Bull Siam Soc 31(2):109–118

Bunyavejchewin S (1985) Analysis of the tropical dry deciduous forest of Thailand: II. Vegetation in relation to topographic and soil gradients. Nat Hist Bull Siam Soc 33(1):3–20

Champion HG (1936) A preliminary survey of the forest types of India and Burma. Indian For Rec 1:1–286

Chinh NN, Chung CT, Can VV, Dung NX, Dung VV, Dao NK, Hop T, Oanh TT, Quynh NB, Thin NN (1996) Vietnam forest trees. Agricultural Publishing House, Hanoi

Dufrene M, Legendre P (1997) Species assemblages and indicator species: the need for a flexible asymmetrical approach. Ecological Monographs 67:345–366

Food and Agriculture Organization (2001) Global forest resource assessment 2000: main report. FAO forestry paper no. 140. FAO, Rome

Forest Cover Monitoring Project (1998) Forest cover assessment of Cambodia, DFW. Phnom Penh

Hiramatsu R, Kanzaki M, Toriyama J, Kaneko T, Okuda Y, Ohta S, Khorn S, Pith P, Lim S, Pol S, Ito E, Araki M (2007) Open Woodland Patches in an Evergreen Forest of Kampong Thom, Cambodia: Correlation of Structure and Composition with Microtopography. In: Sawada H, Araki M, Chappell NA, LaFrankie JV, Shimizu A (eds) Forest Environments in the Mekong River Basin. Springer, Tokyo, pp 222–231

Hong-Narith (1997) Asia Pacific forestry sector outlook study: country paper on some aspects of forestry in Cambodia. Working paper APFSOS/WP/18. FAO, Rome, Italy/Bangkok, Thailand

KimPhat N (2000) Forests and the forest industry in Cambodia. Gifu University, Japan. www.iges.or.jp/en/fc/phase1/ir99/3-3-Nohea.pdf

KimPhat N, Ouk S, Uozumi Y, Ueki T (1999) Forest management problems in Cambodia: a case study of forest management of F company. J Jpn For Plan 5:65–71

Kutintara U (1975) Structure of the dry dipterocarp forest. PhD thesis. Colorado State University, Fort Collins, CO

Legris P, Blasco F (1972) Carte internationale du tapis Végétal a 1/1000000, Cambodge. Notice explicative. Inst Fr Pondichéry Trav Sect Sci Tech Hors série no. 11. Toulouse (France)

MacKinnon J, MacKinnon K (1986) Review of the protected areas system in the Indo-Malayan realm. IUCN/UNEP publication. Gland, Switzerland and Cambridge, UK
McCune B, Mefford MJ (1999) Multivariate analysis of ecological data (version 4.17). MJM Software, Gleneden Beach, OR
Mekong Secretariat (1994) Cambodia land cover atlas 1985/87 1992/93. UNPD/FAO, Rome
Ministry of Forestry (1995) Vietnam forestry. Agricultural Publishing House, Hanoi
Ogawa H, Yoda K, Kira T (1961) A preliminary survey on the vegetation of Thailand. Nat Life Southeast Asia 1:20–158
Rollet B (1953) Note sur les forêts claires du sud de l'Indochine. Bois For Trop 31:3–13. Nogent-sur-Marne, France
Rollet B (1972) La Végétation du Cambodge. Bois For Trop 144:3–15, 145:23–28, 146: 3–20
Royal Forest Department (RFD) (1962) Types of forest of Thailand. No. R 44. Royal Forest Department, Ministry of Agriculture, Bangkok
Santisuk T (1988) An account of the vegetation of Northern Thailand. Steiner, Stuttgart
Schmid M (1974) Végétation du Viet-Nam: Le Massif Sud-Annamitique et les Regions Limitrophes. Memoires ORSTOM No. 74. Paris (France)
Smitinand T (1966) The vegetation of Doi Chiengdao, a limestone massive in Chiangmai, north Thailand. Nat Hist Bull Siam Soc 21:93–128
Smitinand T (1977) Vegetation and ground cover of Thailand. Department of Forest Biology, Kasetsart University, Thailand
Stamp LD (1925) The vegetation of Burma from an ecological standpoint. Thacker, Spink, Calcutta
Suzuki K, Niyomdham C (1992) Phytosociological studies on tropical peat swamps. 1. Classification of vegetation at Narathiwat, Thailand. Tropics 2:49–65
The World Bank, UNDP, FAO (1996) Forest policy assessment, Cambodia. World Bank, Phnom Penh, Cambodia
Trung TV (1978) Vegetation of Vietnam forest, 2nd edn. Science and Technology Publication House, Hanoi
Vidal JE (1960) La Végétation du Laos, Vol. 1 et 2. Travaux du Laboratoire de Toulouse, Toulouse, France
Vidal JE (1997) Paysages Végétaux et Plantes de la Péninsule indchinoise. Karthala, Paris (France)
Whitmore TC (1984) Tropical rain forests of the Far East, 2nd edn. Oxford University Press, Oxford
Wikramanayake E, Dinerstein E, Loucks C, Olson D, Morrison J, Lamoreux J, McKnight M, Hedao P (2002) Terrestrial ecoregions of the Indo-Pacific. Island Press, Washington, DC

Comparison of the Leaf Area Index (LAI) of Two Types of Dipterocarp Forest on the West Bank of the Mekong River, Cambodia

Eriko Ito*, Saret Khorn, Sopheap Lim, Sopheavuth Pol, Bora Tith, Phearak Pith, Akihiro Tani, Mamoru Kanzaki, Takayuki Kaneko, Youichirou Okuda, Naoki Kabeya, Tatsuhiko Nobuhiro, and Makoto Araki

Leaf area index (LAI) is a key biophysical variable in most process-based models of forest ecosystems and water cycles. We compared the LAI of two types of tropical seasonal forest in Kampong Thom Province, Cambodia. The two forest types are extremes of crown-cover density, i.e., closed dry evergreen forest (DEF) and open dry deciduous forest (DDF), suggesting marked spatial variation in forest site conditions such as soil moisture. Monthly changes in LAI were estimated indirectly using a plant canopy analyzer and hemispherical photographs. Both methods of LAI estimation showed instrument errors, i.e., low reproducibility in the plant canopy analyzer data and LAI-saturation in hemispherical photograph data; nevertheless, LAI values differed between DEF and DDF. The average LAI from three years of measurements was about 4.6 times higher in DEF than in DDF. DDF exhibited much greater seasonality than DEF. The annual minimum LAI averaged 76% and 84% of the annual maximum LAI for DDF and DEF, respectively. LAI showed high peaks in the rainy season and decreased in the dry season. However, in DEF, LAI decreased twice annually, at the beginning of the dry season and the beginning of the rainy season. Seasonal changes in LAI could be approximated using a third-degree Fourier-series equation.

1. Introduction

The net primary production of terrestrial ecosystems depends on plant photosynthesis. Because leaves are the primary sites of photosynthesis, both the quantity and quality of leaves are considered basic indices for evaluating ecosystems. Leaf area index (LAI), defined as the total (one-sided) area of photosynthetic tissue per unit ground surface area, has been widely used as an indicator of the quantity of leaves (Jonckheere et al. 2004). Furthermore, LAI is related to the extinction coefficient of light in the chlorophyll absorption band (Jordan 1969). Thus, LAI is a primary

* Forestry and Forest Products Research Institute (FFPRI), Tsukuba, Japan
E-mail: iter@affrc.go.jp

determinant of ecosystem function that governs net primary productivity, water balance, and energy balance (Asner et al. 2003), as well as a key biophysical variable in many process-based models of global forest ecosystems and water cycles (Running and Coughlan 1988; Aber and Federer 1992; Ito and Oikawa 2002; Tanaka et al. 2003; Gerten et al. 2004).

LAI is not spatially stable. Large-scale variation is mainly caused by meteorological conditions such as temperature and precipitation, whereas local-scale variation is affected by nutrient and/or water availability in the soil. LAI is also temporally variable. Temporal patterns in LAI, i.e., seasonal changes, may vary spatially at both large and local scales. Thus, to obtain LAI as basic forest information and as a key biophysical variable in ecosystem models, the quantification of LAI must consider both spatial and seasonal variation. It was within this context that we examined the spatial and temporal variation in LAI in Cambodian lowland tropical forests. We quantified the seasonal variation in LAI across different tree-cover densities in seasonal tropical dipterocarp forests.

2. Site and Methods

Kampong Thom Province, Cambodia, is located on the west bank of the Mekong River and contains large areas of forest. Most of the area consists of dry evergreen forest with high crown-cover density and several other forest types with low crown-cover density, distributed in a mosaic-like pattern (Tani et al., 2007). We compared the LAI between two dipterocarp forest types. Experimental plots (30×80 m) were established in two forest types: dense dry evergreen forest (DEF) and open dry deciduous forest (DDF). The DEF and DDF were located at 12.760° N, 105.474° E, and 12.747° N, 105.419° E, respectively, based on the WGS 1984 reference frame. Dominant species in DEF were *Dipterocarpus costatus*, *Anisoptera costata*, and *Vatica odorata* (all Dipterocarpaceae), whereas those in DDF were *D. obtusifolius* (Dipterocarpaceae) and *Gluta lancifera* (Anacardiaceae). The basal area of DEF ($37.4\,M^2\,ha^{-1}$) was larger than that of DDF ($8.6\,m^2\,ha^{-1}$). DEF and DDF also differed in elevation, at 100 and 70 m, respectively. Fluvial deposit parent materials occurred in these plots. The soil type in DEF was Acrisols, whereas that in DDF was Arenosols (Toriyama et al. 2007).

Meteorological data were collected at two meteorological stations in Kbal Domrey and Bak Snar located 15 km north and 30 km southwest of the experimental plots, respectively, and at a 60-m-high meteorological observation tower located 1.7 km south of the DEF plot and 6.7 km east of the DDF plot. At the Kbal Domrey meteorological station, the mean annual rainfall was 1370 mm in 2003, with a distinct dry season from November to April, and the highest monthly mean air temperature was 30°C in April; it then decreased and was 27°C in November (Kabeya et al. 2007).

Each experimental plot was divided into 10- × 10-m subplots, and we marked ten permanent measuring points at the lattice positions in each plot. We estimated LAI using two indirect methods based on a model of radiative transfer for vegetative canopies: an LAI-2000 plant canopy analyzer (LI-COR, Lincoln, NE, USA) and hemispherical photography. The LAI-2000 estimates LAI by comparing light intensity at

various angles for measurements performed in an open area and below the canopy (LI-COR 1992; Jonckheere et al. 2004). We first performed measurements in an open area, then performed measurements at ten permanent locations below the canopy, and finally performed measurements in an open area again. This series of measurements was repeated three times. The measurements were performed using a 45° view cap to block the silhouette of the operator during measurements and at dusk or dawn during periods of diffuse sunlight. If transmittance >1.0 occurred when measuring LAI under little or no foliage, which often occurred in DDF, it was simply considered to be 1.0, which meant that LAI = 0 in the field of view (LI-COR 1992). Hemispherical photographs taken using a digital camera with fish-eye lens (Nikon COOLPIX 4500 with Nikon Fisheye Converter FC-E8) were analyzed for LAI using GLA software (Frazer et al. 1999). To improve classification during image analysis, we split color images into the blue plane because a clear sky tends to scatter blue light, whereas a canopy absorbs it. Measurements were performed at the end of each month from March 2003 to March 2006, except for hemispherical photographs at DEF and DDF in March and April 2003 and LAI-2000 measurements at DDF in March 2004.

To validate these approaches for estimating LAI, we compared estimates from the two methods for each experimental plot. Consistency between the two measurements was assessed using a Bland–Altman plot. We plotted the differences of the two measured values (i.e., from the different methods) on the y-axis and the means of the two measured values on the x-axis. We then determined whether the slope of the regression $y = a + bx + e$ was significantly different from zero (Bland and Altman 1986).

We used repeated-measures ANOVA to test for differences in the seasonality of LAI between the two forest types (DEF and DDF). The measurement method and location in each experimental plot were blocking factors; month and forest type were fixed factors. Statistical analysis was performed using JMP 5.01a statistical software.

We modeled seasonal changes in LAI in the two forest types using the Fourier series:

$$y = b_0 + \sum_{n=1}^{k} a_n \sin(nx) + b_n \cos(nx)$$

where a_n and b_n are Fourier coefficients, k is the number of harmonics, y is LAI, and x is the day of year (DOY) transformed into radians (0 to 2π). We manually altered the k value to determine the value giving the best fit. We then estimated seasonal changes in LAI using selected parameters giving the best fit and obtained annual averages for LAI while removing measurement-date deviations.

3. Results

LAI measured using the LAI-2000 did not vary significantly from that measured using hemispherical photography ($F_{1,65} = 0.18$, $P = 0.67$; Fig. 1). Jonckheere et al. (2004) also found good consistency between LAI measured using an LAI-2000 and hemispherical photography.

The LAI of DEF was greater than that of DDF (Fig. 2a). The two dipterocarp forests differed significantly in the seasonality in LAI (forest type × time: $F_{32,4573} = 2.74$, $P < 0.0001$). DEF exhibited much greater seasonality than DDF (Fig. 2a). For DEF, the

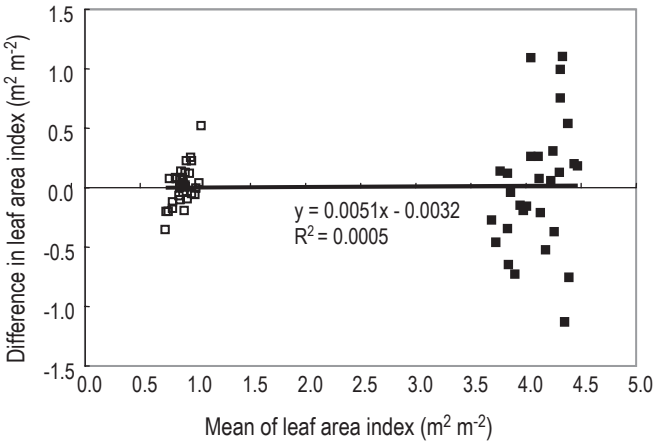

FIG. 1. Bland–Altman plot to compare two approaches, LAI-2000 and hemispherical photography, for estimating leaf area index. We plotted the differences of the two measured values (i.e., from the different methods) on the *y*-axis and the means of the two measured values on the *x*-axis. *Closed squares*, dry evergreen forest; *open squares*, dry deciduous forest. The slope did not differ significantly from zero

highest LAI occurred during the early part of the wet season (June–July); LAI decreased to low values twice seasonally, in the early dry season (October–December) and in the late dry season (February–April; Fig. 2a,b). This seasonal change in LAI corresponded with precipitation. The relatively high LAI occurred in the first half of the rainy season (May–August). LAI then decreased somewhat in the second half of the rainy season and the first half of the dry season (September–December). Finally, LAI gradually decreased in the second half of the dry season (January–April), when no rainfall occurred, and reached the lowest at the end of this period, when some rain again fell (March–April). Leaf fall was relatively substantial in the early and late dry seasons. LAI recovered after the earlier leaf fall and then decreased again at the end of the dry season. Seasonal LAI amplitudes (the percentage of the lowest LAI to the previous adjacent highest LAI) were 87.1% (April 2004/August 2003), 82.6% (April 2005/August 2004), and 79.1% (December 2005/May 2005). In contrast, for DDF, seasonal changes in LAI were not very obvious, although several locations with high LAI showed seasonal variation. Relatively high LAI occurred in the wet season, whereas low LAI was observed in the dry season (Fig. 2). Seasonal LAI amplitudes were 65.6% (March 2004/August 2003), 75.9% (December 2004/May 2004), and 74.0% (February 2006/September 2005). Both study sites were categorized as brevideciduous, i.e., losing 50%–90% of the leaves, following classification in relation to four phenological guilds (Eamus 1999).

A Fourier series with $k = 3$ provided the best fit for seasonal changes in LAI with two annual leaf falls (Fig. 2, Table 1). The annual average LAI for the three observation years modeled using the Fourier series was 4.05 $m^2 m^{-2}$ in DEF and 0.88 $m^2 m^{-2}$ in DDF. Thus, the LAI of DEF was about 4.6 times greater than that of DDF for a similar proportion of tree basal area.

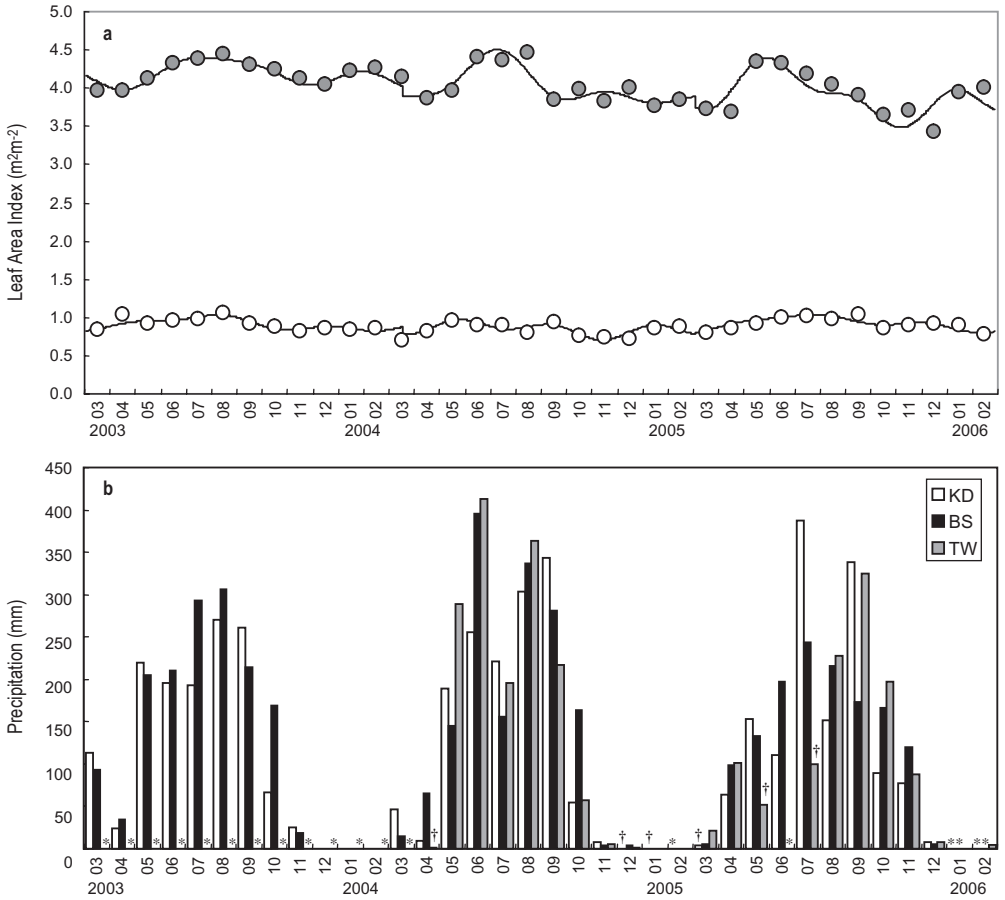

FIG. 2. Seasonality of leaf area index (LAI) and precipitation at the study site. **a** LAI of dry evergreen forest (DEF; *closed circles*) and LAI of dry deciduous forest (DDF; *open circles*). *Solid lines* represent the LAI predicted by a cubic Fourier series ($k = 3$). **b** Monthly precipitation at Kbal Domrey (*KD*), Bak Snar (*BS*), and a meteorological observation tower (*TW*; data from Kabeya et al. 2007 and Nobuhiro et al. 2007). †, Underestimated data, including missing values; *, missing data

TABLE 1. Fourier series parameters providing the best fit to seasonal changes in leaf area index (LAI)

Plot	Period	b_0	a_1	a_2	a_3	b_1	b_2	b_3
DEF	2003/Mar–2004/Mar	4.205	−0.099	0.102	0.045	−0.101	0.047	−0.034
	2004/Mar–2005/Mar	4.030	−0.087	0.070	−0.091	−0.238	0.128	−0.024
	2005/Mar–2006/Mar	3.919	0.045	0.079	0.139	−0.279	0.096	−0.086
DDF	2003/Mar–2004/Mar	0.900	−0.021	0.016	−0.011	−0.081	0.016	0.032
	2004/Mar–2005/Mar	0.836	0.012	0.023	0.073	−0.062	0.010	−0.003
	2005/Mar–2006/Mar	0.915	−0.069	0.009	0.009	−0.057	0.033	0.025

DEF, dry evergreen forest; DDF, dry deciduous forest

Table 2. Monthly average leaf area 3 years of observation

Plot	Month												Annual
	1	2	3	4	5	6	7	8	9	10	11	12	
DEF	3.95	4.01	3.96	3.89	4.06	4.32	4.39	4.26	4.10	3.98	3.87	3.85	4.05
DDF	0.86	0.84	0.81	0.85	0.92	0.95	0.95	0.96	0.94	0.87	0.81	0.83	0.88

We also found interannual changes in LAI. Fourier series modeling indicated that the annual average LAI in DEF decreased to 96% in the second year and 93% in the third year, compared to the first year of study. Similarly, the annual average LAI in DDF in the second year was 91% of that in the first and third years of study. We used the Fourier series model to quantify intraannual variations in LAI considering the interannual variation in LAI, and estimated monthly LAI in the two forest types (Table 2).

4. Discussion

The foliar phenology of seasonal tropical forests is driven largely by moisture periodicity (Reich 1995). However, it is not clear what moisture cues are important for the phenology of trees (Eamus 1999). Leaf fall in savanna often occurs before the beginning of the dry season, whereas leaf flush commonly occurs before the first rains at the end of the dry season (Simioni et al. 2004). Do et al. (2005) reported that interannual variation in canopy phenology in North Senegal is mainly affected by atmospheric conditions and not soil water availability or rainfall. They referred to such behavior as an adaptive trait that maximizes the duration of high photosynthetic activity below a certain threshold of evaporative demand. Although the seasonal variation of LAI in DDF and DEF suggested a dry season effect, it was not very clear, especially in DDF, and did not react to precipitation sensitively.

Seasonal changes in LAI indicate leaf phenology of expansion and shedding. Leaf phenology has been regarded as an optimal strategy for carbon gain in plants (Kikuzawa 1995; Kergoat 1998). Leaf expansion in the wet season and leaf shedding in the dry season have been well documented from the point of view of hydraulic adaptations in leaf phonology (Reich 1995; Jolly and Running 2004). If plant growth is limited only by precipitation, seasonal changes in LAI would indicate this pattern. Our results, however, suggest that LAI in these seasonal tropical forests was affected by not only precipitation but also by water-holding capacity in the soil, and that the moisture limitations in the dry season were not severe enough to prevent the growth of plants or cause complete leaf fall. The maintenance of plenty of leaves in the crown during the dry season may indicate that the start of the dry season is a suitable time for photosynthesis because of the relative abundant solar radiation, cloudless sky, and some soil moisture remaining in the soil layer. We predict that plant photosynthesis was high using the water stored in soil during the dry season, and the amount of leaves was then adjusted according to the amount of water remaining in the soil in the late dry season. Seasonal variation in LAI is usually treated as unimodal in hydroecological modeling (Kang et al. 2004). The bimodal pattern of LAI found here and speculation about seasonal changes in photosynthesis associated with

environmental conditions may provide new insight on how to incorporate seasonal LAI variation into hydroecological models.

From the aspect of the water cycle, interactions between the plant and the environment in the dry season are very important. LAI and moisture conditions are likely closely connected and interact, as the environment affects plant behavior and plants considerably affect subsequent soil moisture conditions, because the amount and/or rate of transpiration during the dry season influences the timing of soil drying. In other words, plants influence their own growth by their responses to the drought brought on by times of low water availability. To understand the mechanisms underlying the determination and maintenance of heterogeneous spatial patterns in dry tropical forests, we need to investigate the causes and effects of feedbacks among rainfall, soil moisture, and LAI at a local scale, following the theoretical study of Baldocchi et al. (2005), which examined vegetation–energy fluxes and interactions associated with heterogeneous savanna landscapes.

Acknowledgments. This study was funded by the "Research Revolution 2002 Project" of MEXT (Ministry of Education, Culture, Sports, Science and Technology), Japan.

References

Aber JD, Federer CA (1992) A generalized, lumped-parameter model of photosynthesis, evapotranspiration and net primary production in temperate and boreal forest ecosystems. Oecologia (Berl) 92:463–474

Asner GP, Scurlock JM, Hicke JA (2003) Global synthesis of leaf area index observations: Implications for ecological and remote sensing studies. Global Ecol Biogeogr 12:91–205

Baldocchi DD, Krebs T, Leclerc MY (2005) "Wet/Dry Daisyworld": a conceptual tool for quantifying sub-grid variability of energy fluxes over heterogeneous landscapes. Tellus 57B:175–188

Bland JM, Altman DG (1986) Statistical methods for assessing agreement between two methods of clinical measurement. Lancet 1:307–310

Do FC, Goudiaby VA, Gimenez O, Diagne AL, Diouf M, Rocheteau A, Akpo LE (2005) Environmental influence on canopy phenology in the dry tropics. Forest Ecol Manag 215:319–328

Eamus D (1999) Ecophysiological traits of deciduous and evergreen woody species in the seasonally dry tropics. Trends Ecol Evol 14:11–16

Frazer GW, Canham CD, Lertzman KP (1999) Gap Light Analyzer (GLA), version 2.0: imaging software to extract canopy structure and gap light transmission indices from true-color fisheye photographs, users manual and program documentation. Copyright© 1999: Simon Fraser University, Burnaby, British Columbia, and Institute of Ecosystem Studies, Millbrook, NY

Gerten D, Schaphoff S, Haberlandt U, Lucht W, Sitch S (2004) Terrestrial vegetation and water balance: hydrological evaluation of a dynamic global vegetation model. J Hydrol 286:249–270

Ito A, Oikawa T (2002) A simulation model of the carbon cycle in land ecosystems (Sim-CYCLE): a description based on dry-matter production theory and plot-scale validation. Ecol Model 151:143–176

Jolly WM, Running SW (2004) Effects of precipitation and soil water potential on drought deciduous phenology in the Kalahari. Global Change Biol 10:303–308

Jonckheere I, Fleck S, Nackaerts K, Muys B, Coppin P, Weiss M, Baret F (2004) Review of methods for in situ leaf area index determination. Part I. Theories, sensors and hemispherical photography. Agric For Meteorol 121:19–35

Jordan CF (1969) Derivation of leaf-area index from quality of light on the forest floor. Ecology 50:663–666

Kabeya N, Shimizu A, Chann S, Tsuboyama Y, Nobuhiro T, Keth N, Tamai K (2007) Stable isotope studies of rainfall and stream water in forest watersheds in Kampong Thom, Cambodia. In: Sawada H, Araki M, Chappell NA, LaFrankie JV, Shimizu A (eds) Forest Environments in the Mekong River Basin. Springer, Tokyo, pp 125–134

Kang S, Lee D, Kimball JS (2004) The effects of spatial aggregation of complex topography on hydroecological process simulations within a rugged forest landscape: development and application of a satellite-based topoclimatic model. Can J For Res 34:519–530

Kergoat L (1998) A model for hydrological equilibrium of leaf area index on a global scale. J Hydrol 213:268–286

Kikuzawa K (1995) Leaf phenology as an optimal strategy for carbon gain in plants. Can J Bot 73:158–163

LI-COR (1992) LAI-2000 Plant Canopy Analyser. Instruction manual. LICOR, Lincoln, NE, USA

Nobuhiro T, Shimizu A, Kabeya N, Tsuboyama Y, Kubota T, Abe T, Araki M, Tamai K, Chann S, Keth N (2007) Year-round observation of evapotranspiration in an evergreen broadleaf forest in Cambodia. In: Sawada H, Araki M, Chappell NA, LaFrankie JV, Shimizu A (eds) Forest Environments in the Mekong River Basin. Springer, Tokyo, pp 75–86

Reich PB (1995) Phenology of tropical forests: patterns, causes, and consequences. Can J Bot 73:164–174

Running SW, Coughlan JC (1988) A general model of forest ecosystem processes for regional applications. I. Hydrologic balance, canopy gas-exchange and primary production processes. Ecol Model 42:125–154

Simioni G, Gignoux J, Le Roux X, Appé R, Benest D (2004) Spatial and temporal variations in leaf area index, specific leaf area and leaf nitrogen of two co-occurring savanna tree species. Tree Physiol 24:205–216

Tanaka K, Takizawa H, Tanaka N, Kosaka I, Yoshifuji N, Tantasirin C, Piman S, Suzuki M, Tangtham N (2003) Transpiration peak over a hill evergreen forest in northern Thailand in the late dry season: assessing the seasonal changes in evapotranspiration using a multilayer model. J Geophys Res 108:D17, 4533, doi:10.1029/2002JD003028

Tani A, Ito E, Kanzaki M, Ohta S, Khorn S, Pith P, Tith B, Pol S, Lim S (2007) Principal forest types of three regions of Cambodia: Kampong Thom, Kratie, and Mondolkiri. In: Sawada H, Araki M, Chappell NA, LaFrankie JV, Shimizu A (eds) Forest Environments in the Mekong River Basin. Springer, Tokyo, pp 201–213

Toriyama J, Ohta S, Araki M, Kanzaki M, Khorn S, Pith P, Lim S, Pol S (2007) Soils under different forest types in the dry evergreen forest zone of Cambodia: morphology, physicochemical properties, and classification. In: Sawada H, Araki M, Chappell NA, LaFrankie JV, Shimizu A (eds) Forest Environments in the Mekong River Basin. Springer, Tokyo, pp 241–253

Open Woodland Patches in an Evergreen Forest of Kampong Thom, Cambodia: Correlation of Structure and Composition with Microtopography

Reiko Hiramatsu, Mamoru Kanzaki*, Jumpei Toriyama, Takayuki Kaneko, Youichirou Okuda, Seiichi Ohta, Saret Khorn, Phearak Pith, Sopheap Lim, Sopheavuth Pol, Eriko Ito, and Makoto Araki

Open woodland patches scattered in dense evergreen forest are a landscape peculiar to Kampong Thom Province. One of these open woodland patches was studied by setting a belt transect, and floral composition, stand structure, and habitat conditions were examined. Based on a census for trees 10 cm or greater in diameter at breast height (DBH), the forest along the transect was divided into three types that varied with topography. Most of the area was covered by gentle slopes and was dominated by *Dipterocarpus obtusifolius*, which displayed 50% canopy openness and poor species richness. The stands were located on rectilinear to convex sloping sites with low clay content that were waterlogged in the rainy season. *Melaleuca cajuputi* stands occurred in a small swamp, whereas on the slope *M. cajuputi* was mixed with *D. obtusifolius*. The *M. cajuputi* stands were geographically isolated from the coastal location more characteristic of the species. Along the stream or beside the swamp, where no waterlogging occurred even in the rainy season, we found *Vatica odorata* stands. Physical habitat conditions associated with the topography, such as clay content and soil water conditions, enable the three forest types with different physiognomies to coexist at this small spatial scale and may also explain the outpost patches of *M. cajuputi*.

1. Introduction

In Cambodia, three main types of forests are recognized along with various transitional types: evergreen, deciduous, and mixed forests (Rollet 1972; Vidal 1997). The dense evergreen forest covers the Cardamon Mountains of provinces of Koh Kong, Kampot, and Pursat, and also the western bank of the Mekong River around Kampong Thom Province. In Kampong Thom Province, dense evergreen forest is most abundant, and the forest is dominated by evergreen dipterocarps such as *Dipterocarpus costatus* (Tani et al. 2007). Within this evergreen forest, sparse woodland appears as scattered patches in the vegetation map (Fig. 1). A surprising constituent of the patches is *Melaleuca cajuputi*, which is a characteristic tree of freshwater swamps in Southeast Asia, sometimes becoming dominant, especially in the secondary forest

* Graduate School of Agriculture, Kyoto University, Kyoto, Japan
E-mail: mkanzaki@kais.kyoto-u.ac.jp

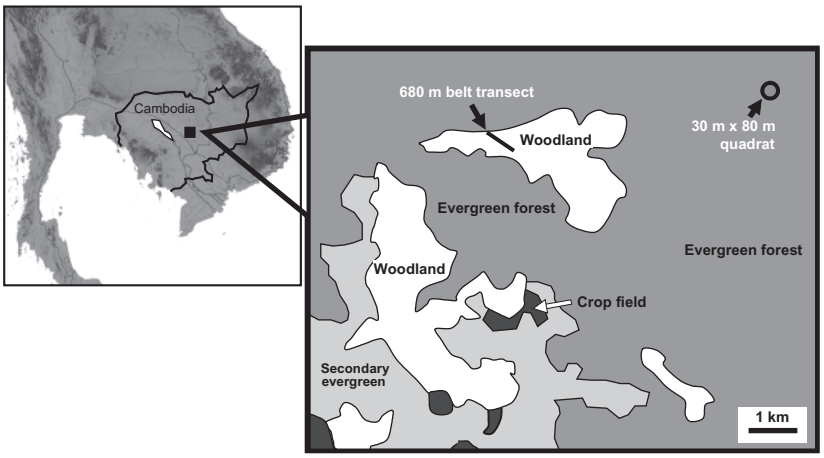

FIG. 1. Map showing the research sites. Woodlands are scattered in evergreen forests and secondary evergreen forests after selective logging and shifting cultivation. (Source: The Department of Forest and Wildlife, Cambodia, 1999)

of peat swamps (Suzuki 1999). The species normally occurs no more than a few kilometers away from the coast (Hozumi et al. 1969; Rollet 1972; Kochummen 1978), and so its appearance in Kampong Thom, some 300 km inland, is unusual and was only previously noted by Rollet (1972) from Kampong Cham and Kratie.

Thus, the most likely explanation for the contrasting composition within these patches lies in the soil and hydrological conditions as they relate to microtopography. We, therefore, examined these relationships and determined the floral composition of a sparse forest patch using a belt transect along a microtopographic gradient.

2. Research Site and Methods

The study site was located in Kampong Thom Province, Cambodia (105°25′ E, 12°45′ N, about 70 m in altitude). The annual mean temperature is 27°C and the mean annual rainfall is 1570 mm at Kampong Thom town, with a strongly seasonal regime wherein 1480 mm is recorded from April to November (Crocker, 1962). In this province, 57% of the land area was covered by forest in 1993 and the forest was under the control of six logging concessions in 1994 (World Bank, UNDP, and FAO 1996). These concessions were halted at least until 2006 to allow Cambodia to renovate its forest management system.

We set a belt transect (10 m × 680 m) so as to cross a microtopographic gradient that included varying forest types (Fig. 1, Photos 1 and 2). To examine dry evergreen forest as a comparative reference point, we set a 30 m × 80 m quadrat about 5 km east from the belt transect (Fig. 1). Within both the transect and the quadrat, all trees ⩾10 cm DBH were enumerated during 2003, with each tree being measured, noted for position, and identified to species. Voucher specimens are kept in the Laboratory of Tropical Forest Resources and Environment, Graduate School of Agriculture, Kyoto University.

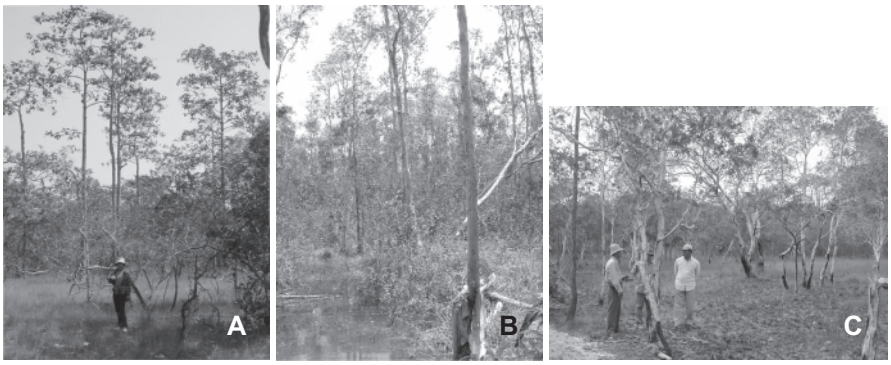

Photo 1. Forest variation in the study site. **A** Open woodland (*Dipterocarpus obtusifolius* stand type). **B** Swamp forest (*Melaleuca cajuputi* stand type). **C** *Melaleuca* stand on a dry habitat

Photo 2. Forest variation in the study site. **A** Evergreen forest overtopped by deciduous trees (*Vatica odorata* stand type). **B** Inside of a *Vatica* stand. **C** Evergreen forest dominated by *Dipterocarpus costatus*

Basic compositional analysis was conducted by dividing the transect into 34 subplots of 10 m × 20 m, while the 30 m × 80 m quadrat was separated into two 30 m × 40 m subplots. Data were analyzed using PC-ORD Version 4.17 for Windows (MjM Software; McCune and Mefford 1999). A presence–absence data matrix of 36 subplots was prepared, and the Sörensen index of similarity was calculated for all the combination of the subplots and subjected to the group averaging cluster analysis. Indicator analysis (Dufrene and Legendre 1997) was then conducted to detect the species with distribution significantly biased to one of the obtained forest types.

Canopy openness was estimated by running Gap Light Analyzer Version 2.0 (Simon Fraser University and Institute of Ecosystem Studies) over hemispheric photographs taken at 36 points arbitrarily selected along the transect. The photographs were taken at 1.0-m height by a digital camera (Nikon Coolpix 990 equipped with fish eye converter FC-E8).

3. Results

The cluster analysis classified the forest into three principal types with strongly contrasting species composition (Fig. 2). Parameters of stand structure, such as basal area and canopy openness, changed sharply at the border between different stand types (Fig. 3). The height of the forest, interpreted as the asymptote of the diameter–height relationship, also differed among the three sites (Fig. 4).

Most of the sparse woodland constituted a stand type that was dominated by *Dipterocarpus obtusifolius* (Dipterocarpaceae) (Fig. 3, Photo 1A). This stand type occurred on the gentle slope stretching 0–100 m and 230–420 m in position along the belt transect. Indicator species of this forest type were *Dipterocarpus obtusifolius* and *Gluta laccifera* (Anacardiaceae) (Table 1). This forest type was species poor with fewer than four species per 10 m × 20 m plot (see Fig. 3). The canopy openness was 50% and basal area (BA) density was 9.3 m^2/ha on average. The canopy height was up to 18 m (see Fig. 4).

The second type was dominated by the sole indicator species of the type, *Melaleuca cajuputi* (Myrtaceae) (see Table 1). This second stand type occurred in a small swamp located 550–680 m along the transect (see Fig. 3, Photo 1B). A stand of intermediate composition was located in a gentle slope (320–360 m position) wherein *M. cajuputi* was mixed with *D. obtusifolius* (see Fig. 3, Photo 1C). The forest structure differed between the stands in the swamp and on the gentle slope. In the swamp habitat, the

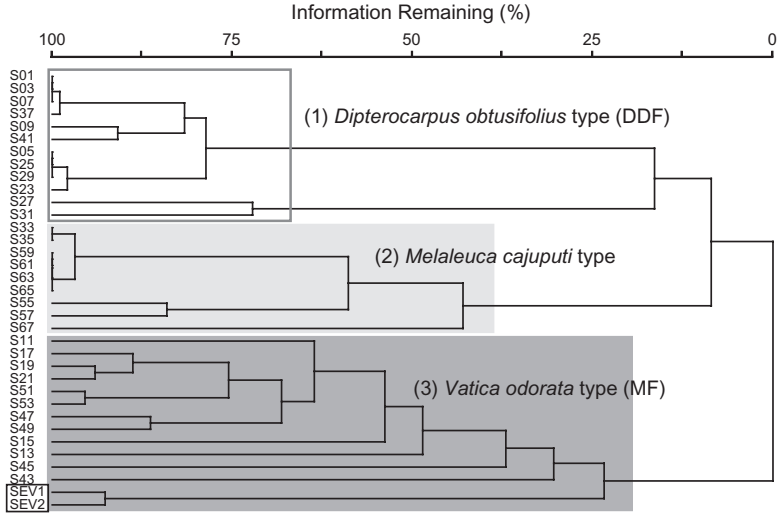

FIG. 2. Dendrogram obtained by the cluster analysis for 35 stands. The stands were separated into three stand types, namely (1) *Dipterocarpus obtusifolius*, (2) *Melaleuca cajuputi*, and (3) *Vatica odorata* types. Two dry evergreen forest subplots (marked by a *box*) were included in *Vatica odorata* type. Types (1) and (2) are also called deciduous dipterocarp forest (*DDF*) and mixed forest (*MF*), respectively

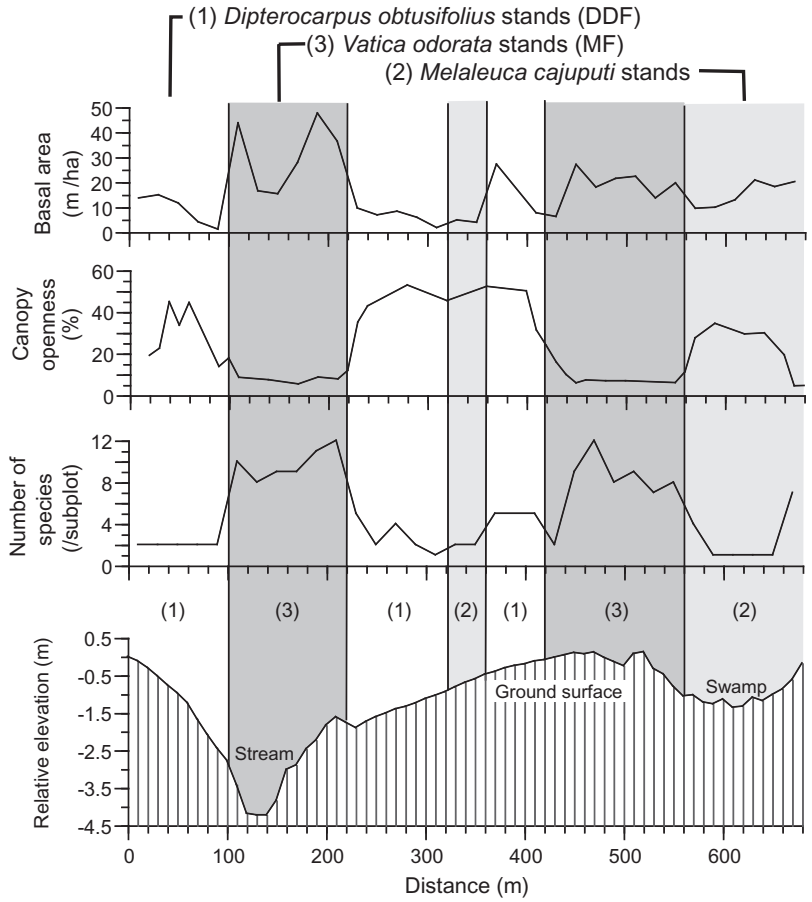

FIG. 3. Topography of the transect and the spatial changes in stand structure and species richness along the transect. Figures in *parentheses* in the *bottom diagram* indicate the stand group shown in Fig. 2

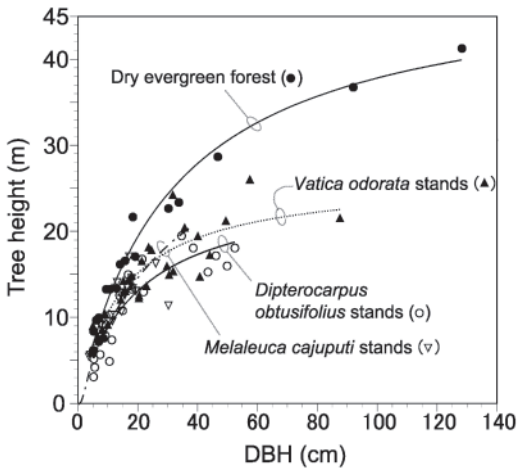

FIG. 4. Relationship between the stem diameter (*DBH*) and tree height

Table 1. Indicator species and habitat condition of each stand type

Stand type	Number of subplots and habitat condition	Indicator species (total number of species recorded)
(1) *Dipterocarpus obtusifolius*	12 subplots Rectilinear or convex slope with minute inclination (<5°)	*Dipterocarpus obtusifolius* *Gluta laccifolia* (11)
(2) *Melaleuca cajuputi*	9 subplots Swamp on concave topography located at the highest part of the transect	*Melaleuca cajuputi* (15)
(3) *Vatica odorata*	12 subplots and 2 evergreen forest subplots Streamside (concave slope) and swamp periphery (convex slope)	*Vatica odorata brevipetiolata* *Syzygium gratum* var. *confertum* *Memecylon edule* *Acronychia pedunculata* *Sindora siamensis* *Symplocos cochinchinensis subsp. laurina* *Garcinia multiflora* (65)

canopy openness was around 30% and BA was 12.5 m^2/ha, whereas on the gentle slope the structure was similar to the *D. obtusifolius* stand. Canopy height was up to 16 m in the swamp site (see Fig. 4).

The third type was dominated by the evergreen species *Vatica odorata subsp. brevipetiolata* (Dipterocarpaceae) and was located along the river and beside the *Melaleuca* swamp (see Fig. 3, Photo 2A,B). The indicator species of the type were *V. odorata* and *Syzygium gratum* var. *confertum* (Myrtaceae) and five other species (see Table 1). The two dry evergreen forest plots (see Photo 2C) were also included into this forest type, suggesting the high similarity of species composition between *Vatica odorata* stands and the dry evergreen forest (see Fig. 2). A deciduous dipterocarp, *Dipterocarpus intricatus*, was also mixed in the stands and formed the upper-canopy layer. This forest was characterized by higher species richness, dense canopy (canopy openness around 8%), and a high basal area of up to 47.5 m^2/ha (see Fig. 3). Canopy height was ≤26 m along the transect and ≤41 m in the evergreen forest stands (see Fig. 4).

4. Discussion

4.1. The Three Forest Stand Groups

The three stand types identified in the microtopographical transect are related to the broader forests types described for Cambodia. The *Dipterocarpus obtusifolius* stands look like open woodland formation and resemble the dry dipterocarp forest or deciduous dipterocarp forest (DDF) (Royal Forest Department 1962). In our large-scale vegetation analysis (Tani et al. 2007), we classified these particular stands as DDF. However, they differed from normal DDF in that they were unusually species poor and lacked those species typical of DDF, such as *Shorea*

obtusa (Dipterocarpaceae), *Pterocarpus macrocarpus* (Fabaceae), and *Xylia xylocarpa* (Fabaceae). Also the ground flora of the stands lacked *Arundinaria* spp. (Graminae) and included *Xyris complanata* (Xyridaceae), which is an indicator species of wetland. These differences are likely the result of the unusual edaphic conditions of the site. For example, the appearance of burnt ground litter and burnt tree bark suggested that ground fires occur during the dry season from November to March. We also observed that the site was waterlogged during the middle of the rainy season, around August–September (Araki et al. 2007). Thus, the peculiar composition of the *D. obtusifolius* stand is most likely caused by the seasonal alteration of the ground condition from dry and prone to fire during the dry spell to waterlogged during the rainy spell. This condition may confirm the finding of Rollet (1972), who recorded *D. obtusifolius* woodland in seasonally flooded conditions in Kampong Cham and Kratie. In Vietnam, the species is also reported to form pure stands at seasonally inundated sites (Nguyen et al. 1996), and this kind of forest is considered to be one type of deciduous dipterocarp forest (Ministry of Forestry 1995).

The composition of the *Melaleuca cajuputi* stand is not surprising because it is well known as an often-dominant species of coastal freshwater swamps, sometimes forming pure stands (Suzuki and Niyomdham 1992). It is also found along coastal sand dunes (Hozumi et al. 1969; Suzuki et al. 2005). However, the location of our site at 300 km inland from the nearest coastline of the Mekong delta or Koh Kong is exceptional. The only inland stands of *Melaleuca* previously recorded were from Kampong Cham and Kratie, about 100 km to the southeast from our study site (Rollet 1972). The stand within the transect was not unique because we also found such stands outside our research site in Kampong Thom, where the local people harvest the timber of *M. cajuputi*.

These inland stands of an essentially coastal species can be explained as either the product of historical biogeography or being caused by more-recent human-related activities. During the hypsithermal period, about 6000 years ago, the mouth of the Mekong River entered the deeper part of the current Mekong delta and reached to the south of Phnom Penh City (Tsukawaki and Sieng 2005). During the period, coastal *Melaleuca* forest would be expected as far inland as Phom Penh. However, our studied stand would still have been 200 km inland from that historical coastline. Because *M. cajuputi* has been reported as a common secondary forest species that invades after forest fires or human disturbance (Suzuki 1999; Tomita et al. 2000), and because it is also planted in the coastal area of Malaysia (Kochummen 1978) and Viet Nam (Ministry of Forestry 1995), it is at least possible that the *M. cajuputi* stand is the result of intentional or inadvertent human activity.

The *Vatica odorata* stands were similar to the dry evergreen forest in floral composition except for the presence of a deciduous dipterocarp, *Dipterocarpus intricatus*, in the upper-canopy layer. Also, the canopy height of *Vatica* stands along the transect was less than 26 m and shorter than that of dry evergreen forest, which may reach up to 40 m. In Cambodia, this kind of forest is frequently called “mixed forests” irrespective of the variation of species composition. The stands located near a stream or a swamp were free from fire in the dry season. The sites were evidently never inundated even in the rainy season, except perhaps the actual streamside (Araki et al. 2007).

4.2. Factors Generating the Pattern

Although the elevation difference along the 680-m transect was only 4.5 m, clear habitat differentiation of three forest types was recognized in our transect study. The overlap of the component species between stand groups was measured by Sörensen's percent similarity using presence–absence data. Similarity was 13.3%, 23.1%, and 20.3% for the combination of clusters (1)–(2), (1)–(3), and (2)–(3), respectively. Species similarity among the stand types was very low in comparison with community differentiation along the topography gradient in a tropical montane forest of Thailand (Kanzaki et al. 2005; Sri-Ngernyuang et al. 2003), where the similarity of species composition among forest stands ranged from 79% to 88% (Kanzaki et al., unpublished data).

The most likely mechanism by which microtopography controls the distribution of forest types is through the interaction of soil water and soil structure. Toriyama et al. (2007) examined the clay content of soils along the transect. The soil of the research site is sandy, and clay content was quite low varying from 2% to 6%. The spatial pattern of clay content showed quite good correspondence with the spatial distribution of two forest types, *Vatica* stands and *D. obtusifolius* stands [mixed forest (MF) and DDF in Fig. 4 of Toriyama et al. 2007]. *Vatica* stands occurred in places with higher clay content and *D. obtusifolius* stands with lower clay content. The difference might be associated with the water and nutrient availability of each stand type.

Araki et al. (2007) monitored the seasonal changes in groundwater level and found that the groundwater level of *Vatica* stands (MF in Araki et al. 2007) and *D. obtusifolius* stands (DDF in Araki et al. 2007) showed no clear difference in the dry season (Fig. 2 in Araki et al.). The difference was most clear in August, when most of the *D. obtusifolius* stand was waterlogged while the *Vatica* stand was never waterlogged. Per humid soil condition, together with low clay content, of *D. obtusifolius* stands seems to critically inhibit the invasion of evergreen species into the stands. The open woodland patches are located at minutely concave topography on flat plains with poor drainage channels. This topography condition results in the waterlogged condition of our research site.

Physical habitat conditions, such as clay content and soil water conditions associated with the topography, enable the three forest types with different physiognomies to coexist at this small spatial scale. The existence of inland outpost patches of *M. cajuputi* is also dependent on the habitat conditions peculiar to the open woodlands. Much attention should be focused on the unique landscape in the study area from the point of view of its biogeography. Conservation measures to protect the outpost patches of biogeographic importance are also required, because this area is experiencing rapid agricultural development.

Acknowledgments. We express our sincere thanks to Mr. Chann Sophal and the Forestry Administration of Cambodia for their kind support during our research activities in Cambodia. The study was financially supported by the Ministry of Education, Culture, Sports, Science, and Technology through Research Revolution 2002, "Model Development for the Prediction of Water Resources Changes Due to Natural Variation and Human Modification in the Asia Monsoon Region."

References

Araki M, Toriyama J, Ohta S, Kanzaki M, Ito E, Sopheap L, Sopheavuth P, Bora T, Saret K, Phearak P, Saila D (2007) Soil moisture conditions in four types of forests in Kampong Thom, Cambodia. In: Sawada H, Araki M, Chappell NA, LaFrankie JV, Shimizu A (eds) Forest environments in the Mekong River basin. Springer, Tokyo, pp 254–262

Crocker, CD (1962) The general soil map of the Kingdom of Cambodia and the exploratory survey of the soils of Cambodia. Royal Cambodian Government Soil Commission/ United States Agency for International Development, Phnom Penh

Dufrene M, Legendre P (1997) Species assemblages and indicator species: the need for a flexible asymmetrical approach. Ecol Monogr 67:345–366

Hozumi K, Kira T, Shinozaki K (1969) Production ecology of tropical rain forests in southwestern Cambodia. I. Plant biomass. Nat Life SE Asia 6:1–52

Nguyen NC, Cao TC, Vu VC, Nguyen XD, Vu VD, Nguyen KD, Tran H, Tran TO, Nguyen BQ, Nguyen NT (1996) Vietnam forest trees. Agricultural Publishing House, Hanoi

Kanzaki M, Hara M, Yamakura T, Tamura MN, Ohkubo T, Sri-ngernyuang K, Sahunalu P, Teejuntuk S, Bunyavejchewin S (2004). Doi Inthanon forest dynamic plot, Thailand. In: Losos EC, Condit R, LaFrankie JV, Leigh EG (eds) Tropical forest diversity and dynamism: findings from a network of large-scale forest dynamics plots. Chicago University Press, Chicago, pp 474–481

Kochummen KM (1978) Myrtaceae. In: Ng FSP (ed) Tree flora of Malaya, vol 3. Longman Malaysia, Kuala Lumpur, pp 169–253

McCune, B, Mefford MJ (1999) Multivariate analysis of ecological data (version 4.17). MJM Software, Gleneden Beach, OR

Ministry of Forestry (1995). Vietnam forestry. Agricultural Publishing House, Hanoi

Rollet B (1972) La Végétation Du Cambodge. Rev Bois For Trop 144, 145, 146

Royal Forest Department (1962) Types of forest of Thailand. No. R 44. Royal Forest Department, Bangkok

Sri-Ngernyuang K, Kanzaki M, Mizuno T, Noguchi H, Teejuntuk S, Sungpalee C, Hara M, Yamakura T, Sahunalu P, Dhanmanonda P, Bunyavejchewin S (2003) Habitat differentiation of Lauraceae species in a tropical lower montane forest in northern Thailand. Ecol Res 18:1–14

Suzuki K (1999) An ecological study of Melaleuca communities in littoral swamps. Eco-Habitat 6:133–141

Suzuki K, Niyomdham C (1992) Phytosociological studies on topical peat swamps. 1. Classification of vegetation at Narathiwat, Thailand. Tropics 2:49–65

Suzuki K, Laongpol C, Sridith K (2005) Phytosociological studies on vegetation of coastal dunes at Narathiwat, Thailand. Tropics 14:229–244

Tani A, Ito E, Kanzaki M, Ohta S, Saret K, Phearak P, Bora T, Sopheavuth P, Sopheap L (2007) Principal forest types of three regions of Cambodia: Kompong Thom, Krache, and Mondolkiri. In: Sawada H, Araki M, Chappell NA, LaFrankie JV, Shimizu A (eds) Forest environments in the Mekong River basin. Springer, Tokyo, pp 201–213

Tomita M, Hirabuki Y, Suzuki K, Hara K, Kaita N, Araki Y (2000) Drastic recovery of Melaleuca-dominant scrub after a severe fire: a three-year period study in a degraded peat swamp, Thailand. Eco-Habitat 7:81–87

Toriyama J, Ohta S, Araki M, Kanzaki M, Saret K, Phearak P, Sopheap L, Sopheavuth P. (2007) Soils under different forest types in the dry evergreen forest zone in Cambodia: morphology, physicochemical properties and classification. In: Sawada H, Araki M, Chappell NA, LaFrankie JV, Shimizu A (eds) Forest environments in the Mekong River basin. Springer, Tokyo, pp 241–253

Tsukawaki S, Sieng S (2005) Formation of the present natural environment on Lake Tonle Sap and the lower course of the Mekong River system in Cambodia: geological history

of Cambodia during the last 20,000 years. In: Proceedings of international conference on forest environment in continental river basins; with a focus on the Mekong River. Sunway Hotel, Phnom Penh, Cambodia, 5th–7th December 2005
Vidal JE (1997) Vegetation types and plants of the Indochinese Peninsula: international environmental databases. Ecocart, http://www.ecocart.com/
World Bank, UNDP, and FAO (1996) Cambodia forest policy assessment. World Bank, Washington, DC

Use of ASTER Optical Indices to Estimate Spatial Variation in Tropical Seasonal Forests on the West Bank of the Mekong River, Cambodia

Eriko Ito*, Sopheap Lim, Sopheavuth Pol, Bora Tith, Phearak Pith, Saret Khorn, Akihiro Tani, Mamoru Kanzaki, Takayuki Kaneko, Youichirou Okuda, and Makoto Araki

Forest ecosystem parameters related to the amount of evapotranspiration and rain interception are key elements to successful hydrological modeling. Thus, we evaluated ASTER (Advanced Spaceborne Thermal Emission and Reflection radiometer) reflectance bands and optical indices for qualitative and quantitative estimation of various characteristics of tropical seasonal forests. Ground conditions were measured in 14 sites in Kampong Thom Province, Cambodia, representing six major tropical seasonal forest types: dry evergreen forest, mixed evergreen-deciduous forest, dry deciduous forest, regrowth of dry evergreen forest, moist evergreen forest, and swamp forest. We performed a discriminant analysis to classify forest types using ASTER reflectance bands and optical indices. We used Visible and near infrared Radiometer (VNIR) and Shortwave Length Infrared Radiometer (SWIR) surface reflectance, four vegetation indices: NDVI (Normalized Difference Vegetation Index); SR (Simple Ratio); DVI (Difference Vegetation Index), and MSAVI2 (Second Modified Soil Adjustment Vegetation Index), and three water content indices: SRWI (Simple Ratio Water Index); NDWI (Normalized Difference Water Index); and LWCI (Leaf Water Content Index), for the discriminant analysis. ASTER image products were acquired on January 12, 2002 in the dry season. We also performed regression analyses to identify an optical index closely correlated with forest qualitative characteristics such as tree density, tree height, basal area, and leaf area index (LAI). Each forest type showed a distinctive pattern in reflectance bands, demonstrating that satellite images can potentially be used for regional forest type classification. Regression analyses showed close agreements between forest qualitative characteristics and optical indices. In particular, ASTER data explained 94% of the variation in LAI. The three most effective indices for estimating LAI were NDVI, MSAVI2, and SR.

1. Introduction

Forest ecosystem parameters related to the amount of evapotranspiration and rain interception are key elements in hydrological modeling (Running and Coughlan 1988;

* Forestry and Forest Products Research Institute (FFPRI), Tsukuba, Japan
E-mail: iter@affrc.go.jp

Aber and Federer 1992; Landsberg and Gower 1997; Engel et al. 2002; Tanaka et al. 2003; Kang et al. 2004; Mo et al. 2004; Yamazaki et al. 2004). Forest ecosystems, however, are not uniform, but are spatially and temporally heterogeneous. Thus, accurate information on forest heterogeneity would be useful for forest ecosystem and water cycle modeling. Remote sensing is a powerful tool with which to obtain general information about forest heterogeneity because it can provide data on a large scale and over time. To determine the heterogeneity by remote sensing, ground truth data must be extrapolated. This process begins by obtaining point data measured on the ground. The next step is to estimate relationships between ground-point data and cell data obtained by remote sensing. The point ground truth data can then be combined with regional-scale remote sensing data, which in turn makes it possible to determine forest heterogeneity. Therefore, to use remote sensing for forest ecological research, we need to determine significant relationships between ground data and remote sensing data. The use of multiple indices in a canonical correlation analysis is more effective than regressions of single optical indices in retrieving normal forest characteristics (Cohen et al. 2003; Wang et al. 2005).

We examined the availability of remote sensing in determining forest heterogeneity in Kampong Thom Province, Cambodia, to achieve two objectives: forest classification using discriminant analysis and forest quantification using multiple regression analysis, i.e., estimating parameter values that express forest characteristics such as tree density, biomass, dominant species, and leaf area index (LAI). We evaluated ASTER reflectance bands and optical indices for the qualita-tive and quantitative estimation of characteristics of various tropical seasonal forest types.

2. Study Site

Dense evergreen forest covers the western bank of the Mekong River in Kampong Thom Province, Cambodia (Hiramatsu et al., this volume). Fourteen sites were chosen in Kampong Thom Province to represent six forest types typical of Cambodian lowland tropical seasonal forest: dry evergreen forest (DEF), mixed evergreen–deciduous forest (MF), dry deciduous forest (DDF), DEF regrowth forest (RDEF), moist evergreen forest (MEF), and swamp forest (SF). DEF had a dense, closed canopy with a mean basal area of 32.2 $m^2 ha^{-1}$ and was dominated by dipterocarp species such as *Dipterocarpus costatus*, *Anisoptera costata*, and *Vatica odorata*. MF had a nearly closed canopy with a mean basal area of 23.0 $m^2 ha^{-1}$ and was also dominated by dipterocarp species such as *D. intricatus* and *V. odorata*. DDF had an open canopy resembling savanna with a mean basal area of 9.6 $m^2 ha^{-1}$ and was dominated by *D. obtusifolius* (Dipterocarpaceae) and *Gluta lancifolia* (Anacardiaceae). RDEF had a dense closed canopy with a basal area of 29.2 $m^2 ha^{-1}$, had no dipterocarp species, and was dominated by *Irvingia malayana* (Simaroubaceae) and *Peltophorum dasyrrhachis* (Leguminosae). MEF had a highly dense canopy with a basal area of 48.8 $m^2 ha^{-1}$, had no dipterocarp species, and was dominated by *Myristica iners* (Myristicaceae). SF had an open canopy with a basal area of 15.5 $m^2 ha^{-1}$ and was a pure stand of *Melaleuca cajuputi* (Myrtaceae). The summary statistics for forest qualitative characteristics by forest type are shown in Table 1. Site details can be found in Hiramatsu et al. (2007), Tani et al. (2007), and Toriyama et al. (2007).

Table 1. Summary statistics for forest characteristics in the different forest types

Forest type	*n*	Basal area ($m^2 ha^{-1}$)	Max, tree height (m)	Tree density (ha^{-1})	LAI ($m^2 m^{-2}$)
		Mean (range)	Mean (range)	Mean (range)	Mean (range)
DEF	5	32.2 (22.5–41.5)	35.8 (32.8–41.4)	617 (271–875)	3.37 (2.79–3.75)
MEF	1	48.8	45.1	1344	3.77
RDEF	1	29.2	26.5	462	3.23
MF	3	23.0 (18.0–31.2)	24.0 (20.2–26.2)	661 (565–717)	3.28 (2.78–3.58)
SF	1	15.5	17.2	782	1.01
DDF	3	9.6 (7.3–12.5)	19.4 (18.2–20.5)	240 (192–283)	0.74 (0.52–0.95)

Forest type was ordered by decreasing leaf area index (LAI)
DEF, dry evergreen forest; MEF, moist evergreen forest; RDEF, DEF regrowth forest; MF, mixed evergreen–deciduous forest; SF, swamp forest; DDF, dry deciduous forest

3. Methods

We measured ground conditions in the 14 sites. In each plot, the diameter at breast height (DBH) of all trees with DBH >10 cm was recorded, and tree density (number of trees ha^{-1}) and basal area ($m^2 ha^{-1}$) were obtained. Maximum tree height was measured. Leaf area index (LAI) was estimated indirectly using a plant canopy analyzer (LAI-2000; LI-COR, Lincoln, NE, USA) and hemispherical photography. The details of LAI measurements are described by Ito et al. (2007). Spatial changes in LAI during the dry seasons were examined from 2003 to 2005.

We used a total of 16 optical indices derived from ASTER image products for analysis: these consisted of three VNIR (Green, Red, and NIR) and six SWIR (SWIR1–6) surface reflectance indices, four vegetation indices (NDVI, SR, DVI, and MSAVI2; Appendix 1), and three water content indices (SRWI, NDWI, and LWCI; see Appendix 1). ASTER surface reflectances acquired on January 12, 2002 (dry season) were extracted from the 15 pixels nearest to the center of the location of each field site, except for nonforest coverage, after adjusting the spatial resolution of SWIR (30 m) to that of VNIR (15 m).

We conducted two analyses of these remote sensing data. First, we performed a forest-type classification using discriminant analysis. Second, we quantified forest characteristics using multiple regression analysis. We then identified optical indices closely correlated with qualitative forest characteristics.

4. Results and Discussion

4.1. Reflectance Pattern in Forests

For patterns of reflectance obtained from the ASTER image, in general, trends in NIR were the opposite to those of other bands; i.e., forest types with higher reflectance in NIR showed lower reflectance in other bands (Table 2). The difference in NIR and Red reflectance among forest types indicates variation in leaf biomass and/or plant activity. Exceptions to this general trend occurred in MEF and SF. Relatively low NIR reflectance was found in MEF, but MEF showed similar reflectance to other bands in high-density forests, such as DEF and RDEF. SF showed a much lower SWIR

TABLE 2. Mean reflectance values (%) and SD in the different forest types

Forest type	No of pixels	Green		Red		NIR		SWIR1	
		Mean	SD	Mean	SD	Mean	SD	Mean	SD
DEF	75	9.11	0.34	4.19	0.27	31.51	2.44	15.24	0.62
MEF	15	8.90	0.27	4.11	0.16	26.80	1.55	14.60	0.25
RDEF	15	8.83	0.32	3.79	0.18	31.15	2.70	15.31	0.18
MF	45	9.65	0.41	4.73	0.39	29.51	2.17	16.81	1.05
SF	15	10.03	—	5.85	—	22.99	2.00	15.75	1.32
DDF	45	10.95	0.78	7.36	1.15	24.48	1.29	22.88	1.32

NIR, Near Infrared Radiometer; ; SWIR1, Short Wave Infrared Radiometer Band 1

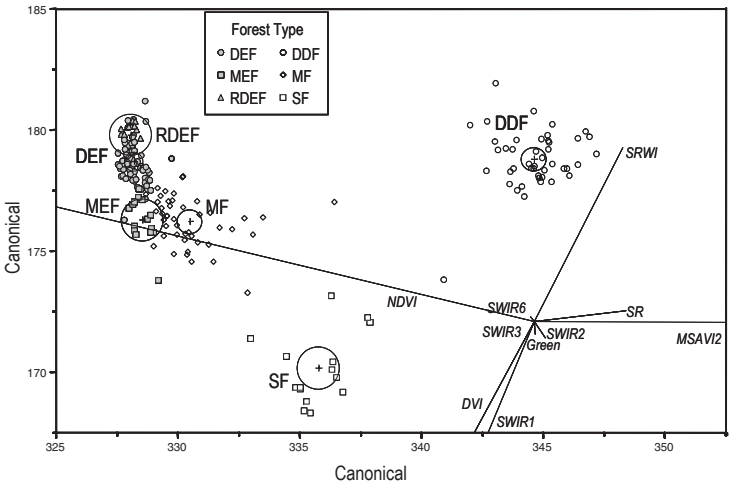

FIG. 1. Two-dimensional canonical plot of the points and multivariate means that best separate the forest-type groups. Each point is one data cell obtained from ASTER; each *labeled circle* is a multivariate mean. The size of the circle corresponds to the 95% confidence limits for the mean. Groups that are significantly different tend to have nonintersecting circles. The directions of the ten best variables in canonical space are shown as *labeled vectors*. *DEF*, dry evergreen forest; *MEF*, moist evergreen forest; *RDEF*, DEF regrowth forest; *DDF*, dry deciduous forest; *MF*, mixed evergreen–deciduous forest; *SF*, swamp forest

reflectance than expected from other reflectance values, suggesting humid ground conditions under the poor vegetation biomass. This observation demonstrates that SWIR can potentially be used for regional forest type classification.

4.2. Forest Classification

Forest classification according to the discriminant analysis is presented in a canonical plot (Fig. 1) showing the points and multivariate means in two dimensions that best separate the groups. We could discriminate more than 95% of cells to the correct forest type using the 16 variables, including VNIR and SWIR surface reflectance indices and vegetation or water content indices. The optical indices are arranged in

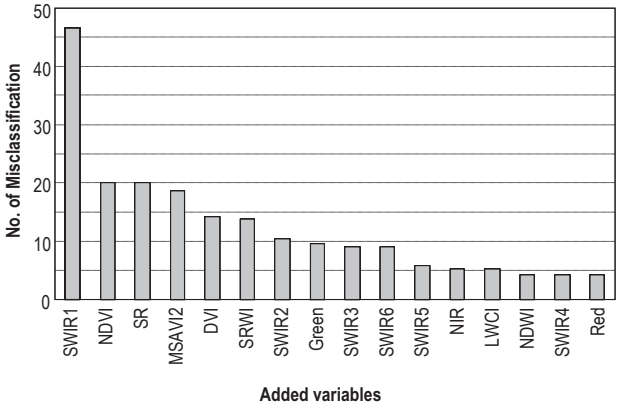

FIG. 2. The number of forest-type misclassifications that occurred in discriminant analysis as optical indices were added cumulatively. Indices are ordered in effectiveness from *left* (most effective) to *right* (least effective). Green, Red, and NIR indicate visible and near infrared radiometer band 1, 2, and 3, respectively. SWIR1-6, Short Wave Infrared Radiometer Band 1-6; NDVI (Nomalized Difference Vegetation Index); SR (Simple Ratio); MSAVI2 (Second Modified Soil Adjustment Vegetation Index); DVI (Difference Vegetation Index); SRWI (Simple Ratio Water Index); LWCI (Leaf Water Content Index); NDWI (Normalized Difference Water Index)

order of effectiveness for forest classification in Fig. 2; when optical indices were added one by one, the number of misclassifications gradually decreased. The discriminant analysis selected SWIR1 as the most effective index. However, when using only SWIR1, 47 of the 210 cells were misclassified. When NDVI, SR, and other indices were added to the analysis, the number of misclassifications decreased; i.e., forest classification improved.

However, misclassifications among the dense forests (DEF, MEF, and RDEF) remained, which indicates that differences in the dominant species (i.e., dipterocarp or other) are not detectable using remote sensing data.

4.3. Forest Quantification

Regression analyses demonstrated that all quantitative forest characteristics showed close agreement with optical indices. A multiple regression model using remote sensing data explained 69% of the variation in basal area (Fig. 3a). Similarly, 69% of the variation in maximum tree height and 61% of the variation in tree density was explained by remote sensing data (Fig. 3b,c). The best estimation was acquired for LAI, with 94% of the variation explained by remote sensing data (Fig. 3d). The optical indices effective for forest classification are shown in Fig. 4. All vegetation indices were positively correlated with LAI, but the strongest relationships with LAI were obtained with NDVI, MSAVI2, and SR. When these three indices were added to the analysis, the adjusted R2 rapidly increased (Fig. 4). Although the best LAI estimates were achieved by multiple regression models, these three indices provided sufficiently accurate estimates of LAI values using simple (single variable) quadratic or linear regression models (Table 3).

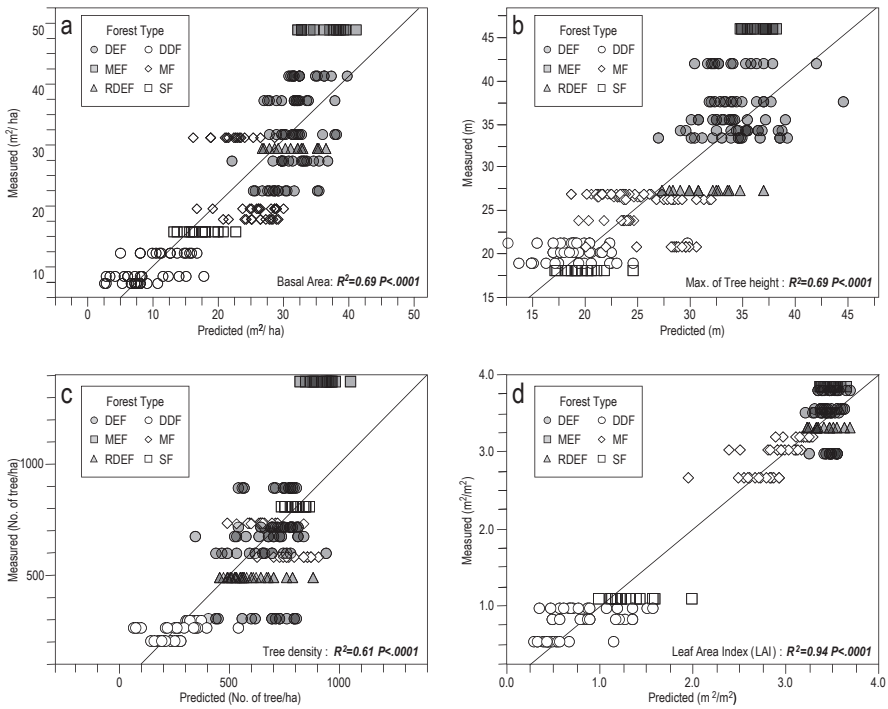

FIG. 3. Relationships between measured and predicted (multiple regression analyses) qualitative forest characteristics: **a** basal area; **b** maximum tree height; **c** tree density; **d** leaf area index (LAI)

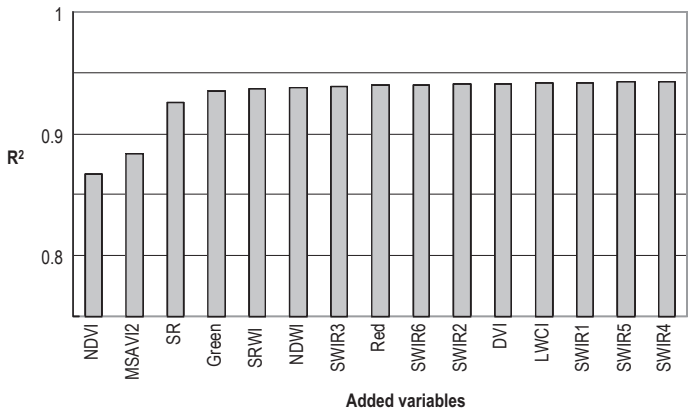

FIG. 4. Adjusted R^2 of multiple regression models as optical indices for LAI estimation were added cumulatively. Indices are ordered by effectiveness from *left* (most effective) to *right* (least effective)

TABLE 3. Best-fit quadratic curve and linear regression models with adjusted R^2 values for predicting LAI by optical indices

Optical index (x)	Quadratic curve regression model	R^2	Linear regression model	R^2
NDVI	$23.2598(x - 0.6942)^2 + 15.5213x - 8.189$	0.89	$13.0328x - 6.2547$	0.87
SR	$-0.1055(x - 6.0959)^2 + 0.5907x - 0.4850$	0.90	$0.7126x - 1.5452$	0.86
DVI	$-0.0156(x - 23.5381)^2 + 0.2276x - 2.2626$	0.84	$0.2779x - 3.7332$	0.82
MSAVI2	$55.3008(x - 0.8126)^2 + 21.9516x - 15.3312$	0.90	$16.9635x - 10.9944$	0.86
SRWI	$-0.6487(x - 1.7267)^2 + 3.0245x - 2.3219$	0.85	$3.2345x - 2.7761$	0.85
NDWI	$11.6102(x - 0.2481)^2 + 11.6798x - 0.2603$	0.86	$10.1841x + 0.2741$	0.84
LCWI	$-523.7168(x - 0.1874)^2 + 26.3673x - 1.5754$	0.85	$13.0328x - 6.2547$	0.77

NDVI (Normalized Difference Vegetation Index); SR (Simple Ratio); DVI (Difference Vegetation Index); MSAVI2 (Second Modified Soil Adjustment Vegetation Index); SRWI (Simple Ratio Water Index); NDWI (Normalized Difference Water Index); LWCI (Leaf Water Content Index)

Water content indices did not show better estimation of LAI than vegetation indices. LCWI achieved the lowest adjusted R^2 among three water content indices. LCWI, however, achieved reasonable estimation in SF, whereas the other two water indices, SRWI and NDWI, overestimated LAI in SF (data not shown). LCWI evaluates only vegetation moisture, in contrast to the other two indices, which may evaluate the moisture of background soil and vegetation collectively (Hunt et al. 1987; Anasawa and Sawada 2001). Therefore, LCWI may have accurately estimated LAI in SF, which has an open canopy and moist forest floor.

5. Conclusion

We examined the spatial variation in forest characteristics in Cambodian lowland tropical forests. We quantified the spatial variation in tree density, biomass, dominant species, and LAI across six types of seasonal tropical forest. Remote sensing was effective for determining forest heterogeneity, and thus remote sensing data could be used for forest classification. In particular, remote sensing could detect differences in the density of trees and basal area among the forest types. However, it could not always distinguish the three types of dense evergreen forest having different dominant species (DEF, MEF, and RDEF). However, this misclassification may be ignored for forest ecosystem and water cycle modeling if few differences in ecosystem function exist among these forest types. It is necessary to determine whether LAI estimates using satellite images, especially in closed forests with high LAI, are sufficiently accurate for application to hydrological models. A large proportion of the variation in forest characteristics was explained by multiple regression models. LAI was predicted with the most accuracy, although its estimation was not perfect. A different approach may be needed to determine LAI in the rainy season, as well as seasonal patterns of LAI.

Acknowledgments. This study was funded by the "Research Revolution 2002 Project" of MEXT (Ministry of Education, Culture, Sports, Science and Technology), Japan.

References

Aber JD, Federer CA (1992) A generalized, lumped-parameter model of photosynthesis, evapotranspiration and net primary production in temperate and boreal forest ecosystems. Oecologia (Berl) 92:463–474

Anasawa M, Sawada H (2001) Moisture environmental map using leaf water content index (LWCI) (in Japanese). Water Sci 257:1–22

Cohen WB, Maiersperger TK, Gower ST, Turner DP (2003) An improved strategy for regression of biophysical variables and Landsat ETM+ data. Remote Sens Environ 84:561–571

Engel VC, Stieglitz M, Williams M, Griffin KL (2002) Forest canopy hydraulic properties and catchment water balance: observations and modeling. Ecol Model 154:263–288

Gao BC (1996) NDWI: a normalized difference water index for remote sensing of vegetation liquid water from space. Remote Sens Environ 58:257–266

Hiramatsu R, Kanzaki M, Toriyama J, Kaneko T, Okuda Y, Ohta S, Khorn S, Pith P, Lim S, Pol S, Ito E, Araki M (2007) Open woodland patches in an evergreen forest of Kampong Thom, Cambodia: correlation of structure and composition with microtopography. In: Sawada H, Araki M, Chappell NA, LaFrankie JV, Shimizu A (eds) Forest Environments in the Mekong River Basin. Springer, Tokyo, pp 222–230

Hunt ER Jr, Rock BN, Nobel PS (1987) Measurement of leaf relative water content by infrared reflectance. Remote Sens Environ 22:429–435

Ito E, Khorn S, Lim S, Pol S, Tith B, Pith P, Tani A, Kanzaki M, Kaneko T, Okuda Y, Kabeya N, Nobuhiro T, Araki M (2007) Comparison of the leaf area index (LAI) of two types of dipterocarp forest on the West Bank of the Mekong River, Cambodia. In: Sawada H, Araki M, Chappell NA, LaFrankie JV, Shimizu A (eds) Forest Environments in the Mekong River Basin. Springer, Tokyo, pp 214–221

Jordan CF (1969) Derivation of leaf area index from quality of light on the forest floor. Ecology 50:663–666

Kang S, Lee D, Kimball JS (2004) The effects of spatial aggregation of complex topography on hydroecological process simulations within a rugged forest landscape: development and application of a satellite-based topoclimatic model. Can J For Res 34:519–530

Landsberg JJ, Gower ST (1997) Applications of physiological ecology to forest management. Academic Press, San Diego

Lillesand TS, Kiefer RW, Chipman JW (2004) Remote sensing and image interpretation, 5th edn. Wiley, New York

Mo X, Liu S, Lin Z, Zhao W (2004) Simulating temporal and spatial variation of evapotranspiration over the Lushi basin. J Hydrol 285:125–142

Qi J, Chehbouni A, Huete AR, Kerr YH, Sorooshian S (1994) A modified soil adjusted vegetation index. Remote Sens Environ 48:119–126

Richardson AJ, Everitt JH (1992) Using spectral vegetation indices to estimate rangeland productivity. Geocartogr Int 1:63–69

Rouse JW, Haas RH, Schell JA, Deering DW (1974) Monitoring vegetation systems in the Great Plains with ERTS. Publication SP-351. NASA, Greenbelt, MD

Running SW, Coughlan JC (1988) A general-model of forest ecosystem processes for regional applications. I. Hydrologic balance, canopy gas-exchange and primary production processes. Ecol Model 42:125–154

Tanaka K, Takizawa H, Tanaka N, Kosaka I, Yoshifuji N, Tantasirin C, Piman S, Suzuki M, Tangtham N (2003) Transpiration peak over a hill evergreen forest in northern Thailand in the late dry season: assessing the seasonal changes in evapotranspiration using a multilayer model. J Geophys Res 108: D17, 4533, doi:10.1029/2002JD003028

Tani A, Ito E, Kanzaki M, Ohta S, Khorn S, Pith P, Tith B, Pol S, Lim S (2007) Principal forest types of three regions of Cambodia: Kampong Thom, Kratie, and Mondolkiri. In:

Sawada H, Araki M, Chappell NA, LaFrankie JV, Shimizu A (eds) Forest Environments in the Mekong River Basin. Springer, Tokyo, pp 201–213

Toriyama J, Ohta S, Araki M, Kanzaki M, Khorn S, Pith P, Lim S, Pol S (2007) Soils under different forest types in the dry evergreen forest zone of Cambodia: morphology, physicochemical properties and classification. In: Sawada H, Araki M, Chappell NA, LaFrankie JV, Shimizu A (eds) Forest Environments in the Mekong River Basin. Springer, Tokyo, pp 241–253

Wang Q, Adiku S, Tenhunen J, Granier A (2005) On the relationship of NDVI with leaf area index in a deciduous forest site. Remote Sens Environ 94:244–255

Yamazaki T, Yabuki H, Ishii Y, Ohta T, Ohata T (2004) Water and energy exchanges at forests and a grassland in eastern Siberia evaluated using a one-dimensional land surface model. J Hydrometeorol 5:504–515

Zarco-Tejada PJ, Rueda CA, Ustin SL (2003) Water content estimation in vegetation with MODIS reflectance data and model inversion methods. Remote Sens Environ 85:109–124

Appendix 1. Formulas and definitions of the four vegetation indices and three water content indices

Vegetation index
SR: Simple Ratio (Jordan 1969) $SR = \rho_{nir}/\rho_{red}$
NDVI: Normalized Difference Vegetation Index (Rouse et al. 1974) $NDVI = (\rho_{nir} - \rho_{red})/(\rho_{nir} + \rho_{red})$
DVI: Difference Vegetation Index (Lillesand et al. 2004, Richardson and Everitt 1992) $DVI = \rho_{nir} - \rho_{red}$
MSAVI2: Second Modified Soil Adjustment Vegetation Index (Qi et al. 1994) $MSAV12 = \rho_{nir} + 0.5 - \sqrt{(\rho_{nir}+0.5)^2 - 2(\rho_{nir} - \rho_{red})}$
Water content index
SRWI: Simple Ratio Water Index (Zarco-Tejada et al. 2003) $SRWI = \rho_{nir}/\rho_{swir}$
NDWI: Normalized Difference Water Index (Gao 1996) $NDWI = (\rho_{nir} - \rho_{swir})/(\rho_{nir} + \rho_{swir})$
LWCI: Leaf Water Content Index (Anasawa and Sawada 2001) LWCI = –log[1 – (a*TM4/A – b*TM5/B)]/–log[1 – (a*TM4ft/A – b*TM5ft/B)] A: Maximum digital number (DN) in [TM4]; B: Maximum DN in [TM5] a: Reflectance correction factor (= 1) b: Reflectance correction factor = ratio of solar radiation in TM4 to that in TM5 (=0.2) ft: Full turgor We used ASTER VNIR 3 and ASTER SWIR 1 instead of TM4 and TM5, respectively

ρ_{red} = red reflectance; ASTER VNIR 2 (band 2) = 0.63–0.69 μm, ρ_{nir} = near-infrared reflectance; ASTER VNIR 3 (band 3) = 0.76–0.86 μm, ρ_{swir} = shortwave-infrared reflectance; ASTER SWIR 1 (band 4) = 1.6–1.7 μm

Soils Under Different Forest Types in the Dry Evergreen Forest Zone of Cambodia: Morphology, Physicochemical Properties, and Classification

Jumpei Toriyama*, Seiichi Ohta, Makoto Araki, Mamoru Kanzaki, Saret Khorn, Phearak Pith, Sopheap Lim, and Sopheavuth Pol

We studied the morphology and physicochemical properties of soils under three different types of forest, i.e., dry evergreen forest (DEF), dry deciduous forest (DDF), and mixed forest with evergreen and deciduous trees (MF), in the dry evergreen forest zone of Kampong Thom Province, Cambodia. The morphological features of soils varied among the three different forest types. The physical characteristics of the soils in the study area were strongly correlated with soil texture. Clay content was clearly higher in DEF soils than in the DDF or MF soils. Bulk density was generally high (1.27–1.92), except in the surface horizons. It was especially high at depths of 100–200 cm and 160–200 cm in the DDF and MF soils, respectively. Total soil porosity was 0.32–0.44 ($m^3 m^{-3}$), except in the surface horizons, and was slightly higher in DEF soils. The DEF soils were characterized by a higher percentage of fine pores (less than −49 kPa) than the other pore classes. DDF soils were characterized by decreasing percentages of coarse pores (0 to −0.2 kPa; the point of capillary saturation), medium pores (−0.2 to −4.9 kPa), and small pores (−4.9 to −49 kPa), and by a concomitant increase in fine pores with depth. In MF soils, the proportion of small pores slightly decreased with depth. The soils were generally poor in cation-exchange capacity (CEC) and exchangeable cations (ECEC). ECEC and CEC were closely related to clay content. The stock of exchangeable Ca^{2+}, Mg^{2+}, and K^+ was larger in DEF soils than in DDF soils. The pH (H_2O) of DDF soils was clearly higher than that of the other soil types at 0–50 cm in depth and showed different patterns in vertical changes. The stock of total carbon at 0–70 cm in depth was highest in MF soils. DEF, DDF, and MF soils were respectively classified into Kanhaplic Haplustults (or Hyperdistic Acrisols, Haplic Acrisols), Arenic Haplustults (Ferrali-Albic Arenosols, Ferralic Arenosols), and Arenic Ultic Alorthods (Haplic Podzols). These results demonstrate a clear relationship between forest type and soil type, suggesting that soil texture is the most important parameter governing soil physicochemical properties, consequently controlling the distribution pattern of the different vegetation types of the study area.

* Graduate School of Agriculture, Kyoto University, Kyoto, Japan
E-mail: tori@kais.kyoto-u.ac.jp

1. Introduction

Understanding the mechanisms that determine the distribution patterns of different forest types under similar climatic conditions is a major focus of ecological and hydrological studies of tropical monsoon forests. Soil properties are considered to be important in affecting the distribution patterns of forest types (Murphy and Lugo 1986). However, the question as to which soil factors are most important remains unanswered. To examine the relationship between soil and forest type, more information on forests soils, with regard to texture, effective depth, and chemical fertility or water retention characteristics, is required.

Although tropical monsoon forest is the most abundant forest type in Cambodia, very few studies have been reported on its soils. Saeki et al. (1959) compared the properties of soils under different forest types such as dense plain forests, teak forests, pine forests, and mixed forests. The U.S. Agency for International Development and the Cambodian Royal Soil Committee compiled a soil map of Cambodia based on an analysis of aerial photographs and field surveys (Crocker 1962). However, neither of these studies presented a detailed discussion of the relationship between soil properties and forest types. Thus, the purpose of this study was to clarify the morphology and fundamental physicochemical properties of soils under different types of forest and the relationship between these properties and the forest types of the tropical monsoon forest region in Cambodia.

2. Site and Methods

2.1. Study Area

The study area was located in Kampong Thom Province, central Cambodia (12°74′–76′ N, 105°41′–48′ E; Fig. 1). The mean annual temperature of the study area was 27°C. The annual rainfall was 1300–1900 mm, with a pronounced dry season from November to February. According to the soil map of Cambodia, red-yellow Podzols (Crocker 1962) are the most predominant soil type in the area. The geology is Quaternary sandy sediment. The elevation ranged from 60 to 100 m a.s.l., and the relief was almost flat

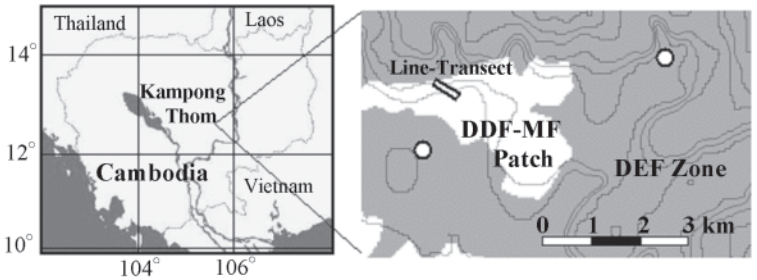

Fig. 1. Location of the study site. The *white circle* in the map on the *right* shows the soil profile. Contour lines are at 4-m intervals. *Gray area*, dry evergreen forest (DEF) zone; *white area*, dry deciduous forest–mixed forest with evergreen and deciduous trees (DDF–MF) patch

to slightly undulating. The most predominant forest type was dry evergreen forest (DEF). Small patches of dry deciduous forest (DDF) and mixed forest with evergreen and deciduous trees (MF) were also distributed throughout the study area (DDF–MF patch; see Fig. 1). The dominant tree species were *Dipterocarpus costatus* in DEF, *D. obtusifolius* in DDF, and *D. intricatus* in MF (Tani et al. 2007).

2.2. Soil Sampling

Soil sampling was conducted in February and May 2003. Based on reconnaissance surveys, two soil pits were dug in DEF (see Fig. 1). Two soil pits were also dug in DDF and in MF on a 500-m line transect in a 10-km^2 DDF–MF patch surrounded by DEF (Fig. 2). In addition, soil samples were collected along the line transect at intervals of 30–90 m and at depths of 0 (topsoil), 50, 100, and 150 cm. Morphological features of the soil profile were described in each pit, and soil samples were collected from each horizon for chemical analysis. In four of the six soil pits (two DEF, one DDF, and one MF plot), undisturbed soil samples for physical analysis were collected from each horizon using three 100-ml (20 cm^2 × 5 cm) metal cylinders.

2.3. Physical and Chemical Analysis

The collected soil samples were analyzed for particle-size distribution using the pipette method, bulk density (BD), particle density (PD) using a pycnometer, pore-size distribution (PSD) using pressure plate extraction (Klute 1986), pH (H_2O, KCl) using a grass electrode, the content of total carbon (T-C) and total nitrogen (T-N) via the dry combustion method, cation-exchange capacity (CEC) and exchangeable bases (Ca, Mg, K, and Na) using ammonium acetate (pH 7), and exchangeable Al and H using 1 M KCl. To classify the soils, free iron and aluminum levels were analyzed using dithionite-citrate and acid oxalate extractions on a proportion of the samples (Blakemore et al. 1981). The stock of T-C (Mg ha^{-1}) or T-N (kg ha^{-1}) was calculated based on the T-C or T-N concentration and BD. ECEC was defined as the sum of exchangeable bases and exchangeable Al and H. ΔpH was calculated as follows:

$$\Delta pH = pH(H_2O) - pH(KCl) \quad (1)$$

Total porosity (TP) was calculated as

$$TP\ (m^3\,m^{-3}) = 1 - BD/PD \quad (2)$$

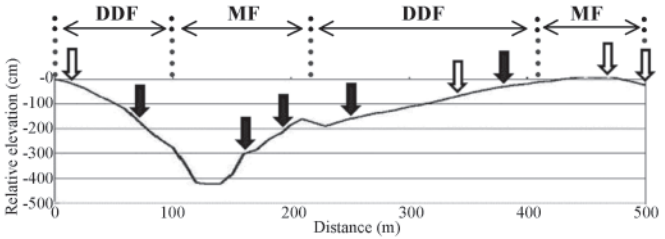

FIG. 2. Sampling plot and relative elevation along the line transect. *White arrows*, soil profile; *black arrows*, soil-auger point

Pore size distribution was calculated using the water content at different matric potential as

$$\text{Large pore} = \{\text{TP} - \text{WC}\ (-0.2)\}/\text{TP} \tag{3}$$

$$\text{Medium pore} = \{\text{WC}\ (-0.2) - \text{WC}\ (-4.9)\}/\text{TP} \tag{4}$$

$$\text{Small pore} = \{\text{WC}\ (-4.9) - \text{WC}\ (-49)\}/\text{TP} \tag{5}$$

$$\text{Fine pore} = \text{WC}\ (-49)/\text{TP} \tag{6}$$

where WC (−0.2) is water content at −0.2 kPa, i.e., capillary saturation; and WC (−4.9) and WC (−49) are water content at −4.9 kPa and −49 kPa, respectively. The water content at −4.9 kPa and −49 kPa has been used in previous studies to define the lower and upper limits of small pores (Arimitsu et al. 1995; Isamoto 2002; Shinomiya et al. 2007).

3. Results and Discussion

3.1. Morphology

3.1.1. DEF Soils

The soil profile consisted of A0 (L layer), A (including Ah), B, and C horizons. The L layer was distributed with 1- to 2-cm thickness. No F or H layers were observed. The A horizon was 30–33.5 cm thick. The colors of the A and B horizons were dull orange or brown (7.5YR5 – 7/2) and light brownish gray (7.5YR7 – 7.5/2 – 3), respectively. The hardness of the B horizon yielded by the Yamanaka handy penetrometer was clearly higher in dry (>8 MPa of penetration resistance) than in moist (0.2–0.8 MPa) conditions. The seasonal change in hardness in the DDF and MF soils was not as clear as in the DEF soils.

3.1.2. DDF Soils

The DDF soil profile consisted of A, E, B, and C horizons. No A_o horizons were observed. The thickness of the A and E horizons was 18–23 cm and 44–52 cm, respectively. The soil colors of the A, E, and B horizons were brownish gray (7.5YR5 – 6/1), dull brown (5 – 7.5YR7 – 8/3), and dull orange (7.5YR7/3) with some redder (2.5YR7/3) parts, respectively.

3.1.3. MF Soils

The MF soil profile consisted of A0 (L layer), A (Ah), E, B (Bh and Bs), and C horizons. The L layer was similar to that of DEF soils. The thickness of the A or Bh horizons was 67–77 cm, and accumulation of humus was observed. The soil color of the A, E, and B horizons was, respectively, grayish brown (5 – 7.5YR5.5 – 6/2), grayish brown (7.5YR5 – 6/2), and dull orange or similar (5 – 7.5YR4 – 8/2 – 4).

3.2. Physical Properties

3.2.1. Particle-Size Distribution

The physical characteristics of soils in the region were characterized by their sandy texture. The clay content of the three types of forest soil generally increased with depth, so much so that the content at 200 cm in depth was 1.7–7.1 times higher than that of the topsoil (Fig. 3a). The clay content of DEF, DDF, and MF soils changed clearly at 0–50 cm, 50–80 cm, and 50–120 cm in depth, respectively. The clay content was clearly higher in DEF soils than in the other two soils at 0–200 cm in depth, and slightly higher in MF soils than in DDF soils at 0–50 cm in depth. The results of the analysis of clay content in DDF and MF soils along the line transect also clearly indicated that DDF occurred on sandy soils (low clay content) at 0–50 cm in depth, whereas MF occurred on relatively finer-textured soils (Fig. 4). The change in clay content along the line transect plot was obvious (within 60–90 m) but was not related to relative elevation. There were no clear differences in silt content among the three soils, and the silt content was less than 0.06 $m^3 m^{-3}$ in all three soils. These results suggest that the distribution pattern of clay content was an important parameter

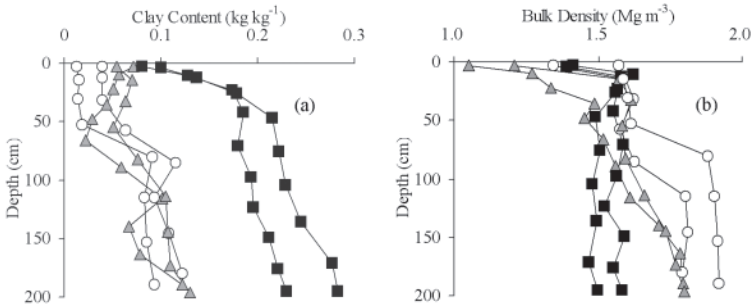

FIG. 3. Changes in clay content (**a**, *left*) and bulk density (**b**, *right*) with depth in the three forest soil types. *Solid squares*, DEF soils; *gray triangles*, MF soils; *open circles*, DDF soils

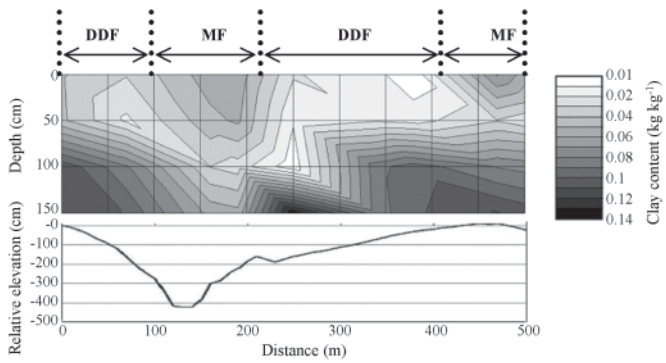

FIG. 4. Changes in clay content along the line transect

characterizing forest soils in the study area. The clay content was closely related to the following results on the physical and chemical properties of the soils.

3.2.2. Bulk Density (BD)

BD was mostly very high (1.4–1.9 $Mg\,m^{-3}$) in the subhorizons, whereas that at 0–50 cm in depth was lower (Fig. 3b). The BD at a depth of 0–50 cm showed a decreasing trend among soil types: DDF ≥ DEF > MF. The vertical trend in BD differed among the three soils. The BD of DDF soils increased at 50–120 cm in depth, whereas that of MF soils increased more gradually than in DDF soils. The change in BD with depth in DEF soils was not clear. The BD of DDF and MF soils at 200 cm in depth reached > 1.75 $Mg\,m^{-3}$, whereas that of DEF soils was 1.5–1.6 $Mg\,m^{-3}$. The BD at 100–200 cm in depth was negatively correlated with clay content, and sandy soils had higher BD (Fig. 5). These results indicate that soils of MF or DDF were more compact than soils of DEF, and the compactness could be attributed to finer soil texture (high clay content).

3.2.3. Pore-Size Distribution (PSD)

Total porosity (TP) of the three types of forest soils was 0.32–0.44 $m^3\,m^{-3}$, except for surface soils (Fig. 6), and was generally comparable to or slightly lower than those of other tropical soils (Sanchez 1976), reflecting the high compactness (high BD). DEF soils were characterized by a slight increase in TP with depth and by lower percentages of small pores (−4.9 to −49 kPa) than the other two soils. The PSD of DEF soils did not change consistently with depth, whereas DDF soils were characterized by a decrease in TP and percentages of large (0 to −0.2 kPa), medium (−0.2 to −4.9 kPa), and small pore with depth, with a concomitant increase in fine pores (less than −49 kPa). The TP of MF soils also decreased with depth, but the PSD of MF soils did not change clearly with depth, except for a slight decrease in small pores. The quantitative relationship between PSD and clay content or BD is not shown; however, clay content and bulk density, known as important parameters of the "pedotransfer

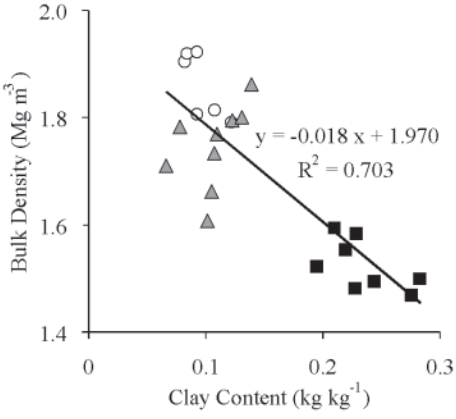

FIG. 5. Relationship between clay content and bulk density (BD) at 100–200 cm in depth. *Solid squares*, DEF soils; *gray triangles*, MF soils; *open circles*, DDF soils

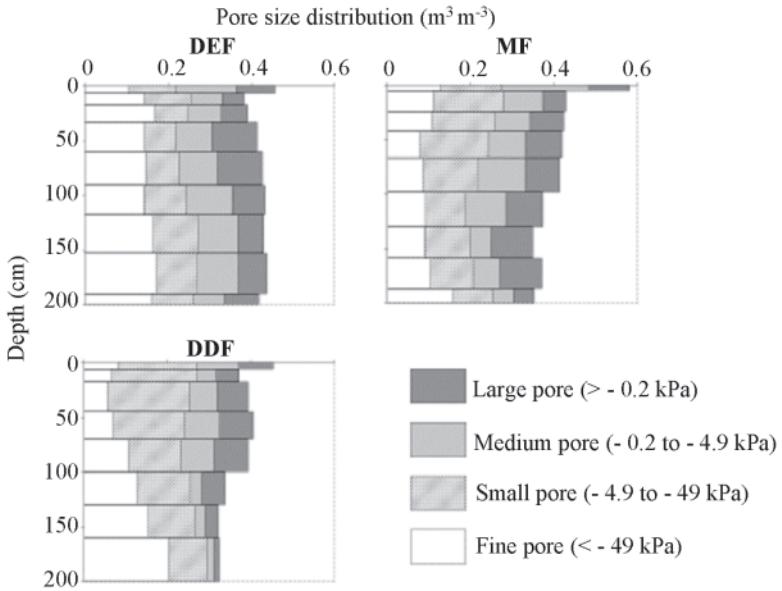

FIG. 6. Pore-size distribution of the three forest soil types. Only one of two profiles is shown for DEF

function" (van den Berg et al. 1997), were considered to regulate PSD considerably. Further studies on clay content, BD, and PSD of these soils over a wider geographic range would enable the formulation of their relationships to one another. Such information could also be used to evaluate the hydrological cycle and edaphic effects on forests.

Water availability is considered to play a major role in the occurrence of deciduous species (Holbrook et al. 1995). Sakurai et al. (1998) found higher clay content and higher water-holding capacity in DEF soils than DDF soils in northeast Thailand. In this study, the difference in the volume of small pores among the soil types was considered to reflect differences in available water capacity. We expected that the volume of small pores would be higher in DEF soils than in DDF soils on the basis that the occurrence of DEF and DDF under the same rainfall regime is affected by the difference in available water capacity in the soils. However, DDF soils showed a larger volume of small pores than DEF soils, and the coexistence of both DEF and DDF in the study area could not be reasonably explained by the capacity to stock available water. Nevertheless, the possibility that the water supply from the soil is related to the distribution of forest types remains because water supply from the soils should be evaluated not only by the amount of available water, but also by the efficiency of water use (or flux). To evaluate the occurrence of drought stress on trees in the study area, seasonal changes in unsaturated water flow in the soil profile will be the subject of a future study. Seasonal changes in soil water content in the study area were reported by Araki et al. (2007).

3.3. Chemical Properties

3.3.1. pH

The pH (H_2O) at 0–50 cm in depth was clearly higher in DDF soils than in the other two soils (Fig. 7a). The pH (H_2O) of DEF and MF soils increased with depth, whereas that of DDF soils decreased. The pH (H_2O) is affected by exchangeable Al^{3+} and H^+ as decreasing factors (Sanchez 1976) and by exchangeable bases as increasing factors. The clay minerals and humus contribute to holding these cations. In the lower horizons (>100 cm in depth) of the studied soils, Al saturation were generally high (>80%), and the pH (H_2O) of DEF soils with high clay contents was lower than those of the other soils (Fig. 7a). In the upper horizons, the difference in pH (H_2O) between DEF and DDF soils became larger than in the lower horizons, reflecting the difference in clay content. In addition, DDF soils were likely to retain less humus because of the markedly sandy texture. Although MF soils were also sandy in the upper horizons, the clay content was slightly higher than in DDF soils, and humus accumulation (characteristics of Podzols or Spodosols) was obvious in Bhs horizons; these were factors decreasing the pH (H_2O) of MF soils. The higher pH (H_2O) in the top horizons of DEF and MF soils (Fig. 7a) was likely caused by accumulated exchangeable bases.

The pH (KCl) of DEF soils did not change consistently at 30–200 cm in depth, whereas those of DDF and MF soils increased with depth in the upper horizons, peaking at around 30 cm and 90 cm in depth, respectively, and then decreased with depth (Fig. 7b). The ΔpH was lower in DDF soils than the other two soils, except for one horizon (Fig. 7c). The ΔpH of DDF soils increased with depth, whereas the ΔpH of DEF and MF soils peaked at around 10 cm and 30 cm, respectively, and then decreased with depth. The peak of pH (KCl) in DDF and MF soils corresponded to the depth of soil with low clay content because exchangeable Al^{3+} and H^+ retained in clay particles was the dominant factor contributing to the low pH (KCl).

3.3.2. Total Carbon (T-C) and Total Nitrogen (T-N)

The stock of T-C ($Mg\,ha^{-1}$) in the soil profiles of the three forest soil types ranged from 37.1 to 148.4 (Fig. 8a) and was similar to those of soils in similar forest types in Thailand, at least in the top 100 cm (Tsutsumi et al. 1966; Sakurai et al. 1998). The

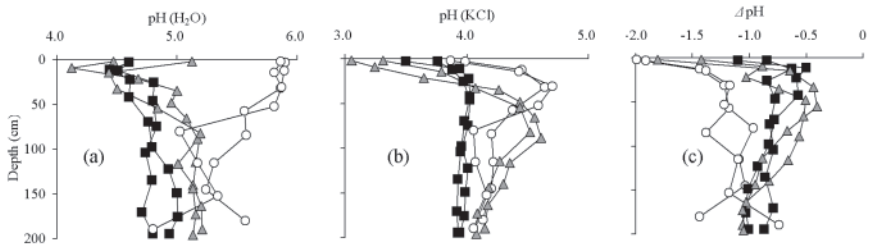

FIG. 7. Change in pH (H_2O, KCl; **a**, **b**) and ΔpH (**c**) with depth in the three forest soil types. *Solid squares*, DEF soils; *gray triangles*, MF soils; *open circles*, DDF soils

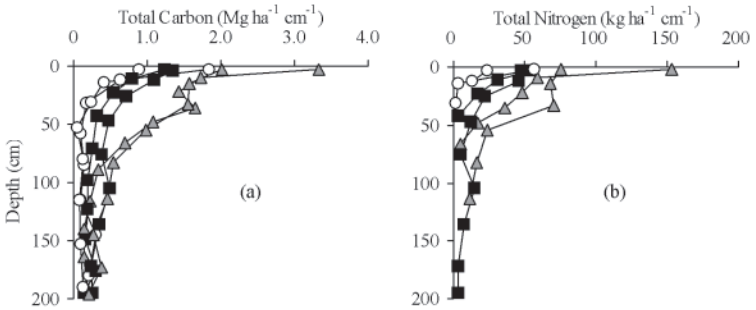

FIG. 8. Change in total carbon (**a**) and total nitrogen (**b**) stock with depth in the three forest soil types. Total nitrogen with concentrations < 0.01 ($mg\,g^{-1}$) was not detected. *Solid squares*, DEF soils; *gray triangles*, MF soils; *open circles*, DDF soils

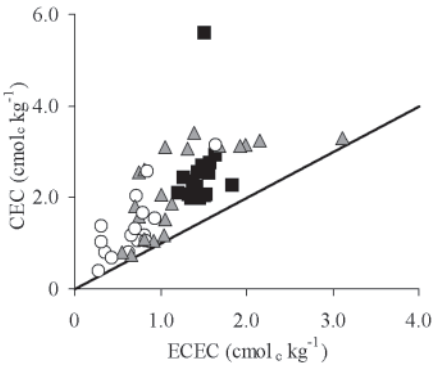

FIG. 9. Relationship between exchangeable cations (*ECEC*) and cation-exchange capacity (*CEC*). *Line* shows a 1:1 ECEC:CEC ratio. *Solid squares*, DEF soils; *gray triangles*, MF soils; *open circles*, DDF soils

stock of T-C at 0–70 cm in depth was of the order of MF > DEF > DDF. The high T-C in MF soils agreed with field observations of soil profiles with spodic horizons. The stock of T-N ($kg\,ha^{-1}$) at the surface horizon of studied soils was in the order of MF > DEF > DDF (Fig. 8b) and lower than in other studies (Tsutsumi et al. 1966). These results showed that the accumulation of organic matter in the study area was small, especially in DDF soils. Most litter fall was decomposed in the A_o horizon, and the inorganic nitrogen was either absorbed by plant roots or leached immediately.

3.3.3. CEC, ECEC, and the Stock of Exchangeable Cations

The CEC of the surface horizons of the studied soils ranged from 2.03 to 5.60 $cmol_c\,kg^{-1}$ soil. The CEC of DEF, MF, and DDF soils decreased with depth to a minimum of 1.98–1.99, 0.75–1.07, and 0.70–0.81 $cmol_c\,kg^{-1}$, respectively. CEC was 0.89 ± 0.68 ($cmol_c\,kg^{-1}$), which was higher than ECEC (Fig. 9). ECEC and CEC were regulated by the clay content, especially at 100–200 cm in depth, where the effect of carbon on the parameters was small (Fig. 10).

The density of exchangeable Ca^{2+}, Mg^{2+}, and K^+ (Ex-Ca^{2+}, -Mg^{2+}, and -K^+) of the studied soils was also highest in the surface horizons and clearly decreased with depth

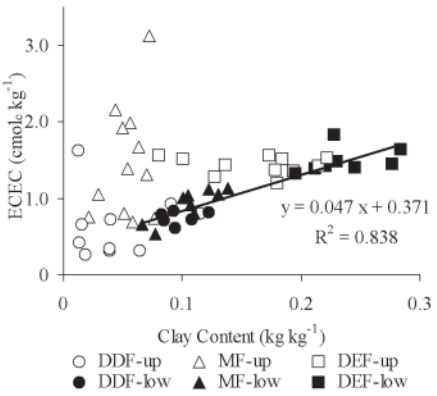

FIG. 10. Relationship between ECEC and clay content. *Open symbols*, upper horizons (≤100 cm in depth); *solid symbols*, lower horizons (>100 cm in depth)

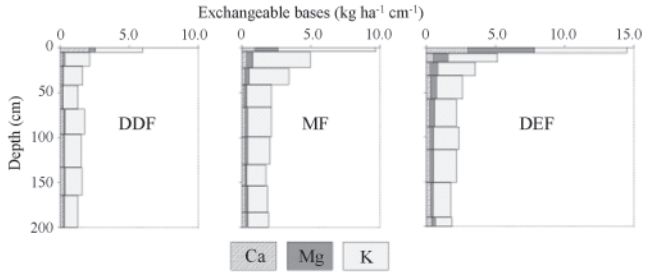

FIG. 11. Stock of exchangeable Ca^{2+}, Mg^{2+}, and K^+ in the studied soils

(Fig. 11), whereas the vertical trend of exchangeable Na^+ was not clear. The stock of Ex-Mg^{2+} and Ex-K^+ in the soil profile was largest in DEF soils, followed by MF and DDF soils. Although the density of Ex-Ca^{2+} in the top horizons was larger in DDF than MF soils, the total stock in the soil profile was comparable (86.3, 58.8, and 58.7 kg ha^{-1} in DEF, DDF, and MF soils, respectively.). The difference in the stock of exchangeable bases among the forest soils was considered to affect the potential productivity of the forests, and the clay had an important role in holding exchangeable bases. Ex-Al^{3+} was higher in DEF than DDF soils and was negatively correlated with pH (H_2O) (Fig. 12). Sanchez (1976) discussed the negative effect of soil acidity, low pH, and concomitantly high Ex-Al^{3+} on plant growth. In this study, pH (H_2O) was lower and Ex-Al^{3+} was higher for DEF soils than for DDF soils (Fig. 12). Soil acidity was not considered to be the cause of the formation of forest types, but rather to be the consequence of clay minerals and humus accumulation, as mentioned earlier in the discussion of pH (H_2O).

3.4. Soil Classification

We divided the soils of the study area using three classification systems [FAO-UNESCO, World Reference Base for Soil Resources (WRB), and the U.S. Soil Taxonomy system], based on their morphology and physicochemical properties (Table 1).

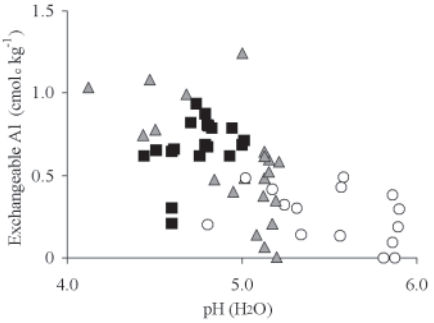

FIG. 12. Relationship between exchangeable Al^{3+} and pH (H_2O). *Solid squares*, DEF soils; *gray triangles*, MF soils; *open circles*, DDF soils

TABLE 1. Classification of the studied soils

Forest type	DEF	DDF	MF
Criteria (soil taxonomy)	• Argillic horizon with base saturation <35% and CEC/clay <24cmol/kg • Ustic moisture regime	• Argillic horizon (same as DEF) • Sandy texture (from topsoil to ≥50 cm in depth)	• Spodic horizon, such as * pH (H_2O) <5.9 * organic carbon >0.6% * color criteria • Iron (by acid oxalate) <0.1%
FAO-UNESCO	Haplic Acrisols	Ferrali-Albic Arensols	Haplic Podzols
WRB	Hyperdystic Acrisols	Ferralic Arenosols	Haplic Podzols
Soil taxonomy	Kanhaplic Haplustults	Arenic Haplustults	Arenic Ultic Alorthods

DEF, dry evergreen forest; DDF, dry deciduous forest (DDF); MF, mixed forest with evergreen and deciduous trees; WRB, World Reference Base for Soil Resources

DEF and DDF soils were characteristic of Ultisols or Acrisols and were classified into the similar classification using the U.S. Soil Taxonomy system (Soil Survey Staff 2003). One of the defining characteristics of Ultisols or Acrisols is the occurrence of argillic horizons that signify the eluvi-illuviation of clay particles. The detailed properties of DEF and DDF soils, however, clearly differed. Although DDF soils had argillic horizons, the physicochemical properties, more specifically their very sandy texture, resembled those of Entisols or Arenosols, as opposed to Ultisols or Acrisols. MF soils were classified as Spodosols or Podzols because of their low pH (H_2O), red color, movement of organic matter, and accumulation of iron and aluminum at 40–70 cm in depth (spodic B horizon). The three types of forest soils were classified differently using the WRB (FAO et al. 1998a) and the FAO-UNESCO system (FAO et al. 1988b). These results indicated the occurrence of a specific pattern of combination of soils and forest types in the study area.

4. Conclusion

The soils in the study area were generally characterized by a sandy texture, high compactness, and paucity in CEC and exchangeable bases compared to soils under similar forest types in Thailand.

A clear relationship between the forest and soil types was demonstrated and was characterized by the clay content of the soils. DEF soils were finest in texture, followed by MF and DDF soils. The clay content affected other soil physicochemical properties. Increasing clay content led to a decrease in bulk density (lower compactness). In terms of chemical properties, increasing clay content led to increasing exchangeable Al and H and decreasing pH (H_2O). The clay content was also closely related to ECEC, CEC, and the stock of exchangeable bases. As a result, DEF soils were classified as Kanhaplic Haplustults (or Hyperdistic Acrisols, Haplic Acrisols), with a low pH (H_2O), relatively high percentages of fine pores, and a larger stock of exchangeable bases than other soils. Similarly, DDF soils were classified as Arenic Haplustults (Ferrali-Albic Arenosols, Ferralic Arenosols), with relatively high percentages of coarser pores, higher compactness, and a smaller stock of nutrients. MF soils were classified as Arenic Ultic Alorthods (Haplic Podzols), with intermediate properties. According to these results, clay content was considered to be the most important parameter governing soil physicochemical properties and, consequently, affecting the distribution pattern of different forest types in the study area.

The pore-size distribution clearly differed among the three types of forest soil. However, its ecological implications remain obscure. Further work on seasonal changes in water flux in the soils is necessary to evaluate the effect of soil physical properties on forests and clarify the distribution patterns of forest–soil combinations in the monsoon tropics.

Acknowledgments. We thank the staff members of Cambodian Forestry Administration for cooperation in research in Cambodia and the staff members of Kansai Research Center, Forestry and Forest Products Research Institute, for use of their laboratory for measurement of soil physical properties. This study was funded by the "Research Revolution 2002 Project" of MEXT (Ministry of Education, Culture, Sports, Science and Technology), Japan.

References

Araki M, Toriyama J, Shimizu A, Ito E, Kabeya N, Nobuhiro T, Lim S, Pol S, Tith B, Khorn S, Pith P, Det S, Ohta S, Kanzaki M (2007) Changes of vertical soil moisture conditions of a dry evergreen forest in Kompong Thom, Cambodia. In: Sawada H, Araki M, Chappell NA, LaFrankie JV, Shimizu A(eds) Forest Environments in the Mekong River Basin. Springer, Tokyo, pp 112–124

Arimitsu K, Araki M, Miyakawa K, Kobayashi S, Kato M (1995) Water holding capacities estimated by soil pore capacities of Takaragawa Experiment Station: comparison of No. 1 and No. 2 experimental watersheds. Jpn J For Environ 37:49–58

Blakemore LC, Searle PL, Daly BK (1981) Methods for chemical analysis of soils. Scientific report 10A. New Zealand Soil Bureau, Lower Hutt, New Zealand

Crocker CD (1962) Exploratory survey of the soils of Cambodia, Royal Cambodian Government Soil Comittion and U.S. Agency for International Development, Phnom Penh

FAO, ISRIC, ISSS (1998a) World reference base for soil resources. FAO, Rome

FAO, UNESCO, ISRIC (1988b) Soil map of the world, revised legend. FAO-UNESCO, Rome

Holbrook NM, Whitbeck JL, Mooney HA (1995) Drought responses of neotropical dry forest trees. In: Bullock SH, Mooney HA, Medina E (eds) Seasonally dry tropical forests. Cambridge University Press, Cambridge, pp 243–276

Isamoto N (2002) Estimation of the water holding capacity of forest stands using soil pore distribution and an analysis of the related factors. Jpn J For Environ 44:31–36

Klute A (1986) Water retention: laboratory methods. In: Klute A (ed) Method of soil analysis, part 1. Physical and mineralogical methods. ASA and SSSA, Madison, WI, pp 635–662

Murphy PG, Lugo AE (1986) Ecology of tropical dry forest. Annu Rev Ecol Syst 17:67–88

Saeki H, Okamoto M, Azuma J, Inoue H, Takiuchi M, Tarumi H (1959) Physical and chemical properties of Cambodian soil. The scientific reports of the agricultural expedition to Cambodia, part 2. Hyogo University of Agriculture, Sasayama, Hyogo, Japan, pp 1–50

Sakurai K, Tanaka S, Ishizuka S, Kanzaki M (1998) Difference in soil properties of dry evergreen and deciduous forests in the Sakaerat Environmental Research Station. Tropics 8:61–80

Sanchez PA (1976) Properties and management of soils in the tropics. Wiley-Interscience, New York

Shinomiya Y, Araki M, Toriyama J, Ohnuki Y, Shimizu A, Kabeya N, Nobuhiro T, Kimhean C, So S (2007) Effect of soil water content on water storage capacity: comparison between the forested areas in Cambodia and Japan. In: Sawada H, Araki M, Chappell NA, LaFrankie JV, Shimizu A (eds) Forest Environments in the Mekong River Basin. Springer, Tokyo, pp 273–280

Soil Survey Staff (2003) Keys to soil taxonomy, 9th edn. Natural Resources Conservation Service, USDA, Washington, DC

Tani A, Ito E, Kanzaki M, Ohta S, Khorn S, Pith P, Tith B, Pol S, Lim S (2007) Principal forest types of three regions of Cambodia: Kampong Thom, Kratie, and Mondolkiri. In: Sawada H, Araki M, Chappell NA, LaFrankie JV, Shimizu A (eds) Forest Environments in the Mekong River Basin. Springer, Tokyo, pp 201–213

Tsutsumi T, Kan M, Khemanark C (1966) The amount of plant nutrients and their circulation in the forest soils in Thailand: carbon and nitrogen contents and some physical properties of the forest soils (in Japanese). Southeast Asian Stud 4:327–366

van den Berg M, Klamt E, van Reeuwijk LP, Sombroek WG (1997) Pedotransfer functions for the estimation of moisture retention characteristics of Ferralsols and related soils. Geoderma 78:161–180

Soil Moisture Conditions in Four Types of Forests in Kampong Thom, Cambodia

Makoto Araki*, Jumpei Toriyama, Seiichi Ohta, Mamoru Kanzaki, Eriko Ito, Bora Tith, Sopheavuth Pol, Sopheap Lim, Saret Khorn, Phearak Pith, and Seila Det

Soil moisture conditions were observed in four types of forest in central Cambodia, where dry evergreen forests are distributed widely, to investigate differences of soil moisture in each forest and to clarify relationships between forest types and soil moisture conditions. Observations revealed that soil water contents were high during the rainy season in dry deciduous forest (DDF) and mixed forest (MF), which contained both evergreen and deciduous trees. Those areas have thinner tree crown density and less stand biomass than a dry evergreen forest (DEF). In contrast, during the dry season, water content was low in DDF and MF. That difference is attributable to the disparate evapotranspiration rates of forests caused by the tree crown density and stand biomass. Moreover, soil temperatures were affected by the type of forest. In areas with DDF forests, the temperatures were high in the months of April and May but were lower in MF, DEF, and DEFlog forests. Those differences were caused by inhibition of temperatures through shading effects of tree crowns and evapotranspiration by trees. Based on those observed data, this study clarified a relationship between forest stand type and soil moisture conditions in Kampong Thom forest area.

1. Introduction

The Mekong River basin, which has a rainy season and a dry season, is in a biannual change monsoon climate zone. Tropical seasonal forests, which defoliate during the dry season, are dominant there. Cambodia, with 181 000 km^2 land area, has forests occupying about 60% (106 000 km^2) of that area (World Bank et al. 1996). Those forests are evergreen (38% of total forest area), deciduous (40%), and mixed (14%); in addition, a unique type of forest is distributed there, so-called *flooded forests*, which cover 7% of the total forest area. Dry evergreen forests are distributed widely in central Cambodia. These forests are extremely important because of their high species diversity and rarity in Indochina, where most forests are deciduous and are developed and used for human activities. For those reasons, clarifying

* Forestry and Forest Products Research Institute (FFPRI), Tsukuba, Japan
E-mail: makot@ffpri.affrc.go.jp

features of vegetation, characteristics of forest ecology, and properties of the site environment hold high importance to establish and improve sustainable forest management.

Top et al. (2004) reported increased forest biomass in Kampong Thom, Cambodia. That report estimated the biomass of dry evergreen forests and gave valuable results from a survey of 32 permanent experimental plots located in central Cambodia. Kim et al. (2006) estimated revenues from timber harvesting in Cambodia, which represents the importance of forest resources there. Tani et al. (2007) surveyed forests in Kampong Thom, Kratie, and Mondulkiri in Cambodia and reported vegetation characteristics of each forest. Hiramatsu et al. (2007) investigated vegetation and clarified tree compositions and site environment conditions in Kampong Thom. Toriyama et al. (2007) surveyed soils in Kampong Thom forests, diagnosed soil types, and clarified physical and chemical soil properties of each forest in Kampong Thom. In addition, Ohnuki et al. (2007) investigated the thickness and hardness of soil layers in Kampong Thom forests. That study in particular yielded original and valuable results.

In the present study, soil moisture conditions of four stand types of dry evergreen forests in Kampong Thom were revealed through year-round observation of groundwater levels and soil water contents. Furthermore, we studied the relationship between forest vegetation and soil moisture conditions, which is a major environment factor for vegetation.

2. Site and Methods

The research site was in central Cambodia, where dry evergreen forests are distributed (12°45′ N, 105°25′ E). The surrounding area is a flat alluvial plain, gently varying in topography, with altitude of 60–100 m a.s.l. The surficial geology in the area is alluvial deposits. Acrisols are dominant there; Podzols and Histosols are also distributed within the research site. Forests are dominated by evergreen dipterocarps such as *Dipterocarpus costatus*. Within this evergreen forest, sparse woodland that is dominated by *Dipterocarpus obtusifolius* appears as scattered patches at the site. In addition, there is another patch that consists of *Melaleuca cajuputi*, which is a characteristic tree of Southeast Asian freshwater swamps, in the site (Hiramatsu et al. 2007). Annual precipitation is 1500–1600 mm, of which more than 90% occurs during the rainy season (May–October). The annual mean air temperature was 26.4°C during October 2003 to October 2004 (Nobuhiro et al. 2007).

At this research site, the following observation plots were established (Fig. 1).

1. Dry deciduous forest (DDF plot: 12.7470° N, 105.4189° E, 69 m a.s.l.) consists of *Dipterocarpus obtusifolius* and *Gluta laccifera*. Heights of dominant trees are 10–20 m. Soils are Arenosols.
2. Mixed forest (MF plot: 12.7493° N, 105.4152° E, 70 m a.s.l.) consists of *Dipterocarpus intricatus*, *Vatica odorata*, *Syzygium gratum*, *Parinari annamense*, etc. Heights of predominant trees are 15–25 m. Soils are Podzols.

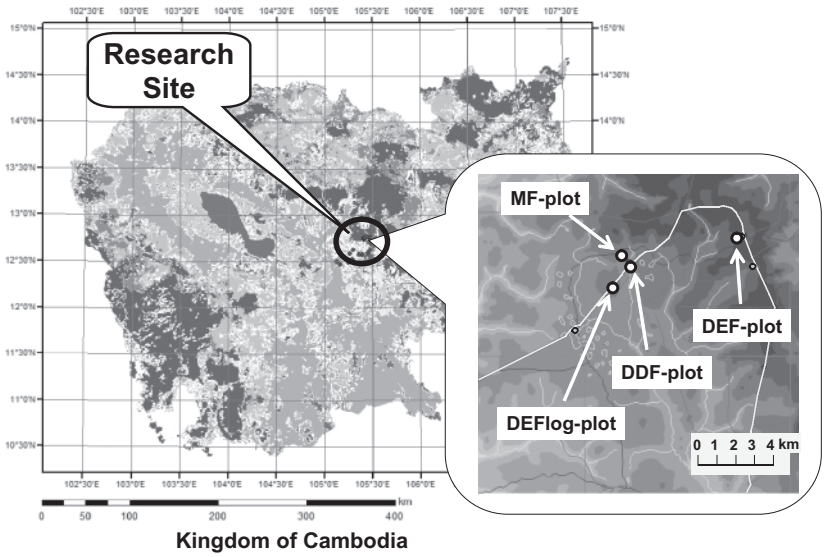

Fig. 1. Layout of experimental plots in Kampong Thom. *DEF*, dry evergreen forest; *DEFlog*, logged dry evergreen forest; *DDF*, dry deciduous forest; *MF*, mixed forest

3. Dry evergreen forest (DEF plot: 12.7594° N, 105.4739° E, 100 m a.s.l.) consists of *Dipterocarpus costatus*, *Anisoptera costata*, *Vatica odorata*, etc. Heights of dominant trees are 30–40 m. Soils are Acrisols.
4. Logged dry evergreen forest (DEFlog plot: 12.7352° N, 105.4106° E, 73 m a.s.l.) is a dry evergreen forest where tall trees (*Dipterocarpus costatus*) are logged; it consists of *Anisoptera costata*, *Vatica odorata*, small *Dipterocarpus costatus*, etc. Soils are Acrisols.

The DDF plot and MF plots were located contiguously along a belt transect line, which included a swamp forest in which *Melaleuca cajuputi* was dominant; the transect line plot was surveyed by Hiramatsu et al. (2007). Groundwater levels were measured every day with alarm measuring tape at observation wells that had been set along the transect line plots from November 2003. Moreover, groundwater table appearances were checked through simple wells at the DEF plot and DEFlog plot.

Soil water content at depths of 30 cm and 100 cm was measured automatically every hour at DDF, MF, DEF, and DEFlog plots (UIZ-ECH20; Uizin). Soil temperatures at those depths were also measured automatically every hour on each plot (UIZ3633; Uizin). For this study, measured data at 100 cm depth were used. Missing data were those for less than 30 cm depth. At 100 cm depth, short-term fluctuation according to rainfall events or other environmental conditions was less than at 30 cm depth. Therefore, comparisons of seasonal changes were clarified using data of soil water content and soil temperature measured at the 100 cm depth.

3. Results and Discussion

3.1. Seasonal Change of Groundwater Level

Seasonal groundwater levels in 2005 in the transect line plot, DDF and MF plots, and those of swamp forest are shown in Fig. 2. Those values were mostly equal to values of 2004. Groundwater levels were at 240–290 cm depth from the ground surface at the DDF plot and 290 cm deep at the MF plot in February, late in the dry season. At the beginning of the rainy season, in May, groundwater levels at each point along the transect line plot were lowest. Although May is a period when the rainy season begins and it had rained several times, the groundwater level was recorded as minimum, as a lag pertains between rainfall and the groundwater rise. In August, in the middle of the rainy season, the DDF plot was waterlogged; the MF plot groundwater level was at 40 cm depth. The swamp forest was under water during the rainy season. There, the groundwater level remained at 20–30 cm depth even in the dry season. Each plot along the transect line shows different seasonal changes of groundwater level. Those seasonal variations strongly influenced vegetation and plant growth in the transect line plot (Hiramatsu et al. 2007). Correspondence that was apparent between vegetation and soil moisture conditions was derived from groundwater level data.

At the DEF plot and DEFlog plot, groundwater levels were not detected within 400 cm depth, even in the rainy season: the groundwater level was deeper than 400 cm at both plots. However, as described later, soil water contents at both of plots were greater than at the DDF plot and MF plot during the dry season. We infer that rain water was retained longer during the dry season and that the capillary rise from the deep groundwater table was maintained throughout the dry season. The soil at DEF and DEFlog has more fine pores, which resulted in better water retention than at DDF and MF. To clarify soil moisture conditions in DEF in detail, year-round data of groundwater levels at the DEF area are needed. For that purpose, a new deeper observation well is needed in the DEF area.

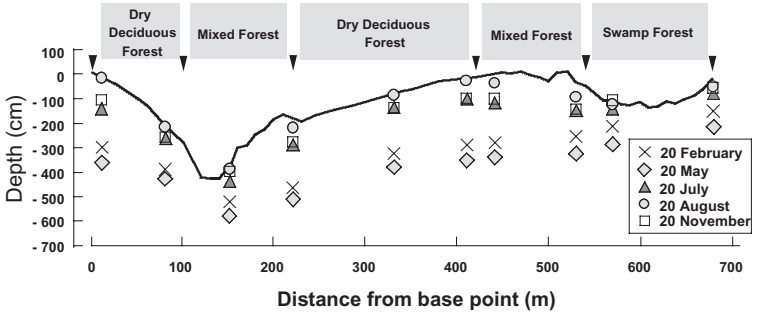

FIG. 2. Seasonal changes of groundwater level along the transect line

3.2. Soil Moisture Conditions

Figure 3 shows monthly mean soil water contents at 100 cm depths at DDF, MF, DEF, and DEFlog plots. Soil water contents at all plots showed, fundamentally, a cycle of rise and decline in rainy and dry seasons, respectively. Soil water content at the DDF plot was greater than 0.35 $m^3 m^{-3}$ in the rainy season and greater than 0.15 $m^3 m^{-3}$ in the dry season. At the MF plot, soil water content was greater than 0.37 $m^3 m^{-3}$ in the rainy season and decreased to 0.17 $m^3 m^{-3}$ in the dry season. Meanwhile, soil water content at the DEF plot was 0.25–0.30 $m^3 m^{-3}$ in the rainy season and 0.16–0.20 $m^3 m^{-3}$ in the dry season. At the DEFlog plot, soil water content was 0.25–0.28 $m^3 m^{-3}$ in the rainy season and 0.16–0.23 $m^3 m^{-3}$ in the dry season. The ground surface was waterlogged several times at the DDF plot and MF plot in the rainy season. The monthly mean soil water content showed saturated conditions at those plots in the rainy season, and soil water content was extremely low in the dry season. Although soil water content at the DEF plot and DEFlog plot was less than at the DDF plot and MF plot in the rainy season, the values were greater in the dry season. In other words, ranges of seasonal differences at the DDF and MF plots were greater than at the DEF and DEFlog plots.

Those results were attributable to differences of tree biomass and soil pore properties among plots. Biomass of trees at DEF was greater than at DDF and MF plots (Hiramatsu et al. 2007). During the rainy season, evapotranspiration rates at DEF were greater than at DDF and MF plots because of differences of biomass. Evapotranspiration helped prevent increased soil water content at the DEF plot. In addition, in the DEFlog area, where some tall trees (*Dipterocarpus costatus*) were cut selectively, there was less biomass than at the DEF plot, but considerably more than in the DDF or MF plot. The DEFlog plot biomass more closely resembled that of DEF than DDF and MF plots. Toriyama et al. (2007) reported that total fine soil pores at a depth of 100 cm at the DEF and DEFlog plots (Acrisols) were greater than at the DDF (Arenosols) or MF (Podzols) plot. In the dry season, when there was almost no precipitation, the soil at the DEF and DEFlog plots retained more water than that at the

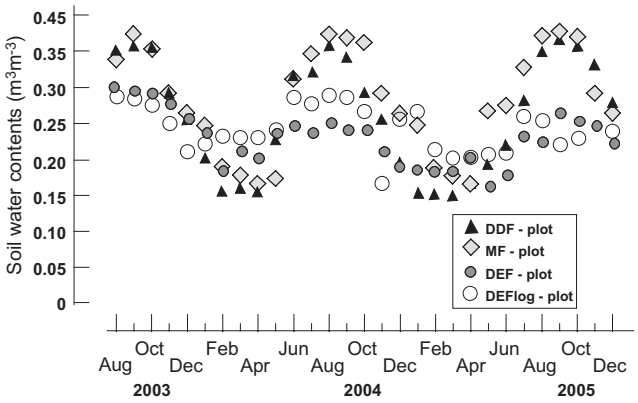

FIG. 3. Monthly changes of soil water content (100 cm depth)

DDF and MF plots because of fine pores that had high water retention capacity. Soil types and properties of the DEF plot were similar to those of the DEFlog plot: they also had equivalent water retention capacities. However, the stand density of tall trees in the DEFlog plot was lower than that of the DEF plot because of selective cutting of tall trees. Even in the dry season, evapotranspiration by trees occurred (Nobuhiro et al. 2007); the DEFlog plot, where the crown density was not greater than that at the DEF plot, had a lower evapotranspiration rate than that of the DEF plot in that period: soil water content at the DEFlog plot was slightly higher than at the DEF plot. Nevertheless, systematic differences between soil water content at DEFlog and DEF plots were not apparent in the rainy season because rainfall intervals and rainfall intensities, which strongly affected soil moisture conditions, were not uniform among years.

Daily mean soil water content at the start of the dry season is shown in Fig. 4a. Soil water content at the DDF plot and MF plot was 0.35 $m^3 m^{-3}$ in mid-October and decreased to 0.25 $m^3 m^{-3}$ by mid-December; that at the DEF plot and DEFlog plot was 0.30 $m^3 m^{-3}$ in mid-October and decreased to 0.26 $m^3 m^{-3}$ by mid-December. At the start of the dry season, soil water content at the DDF plot and MF plot decreased more rapidly than at the DEF plot and DEFlog plot. In addition, at the end of the dry season, soil water content at DDF and MF plots was less than at DEF and DEFlog plots. At the start of the rainy season, May–June daily mean soil water content is shown in Fig. 4b. The soil at the DDF and MF plots, which was dried up during the dry season, had a water content of 0.16 $m^3 m^{-3}$ at the beginning of May, and the soil at the DEFlog plot had a water content of 0.23 $m^3 m^{-3}$ during that period. Although the DEF plot had not been measured during that period, it was estimated to be little different from the DEFlog plot. It rained constantly during May–June; soil water content increased in each plot. Soil water content at DDF, MF, DEF, and DEFlog plots increased to 0.22–0.28 $m^3 m^{-3}$ by the end of May and that at the DDF plot and MF plot increased to 0.37–0.38 $m^3 m^{-3}$ by mid-June. However, at the DEF plot and DEFlog plot, soil water content was stable, at 0.25–0.30 $m^3 m^{-3}$, after the end of May.

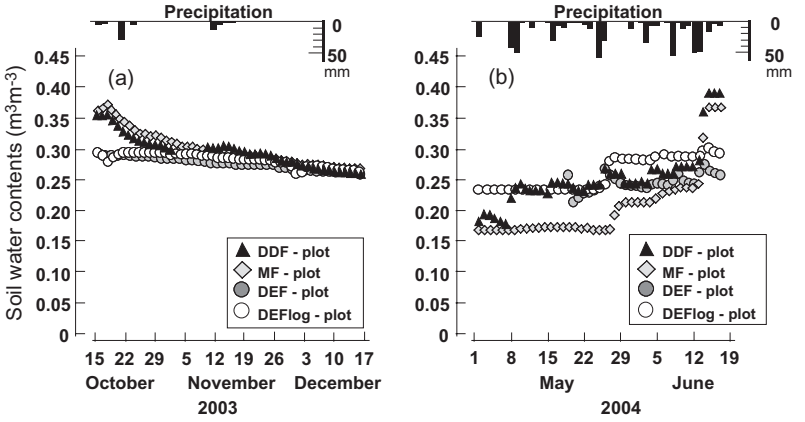

FIG. 4. Changes of soil water content (100 cm depth): start of the dry season and the rainy season

During the dry season, when water supply through rainfall ceased, soil water content was regulated by groundwater. Especially, the soils of DDF and MF plots, where groundwater levels rose to levels that were above the ground surface during the rainy season, had fewer fine pores, which have great water retention capacity, than at the DEF plot (Toriyama et al. 2007). The soil of the DEF plot contained double the rate of clay content of DDF and MF plots, implying that the DDF and MF plots had better drainage instead of water retention. Soil water content at the DDF and MF plots decreased with groundwater level declination, which was attributable to the dry season. Groundwater levels at the DEF plot were deeper than 400 cm year round; the soil water of the DEF and DEFlog plots at 100 cm depth was retained during the rainy season and supplied through capillary rise from the groundwater table. In other words, soil water at the DEF and DEFlog plots was retained by fine pores and water retention capacity, which provided a greater rate of clay content than at the DDF and MF plots. For that reason, soil water content at the DEF and DEFlog plots decreased more slowly than at the DDF and MF plots. By the end of the dry season, DEF and DEFlog plot soils had retained water better than those of the DDF and MF plots.

3.3. Soil Temperature

Monthly mean soil temperatures of each plot at 100 cm depth are represented in Fig. 5. Each plot showed a peak during April–June and lowest values in December–January. The fluctuation curve was the same pattern as the air temperature (Nobuhiro et al. 2007), although the phase of the soil temperature curve was shifted later by about 1 month. Soil temperatures at the DDF plot were 30°C in April–May and 26°C in December. At the MF plot, the plot soil temperatures were 27°–28°C in May–June and 25°–26°C in January. Soil temperatures at the DEF plot and DEFlog plot were 27°–28°C in May–June and 24°C in January. Seasonal differences, showing the range of soil temperatures, were 4°C in the DDF plot, whereas those in the MF, DEF, and DEFlog plots were 3°C. Those values were derived from inhibition of temperature increases through shading effects by tree crowns and evapotranspiration by trees.

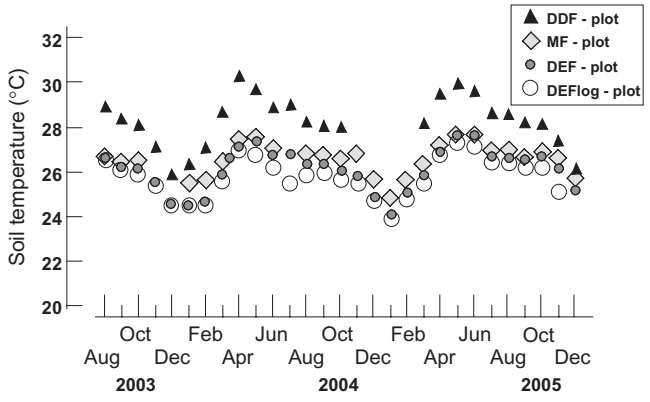

FIG. 5. Monthly changes of soil temperature (100 cm depth)

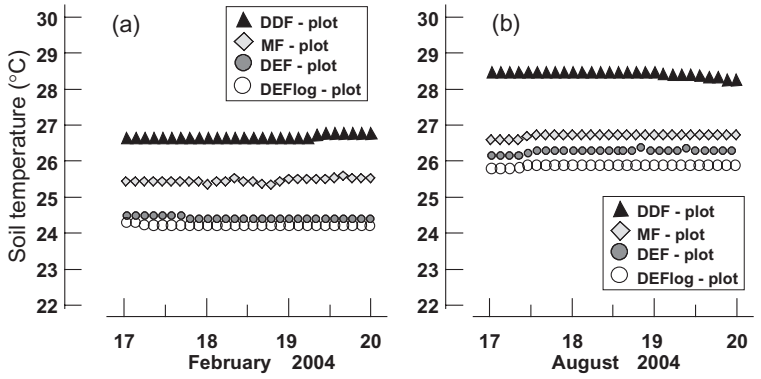

FIG. 6. Changes of soil temperature (100 cm depth): in the dry season and in the rainy season

Those effects were influenced by tree biomass, which was lower in DDF than in the other plots (Hiramatsu et al. 2007). Soil temperatures at MF plots were highest among the three plots, except DDF, in the low temperature period of December–February. That result is attributable to inhibition of cooling by the exuberant trees of mixed forests, which are characterized by species richness and a dense canopy (Hiramatsu et al. 2007). Daily mean soil temperatures at extremes of the dry season and rainy season, February 17–20, 2004 and August 17–20, 2004, respectively, are represented in Fig. 6a,b. Respective soil temperatures at the DDF, MF, DEF, and DEFlog plots were 26.7°, 25.5°, 24.4°, and 24.2°C in February: each was almost steady. In addition, in August, respective soil temperatures at the DDF, MF, DEF, and DEFlog plots were 28.4°, 26.6°, 26.3°, and 25.9°C: they were almost constant.

Air temperatures during those periods were 23°–27°C in February and 25°–29°C in August (Nobuhiro et al. 2007). Generally, the daily amplitude of soil temperature is less than that of air temperature and less with increasing soil depth. The phase of the temperature curve lags that of the air temperature. Air temperature diurnal variation was about 4°C at the research site, which was an extremely small range. Consequently, soil temperatures had no diurnal variation. Each plot showed seasonal variation. Soil temperatures at DDF were higher than at other plots through the years and had a slightly wider range than others. Soil temperatures were affected by sunlight on the forest floor, air temperature in the forests, and other environmental factors. Soil temperatures differed among plots that had different stand types. Therefore, each forest had different temperature conditions.

4. Conclusion

Soil water content and temperature were observed in four forests, which were categorized by their different stand types through a vegetation survey. Soil water content of different forests represented each forest type. Especially, the fluctuation and range of soil water content differed among forest stand types. Forest stand types were derived from microtopography, soil properties, groundwater levels, soil water content, etc. In particular, soil moisture conditions are among the most important factors affecting

forest stand types (Hiramatsu et al. 2007). Soil moisture conditions were affected by plant biomass, tree crown densities, stand structures, tree composition, and other conditions, mainly through evapotranspiration. Some relationship exists between the forest stand type and soil moisture conditions. This study clarified the relationships in the Kampong Thom forest area. In addition, the soil temperatures of each type of forest displayed a pattern.

Future studies should examine detailed soil moisture conditions of dry evergreen forests, which were most dominant in the Kampong Thom forest area. Furthermore, seasonal groundwater level variation must be observed using deep observation wells. In addition, estimation of regional soil water content in Kampong Thom forest area should be conducted using obtained results of the relationships between forest stand types and soil moisture conditions.

Acknowledgments. We thank Mr. Chann Sophal and staff members of the Forestry Administration, Cambodia for their arrangement and help of field surveys of Cambodian forests. This research was carried out as a part of a research project "Model Development for the Prediction of Water Resources Changes due to Natural Variation and Human Modification in the Asia Monsoon Region," funded by Ministry of Education, Culture, Sports, Science, and Technology, Japan.

References

Hiramatsu R, Kanzaki M, Toriyama J, Kaneko T, Okuda Y, Ohta S, Khorn S, Pith P, Lim S, Pol S, Ito E, Araki M (2007) Open woodland patches in an evergreen forest of Kampong Thom, Cambodia: Correlation of structure and composition with microtopography. In: Sawada H, Araki M, Chappell NA, LaFrankie JV, Shimizu A (eds) Forest Environments in the Mekong River Basin. Springer, Tokyo, pp 222–231

Kim S, Kim PN, Koike M, Hayashi H (2006) Estimating actual and potential government revenues from timber harvesting in Cambodia. For Policy Econ 8:625–635

Nobuhiro T, Shimizu A, Kabeya N, Tsuboyama Y, Kubota T, Abe T, Araki M, Tamai K, Chann S, Keth N (2007) Year-round observation of evapotranspiration in an evergreen broadleaf forest in Cambodia. In: Sawada H, Araki M, Chappell NA, LaFrankie JV, Shimizu A (eds) Forest Environments in the Mekong River Basin. Springer, Tokyo, pp 75–86

Ohnuki Y, Kimhean C, Shinomiya Y, Sor S, Toriyama J, Ohta S (2007) Seasonal change of soil depth and soil hardness at forested areas in Kampong Thom Province, Cambodia. In: Sawada H, Araki M, Chappell NA, LaFrankie JV, Shimizu A (eds) Forest Environments in the Mekong River Basin. Springer, Tokyo, pp 263–272

Tani A, Ito E, Kanzaki M, Ohta S, Khorn S, Pith P, Tith B, Pol S, Lim S (2007) Principal forest types of three regions of Cambodia: Kampong Thom, Kratie, and Mondolkiri. In: Sawada H, Araki M, Chappell NA, LaFrankie JV, Shimizu A (eds) Forest Environments in the Mekong River Basin. Springer, Tokyo, pp 201–213

Top N, Mizoue N, Kai S (2004) Estimating forest biomass increment based on permanent sample plots in relation to woodfuel consumption. J For Res 9:117–123

Toriyama J, Ohta S, Araki M, Kanzaki M, Khorn S, Pith P, Lim S, Pol S (2007) Soils under different forest types in dry evergreen forest zone in Cambodia: morphology, physicochemical properties and classification. In: Sawada H, Araki M, Chappell NA, LaFrankie JV, Shimizu A (eds) Forest Environments in the Mekong River Basin. Springer, Tokyo, pp 241–253

World Bank, UNDP, and FAO (1996) Cambodia forest policy assessment. World Bank, Washington, DC

Apparent Change in Soil Depth and Soil Hardness in Forest Areas in Kampong Thom Province, Cambodia

Yasuhiro Ohnuki*, Chansopheaktra Kimhean, Yoshiki Shinomiya, Sethik Sor, Jumpei Toriyama, and Seiichi Ohta

In the evergreen forests in Kampong Thom Province, Cambodia, soil depth and soil hardness apparently change from the rainy season to the dry season. In contrast, in deciduous and mixed forests, these parameters hardly change in either season. The apparent changes in soil depth and hardness would be strongly affected in the dry season by physical properties, including clay content and transpiration rates. At the DEFlog plot, hard soils were confirmed in the dry season from just below the surface to 4 m in depth. This fact suggests that the roots siphon off soil water from very deep under the surface of the ground. Assuming that the effective porosity of the soils was 0.09 $m^3 m^{-3}$, the soil water consumption rate in the dry season from just below the surface to 4.1 m in depth, occurring mainly by transpiration, was approximately 369 mm. In addition to this, a deeper soil layer above the groundwater level loses considerable soil water in the dry season.

1. Introduction

Soil layers play an important role in hydrological processes, especially in forest basins. Thick soil layers store rainwater temporarily and let it drain off gradually. Recent studies of the roles of soil layers have dealt with unchannelized valleys. These so-called "zero-order basins" (Tsukamoto 1973; Tsukamoto et al. 1982) are thought to play important roles in the hydrological processes that occur in headwater areas (Asano et al. 2002; Katsuyama and Ohte 2002; Uchida et al. 2003). In temperate humid Asia, several studies have been conducted on the distribution of soil depth (colluvium plus saprolite) and on soil physical properties in small basins in coniferous and deciduous forests in Japan (Ohnuki et al. 1994, 1997, 1999). However, we have no data on soil depth and related information (water permeability of the soil surface, etc.) in the Mekong River Basin. Especially in Cambodia in tropical monsoon Asia, evergreen and deciduous forests are widely distributed, and the water balance changes drastically between rainy and dry seasons.

* Kyushu Research Center, Forestry and Forest Products Research Institute (FFPRI), Kumamoto, Japan
E-mail: bchankan@ffpri.affrc.go.jp

Recent studies concerned with soil depth have been carried out using a variety of techniques, such as extensive use of boring data (Dietrich and Dorn 1984) or by observing the features of the bedrock at the site of a landslide (Reneau et al. 1984). Dengler et al. (1987) evaluated the boundaries of soil layers and bedrock using the seismic refraction method, which requires some calibration adjustment to the field site because the velocity varies in response to the soil water content in deep sites. Fernandes et al. (1994) measured the colluvium thickness using a hand auger. This portable device can be used to measure thickness at many points, but it cannot measure saprolite thickness. Recently, the radiomagnetotelluric-resistivity (Radio-MT) method was applied to separate hydromorphic horizons (Chaplot et al. 2001), but this method failed to measure soil horizons deeper than 10 m.

Considering these limitations in field methods, we investigated the structure of soil layers using a handy dynamic cone penetrometer (Iida and Okunishi 1983; Onda 1992; Ohnuki et al. 1997, 1999), which is often used in landslide surveys in Japan. By applying this method at many points, areal interpretations of the internal structure of an unchannelized valley can be made. Because the measured values are proportional to the bulk density and total porosity of the soil (Yoshinaga and Ohnuki 1992, 1995; Ohnuki et al. 1997, 1999), this method can be used when the bulk densities of colluvium, saprolite; and bedrock are different. Regarding the physical properties of saprolite, several studies have dealt with weathered metamorphic rocks (Schoeneberger and Amoozeger 1990; Schoeneberger et al. 1995; Vepraskas et al. 1991) and weathered granite (Johnson-Maynard et al. 1994; Jones and Graham 1993). However, these studies have focused on hydraulic conductivity. Only Schoeneberger et al. (1995) examined water retention.

The present study has three objectives: (1) to gain an understanding of the soil depth and hardness using a handy dynamic cone penetrometer in rainy and dry seasons at evergreen, mixed, and deciduous forests in Kampong Thom Province in central Cambodia; (2) to comprehend the difference in soil hardness in different seasons between the evergreen forests and the deciduous forests; and (3) to evaluate water consumption from the deep soil layer in an evergreen forest in the dry season.

2. Study Area

Survey sites were located in Kampong Thom province, Cambodia (Toriyama et al. 2007). The sites are 69–101 m in elevation and in an evergreen forest area, where deciduous forests and mixed forests exist in a mosaic-like pattern; there, a transect line plot (length, 680 m) was established (Fig. 1). The surface geology there is Quaternary and consists of river terraces overlaid with sedimentary rocks. The distributed soils are Acrisols, Podosols, and Histosols based on the Food and Agriculture Organization (FAO) classification. Five types of plots were established in the survey sites as follows (Tani et al. 2007; Hiramatsu et al. 2007).

1. Dry evergreen forest plot (DEF; KPT2; soil type, Acrisols). DEF consists of *Dipterocarpus costatus*, *Anisoptera costata*, *Vatica odorata*, etc. The height of the predominant trees is 30–40 m.

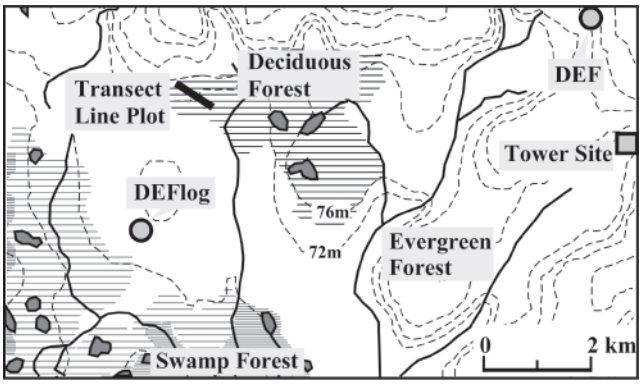

FIG. 1. Study area in Kampong Thom Province. *DEF*, dry evergreen forest; *DEFlog*, logged DEF

2. Logged dry evergreen forest plot (DEFlog; KPT7; soil type, Acrisols). Similar to DEF (1) except the tall trees were logged. DEF consists of *Dipterocarpus costatus*, *Anisoptera costata*, *Vatica odorata*, etc. The height of predominant trees is 30–40 m.
3. Dry deciduous forest (DDF; KPT1 & KPT6, in the transect line plot; soil type, Arenosols). DDF consists of *Dipterocarpus obtusifolius* and *Gluta laccifera*. Height of predominant trees is 10–20 m.
4. Mixed forest (MF; KPT5, in the transect line plot; soil type, Podzols) where evergreen species and deciduous species grow together. MF consists of *Dipterocarpus intricatus*, *Vatica odorata*, *Parinari annamensis*, etc. Height of predominant trees is 15–25 m.
5. Swamp forest (SF; KPT3, in the transect line plot; soil type, Histosols) where the water table is close to a ground surface, even in the dry season. SF predominantly consists of *Melaleuca cajuputi*. Height of predominant trees is 10–15 m.

In addition to these sites, soil depths were measured at three points: at observation wells (TW-W6, TW-W7, and TW-W8); near a tower site; and at an interception observation plot, where evapotranspiration rates and interception rates of the forest have been observed since November 2003 (Nobuhiro et al. 2007). The three points were located along a straight line; the relative heights from the lowest point (TW-W6) near a small stream were 0.5 m (TW-W7) and 1.2 m (TW-W8), respectively. At these points the groundwater levels have been measured since January 2004, and each point has shown different groundwater levels corresponding to their relative heights (Nobuhiro et al. 2007).

3. Methods

Soil depths and soil hardness were measured using a handy dynamic cone penetrometer in each forest area in different seasons. The apparatus consists of four parts: a top cone at a sharp (60°) angle with a diameter of 25 mm, a guide rod, a knocking

head, and a 5-kg weight. The soil profiles were expressed by Nc values obtained from the penetrometer test. The values were measured by counting the number of times the weight must be dropped from a height of 50 cm to drive the cone 10 cm into the soil. In resent studies in Japan, a humid temporal area, such values were used to define the thickness of colluvium ($0 < Nc \leq 5$) and saprolite ($5 < Nc \leq 40$) based on a detailed examination of selected soil profiles (Ohnuki et al. 1999; Yoshinaga and Ohnuki 1995). However, in our test areas in Cambodia, we could not determine the borders of colluvium and saprolite because the distributed soils and weathered rocks each have a different hardness, and the hardness is often changed by the soil water content in the rainy and dry seasons. In this study, we divided the soil layer into soft soil ($0 < Nc \leq 5$), fairly hard soil ($5 < Nc \leq 10$), and hard soil ($10 < Nc \leq 50$).

At DEF and DEFlog plots in Kampong Thom Province, we measured soil depths and soil hardness three times: May 2003 (the beginning of rainy season), October 2003 (rainy season), and February 2004 (dry season). At the transect line plot, which includes DDF, MF, and SF, the measurements were carried out in May 2003 and February 2004. In the rainy season, we could not use the device because the soils were filled with water. Near the tower site, soil depths and soil hardness were measured in February 2005 (dry season).

4. Results

Representative soil depths and soil hardness along the transect line plot in different seasons are shown in Fig. 2. The distributed soil at DDF (KPT1) is Arenosols; at MF (KPT5), Podosols; and at SF (SWAMP), Histosols. The black lines (May 2003, beginning of the rainy season) and gray lines (February 2004, dry season) in this figure show a similar distribution of soil depth and soil hardness. Surface soils were rather soft even in the dry season except for KPT5, which had very hard soil from 1.1 to 1.6 m in depth. Deeper soil layers showed greater soil hardness even in the swamp forest.

In contrast, in the evergreen forests that are located on Acrisols, we observed a seasonal apparent change in soil depths and hardness. For instance, at DEFlog (KPT7), the apparent soil depth and hardness changed from the beginning of the rainy season to the dry season (Fig. 3). First, at the beginning of the rainy season (May 2003), soft soils were distributed from the surface to a depth of 1 m; a deeper hard soil layer extended to a depth of 4.2 m. Next, in the rainy season (October 2003), extremely low penetration values were observed from the surface to a depth of 3 m. The apparent soil layer continued to more than 8 m depth. Last, in the dry season (February 2004), we observed low penetration values from 4 to 9 m in depth; the former was about the limit of penetration at the beginning of the rainy season, whereas the latter was just above the water table in the dry season. A hard thick soil layer from 0 to 4 m in depth was observed. The penetration value could be reflected in the water content of the soil layer.

Besides the DEFlog plot, low penetration values in a deep soil layer were observed in the dry season near the tower site (Fig. 4). There, point TW-W6 is located near the spring, point TW-W7 is higher in elevation by 0.5 m, and point TW-W8 is higher by 1.2 m. Point TW-W6 had no high penetration values near the surface; in contrast, the

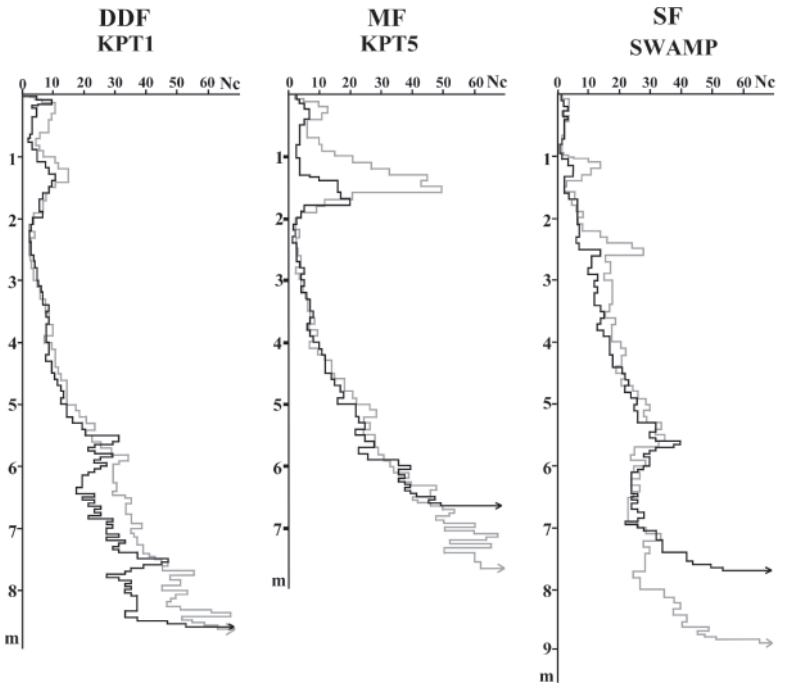

FIG. 2. Soil depths and soil hardness along the transect line plot. *DDF*, dry deciduous forest; *MF*, mixed forest; *SF*, swamp forest

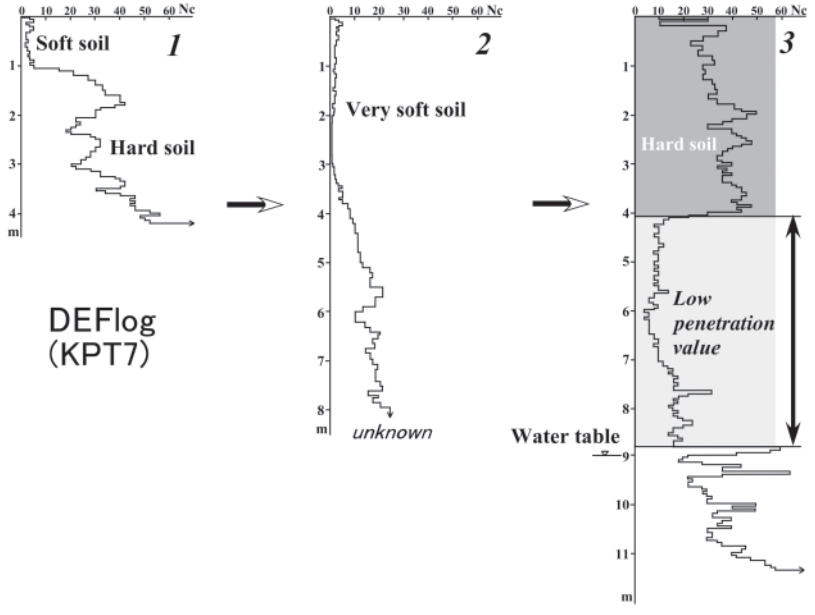

FIG. 3. Apparent change of soil depths and soil hardness at DEFlog: 1, beginning of a rainy season (May 2003); 2, end of a rainy season (October 2003); 3, end of a dry season (February 2004)

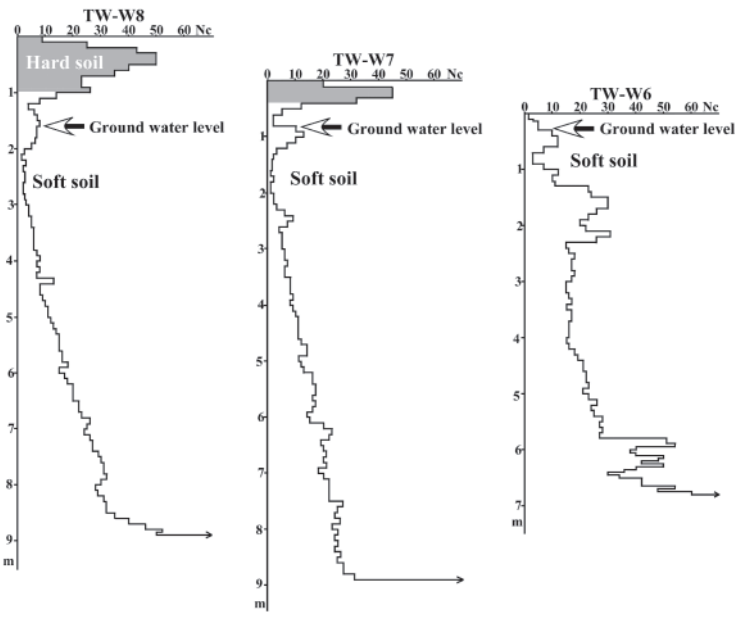

FIG. 4. Soil depth and soil hardness at the tower site in the dry season. Each *horizontal line* indicates ground level

other two points had a very hard soil layer near the surface and a very soft one in a deeper horizon. The groundwater level was shallow (from −0.4 to −1.7 m in depth), even in the dry season, and the hard soil zone was thin.

5. Discussion

As seen here, we observed obvious differences in soil depths, apparent seasonal changes in penetration values, and a great change in penetration values between the transect line plot and the evergreen forests. The altitudes of the evergreen forests (73–101 m) are higher than those of the transect line plot (64–70 m).

Seasonal changes in penetration values in the transect line plot were very small, and soil hardness was greater in the deeper horizons in the rainy and dry seasons. Arenosols at DDF and Podosols at MF that contain less clay content and less bonding power hardly changed in soil hardness with differences in the water content (Fig. 5). In the evergreen forests, apparent changes in soil depths and seasonal changes in penetration values were large, especially 4 m below the surface; the shallowest soil depth was observed at the beginning of the rainy season and the deepest at the end of the dry season. This phenomenon would have been a consequence of water consumption by the soils in the evergreen forest and the grain-size distribution (clay content) of the soil layer of Acrisols. The effect of soil water consumption would for the most part be great to a depth of about 4 m, and the soil particles (clay fraction) in the soil to that depth could have much bonding power (Fig. 5). Near the tower site,

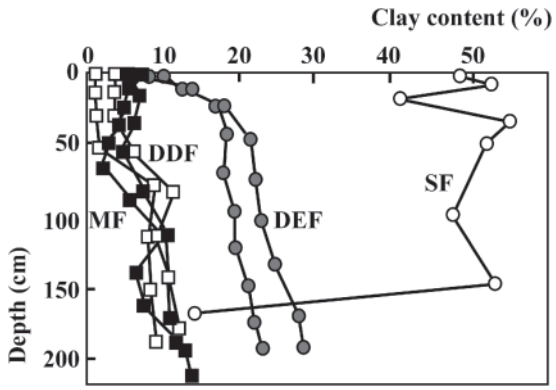

FIG. 5. Clay content of soils in different vegetation types

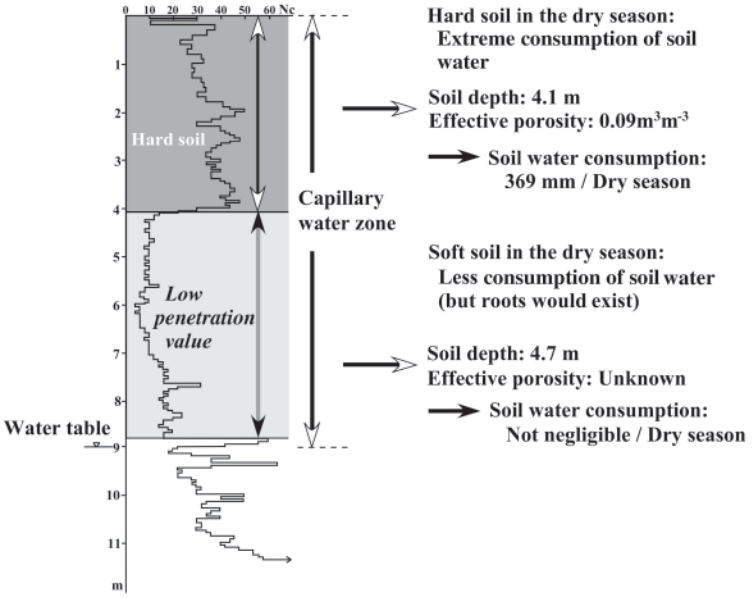

FIG. 6. Estimation of soil water consumption from the deep soil (DEFlog plot)

each measuring point had a different hard soil thickness because the groundwater levels were shallow and at a different depth from the surface.

We estimated the soil water consumption in the dry season at the DEFlog plot using data for soil depth, penetration value, effective porosity of soil, and the groundwater level (Fig. 6). At first, we assumed that the deep hard soil just below the surface in the dry season would have resulted from extreme consumption of soil water. We also assumed that the low penetration value zone below the hard soil and above the water table, with values less than those in the upper hard soil, could result from partially lost soil water. The hard soil depth was 4.1 m; the average effective porosity was $0.09\,m^3\,m^{-3}$, and the soil water consumption is the product of these: 369 mm in the

dry season. The depth of the low penetration value zone was 4.7 m; the average effective porosity was unknown because it was impossible to take samples without a deep soil pit. Thus, we could not make an assumption about the soil water consumption of this zone, but we knew it could not be negligible because the fine roots that can siphon off water could intrude deep into the soil.

The vegetation is an especially relevant factor because it plays an important role in consuming rainwater in this tropical monsoon area, and it can change apparent soil depths and soil hardness. Therefore, in this tropical monsoon area, it is easier to estimate the soil depths in some kinds of forests and construct a model for evaluating the distribution of soil depth and soil hardness than a humid temperate area (Dietrich et al. 1995).

In addition, for the purpose, in a further study, of constructing a model of the water storage capacity of forest-covered basins, we need more information: in-depth data on soil physical properties, including soil water content, grain-size distribution, and the soil moisture retention curve. Also for this purpose, the distribution of vegetation types and their transpiration rates would be important factors in evaluating soil water movement.

6. Conclusions

The main conclusions from our study can be summarized as follows: In the evergreen forests in Kampong Thom, the soil depth and soil hardness apparently change from the rainy season to the dry season. In contrast, in the deciduous and mixed forests, they hardly change in both seasons. The apparent seasonal change in soil depth and hardness is strongly affected by physical properties, including the clay content and the transpiration rates in the dry season. In the DEFlog plot, hard soils were confirmed to extend from just below the surface to 4.1 m depth in the dry season. This fact suggests that the roots siphon off soil water from a very deep level under the ground. Assuming the effective porosity of soils to be 0.09 $m^3 m^{-3}$, the soil water consumption rate from just below the surface to a depth of 4.1 m, occurring mainly by transpiration in the dry season, was approximately 369 mm. In addition, a deeper soil layer above the groundwater level loses considerable soil water in the dry season.

Acknowledgments. We wish to express our gratitude to the staff members of the Forestry Administration of the Kingdom of Cambodia for allowing us to use the study area. We also thank Dr. Eriko Ito, Mr. Makoto Araki, Mr. Akihiro Tani, and Mr. Pol Sopheavuth for their help in measuring soil depths. This study was funded by the "Research Revolution 2002 Project" of MEXT (Ministry of Education, Culture, Sports, Science and Technology), Japan.

References

Asano Y, Uchida T, Ohte N (2002) Residence time and flowpath dynamics at a forested headwater catchment, central Japan. J Hydrol 261:173–192

Chaplot V, Walter C, Curmi P, Hollier-Larousse A (2001) Mapping field-scale hydromorphic horizons using Radio-MT electrical resistivity. Geoderma 102:61–74

Dengler L, Lehre AK, Wilson CJ (1987) Bedrock geometry of unchannelized valleys. In: Erosion and sedimentation in the Pacific Rim. Proceedings of the Corvallis symposium, August 1987, Corvallis, pp 81–90

Dietrich WE, Dorn R (1984) Significance of thick deposits of colluvium on hillslopes: a case study involving the use of pollen analysis in the coastal moutains of northern California. J Geol 92:147–158

Dietrich WE, Reis R, Hsu ML, Montgomery DR (1995) A process-based model for colluvial soil depth and shallow landsliding using digital elevation data. Hydrol Process 9:383–400

Fernandes, NF, Coelho Netto AL, Lacerda, WA (1994) Subsurface hydrology of layered colluvium mantles in unchannelled valleys: south-eastern Brasil. Earth Surf Proc Land 19:609–626

Hiramatsu R, Kanzaki M, Toriyama J, Kaneko T, Okuda Y, Ohta S, Khorn S, Pith P, Lim S, Pol S, Ito E, Araki M (2007) Open woodland patch and the isolated stand of *Melaleuca cajuputi* in an evergreen forest of Kampong Thom, Cambodia: a transect study along a microtopography gradient. In: Sawada H, Araki M, Chappell NA, LaFrankie JV, Shimizu A (eds) Forest Environments in the Mekong River Basin. Springer, Tokyo, pp 222–231

Iida T, Okunishi K (1983) Development of hillslopes due to landslides. Z Geomorphol (Suppl) 46:67–77

Johnson-Maynard J, Anderson MA, Green S, Graham RC (1994) Physical and hydraulic properties of weathered granitic rock in southern California. Soil Sci 158:375–380

Jones DP, Graham RC (1993) Water-holding characteristics of weathered granitic rock in chaparral and forest ecosystems. Soil Sci Soc Am J 57:256–261

Katsuyama M, Ohte N (2002) Determining the sources of stormflow from the fluorescence properties of dissolved organic carbon in a forested headwater catchment. J Hydrol 268:192–202

Nobuhiro T, Shimizu A, Kabeya N, Tsuboyama Y, Kubota T, Abe T, Araki M, Tamai K, Chann S, Keth N (2007) Year-round observation of evapotranspiration in an evergreen broadleaf forest in Cambodia. In: Sawada H, Araki M, Chappell NA, LaFrankie JV, Shimizu A (eds) Forest Environments in the Mekong River Basin. Springer, Tokyo, pp 75–86

Ohnuki Y, Terazono R, Ikuzawa H, Hirata I (1994) Distribution and physical properties of surficial soils in Minami-Meijiyama Experimental Watershed in Okinawa Island, Japan (in Japanese). J Jpn For Soc 76:355–360

Ohnuki Y, Terazono R, Ikuzawa H, Hirata I, Kanna K, Utagawa, H (1997) Distribution of colluvia and saprolites and their physical properties in a zero-order basin in Okinawa, southwestern Japan. Geoderma 80:75–93

Ohnuki Y, Yoshinaga S, Noguchi S (1999) Distribution and physical properties of colluvium and saprolite in unchannelized valleys in Tsukuba Experimental Basin, Japan. J For Res 4:207–215

Onda Y (1992) Influence of water storage capacity in the regolith zone on hydrological characteristics, slope processes and slope form. Z Geomorphol 36:165–178

Reneau SL, Dietrich WE, Wilson CJ, Rogers JD (1984) Colluvial deposits and associated landslides in the northern San Francisco Bay area, California, USA. In: Proceedings of the IVth international symposium on landslides, Toronto, Canada, pp 425–430

Schoeneberger P, Amoozeger A (1990) Directional saturated hydraulic conductivity and macropore morphology of a soil-saprolite sequence. Geoderma 46:31–49

Schoeneberger PJ, Amoozegar A, Boul SW (1995) Physical property variation of a soil and saprolite continuum at three geomorphic positions. Soil Sci Soc Am J 59:1389–1397

Tani A, Ito E, Kanzaki M, Ohta S, Khorn S, Pith P, Tith B, Pol S, Lim S (2007) Principal forest types of three regions of Cambodia: Kampong Thom, Kratie, and Mondul Kiri. In: Sawada H, Araki M, Chappell NA, LaFrankie JV, Shimizu A (eds) Forest Environments in the Mekong River Basin. Springer, Tokyo, pp 201–213

Toriyama J, Ohta S, Araki M, Kanzaki M, Khorn S, Pith P, Lim S, Pol S (2007) Soils under different forest types in dry evergreen forest zone in Cambodia: morphology, physiochemical properties and classification. In: Sawada H, Araki M, Chappell NA, LaFrankie JV, Shimizu A (eds) Forest Environments in the Mekong River Basin. Springer, Tokyo, pp 241–253

Tsukamoto Y (1973) Study on the growth of stream channel (I). Relationship between stream channel growth and land slides occurring during heavy storm (in Japanese with English summary). J Jpn Soc Erosion Control Eng 25:4–13

Tsukamoto Y, Ohta T, Noguchi H (1982) Hydrological and geomorphological studies of debris slides on forested hillslopes in Japan. In: Proceedings of the Exeter symposium, July, 1982, vol 137. International Association of Hydrological Scientists, Exeter, pp 89–98

Uchida T, Asano Y, Ohte N (2003) Analysis of flowpath dynamics in a steep unchanneled hollow in the Tanakami Mountains of Japan. Hydrol Process 17:417–430

Vepraskas MJ, Jongmans AG, Hoover MT, Bouma J (1991) Hydraulic conductivity of saprolites as determined by channelsand porous groundmass. Soil Sci Soc Am J 55:932–938

Yoshinaga S, Ohnuki Y (1992) Estimation of water storage capacity of weathered zone in forested mountain (in Japanese). In: Proceedings of 4th symposium on water resourses. Commitee of the Symposium on water resources, pp 661–666

Yoshinaga S, Ohnuki Y (1995) Estimation of soil physical properties from a handy dynamic cone penetrometer test (in Japanese with English summary). J Jpn Soc Erosion Control Eng 48:22–28

Effect of Soil Water Content on Water Storage Capacity: Comparison Between the Forested Areas in Cambodia and Japan

Yoshiki Shinomiya*, Makoto Araki, Jumpei Toriyama, Yasuhiro Ohnuki, Akira Shimizu, Naoki Kabeya, Tatsuhiko Nobuhiro, Chansopheaktra Kimhean, and Sethik Sor

Water storage capacity (WSC), which is based on effective porosity in a soil profile or watershed scale, is one of the indicators for evaluating the water conservation function in a forested area. The effect of soil water content (SWC) on WSC was compared in this study between Cambodia and Japan. We studied four experimental plots. The DEF-plot is located in dry evergreen forest, the DEFlog-plot, in selectively logged dry evergreen forest, and the MF-plot, in mixed (evergreen and deciduous trees) forest in Kampong Thom Province, Cambodia. The JPN-plot is located in a natural forest consisting of fir and Japanese hemlock in Kochi Prefecture, Japan. The effect was evaluated using the index for the effect of SWC on WSC (ESW = WSC_b/WSC_a); WSC_a is the typical WSC calculated from the effective porosity (estimated by the difference in SWC at saturation and −49 kPa), examined using the pressure plate method and soil thickness based on a soil survey. WSC_b is a modified WSC that considers soil water in a WSC evaluation, which is computed by removing the effective porosity filled with water from WSC_a. SWC was measured using a soil moisture gauge and was observed at depths of 30 and 100 cm from the surface in the three plots in Cambodia and at depths of 10, 30, and 50 cm in the JPN-plot. The ESW in the three plots in Cambodia was in the range of 0.6 to 0.8 from January through April and below 0.5 from June through October. In contrast, the ESW for the JPN-plot remained almost constant at 0.5 to 0.7 throughout the year. Seasonal variations in the ESW were considerable in the three plots in Cambodia and small at the JPN-plot. These results suggest that although the capacity for temporal rainwater storage was almost the same throughout the year in Japan, it decreased greatly in the rainy season in Cambodia. This variance is fundamentally influenced by the difference in climate properties, particularly the seasonal variation of rainfall between Cambodia and Japan. This fact implies that the effect of the SWC on the WSC in forested areas is greater in Cambodia than in Japan.

* Shikoku Research Center, Forestry and Forest Products Research Institute (FFPRI), Kochi, Japan
E-mail: sinomiya@affrc.go.jp

1. Introduction

Water storage capacity (WSC), based on effective porosity and soil depth in a soil profile or a watershed scale, is one of the familiar indicators for evaluating the water conservation function in a forested area. For example, Arimitsu et al. (1995) explained the difference in the runoff properties between two adjacent forested watersheds using the WSC. Ohnuki et al. (1999) investigated the effective porosity and thickness of saprolite in a forested watershed and described the importance of saprolite to the WSC. Isamoto (2002) evaluated the WSC in 246 forests in Oita Prefecture, Japan, and analyzed the related factors.

The WSC is determined by integrating the effective porosity in a soil profile or watershed scale. Thus, the effect of the soil water content (SWC) on the WSC is not considered, even though some of the soil pores are typically filled with soil water. The effect of the SWC on the WSC should be verified more strictly when evaluating the water conservation function in a forested area. This study attempts to evaluate the effect of the SWC on the WSC in a soil profile scale in forested areas and compares the effect of the SWC on the WSC in a soil profile scale between forested areas in Cambodia and those in Japan.

2. Site and Methods

2.1. Experiment Sites

We studied forested areas in Cambodia and Japan. The experimental plots in Cambodia were located in Kampong Thom Province (Fig. 1). There were three plots: the DEF-plot, DEFlog-plot, and MF-plot. The vegetation at the DEF-plot was dry evergreen forest. The DEFlog-plot consisted of dry evergreen forest in which the upper-story trees have been logged. The vegetation of the MF-plot was a mixed forest that included dry evergreen and deciduous trees. The soil morphological properties are described in Toriyama et al. (2007).

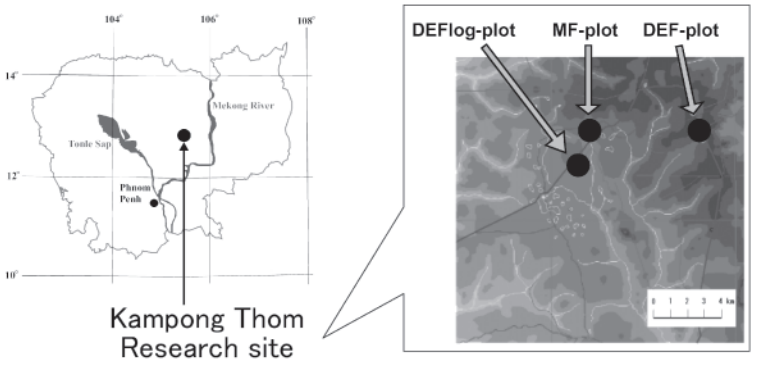

Fig. 1. Location of the experimental plots in Cambodia

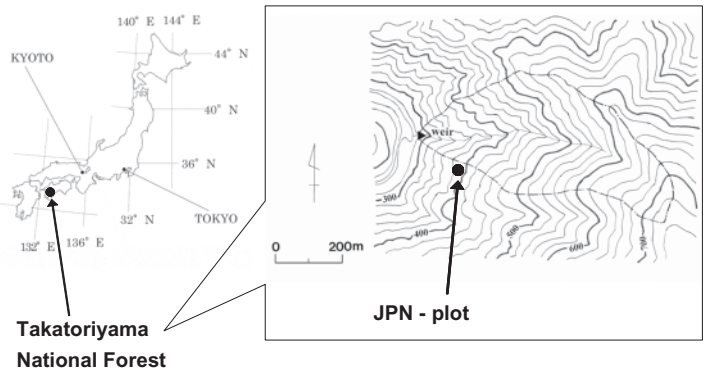

FIG. 2. Location of the experimental plot in Japan

TABLE 1. Summaries of the experimental plots

Country	Cambodia			Japan
Plot	DEF	DEFlog	MF	JPN
Geology		Sandy alluvium		Mudstone, sandstone
Annual rainfall (mm year^{-1})		~1600		2556
Annual mean air temperature (°C)		~27		13.1
Elevation (m)		70		400
Vegetation	Dry evergreen forest	Dry evergreen forest	Mixed forest	Natural forest
Soil type	Acrisol	Acrisol	Podosol	Cambisol

DEF, dry evergreen forest; DEFlog, logged DEF; MF, mixed forest; JPN, Japan

The experimental plot in Japan (JPN-plot) was located in Takatoriyama National Forest, Kochi Prefecture, Shikoku Island, in southwestern Japan (Fig. 2). The vegetation of the JPN-plot is a natural forest consisting of fir and Japanese hemlock about 180 years old. A description of the experimental plots is summarized in Table 1. Rainfall was measured near the DEF-plot (Cambodia) and the JPN-plot (Japan) by an automatic rain gauge of the tipping-bucket type.

2.2. Calculation of ESW

The effect of SWC on WSC was evaluated using an index for the effect of SWC on WSC (ESW), as expressed below.

$$\mathrm{ESW} = \mathrm{WSC_b}/\mathrm{WSC_a} \tag{1}$$

$$\mathrm{WSC_a} = \sum_{i=1}^{n} (P_i H_i) \tag{2}$$

$$\mathrm{WSC_b} = \sum_{i=1}^{n} [\{P_i - (W_i - C_i) H_i\}] \tag{3}$$

Here, P_i is the effective porosity at soil layer i ($m^3 m^{-3}$), H_i is the thickness of soil layer i (mm), W_i is the observed volumetric water content at soil layer i ($m^3 m^{-3}$), and C_i is the water content at soil layer i when the soil matric potential (ψ) is –49 kPa. WSC_a (mm) was the typical WSC, calculated from the effective porosity and soil thickness based on a soil survey. WSC_b (mm) was a modified WSC to take soil water into consideration in the evaluation of the WSC, computed by subtracting the effective porosity filled with water from WSC_a. The monthly averaged volumetric water content at soil layer i ($m^3 m^{-3}$) was substituted here for W_i, the observed water content. WSC was calculated to a depth of 60 cm from the surface.

2.3. Effective Porosity

The effective porosity is defined here as the difference between the SWC at capillary saturation and SWC at $\psi = -49$ kPa, in accordance with numerous previous studies (Takeshita 1985; Arimitsu et al. 1995; Isamoto 2002). The effective porosity was examined by the pressure plate method (Nakano et al. 1995). The soil thickness of the three plots in Cambodia was determined from a soil survey undertaken by Toriyama et al. (2007).

2.4. Soil Water Content

SWC was measured every hour automatically by time domain reflectometry (TDR) probes at depths of 30 and 100 cm from the surface in the DEF-plot, DEFlog-plot, and MF-plot, and at 10, 30, and 50 cm from the surface in the JPN-plot. Outputs from the TDR probes were stored in a data logger (Hioki E.E., 3639 or Campbell Scientific, CR10X) and converted to volumetric water content using a calibration curve at each plot. Taking the soil morphological properties and SWC observation depth into consideration, WSC was calculated with two (upper and lower) layers at the three plots in Cambodia. The observed SWC at 30 cm and the mean of the observed SWC at 30 and

Table 2. Parameter values for calculation of ESW (the index for the effect of SWC on WSC)

Plot	Layer	Soil thickness (cm)	SWC at saturation ($m^3 m^{-3}$)	SWC at $\psi = -49$ kPa ($m^3 m^{-3}$)	Effective porosity ($m^3 m^{-3}$)	WSC (mm)
DEF	Upper	0–30	0.308	0.145	0.163	48.8
	Lower	30–60	0.309	0.140	0.169	50.5
					Total (= WSC_a)	99.3
DEFlog	Upper	0–33.5	0.330	0.170	0.160	53.5
	Lower	33.5–60	0.306	0.145	0.161	42.7
					Total (= WSC_a)	96.2
MF	Upper	0–42	0.343	0.109	0.234	98.1
	Lower	42–60	0.331	0.080	0.252	45.3
					Total (= WSC_a)	143.4
JPN	Upper	0–20	0.550	0.259	0.291	58.2
	Middle	20–40	0.486	0.270	0.216	43.2
	Lower	40–60	0.508	0.293	0.215	43.0
					Total (= WSC_a)	144.4

SWC, soil water content; WSC_a, typical water storage capacity

100 cm were used as the SWCs at the upper and lower layers. The soil profile at the JPN-plots was divided into three (upper, middle, and lower) layers. The SWCs observed at 10, 30, and 50 cm were used for the upper, middle, and lower layers, respectively.

3. Results

When ESW is 1, SWC_b is equal to SWC_a; this means that SWC does not affect WSC. ESW ranged from 0.31 to 0.89 (DEF-plot), 0.25 to 0.75 (DEFlog-plot), 0.37 to 0.83 (MF-plot), and 0.54 to 0.80 (JPN-plot). ESW was less than 1 for all months in all plots, indicating that the actual WSC is less than the WSC computed by the procedure used in previous studies.

The ESW in the three plots in Cambodia ranged from 0.6 to 0.8 from January through April and was below 0.5 from June through October. The ESW returned to greater than 0.6 from October through December. Thus, ESW in the Cambodian plots was high during the dry season but low during the rainy season (Fig. 3). Figure 4

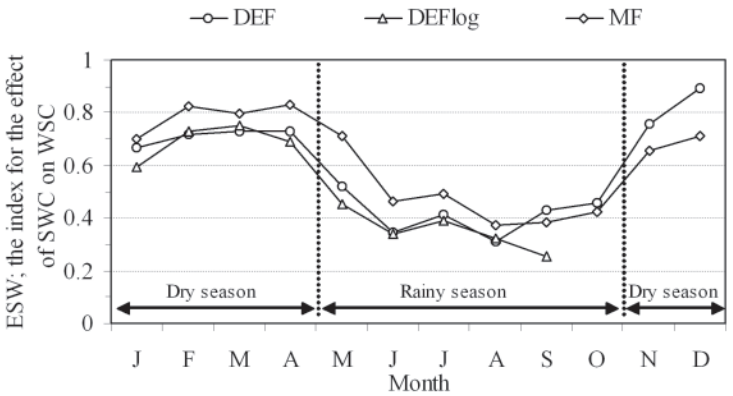

Fig. 3. Monthly variation in ESW (the index for the effect of SWC on WSC) in Cambodian plots in 2004

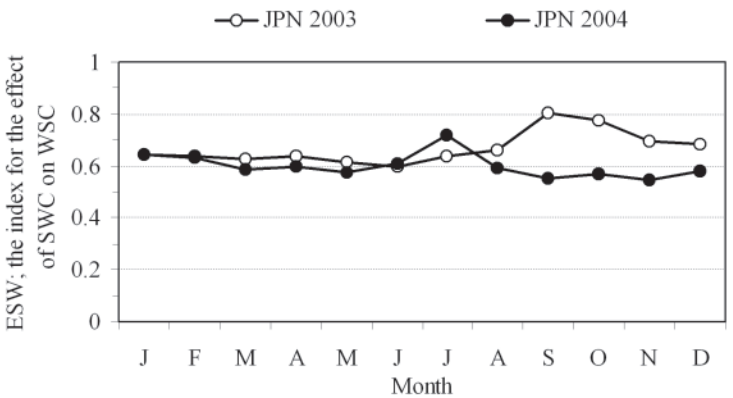

Fig. 4. Monthly variation in ESW in the JPN-plot (Japan) in 2003 and 2004

illustrates the monthly variation in ESW in the JPN-plot in 2003 and 2004. In contrast to the Cambodian plots, the ESW for the JPN-plot remained almost constant in a range of 0.5–0.7 throughout the year. The ESW was slightly greater than 0.7 from September through October 2003 and in July 2004. The monthly rainfall was about 67% (45%) of the mean monthly precipitation in September 2003 (July 2004). The soil water conditions tended to be dry in the JPN-plot. The difference in ESW between 2003 and 2004 was evident from September through December. However, it gradually decreased as the months passed from September to December. The soil water deficiency caused by the minimal rainfall in September 2003 slowly reduced the difference. The ESW in the JPN-plot appeared to be slightly higher under conditions of little rainfall in summer or fall. The differential between the maximum and minimum ESW was 0.20 in 2003 and 0.17 in 2004. These values were smaller than those in the three plots in Cambodia (0.58 at the DEF-plot, 0.50 at the DEFlog-plot, and 0.46 at the MF-plot). Although ESW in the JPN-plot was slightly higher when there was little rainfall in summer or fall, seasonal variations in the ESW were no greater in the JPN-plot than in the three plots in Cambodia.

4. Discussion

These results suggest that although the capacity for temporal rainwater storage remains approximately the same during the year in Japan, the capacity decreases significantly during the rainy season in Cambodia. This difference is fundamentally influenced by the difference in climate, particularly the seasonal variation of rainfall between Cambodia and Japan (Fig. 5). The rainfall in Cambodia during the dry season (November through April) was only 5% of the total precipitation (1621 mm) in 2004. There was no rainfall at all in January and February of 2004. In contrast, rainfall in the JPN-plot from November through April was 29% and 19% of the total precipitation (3015 mm and 4297 mm) in 2003 and 2004, respectively. Therefore, the seasonal variation in rainfall is greater in the Cambodian plots than in the JPN-plot. We assume that this difference in input affects ESW. Regarding vertical variation of permeability in the soil profile, the saturated hydraulic conductivity in the three plots in Cambodia was 10^{-5} to 10^{-6} ($m\,s^{-1}$), while it exceeded 4×10^{-4} ($m\,s^{-1}$) in the JPN-plot (Fig. 6). The saturated hydraulic conductivity was almost 10 to 100 times greater in the JPN-plot than in the three plots in Cambodia. Araki et al. (2007) demonstrated that the soil matric potentials calculated by HYDRUS–2D using soil physical properties in the DEF-plot corresponded approximately to the observed values. This result indicates that the matrix flow is predominant in the vertical water dynamics in the three plots in Cambodia. In contrast, it is estimated that the preferential flow takes priority in the JPN-plot from high permeability and aggregated clayey soil. These facts suggest that the drainage properties in the three plots in Cambodia may be inferior to those of the JPN-plot. Furthermore, the forested area in the JPN-plot was not as flat as it in the three plots in Cambodia. It is possible that the gravitational potential tends to be less in the three plots in Cambodia than in the JPN-plot. Thus, the topographical properties may have contributed to the result of this study.

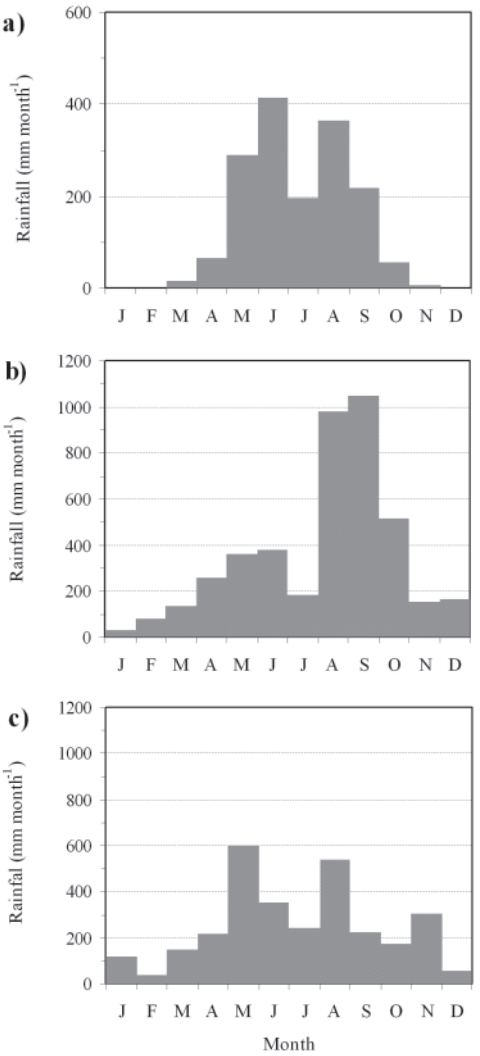

FIG. 5. Monthly variation in rainfall near (**a**) the dry evergreen forest (DEF)-plot, Cambodia, in 2004, (**b**) the JPN-plot, Japan, in 2004, and (**c**) the JPN-plot in 2003

5. Conclusion

When SWC was taken into consideration, the actual WSC becomes less than the common WSC used in previous studies. The ESW exhibited significant seasonal variation in the three plots in Cambodia, while the ESW in the JPN-plot did not change throughout the year. We thus concluded that the effect of SWC on WSC in forested

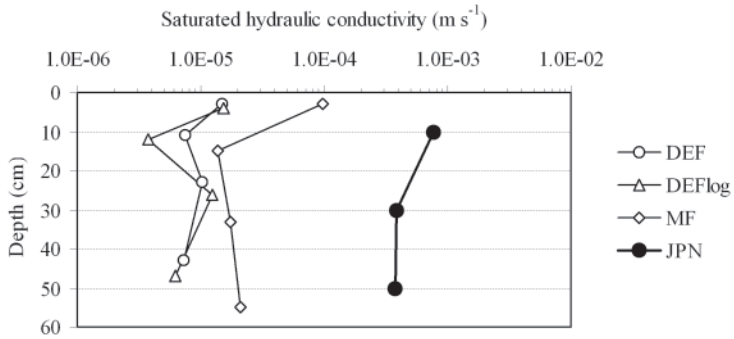

FIG. 6. Vertical variation in saturated hydraulic conductivity in the four plots in this study

areas is greater in Cambodia than in Japan, which we attribute to differences in seasonal rainfall variation, soil physical properties, and other factors.

Acknowledgments. The authors thank the members of the Cambodian Forestry Administration for their cooperation during research in Cambodia. This study was funded by the "Research Revolution 2002 Project" of MEXT (Ministry of Education, Culture, Sports, Science and Technology), Japan.

References

Araki M, Shimizu A, Toriyama J, Ito E, Kabeya N, Nobuhiro T, Tith B, Pol S, Lim Sp, Khorn S, Pith P, Det S, Ohta S, Kanzaki M (2007) Changes of vertical soil moisture conditions of a dry evergreen forest in Kampong Thom, Cambodia. In: Sawada H, Araki M, Chappell NA, Lafrankie JV, Shimizu A (eds) Forest Environments in the Mekong River Basin. Springer, Tokyo, pp 112–124

Arimitsu K, Araki M, Miyakawa K, Kobayashi S, Kato M (1995) Water holding capacities estimated by soil pore capacities of Takaragawa Experiment Station: comparison of No. 1 and No. 2 experimental watersheds. Jpn J For Environ 37:49–58

Isamoto N (2002) Estimation of the water holding capacity of forest stands using soil pore distribution and analysis of the related factor. Jpn J For Environ 44:31–36

Nakano M, Miyazaki T, Shiozawa S, Nishimura T (1995) Physical and environment analysis of soils. University of Tokyo Press, Tokyo

Ohnuki Y, Yoshinaga S, Noguchi S (1999) Distribution and physical properties of colluvium and saprolite in unchannelized valleys in Tsukuba Experimental Basin, Japan. J For Res 4:207–215

Takeshita K (1985) Some consideration on the relation between forest soil and control function to river discharge. Jpn J For Environ 27(2):19–26

Toriyama J, Ohta S, Araki M, Kanzaki M, Khorn S, Pith P, Lim S, Pol S (2007) Soils under different forest types in the dry evergreen forest zone of Cambodia: morphology, physicochemical properties and classification. In: Sawada H, Araki M, Chappell NA, LaFrankie JV, Shimizu A (eds) Forest Environments in the Mekong River Basin. Springer, Tokyo, pp 241–253

Influence of Large Seasonal Water Level Fluctuations and Human Impact on the Vegetation of Lake Tonle Sap, Cambodia

Yuji Araki*, Yoshihiko Hirabuki, Dourng Powkhy, Shinji Tsukawaki, Chay Rachna, Mizuki Tomita, and Kunio Suzuki

Lake Tonle Sap, the largest inland water body in Southeast Asia, encompasses unique ecosystems and wildlife adapted to large seasonal fluctuations in water level. The permanent waterlogged area of the lake is encircled by a vast floodplain, the inundated woodland being dominated by *Barringtonia acutangula* (Lecythidaceae), probably a major vegetation type of this ecotone, although human impact has degraded the floodplain vegetation and developed forest is restricted to a narrow band along the shore in the lowest water season. The aspects of seasonally inundated vegetation (i.e., variations in physiognomy, species composition, stratification, and distribution) on the coastal side of the floodplain (approximately 4 km in depth), located adjacent to the southern part of Siem Reap, was analyzed. Quantitative data for phytosociological evaluation were collected at 67 quadrats (10 m × 10 m each) during the low water seasons in 2005 and 2006, the sampling plots being classified by Two-Way Indicator Species Analysis (TWINSPAN) and ordinated by Detrended Correspondence Analysis (DCA). Two vegetation zones (i.e., extensive cropland and disturbed woodland), seven vegetation types (i.e., "Cultivated field," "Fallow field," "Shrub," and "Tall-shrub" in the extensive cropland zone and "Scrub," "Open forest," and "Closed forest" in the disturbed woodland zone), and vigorous invasion and/or regeneration of *Barringtonia acutangula* over the study area were identified. Human impact (e.g., plowing, burning, and cutting for firewood) seemed to be inversely related to both duration of flooding and maximum water depth and to be the main cause of degradation of seasonally inundated vegetation.

1. Introduction

Lake Tonle Sap, the largest inland water body in Southeast Asia and the natural reservoir of the Mekong River, has been found to contain unique wildlife and ecosystems adapted to its large seasonal fluctuations in water level (Mekong River Commission 1997; CNMC/NEDECO 1998a,b). In the highest water season (October–November),

* Graduate School of Environment and Information Sciences, Yokohama National University, Yokohama, Japan
E-mail: d02td002@ynu.ac.jp

the waterlogged area expands to four times the size of that in the lowest water season (April–May), the maximum depth reaching to more than 8 m from a minimum of about 1 m. The lake (including its floodplain) also plays an important role in the everyday life of local people, and in the economy and culture of Cambodia, being a major source of fish, wood, fertile agricultural land, and some natural resources (CNMC/NEDECO 1998a,b; Bailleux 2003).

Unfortunately, during the past approximately 50 years, most areas of floodplain vegetation have been severely disturbed by human activities. At the same time, scientific research, such as biological inventories, phytosociological analyses, life history investigations of adapted species, and hydrological surveys, have fallen behind. For example, only a few studies have been conducted on the flora and vegetation of the floodplain (McDonald et al. 1997; Sokhun 1997; CNMC/NEDECO 1998b), although researchers have indicated that floodplain vegetation was an important factor in (1) fish habitat and breeding sites, (2) biological productivity and water purification, and (3) the high biodiversity.

The remnant forest fringing the shore in the lowest water season is the standout vegetation of the floodplain, *Barringtonia acutangula* (Lecythidaceae), which is dominant and grows to a maximum height of about 15 m (maximum DBH, about 55 cm), in addition to stunted examples of *Diospyros cambodiana* and *Coccoceras anisopodum* (McDonald et al. 1997). On the other hand, large areas of the floodplain are covered with various vegetation types, including woodland, scrub, shrub, meadow, aquatic herbaceous communities, and cultivated fields, and are recognized as mosaics of these types.

In the present study, we analyzed aspects of the seasonally inundated vegetation (i.e., variations in physiognomy, species composition, stratification, and distribution) on the coastal side of the floodplain (about 4 km in depth), being our first step toward the scientific evaluation of the lake ecosystem for its preservation, conservative management and use of its biological resources.

2. Study Area

The study area was adjacent to the southern part of Siem Reap, Cambodia, situated on the northwest side of Lake Tonle Sap (13°16′ N, 103°49′ E; about 1–6 m a.s.l.; Fig. 1). As in the other lakeside lowlands, the flooding pulse, originating mainly in the Mekong River, took place in April–May, increasing sharply before decreasing in October–November. In the study area, floodwaters reached about 8 km inland from the shore of the permanent lake at their peak. Accordingly, both maximum water depth and duration of flooding gradually changed from south to north, microscale landform undulations (e.g., banks, channels and shallow ponds) probably influencing site conditions. The climate of terrestrial areas surrounding the floodplain was seasonal dry tropical, with the result that in the dry season (corresponding to low water level in the lake) many plants, especially those growing on the upper floodplain, seemed to suffer from drought conditions (McDonald et al. 1997). Annual mean temperature was 28.2°C, with only 12% of annual precipitation (1425 mm/year) falling during the dry season in Siem Reap(MRCS 2003). The surface soil of the floodplain was reddish-brown or yellowish-brown soft sandy clay and clayey sand. Soil

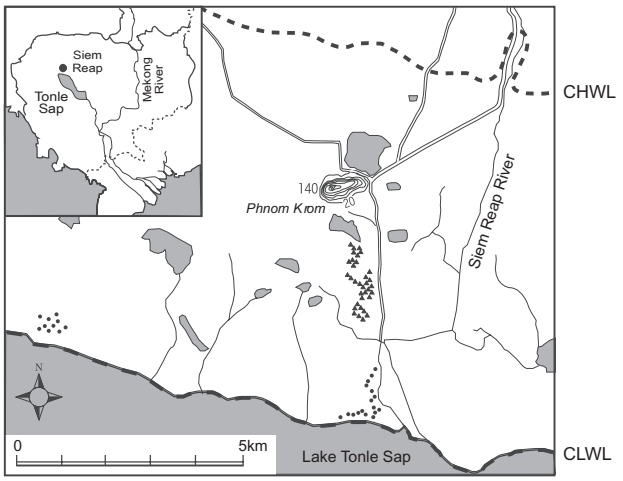

FIG. 1. Location of the study area (*upper left*) and 67 quadrats for phytosociological survey: ▲, quadrats of extensive cropland zone; •, quadrats of disturbed woodland zone; *CHWL*, coastline at the highest water level; *CLWL*, coastline at the lowest water level

deposition was estimated to be minute, owing to the seasonal rising and receding of the high volume of lake water.

Natural vegetation and landform conditions characterized the coastal side of the study area (about 4 km in depth), the upper reaches on the other hand having been largely reclaimed as paddy fields, enclosed by artificial banks and channels of various sizes. Reasons why local people have not caused large-scale modifications to the original inundated vegetation on the coastal side are though to be (1) the woodland, especially the forest consisting of stunted *Barringtonia acutangula* and *Diospyros cambodiana*, is essential for weakening waves and currents surging from the permanent lake to the littoral zone where they normally persist during the flood season, and (2) the location is unsuitable for agricultural use because of the long duration of submergence and its distance from villages (McDonald et al. 1997; CNMC/NEDECO 1998a,b). During the low water season, the various vegetation types already described can be distinguished physiognomically within the study area.

3. Methods

3.1. Survey Procedures

The phytosociological field surveys were carried out in the low water seasons (February–August) of 2005 and 2006. After general observations of the floodplain vegetation, we established 67 quadrats (10 m × 10 m each) on the coastal side of the floodplain, covering the major vegetation types (see Fig. 1). In each quadrat, the height and coverage of each layer (tree, short-tree, shrub, and herb), and species name and dominance sensu Braun-Blanquet (1964) for every component species, were checked. Maximum height and diameter at breast height (DBH) were measured

by measuring poles and diameter tape, and the location of the quadrat determined by GPS (Global Positioning System) (GPSMAP76; GARMIN Corporation) for calculating the distance from the coastline at the lowest water level (CLWL). Voucher herbarium specimens were collected for each of the 122 plant species recorded (including unidentified species of low frequency and dominance).

3.2. Data Analysis

Two-Way Indicator Species Analysis (TWINSPAN; Hill 1979) and Detrended Correspondence Analysis (DCA; Hill and Gauch 1980) were used to analyze vegetation data. After omitting rare species that had been recorded less than three times, a data matrix consisting of 67 sampling plots versus 89 indicator species was prepared, the calculation being performed by PC-ORD for Windows Version 4.00 (McCune and Mefford 1999). In TWINSPAN, pseudospecies cut levels were set at 0, 1, 5, 25, 50, and 75, according to the dominance scale of Braun-Blanquet (1964) for each layer.

The following parameters were used to assess species richness and diversity of vegetation type: density of species (total number of species per quadrat), Simpson diversity index (*D*'; Simpson 1949), Shannon diversity index (*H*'; Shannon and Weaver 1949) and Pielou evenness index (*J*'; Pielou 1975).

4. Results

4.1. Classification of Seasonally Inundated Vegetation

Using TWINSPAN, 67 phytosociological samples were classified into two categories in the first division and eventually into seven categories in the third division (Fig. 2). The former was clearly characterized by the location of stands in the study area, the latter varying in respect to physiognomy, species composition and vegetation strati-

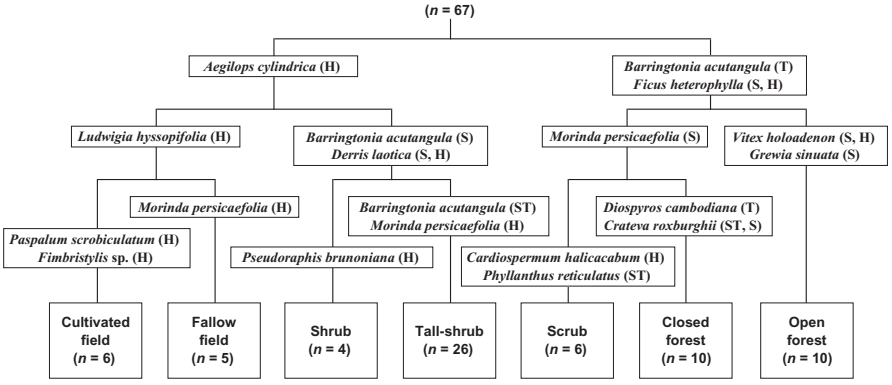

FIG. 2. Two-Way Indicator Species Analysis (TWINSPAN) dendrogram of 67 quadrats identifying seven vegetation types with indicator species listed at divisions. The number of quadrats in each vegetation type is indicated in *parentheses*. Abbreviations following species names are layers to which indicator species belonged: *T*, tree layer; *ST*, short-tree layer; *S*, shrub layer; *H*, herb layer

TABLE 1. Comparison of the mean distance from CLWL, mean height of vegetation, mean density of species (/100 m^2), and diversity indices among seven vegetation types

Vegetation types	Number of quadrats	Mean distance from CLWL (km)	Mean height of vegetation (m)	Mean density of species (/100 m^2)	Simpson D'	Shannon H'	Pielou J'
Cultivated field	6	4.1	0.3	11.2	0.577	2.103	0.887
Fallow field	5	4.5	1.1	13.0	0.333	1.171	0.456
Shrub	4	3.4	3.8	13.5	0.395	1.340	0.515
Tall shrub	26	3.6	6.3	15.9	0.428	1.559	0.567
Scrub	6	0.9	6.9	8.8	0.356	1.122	0.516
Open forest	10	0.2	10.8	8.0	0.390	1.177	0.583
Closed forest	10	0.6	13.8	8.0	0.439	1.354	0.658

CLWL, coastline at the lowest water level

fication (Fig. 1, Table 1, Table 2). Therefore, they were regarded as vegetation zones and vegetation types, respectively.

4.1.1. Vegetation Zones

Vegetation zones consisted of extensive cropland occupying the upper part of the study area (about 2–3 km in depth) and disturbed woodland fringing the coastal side of the study area (about 1–2 km in depth).

Stands of extensive cropland (n = 41) were separated from those of disturbed woodland (n = 26) by reference to *Aegilops cylindrica* (herb layer), a pioneer grass in seasonally dry habitats, as the indicator species (Fig. 2), and characterized by the growth of (1) similar pioneer herbaceous species such as *Melochia corchorifolia*, *Ludwigia hyssopifolia*, *Fimbristylis* sp., and *Lindernia crustacea*; (2) pioneer or early successional lianas such as *Derris laotica*, *Merremia hederacea*, *Phyllanthus reticulatus*, *Gmelina asiatica*, and *Hiptage triacantha*; and (3) pioneer or early successional woody shrubs and short-trees such as *Mimosa pigra*, *Croton krabas*, and *Hymenocardia wallichii* (Fig. 2, Table 2). This vegetation zone was subdivided into four categories of vegetation types (Fig. 2), both the mean distance from CLWL and mean density of species in stands in extensive cropland being larger than those in stands in disturbed woodland, while the mean vegetation height was lower (Table 1). The landscape of the extensive cropland was a mosaic of cultivated fields, abandoned fields of various successional stages, and agricultural infrastructure such as banks, channels, shallow ponds, and footpaths (Photo 1).

The indicator species utilized for the disturbed woodland were *Barringtonia acutangula* (tree layer) and *Ficus heterophylla* (shrub and herb layers). Tree and short-tree species such as *Diospyros cambodiana*, *Coccoceras anisopodum*, and *Crateva roxburghii*, shrubs such as *Morinda persicaefolia* and *Grewia sinuate*, and lianas such as *Combretum trifoliatum* and *Vitex holoadenon* occasionally accompanied these (Fig. 2, Table 2, Photo 2). This vegetation zone was subdivided into three vegetation types (see Fig. 2), "Scrub" indicating transitional vegetation over a wide area between the extensive cropland and seasonally inundated forest. The density of thick trees tended to increase toward the coastal side of the study area, whereas "Closed forest,"

TABLE 2. Synoptic table of indicator and preferential species in the seven vegetation types by Two-Way Indicator Species Analysis (TWINSPAN)

Vegetation types		Cultivated field	Fallow field	Shrub	Tall shrub	Scrub	Open forest	Closed forest
Number of quadrats		6	5	4	26	6	10	1 0
Mean density of species		11.2	13.0	13.5	15.9	8.8	8.0	8.0
Paspalum scrobiculatum	G	IV_{+}	-	-	I_{+}	-	-	-
Oryza sativa	G	II_{+}	-	-	-	-	-	-
Sesbania roxburghii	H	I_{+}	-	-	I_{+}	-	-	-
Aeschynomene indica	H	I_{+}	-	-	I_{+}	-	-	-
Passifora foetida	L	II_{+}	I_{+}	-	I_{+}	-	-	-
Cyperus pilosus	G	I_{+}	II_{+-1}	-	I_{+-1}	-	-	-
Brachiaria reptans	G	III_{+}	I_{+}	-	I_{+}	-	-	-
Nymphoides indica	H	III_{+}	III_{+}	1_{+}	-	-	-	-
Melochia corchorifolia	H	IV_{+}	III_{+-1}	-	I_{+}	-	-	-
Ludwigia hyssopifolia	H	V_{+-1}	III_{+-1}	1_{+}	I_{+}	-	-	-
Fimbristylis sp.	G	V_{+}	II_{+-3}	1_{+}	I_{+}	-	-	-
Lindernia crustacea	H	III_{+}	II_{+}	2_{+}	I_{+}	-	-	-
Aegilops cylindrica	G	III_{+}	III_{+}	3_{+}	IV_{+-1}	-	-	-
Mimosa pigra	S	III_{+}	III_{+}	4_{+-3}	IV_{+-2}	I_{+}	-	-
Pseudoraphis brunoniana	G	II_{+}	V_{+-5}	4_{1-5}	III_{+-3}	-	III_{+-1}	-
Derris laotica	L	II_{+}	I_{+}	1_{+}	V_{+-3}	III_{+-1}	-	-
Merremia hederacea	L	V_{+-1}	V_{+-4}	4_{+}	IV_{+-3}	IV_{+}	V_{+}	-
Barringtonia acutangula	T	V_{+}	V_{+-3}	4_{+-5}	V_{+-5}	V_{+-5}	V_{+-5}	V_{+-5}
Morinda persicaefolia	S	III_{+}	V_{+-1}	3_{+-2}	V_{+-2}	V_{1-5}	IV_{+-2}	V_{1-5}
Combretum trifoliatum	L	I_{+}	IV_{+}	3_{+-3}	IV_{+-3}	V_{+-2}	II_{+-1}	III_{+-2}
Phyllanthus reticulatus	L	I_{+}	IV_{+-3}	4_{+-2}	V_{+-5}	V_{+-1}	-	-
Gmellina asiatica	L	-	III_{+-1}	2_{+}	IV_{+-3}	III_{+-1}	-	-
Croton krabas	ST	-	III_{+}	4_{+}	IV_{+-3}	I_{+}	-	-
Hymenocardia wallichii	ST	-	II_{+}	-	II_{+-1}	I_{+}	-	-
Hiptage triacantha	L	-	II_{+}	2_{+-1}	IV_{+-2}	-	I_{+}	-
Dalbergia entadoides	L	-	-	1_{1}	III_{+-2}	-	-	-
Ipomoea aquatica	L	-	-	2_{+}	II_{+}	-	-	-
Ludwigia adscendens	H	-	-	-	I_{+-1}	-	-	-
Uvaria pierrei	S	-	-	-	I_{+-2}	-	-	-
Brownlowia paludosa	ST	-	-	-	II_{+-1}	I_{1}	-	-
Acacia thallandica	L	-	-	-	III_{+-2}	-	I_{2}	-
Cardiospermum halicacabum	H	-	-	-	I_{+}	V_{+}	I_{+}	-
Vitex holoadenon	L	-	-	2_{+-1}	IV_{+-5}	II_{2}	V_{2-5}	III_{1-2}
Crateva roxburghii	ST	-	-	-	I_{+}	I_{1}	III_{+}	V_{+-2}
Ficus heterophylla	S	-	-	-	-	IV_{1-2}	V_{+-1}	II_{+-1}
Diospyros cambodiana	T	-	-	-	-	I_{1}	I_{2}	V_{+-4}
Grewia sinuata	S	-	-	-	-	-	IV_{1-3}	I_{+}
Coccoceras anisopodum	T	-	-	-	-	-	-	II_{1-3}
Xanthophylum anisopodum	T	-	-	-	I_{+-1}	-	-	I_{4}

Roman numbers are appearance frequency; I, 1%–20%; II, 21%–40%; III, 41%–60%; IV, 61%–80%; V, 81%–100%

Symbols following appearance frequency indicate Braun–Blanquet's dominant scale (+, 1, 2, 3, 4, 5)
Growth forms; G, graminoids; H, herbs; S, shrubs; ST, short-trees; T, trees; L, lianas

Photo 1. Landscape of the extensive cropland zone in the lowest water season (May 2005)

Photo 2. Landscape of the disturbed woodland zone in the highest water season (November 2003)

PHOTO 3. Aspect of emergent "Closed forest" fringing the shore in the lowest water season (February 2005). *Arrow* indicates the highest water level in the flood season

the most developed stage with the highest (mean height, 13.8 m) and most continuous (mean coverage, 92%) canopy, was only found on the coastal side located far from villages (Fig. 1, Table 1, Photo 3).

4.1.2. Vegetation Types

Seven categories of vegetation types, classified by TWINSPAN, included "Cultivated field," "Fallow field," "Shrub," and "Tall-shrub" in the extensive cropland zone and "Scrub," "Open forest," and "Closed forest" in the disturbed woodland zone (see Fig. 2). Vegetational characteristics of each type are summarized next.

"Cultivated field" (n = 6) was almost entirely occupied by paddy fields located in the comparatively high elevation area of the floodplain (waterlogged period, September–January) and cultivated extensively during the early part of the dry season. Under wet soil conditions just before flooding, the mean vegetation height was 0.3 m and the mean herb layer coverage scarce (2%). On the other hand, this type included large numbers of herbaceous species, such as *Merremia hederacea*, *Ludwigia hyssopifolia*, *Fimbristylis* sp., *Paspalum scrobiculatum*, *Melochia corchorifolia*, *Brachiaria reptans*, *Lindernia crustacea*, and *Aegilops cylindrica* (see Table 2). Current-year seedlings and/or sprouts of woody plants (e.g., *Barringtonia acutangula*, *Mimosa pigra*, and *Morinda persicaefolia*) and water plants (e.g., *Nymphoides indica* and *Pseudoraphis brunoniana*) also emerged (Table 2), the large variations in species composition among quadrats increasing the species diversity indices (see Table 1).

"Fallow field" (n = 5) referred to cultivated fields that had been abandoned for relatively few years and were characterized by a herb layer only, the mean height and coverage of recovered vegetation being greater than those of "Cultivated field" (1.1 m and 73% in the former, respectively). Herbaceous species, such as *Pseudoraphis*

brunoniana and *Merremia hederacea*, and seedlings and/or sprouts of *Barringtonia acutangula*, *Combretum trifoliatum*, and *Phyllanthus reticulatus* occurred more frequently (Table 2), although *Paspalum scrobiculatum* was not recorded. Stands of this vegetation type were scattered in the upper part of the study area, the mean distance from CLWL being 4.5 km (Table 1).

"Shrub" ($n = 4$) was characterized by a shrub layer in which *Barringtonia acutangula* dominated (mean height, 3.8 m; mean coverage, 75%) and a large number of liana species flourished (Table 2). Shrubby species, such as *Mimosa pigra*, *Morinda persicaefolia*, and *Croton krabas*, and liana species, such as *Phyllanthus reticulatus*, *Combretum trifoliatum*, *Vitex holoadenon*, *Hiptage triacantha*, and *Merremia hederacea*, also occurred in the canopy. In the herb layer, *Pseudoraphis brunoniana* dominated and *Aegilops cylindrica*, *Lindernia crustacea*, and current-year seedlings of *Barringtonia acutangula* were occasionally recorded (Table 2). The distributional pattern of "Shrub" was mosaic in the "Cultivated field" range and sometimes comprised large patches.

In general, "Tall-shrub" ($n = 26$) was also a crowded vegetation type, with flourishing liana species as found in "Shrub." The height of the former reached to 6.3 m on average (Table 1), the maximum DBH in each quadrat attaining between 11.9 cm and 26.7 cm. Scattered individuals of *Barringtonia acutangula* were predominant in the canopy (note: in the present study, we regarded this developing foliage not as a shrub layer but as a short-tree layer), accompanied by *Croton krabas* and many woody liana species, such as *Phyllanthus reticulatus*, *Dalbergia entadioides*, *Gmelina asiatica*, *Combretum trifoliatum*, *Vitex holoadenon*, and *Acacia thailandica* (Table 2). Shrub and herb layers were composed of *Morinda persicaefolia*, *Derris laotica*, *Croton krabas*, *Hiptage triacantha*, *Mimosa pigra*, *Hymenocardia wallichii*, *Merremia hederacea*, *Pseudoraphis brunoniana*, and *Aegilops cylindrica*. The mean number of emergent species in a single quadrat (15.9 species/100 m^2) was the largest among the seven categories of vegetation types recognized (Table 1). Moreover, large numbers of indicator and preferential species overlapped with those of other vegetation types (see Table 2). "Tall-shrub" was widely distributed over the middle part of the study area (mean distance from CLWL, 3.6 km; Table 1), accompanied by phenomena such as isolated stands created by reclamation and degraded stands by selective logging. Therefore, from the point of view of vegetation succession, "Tall-shrub" was considered as a transitional stage between shrub and forest, showing relatively high species diversity (see Table 1) under varying human impacts.

"Scrub" ($n = 6$) was physiognomically a dense, shrubby vegetation located in the disturbed woodland zone (mean height of vegetation, 6.9 m; mean distance from CLWL, 0.9 km; Table 1). Compared floristically with "Tall-shrub" and "Shrub," "Scrub" was characterized by (1) disappearance or decrease in dominance of many herbaceous and liana species (e.g., *Aegilops cylindrica*, *Pseudoraphis brunoniana*, *Hiptage triacantha*, *Dalbergia entadioides*, and *Acacia thailandica*); (2) emergence of important species of seasonally inundated forest (e.g., *Ficus heterophylla* and *Diospyros cambodiana*); (3) frequent growth of *Cardiospermum halicacabum*, a perennial herb species; and (4) lower density of species (8.8 species/100 m^2; see Table 2). Predominant species coinciding with those of "Tall-shrub" were *Barringtonia acutangula*, *Combretum trifoliatum*, *Vitex holoadenon*, and *Phyllanthus reticulatus* in the short-tree layer and *Morinda persicaefolia*, *Gmelina asiatica*, *Derris laotica*, and *Merremia hederacea* in the shrub and herb layers.

The canopy of "Open forest" reached to 10.8 m on average ($n = 10$; Table 1), the stunted examples of *Barringtonia acutangula* (maximum DBH, 27.6–46.8 cm) having abundantly extended crowns (mean coverage of tree layer, 67%). Short-tree and shrub layers, which frequently appeared as dense bushes or blankets of foliage, contained *Morinda persicaefolia* and species characteristic of disturbed woodland zones, such as *Vitex holoadenon*, *Ficus heterophylla*, *Grewia sinuate*, and *Crateva roxburghii* (see Table 2). On the other hand, the herb layer was poor (mean coverage, 22%) under dark conditions, and several species such as *Merremia hederacea* and *Pseudoraphis brunoniana* were infrequently recorded. Species density was only 8.0 species/100 m^2. "Open forest" occurred along the shore of the lowest water season (mean distance from CLWL, 0.2 km; Table 1), a habitat in which waterlogged conditions continued for about 6 months, from the end of July to early in February. Stumps left over from selective logging were apparent, and branches had also been cut by local people for firewood and fish-catching materials, even in the flood season.

"Closed forest" ($n = 10$) was the most developed stand of seasonally inundated forest; namely, the mean canopy height (13.8 m, Table 1) and coverage (92%), and maximum DBH in each quadrat (38.9–63.5 cm), were greater than those of "Open forest," although species density (8.0 species/100 m^2), species indices, and locations of stands (mean distance from CLWL, 0.6 km) were similar between the two vegetation types (Table 1). The dominant canopy species was *Barringtonia acutangula*, accompanied by water-durable trees (*Diospyros cambodiana*, *Coccoceras anisopodum*, and *Xanthophyllum glaucum)* and the liana *Combretum trifoliatum* (Table 2). In the short-tree layer, a small number of *Vitex holoadenon* and *Crateva roxburghii* occurred (mean coverage, 13%), the shrub layer being almost entirely occupied by *Morinda persicaefolia* (mean coverage, 75%). The herb layer was also poor, including primarily *Morinda persicaefolia*, *Vitex holoadenon*, and *Crateva roxburghii* (mean coverage, 10%). In the present study, "Closed forest" was infrequently found, occurring as remnant patches far from villages (about 7 km west from main sampling area; see Fig. 1).

4.2. Ordination of Seasonally Inundated Vegetation

The ordination of 67 quadrats on the two principal axes of DCA is given by Fig. 3, in which seven categories of vegetation types classified by TWINSPAN were overlaid. Table 3 shows correlations between DCA scores and parameters of stand characteristics.

Axis 1 (eigenvalue, 0.794) had negative correlations with vegetation height and tree layer coverage (Table 3; $P < 0.001$, Spearman's ranking correlations). Additionally, Axis 1 also had positive correlations with species density, short-tree layer coverage, Shannon H, and distance from CLWL (Table 3; $P < 0.05$, Spearman's ranking correlations). Axis 2 (eigenvalue, 0.427) had negative correlations with tree layer coverage, short-tree layer coverage, and vegetation height (Table 3; $P < 0.05$, Spearman's ranking correlation), but a positive correlation with Shannon H' (Table 3; $P < 0.05$, Spearman's ranking correlation).

Along Axis 1, seven vegetation types roughly followed the order "Closed forest", "Open forest", "Scrub", "Tall-shrub", "Shrub", "Fallow field", and "Cultivated field" (Fig. 3). Comparing the distributional ranges of the vegetation types on the two prin-

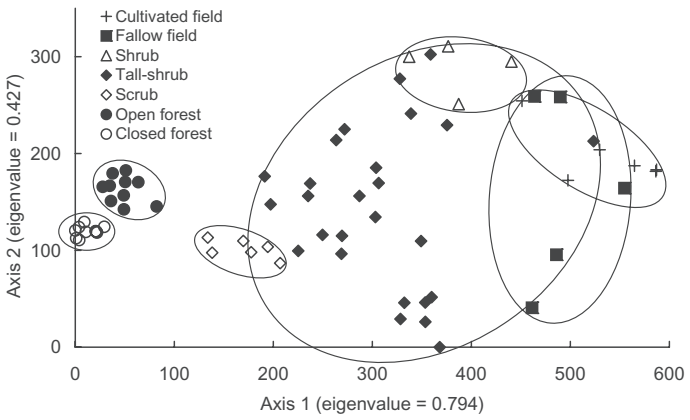

FIG. 3. Detrended Correspondence Analysis (DCA) ordination of 67 quadrats. The different vegetation types classified by TWINSPAN are *overlaid* and *encircled*

TABLE 3. Correlations between DCA scores and parameters of stand characteristics

Parameter	Axis 1	Axis 2
Height of vegetation	−0.942***	−0.315**
Density of species	0.447***	0.200
Simpson D'	0.088	0.220
Shannon H'	0.242*	0.266*
Pielou J'	−0.126	0.139
Coverage of T	−0.728***	−0.873***
Coverage of ST	0.390**	−0.331*
Coverage of S	−0.018	−0.098
Coverage of H	0.144	0.233
Distance from CLWL	0.803***	0.061

T, tree layer; ST, short-tree layer; S, shrub layer; H, herb layer; CLWL, coastline at the lowest water level

* $P < 0.05$, ** $P < 0.01$, *** $P < 0.001$; Spearman's ranking correlations

cipal axes, three vegetation types constituted a disturbed woodland zone, which was characterized by the existence of a tree and/or short-tree layer and a limited number of woody species adapted to long-term inundation, closely clustered.

5. Discussion

5.1. Structure of Seasonally Inundated Vegetation

Seasonally inundated vegetation covering the vast floodplain of the study area was clearly affected by flooding stress and man-made disturbances. CNMC/NEDECO (1998b) listed up to about 200 vascular plant species in the Tonle Sap area, describing

the introduced floodplain vegetation as comprising three major habitat types (McDonald et al. 1997): (1) short-tree and shrubland vegetation, covered by semicontinuous, locally homogeneous stands of short trees and large shrubs; (2) stunted swamp forest, comprising trees 7–15 m in height and dense gallery forests that commonly skirted the lake shoreline of the floodplain; and (3) aquatic herbaceous vegetation, being either floating or emergent (1–3 m tall). In the present study, based on phytosociological data from 67 quadrats (10 m × 10 m each), we recorded 122 vascular plant species and seven vegetation types on the coastal side of the floodplain (about 4 km in depth; about 1–6 m a.s.l.).

Of the 122 plant species, indicator and preferential species of the seasonally inundated forest, namely, "Closed forest" and "Open forest" in our study, were limited to taller trees such as *Barringtonia acutangula*, *Diospyros cambodiana*, *Coccoceras anisopodum*, and *Xanthophyllum glaucum*, shorter trees such as *Crateva roxburghii*, shrubs such as *Morinda persicaefolia*, *Ficus heterophylla*, and *Grewia sinuate*, and lianas such as *Vitex holoadenon* and *Combretum trifoliatum* (see Table 2). On the other hand, it should be noted that *Mimosa pigra*, a prickly woody shrub originating from tropical America, has spread extensively in the cropland zone. It is currently considered to be one of the most invasive and problematic species in the seasonally inundated vegetation (Tim et al. 2005).

Two types of wooded vegetation distinguished by McDonald et al. (1997), namely short-tree and shrubland vegetation, and stunted swamp forest, seemed to roughly correspond to "Shrub" + "Tall-shrub" and "Scrub" + "Open forest" + "Closed forest" in the present study, respectively. However, "Shrub" constituted crowded recovery areas neighboring "Cultivated field", and "Tall-shrub" consisted of 26 dense stands with large floristic and architectural variations in disturbed areas (see Table 1, Fig. 3). Because of stumps and selective cuts on branches, "Scrub" and "Open forest" are also implicated in degraded vegetation suffering from human impact. Therefore, these vegetation types, excepting "Closed forest", might be seminatural and still developing. Accordingly, to reconstruct the original vegetation structure of the inundated area, both distributional patterns along the waterlogged versus drought condition gradient, not subject to human impact, and regeneration traits for key species (see Table 2) should be examined carefully.

5.2. Importance of Barringtonia acutangula

The genus *Barringtonia* (Lecythidaceae) is distributed in tropical regions from East Africa to the Pacific Islands and frequently occurs in freshwater swamps near rivers and lakes (Payens 1967). In the lowland areas of Cambodia, *Barringtonia acutangula* is highly useful, providing firewood, edible young shoots, and medicinal bark, roots, and fruits (McDonald et al. 1997; Dy phon 2000; Kham 2004).

The present survey revealed that *Barringtonia acutangula* grew vigorously, becoming the dominant species in six vegetation types, excluding "Cultivated field". The species regenerated from seedlings (growing from floating fruits) and also sprouted from stumps or floated twigs, thereby achieving maturity even in interior sites in the extensive cropland zone. Considering these phenomena, it can be concluded that *Barringtonia acutangula* had originally prevailed even more than presently over the floodplain, and that an investigation of the life history strategies of this species should

be a priority in the restoration of disturbed sites and the wise management of seasonally inundated vegetation.

Acknowledgments. We would like to thank the Authority for the Protection of the Site and Management of Angkor and Region of Siem Reap, Angkor Conservation Compound, Kingdom of Cambodia, for local research support. Many thanks are also due to the staff of the Department of Geology, General Department of Mineral Resources, Ministry of Industry, Mines and Energy, Kingdom of Cambodia, for help during the field survey. We also thank M. Kanzaki, M. Araki, P. Chhang, and K. Saret for their encouragement. This study was supported financially by UNESCO MAB-IHP Japanese Fund-in Trust, JSPS Grant-in-Aid for International Scientific Research (15405004), Kanazawa University 21st Century COE Program, The 21st Century COE Program "Environmental Risk Management for Bio/Eco-Systems," and a Grant-in-Aid for Scientific Research from the Ministry of Education, Culture, Sports, Science and Technology of Japan (18650236).

References

Bailleux R (2003) The Tonle Sap great lake: a pulse of life. FAO. Asia Horizons Books, Bangkok

Braun-Blanquet J (1964) Pflanzensoziologie: Grundzüge der Vegetations-kunde, 3 Aufl. Springer-Verlag, Wien and New York

CNMC/NEDECO (1998a) Natural resources-based development strategy for the Tonle Sap Area, Cambodia (CMB/95/003). Final report, vol 1. Main report. Cambodian National Mekong Committee, Phnom Penh

CNMC/NEDECO (1998b) Natural resources-based development strategy for the Tonle Sap Area, Cambodia (CMB/95/003). Final report, vol 2. Sectoral studies: Environment in the Tonle Sap area. Cambodian National Mekong Committee, Phnom Penh

Dy phon P (2000) Dictionary of plants used in Cambodia. Imprimerie Olympic, Phnom Penh

Hill MO (1979) TWINSPAN, a FORTRAN program for arranging multivariate data in an ordered two-way table by classification of the individuals and attributes. Ecology and Systematics, Cornell University, Ithaca, NY

Hill MO, Gauch HG (1980) Detrended correspondence analysis, an improved ordination technique. Vegetatio 42:47–58

Kham L (2004) Medical plants of Cambodia: habitat, chemical constituents and ethnobotanical uses. Bendigo, Golden Square, Australia

McCune B, Mefford MJ (1999) PC-ORD for windows. Multivariate analysis of ecological data, version 4.00. MjM Software, Gleneden Beach, OR

McDonald JA, Pech B, Phauk V, Leeu B (1997) Plant communities of the Tonle Sap floodplain. Final report in contribution to the nomination of Tonle Sap as a biosphere reserve for UNESCO's Man in the Biosphere Program. UNESCO, Paris

Mekong River Commission (1997) Mekong River basin diagnostic study. Final report. Mekong River Commission, Bangkok

MRCS (2003) Database for precipitation and water stage data. Mekong River Commission Secretariat, Phnom Penh

Payens JPDW (1967) A monograph of the genus *Barringtonia* (Lecythidaceae). Blumea 15:157–263

Pielou EC (1975) Ecological diversity. Wiley Interscience, New York

Shannon CE, Weaver W (1949) The mathematical theory of information. University of Illinois Press, Urbana

Simpson EH (1949) Measurement of diversity. Nature (Lond) 163:688

Sokhun T (1997) Review of the forestry sector in Cambodia. Prepared for the Project CMB/95/003: Natural resources-based development strategy for the Tonle Sap area, Cambodia. UNDP, Mekong River Commission and Cambodian National Mekong Committee, Phnom Penh

Tim AH, Quentin P, Richard C, Areli M (2005) *Malacorhinus irregularis* for biological control of *Mimosa pigra*: host-specificity, life cycle, and establishment in Australia. Biol Control 32:252–262

Subject Index

a
Acacia thailandica 289
Acrisols 189, 196, 197, 251, 264, 275
Aegilops cylindrica 285
air temperature 75, 80, 81, 84
albedo 80, 81, 84
Anisoptera 215
aquifer 19
Arenosols 189, 196, 197, 199, 265
Asia 3, 6, 10, 18, 19
ASTER 232, 234
atmospheric stability 93, 94
available water capacity 247

b
bamboo and palms 189, 194
bamboos 211
Barringtonia acutangula 281
basal area 232–234, 237
bonding power 268
Bowen ratio 75, 78, 79, 84
BREB 139
bucket model 38
buffer zone 186
bulk density 246, 264

c
Cambisol 275
Cambodia 135, 149, 150, 157, 160, 214, 215, 232, 273
canopy 210
capacity inflow 170
CEC 249
Central Indochina Dry Forest 209
Chap chon 181
Chi River basin 24
clay content 229, 245, 268
clay mineralogy 3, 8, 18
climate properties 273
closed evergreen lowland forests 192
closed mountain forests 193
cluster analysis 205, 224, 225
coastal forests 194
Coccoceras anisopodum 285
colluvium 263
Combretum trifoliatum 285
community forestry 183
confusion matrix 155, 156
coniferous forests 189, 195
correlation coefficient 33
Crateva roxburghii 290

d
Dalbergia entadioides 289
dead storage 177
decentralization 182
deciduous dipterocarp forest 209, 225, 227
deciduous forest 57, 189, 194, 205
deep seepage 33
deforestation 25
degradation 281
DEM 162
Derris laotica 289
deuterium excess 128
Diospyros cambodiana 285
Dipterocarpaceae 209, 215, 233
Dipterocarpus costatus 222, 224
Dipterocarpus intricatus 228
Dipterocarpus obtusifolius 222, 224, 225, 227
discharge 27, 67, 70, 71
discriminant analysis 234, 235
disturbed woodland zone 288

diversity 284
drainage properties 278
drought 31, 45, 292
dry deciduous forest (DDF) 97, 98, 112, 113, 123, 214, 243, 254–256, 275
dry dipterocarp forest 227
dry evergreen forest (DEF) 97, 98, 112, 113, 123, 204, 214, 223, 225, 227, 243, 254, 256, 275
dry season 59, 67, 112, 113, 115–118, 120–123, 254, 257–261, 277
dry season irrigation 67
dryness 105, 108, 109

e
ECEC 249
ecoregions 202
effective porosity 269, 276
El Niño 45
energy, water, and carbon budget 65
erosion 168, 169, 176, 177
evapotranspiration 32, 33, 40, 75–80, 82–84, 137
evergreen broadleaf forest 75, 84, 137
evergreen forest 189, 192, 194, 205
exchangeable cations 249
experimental watershed 137
extensive cropland zone 288

f
Ferralsols 189, 196–198
Ficus heterophylla 289
firewood 290
flooding pulse 282
floodplain 281
flow/rainfall (Q/P) ratio 26
Fluvisols 189, 197–199
forest classification 235
forest composition 202
forest soils 189, 196
forest type 39, 202
forest vegetation 189, 190, 192, 202
forested area 29, 36, 274
frequency distributions 137
freshwater swamps 292

g
GAME reanalysis data 37
geographic information system (GIS) 36, 136
GLC2000 159, 161–164
global meteoric water line (GMWL) 125, 128, 130, 133
Grewia sinuate 285
ground fires 228
groundwater level 79, 82–84, 112, 113, 115–118, 120–123, 229, 257, 260, 262, 268
growing season 56
GTOPO30 37, 161, 162

h
heat pulse velocity 58
heat-balance method 75, 78, 79, 84
hemispherical photography 215–217
high flow 31
hill evergreen forest 65, 208
Hiptage triacantha 289
Histosols 265
human impact 281
hydrological processes 32
hypsitsermal 228

i
image segmentation 149, 152, 153, 157
indicator species analysis 204, 224
Indochina bioregion 201
infiltration 115, 117, 121, 123
interannual variability 56, 64
International Satellite Land Surface Climatology Project (ISLSCP) Initiative 1 data 37
Irvingia malayana 210

j
Jarvis-type model 97, 98, 100, 102, 106, 108

k
Kampong Thom 112, 113, 214, 215, 242, 254, 255, 262
Khat statistics 149, 155
Kog-Ma 67

l
LAI-2000 215
Lake Tonle Sap 281
land cover 67
land cover map 149, 150, 155–157 159, 160, 162, 163, 165

land tenure 181
land-use 24, 27, 34, 180
landform 282
Landsat 150–152
Laos 160, 164
leaf area index (LAI) 59, 60, 99, 101, 102, 214, 215, 232, 234, 237
leaf fall 62
leaf flushing 62
leafless period 210
Leptosols 199
life history strategies 292
lifespan 168, 169, 171, 177
light saturation 102
line transect 243
Local Maximum Fitting with Kalman Filter (LMF-KF) 159–161, 163, 164
local meteoric water line (LMWL) 125, 126, 128–130, 133
low flow 73

m
Mae Chaem 67
Mae Tia 67
mangrove swamps 193
matric potential 114, 115, 117, 118, 120–122, 278
matrix flow 278
maximum stomatal conductance (g_{smax}) 97, 98, 100, 102, 104, 105
Mekong River basin 36, 149, 150, 159, 165
Melaleuca cajuputi 209, 222, 224, 225, 228
Merremia hederacea 285
meteoric water line (MWL) 128–130
meteorological observation tower 75, 76, 78, 137
microtopography 222, 229
Mimosa pigra 285
minimum flow 70, 72, 73
mixed forest 209, 225, 243, 254, 255, 275
MOD12Q1 37
modified HYCY model 140
monsoon winds 93
Morinda persicaefolia 285
MSAVI2 234, 236
multitemporal image 150, 157, 158
Myanmar 160

n
National Economic Social Development Board (NESDB) 181
nationalization 179
natural forest 275
nearest neighbor classification 152, 153
net radiation 75, 79, 80, 84
neutral stability 94
NOAA Pathfinder AVHRR 8-km land (PAL) dataset 159, 160, 164, 165
Nontimber Forest Products (NTFPs) 184
Normalized Differential Vegetation Index (NDVI) 159–164, 234, 236
northeast monsoon 88, 93
northern Thailand 57
numerical classification 211

o
object-oriented classification 149, 150, 153, 157
one-dimensional 112–114, 118, 122
open broad-leaved forests 189, 195
open woodlands 211

p
PAR 100–102, 105, 106, 108, 109
Participatory Learning and Action (PLA) 184
peat swamps 223
Pelthophorum dasyrrhachis 208
penetration (Nc) value 266, 269
penetrometer 264, 265
permanent lake 282
permeability 278
pH 248
Phyllanthus reticulatus 285
physiognomy 282
phytosociological evaluation 281
Ping River 68
pioneer species 208
plant phenology 38
Podzols 265, 275
pore-size distribution (PSD) 246
precipitation 76, 80, 84
preferential flow 278
Priestley–Taylor (PT) equation 37
Pseudoraphis brunoniana 289

r
radiative transmittance 59
rainfall 25, 27, 29, 67, 68, 139, 278
rainwater 270

rainy season 59, 112, 114–118, 120, 122, 123, 254, 255, 257–261, 277
range line 176
rangeline 176
rating curve 172
recession 26
regeneration traits 292
regolith 3, 6, 10, 18, 19
remnant forest 282
restoration 293
retention curve 270
Richards' equation 112–114, 118, 119, 123
riparian forests 194
river discharge 31
rock type 3
roughness length 93–95
runoff 3, 76, 79, 83, 84, 136, 172, 174, 175

s
Salic Fluvisols 198
sap flow 45
sap flux 57
saprolite 263
saturated hydraulic conductivity 278
saturation deficit 75, 79–84
scale 67
Schima wallichii 208
scrub 189, 196
seasonal 75, 76, 80–84, 150, 163, 216, 218, 268, 278, 281
seasonal and annual flows 34
seasonal spectral 151, 154, 157
seasonally flooded forest 180, 183
seasonally inundated 284
secondary evaporation 125, 128–131
sediment yield 173
sedimentation 168, 169, 177
selective logging 289, 290
semideciduous broad-leaved forests 189, 192
shifting cultivation 67
shortwave radiation 75, 79, 80, 84
silt content 245
siltation 168, 169, 177
soil classification 250
soil colors 244
soil depth 266, 269
soil hardness 266
soil layer 263, 276
soil loss 174, 175
soil moisture 60, 62, 64, 112, 113, 119, 121, 122, 254, 255, 257–259, 261, 262
soil Morphology 244
soil particle-size distribution 245
soil texture 169, 245
soil thickness 244, 276
soil type 6
soil water content 41, 82, 256, 258–262, 273
Songkhram River 179, 180
Southeastern Indochina Dry Evergreen Forest 209
Southern Annamites Montane Rain Forest 209
southwest monsoon 88
species composition 282
stability length 93
stable isotope 125, 126, 128, 132, 133
stand characteristics 290
stem density 137
stomatal conductance (g_s) 97–102, 105, 106, 109
stomatal control 63, 65
stomatal response 97, 98, 104
storage capacity 169, 171
stratification 282
streamflow 29
swamp forest 193, 209

t
tambon 182, 183
Tectona grandis (teak) 57
Tha Bo village 185
Tha Koon village 184
Thailand 24, 67, 160
Thionic Fluvisols 198
time-series analysis 25, 28
topographical properties 278
total carbon 248
total nitrogen 248
total porosity (TP) 246, 264
transpiration period 58, 62, 64
transpiration 45, 56, 58, 60, 63, 97–99, 108, 109
trap efficiency 170
tree crown density 254
tree model 162–164
tropical 3, 6, 8, 18
tropical monsoon Asia 263
tropical rainforests 3
tropical seasonal forest 56, 214, 232, 233

u
Ultisols 251

v
vapor pressure deficit (*VPD*) 97, 98, 100–102, 104–106, 108, 109
Vatica odorata 204, 215, 222, 224, 227, 228
vegetation index 234, 240
vegetation map 203
vegetation type 288
vegetation zone 285
vertical variation 280
Vietnam 160
Vitex holoadenon 285

w
water balance 24, 26, 27, 32
water budget 34, 65, 75, 76, 83, 84
water conservation function 274
water content index 234, 240
water demand 67
water level 281
water loss 27, 75, 76, 84
water pathway 3, 8, 18
water potential 45
water storage capacity 270, 274
water yield 26
waterlogged 211, 228, 229, 288, 290
wise management 293

x
Xanthophyllum glaucum 290
Xylia xylocarpa 208

y
Yang Ngoy village 185

z
zero plane displacement height 93–95